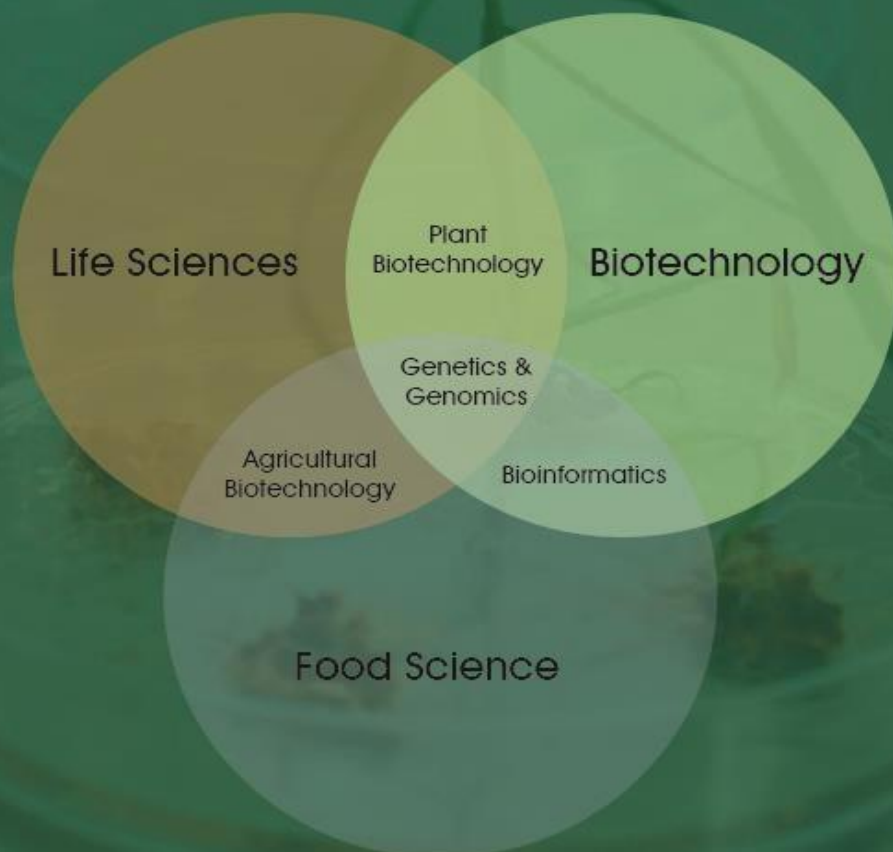


International Journal of Life Sciences and Biotechnology

e-ISSN:2651-4621



Editor in Chief / Baş Editör**Asst. Prof. Dr. Yılmaz Kaya**

Ondokuz Mayıs University, Turkey

Section Editors / Bölüm Editörleri*

* sıralama akademik unvan içinde alfabetik sıralamaya göre. * The ranking is arranged alphabetically within the academic title.

Prof. Dr. Ali ASLAN, PhD, Van Yuzuncuyıl University

Prof. Dr. Ercan BURSAL, PhD, Muş Alparslan University

Prof. Dr. Hasan AKAN, PhD, Harran University

Prof. Dr. Nermin GOZUKİRMİZİ, PhD Istinye University

Prof. Dr. Tengku Haziyaamin TENGKU ABDUL HAMİD, PhD, International Islamic University Malaysia

Assoc. Prof. Dr. Ayhan HORUZ, PhD Ondokuz Mayıs University

Assoc. Prof. Dr. Hasan Murat AKSOY, PhD, Ondokuz Mayıs University

Editorial Board / Editör Kurulu

Prof. Dr. İsmail KOCAÇALIŞKAN, PhD, Yıldız Technical University

Prof. Dr. Kasim BAJROVIĆ, University of Sarajevo

Prof. Dr. Muhammet KURULAY, PhD, Yıldız Technical University

Assoc. Prof. Dr. Gulbubu KURMANBEKOVA, Kyrgyz-Turkish Manas University

Assoc. Prof. Dr. İsmail ERPER, PhD, Ondokuz Mayıs University

Assoc. Prof. Dr. Muhammad Arshad JAVED, PhD, Universiti Teknologi Malaysia

Assoc. Prof. Dr. Roswanira AB. WAHAB, PhD, Universiti Teknologi Malaysia

Assoc. Prof. Dr. Sevgi MARAKLI, PhD, Amasya University

Asst. Prof. Dr. Abdussamat GÜZEL, PhD, Inonu University

Asst. Prof. Dr. Ali Yuksek, PhD, Ondokuz Mayıs University

Asst. Prof. Dr. Cihan İNAN, PhD, Karadeniz Technical University

Asst. Prof. Dr. Ertan ERMİŞ, PhD, Istanbul Sabahattin Zaim University

Asst. Prof. Dr. Feyza TUFAN, PhD, Halic University

Asst. Prof. Dr. Harun ÖZER, PhD, Ondokuz Mayıs University

Asst. Prof. Dr. Kasım TAKIM, PhD, Harran University

Asst. Prof. Dr. Mohamed EDBEİB, PhD, Baniwalid University, Libya

Asst. Prof. Dr. Muhammed YÜCEER, PhD, Canakkale Onsekiz Mart University,

Dr. Aliyu ADAMU, PhD, Kaduna State University

Dr. Abdulwali ABLAT, University of Malaya

Dr. Lect. Abdulgani DEVLET, PhD, Bilecik Seyh Edebali University

Dr. Nedim UZUN, PhD, Taksim Education and Research Hospital, Turkey

Dr. Res. Asst. Kiran NAWAZ, PhD, University of Arizona

Advisory Board / Danışma Kurulu

Prof. Dr. Ahmet OKUMUŞ, PhD, Aydın Adnan Menderes University

Prof. Dr. Didem ÖZÇİMEN, PhD, Yıldız Technical University

Prof. Dr. Fahrul Zaman HUYOP, PhD, Universiti Teknologi Malaysia

Prof. Dr. İbrahim İlker ÖZYİĞİT, PhD, Marmara University

Assoc. Prof. Dr. Funda ARSLANOĞLU, PhD, Ondokuz Mayıs University

Assoc. Prof. Dr. Kadyrbay CHEKİROV, Kyrgyz - Turkish Manas University, Kyrgyzstan

Assoc. Prof. Dr. Sibel YILMAZ, PhD, Yeni Yuzyil University

Assoc. Prof. Dr. Zarina Bt ZAINUDDİN, PhD, International Islamic University Malaysia

Language Editors/ Dil Editörleri

Assoc. Dr. Sevgi Maraklı, Amasya University, Turkey

Res. Assist. Bermet Kıdıralyeva, Kyrgyz - Turkish Manas University, Kyrgyzstan

Specialist Nurjamal Omurzakova, Kyrgyz - Turkish Manas University, Kyrgyzstan

Managing Editor / Yönetici Editör

Dr. Yunus Emre ARVAS, PhD, Yildiz Technical University

Yönetim Ofisi/ Management Office

Yildiz Technical University, Faculty of Chemical and Metallurgical Engineering.
ESENLER/ISTANBUL

Yasal Sorumluluk

Yazıların yasal ve hukuki sorumluluğu yazarlara aittir.

Tüm hakları saklıdır. Derginin hiçbir bölümü, yazılı ön izin olmaksızın ve dergi adına referans gösterilmeden herhangi bir formatta çoğaltılamaz veya kullanılamaz.

Legal Responsibility

The legal responsibility of the articles belongs to the authors. All rights reserved. No part of this journal may be reproduced or used in any form without the prior written permission and a reference to name of the journal.

Editörden;

Değerli okurlar ve yazarlar,

“International Journal of Life Sciences and Biotechnology” olarak dergimizin on dördüncü sayısını yayın hayatına sunmaktan mutluluk ve onur duyuyoruz. “International Journal of Life Sciences and Biotechnology” dergisi araştırma- geliştirme ve uygulama ilkeleri baz alınarak yayınlanan uluslararası hakemli açık erişimli akademik bir elektronik dergidir.

“International Journal of Life Sciences and Biotechnology” dergisi Yaşam Bilimleri, Biyoloji, Biyoteknoloji, Biyomühendislik, Ziraat Bilimleri, Gıda Biyoteknolojisi ve Genetik alanlarındaki ilgili araştırmacılara, kurum ve kuruluşlara teorik ve pratik uygulamalarda katkı sağlamayı, tarafsızlık ve bilim etiği ilkelerine bağlı kalarak çözüm temelli, yenilikçi ve katma değeri olan çalışmalara odaklanan, günceli ve geleceği tartışan çalışmaların yayınlanmasını hedeflemektedir.

Bu düşüncelerle 2022 yılı üçüncü sayısını yayınladığımız “International Journal of Life Sciences and Biotechnology” dergisini, makaleleri ile onurlandıran akademisyenlere, Fikir / Görüş / Öneri / Katkı ve Eleştirileri ile değerlendirme süreçlerine katkılarından dolayı hakem ve yayın kurullarında yer alan kıymetli bilim insanlarına yürekten teşekkür ediyoruz. Bir sonraki sayıda görüşmek ümidiyle...

15.12. 2022
Editör
Dr. Öğrt. Üyesi Yılmaz KAYA

From The Editor;

Dear Readers and Authors,

As “International Journal of Life Sciences and Biotechnology”, we are pleased and honored to present the 14th issue of the journal. "International Journal of Life Sciences and Biotechnology" is an international double peer-reviewed open access academic journal published on the basis of research- development and code of practice.

The aims of this journal are to contribute in theoretical and practical applications in relevant researchers of Life Sciences, Biology, Biotechnology, Bioengineering, Agricultural Sciences, Food Biotechnology and Genetics institutions and organizations in Turkey, and to publish solution based papers depending on the principle of impartiality and scientific ethics principles, focusing on innovative and added value work, discussing the current and future.

With these thoughts, We are especially thankful to academicians honoring with the articles, valuable scientists involved in editorial boards and reviewers for their contributions to the evaluation processes with through their opinions/ideas/contributions/criticisms in the third issue of 2022 "International Journal of Life Sciences and Biotechnology". Hope to see you in the next issue...

15. 12. 2022

Editor in Chief

Assist. Prof. Dr. Yilmaz KAYA

Sayının Hakemleri / Reviewers of the Issue*

* sıralama akademik unvan içinde alfabetik sıralamaya göre. * The ranking is arranged alphabetically within the academic title.

Prof. Dr. Anisur Rahman, Ph. D.	Jashore University of Science and Technology, Bangladesh
Prof. Dr. Ayşegül Çerkezayabekir, Ph. D.	Trakya University, Turkey
Prof. Dr. Erol Bayhan, Ph. D.	Dicle University, Turkey
Prof. Dr. Fahrul Zaman Huyop, Ph. D.	Universiti Teknologi Malaysia
Prof. Dr. Ferat Uzun, Ph. D.	Ondokuz Mayıs University, Turkey
Prof. Dr. Feyzi Çelik, Ph. D.	Dicle University, Turkey
Prof. Dr. Hasan Yetim, Ph. D.	Istanbul Sabahattin Zaim University, Turkey
Prof. Dr. İbrahim İlker Özyiğit, Ph. D.	Marmara University, Turkey
Prof. Dr. İzzet Akça, Ph. D.	Ondokuz Mayıs University, Turkey
Prof. Dr. Seyit Ahmet Oymak, Ph. D.	Marmara University, Turkey
Prof. Dr. Subrata Mondal, Ph. D.	Jashore University of Science and Technology, Bangladesh
Assoc. Prof. Dr. Alı Taghızadehghalehjoughı, Ph. D.	Bilecik Seyh Edebali University, Turkey
Assoc. Prof. Dr. Abdullah Özkan, Ph. D.	Iskenderun Technical University, Turkey
Assoc. Prof. Dr. Behiye Banu Bilgen, Ph. D.	Namik Kemal University, Turkey
Assoc. Prof. Dr. Erdem Gülümser, Ph. D.	Bilecik Sheikh Edebali University, Turkey
Assoc. Prof. Dr. Figen Çalışkan, Ph. D.	Eskisehir Osmangazi University, Turkey
Assoc. Prof. Dr. Gülsüm Yaldız, Ph. D.	Abant İzzet Baysal University, Turkey
Assoc. Prof. Dr. Hatice Aysun Mercimek Takcı, Ph. D.	Kilis 7 Aralık University, Turkey
Assoc. Prof. Dr. M. Aydın Akbudak, Ph. D.	Akdeniz University, Turkey
Assoc. Prof. Dr. Murat Bilgi, Ph. D.	İzzet Baysal Education And Research Hospital, Turkey
Assoc. Prof. Dr. Recep Taş, Ph. D.	Bartın University, Turkey
Assoc. Prof. Dr. Sibel Yılmaz, Ph. D.	Yeni Yuzyıl University, Turkey
Assoc. Prof. Dr. Soner Çakar, Ph. D.	Zonguldak Bulent Ecevit University, Turkey
Assoc. Prof. Dr. Songül Sever Mutlu, Ph. D.	Akdeniz University, Turkey
Assoc. Prof. Dr. Tuba Aydın, Ph. D.	Agri Ibrahim Cecen University, Turkey
Assist. Prof. Dr. Ayşe Feyza Tufan Dülger, Ph. D.	Ondokuz Mayıs University, Turkey
Assist. Prof. Dr. Abdussamat Güzel, Ph. D.	Inonu University, Turkey
Assist. Prof. Dr. Benan İnan, Ph. D.	Yildiz Technical University, Turkey
Assist. Prof. Dr. Cihan İnan, Ph. D.	Karadeniz Technical University, Turkey
Assist. Prof. Dr. Çiğdem Yamaner, Ph. D.	Isparta University of Applied Sciences, Turkey
Assist. Prof. Dr. Deniz Kırış, Ph. D.	Yeditepe University, Turkey
Assist. Prof. Dr. Elif Karlık, Ph. D.	Istinye University, Turkey
Assist. Prof. Dr. Fatih Öner, Ph. D.	Ordu University, Turkey
Assist. Prof. Dr. Gülşah Koç, Ph. D.	Aydin University, Turkey
Assist. Prof. Dr. Handan Özlü Torun, Ph. D.	Kahramanmaraş İstiklal University, Turkey
Assist. Prof. Dr. Hüseyin Uysal, Ph. D.	Akdeniz University, Turkey
Assist. Prof. Dr. Kasım Takım, Ph. D.	Harran University, Turkey
Assist. Prof. Dr. Mehmet Tütüncü, Ph. D.	Ondokuz Mayıs University, Turkey
Assist. Prof. Dr. Meltem Kızılcı Çoruh, Ph. D.	Ataturk University, Turkey
Assist. Prof. Dr. Muhammed Yaşar Dörtbudak, Ph. D.	Harran University, Turkey
Assist. Prof. Dr. Pınar Bozbeyoglu, Ph. D.	Gumushane University, Turkey
Assist. Prof. Dr. Selman Uluşık, Ph. D.	Mehmet Akif Ersoy University, Turkey
Assist. Prof. Dr. Vildan Özkan, Ph. D.	Iskenderun Technical University, Turkey
Assist. Prof. Dr. İbrahim Saygılı, Ph. D.	Tokat Gaziosmanpasa University, Turkey
Dr. Daniel Kimsanaliev, Ph. D.	Kyrgyz - Turkish Manas University, Kyrgyz Republic
Dr. Muhammed Said Yolcu, Ph. D.	Van Yuzuncu Yil University, Turkey
Dr. Nurbek Aldayarov, Ph. D.	Kyrgyz - Turkish Manas University, Kyrgyz Republic
Dr. Nurjamal Omurzakova, Ph. D.	Kyrgyz - Turkish Manas University, Kyrgyz Republic
Dr. Sahın İnjamamul İslam, Ph. D.	Raiganj University, West Bengal India, Turkey
Dr. Sibel Kalyoncu Uzunlar, Ph. D.	İzmir Biomedicine and Genome Center, Turkey
Dr. Sk İnjamamul İslam, Ph. D.	Jashore University of Science and Technology, Bangladesh
Res. Assist. Dr. Gamze Gundogdu, Ph. D.	Uludag University, Turkey
Res. Assist. Dr. Latife Betül Gül, Ph. D.	Giresun University, Turkey
Res. Assist. Dr. Özlem Bakır, Ph. D.	Ataturk University, Turkey
Dr. Bashir Sajo Mienda, Ph. D.	Eberhard Karls Universität Tübingen, Germany

İçindekiler/ Contents

Research Articles/ Araştırma Makaleleri

An In-silico approaches for identification of potential natural antiviral drug candidates against Erythrocytic necrosis virus (Iridovirus) by targeting Major capsid protein: A Quantum mechanics calculations approach	
Saloa SANJIDA Moslema Jahan MOU Sk Injamamul ISLAM Md. SAROWER-E-MAHFUJ	294-315
Assessment of the protective culture potential of the Lactococcus lactis Ganee-5 strain as a preservative against spoilage bacteria in tomato pastes	
Abdullahi AJAO Ganiyat ALASİNRİN	316-334
Schizosaccharomyces pombe' de Magnezyum Kısıtlamasının Glukoz Transportu Üzerine Etkisinin Araştırılması	
Gülşen UZ Tuğba PESEN Ahsen BERBER Cenk KIĞ Bedia PALABIYIK Ayşegül TOPAL SARIKAYA	335-345
Characterization of Omega-3 and Omega-6 Fatty Acid Accumulation in Chlorococcum novae-angliae Microalgae Grown under Various Culture Conditions	
Elifcan ÇALIŞKAN Berat Zeki HAZNEDAROĞLU	346-369
Discrimination of two species (Androctonus crassicauda and Leiurus abduhbayrami; Buthidae Scorpions) by MALDI-TOF- MS-based PCA	
Yasemin NUMANOĞLU ÇEVİK Mehmet Ali KANAT	370-385
Determination of Yield and Quality Characteristics of Various Genotypes of Black Cumin (Nigella Sativa L.) Cultivated Through Without Fertilizers	
Çiğdem BOZDEMİR Reyhan BAHTİYARCA BAĞDAT İlhan SUBAŞI Nilüfer AKCİ Nurettin ÇİNKAYA	386-406
Antitumor Activity of Etoposide, Puerarin, Galangin and Their Combinations in Neuroblastoma Cells	
Çağatay OLTULU Melek AKINCI Elvan BAKAR	407-423
Investigation of The Potential Inhibitor Effects Of Lycorine On Sars-Cov-2 Main Protease (Mpro) Using Molecular Dynamics Simulations and MMPBSA	
Barış KURT	424-435
Karadeniz Bölgesinin İl Düzeyinde Süs Bitkileri Üretimini İncelenmesi	
Ömer SARI Fisun Gürsel ÇELİKEL	436-458
Antioxidant, Antimicrobial Properties and In Silico Study of a N,N'-(ethane-1,2-diyl)bis(1-(9H-fluoren-2-yl)methanimine)	
İlter DEMİRHAN Erkan ÖNER Adem NECİP Aydın AKTAŞ Medine ÇOTAK Yetkin GÖK.....	459-479
Evaluation of LC-MS/MS Analysis and In Vitro Biological Activities of Rosa pimpinellifolia Root, Pseudo-fruit, and Seed extracts	
Leyla GÜVEN Ufuk ÖZGEN Handan SEVİNDİK İclal AĞAN Mehmet KOCA İbrahim TURAN Selim DEMİR Yüksel ALİYAZICIOĞLU	480-503
Diversity Analysis of Common Vetch (Vicia Sativa L.) Lines and Cultivars Using Pairwise Combinations of Universal Rice Primers	
Mustafa TOPU İskender TİRYAKİ.....	504-518
Controlling with Mass Trapping and Determination of Damage Rates of Codling Moth, Cydia pomonella L. (Lepidoptera: Tortricidae) at Good Agricultural Practices of Walnut Orchards in Hatay Province	
Mustafa SÜRMEİ Nihat DEMİREL	519-525
mtDNA COI and Cyt b Analysis of Carassius auratus (Linnaeus, 1758) Species Living in Atatürk Dam Lake (Turkey)	
Arif PARMAKSIZ Aynur DEMİR Dilara ULUSAL	526-532
Developing selection strategy for CHO-K1 cell line that secretes scfv-Fc fusion antibodies using ClonePix2	
Aylin ÖZDEMİR BAHADIR	533-545

Comparison of Modified DNA Isolation Methods for the Detection of GMO in Processed Foods	
Begüm TERZİ AKSOY Özlem ATEŞ SÖNMEZOĞLU	546-561
A Current and Common Cause of Secondary Spontaneous Pneumothorax: Covid- 19 Pneumonia	
Nurmuhammet TAŞ Muhammet NALDAN Fatih ÖNER Hülya NALDAN Yener AYDİN	562-571
Antibacterial Activity of Ethanol Leaf Extract of <i>Sida acuta</i> Against Some Clinical Bacterial Isolates	
Maimuna HASSAN Fatima M. MUSA Firdausi ALİYU Aliyu ADAMU	572-580
Nitrogen-Doped Carbon Quantum Dots-Gellan Gum As An Innovative Self-Healable Hydrogel Composite	
Serbülent TÜRK Mahmut ÖZACAR.....	581-590
Homology Modeling of L18F Mutation on SARS-CoV-2 Spike Protein Receptor-Binding-Domain	
Gizem KÖPRÜLÜLÜ KÜÇÜK Nazlı Irmak GİRİTLİOĞLU	591-601
Meralarda Kentsel Dönüşüm ve Gelişim Amaçlı Tahsis Amacı Değişikliği Talebinin Değerlendirilmesi: Doyran ve Kızılcaören Örneği	
Ömer Faruk UZUN Fatih ALAY	602-610
L-Askorbik asit (C vitamini) Tayinine Yönelik Kalem Grafit Elektrot-Askorbat Oksidaz Temelli Yeni Bir Biyosensör Geliştirilmesi	
Burhan BUDAK Erhan DİNCKAYA	611-626

Review Articles / Derleme Makaleler

Fritillaria cinsinin ve bu cinsin bir üyesi olan Aygül lalesi'nin (<i>Fritillaria eduardii</i>) dünü, bugünü ve yarını	
Daniel KİMSANALİEV Sevgi MARAKLI Yılmaz KAYA	627-642
Hava Bazlı Proteinin Alternatif Bir Protein Kaynağı Olarak Kullanım Olanaklarının İncelenmesi	
Büşra ÇAKALOĞLU EBCİM Elif ERDOĞAN Esra DERİN Orhan KAYA	643-668
Karbon noktaların tarımsal üretimde kullanılması	
Mehmet Han BAŞTÜRK Şahane Funda ARSLANOĞLU Rumeysa ÖZTÜRK.....	669-679

Sanjida, S., et al., Identification of potential antiviral drug compound against Erythrocytic necrosis virus by targeting Major capsid protein. International Journal of Life Sciences and Biotechnology, 2022. 5(3): p. 294-315. DOI: 10.38001/ijlsb.1074392

Identification of potential antiviral drug compound against Erythrocytic necrosis virus by targeting Major capsid protein

Saloa Sanjida ¹ , Moslema Jahan Mou ² , Sk Injamamul Islam^{3*} , Sarower Mahfuj ³ 

ABSTRACT

A member of the Iridoviridae family has been detected as the erythrocytic necrosis virus (ENV), which causes viral erythrocytic necrosis (VEN) in 20 marine and anadromous fishes. The major capsid protein (MCP) is the main structural protein of iridoviruses and is responsible for causing disease in various fishes. It has been found that the VEN utilizes major capsid protein (MCP) to enter the host cell and blocking the virus entry by targeting the protein can reduce the economic losses caused by the pathogen. The main objective of the study was to evaluate the inhibitory potentiality of 48 compounds *Allium sativum* is one of the medicinal plants which has been reported to show potential antiviral activity against various pathogens, but activity against the capsid protein promoted pathogens has not yet been reported. The MCP was retrieved, modeled, refined, and validated in this experiment. The binding affinity of 48 compounds was calculated against the MCP with the docking, ADMET, and molecular dynamics (MD) simulation approaches which predict PubChem CID 12303662 inhibitory compound that binds strongly with the major capsid protein with a binding affinity of -9.7 after optimization. For theoretical calculation, the HOMO-LUMO gap score was also calculated. The best ADMET compounds were selected for the optimization analysis and re-docking. As a result of the research, it is possible to deduce that these *Allium sativum* phytochemicals might act as significant inhibitors of the MCP. More in-vitro testing is needed to establish their effectiveness.

ARTICLE HISTORY

Received

16 February 2022

Accepted

22 May 2022

KEYWORDS

MCP,
Iridovirus,
Allium sativum,
Molecular docking
and ADMET,
HOMO and LUMO

Introduction

Iridoviruses are big cytoplasmic DNA viruses with particular hosts in insects or vertebrates. The major capsid protein (MCP) is the main constituent of non-enveloped icosahedral viral particles that appears to be highly conserved across members of the Iridoviridae,

¹ Department of Environment Science and Technology, Faculty of Applied Science, Jashore University of Science and Technology, Bangladesh

² Department of Genetic Engineering and Biotechnology, Faculty of Earth and Life Science, University of Rajshahi, Bangladesh

³ Department of Fisheries and Marine Bioscience, Faculty of Biological Science, Jashore University of Science and Technology, Jashore-7408, Bangladesh

*Corresponding author: Sk Injamamul Islam. 6378506331@student.chula.ac.th

Phycodnaviridae, and African swine fever virus families [1]. MCP genes have only been cloned and described in a small number of fish species, in comparison to higher vertebrates. The MCP is a late gene expressed during viral infection, and it forms aggregated in both the nucleus and cytoplasm of infected cells [2]. Each MCP domain in different fish species has a distinct mix of essential amino acid residues for signal transduction pathway inhibition [3]. Following infection of rainbow trout, grouper fish species with Erythrocytic necrosis virus, distinct expression patterns of the MCP gene have been described [4]. Economic loss from this disease will affect the aquaculture industries and thus prevention of any viral pathogens is pivotal for sustainability.

Medicinal plants can play a critical role in the treatment of a variety of ailments, particularly in areas where resources are scarce. Because they have been implicated in treatments for several infectious and non-infectious disorders, they are viewed as a supplemental approach to controlling viral diseases [5]. Traditional remedies are mostly advocated given the abundance of these plants all over the world [5, 6]. For example, an ethnobotanical study of medicinal plants used to treat human and livestock ailments in Hulet Eju Enese Woreda, East Gojjam Zone of Amhara Region, Ethiopia [7]. Before anything, traditional drugs have less detrimental consequences than modern drugs, which is one of the main reasons why essential chemicals are extracted and produced from plants [8]. *Allium sativum* typical medicinal plant whose importance has risen steadily in recent years around the world. It contains a large number of biologically active compounds with a variety of structures [9]. For centuries it was used as a traditional remedy for most health-related disorders [10]. In many nations, garlic and its products are primarily used for culinary and therapeutic purposes [10]. As evidenced by the study, over 100 beneficial chemical compounds have been recorded and isolated from various components of this plant, including leaves, flowers, seeds, roots, fruits, and bark. These components have been utilized traditionally as a treatment for a range of ailments. Garlic is one of the world's oldest cultivated plants [11, 12]. For over 4000 years, it has been used as a spice, food, and traditional medicine, and it is the most extensively investigated medicinal plant.

Garlic is a fragrant herbaceous plant that is used as a food and a traditional cure for a variety of ailments across the world [12, 13]. It has been reported to possess several biological

properties including anticarcinogenic, antioxidant, antidiabetic, renoprotective, anti-atherosclerotic, antibacterial, antifungal, and antihypertensive activities in traditional medicines. Sulfur-containing phytoconstituents including alliin, allicin, ajoenes, vinyldithiins, and flavonoids like quercetin are abundant in *A. sativum*. *A. sativum* extracts and isolated chemicals have been tested for antibacterial, antiviral, antifungal, antiprotozoal, antioxidant, anti-inflammatory, and anticancer properties, among other biological activities [14].

Introducing effective medicines in a conventional or standard manner can take a long time, be expensive, and require a significant amount of effort [15]. For example, high-throughput screening (HTS) is a technique that integrates multiple-well microplate with automated processing to improve drug development by assaying a large number of putative drug-like molecules [16]. Additionally, HTS should have abundant resources, as processing a particular HTS program is expensive and involves the use of robotic devices [17]. On the contrary, computer-aided drug design, also known as *in silico* drug design, is a relatively new technology for screening a large database of compounds using a high-throughput approach [18]. The *in silico* virtual screening approach aids in the discovery of novel medicines by generating hits for lead compounds in a shorter period and at a cheaper cost [19]. As a result, improved *in silico* drug design reduces the time required to develop, design, and optimize a novel drug. The virtual screening approach has been used for decades to find the best lead compounds with various structural properties for use with a given biological target [20]. Furthermore, computer-aided drug design has been used to find a wide variety of interesting drug applications and hits utilizing virtual screening, molecular docking, and dynamics simulation techniques [21]. In light of the above-mentioned *Allium sativum* drugs, the goal of this study is to use molecular docking, geometry optimization of highest docked compounds, and molecular dynamics simulation to screen active compounds of *Allium sativum* against the Erythrocytic necrosis virus (Iridovirus) and investigate their interaction pattern. As a result, the goal of this work was to combine virtual screening, molecular docking, and ADMET (absorption, distribution, metabolism, excretion, and toxicity) features strategies to screen potential natural anti-fish drugs.

Materials and Methods

Retrieving the sequence

The Uniprot database (<https://www.uniprot.org/uniprot/>) was used to retrieve the amino acid (aa) sequence of the major capsid protein (Accession No.: A0A4D6QIF4) found in Erythrocytic necrosis virus (Irido Virus) and downloaded in FASTA format.

Assessment of Secondary Structure

The secondary structural elements of the toll receptor protein were predicted through the SOPMA tool [22-24] using the default parameters (window width of 17, number of states of 4, and similarity threshold of 8).

Prediction, Refinement, and Validation of Three-Dimensional Structures

The three-dimensional structure of the target protein was predicted using the RaptorX server (<http://raptorx.uchicago.edu/>) [25-27]. The protein 3D structure was refined by the GalaxyWeb server. The structure validity is a crucial stage in homology modeling, which is based on the experimentally validated structure of 3D proteins. The proposed toll receptor protein model was uploaded to ProSA-web for basic confirmation [28, 29]. The server foresaw the overall character of the model, which is represented by the z-score. If the expected models' z-scores are outside the scale of the property for local proteins, it indicates that the structure is erroneous [28, 30]. To determine the overall quality of the suggested drug, a Ramachandran plot analysis was performed using the Ramachandran Plot Server (<https://zlab.umassmed.edu/bu/rama/>) [31].

Preparation of protein

The 3D structure of the protein was modeled and developed using the following criteria: water, metal ions, and cofactors were removed, polar hydrogen atoms were introduced, nonpolar hydrogen was combined, and gasteiger charges were calculated using AutoDockTools [32, 33].

Retrieval and preparation of compounds

Phytochemicals derived from naturally occurring medicinal plants cover a wide range of chemical spaces that can be used in drug development and discovery. IMPPAT stands for Indian Medicinal Plants, Phytochemistry, and Therapeutics, a manually curated database of over 1742 Indian medicinal plants and over 9500 phytochemical compounds that uses

cheminformatic methodologies to improve natural product-based drug discovery [34]. Because of virtual screening, the phytochemical of the ginger plant (*Allium sativum*) has been discovered and obtained from the database. The compounds found from the database were created by assigning accurate AutoDock 4 atom types, merging nonpolar hydrogens, detecting aromatic carbons, and establishing a 'torsion tree. It has been discovered that the AD4 atom type is the same as the elements of the compound for the majority of atoms.

Molecular docking and receptor grid generation

The PyRx virtual screening tool AutoDock Vina was used to create a protein receptor grid [35]. The molecular docking investigation was carried out using the PyRx virtual screening program AutoDock Vina to find the binding mechanism of the required protein with chosen phytochemicals. PyRx is an open-source virtual screening application that can screen libraries of compounds against a given therapeutic target and is primarily used in CADD techniques. PyRx integrates AutoDock 4 and AutoDock Vina as docking wizards with an intuitive user interface, making it a more trustworthy CADD tool [24]. This experiment used PyRx's AutoDock Vina wizard for molecular docking to find the optimum protein and ligand binding poses. For docking objectives, the default configuration parameters of the PyRx virtual screening tools were utilized, and the highest binding energy (kcal/mol) with the negative sign was chosen for further investigation. Subsequently, using the BIOVIA Discovery Studio Visualizer v19.1.0.18287, the binding interaction of the protein–ligands complex was seen.

ADME Analysis

The physicochemical, pharmacokinetics, metabolism, and excretion properties of molecules in urine and feces are all listed in the ADME of a substance [47]. The Swiss-ADME server (<http://www.swissadme.ch/>) was used to forecast the various pharmacokinetic and pharmacodynamic parameters for the experiments [25].

Toxicity Test

In the area of drug discovery and development, an initial analysis of a compound's toxicity is critical [48]. Toxicology profiles of drug candidates provide information about the hazards to human health and the environment, as well as the safety and toxicity of chemical constituents. Chemical toxicity is now assessed using computer-assisted in-silico testing without the need for animal experiments. As a result, the ProTox-II ([298](http://tox.</p></div><div data-bbox=)

charite.de/protox II) website was used to assess the early-stage toxicity of the chosen medication candidates [11]. With ProTox-II, you can identify compounds that are acutely toxic, hepatotoxic, cytotoxic, carcinogenic, mutagenic, and immunotoxic [49]. Using Quantitative Structure-Activity Relationships (QSARs) techniques, the software estimates the toxicity of specified compounds.

Quantum Mechanics (QM)-Based Calculation

An important element of identifying possible active conformation, binding affinity, and strain discipline related to the binding process is the confirmation study of a ligand to the binding site of a protein. The computation of lowest energy conformation and structural optimization, which is based on the solution phase and related gas-phase energy, can be used to accomplish this sort of binding. Because metal ions are present in a ligand-protein complex system, conventional molecular mechanics (MM) cannot adequately describe the process [36]. In the last few years, QM-based calculations have helped to improve the scoring functions that can represent the electronic structure, electronic alterations, and reaction-specific charges in a molecular system. Surprisingly, density functional theory (DFT) is currently used to answer more than 80–90% of all QM-based computations. As a result, the DFT methods-based QM calculations of three substances were done in this work. After optimizing bond lengths, bond angles, and dihedral angles for possible compounds, the DFT of the compounds was computed using the ORCA quantum chemistry software package (Version 4.1.1) [37, 38]. DFT was calculated by combining Becke's three parameters with Lee-Yang-Parr functionals (B3LYP) and a dispersion correction energy term D3 (B3LYP-D3). The usual combination of functionalities B3LYP-D3 was chosen for this investigation because it does not directly affect the wavefunction or any other molecular characteristic, and 6-31G**, also known as 6-31G (d, p), was chosen as a basis set to describe all the molecules electronic wave function.

Frontier Molecular Orbital HOMO/LUMO Calculation

Kenichi Fukui's frontier molecular orbital (FMO) theory or Fukui functions, created in the 1950s, relies on the highest energy occupied (HOMO) and lowest energy unoccupied molecular orbital (LUMO). The FMO of a molecule is the “frontier” of an electron that helps to identify the energy difference between two orbitals HOMO and LUMO. HOMO is predominantly an electron donor (nucleophilic) and LUMO is an electron acceptor

(electrophilic) in nature and the interaction between electron donor and electron acceptor pair can control other chemical reactivity of a molecule [39]. Electrons from the HOMO move to the LUMO during the electrophilic-nucleophilic process, creating an energy difference between two molecular orbitals. The energy difference between two molecular orbitals is termed the HOMO-LUMO gap, which illustrates the photochemistry and the strength and balance of transition metal complexes of organic compounds. To comprehend the sensitivity of atoms against electrophilic and nucleophilic interactions, the HOMO and LUMO energy were computed by using the Avogadro Software and visualized by Avogadro and Chemcraft software [38], and the following equation was used to determine the energy difference between two molecular orbital HOMO-LUMO gaps. (1).

$$\Delta E(\text{gap}) = E_{\text{LUMO}} - E_{\text{HOMO}} \dots\dots\dots (1)$$

here, ΔE is the HOMO-LUMO gaps, E_{LUMO} is the lowest energy unoccupied molecular orbital energy, and E_{HOMO} is the highest energy occupied molecular orbital energy.

Molecular dynamics simulation

Molecular dynamics is a computational approach that was applied to describe the molecule's behavior as well as to measure the stability of protein-protein complexes [40]. The binding stability and flexibility of the protein and ligand complex were analyzed using the iMODS server (<http://imods.Chaconlab.org/>) which performs Normal Mode Analysis (NMA) in internal (dihedral) coordinates using an elastic network model (ENM) [41]. This tool estimates the direction and range of the basic motions of the protein-ligand complex by measuring four main factors: deformability, eigenvalues, B-factors, and covariance. Generally, deformation is much harder when the eigenvalue is high [41].

Result and Discussion

Sequence Retrieval

The amino acid (aa) sequence of the Erythrocytic necrosis virus (Irido Virus) (Accession No.: A0A4D6QIF4) was obtained from the Uniprot database. There are 388 amino acids in the protein. Fig. 1 provides additional information on the protein.

Amino acid sequence:

MSSNNPATYLPAYVDLATFKNSVLEEDYMYSLSNSMTYFMREVRKCTPLTQIPTIFTIQ
SGQPSFGNNFVSVLRSRSTDYLLNCWLRVTIPEVTLLDTNPHGADGRIRWTKNLMHNLIEE
VTLSEADFPTQTIDSYFLDFWAAFTTSASKKSGYDTMIGNVDDLISPHGPNPLKSKILN
LPIPIFFFSRDSGIALPTGALLYTETRISFKLRNWNQLLILENANPLPNTPNGGVPMVGPS
IERAPMLTGVTVWGDVAADPLERSYMATCERDLLIEQVKQAPAQTYEPVNNPNKSFVDR
FSHAVKALLFGVRNITYPNVWSNWTASPVIDDRLLIMLEPSGAYDPINDVTIKYDSTTRL
QNVGADYFSHVNPYYHAPTIPDSIGYHMYSYALDLMGIDPQGSTNFGRLNNVTIVPNASN
EAKIGYQGTGAVGSGRDHPQRY

Fig 1. The amino acid (aa) sequence of the Erythrocytic necrosis virus (Irido Virus).

Secondary Structure Inquiry

The alpha helix (Hh), extended strand (Ee), beta-turn (Tt), and random coil (Cc) of the protein (A0A4D6QIF4) were predicted by the SOPMA software to be 101 (22.85%), 95 (21.49%), 15 (3.39%), and 231 (52.26%), accordingly Fig. 2

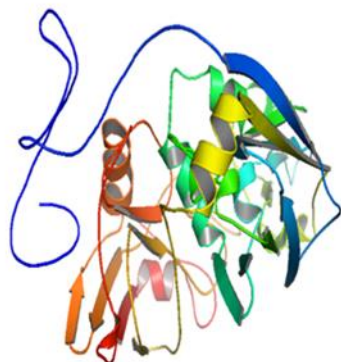
SOPMA :

Alpha helix (Hh)	:	101 is 22.85%
310 helix (Gg)	:	0 is 0.00%
Pi helix (Ii)	:	0 is 0.00%
Beta bridge (Bb)	:	0 is 0.00%
Extended strand (Ee)	:	95 is 21.49%
Beta turn (Tt)	:	15 is 3.39%
Bend region (Ss)	:	0 is 0.00%
Random coil (Cc)	:	231 is 52.26%
Ambiguous states (?)	:	0 is 0.00%
Other states	:	0 is 0.00%

Fig 2. Secondary structural elements

Three-Dimensional Structure Prediction and Refinement

The Galaxy Refine server (RMSD .509) was used to refine the protein's projected tertiary structure, yielding five refined models and increasing the number of amino acid residues in the favored location. When compared to the other models, the scores listed above indicate the improved model's caliber. Crude model and refine model 2 were chosen and visualized in Pymol Fig. 3.

(A) Crude Model**(B) Refine Model****Fig 3.** (A) 3D structure of the crude model and (B) 3D structure of refining the model

Validation of a three-dimensional structure

Ramachandran Plot Server and ProSA-Web online server were used to validate the before and after revised major capsid protein model. Ramachandran plot analysis of the before refine structure revealed that 94.474% of the structure was in the favorable zone, as per the Ramachandran plot server. After refining, the rampage server produced a better result, with 96.842% of residues in the preferred regions Table 1. The validation quality and potential faults in a basic tertiary structure model are assessed using the ProSA-web server. Validation of the final protein model reveals a Z-score of -5.59 Table 1.

Table 1. Validation of selected protein model by Ramachandran and z-score studies.

Parameters		Initial Model	Refine Model	Remarks
Ramachandran	Highly Preferred	94.474%	96.842%	Significant
	Preferred	4.211%	3.158%	Significant
	Questionable	1.316%	0.000%	Significant
ProSA Web	Z-Score	-5.24	-5.59	Significant

Retrieval and preparation of phytochemicals

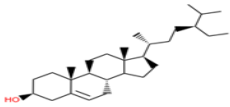
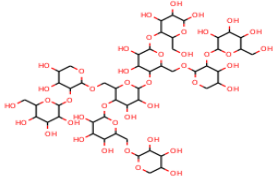
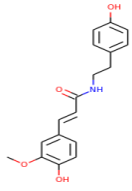
The IMPPAT database, an Indian natural, and the medicinal phytochemical compound library were used to find the accessible compounds of the required plant. The phytochemical components found in *Allium sativum* were extracted and recorded in a 2D (SDF) file format.

During the ligand preparation procedures, the compounds were produced and optimized, then converted to pdbqt file format for further assessment.

Molecular docking analysis

A molecular docking study was first conducted to screen and identify the optimal intermolecular interaction among the desired protein and phytochemical substances. PyRx tools AutoDock Vina wizard were used to perform molecular docking between 48 phytochemical compounds and the protein of choice. The binding affinities discovered during molecular docking of the phytochemical molecule ranged from -3.1 kcal/mol to -9.2 kcal/mol, as reported in Supplementary Table 1. Based on the binding affinity top 3 of 48 phytochemical (total 3) compounds have been chosen in Table 2. The docking methods predict 3 (PubChem CID: 12303662, 44630412, and 5280537) inhibitory compounds that bind strongly with the major capsid protein with a binding affinity of -8.8, -8.7, and -9.2 kcal/mol, respectively Table 2.

Table 2. The top 3 compounds molecular docking score and ligand structure

Ligand	Molecule Name	Formula	Binding Affinity (kcal/mol)	Structure
CID 12303662	Phytosterols	$C_{58}H_{98}O_2$	-8.8	
CID 44630412	Monosaccharide Glc4Xyl13Gal2	$C_{51}H_{86}O_{43}$	-8.7	
CID 5280537	Moupinamide	$C_{18}H_{19}NO_4$	-9.2	

Absorption, distribution, metabolism, and excretion (ADME) analysis

The ADME characteristics of chemical compounds are crucial in determining a drug's effectiveness. Pharmacokinetics-related failure in clinical stages can be reduced by optimizing ADME characteristics, which is complex and demanding in the drug design and trial process [25]. It has been discovered that assessing ADME at an early stage in the clinical drug development process can lower attrition rates. As a result, the SwissADME online tool was used to conduct an early-stage evaluation of ADME characteristics for four drugs. Focusing on hydrophilic nature, solubility, pharmacokinetics, medicinal chemistry, and drug-likeness characteristics, the server assessed the ADME qualities of three compounds (PubChem CID: 12303662, 44630412, and 5280537). All the compounds have maintained an optimum pharmacokinetics property Table 3.

Table 3. List of absorption, distribution, metabolism, and excretion (ADME) and toxicity of compounds

Properties		CID 12303662	CID 44630412	CID 5280537
Physio-chemical properties	MW (g/mol)	827.40	1387.20	313.35
	Heavy atoms	60	94	23
	Aro. atoms	0	0	12
	Rotatable bonds	15	22	7
	H-bond acceptors	2	43	4
	H-bond donors	2	26	3
	TPSA (Å ²)	40.46	20.23	78.79
Lipophilicity	Log Po/w (Cons)	13.48	-14.63	3.25
Water solubility	Log S (ESOL)	Moderately Soluble	Soluble	Moderately Soluble
Pharmacokinetics	GI absorption	Low	Low	High
	BBB permeant	No	No	No
	P-GP substrate	No	Yes	No
Drug likeness	Lipinski violations	0	3	0
Medi. chemistry	Synth. accessibility	Very Easy	Easy	Medium

Toxicity Test

Toxicity testing is an essential and crucial phase in pharmaceutical development that aids in determining the adverse levels of toxic compounds on people, wildlife, plants, and the surroundings. Traditional toxicity testing of chemicals necessitates the use of an in vivo

animal model, which is time-consuming, costly, and fraught with ethical issues [42]. As a result, computer-aided in silico toxicity measurements of chemical compounds might be regarded beneficial in the drug development phase. The study used the ProTox-II webserver to compute the toxicity of the chemical since it is quick, inexpensive, and does not need any ethical concerns. The three compounds (PubChem CID: 12303662, 44630412, and 5280537) selected previously through different screening processes have been submitted to the ProTox-II web server that determines the acute toxicity, hepatotoxicity, cytotoxicity, carcinogenicity, and mutagenicity of the compounds listed in Table 4. All the compounds have shown no oral toxicity or organ toxicity effect.

Table 4. The toxicity endpoints of chosen four chemicals include acute toxicity, hepatotoxicity, cytotoxicity, carcinogenicity, and mutagenicity

Classification	Target	CID 12303662	CID 44630412	CID 5280537
Oral toxicity	LD50 (mg/kg)	1190	3140	500
	Toxicity Class	4	4	4
Organ toxicity	Hepatotoxicity	Inactive	Inactive	Active
Toxicity endpoints	Carcinogenicity	Inactive	Inactive	Active
	Mutagenicity	Inactive	Inactive	Inactive
	Cytotoxicity	Inactive	Active	Inactive

Selection of the compound

The best ADMET compound was selected for further analysis. Although ADME qualities of the selected three compounds showed good results as a suitable drug candidate toxicity test found only the CID 12303662 compound of *Allium sativum* with the best qualities (Table-4). The other compounds CID 44630412 and CID 5280537 showed cytotoxicity and hepatotoxicity respectively. As a result, for further calculation, we selected only CID 12303662 for geometry optimization and molecular dynamics simulation analysis.

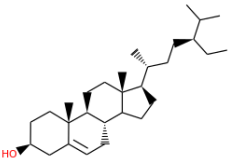
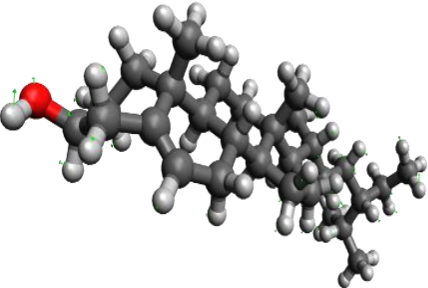
Theoretical Calculation

Geometry Optimization

Most computational biologists, chemists, academics, and researchers use geometry optimization, a quantum chemical technique, to find the configuration of minimum energy with the most stable form of a chemical structure. It is a technique for getting as close to

accurate geometric measurements as feasible by using rough estimates [43]. Because molecules in the lowest energy state spontaneously reduce their energy by emitting, the geometry with the lowest energy is the most stable. By using the default basis set 6-31G (d,p) in Avogadro, the molecular geometry with the lowest energy value has been selected as the best-optimized one. The 2D structures and 3D optimized geometries of the compound CID 12303662 have been plotted in Table 5.

Table 5. Geometry optimization of compounds

Compound ID	Crude (2D)	Optimized (3D)
CID 12303662		

Frontier Molecular Orbital HOMO/LUMO Calculation

Molecular structure and reactivity are now explained largely using the FMO in organic chemistry. Through the use of HOMO-LUMO bandgap energy, electronic and optical properties of molecules can be described. In addition to determining atom sensitivity to electrophilic and nucleophilic attacks, chemical kinetic stability, chemical hardness, and softness of molecules, the gap between HOMO and LUMO helps to determine the stability of chemical bonds [43]. In the nucleophilic reaction, the electrons located from the HOMO orbital are freer, while the electrons located from the LUMO orbital are freer to participate. Soft molecules have low HOMO-LUMO gap energies, the lowest kinetic stability, and high chemical reactivity. Because there is a low probability of electron addition to the high-energy LUMO orbital gap, molecules with high frontier (HOMO/LUMO) orbital gaps should have low chem-reactivity or bioactivity and high kinetic stability. Low chemical reactivity and high kinetic stability are responsible for the energetic stability of molecules with a high FMO

energy gap compared to molecules with a low kinetic energy gap [44]. Therefore, to evaluate the chemical reactivity and kinetic stability of the selected three compounds the HOMO, LUMO, and HOMO-LUMO, gap energy was calculated from Equation (1) and shown in Figure 4. The calculated FMO energy band gap value found for the compound CID 12303662 was 3.332 eV, which was considerably higher, indicating kinetic stability and low chemical reactivity of the molecules.

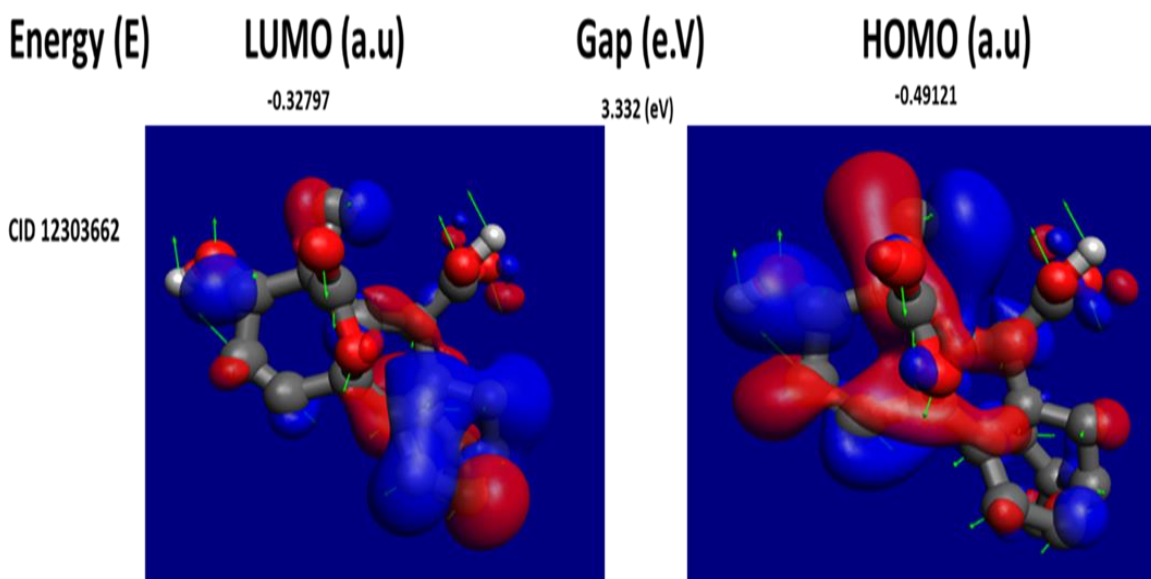


Fig 4. The molecular frontier orbital wave function is shown with negative and positive phases for selected *Allium sativum* compound CID 12303662, representing asymmetric HOMO, LUMO, and HOMO-LUMO gaps

Re-Docking and Interaction

Redocking Score

Utilizing the previously obtained binding sites of the protein, re-docking has been performed to identify possible docking poses in a restricted area. The geometry optimized structure has been docked and the score found for the selected three compounds CID 12303662 was -9.7 kcal/mol, which was better than the previously obtained binding score (Table 3). Therefore, it can be considered that the QM-based optimization of the compounds changed into effective for the chosen three compounds.

Protein–Ligands Interaction Interpretation

With the target protein, compound CID:12303662 has been found to create a conventional hydrogen bond at the positions of ALA:216 (2.49), ALA:216 (4.42), ALA:216 (4.41) androgen bond ALA:216 (4.27), where Alkyl bonds have been noted at the positions of LEU:36 (5.03), ILE:7 (5.0) and TYR:76 (4.25) Fig. 5C and Table 6.

Pi-Alkyl bonds were observed to form exclusively at the VAL:180 (3.77) and PRO:180 (5.07) position of the molecule CID:12303662 as shown in Fig. 5 and Table 6.

Table 6. List of the interaction between the selected compound and major capsid protein found during the complex structure analysis and generated through the docking simulation

Compound	Residues	Bond Distance (Å)	Category	Bond Types
CID:12303662	ALA:216	2.49	Hydrogen Bond	Conventional H-B
	ALA:216	4.42	Hydrogen Bond	Conventional H-B
	ALA:216	4.41	Hydrogen Bond	Conventional H-B
	ALA:216	4.27	Hydrogen Bond	Conventional H-B
	LEU:36	5.03	Hydrophobic	Alkyl
	ILE:7	5.0	Hydrophobic	Alkyl
	TYR:76	4.25	Hydrophobic	Alkyl
	VAL:180	3.77	Hydrophobic	Pi-Alkyl
	VAL:180	3.91	Hydrophobic	Pi-Alkyl
PRO:183	5.07	Hydrophobic	Pi-Alkyl	

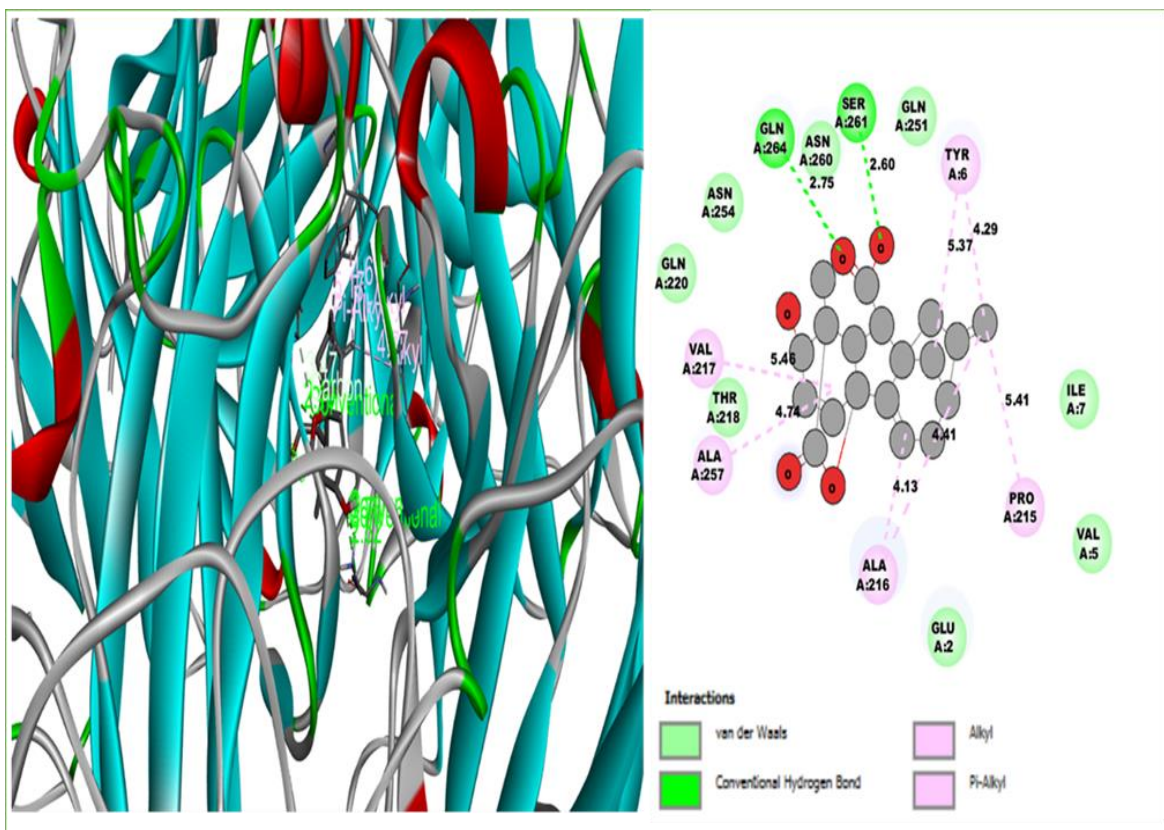


Fig 5. The interaction between the major capsid protein and CID 12303662 compound. The 3D interaction has represented on the left side of the figure, whereas the 2D interaction has been depicted on the right side of the figure accordingly.

Molecular Dynamic Simulation

Molecular dynamic simulation results showed that major capsid protein binds with CID 12303662. Here highest binding affinity complex is approved for molecular dynamic simulation analysis.

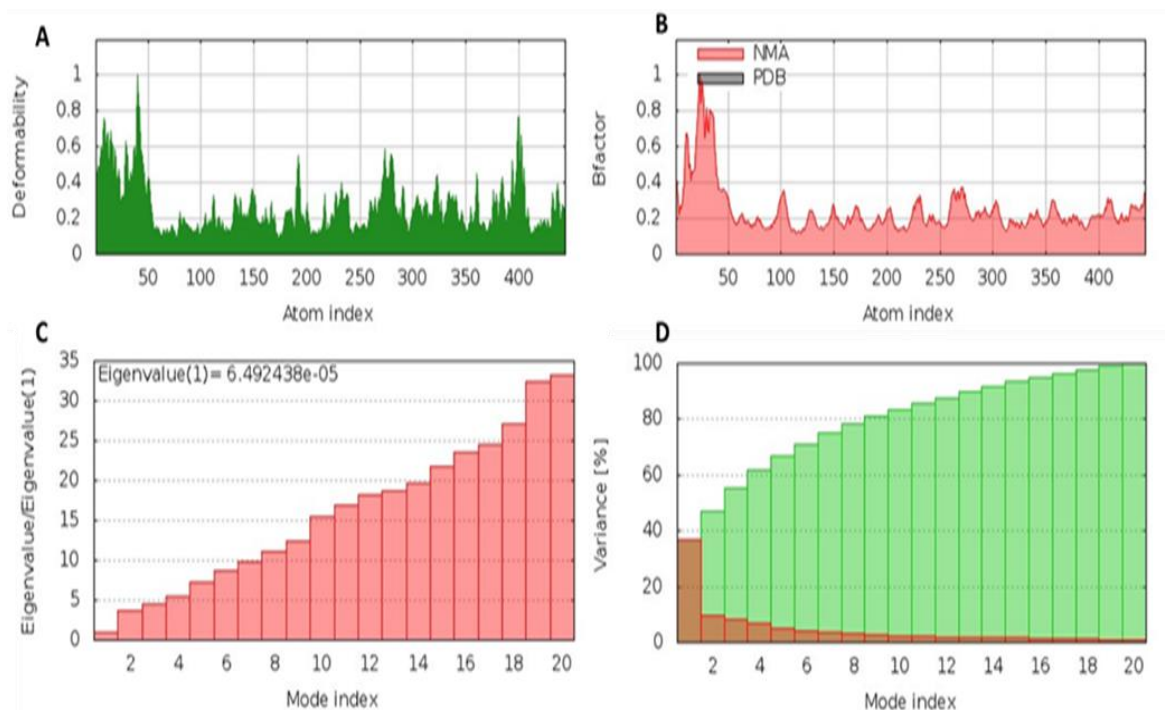


Fig 6. The molecular dynamics simulation of the major capsid protein- CID 12303662 docked complex (A) Deformability simulations on main chains show high deformability in hinges (B) Normal mode analysis generates B-factor values, which measure each atoms uncertainty (C) The eigenvalue of the docked complex, showing the energy required to deform the structure (D) The variance matrix between complex and residue

Discussion

The differential expression patterns of the MCP gene have been reported in numerous viral infections in fish species (Shan et al., 2016; Lu et al., 2013; Huang et al., 2012). According to several studies, Ginger is one of the most beneficial traditional medicinal plants on the planet [45, 46]. From antiquity, almost all components of the plant have medicinal characteristics and have been utilized as traditional medicine or cures for a variety of diseases [47]. It is now regarded as a valuable source of unique natural compounds for the creation of medications to treat a variety of illnesses. Furthermore, phytochemicals found in plants may boost the innate immune system, have antibacterial properties, and are redox-active molecules with antioxidant properties, all of which may aid in improving the fish species' overall physiological state. Many researchers have looked into the benefits of phytochemicals in disease prevention [32, 48].

Computer-Aided Drug Design (CADD) is one of the most promising tools for the selection of novel compounds against a specific protein as it includes different advanced features and techniques [49]. The CADD approach has minimized the required time and costs involved in the entire drug discovery process making the virtual screening process includes molecular docking, molecular dynamic simulation, ADMET, etc. as integral parts of drug designing [50].

A 3D structure prediction was performed (the lowest energy score was used to choose the best model) and the result was the achievement of the best model among the discovered models. For the Ramachandran plot, we observed a good number of Z-scores (-5.59) and the most favored, accepted, and disallowed regions.

In this study, we identified potential drugs by molecular docking and another process. Initially, the molecular docking process has used to screen the compounds, where the top 3 compounds have been selected with the highest binding affinities of -9.2 to -8.7 kcal/mol from which only one compound was selected for further validation. The RO5 demonstrated the drug-like properties of the selected compounds [51, 52]. Only one compound was found to follow the five Lipinski's rules of drug-likeness properties. The toxicity qualities of the chemical with good ADME properties were used to quantify the detrimental impact on humans or animals [53]. After toxicity testing, we confirmed that the CID 12303662 compound selected is non-toxic or low-toxic.

The compounds were investigated and optimized by a computational DFT-based QM simulation. We retrieved and re-docked the geometry optimized by DFT with the desired protein, and the docking energy was significantly above >9.00 kcal / molecular. To determine the reactivity of the compounds, the HOMO-LUMO energy gap was calculated using an FMO model. The HOMO-LUMO gap energy found for compound CID 12303662 was high >3.00 eV which confirms the low reactivity correspondence to the bioactivity of the compound.

Using the MD simulation approach on the geometry-optimized re-docked complex structure, we have investigated the stability of the compound concerning the binding sites of the protein. Molecular dynamics simulation is used to confirm the stability of a protein in a complex with ligands [50, 53]. Also, it can determine the stability and rigidity of protein-

ligand complexes in a specific artificial environment like the body [50]. The B-factor, main-chain deformability simulation, and eigenvalue of the selected protein – CID 12303662 complex systems indicate the best stability of the compound.

Conclusion

The study is the first to identify potential antibacterial drug candidates targeting major capsid protein using compressed *in-silico* approaches, to the best of our knowledge. An integrative molecular modeling, virtual screening, molecular docking, ADMET, and MD simulation approaches revealed CID 12303662 as a potential drug candidate that will help to inhibit the activity of the major capsid protein. By determining the activity of the compound through a variety of lab-based experiments, researchers will be able to identify alternative methods for the treatment of viral infections.

Acknowledgments

The author thanks Dr. Foysal Ahmed Sagore and Dr. Kazi Abdus Samad for helpful comments.

References

1. Tidona, C.A., et al., Is the Major Capsid Protein of Iridoviruses a Suitable Target for the Study of Viral Evolution? *Virus Genes*, 1998. 16(1): p. 59-66.
2. Lin, H.-Y., et al., Development and application of a monoclonal antibody against grouper iridovirus (GIV) major capsid protein. *Journal of Virological Methods*, 2014. 205: p. 31-37.
3. Huang, R., et al., Identification, characterization and the interaction of Tollip and IRAK-1 in grass carp (*Ctenopharyngodon idellus*). *Fish Shellfish Immunol*, 2012. 33(3): p. 459-67.
4. Yu, Q., et al., Identification of Major Capsid Protein as a Potential Biomarker of Grouper Iridovirus-Infected Cells Using Aptamers Selected by SELEX. *Frontiers in Microbiology*, 2019. 10(2684).
5. Raza, A., et al., Antiviral and immune-boosting activities of different medicinal plants against Newcastle disease virus in poultry. *World's Poultry Science Journal*, 2015. 71(3): p. 523-532.
6. Jalil, A., et al., Screening and design of anti-diabetic compounds sourced from the leaves of neem (*Azadirachta indica*). *Bioinformation*, 2013. 9(20): p. 1031-5.
7. Marakli, S., et al., Vista de Actividad antibacteriana de los extractos de *Calendula officinalis* y *Echinacea purpurea* contra el agente causal del cancro bacteriano del tomate *Clavibacter michiganensis* subsp. *Michiganensis*. 2021.
8. Akanksha, A.K. Srivastava, and R. Maurya, Antihyperglycemic activity of compounds isolated from Indian medicinal plants. *Indian J Exp Biol*, 2010. 48(3): p. 294-8.
9. Majewski, M., *Allium sativum*: facts and myths regarding human health. *Rocz Panstw Zakl Hig*, 2014. 65(1): p. 1-8.
10. Sasi, M., et al., Garlic (*Allium sativum* L.) Bioactives and Its Role in Alleviating Oral Pathologies. *Antioxidants (Basel, Switzerland)*, 2021. 10(11): p. 1847.

11. Islam, S., et al., An In-silico Approach for Identifying Phytochemical Inhibitors Against Nervous Necrosis Virus (NNV) in Asian Sea Bass by Targeting Capsid Protein. *Genetics of Aquatic Organisms*, 2022. 6: p. 487.
12. Gurib-Fakim, A., Medicinal plants: Traditions of yesterday and drugs of tomorrow. *Molecular Aspects of Medicine*, 2006. 27(1): p. 1-93.
13. Mukhtar, M., et al., Antiviral potentials of medicinal plants. *Virus research*, 2008. 131(2): p. 111-120.
14. El-Saber Batiha, G., et al., Chemical Constituents and Pharmacological Activities of Garlic (*Allium sativum* L.): A Review. *Nutrients*, 2020. 12(3): p. 872.
15. Lim, S.M., et al., Development of small molecules targeting the pseudokinase Her3. *Bioorg Med Chem Lett*, 2015. 25(16): p. 3382-9.
16. Hughes, J.P., et al., Principles of early drug discovery. *Br J Pharmacol*, 2011. 162(6): p. 1239-49.
17. Szymański, P., M. Markowicz, and E. Mikiciuk-Olasik, Adaptation of high-throughput screening in drug discovery-toxicological screening tests. *Int J Mol Sci*, 2012. 13(1): p. 427-52.
18. Liang, P.H., et al., Novel five-membered iminocyclitol derivatives as selective and potent glycosidase inhibitors: new structures for antivirals and osteoarthritis. *Chembiochem*, 2006. 7(1): p. 165-73.
19. Wichapong, K., et al., Identification of potential hit compounds for Dengue virus NS2B/NS3 protease inhibitors by combining virtual screening and binding free energy calculations. *Trop Biomed*, 2013. 30(3): p. 388-408.
20. Wu, J., et al., In silico study reveals existing drugs as α -glucosidase inhibitors: Structure-based virtual screening validated by experimental investigation. 2020. 1218: p. 128532.
21. Wu, C., et al., Analysis of therapeutic targets for SARS-CoV-2 and discovery of potential drugs by computational methods. *Acta Pharm Sin B*, 2020. 10(5): p. 766-788.
22. Combet, C., et al., NPS@: Network Protein Sequence Analysis. *Trends in Biochemical Sciences*, 2000. 25(3): p. 147-150.
23. Jahan, M., S. Islam, and M.s.E. Mahfuj, In Silico Functional Annotation of VP 128 Hypothetical Protein from *Vibrio parahaemolyticus*. 2021.
24. Islam, S. and M. Jahan, Functional Annotation of Uncharacterized Protein from *Photobacterium damsela* subsp. *piscicida* (*Pasteurella piscicida*) and Comparison of Drug Target Between Conventional Medicine and Phytochemical Compound Against Disease Treatment in Fish: An In-silico Approach. *Genetics of Aquatic Organisms*, 2022. 6: p. 453.
25. Xu, J., M. McPartlon, and J. Li, Improved protein structure prediction by deep learning irrespective of co-evolution information. *Nature Machine Intelligence*, 2021. 3(7): p. 601-609.
26. Mou, M., S. Islam, and M.s.E. Mahfuj, In Silico Functional Annotation of VP 128 Hypothetical Protein from *Vibrio parahaemolyticus*. 2021.
27. Islam, S., et al., An In-silico analysis of the molecular interactions between PmCBP-VP24 and PmCBP-VP28 protein complex to understand the initial initiating events of shrimp WSSV infection. *International Journal of Life Sciences and Biotechnology*, 2022.
28. Wiederstein, M. and M.J. Sippl, ProSA-web: interactive web service for the recognition of errors in three-dimensional structures of proteins. *Nucleic acids research*, 2007. 35(suppl_2): p. W407-W410.
29. Islam, S., et al., In-silico functional annotation of a hypothetical protein from *Edwardsiella tarda* revealed Proline metabolism and apoptosis in fish. *International Journal of Life Sciences and Biotechnology*, 2022. 5: p. 78-96.
30. Islam, S., et al., In-silico functional annotation of a hypothetical protein from *Edwardsiella tarda* revealed Proline metabolism and apoptosis in fish. *International Journal of Life Sciences and Biotechnology*, 2022. 5: p. 78-96.
31. Biol, 攀.J.J.m., Stereochemistry of polypeptide chain configurations. 1963. 7: p. 95-99.

32. Malekmohammad, K., et al., Effective Antiviral Medicinal Plants and Biological Compounds Against Central Nervous System Infections: A Mechanistic Review. *Curr Drug Discov Technol*, 2020. 17(4): p. 469-483.
33. Islam, S., et al., An In-silico Approach for Identifying Phytochemical Inhibitors Against Nervous Necrosis Virus (NNV) in Asian Sea Bass by Targeting Capsid Protein. *Genetics of Aquatic Organisms*, 2022. 6: p. 487.
34. Mohanraj, K., et al., IMPPAT: A curated database of Indian Medicinal Plants, *Phytochemistry And Therapeutics*. *Scientific Reports*, 2018. 8(1): p. 4329.
35. Dallakyan, S. and A.J. Olson, Small-molecule library screening by docking with PyRx. *Methods Mol Biol*, 2015. 1263: p. 243-50.
36. Friesner, R.A. and V. Guallar, Ab Initio Quantum Chemical And Mixed Quantum Mechanics/Molecular Mechanics (Qm/Mm) Methods For Studying Enzymatic Catalysis. *Annual Review of Physical Chemistry*, 2005. 56(1): p. 389-427.
37. Maity, A., et al., Studies on nanoconfinement effect of NiO-SiO₂ spin glass within mesoporous Al₂O₃ template. *Journal of Alloys and Compounds*, 2021. 887: p. 161447.
38. Hanwell, M.D., et al., Avogadro: an advanced semantic chemical editor, visualization, and analysis platform. *Journal of Cheminformatics*, 2012. 4(1): p. 17.
39. Li, Y. and J.N.S. Evans, The Fukui Function: A Key Concept Linking Frontier Molecular Orbital Theory and the Hard-Soft-Acid-Base Principle. *Journal of the American Chemical Society*, 1995. 117(29): p. 7756-7759.
40. Pandey, R.K., et al., High-throughput virtual screening and quantum mechanics approach to develop imipramine analogues as leads against trypanothione reductase of leishmania. *Biomedicine & Pharmacotherapy*, 2016. 83: p. 141-152.
41. López-Blanco, J.R., et al., iMODS: internal coordinates normal mode analysis server. *Nucleic acids research*, 2014. 42(W1): p. W271-W276.
42. Banerjee, P., et al., ProTox-II: a webserver for the prediction of toxicity of chemicals. *Nucleic Acids Res*, 2018. 46(W1): p. W257-w263.
43. Bharadwaj, S., et al., Exploration of natural compounds with anti-SARS-CoV-2 activity via inhibition of SARS-CoV-2 Mpro. *Briefings in Bioinformatics*, 2021. 22(2): p. 1361-1377.
44. Miara, M., et al., Theoretical investigations on the HOMO–LUMO gap and global reactivity descriptor studies, natural bond orbital, and nucleus-independent chemical shifts analyses of 3-phenylbenzo[d]thiazole-2(3H)-imine and its para-substituted derivatives: Solvent and substituent effects. *Journal of Chemical Research*, 2021. 45(1-2): p. 147-158.
45. Mukhtar, M., et al., Antiviral potentials of medicinal plants. *Virus Res*, 2008. 131(2): p. 111-20.
46. Khan, T., et al., Therapeutic potential of medicinal plants against COVID-19: The role of antiviral medicinal metabolites. *Biocatalysis and agricultural biotechnology*, 2021. 31: p. 101890-101890.
47. Ben-Shabat, S., et al., Antiviral effect of phytochemicals from medicinal plants: Applications and drug delivery strategies. *Drug delivery and translational research*, 2020. 10(2): p. 354-367.
48. Chakraborty, S.B., P. Horn, and C. Hancz, Application of phytochemicals as growth-promoters and endocrine modulators in fish culture. *Reviews in Aquaculture*, 2014. 6(1): p. 1-19.
49. Sastry, G.M., et al., Protein and ligand preparation: parameters, protocols, and influence on virtual screening enrichments. *J Comput Aided Mol Des*, 2013. 27(3): p. 221-34.
50. Bharadwaj, S., et al., Exploration of natural compounds with anti-SARS-CoV-2 activity via inhibition of SARS-CoV-2 Mpro. *Brief Bioinform*, 2021. 22(2): p. 1361-1377.
51. Lipinski, C.A., Lead- and drug-like compounds: the rule-of-five revolution. *Drug Discovery Today: Technologies*, 2004. 1(4): p. 337-341.

52. Pollastri, M.P., Overview on the Rule of Five. *Current Protocols in Pharmacology*, 2010. 49(1): p. 9.12.1-9.12.8.
53. Aljahdali, M.O., M.H. Molla, and F. Ahammad, Compounds Identified from Marine Mangrove Plant (*Avicennia alba*) as Potential Antiviral Drug Candidates Against WDSV, an In-Silico Approach. *Marine Drugs*, 2021. 19(5).

Ajao, A. and G. Alasinrin, Assessment of the Protective Culture Potential of the *Lactococcus lactis* Ganee-5 strain as a Preservative against Spoilage Bacteria in Tomato Pastes. International Journal of Life Sciences and Biotechnology, 2022. 5(3): p. 316-334. DOI: 10.38001/ijlsb.1091980

Assessment of the Protective Culture Potential of the *Lactococcus lactis* Ganee-5 strain as a Preservative against Spoilage Bacteria in Tomato Pastes

Abdullahi Ajao*¹ , Ganiyat Alasinrin² 

ABSTRACT

This study investigated the spoilage patterns and biopreservation of tomato paste by lactic acid bacteria isolated from fermented milk products. All the isolates were screened for hydrogen peroxide, diacetyl, and lactic acid production. Isolate with the highest mean values of evaluating parameters was selected as protective culture for the biopreservation. The isolate was identified as *Lactococcus lactis* strain Ganee-5 using molecular techniques, and the sequences were submitted to the Genbank Database to obtain the accession number (MH571417). Antimicrobial properties of the protective culture were evaluated against some selected spoilage bacteria *E. coli* (ATCC 25922), *Listeria monocytogenes* (ATCC 15313), *Salmonella typhimurium* (IFO 12529), and *Staphylococcus aureus* (ATCC 12600), varying zone of inhibitions ranged from 18-25 mm were detected. The potato paste was preserved with *L. lactis* culture, sodium benzoate and control samples while the control samples were left without preservatives. All the experimental set-up was left for 16 days. Physicochemical and nutritional analysis showed that tomato paste with *L. lactis* was preserved closely as much as sodium benzoate ($p < 0.005$). Therefore, *L. lactis* can be adopted for the preservation of the tomato paste to replace chemical preservatives.

ARTICLE HISTORY

Received

23 March 2022

Accepted

21 May 2022

KEYWORDS

Protective culture, nutritional values, tomato paste, chemical preservatives, lactic acid, spoilage bacteria

Introduction

Tomato (*Solanum lycopersicum* L) is one of the most important vegetables produced globally, comprising approximately 14 % of world vegetable production [1,2]. It is one of the highly nutritious food ingredient used in the preparation of foods all over the world [3,4]. The following procedures for the treatment of vegetables such as pre and post-harvest methods, use of unsafe water for rinsing the vegetables and sprinkling to keep them fresh are the major predisposing factors responsible for the contaminations [5].

¹ Department of Microbiology, Faculty of Pure and Applied Sciences, Kwara State University, Malete, Nigeria.

²Department of Microbiology, Science Laboratory Technology, Federal Polytechnic, Nasarawa, Nigeria

*Corresponding E-mail Address: abdullahi.ajao@kwasu.edu.ng

The high water content in tomatoes makes it susceptible to spoilage by bacteria and fungi during storage, harvesting and transportation [6]. Spoilage accounts for the annual loss of the large proportion of the vegetable produce [7].

Spoilage bacteria or fungi are responsible for the postharvest decay and rapid deterioration which in turn affects the quality and shortens the shelf life of fruits and vegetables [8]. Vegetables have been associated with outbreaks of foodborne disease in many countries with varying magnitude from a few affected persons to many thousands [9].

Spoilage and pathogenic bacteria such as *Bacillus* spp, *Clostridium* spp, *Staphylococcus aureus*, *Escherichia coli* and *Salmonella* spp are responsible for the short shelf-life of food products and food-borne illnesses. In order to achieve improved food safety against such pathogens, food industry makes use of chemical preservatives or physical treatments (e.g. different chemicals and high temperatures). Food preservation is the process of treating food to stop or slow down spoilage, loss of quality, edibility or nutritional value. Food preservation is paramount to food safety and storage and has an impact on food security [10]. There have been growing global safety and health concerns over the use of synthetic chemical and artificial food preservatives and additives such as nitrites and sulphites in foods which have been found to be mutagenic and capable of triggering allergies and intolerances respectively [11]. This has called for the need for natural and safer approaches to food preservation and a lot of effort has been put towards moving away from the use of chemical food preservatives [12].

These preservation techniques have many drawbacks which include the proven toxicity of the chemical preservatives (e.g. nitrites), the alteration of the organoleptic and nutritional properties of foods, and especially recent consumer demands for safe but minimally processed products without additives. Therefore, there is an intense interest in developing novel antimicrobial agents for use in vegetable foods preservation to avoid spoilage.

Bio-preservation is defined as technique of extending the shelf life of food by using natural or controlled microbiota or antimicrobials [13].

Lactic acid bacteria and their metabolites are envisaged to be potential alternatives to chemical preservatives since they exhibit antimicrobial effects against spoilage and pathogenic bacteria. In addition, lactic acid bacteria are safer to consumers since they have

a generally recognized as safe' (GRAS) status [14]. Consumers' growing awareness of the health risks associated with the use of preservatives has resulted in a demand for the availability of chemical-free food on the market. As a result, there is a need to look for new alternatives that are natural but efficient and do not pose a health risk.

Materials and Methods

Sample Collection

A fermented dairy product (“Fura da nono”) was obtained from Fulani herdsmen in Ilorin around Abayawo area, Nigeria. It was collected in sterile universal bottle and kept at temperature of 4 °C before being taken to the laboratory for microbial analysis. While, ripe and wholesome tomatoes known as Roma tomatoes were purchased from Mandate Market, Ilorin, used in this research. The tomatoes were thoroughly cleaned and blended, then stored before being used.

Physicochemical Parameters of Tomato Paste

pH Determination

The pH meter was calibrated using a buffer solution of pH 4 and 7. A beaker was filled with about 25 ml of tomato paste, pH meter probe was dipped into the beaker and the pH of the sample was taken as described by Akinola *et al.* [15].

Determination of Lycopene Content

Lycopene of the tomato paste was extracted and estimated as described by Suwanaruang [16] using hexane:ethanol:acetone (2:1:1) (v/v). They were vortexed for 1 hour at 30°C in hexane and cooled to room temperature. Lycopene levels in the hexane extracts were calculated according as follow: $\text{Lycopene (mg/kg)} = \text{Abs } 503 \text{ nm} \times 137.4$

Determination of β -Carotene content

The β -carotene content was estimated following the method of Owolade *et al.* [17]. The beta-carotene content of Tomato paste samples was determined by analyzing the absorbance at 452 nm using 3% acetone in petroleum ether and 1% chloroform. The standard curve was used to determine the concentration of beta-Carotene in the Tomato paste. The amount of β -Carotene content was expressed in mg/kg of Tomato paste.

Determination of Ascorbic Acid Content

Ascorbic acid content of tomato paste was determined by iodometric titration as described by Dioha *et al.* [18]. Briefly, Ten milliliters of the tomato paste was added into a pre-washed conical flask, which was then filled with 5 milliliters of 10 % potassium iodide (KI) and 2 milliliters of 0.3 M sulphuric acid (H₂SO₄). In addition, 10 mL of 0.01 M potassium iodate was added to the flask (KI₃). A solution of 0.01 M sodium thiosulphate was used to titrate the excess iodine (Na₂S₂O₃). A blank titration was performed with 10 mL of distilled water. The amount of ascorbic acid was expressed in mg/L of Tomato paste.

Determination of Titratable Acidity

Titratable acidity was estimated following standard procedure [19] as percentage of citric acid monohydrate.

Total Bacterial Counts

The bacterial load of the tomato paste was carried out using pour plate method as described by Cheesbrough [20]. The total counts were taken as colony forming unit per milliliter (cfu/ml) of the sample [21].

Enumeration and isolation of Lactic acid Bacteria (LAB) from Fermented dairy products (“Fura da nono” and “wara”)

Enumeration and isolation of LAB was carried out following method of Wang *et al.* [22]. Fermented dairy products (“Fura da nono” and “wara”) were cultivated in De Man Rogosa and Sharpe (MRS) broth at 30 °C for 24 h for enrichment. One milliliter of a sample was mixed with 9 mL sterile physiological saline (0.85% w/v, NaCl) to make an initial dilution. Then subsequently, serially diluted and 1ml of the aliquot was inoculated using pour plate method on molten De Man Rogosa and Sharpe (MRS) agar Cycloheximide at a concentration of 0.01% (v/v) was added to the MRS plates in order to prevent the fungal growth, The plates were packed and sealed in an anaerobic jar then incubated under anaerobic condition at 30 °C for 48-72 h. Colonies with distinct morphological differences (based on color, shape, size, rough or smooth surface) were selected. The catalase activity and Gram reaction of the isolates were assessed. Gram-positive, catalase-negative and non-motile microorganisms were preserved in 10% (w/v) skim milk containing 0.1% (w/v)

sodium glutamate and maintained on agar slant for further characterization and identification.

Evaluation of the LAB Strains for the Production metabolites

The LAB isolates were screened for the production of metabolites following modified method of Ishola and Adebayo-Tayo [23]. The isolates were cultivated in MRS medium and incubated for 8 hours to attain stationary phase. One milliliter of each of the working cultures was transferred into 10 ml of MRS broth in 100 ml conical flasks incubated in an anaerobic jar for 24 hrs at 30 °C. Ten milliliter Inocula ($OD_{600}=1.0$) were inoculated into 200-ml conical flasks containing 90 ml of MRS broth and incubated at 30 °C for 36 hrs. Samples were taken and analyzed for lactic acid, diacetyl, hydrogen peroxide, pH development following methods of Awojobi *et al.*, [24] as follows:

Determination of Hydrogen Peroxide Production

Twenty five milliliter of diluted sulphuric acid was added to the isolates' broth culture. Titration of 0.1 N potassium permanganate was carried out The sample's decolorization was taken as the end point (AOAC, 1990).

Determination of Lactic Acid Production

A titration using 3 drops of phenolphthalein as an indicator was carried out with the NaOH (0.1 N) against a 25 ml broth culture of the isolates. The NaOH was gradually added until the color turned pink. Each milliliter of NaOH equals 90.08 milligrams of lactic acid.

Determination of Diacetyl Production

Twenty five milliliter of the isolate broth culture and 7.5 ml hydroxylamine solution were added to conical flasks for residual titration. HCl of 0.1 N was titrated with the bromophenol blue as an indicator which turned to a greenish end point; 21.5 mg HCl = diacetyl.

Molecular Identification of the LAB Isolate

The isolate was identified using molecular technique. Bacterial DNA was extracted from 18 hours old cultures using the Microbial DNA Isolation Kit (MO BIO, Laboratories, Inc.) according to manufacturer's instructions. The 16S rRNA was amplified by PCR for all the isolates using the primers: 16S forward primer (5'-AGAGTTTGATCCTGGCTCAG-3) and 16S reverse primer (5'ACGGCTACCTTGTTACGACTT-3'). PCR was performed. Each

PCR reaction was run with a negative control (no DNA). The PCR products was electrophoresed on 1.5% agarose gels, stained with 0.4 µg/ml ethidium bromide, and bands visualized with a UV illuminator [25].

Sequence analysis

PCR product was cleaned utilizing ExoSAP- 1T (Affymetrix, Inc., USA). The 5 µl of post-PCR reaction and 2 µl ExoSAP-IT reagents was mixed. The mix was incubated at 37 °C for 15 minutes followed by incubation at 80 °C for 15 minutes. Each purified template was sequenced on both strands using 16s primers. The sequences of ITS 3 and 4 regions, 16s of the tested isolates was edited in order to generate a consensus sequence from forward and reverse sequence in the amplicon using sequence assembly software (DNA BASER). A consensus sequence was analyzed by NCBI BLAST database for bacterial identities [26].

Antimicrobial properties of Bioactive Metabolites Produced by LAB isolates

Production of Bioactive Metabolites

The isolated strain of *Lactococcus* was grown in MRS broth (Hi Media, Mumbai) and maintained anaerobically at 34 °C for 24 h. After incubation, cells were removed from the growth medium by centrifugation (10,000 x g for 30 min, 4 °C) and passed through 0.2 mm filter. The cell-free supernatant was adjusted to pH= 6.0 using 1N NaOH and used as crude metabolite.

Determination of antibacterial effect of the bioactive metabolites

Antibacterial properties of the metabolites was determined by the agar well diffusion method using standard organisms *E.coli* (ATCC 25922), *Listeria monocytogenes* (ATCC 15313), *Salmonella typhimurium* (IFO 12529), *Staphylococcus aureus* (ATCC 12600) as the indicator strains. Nutrient agar was previously streaked with the test organisms on different plates and they were incubated at 37 °C for 24 hours, after which a cockborer was used to make hole of 6mm on each plate and 5 ml of bioactive metabolites was introduced into the hole and plates were incubated for 24 hours to observe the zone of inhibition. Zone of inhibition was measured in mm using ruler.

Comparative Evaluation of Biopreservatative activities of LAB and Sodium benzoate on Tomato pastes

The tomato pastes were then distributed into different sterile McCartney bottles. Prepared Tomato paste was then pasteurized using High –Temperature-Short time method with water bath pasteurizer at 85 °C for 15 mins [27]. One milliliter of the inoculum at ($OD_{600}=1.0$) was aseptically pipetted into 10ml of the pasteurized tomato paste inside McCartney bottles. Similarly chemical preservative (Sodium benzoate) at 0.1% was mixed with 10ml of the pasteurized tomato paste inside McCartney bottles. The treated tomato samples were then stored under ambient conditions (25°C). The physicochemical parameters were monitored as mentioned above for a period of 16 days for the assessment preservative activities of the LAB isolate [24].

Data Analysis

After data collection, the instruments were checked for completeness and consistency. The data was analyzed using statistical package for social sciences (SPSS) and Microsoft excel 2010. Analysis of variance (ANOVA) statistical test was used to determine the mean difference between the treatments conditions used for the research. A 95% confidence level was used and $p \leq 0.05$ or statistical value greater than 1.960 was considered statistically significant. Descriptive statistics like frequencies and percentages were used to present the result. Some results were expressed as mean \pm standard deviation, while others were presented in clustered bar chart.

Results and Discussion

The physicochemical and nutritional values obtained were within the range documented in the literature thus the nutritional and bioactive composition of tomatoes such as lycopene, β -carotene and ascorbic acid presents tomatoes as a food of great interest all over the world [28]. Current study evaluated the physicochemical, nutritional properties and bacteriological load of the experimental tomato paste as presented in Table 1.0.

Table 1. Physicochemical characteristics, Nutritional and Bacteriological Load of Tomato paste

Parameters	Values
pH	4.0 ± 0.25
β-Carotene (mg/kg)	12.35 ± 1.60
Lycopene (mg/kg)	290.04 ± 4.56
Ascorbic Acid (mg/L)	12.10 ± 0.33
Titrateable Acidity (%)	69.56 ± 2.40
Log Total Bacterial Counts (cfu/ml)	5.0 ± 0.55

Values are means ± SEM (n=3) per treatment

The pH of the sampled tomato paste obtained in this study ranged from 4.8 – 5.0 fallen within the expected range of 3-5 for fruits and vegetable juices [29,30]. The low pH of the tomato has been attributed to the abundance of organic acid largely citric and malic acids [31]. This result seemed to validate the literature information available on the pH values of tomato fruit [32]. Stevens [33] reported that although the pH of ripe tomatoes may exceed 4.6, tomato products are generally classified as acidic foods (pH < 4.6).

pH below 4.5 is a desirable trait, because it effectively inhibits the proliferation of microorganisms [34]. Lycopene is a natural pigment which is responsible for the reddish coloration of tomatoes and other fruits [16]. The average lycopene content of raw tomatoes has been reported at 30 mg kg⁻¹ [35]. However, higher values were obtained in this study, this variance in lycopene accumulation could be attributed to the environmental factors (temperature, light, growing season and location), and the agricultural techniques [36,37] (Dumas *et al.*, 2003; Toor *et al.*, 2006). Similarly, the average β-carotene content of raw tomatoes has been reported at 3.9 mg kg⁻¹ [38].

The presence of Vitamin C in the fruit and vegetable is highly essential since it plays a crucial role in the body forms and metabolic functions[39], and as such the mean values of ascorbic acid content as evaluated was 46.33 ± 2.98 mg/cm³ significantly in high proportion. Again, high bacterial load of the tomato paste recorded in the study could be a contamination from either water, equipment used during processing, airborne, soil borne bacteria or tomato flora. Fermented diary product fura do nono used in this study provided a good source for isolating Lactic acid bacteria. The LABs with the highest frequency of

occurrence in the fura do nono was selected for the experiment. The occurrence of this organism has been reported by various researchers [40,41]. This study demonstrated that the selected LAB produced different biomolecules in sufficient quantities such as hydrogen peroxide, diacetyl and lactic acid productions. The ability of this LAB strains to secrete antimicrobial compounds confers the potential ability on them to extend the shelf life of tomato paste and reduce the microbial load [24].

The phylogenetic relationship among the strain GANEE-5 and other related bacteria downloaded from the GenBank database was constructed. The strain was in the phylogenetic branches of the *Lactococcus lactis*. Strain exhibited a maximum identity (100 %) to *Lactococcus lactis* strain NBRC 100933 (NR 113960.1) showed in Fig. 1.0. The bacterial isolate clustered with the members of the genera *Lactococcus*, thus differentiating the bacterial isolate on the genetic basis. Incidentally, Biscola *et al.* [42] had earlier reported that *Lactococcus lactis* 69 harbor no virulence genes which implies that the safety and potential technological application of this strain to inhibit undesirable microbial growth is promising.

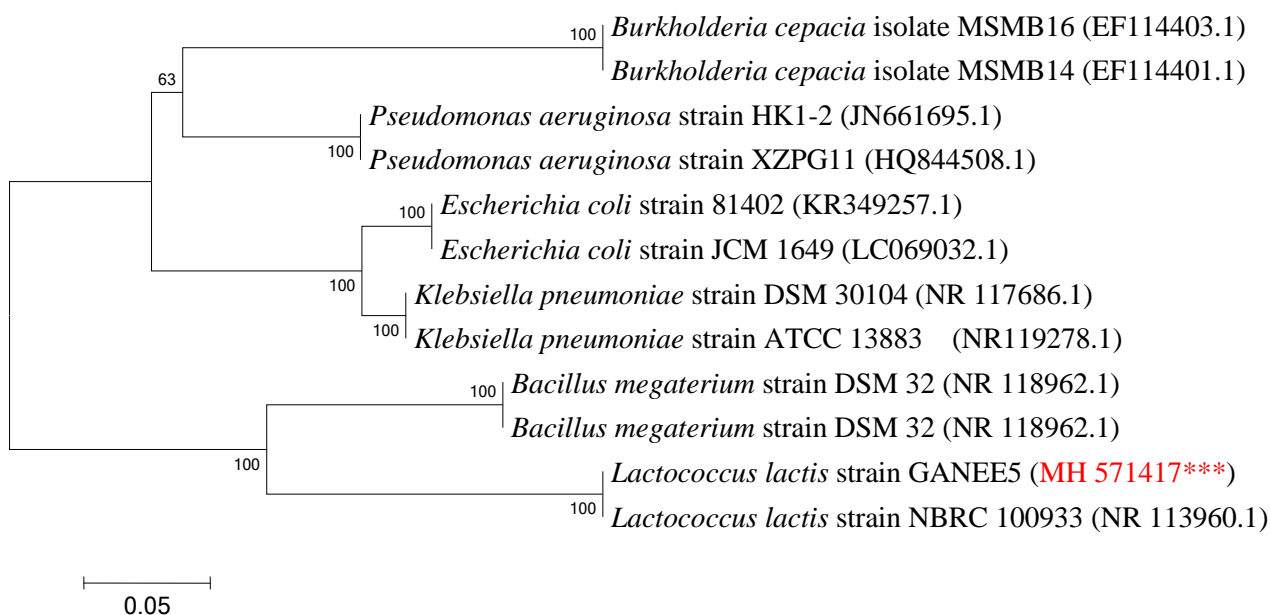


Fig 1. Phylogenetic tree constructed by Neighbor-Joining method derived from analysis of the 16S rRNA gene sequences of native isolates and related sequences obtained from NCBI. Scale bar, 0.05 substitutions per nucleotide position and numbers in parenthesis represent GeneBank accession numbers.

Current study also evaluated the inhibitory effect of the isolated *Lactococcus lactis* sp. lactis Ganee-5 against some selected bacteria. The result showed that the isolate produced inhibitory compound against test organism namely *E.coli* (ATCC 25922), *Listeria monocytogenes* (ATCC 15313), *Salmonella typhimurium* (IFO 12529), *Staphylococcus aureus* (ATCC 12600). The diameter of zone of inhibition ranged from 18-25mm. The mean values of the diameter of the zone of inhibition against *Listeria monocytogene* (ATCC 15313) and *Salmonella typhimorium* (IFO 12529) was 18.72 mm and 25.44 mm respectively. The test organisms' sensitivity to bioactive metabolites varies greatly. The bioactive compound impacts test organisms in varying degrees. The mean values recorded for the zone of inhibition was 25.00 mm and 22.00 mm for both *Staphylococcus aureus* (ATCC 12600) and *E.coli* (ATCC 25922) respectively (Table 2.0). These findings are in line with the work of Sahraoui *et al.* [43] who reported that *Lactococcus lactis ssp. lactis* KJ660075 strain showed a remarkable antibacterial inhibition almost against several food borne pathogens and spoilage bacteria. Also, Yang *et al.* [44] also found that inhibitory effect against several foodborne pathogens e.g. *Listeria innocua*, *B. cereus*, *P. fluorescens*, *Erwinia carotovora* and *Leuconostoc mesenteroides* subsp. *mesenteroides* LAB isolated from cheese and yogurt. Several Authors have reported the inhibitory properties of Lactic acid bacteria against various spoilage and pathogenic bacteria [45,46].

Table 2. Inhibitory effect of the *Lactococcus lactis* strain GANEE5 against selected test organisms

Test organisms	Zone of inhibition (mm)
<i>E.coli</i> (ATCC 25922)	22.00 ± 1.60
<i>Listeria monocytogenes</i> (ATCC 15313)	18.00 ± 0.72
<i>Salmonella typhimurium</i> (IFO 12529)	20.00 ±1.10
<i>Staphylococcus aureus</i> (ATCC 12600)	25.00 ^a ±1.44

Several Authors have hypothesized different mechanisms for the antagonistic activity of LAB metabolites against the spoilage bacteria. The inhibitory effect of lactic acid is due to undissociated forms of the acids which penetrates the pathogen's membrane and liberate hydrogen ion in the neutral cytoplasm thus inhibiting vital cell functions [47]. Diacetyl is

known to have a very effective and strong oxidizing effect on organism's cell especially bacteria [48]. In the same way, the antibacterial activity of the LAB was presumed to be associated with synthesis of organic acid, hydrogen peroxide and bacteriocins and this fact may contribute to their colonizing and competitive ability [49]. The authors also claimed the bacteriostasis and death of susceptible bacteria were indeed due to the neutralization of organic acids on the cytoplasmic membrane, and thus increasing its permeability. This mechanism causes the cell ruptures and eventually kills the bacteria [50].

On the whole, inhibitory activity of LAB has been reported to be due to a combination of many factors such as production of lactic acid which brings about reduction of pH of the fermentation medium [51] and production of inhibitory bioactive compounds such as hydrogen peroxide and bacteriocins which are responsible for most antimicrobial activity [4,23]. Lactic acid bacteria (LAB) play a major part in most fermentation processes, not only because of their ability to improve the flavour and aroma but especially for their preservative effects on food. LAB contributes to preservation by the production of a vast array of antimicrobial compounds and proteins [52,53].

The bio-preservative potential of LAB metabolites has been tested on other food product like suya [54] and chicken meat [55]. A major advantage in the use of lactic acid bacteria and their metabolites is that they are considered as generally recognized as safe (GRAS) and comply often with the recommendations for food products [56]. Unlike some chemical preservatives, LAB metabolites have not been reported to have residual effect on the food product or the consumer's health.

The effect of *Lactococcus lactis* strain Ganee-5 biomolecules and sodium benzoate on the ascorbic acid in preserved tomato paste is presented in Fig. 2. The Ascorbic acid decreased as the number of days of storage increased in the control samples while samples preserved with both sodium benzoate and *Lactococcus lactis spp lactis* as preservatives was stable throughout the 16 days of storage. However, on the 10th days of storage, the ascorbic acid of the control sample decreased and was significantly different to other samples ($p \geq 0.05$). Incidentally the ascorbic acid of both the sodium benzoate and *Lactococcus lactis spp lactis* preserved tomato paste was maintained throughout the storage period. This may be due to

the degradation of tomato paste when exposed to heat, light, or oxygen, as suggested by Akinola et al. [15] on an orange, watermelon, carrot, and ginger juice blend.

The ascorbic acid level in samples decreased with time. This observed diminution in vitamin C content is in agreement with what was reported in literature. Vitamin C content is known to be an important parameter for assessing the nutritional quality of fruits blends as it degrades during storage [57]. This degradation is perhaps due to the high sensitivity of ascorbic acid to oxygen, light and heat - and consequential oxidation in the presence of oxygen by both enzymatic and non-enzymatic catalyst [59]. At 16th day, sample with sodium benzoate gave higher ascorbic acid level (12.10 mg/100 g) than sample with metabolite (10.26mg/100 g); this implies that sodium benzoate preserved ascorbic acid more than metabolite during the storage period. Consequently, vitamin C contents of tomato paste can be enriched using sodium benzoate as preservative, although, the abuse (excess addition) of such preservative has been linked to food poisoning/toxicity, immune depression and cancer in human [60].

The effect of *Lactococcus lactis spp lactis* strain Ganee-5 biomolecules and sodium benzoate on the β -carotene in preserved tomato paste is presented in Fig. 3. The beta carotene content of the preserved tomato paste both with the sodium benzoate and *Lactococcus* metabolite preservatives showed slightest decrease in β -carotene content in both preservatives significantly not different ($p \geq 0.05$) throughout the storage time. While, there was remarkable decrease in the β -carotene of the control sample. Incidentally, β -carotene was not detected after 16 days of storage. The gradual decrease in beta-carotene as observed in result presented in (Fig 3) may be due to changes in surrounding storage temperature. This gradual decrease in beta-carotene during storage was also observed by Awsi [67].

The effect of *Lactococcus lactis spp lactis* strain Ganee-5 biomolecules and sodium benzoate on the titratable acidity in preserved tomato paste is presented in Fig.4. The titratable acidity increased as number of days of storage increased and the highest values was recorded in the sodium benzoate preserved samples followed by *Lactococcus lactis spp lactis* strain Ganee-5 biomolecules preserved sample and the lowest in control sample.

The effect of *Lactococcus lactis* spp *lactis* strain Ganee-5 biomolecules and sodium benzoate on the lycopene in preserved tomato paste is presented in Fig. 4. Result showed that lycopene retention was lowest in control sample whereas treatment with metabolite recorded high lycopene content (Fig. 5), although retention of lycopene was higher in sodium benzoate. Lycopene retention of the control sample ranged from 1.56 mg/kg –14.3 mg/kg on the 12th day. The lycopene content was not detected in day 14-16 of the control samples. Lycopene content in tomato paste preserved with metabolites ranged from 12.22 mg/kg – 14.3 mg/kg while sodium benzoate treated tomato paste recorded ranged from 13.0 mg/kg – 14.3 mg/kg. Lycopene content was decreased during storage period for all samples. The loss of lycopene at all conditions might be due to oxidation which depends on temperature, moisture etc [69].

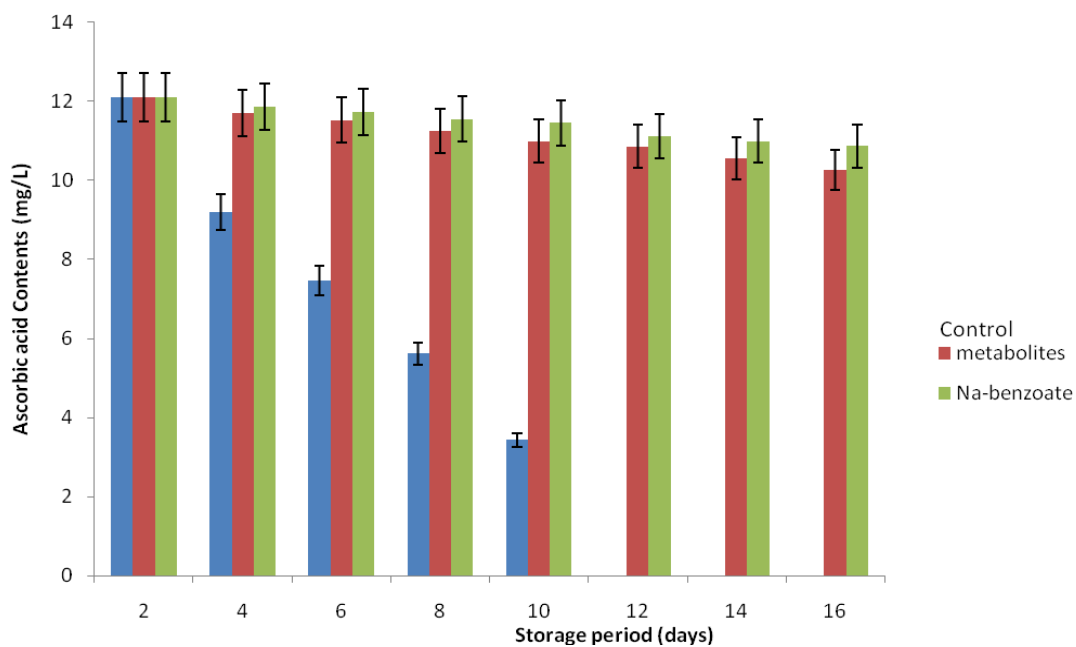


Fig 2. Effect of *Lactococcus lactis* metabolite and sodium benzoate on the ascorbic acid content of tomato paste over a storage time

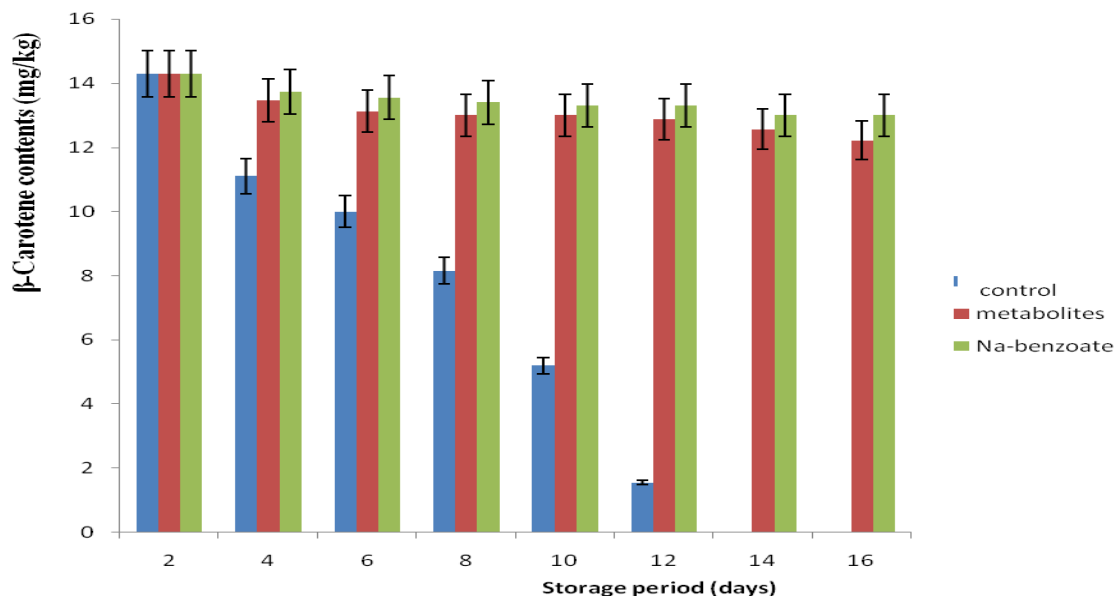


Fig 3. Effect of *Lactococcus lactis* metabolite and sodium benzoate on the β -carotene contents of tomato paste over a storage time

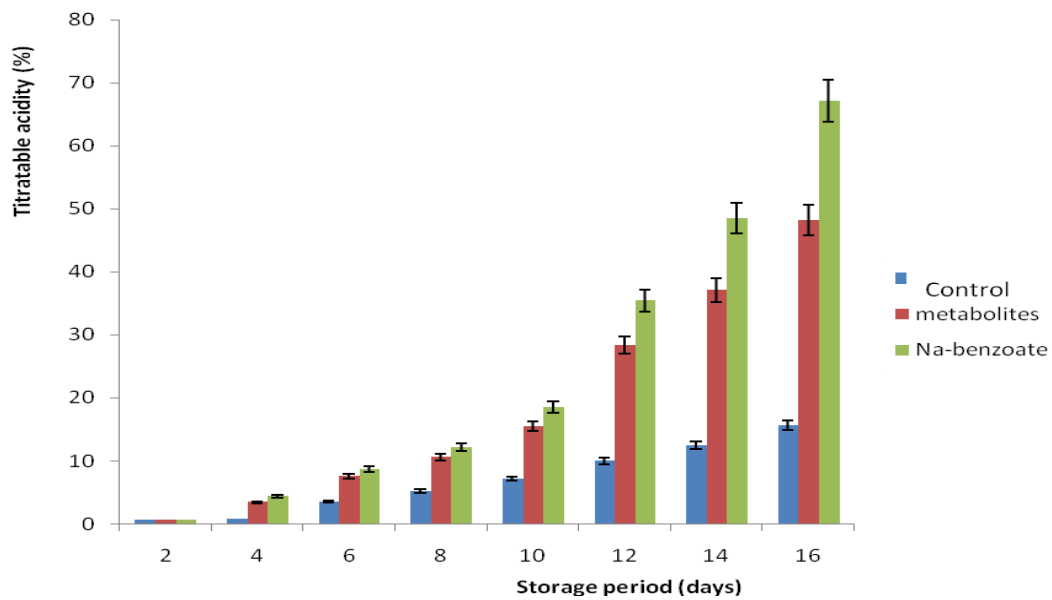


Fig 4. Effect of *Lactococcus lactis* metabolite and sodium benzoate on the titratable acidity content of tomato paste over a storage time

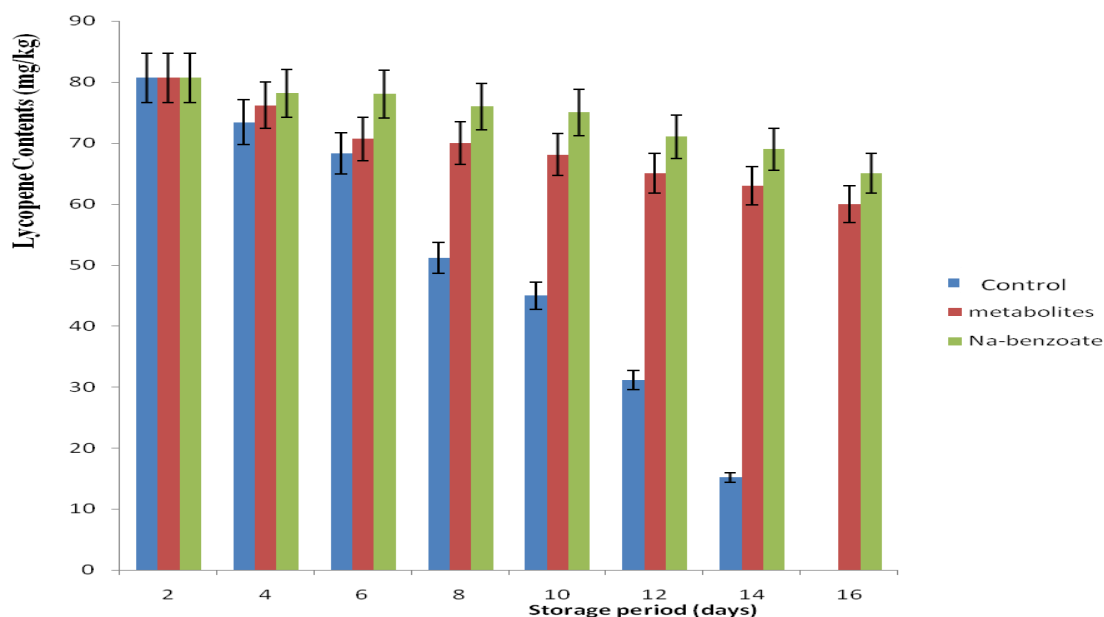


Fig 5. Effect of *Lactococcus lactis* metabolite and sodium benzoate on the Lycopene contents of tomato paste over a storage time

The use of lactic metabolites with biopreservative activity could improve the quality of food and increase its safety by inhibiting the food-borne pathogens and spoilage microorganisms.

Conclusion

This research work confirmed and supported the fact that vital physicochemical property of tomato paste such as ascorbic acid, pH, titratable acidity, β -carotene and lycopene decrease with advancement of storage time. Addition of preservatives (natural and synthetic) was noted not to prevent the loss of ascorbic acid from the result, even though sodium benzoate preserved better than *L.Lactis* metabolite, natural preservative (*L.lactis* metabolites) maybe said to be better than synthetic preservative as no negative impact on humans has been ascribed to its use in tomato paste while use of preservative have been proved to mutagenic. Finally, physicochemical analysis revealed that the tomato paste has good quality characteristics without the addition of preservatives. Therefore, tomato should be consumed fresh. It is therefore recommended that more research needs to be conducted to prove and establish the results reported in this work, especially on the effect of preservatives (natural

and synthetic). Also, storage period should be increased and mineral composition should be analyzed in tomato paste and other vegetables.

References

- 1 Food and Agriculture Organization of the United Nations. Summary of food and agricultural statistics, 2003. Rome, Italy. p. 67-69.
2. Kader, A.A. Increasing food availability by reducing postharvest losses of fresh produce. Paper presented at the International Postharvest Symposium, 2004. P 682:2169-2176.
- 3 Ogunniyi, L.T. and J.A. Oladejo, Technical efficiency of tomato production in Oyo State Nigeria. *Agricultural Science Research Journal*, 2011. 1(4): p. 84-91.10.1042/BST20120183.
4. Ogunbanwo, S.T., I.F. Fadahunsi, and A.J. Molokwu, Thermal stability of lactic acid bacteria metabolites and its application in preservation of tomato pastes. *Malaysian Journal of Microbiology*, 2014. 10 (1): p. 15-23.
5. Hamed, H.A., Y.A. Moustafa, and S. M. Abdel-Aziz, In vivo Efficacy of Lactic Acid Bacteria in Biological Control against *Fusarium oxysporum* for Protection of Tomato Plant. *Life Science Journal*, 2011. 8 (4): p. 462-467.
6. Spadaro, D. and M.L. Gullino, State of the art and future prospects of the biological control of post-harvest fruit diseases. *International Journal of Food Microbiology*, 2004. 91 (2): p. 185-194.
7. Barth, M., et al., *Microbiological Spoilage of Fruits and Vegetables*. W.H. Sperber, M.P. Doyle (eds.), *Compendium of the Microbiological Spoilage of Foods and Beverages*, Food Microbiology and Food Safety. 2009. C Springer Science+Business Media, LLC, 2009; p. 135-183.
8. Jang, M. and G.H. Gun-Hee Kim, Inhibitory effect of novel thioflavone derivatives against foodborne and spoilage microbes on fresh fruit. *Journal of food safety*, 2016; 1–7DOI 10.1111/jfs.12337.
9. Hwanhlem, N.et al., Bacteriocin-producing lactic acid bacteria isolated from mangrove forests in southern Thailand as potential bio-control agents: Purification and characterization of bacteriocin produced by *Lactococcus lactis* subsp. *Lactis* KT2W2L, *Probiotics and Antimicrobial Proteins*, 2013. 5 (4): p. 264-278.
10. Ahmed, F.A.et al., Postharvest diseases of tomato and natural products for disease management. *African Journal of Agricultural research*, 2017. 12 (9): p. 684-691.
11. Agharkar, M. S.,et al., Trends in green reduction of graphene oxides, issues and challenges: A Review.*Resources Bulletin*, 2014. 59: p. 323- 324.
12. Bhakya, S. et al., Biogenic synthesis of silver nanoparticles and their antioxidant and antibacterial activity. *Applied Journal of Nanoscience*, 2015. 12: p. 44-47.
13. Veer, P.S., Recent approaches in food bio-preservation- A review. *Open Veterinary Journal*, 2018. 8 (1): p. 104-111.
14. Luz, C.,et al., In vitro antifungal activity of bioactive peptides produced by *Lactobacillus plantarum* against *Aspergillus parasiticus* and *Penicillium expansum*. *Food Science and Technology*, 2017. 10: p. 12-15.
15. Akinola, O.T., T. O. Ogunbode, and E. O. Akintunde, Borehole Water Quality Characteristics and Its Potability in Iwo, Osun State, Nigeria. *Journal of Scientific Research & Reports*, 2018. 18(1): p. 1-8
16. Suwanaruang, T. Analyzing Lycopene Content in Fruits. *Agriculture and Agricultural Science Procedia.*, 2016. 11: p. 46 – 48.

17. Owolade, S.O. et al., Study on physico-chemical properties, antioxidant activity and shelf stability of carrot (*Daucus carota*) and pineapple (*Ananas comosus*) juice blend. *International Food Research Journal*, 2017. 24 (2): p. 534-540.
18. Dioha, J. et al., Determination of ascorbic acid content of some tropical fruits by iodometric titration. *Int. J. Biol. Chem. Sci.*, 2011. 5 (5): p. 2180-2184.
19. AOAC.. *Official Methods of Analysis 17th ed.* Association of Official Analytical Chemists International. 2000. Washington, DC, USA.
20. Cheesbrough, M. *District Laboratory Practice in Tropical Countries, Part 2.* Cambridge University Press, 2000. Edinburgh, Uk. P .52-70.
21. Oyeleke S.B. and SB. *Manga Essentials of Laboratory Practicals in Microbiology.* Tobest publisher, Minna, Nigeria, 2008; p.36-75.
22. Wang, D.et al., Isolation and Identification of Lactic Acid Bacteria from Traditional Dairy Products in Baotou and Bayannur of Midwestern Inner Mongolia and q-PCR Analysis of Predominant Species. *Korean J. Food Sci. An.*, 2016. 36 (4): p. 499-507.
23. Ishola, R.O. and B.C. Adebayo-Tayo,. Screening of Lactic Acid Bacteria Isolated from Fermented Food for Bio-molecules Production. *AU J.T.*, 2012. 15 (4): p. 205-217.
24. Awojobi, K. O., S. M. Adeyemo, and O. O. Sanusi,. Biosynthesis of Antimicrobial Compounds by Lactic Acid Bacteria and Its Use as Biopreservative in Pineapple Juice. *Frontiers in Science*, 2016. 6 (1): p. 17-24.
25. Bromberg, R., S.A Barnby, and F.M. George,. Isolation of Bacteriocin-producing Lactic acid bacteria from meat products and its spectrum of inhibitory activity. *Brazilian Journal of Microbiology*, 2004. 35: p. 21-27.
26. Bhutia, M. O., N. Thapa, and J. P. Tampang,. Molecular characterization of Bacteria, Detection of Enterotoxin Genes, and Screening of Antibiotic susceptibility patterns in Traditionally processed meat products of Sikkim, India *Frontiers in microbiology.* (2021) 11(599606): p. 1 – 8.
27. Odebumi, E.O., O.O Dosumu, and O.O. Shoga, Comparative Analysis of soboextract, orange and pineapple juices. *Journal of Chemical Society of Nigeria*, (2003. 28: p. 65-69.
28. Adalid, A.M., S. Salvador Rosello, and F. Nuez, Evaluation and selection of tomato accessions (*Solanum section Lycopersicon*) for content of lycopene, β -carotene and ascorbic acid. *Journal of Food Composition and Analysis*, 2010. 23 (2010): 613–618.
29. Harris, A., J. Key, and B. Silcocks,. *Dietary carotene.* 3rd ed. Prentice hall press, NY. 1991: p. 63-68.
30. Adubofuor, J.et al., Comparative study related to physicochemical properties and sensory qualities of tomato juice and cocktail juice produced from oranges, tomatoes and carrots. *African Journal of Food Science*, 2010. 4 (7): p. 427-433.
31. Wilkerson, E. D. Rapid assessment of quality parameters in processing tomatoes using hand-held and benchtop infrared spectrometers and multivariate analysis. *Journal of Agricultural and Food Chemistry*, 2013. 61(9): p. 2088–2095.
32. Mohammed M, LA, Wilson, P.L. Gomes, Postharvest sensory and physiochemical attributes of processing and non-processing tomato cultivar. *J Food Qual.*, 1999. 22: p. 167–182.
33. Stevens, M.A. Relationships between components contributing to quality variation among tomato lines. *J. Amer. Soc. Hort. Sci.*, 1972. 97: p. 70–73.
34. Tigist, M., T. S., Workneh, & K. Woldetsadik,. Effects of variety on the quality of tomato stored under ambient conditions. *Journal of food science and technology*, 2013. 50(3): p. 477–486. <https://doi.org/10.1007/s13197-011-0378-0>
35. Kuti, J.O., H.B. Konuru,. Effects of genotype and cultivation environment on lycopene content in red-ripe tomatoes. *J. Sci. Food Agric.*, 2005. 85(12): p. 2021-2026.

36. Dumas, Y. et al., Effects of environmental factors and agricultural techniques on antioxidant content of tomatoes. *J. Sci. Food Agric.*, 2003: 83(5): p. 369-382.
37. Toor, R.K., G.P. Savage, C.E. Lister., Seasonal variations in the antioxidant composition of greenhouse grown tomatoes. *J. Food Compost. Anal.*, 2006. 19(1): p. 1-10.
38. Holden, J. M. et al., carotenoid content of US Foods: an update of the database. *J. Food Comp. Anal.*, 1999. 12: p. 169–196.
39. Chambial, S. et al., Vitamin C in disease prevention and cure: an overview. *Indian journal of clinical biochemistry : IJCB*, 2013. 28(4): p. 314–328.
40. Enan, E. et al., Novel Antibacterial Activity of *Lactococcus Lactis* Subspecies *Lactis* Z11 Isolated from Zabady. *International journal of Biomedical science*, 2013. 9 (3): p. 174-180.
41. Wang, D. Isolation and Identification of Lactic Acid Bacteria from Traditional Dairy Products in Baotou and Bayannur of Midwestern Inner Mongolia and q-PCR Analysis of Predominant Species. *Korean J. Food Sci. An.*, 2016. 36 (4): p. 499-507.
42. Biscola, V. Effect of autochthonous bacteriocin-producing *Lactococcus lactis* on bacterial population dynamics and growth of halotolerant bacteria in Brazilian charqui. *Food Microbiology*, 2014. 44 (2014): 296-301.
43. Sahraoui, Y. et al., Antibacterial and technological properties of *Lactococcus lactis* ssp. *lactis* KJ660075 strain selected for its inhibitory power against *Staphylococcus aureus* for cheese quality improving, *J. Food Sci. Technol.*, 2015. DOI 10.1007/s13197-015-1845-9
44. Yang, E. et al., Antimicrobial activity of bacteriocin-producing lactic acid bacteria isolated from cheeses and yogurts. *AMB Express*, 2012. 2 (1): 48.
45. Jalilsood, T. et al., Inhibition of pathogenic and spoilage bacteria by a novel biofilm-forming *Lactobacillus* isolate: a potential host for the expression of heterologous proteins. *Microbial cell factories*, 2015. 14: p. 96. <https://doi.org/10.1186/s12934-015-0283-8>
46. Ibrahim, S.A. et al., Lactic Acid Bacteria as Antimicrobial Agents: Food Safety and Microbial Food Spoilage Prevention. *Foods*, 2021. 10: p.3131. <https://doi.org/10.3390/foods10123131>
47. Adeniyi, B.A., F.A. Ayeni, and S.T. Ogunbanwo, Antagonistic Activities of Lactic Acid Bacteria Isolated from Nigerian Fermented Dairy food against Organisms Implicated in Urinary Tract Infection. *Biotech.*, 2006. 5: p. 183- 188.
48. Sangorrín, M.P., Cold-adapted yeasts as biocontrol agents: Biodiversity, adaptation strategies and biocontrol potential. 2014. Book Part. p. 441-464
49. Cosentino, S. Antilisterial activity of nisin-like bacteriocin-producing *Lactococcus lactis* subsp. *lactis* isolated from traditional Sardinian dairy products. *Journal of Biomedicine and Biotechnology*, 2012. doi:10.1155/2012/376428.
50. Loh, J.Y., In vitro assessment on intestinal microflora from commonly farmed fishes for control of the fish pathogen *Edwardsiella tarda*. *Turkish Journal of Veterinary and Animal Sciences*, 2014. 38: p. 257–263.
51. Adebayo-Tayo, B.C. and A.A Onilude,.. Screening of lactic acid bacteria strains isolates from some Nigeria fermented foods for EPS production. *World Applied Sciences Journal*, 2008. 4(5): p. 741-47.
52. Ray, B. and M. Daeschel, *Food Biopreservatives of Microbial Origin*. CRC Press, Boca Raton, 1992. FL, USA. P. 3-11.
53. Elliason, D.J., S.R. Tatini, 1999. Enhanced inactivation of *Salmonella typhimurium* and verotoxigenic *Escherichia coli* by nisin at 6.5 °C. *Food Microbiol.*, 16(3): p. 257-67.
54. Adesokan IA, B. B.Odetoyinbo, A.O. Olubamiwa, Biopreservative activity of lactic acid bacteria on suya produced from poultry meat. *Afr. J. Biotechnol.*, 2008. 7(20): p.3799-3803.

55. Ogunbanwo, ST., A .I. Sanni, and A.A..Onilude,. Influence of cultural conditions on the production of bacteriocin by *Lactobacllus brevis* OG1. *African Journal of Biotechnology*, 2003. 7: p. 179 –184.
56. Stiles EM, W.H. Holzapfel, Lactic acid bacteria of foods and their current taxonomy. *Int. J. Food. Microbiol.* 1997. 36(1): 1-2.
57. Corina, C., D. Parvu, and A. Ravis, The determination of some physicalchemical characteristics for orange, grapefruit and tomato juices. *Journal of Agro alimentary Processes and Technologies*, 2006. 12 (2): p. 429-432.
58. Vwioko DE, O.O. Osemwegie, J.N. Akawe, The effect of garlic and ginger phytochemicals on the shelf life and microbial contents of homemade soursop (*Annona muricata*) fruit juice. *Biokemstri.*, 2013. 25 (2): p. 31-38.
59. Awsi, J. and M. Dorcus, Development and Quality of Evaluation of Pineapple Juice Blend with Carrot and Orange Juices. *International Journal of Scientific and Research Publications*, 2012. 6: p. 1-8.
60. Trifiro A.S. et al., Quality changes in tomato concentrate production: Effects of heat treatment. *Industrial Conserve*, 1998. 73(1): p. 30-41.

Uz, G., et al., *Schizosaccharomyces pombe*' de Magnezyum Kısıtlamasının Glukoz Transportu Üzerine Etkisinin Araştırılması. International Journal of Life Sciences and Biotechnology, 2022. 5(3): p. 335-345. DOI: 10.38001/ijlsb.1103724

Schizosaccharomyces pombe' de Magnezyum Kısıtlamasının Glukoz Transportu Üzerine Etkisinin Araştırılması

Gülşen Uz^{1,2*}, Tuğba Pesen¹, Ahsen Berber¹, Cenk Kığı³,
Bedia Palabıyık⁴, Ayşegül Topal Sarıkaya³

ÖZET

Magnezyum, enerji metabolizması, nükleik asit ve protein sentezi, sinyal iletimi, hücre bölünmesi gibi birçok biyolojik süreç için hayati önem taşır. Magnezyum homeostasisinin bozulması, kardiyovasküler hastalıklar, hipertansiyon, tip 2 diyabet ve kanser başta olmak üzere çok sayıda hastalıkla ilişkilendirilmiştir. Dünya çapında 300 milyondan fazla insan tip 2 diyabet ile mücadele etmektedir ve bu sayı katlanarak artmaktadır. Klinik çalışmalar, tip 2 diyabetli hastalarda serum magnezyum seviyesinin düştüğünü ve magnezyum takviyesinin glukoz metabolizması üzerine olumlu etkileri olduğunu göstermiştir. Bu çalışmada, biyolojik süreçler ve genetik mekanizmalar bakımından memeli hücreleriyle benzerlik gösteren *Schizosaccharomyces pombe* mayasının magnezyum transportu kısıtlı mutant suşunda glukoz tüketimi ve glukoz taşıyıcılarının (*ght1*, *ght2*, *ght5*) anlatım seviyeleri araştırılmıştır. Magnezyum transportu kısıtlı olan mutant suşta, besi ortamına ilave edilen magnezyum artışına bağlı olarak glukoz tüketimi artmıştır. Glukoz taşıyıcılarından *ght1*, *ght2*'nin anlatım düzeyi, 30 mM Mg⁺² destekli ortamda artmış, suş için optimum üremenin görüldüğü daha yüksek magnezyum konsantrasyonunda (75 mM) azalmış, *ght5*'in anlatım düzeyinde ise anlamlı bir değişim bulunmamıştır. Bulgularımız, glukoz taşıyıcılarından *ght1* ve *ght2*'nin *ght5*'ten farklı bir mekanizma ile düzenlendiğini işaret etmektedir.

MAKALE GEÇMİŞİ

Geliş

18 Nisan 2022

Kabul

27 Nisan 2022

ANAHTAR KELİMELER

magnezyum eksikliği, glukoz transportu, *S. pombe*

¹İstanbul Yeni Yüzyıl University, Faculty of Science and Literature, Department of Molecular Biology and Genetics, İstanbul / Turkey

²İstanbul University, Institute of Science, Department of Molecular Biology and Genetics, İstanbul/ Turkey

³İstanbul Yeni Yüzyıl University, Faculty of Medicine, Department of Medical Biology and Genetics, İstanbul / Turkey

⁴İstanbul University, Faculty of Science, Department of Molecular Biology and Genetics, İstanbul/ Turkey

* Corresponding Author: Gülşen Uz, E-mail: gulsen.uz@yeniuyuzuil.edu.tr

Investigation of the Effect of Magnesium Restriction on Glucose Transport in *Schizosaccharomyces pombe*

ABSTRACT

Magnesium is vital for many biological processes such as energy metabolism, nucleic acid, and protein synthesis, signal transduction, and cell division. Impairment of magnesium homeostasis is associated with many diseases, especially cardiovascular diseases, hypertension, type 2 diabetes, and cancer. More than 300 million people worldwide struggle with type 2 diabetes, and this number is growing exponentially. Clinical studies have shown that serum magnesium levels were decreased in patients with type 2 diabetes and that magnesium supplementation has positive effects on glucose metabolism. In this study, glucose consumption and the expression levels of glucose transporters (*ght1*, *ght2*, *ght5*) were investigated in magnesium transport-restricted mutant strain of *Schizosaccharomyces pombe* yeast, which is similar to mammalian cells in terms of biological processes and genetic mechanisms. In mutant strain with limited magnesium transport, glucose consumption increased due to the increase in magnesium added to the medium. The expression level of *ght1*, *ght2*, one of the glucose transporters, increased in 30 mM Mg²⁺ supplemented medium, decreased at higher magnesium concentration (75 mM), where optimum growth was observed for the strain, and there was no significant change in the expression level of *ght5*. Our findings indicate that the glucose transporters *ght1* and *ght2* are regulated by a different mechanism than *ght5*.

ARTICLE HISTORY

Received

18 April 2022

Accepted

27 April 2022

KEY WORDS

magnesium deficiency, glucose transport, *S. pombe*

Giriş

Magnezyum (Mg²⁺), ökaryotik hücrelerde potasyumdan sonra en fazla bulunan katyondur [1]. Memeli hücrelerinde magnezyum konsantrasyonu ~10-30 mM civarındadır. Hücrede magnezyum negatif yüklü yapılara; ATP, DNA ve RNA gibi fosfat grupları taşıyan makromoleküllere, ribozomlara ve hücre membranına bağlı olup, ~0.5-1.2 mM düzeyinde de serbest iyon olarak bulunur [2]. Bununla birlikte, negatif yüklü gruplar taşıyan yapılara bağlanarak yapısal kararlılık sağlamanın yanında, nükleik asit, protein, lipid, glukoz ve enerji metabolizması gibi önemli biyolojik süreçlerde yer alan 600' den fazla enzimin kofaktörü/allosterik düzenleyicisi olarak hayati önem taşır [2].

Magnezyum, evrensel enerji molekülü ATP' ye bağlanıp, fosfat transferini kolaylaştırarak ATP' yi biyolojik olarak aktif duruma getirir [3]. Glukoz, prokaryotlardan tek hücreli ökaryotlara ve omurgalılara kadar çok çeşitli canlı türünde, hücrenin biyosentez ve fonksiyonel işlevleri için gerekli ATP' nin sağlanmasında başlıca karbon kaynağıdır.

Glukozdan ATP sentezi sürecinde yer alan reaksiyon basamaklarında, glikoliz evresi (heksokinaz, fosfofruktokinaz, fosfogliserat kinaz, piruvat kinaz), krebs döngüsü (izositrat dehidrogenaz, α -ketogluterat dehidrogenaz, pirüvat dehidrogenaz) ve oksidatif fosforilasyonda (ATP-sentaz) magnezyuma bağımlı çok sayıda enzim görev alır [4]. Magnezyum ATP sentez süreci dışında, pankreas beta hücrelerinde hücreye Ca^{+2} girişini ve buna bağılı insülin salınımını kontrol eder [5]. İnsüline duyarlı pankreas, karaciğer, kas, yağ ve beyin hücrelerinde, insülinin reseptörüne bağlanması, insülin reseptör tirozin kinazın fosforilasyonu ve devamında gerçekleşen bir dizi fosforilasyon reaksiyonu Mg-ATP kompleksine bağılıdır; bu reaksiyonlar sonrasında glukoz transportu, glikojen, yağ ve protein sentezi gibi hayati hücresel süreçler gerçekleşir [5].

Magnezyum homeostasisini ve glukoz metabolizması ile ilişkisini araştıran çok sayıda klinik araştırma bulunmaktadır. Bu çalışmalardan birinde, insülin direnci, şişmanlık, hipertansiyon ve dislipidemi ile karakterize edilen metabolik sendrom tanısı konulmuş hastalarda, sağlıklı bireylere kıyasla, serum magnezyum seviyesi fizyolojik alt sınır 0.75 mmol/L' den daha düşük bulunmuştur [6]. 10 yıl süre ile takip edilen 817 katılımcının yer aldığı başka bir çalışmada, şiddetli hipomagnezemi bulunan bireylerde (serum $Mg^{+2} < 0.5$ mmol/L) açlık glukoz düzeyinin yüksek olduğu belirtilmiştir [7]. 7 yıl süre ile takip edilen 2582 katılımcının yer aldığı diğer bir çalışmada diyet ve takviye ile birlikte yüksek magnezyum alınmasının (365 mg/gün), glukoz metabolizması ile ilişkili hastalıkların gelişme riskini ~%30-40 oranında düşürdüğü belirtilmiştir [8].

22.900 diyabet tanılı hastanın yer aldığı yaklaşık 21 bağımsız çalışmada, serum Mg^{+2} konsantrasyonu düşük bulunmuştur [9,10,11]. Benzer şekilde başka çalışmalarda, diyabetiklerde hipomagnezemi görülme sıklığının sağlıklı kontrol grubuna kıyasla oldukça yüksek olduğu gösterilmiştir [12,13]. Çalışma grubumuzun 2020 yılında yaptığı bir araştırmada normal referans aralığında bulunduğu halde, kandaki Mg^{+2} düzeyinin alt sınıra yakın değerlerde bulunduğu bireylerde diyabete yatkınlık riski oluşabileceği yönünde bulgular elde edilmiştir [14].

Diyabet hastalarında kan damarlarında meydana gelen hasar nedeniyle yüksek kan basıncına bağılı olarak böbrek yetmezliği gelişme riski yüksektir [15]. Diyabete bağılı böbrek fonksiyonlarındaki bozukluğun sonucu olarak hipomagnezemi gelişmektedir. Ayrıca

tedavide kullanılan insülin duyarlılığını artıran ilaçlar da diyareye neden olarak hipomagnezemiye neden olmaktadır [16]. Bununla birlikte insülin tedavisi de magnezyumun hücre içine girmesine neden olarak serum magnezyum konsantrasyonunun azalmasına neden olur [17]. Hipomagnezemi, diyabet hastalığının bir sonucu olarak görülse de TRPM (Transient Receptor Potential Melastatin) gibi magnezyum kanal proteinlerini kodlayan genlerdeki mutasyonların bir sonucu olarak da gelişebilmektedir [18, 9].

Schizosaccharomyces pombe (*S. pombe*) mayası yetiştirilmesi kolay, genom yapısı aydınlatılmış [32] ökaryotik bir model organizma olup, kromozom organizasyonu [19], rekombinasyon [33], stres yanıt mekanizmaları [34], hücre döngüsü [35], mRNA kırılma mekanizmaları [36] bakımından yüksek ökaryotlarla benzerlik taşıması nedeniyle glukoz ve magnezyum metabolizmasının araştırılmasında tercih edilmektedir. *S. pombe*' de, 8 heksoz taşıyıcı protein (Ght1-Ght8) tanımlanmıştır [20]. Bunlardan Ght5, yüksek afiniteli glukoz/fruktoz:proton taşıyıcısıdır ve başlıca glukoz transportundan sorumludur. Ght1 ve Ght2, glukoz afinitesi Ght5' den daha düşük olan glukoz taşıyıcılarıdır. Diğer heksoz taşıyıcıları fruktoz, glukonat gibi farklı heksozların taşınmasından sorumludur [21]. Ght5' in transkripsiyonu ve lokalizasyonu insandaki glukoz transport proteinlerine (GLUT) benzer şekilde düzenlenir. Yüksek glukoz içeren besi ortamında (%3) Scr1 baskılayıcı protein *ght5*' in anlatımını baskılar, düşük glukoz ortamında (%0.1) baskılayıcı protein nukleustan ayrılır ve *ght5* anlatım yapar [21].

S. pombe mayasında magnezeyum transportu tamamen aydınlatılamamıştır. Magnezyum transportundan sorumlu proteinler, hücre membranında *Saccharomyces cerevisiae* mayasındaki CorA protein ailesine ait ALR1 (Aluminum resistance protein 1) homoloğu (SPBC27B12.12c) kanal proteini, mitokondri membranında MRS2 (Mitochondrial RNA Splicing 2) homoloğu (SPBC25H2.08c) [22] ve vakuol membranında MNR2 (MaNganese Resistance 2) homoloğudur (SPAC17A2.14) [23, 24, 25]. Hücre membranındaki ALR1 homoloğu olarak bilinen Mg^{+2} kanal proteinini taşımayan mutant *S. pombe* suşu, besi ortamına oldukça yüksek konsantrasyonda Mg^{+2} eklendiğinde bölünebilmekte ve canlılığını sürdürebilmektedir [24]. Bu çalışmada, *S. pombe*' nin plazma membranındaki ve vakuol membranındaki Mg^{+2} kanal proteinlerini taşımayan, hipomagnezemi için model oluşturan suşunda, glukoz transportunun ve glukoz tüketiminin araştırılması amaçlanmıştır.

Materyal ve Metot

Kullanılan suşlar ve besi ortamları

Çalışma kapsamında bilinen iki Mg²⁺ kanal proteinini kodlayan genler bakımından PCR temelli delesyon yapılmış GA2 suşu (Δ SPAC17A2.14 Δ SPBC27B12.12 leu1-32 ura4-D18 ade6-M216 kanr) ve kontrol grubu olarak bu suşun elde edildiği atasal suş Sp292 (leu1-32 ura4-D18 ade6-M210 h-) kullanıldı. Sp292 suşunun üretilmesinde maya ekstreli sıvı besi ortamı (YEL: yeast extract 5g/L, glukoz 30 g/L), maya ekstreli katı besi ortamı (YEA: yeast extract 5g/L, glukoz 30 g/L, 20 g/L) kullanıldı. GA2 suşunun üretilmesinde, YEA besi ortamına suşun optimum üreyebildiği miktarda 200 mM MgCl₂, YEL besi ortamına 75mM MgCl₂ eklendi.

Glukoz tüketim analizi

20 ml YEL besi yerine 30 mM ve 75 mM düzeyinde MgCl₂ eklenerek hazırlanan deney ortamlarına 0.1 OD (600nm), $\sim 1 \times 10^6$ hücre/mL, olacak şekilde hücre ekimi yapıлып, 24 saat sonundaki hücre süspansiyonlarından elde edilen üst fazlar, Nzytec marka GOD-POD kolorimetrik glukoz analiz kiti kullanılarak glukoz tüketim miktarları (g/L) belirlendi. Üç biyolojik tekrardan elde edilen veriler GraphPad Prism 6 istatistik analiz programında, one-way ANOVA ve Tukey's Multiple Comparison Post testi ile değerlendirildi.

RNA izolasyonu ve cDNA sentezi

Logaritmik fazdaki ~ 0.6 OD (600nm) yoğunluğundaki hücre süspansiyonlarından, fenol-kloroform yöntemi ile RNA izolasyonu yapıldı [26]. Genomik DNA' yı uzaklaştırmak için (Zymoresearch) DNase I (1 U/ μ l) örnekler üzerine uygulandı. Spektrofotometrik olarak saflık ve miktar analizi yapıldıktan sonra, 20 ng RNA örneklerinden (GeneMarkBio) cDNA sentez kiti ile cDNA sentezi gerçekleştirildi.

Real-Time PCR

Gen ekspresyonlarının göreceli analizinde SYBR temelli Real-time PCR kullanıldı. SybrGreen I (GeneMarkBio), 5 pmol forward ve revers primerler kullanılarak, 20 ng RNA'ya denk gelen miktarda cDNA olacak şekilde toplam 20 μ l hacimde reaksiyon bileşenleri hazırlandı. Reaksiyon Applied Biosystem QuantStudio5 Real-time PCR cihazında, 95 °C'de

5 dakikalık bir ön denatürasyonu takiben, 45 döngüden oluşan 95 °C’de 15 saniye, 59 °C’de 15 saniye, 72 °C’de 15 saniye ve 60 °C’de 1 dk erime eğrisi basamakları ile gerçekleştirildi. Referans olarak *act1* geni kullanılarak *ght1*, *ght2* ve *ght5* genlerinin anlatım düzeyi $2^{-\Delta\Delta Ct}$ yöntemi [27] ile hesaplandı. Gen ekspresyonlarının istatistiksel anlamlılık düzeyleri GraphPad Prism 6 programında, two-way ANOVA ve Bonferroni Post testi ile belirlendi. Çalışmada kullanılan primerlere ait dizi bilgisi Tablo 1’ de verildi.

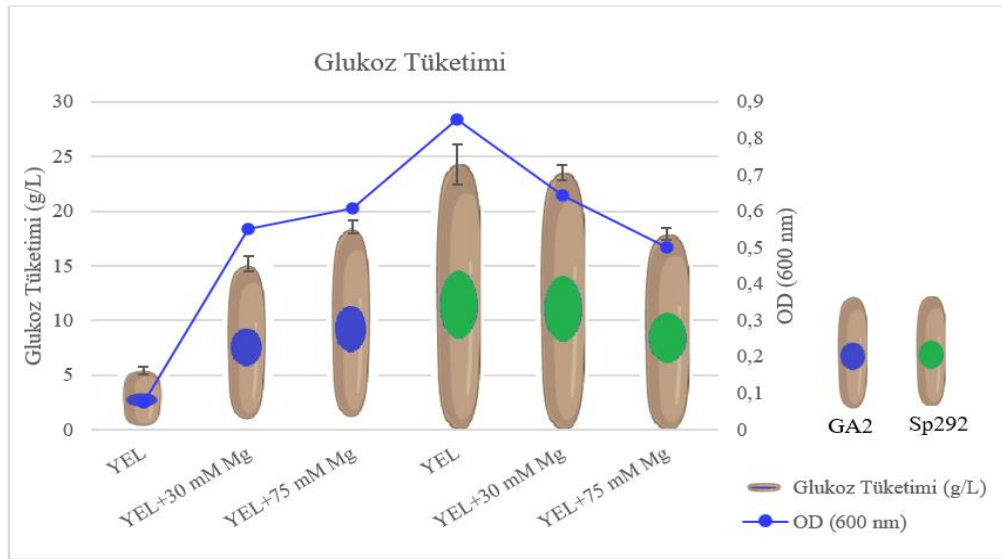
Tablo 1 Çalışmada kullanılan primer dizileri

	Forward primer	Reverse primer
Act1	TCATGCGTCTTGATCTCGCC	ATTTCACGTTTCGGCGGTAGT
Ght1	TTCAAGTCACCGCTGTTCCA	CGAATATGGGGAGGAGCCAC
Ght2	TACCGGTTCCATTGGTGGTG	AAGACCTTGACGAGCCGAAG
Ght5	CGTGGTGTTCAAGGCGAAAG	CGTGGTAGCTAGATTCCGGC

Bulgular ve Tartışma

Farklı magnezyum konsantrasyonları içeren besi ortamlarında glukoz tüketimi

Schizosaccharomyces pombe’ nin bilinen Mg^{+2} kanal proteinlerini ($\Delta alr1 \Delta mnr2$) taşımayan GA2 suşunda Mg^{+2} ilavesi yapılmayan YEL besi ortamında (Mg: ~ 0.2 mM) glukoz tüketimi en düşük bulundu (5.4 g/L). En yüksek glukoz tüketiminin ise Sp292’ nin YEL ve 30 mM Mg^{+2} destekli YEL besi ortamında (24.3-23.5 g/L) olduğu belirlendi (Şekil 1).



Şekil 1 GA2 ve Sp292 suşlarında YEL, 30 ve 75 mM Mg^{+2} ilave edilen YEL besi ortamlarında glukoz tüketimi (g/L) ve hücre yoğunlukları (OD_{600nm})

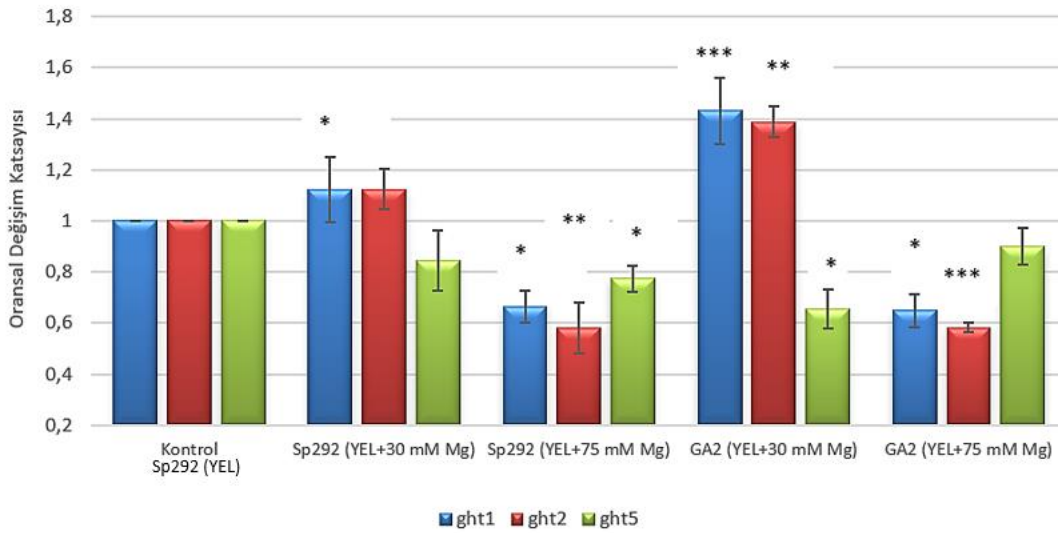
Sp292 suşunda 30 ve 75 mM Mg⁺² ilavesinin hücre yoğunluğunu anlamlı bir şekilde azalttığı belirlendi (p<0.05). Buna karşın, YEL ve 30 mM Mg⁺² destekli YEL besi ortamındaki glukoz tüketimi arasında istatistiksel olarak anlamlı bir fark bulunamadı. GA2 suşu besi ortamına Mg⁺² ilave edilmeden çoğalamamaktadır. Besi ortamına artan konsantrasyonlarda Mg⁺² ilave edildiğinde hücre yoğunluğu ile birlikte glukoz tüketiminin de arttığı belirlendi. 75 mM Mg⁺² ilave edilen besi ortamında, Sp292 suşunun hücre yoğunluğu GA2 suşuna kıyasla daha düşük olmasına rağmen, iki suşun 75 mM Mg⁺² destekli besi ortamında glukoz tüketimi bakımından anlamlı bir fark bulunamadı.

Çalışmamızda magnezyumu dış ortamdan hücre içine alamayan, hücrede Mg⁺² deposu olan vakuolden sitoplazmaya çıkışı olmayan, dolayısıyla depo organeldeki magnezyumu kullanamayan *S. pombe* suşu kullanılarak uzun süreli magnezyum eksikliğinin glukoz tüketimi ve glukoz transportu üzerine etkisi araştırılmıştır. Bu suş ~0.2 mM Mg⁺² içeren zengin besi ortamında (YEL) çoğalamamaktadır, besi ortamına 75 mM Mg⁺² ilave edildiğinde çoğalması ~%50 oranında iyileşmektedir [25]. Besi ortamına 30 ve 75 mM olarak ilave edilen Mg⁺², atasal suşun (Sp292) çoğalmasını olumsuz yönde etkilerken, magnezyum transportundan sorumlu genler bakımından delesyonlu GA2 suşunda belirtilen konsantrasyonlar hücre çoğalmasını iyileştirmektedir. Atasal suşun (Sp292) çoğalmasını olumsuz yönde etkileyen yüksek konsantrasyondaki Mg⁺²'nin, henüz belirlenememiş bir taşıyıcı sistemle GA2 suşunda hücreye kısıtlı oranda girdiği düşünülmektedir.

Magnezyum eksikliği, karbonhidrat intoleransı ve insülin direnci ile de ilişkili olup, diyabetin gelişmesinde ve ilerlemesinde etkili olduğu belirtilmektedir [28, 10]. Yapılan epidemiyolojik çalışmalar, diyetle magnezyum takviyesi yapılmasının glukoz metabolizması ve insülin duyarlılığı üzerine olumlu etkileri olduğunu [29] tip 2 diyabet gelişme riskini azalttığını [30] göstermektedir. Diğer taraftan, diyabet tedavisinde kullanılan insülin duyarlılığını artıran metformin vb. ilaçlar, insülin tedavisi, diyabete bağlı gelişen böbrek fonksiyon bozuklukları, hipomagnezemiye neden olur. Bu nedenle de hipomagnezemi diyabet hastalarında sıklıkla rastlanan durumdur.

Farklı magnezyum konsantrasyonlarında glukoz taşıyıcılarının (*ght1*, *ght2*, *ght5*) anlatım düzeyleri

Zengin besi ortamına (YEL) 30 mM Mg⁺² ilave edildiğinde, Sp292 suşunda sadece *ght1*' in ekspresyonu anlamlı olarak artmıştır (oransal kat artışı: 1,12), GA2 suşunda ise *ght1* ve *ght2* genlerinin ekspresyonu artmış, *ght5* geninin ekspresyonu azalmıştır. 75 mM Mg⁺² ilave edildiğinde Sp292 suşunda, *ght1*, *ght2* ve *ght5* genlerinin ekspresyonu anlamlı olarak azalmış, GA2 suşunda *ght1* ve *ght2* genlerinin ekspresyonu azalmış, *ght5* geninin anlatımında anlamlı bir değişme bulunamamıştır (Şekil 2, Tablo 3).



Şekil 2 Farklı Mg⁺² konsantrasyonlarında *ght1*, *ght2* ve *ght5* gen ekspresyonu oransal kat değişimlerinin karşılaştırılması (***:P<0.001, **: P<0.01, *: P <0.05)

Tablo 3 GA2 ve Sp292 suşlarında 30 ve 75 mM Mg⁺² ilave edilen YEL besi ortamlarında *ght1*, *ght2* ve *ght5* gen ekspresyonlarının oransal kat değişimleri

	Sp292 (YEL+30 mM Mg)	Sp292 (YEL+75 mM Mg)	GA2 (YEL+30 mM Mg)	GA2 (YEL+75 mM Mg)
<i>ght1</i>	1.122± 0.128	0.664± 0.063	1.43± 0.131	0.648± 0.06
<i>ght2</i>	1.124± 0.077	0.579± 0.099	1.387± 0.058	0.582± 0.019
<i>ght5</i>	0.843± 0.116	0.773± 0.052	0.654± 0.074	0.899± 0.071

GA2 suşunda zengin besi ortamına 30 ve 75 mM olarak ilave edilen Mg⁺²' nin, hücre bölünmesini teşvik etmesi nedeniyle glukoz tüketimini arttırdığı görülse de suşun bölünmesi

için optimum Mg^{+2} konsantrasyonunda (75mM) glukoz taşınmasından sorumlu iki genin (*ght1* ve *ght2*) ekspresyonu azalmış, başlıca glukoz taşınmasından sorumlu *ght5*' in ekspresyonunda ise anlamlı değişim bulunamamıştır. 30 mM Mg^{+2} ilavesi ise *ght1* ve *ght2*' nin anlatımını arttırmış, *ght5*' in anlatımını azaltmıştır. Atasal suşta ise, besi ortamına 30 mM Mg^{+2} ilavesi *ght1*' in anlatımını arttırmış, 75 mM Mg^{+2} ilavesi her üç glukoz taşıyıcısının anlatımında azalmaya neden olmuştur. Bu bulgular bize *ght1* ve *ght2*' nin anlatımının *ght5*' ten farklı bir mekanizmayla düzenlendiğini işaret etmektedir. Çalışmanın diğer önemli bulgusu, 30 mM Mg^{+2} ilavesinin atasal suşun çoğalmasında olumsuz yönde etkilemesine rağmen glukoz tüketimini azaltmamasıdır. Bu da daha az sayıdaki hücrenin daha fazla glukoz tükettiğini göstermektedir. Bu bulgu ise 30 mM Mg^{+2} ilavesinin, magnezyum transport sistemi bakımından sağlıklı olan suşta çevresel stres yanıtının aktifleşmiş olabileceğini düşündürmekle birlikte aday stres yanıt yollarının (osmotik stres, oksidatif stres, ağır metal, ısı şoku vb.) araştırılması gerekmektedir.

Sonuç

Dünya Sağlık Örgütü' nün 2016 yılındaki raporuna göre; dünya genelinde 400 milyondan fazla diyabet hastası vardır, diyabet nedeniyle 1.5 milyondan fazla kişi ve buna ek olarak diyabete bağlı gelişen özellikle kardiyovasküler hastalıklar ve böbrek yetmezliği nedeniyle 2.5 milyondan fazla kişi hayatını kaybetmiştir [31]. Bu kronik hastalığın başarılı bir şekilde yönetilmesi için altında yatan patofizyolojik mekanizmaların aydınlatılması önem taşımaktadır. Hipomagnezemi için önemli bir model teşkil eden maya suşu ile yaptığımız bu çalışma, magnezyum homeostasisi ile ilişkili diyabet başta olmak üzere çeşitli hastalıkların hücrel mekanizmalarının aydınlatılması bakımından yapılacak çalışmalara ışık tutacaktır.

Açıklama ve Teşekkür

Bu çalışma TÜBİTAK 2209-A Üniversite Öğrencileri Araştırma Projeleri Destekleme Programının, 1919B011702923 numaralı projesi ile desteklenmiştir.

Kaynaklar

1. Jahnen-Dechent, W. and Ketteler, M., Magnesium basics. CKJ: Clinical Kidney Journal, 2012. 5: p.3-14.
2. De Baaij, J., Hoenderop, J. and Bindels, R., Magnesium in man: implications for health and disease. Physiol. Rev., 2015. 95: p.1-46.

3. Fiorentini, D., et al., Magnesium: Biochemistry, Nutrition, Detection, and Social Impact of Diseases Linked to Its Deficiency. *Nutrients*, 2021.13(1136): p. 1-44.
4. Pilchova, I., et al., The Involvement of Mg⁺² in Regulation of Cellular and Mitochondrial Functions. *Oxidative Medicine and Cellular Longevity*, 2017. 6797460: p.1-8.
5. Kostov, K., Effects of Magnesium Deficiency on Mechanisms of Insulin Resistance in Type 2 Diabetes: Focusing on the Processes of Insulin Secretion and Signalling. *Int. J. Mol. Sci*, 2019. (20)1351: p. 1-15.
6. Guerrero-Romero, F., and Rodríguez-Morán, M., Low serum magnesium levels and metabolic syndrome. *Acta Diabetol*, 2002. 39: p. 209–213.
7. Guerrero-Romero, F., et al., Hypomagnesaemia and risk for metabolic glucose disorders: a 10-year follow-up study, *European journal of clinical investigation*, 2008. 38(6): p. 389–396.
8. Hruby, A., et al., Higher magnesium intake reduces risk of impaired glucose and insulin metabolism and progression from prediabetes to diabetes in middle-aged Americans. *Diabetes care*, 2014. 37 (2): p. 419-427.
9. Mooren, F.C., Magnesium and disturbances in carbohydrate metabolism. *Diabetes, obesity & metabolism*, 2015. 17(9): p. 813–823.
10. Barbagallo, M., et al., Serum ionized magnesium in diabetic older persons. *Metabolism: clinical and experimental*, 2014. 63(4): p. 502–509.
11. Wälti, M.K., et al., Low plasma magnesium in type 2 diabetes. *Swiss medical weekly*, 2003. 133(19-20): p. 289–292.
12. Lecube, A., et al., Diabetes is the main factor accounting for hypomagnesemia in obese subjects. *PLoS one*, 2012. 7(1): p. 1-7.
13. Chambers, E.C., et al., Serum Magnesium and Type-2 Diabetes in African Americans and Hispanics: A New York Cohort. *Journal of the American College of Nutrition*, 2006. 25(6): p. 509-513.
14. Kılıç, C., et al., Magnesium Deficiency Can Be a Sign for Predisposition to Diabetes. *Yeni Yüzyıl Journal of Medical Sciences*, 2020. 2: p. 32-38.
15. Nathan, D.M., et al., Intensive diabetes treatment and cardiovascular disease in patients with type 1 diabetes. *N. Engl. J. Med.*, 2005. 353: p. 2643–2653.
16. Svare, A., A patient presenting with symptomatic hypomagnesemia caused by metformin-induced diarrhoea: a case report. *Cases J*, 2009. 2: p. 156.
17. Paolisso, G., et al., Insulin induces opposite changes in plasma and erythrocyte magnesium concentrations in normal man. *Diabetologia*, 1986. 29: p. 644-647.
18. Song, Y., et al., Common genetic variants of the ion channel transient receptor potential membrane melastatin 6 and 7 (TRPM6 and TRPM7), magnesium intake, and risk of type 2 diabetes in women. *BMC medical genetics*, 2009. 10: p. 4.
19. Cam, H., and Whitehall, S., Analysis of heterochromatin in *Schizosaccharomyces pombe*. *Cold Spring Harbor Protocols*, 2016. 11: p. 920-927.
20. Heiland, S., et al., Multiple hexose transporters of *Schizosaccharomyces pombe*. *J Bacteriol*, 2000. 182: p. 2153–2162.
21. Saitoh, S., et al., Mechanisms of expression and translocation of major fission yeast glucose transporters regulated by CaMKK/phosphatases, nuclear shuttling, and TOR. *Molecular biology of the cell*, 2015. 26(2): p. 373–386.
22. Matsuyama, A., et al., ORFeome cloning and global analysis of protein localization in the fission yeast *Schizosaccharomyces pombe*. *Nature biotechnology*, 2006. 24(7): p. 841–847.
23. Kim, D., et al., Analysis of a genome-wide set of gene deletions in the fission yeast *Schizosaccharomyces pombe*. *Nat Biotechnol*, 2010. 12(1308): p. 617-623.

24. Topal Sarikaya, A., Akman, G., and Temizkan, G., Nickel resistance in fission yeast associated with the magnesium transport system. *Molecular Biotechnology*, 2006. 32: p.139-145.
25. Uz, G. and Topal Sarikaya, A., The effect of magnesium on mitotic spindle formation in *Schizosaccharomyces pombe*. *Genetics and Molecular Biology*, 2016. 39(3): p.459-464.
26. Bähler, J. and Wise, J., Preparation of total RNA from fission yeast. *Cold Spring Harbor Protocols*, 2017. 4: p. 306-310.
27. Livak, K. and Schmittgen, T., Analysis of relative gene expression data using real-time quantitative PCR and the 2(-Delta Delta C(T)) Method. *Methods*, 2001. 25 (4): p. 402-408.
28. Weisinger, J.R., and Bellorín-Font, E., Magnesium and phosphorus, *Lancet*, 1998. 352: p. 391-396.
29. Rodríguez-Morán, M., and Guerrero-Romero, F., Oral magnesium supplementation improves insulin sensitivity and metabolic control in type 2 diabetic subjects: a randomized double-blind controlled trial. *Diabetes Care*, 2003. 26: p.1147–1152.
30. Dong, J.Y., et al., Magnesium intake and risk of type 2 diabetes: meta-analysis of prospective cohort studies. *Diabetes Care*, 2011. 34: p. 2116-2122.
31. World Health Organization, Global report on diabetes, 2016.
32. Wood, V., Gwilliam, R., Rajandream, M. A. et al., The genome sequence of *Schizosaccharomyces pombe*. *Nature*, 2002. 415: p. 871–880.
33. Fowler K. R., Sasaki M., Milman N. et al., Evolutionarily diverse determinants of meiotic DNA break and recombination landscapes across the genome. *Genome Res.*, 2014. 24: p.1650–1664.
34. Papadakis, M. A., Workman, C. T., Oxidative stress response pathways: Fission yeast as archetype. *Critical Reviews in Microbiology*, 2015. 41:4 p. 520-535.
35. Nurse P., Thuriaux P., Nasmyth K., Genetic control of the cell division cycle in the fission yeast *Schizosaccharomyces pombe*. *Mol. Gen. Genet.*,1976.146: p. 167–178.
36. Hoffman, C.S., Wood, V., Fantes, P. A., An Ancient Yeast for Young Geneticists: A Primer on the *Schizosaccharomyces pombe* Model System. *Genetics*, 2015. 201(2): p. 403–423.

Caliskan, E. and B. Z. Haznedaroglu, Characterization of Omega-3 and Omega-6 Fatty Acid Accumulation in *Chlorococcum novae-angliae* Microalgae Grown under Various Culture Conditions. International Journal of Life Sciences and Biotechnology, 2022. 5(3): p. 346-369. DOI: 10.38001/ijlsb.1082112

Characterization of Omega-3 and Omega-6 Fatty Acid Accumulation in *Chlorococcum novae-angliae* Microalgae Grown under Various Culture Conditions

Elifcan Caliskan¹ , Berat Z. Haznedaroglu^{1*} 

ABSTRACT

Chlorococcum novae-angliae is a terrestrial green microalgae species with remarkable potential to synthesize omega-3 (ω -3) and omega-6 (ω -6) fatty acids. In this study, *Chlorococcum novae-angliae* has been subjected to varying growth conditions (light, nitrogen, salinity, and temperature) to investigate the accumulation of ω -3 and ω -6 fatty acids. Among tested growth conditions, eicosapentaenoic acid, α -linoleic acid, γ -linoleic acid, and arachidonic acid were enhanced by nitrogen limitation. Significant increases were observed in concentration of linoleic acid, an essential precursor molecule for the production ω -6 fatty acids under decreased nitrogen concentrations. Despite the lowest biomass growth, monounsaturated fatty acids and docosahexaenoic acid were increased by 14.4% and 8.7% under low light intensities, respectively. Meanwhile, the highest concentrations of palmitic acid (C16:0), stearic acid (C18:0), and oleic acid (18:1cis-9) were also detected under nitrogen limitation. Total accumulation of ω -3 fatty acids was highest in the control group, followed by nitrogen limitation, whereas total ω -6 fatty acid accumulation was highest under nitrogen limitation followed by the control group. Total lowest fatty acid concentrations were obtained under increased salinity while low temperature conditions heavily inhibited cellular growth.

ARTICLE HISTORY

Received

07 March 2022

Accepted

20 May 2022

KEY WORDS

Chlorococcum novae-angliae, essential fatty acids, microalgal lipids, omega fatty acids

Introduction

Fatty acids are essential components of cellular membranes composed of long aliphatic carbon chains with carboxylic acid and methyl group at both ends [1, 2]. Long chain polyunsaturated fatty acids (LC-PUFAs), in particular, play considerable roles in important metabolic processes as storage and transport of energy, regulation of gene functions, generation of eicosanoids, lipid peroxidation, acylation of proteins, cell signaling, and inflammatory processes [3, 4]. Many LC-PUFAs also play prophylactic roles against various diseases such as coronary artery, diabetes, cardiac arrhythmias, atherogenesis, and hyperlipidemia [5]. Specifically, ω -3 and ω -6 fatty acids are required for cognitive functions

¹Institute of Environmental Sciences, Bogazici University, Istanbul, Turkey

*Corresponding Author: Berat Z. Haznedaroglu, e-mail: berat.haznedaroglu@boun.edu.tr

and neural network as they maintain cell signaling [6]. A recent study reported that regular intake of ω -3 and ω -6 fatty acids hinders developing major depression and Alzheimer's disease [7]. Among them, linoleic acid (LA) and α -linoleic acid (ALA) were recommended to be included in daily diets of humans as they cannot be synthesized *de novo* due to lack of Δ 12 and Δ 15 desaturase enzymes [8]. Linoleic acid and ALA are important precursors of ω -3 and ω -6 fatty acids respectively. Alpha-linoleic acid is a key structural component required for biosynthesis of eicosapentaenoic acid (EPA) and docosahexaenoic acid (DHA) and produced in mammals in very limited quantities [2]. Alpha-linoleic acid and arachidonic acid (AA) are precursors for prostaglandins, critical immune response mediators such as inflammation, patent vasodilators regulating the body's defense mechanism after injuries and infections [9]. Both EPA and DHA are recommended as dietary supplements for brain and nervous system development, cardiovascular health, visual function, memory and learning and cognitive maintenance and infant development [6]. Impulses generated between the brains cells are significantly affected by DHA [10]. In addition, DHA is one of most substantial components which take place in retina membrane and play role in signaling mechanisms in the eye [11]. Recent studies indicate the presence of the EPA at certain doses in the entire human body promotes inflammation control and enhances the immune system [12]. Substances obtained from EPA also play vital roles in combating heart disease, and chronic and inflammatory processes [10]. EPA and DHA also play a strong role in the body's defense mechanism in reducing inflammation and eliminating reactive oxygen species (ROS) at the cellular level [13]. Meanwhile, LDL (High density lipoprotein) and VLDL (very low density lipoprotein) levels in human blood plasma are considerably related with ω -3 fatty acids that have significant impacts on TAG (triacylglycerol) production [4].

Stearidonic acid (SDA, C18:4n3) and docosapentaenoic acid (DPA, C22:5n3) are other notable ω -3 fatty acids which have been identified as important needs for human well-being in addition to EPA, DHA and ALA [14]. Arachidonic acid and γ -linoleic acid (GLA) are considered to be essential ω -6 fatty acids made from LA [1]. Gamma-linoleic acid is the initial product of a synthesis of ω -6 fatty acids which is further synthesized with DGLA after LA reaches the human body. This fatty acid is essential for the metabolism of ω -6 fatty acids where homo- γ -linolenic acid (DH-GLA) is converted to AA through the action of Δ 5

desaturase enzyme [15]. Certain diseases like cancer and diabetes have been reported to have disruptive effects on the conversion of LA to GLA [16]. In fact, some studies suggest that daily intake of GLA may be a possible solution for the circulation of the metabolism of ω -6 fatty acids [17-19].

All these potential health benefits has created a growing market demand for ω -3 and ω -6 fatty acids leading to overfishing and decreased fish stocks [20]. While the demand for fish oil as a source of ω -3 and ω -6 fatty acids increased, some serious issues also emerged in recent years. Unwanted odors and burping of fish oil, bioaccumulation of heavy metals and organic pollutants into fish bodies, diminished fish stocks due to overfishing are some of the key issues. Meanwhile, fish oil cannot to be recommended as the sole source of EPA and DHA due to the possible accumulation of toxic chemicals, heavy metals (i.e. copper, mercury) and other synthetic pollutants (i.e. PCB and dioxin) present in water bodies due to industrial and agricultural discharges and other anthropogenic activities contributing to environmental pollution [21]. Such overarching issues related to fishing and aquaculturing suggest vegan sources of ω -3 and ω -6 fatty acids such as microalgae as sustainable alternative strategies to meet consumer needs in a much broader range [14]. As such, most biotechnology companies have started to prefer microalgae feedstock for large-scale production of EPA and DHA, as they are primary producers of ω -3 and ω -6 fatty acids [22, 23]. As a reliable source of bioactive compounds, microalgae have tremendous capability to produce substantial amounts of EPA and DHA and are regarded as important sources of LC-PUFAs.

Additional benefits of using microalgae feedstock include their faster growth rates and higher production of biomass relative to other omega-rich plants and crops [24]. Microalgal production systems do not compete arable land space for agricultural activities, and freshwater resources are not required if marine or brackish species are preferred [25]. Microalgae also offer the most promising results for conservation benefits as they can be grown with sustainable inputs such as solar light, atmospheric carbon dioxide and recycled nitrogen and phosphorous from pasteurized/pre-treated waste streams.

Microalgae also display exceptional versatility with highly adaptive capacities to complex environmental conditions [26]. However, in order to achieve economical, efficient and sustainable large-scale production for ω -3 and ω -6 fatty acids, microalgal production metrics

need to be optimized. Several cultivation parameters including nutrients (particularly nitrogen and phosphorus), light intensity, temperature, pH, and salinity have considerable impacts on biochemical characteristics of microalgae, and influence biomass growth and ω -3 and ω -6 fatty acid accumulation. Among these parameters, shifts in temperature influence cellular structural components such as membranes and organelles by changing composition of lipids and proteins. Also, temperature changes have strong impacts of enzymatic activities as a result of oscillations in reaction kinetics [27]. Light is another vital parameter for photosynthesis which significantly affects metabolic activities of microalgae [28]. High light intensity is a favorable condition for microalgal growth and production of pigments as it increases photosynthetic activity, however, it might not be favorable for all types of fatty acids. As another important parameter, salt stress could be applied as some studies show that high salt levels in the growth media promotes production of lipid-based pigments, specifically carotenoids. However, increased levels of salt in media reduces microalgal growth [29]. As a macronutrient, nitrogen plays an important role in microalgae cells since accessory pigments such as chlorophylls a and b, vital for photosynthetic efficiency and non-photochemical active pigments such as carotenoids contain nitrogen. In the absence of nitrogen, while protein rich compounds such as chlorophylls a and b are consumed to maintain cell growth and serve as nitrogen pools for vital proteins, lipids and carbohydrates are increased for long term energy storage as a response to nitrogen stress [30]. It should be noted that the effects of these parameters are mostly species/strain specific, and optimal conditions for one species/strain may not always be beneficial for others [3]. Therefore, it is important to understand the roles of these parameters play in different microalgae species' metabolic responses and overall accumulation of desired bioproducts. With respect to lipid and fatty acid metabolism, one of the common strategies is to expose microalgae to different growth conditions by varying temperature, light, salinity, and nutrient levels [27, 28, 31, 32]. This study examined the effects of four varying growth parameters (light, nitrogen, salinity, and temperature) on a terrestrial green microalgae *Chlorococcum novae-angliae* strain SAG 5.85 in an effort to characterize accumulation of ω -3 and ω -6 fatty acids. The rationale for choosing this strain was The Culture Collection of Algae at Georg-August-Universität (SAG, Göttingen, Germany), where the seed culture was obtained, has listed this strain as a potential

oleaginous species in a large scale screening study [33], yet, this is the first study comprehensively investigating fatty acid profile of terrestrial *C. novae-angliae* SAG 5.85 grown in liquid culture medium with varying light, nitrogen, salinity, and temperature. The results shed light on optimal conditions for this green microalgae species to achieve commercial scale ω -3 and ω -6 fatty acids production goals.

Materials and Methods

Microalgal strain selection and culture maintenance

Chlorococcum novae-angliae strain SAG 5.85 was originally isolated from soil samples of semi-desert ecosystem of Cahuilla Reservation (Arizona, USA) and deposited at SAG. Obtained seed cultures were transferred to modified Bold's 3N (MB3N) liquid culture medium [34]. Seed cultures were maintained in 500 mL gas wash bottles with a working volume of 350 mL until they reach mid-exponential growth phase (i.e. 4-5 days) prior to experimental conditions. Cultures were supplied with 0.22 μ m filtered air at 0.5 L/min and illuminated with 16000 \pm 200 lux light intensity for 14:10 h (light:dark) cycles. Reactor pH levels were maintained at 7.5 \pm 0.5. As air diffusers have provided sufficient homogenization, no further mixing has been provided to reactors. Seed cultures reaching mid-exponential phase were harvested at 4500 rpm for five min at 4°C by centrifugation (U-320R, Boeco, Germany) and washed twice with phosphate buffered saline. Concentration of seed culture were determined using a hemocytometer (Neubauer, Isolab, Wertheim, Germany) and were inoculated into experimental reactors at a starting concentration of 3 \times 10⁶ cells/mL.

Experimental set-up and culture growth conditions

All experimental conditions were conducted in a temperature controlled 6L flat panel photobioreactor (PBR) system (Subitec, Germany) (Fig. 1). Reactor pH values were maintained at 7.5-8.0 by pure filtered CO₂ intermittently pumped into the reactors via automated solenoid system. The reactor was supplied with 0.22 μ m filtered air at 0.5 L/min. Temperature was kept at 25°C \pm 1 for all experimental conditions except the temperature test condition (17°C \pm 1).

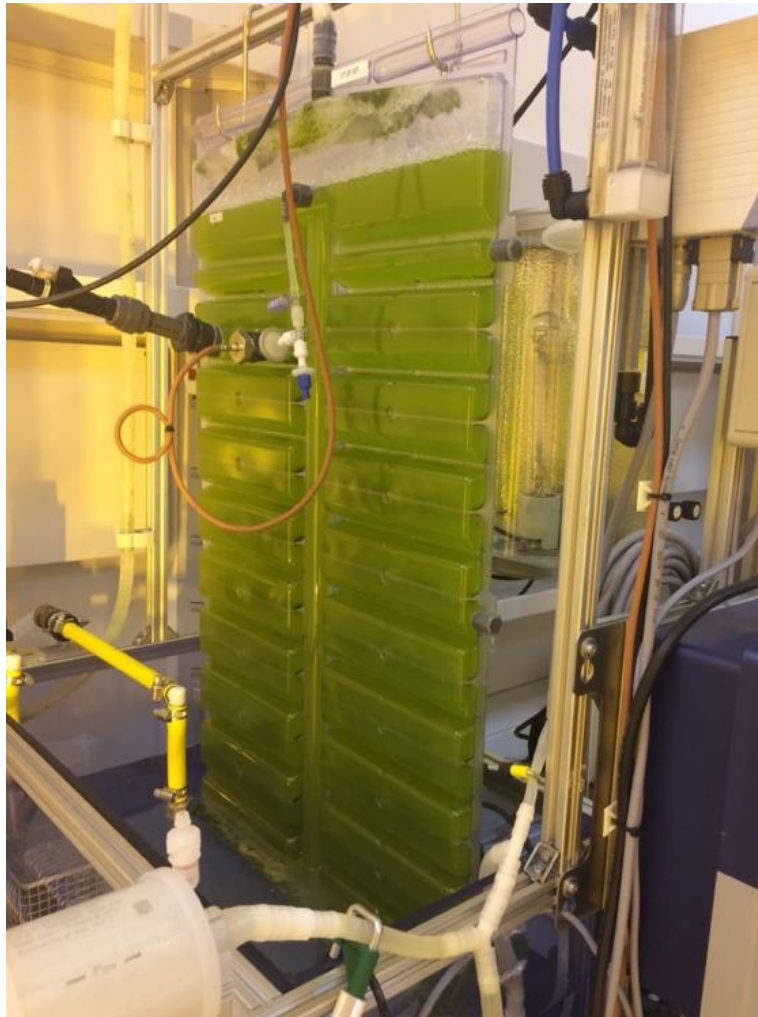


Fig 1 Six-liter capacity photobioreactor systems used for experimental cultures

For nitrogen test, concentration of NaNO_3 in MB3N medium were decreased to 1.47 mM (original recipe was 8.82 mM). Light intensity applied to PBR through a sodium lamp was kept at 11100 lux except light test condition where intensity was decreased to 5500 lux. For salinity test, NaCl concentration was increased 2X fold (0.86 mM compared to 0.43 mM in original recipe). All experimental growth conditions and the control group can be seen in Table 1.

Table 1 Culture growth parameters of *Chlorococcum novae-angliae* for each tested condition (**Bold** indicates changed parameter with respect to the control group)

Parameter	Control	Light	Nitrogen	Salinity	Temperature
Light intensity	11100 lux	5500 lux	11100 lux	11100 lux	11100 lux
Aeration rate	100 L/min	100 L/min	100 L/min	100 L/min	100 L/min
Temperature	25°C±1	25°C±1	25°C±1	25°C±1	17°C±1
NaNO ₃ conc.	8.82 mM	8.82 mM	1.47 mM	8.82 mM	8.82 mM
NaCl conc.	0.43 mM	0.43 mM	0.43 mM	0.86 mM	0.43 mM

All experiments were completed in biological triplicates. Optical density measurements were taken at 680 nm wavelength using a spectrophotometer (DR3900, Hach Lange, Manchester, UK) and cell counts were determined every two days using a hemocytometer. Growth rates were compared in exponential phase based on the equation given below.

$$\text{Growth rate} = \ln(X_1) - \ln(X_0) / N_1 - N_2$$

where

X₁: Cell number at the end of exponential phase

X₀: Cell number at the beginning of exponential phase

N₁: Number of days at the end of exponential phase

N₂: Number of days at the beginning of exponential phase.

Cultures were harvested by on Day 6 at early stationary phase by centrifugation, washed twice and the biomass pellets were lyophilized at -80°C (Hypercool, Gyrozen, Frankfurt, Germany) and stored at -80°C ultra-low temperature freezers prior to lipid and fatty acid analyses. An aliquot from each reactor was processed for dry cell weight (DCW) measurements [35].

Lipid extraction

For total lipid extraction a modified protocol was adopted from Breuer et al. and Bligh and Dyer [35, 36]. One mL of extraction solution with 50 mM Tris and 1M NaCl was prepared

at pH 7 and added to 100 mg lyophilized algal biomass. For cell wall disruption and homogenization, acid-washed and autoclaved glass beads were added to extraction vials (for each extraction 0.3 g of 0.1 mm and 0.1 g of 0.5 mm diameter glass beads were used). As internal standard, a mixture of nonadecanoic acid (C19:0) and chloroform: methanol 4:5 (v/v) was prepared at 50 mg/L concentration and processed with each extraction. Samples were homogenized using a bead beater (Minilys, Bertin Technologies, France) for 60 seconds for 8 times with 60 seconds of cooling intervals on ice. Following the homogenization, samples were transferred into 50 mL glass centrifuge tubes with Teflon insert screw caps. A mixture of 2.5 mL de-ionized water (DIW) containing 50 mM Tris and 1 M NaCl was added into glass tubes, vortexed briefly and sonicated for 10 min (Sonorex Super RK 102 H, Bandelin, Germany). Next, tubes were centrifuged at 1200Xg for 5 min. Bottom phases were transferred into new clean glass tubes by glass Pasteur pipettes. Extraction process steps were repeated with chloroform addition to fully recover lipids. Lastly, chloroform was evaporated under N₂ gas stream and the weights of lipid extract tubes were measured. The initial record (tare tube weight) was removed from final measurement providing the amount of total lipids extracted.

Transesterification reactions

Three mL of methanol with 5% sulfuric acid (v/v) were added to dried lipid samples and tightly closed. The samples were incubated in a water bath (Maxturdy-30, Daihan Scientific, Wonju, South Korea) at 70°C for 3 h and vortexed in every 30 minutes to avoid boiling. Once samples were cooled, 3 mL of DIW water and 3 mL of hexane were added, briefly vortexed and rotated at 15 rpm for 15 min (Wisemix RT-10, Witeg, Wertheim, Germany). Following, samples were centrifuged at 1200Xg for 5 min, and upper 2 mL of organic phase were collected and transferred into clean glass tubes. A washing step was done using 2 mL DIW added to each collected sample. Finally, the tubes were vortexed and centrifuged at 1200Xg for 5 min, transferred to GC vials and stored at -20°C until analytical measurements.

Analytical measurements and fatty acid methyl ester (FAME) profiling

Identification and quantitation of FAMES were conducted on a GC system (7820A, Agilent, Santa Clara, CA, USA) equipped with a flame ionization detector (FID). Five µl of FAME samples were injected in splitless mode into HP-88 column (Agilent) with dimensions of 100

m length x 0.25 mm diameter x 0.2 µm film thickness. The temperature program was as follows: initial 140°C hold for 5 min; followed by 4°C/min ramp to 240°C with a 15 min hold. Column flow was set at 1 mL/min and nitrogen was used as carrier gas set at 280°C. Run time for each sample was appx. 45 min. Identification and quantification of individual FAMES were done using a standard calibration mix (Supelco 37 FAME Mix, Sigma Aldrich, St. Louis, MO, USA) injected at 1 µl using same run method. By comparing peak area of reference standard with peak area of the target, concentrations of each FAME were calculated.

Statistical analysis

All experiments were conducted in biological triplicates and the calculated data values were reported as mean ± standard deviation. Statistical analyses were based on two-tailed paired t-test computed in MS Excel (version 16.42 Microsoft, Redmond, Washington, USA). Results were considered statistically significant only if $P \leq 0.05$.

Results

Culture growth metrics and total lipid content

Growth metrics of *C. novae-angliae* under each experimental condition were monitored and evaluated based on optical density, cell counts, growth rates and dry cell weight (DCW). As presented in Fig. 2, on harvest Day-6, all experimental conditions except salinity test resulted in lower cell counts than the control group, followed by nitrogen and light variations (Fig. 2A). Absorbance values measured under salinity test were slightly higher than the control group (Fig. 2B). Decreased temperature condition completely suspended cellular growth with no increase in optical density and cellular count (Fig. 2). Accordingly, lower temperature exposed cultures were not pursued for further characterization.

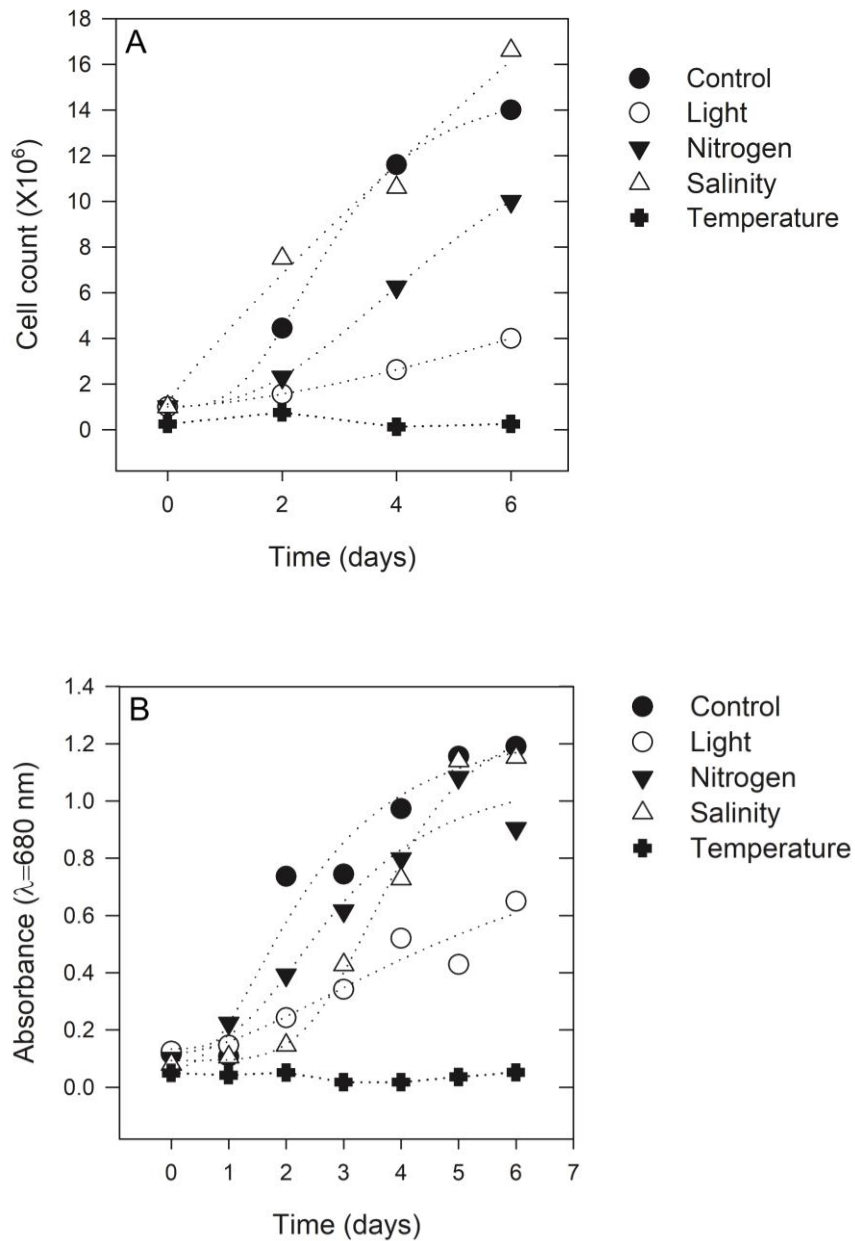


Fig 2 Cell count (A) and optical density (B) measurements of *Chlorococcum novae-angliae* for each tested condition

Growth rates were highest for increased salinity and calculated as 1.32 cells/day followed by the control group (0.61 cells/day), decreased nitrogen (0.45 cells/day), and light (0.23 cells/day) test conditions (Table 2). Average DCW measurements on harvest Day-6 indicated control group had the highest biomass concentration at 0.48 g/L, followed by nitrogen (0.37

g/L), salinity (0.28 g/L) and light test conditions (0.14 g/L) (Table 2). Despite marginally better performance in final cell counts (Fig. 2A), average total lipid content was higher in the control group (21.77%) compared to increased salinity (17.40%) followed by decreased light (16.33%) and nitrogen (13.93%) test conditions (Table 2). Changes in total lipid contents compared to control group were not statistically significant except decreased light condition.

Table 2 Culture growth metrics and total lipid accumulation of *Chlorococcum novae-angliae* under tested conditions

Test condition	Growth rate (cells/day)	Dry cell weight (DCW) (g/L)	Total lipid content (% DCW)
Control	0.61	0.48±0.34	21.77±3.48
Light	0.23	0.14±0.13	16.33±0.71*
Nitrogen	0.45	0.37±0.01	13.93±7.04
Salinity	1.32	0.28±0.06	17.40±2.90
Temperature	-	-	-

*Change is statistically significant ($P \leq 0.05$).

Saturated fatty acid profiles

Palmitic acid (C16:0) and stearic acid (C18:0) were the most dominant saturated fatty acids (SFAs) with highest concentrations among all experimental conditions including the control group (Table 3). The highest total saturated fatty acid (SFA) concentration was observed under decreased nitrogen (700.5 ng/μl) which was 71% higher than the control group where total SFA concentration was 497.81 ng/μl. Cultures exposed to low light intensity resulted in a total saturated fatty acid (SFA) concentration of 366.11 ng/μl, which was 26.4% lower than the control group. Cultures grown in increased salinity accumulated the lowest amount of SFAs at 148.23 ng/μl, 29.78% lower than the control group (Table 3). Changes in total SFA concentrations were statistically significant ($P \leq 0.05$) for all experimental conditions compared to the control group.

Table 3 Saturated fatty acid (SFA) profiles of *Chlorococcum novae-angliae* under tested conditions

Fatty Acid	Fatty Acid Concentration (ng/μl)			
	Control	Light	Nitrogen	Salinity
C6:0	1.62±2.8	2.20±3.12	0.47±0.82	1.62±1.23
C8:0	6.04±0.68	3.07±0.9	5.94±2.42	0.51±0.22
C10:0	0.64±0.55	0.33±0.3	0.2±0.02	0.75±0.22
C11:0	0.33±0.05	0.3±0.08	0.07±0.12	0.03±0.05
C12:0	0.74±0.31	0.45±0.18	1.28±0.23	0.17±0.07
C13:0	1.49±1.43	1.84±0.78	0.22±0.03	0.54±0.69
C14:0	38.83±3.46	27.03±9.37	46.45±6.58	7.92±4.64
C15:0	4.55±0.85	3.49±1.25	5.65±0.76	1.25±0.65
C16:0	344.1±20.57	270.45±81.12	492.46±61.26	87.65±45.92
C17:0	17.44±3.35	10.33±4.64	19.87±19.87	3.88±2.09
C18:0	47.28±3	28.87±10.01	78.45±8.11	21.06±10.54
C20:0	13.21±1.97	7.53±1.89	17.52±2.55	3.44±1.63
C21:0	2.72±0.3	1.16±1.11	1.84±1.05	0.75±0.95
C22:0	5.32±1.24	3.53±2.64	6.51±0.81	6.25±5.84
C23:0	9.24±8.88	4.38±3.93	10.88±15.68	3.39±2.02
C24:0	9.24±4.52	1.15±0.44	12.68±19.68	9.02±10.6
Sum of SFAs	497.81±27.40	366.11±103.92	700.50±96.3	148.23±77.3

Under decreased nitrogen test condition, palmitic acid and stearic acid levels, which are essential precursors SFAs for the biosynthesis of polyunsaturated fatty acid (PUFA) were increased by 69.88% and 60.26% compared to control group respectively, whereas decreased by 21.41% and 38.94% under decreased light and 74.53% and 55.46%, increased salinity test conditions compared to control group respectively (Table 3).

Monounsaturated fatty acid profiles

Similar to total SFA content, highest total average monounsaturated fatty acid (MUFA) concentration (747.79 ng/μl) were obtained under decreased nitrogen condition, 54% higher than the control group (343.92 ng/μl) (Table 4). Total average MUFA content was measured as 393.61 ng/μl under decreased light condition, slightly higher than the control group

(12.62%), whereas increased salinity condition resulted a major decrease in total MUFA content and measured as 31.46 ng/μl (or 98.86% lower compared to the control group) (Table 4). Changes in total MUFA contents compared to control group were not statistically significant except increased salinity test condition.

Table 4 Monounsaturated fatty acid (MUFA) profiles of *Chlorococcum novae-angliae* under tested conditions

Fatty Acid	Fatty Acid Concentration (ng/μl)			
	Control	Light	Nitrogen	Salinity
C14:1	28.53±6.68	18.29±13.39	10.42±2.12*	0.97±0.55*
C15:1	0.38±0.28	0.29±0.05	0.46±0.32	4.17±3.69
C16:1	11.04±1.32	8.32±2.81	27.2±5.24*	3.08±1.74*
C17:1	1.87±0.74	1.42±0.81	2.52±0.32*	0.73±0.34
C18:1n9t	32.73±55.57	11.71±19.28	0.67±0.25	12.46±13.38
C18:1n9c	32.70±5.19	26.60±7.2	136.17±18.89*	4.24±2.14*
C20:1	235.01±403.15	325.84±323.94	566.10±489.5	1.25±1.41*
C24:1	1.67±1.89	1.15±0.71	4.25±1.96	4.56±2.01
Sum of MUFAs	343.92±377.88	393.61±327.42	747.79±512.61	31.46±13.48*

*Change is statistically significant ($P \leq 0.05$).

Notably, oleic acid (C18:1n9c), an essential ω-9 fatty acid, content was increased more than four fold under decreased nitrogen compared to the control (136,17 ng/μl). Decreased light conditions caused an accumulation of 26.6 ng/μl of oleic acid whereas increased salinity resulted in only 4.24 ng/μl of oleic acid (Table 4).

Polyunsaturated fatty acid profiles

Overall average PUFA accumulation was the highest in the control group (803.55 ng/μl) followed by a slight decrease under decreased nitrogen test condition (741.1 ng/μl) (Table 5). Decreased light condition resulted in average total PUFA concentration (522.59 ng/μl), while the lowest PUFA accumulation was observed in increased salinity conditions (263.88 ng/μl) (Table 5). Changes in total PUFA contents compared to control group were not statistically significant except increased salinity condition.

Table 5 Polyunsaturated fatty acid (PUFA) profiles of *Chlorococcum novae-angliae* under tested conditions

Fatty Acid	Fatty Acid Concentration (ng/μl)			
	Control	Light	Nitrogen	Salinity
C18:2n6t	85.08±7.97	53.6±17.74	75.19±10.95	38.54±14.48
C18:2n6c (LA)	222.50±63.13	152.54±70.18	311.25±48.58*	38.33±18.28*
C18:3n6 (GLA)	98.23±20.97	74.2±31.73	137.15±21.41*	23.81±11.84*
C18:3n3 (ALA)	381.09±334.90	191.08±329.27	164.92±285.01	134.18±60.67
C20:2	1.09±0.38	0.61±0.5	0.72±0.24	3.05±2.56
C20:3n6 (DGLA)	1.22±1.07	0.85±0.04	0.73±0.40	0.21±0.06
C20:3n3/C22:1n9	4.46±1.41	7.57±7.24	3.35±0.36	1.91±1.75
C20:4n6 (AA)	1.24±1.14	13.60±9.15	13.95±11.81	6.32±9.30
C22:2	24.97±22.20	3.41±4.88	0.32±0.05	2.35±1.98
C20:5n3 (EPA)	5.58±7.14	17.62±24.15	32.76±23.77	15±23.63
C22:6n3 (DHA)	2.87±2.90	3.12±4.29	0.76±0.35	0.21±0.25
Sum of PUFAs	803.35±272.857	522.59±402.67	741.10±222.7	263.88±120.51

*Change is statistically significant ($P \leq 0.05$).

Omega-3 fatty acid profiles

Concentration of essential fatty acid ALA (C18:3n3) was decreased under all tested conditions compared to the control group (381.09 ng/μl) (Table 5). Alpha-linoleic acid concentration under decreased light intensity was 191.08 ng/μl. Under decreased nitrogen condition, the cells also lowered ALA concentration to 164.92 ng/μl. The lowest ALA concentration was seen under increased salinity condition at 134.18 ng/μl. Concentration of EPA (C20:5n3) was the highest under decreased nitrogen condition and accumulated at 32.76 ng/μl, more than five fold higher than the control group. Decreased light and increased salinity test conditions resulted in similar EPA concentrations at 17.62 and 15 ng/μl respectively, while the control group had the lowest EPA content at 5.58 ng/μl (Table 5). The other major ω-3 fatty acid, DHA (C22:6n3), was accumulated in minute amounts in all growth conditions, where decreased light condition had 3.12 ng/μl, 8.7% higher compared to the control group. Decreased nitrogen and increased salinity test conditions caused DHA

accumulation to 0.76 and 0.21 ng/ μ l, respectively (Table 5). As chromatographic separation of eicosatrienoic acid (ETE) (20:3n3) was not possible from erucic acid (C22:1n9), their accumulation is reported as lump sum, with the highest accumulation under decreased light (7.57 ng/ μ l), followed by control group (4.46 ng/ μ l), decreased nitrogen (3.35 ng/ μ l), and the lowest under increased salinity (1.91 ng/ μ l) test conditions (Table 5).

Omega-6 fatty acid profiles

Among all tested conditions, concentration of LA (C18:2n6c), an essential ω -6 fatty acid, was positively affected by decreased nitrogen and significantly increased by 39.89% compared to the control group with an overall accumulation of 311.25 ng/ μ l (Table 5). Decreased light condition also caused 45.86% decrease in LA content compared to the control and calculated as 152.54 ng/ μ l. Increased salinity resulted in 38.33ng/ μ l LA accumulation, significantly decreased by 82.77% compared to the control group (Table 5). Cells grown in decreased nitrogen conditions showed significant increase in concentration of GLA (C18:3n6) by 39.62% compared to control group and reported at 137.15ng/ μ l. However, both decreased light and increased salinity test conditions caused lower GLA content compared to the control group, 74.2 ng/ μ l (24.46% decrease) and 23.81 ng/ μ l (75% decrease) respectively (Table 5).

Discussion

Average total lipid contents from *Chlorococcum novae-angliae* obtained in all experimental conditions were between 14-22% in this study. The lipid contents of closest sister species of *C. novae-angliae*, i.e. *Chlorococcum sp.*, were found to be 6-28% in previous studies [37, 38], comparable to our findings. The cells under decreased light test condition (5500 lux compared to 11000 of the control group) caused lower total lipid content and growth rate compared to the control group. Ota et al., reported that the highest growth rate of *Chlorococcum littorale* was observed under 100 μ mol $m^{-2}s^{-1}$ (~7400 lux) [39]. In another study by Rehman and Anal, optimal light intensity was determined as 4340 lux for the growth of *Chlorococcum sp.* TISTR 8583 [40]. In alignment with these studies, lowered light intensity negatively affected cellular growth and suppressed overall lipid accumulation of *C. novae-angliae* in this study. The cells in control reactor grown under 11000 lux provided

highest dry cell weight, total lipid, and reactor productivity which could be interpreted as optimal for the cultivation of *C. novae-angliae* SAG5.85. With respect to FAME profiles, total saturated fatty acid concentrations were decreased under lowered light intensity although Seyfabadi and colleagues found that increased light conditions improve levels of SFAs in *Chlorella vulgaris* [41]. Similarly, all MUFA concentrations were decreased under low light conditions compared to the control except eicosenoic acid (C20:1) which was the only fatty acid increased. This might be due to difficulties in chromatographic separation of C20:1 from heneicosanoic acid (C21:0) as evident from higher deviation among samples. Sukenik and coworkers reported that decreasing light intensity during the cultivation of *Nannochloropsis* sp. increased total PUFA content [42], which was not observed for *C. novae-angliae* as the cells under low light intensity decreased total PUFA content compared to the control. The only deviation was in DHA, EPA, and AA contents that were increased under low light intensity. Although Lang and colleagues stated that *C. novae-angliae* had the second highest DHA levels (18.9% of total fatty acids) among SAG strains [33], that was not confirmed by this study.

Second tested growth parameter was decreased nitrogen concentration as one of the most essential nutrients that limits the growth of microalgae while improving the accumulation of lipids. Numerous literature studies suggest that nitrogen limitation increases the accumulation of lipids in microalgae [43-45]. For instance, enhanced lipid accumulation, i.e. 29.59% higher, in *Chlorococcum* sp. TISTR 8583 cells was observed under nitrogen limited conditions, however, DCW was reduced during the cultivation [40]. Li and colleagues examined the effects of nitrogen concentration on lipid accumulation in *Ettlia oleoabundans* (aka *Neochloris oleoabundans*) cells and reported increased lipid accumulation with biomass reduction [30]. In another study, Bona and coworkers reported that nitrogen deplete conditions (2.9×10^{-4} M), enhanced lipid accumulation in *E. oleoabundans* cells [46]. Kiran and colleagues also reported that higher lipid accumulation was observed in *Chlorella* sp. grown under 5 mM NaNO_3 (corresponding to one third of nitrogen of original medium) [47]. In this study, both cellular growth and total lipid content of *C. novae-angliae* was lowered under decreased nitrogen test condition compared to the control group. With respect to growth, nitrogen is a critical nutrient as it takes part in the structures of algal chlorophylls,

and amino acids as the key building blocks of proteins. Therefore, decreased nitrogen concentrations lead to inhibited growth rates in *C. novae-angliae*. Meanwhile, contrary to majority of green microalgae species' response, reduction in the concentration of nitrogen also reduced overall accumulation of lipids in this study. However, despite decreased total lipid content, free fatty acid content was the highest under decreased nitrogen. Notably, total SFAs were increased, which was also observed in *E. oleoabundans* [48] and *Nannochloropsis* CCAP 211/78 [49] grown in limited nitrogen. Under decreased nitrogen exposure, total MUFAs of *C. novae-angliae* were also increased compared to the control group. Despite lower than the control group, second highest level of total PUFAs was obtained under decreased nitrogen. In particular, DHA and ALA were decreased while EPA was increased. Contradictive to our findings, Bona and colleagues observed that ALA contents in *E. oleoabundans* cells were increased on the under nitrogen stress [46]. The highest increases in EPA levels were also observed under nitrogen stress in *Nannochloropsis* 211/78 (CCAP) [49]. Meanwhile, Breuer and colleagues reported that LA concentrations were decreased under nitrogen limited conditions in *C. vulgaris*, *C. zofingiensis*, *Dunaliella tertiolecta*, *Isochrysis galbana*, *Nannochloropsis* sp., and *E. oleoabundans* [35].

The third tested growth parameter *C. novae-angliae* cells were exposed was increased salinity, known to impose considerable effect on growth and biochemical composition of microalgae. As osmotic regulation is an important parameter for the survival of microalgal cells, optimal salinity ranges exist for different species [50-52]. In most species, salinity increase usually promotes overall cellular growth up to a certain threshold where salt concentrations start to negatively affect overall homeostasis [53, 54]. In *C. novae-angliae*, doubled salinity levels compared to control group was within optimal levels and had positive impacts on the overall growth. There are several studies showing increased salinity could trigger enhanced lipid production in microalgae [27, 55, 56]. Despite slight decrease compared to the control group, second highest average total lipid accumulation was observed under increased salinity conditions. Rismani and Shariati reported that 200 mM NaCl exposure caused 82% increase in total lipid productivity of *C. vulgaris* [57]. Takagi and Yoshida have shown that *D. tertiolecta* cells increased their lipid accumulation when NaCl in culture media was increased from 0.5 to 1 M [58]. Despite being a freshwater microalgae

species, salt stress adapted *Botryococcus braunii* showed increased growth rate, and lipid content [59], both in compatible with this study. Similarly, Ben-Amotz and colleagues achieved increased lipid content in *B. braunii* exposed to 0.5 M NaCl [60].

Despite relatively higher total lipid content, total SFA accumulation of *C. novae-angliae* was the lowest when exposed to increased salinity compared to the other test conditions and the control group. This was conflicting with total SFAs production enhanced in *Dunaliella* sp. cells when NaCl concentration was increased from 0.4 to 4 M [61]. As *Dunaliella* sp. are robust marine microalgae, it is possible that general adaptive capacity of terrestrial *C. novae-angliae* may not be as strong as *Dunaliella* sp. Total MUFAs were also decreased in increased salinity compared to the control and other test conditions. In literature, Azachi and colleagues showed increased salt stress induced oleic acid production in *B. braunii* and *I. galbana* [60], which was also not the case with *C. novae-angliae*. Similar to other fatty acid fractions, lowest levels of PUFAs content were also observed under increased salinity exposure. Meanwhile, Xu and Beardall observed that NaCl levels led to reductions in total PUFAs content in *Dunaliella* sp., indicating SFA, MUFA and PUFA trends might differ under the same salinity stress exposure [61]. Among PUFA of particular interest, DHA accumulation in *C. novae-angliae* were negatively impacted by increased salinity. Some studies also reported that DHA was below detectable levels in different microalgae species exposed to increased salinity [57, 60]. Moreover, LA and ALA concentration were also the lowest when exposed to increased salinity. This was in agreement with the study by Rao and colleagues where *B. braunii* 572 cells showed decreased LA concentration under increased salinity [59]. In another study, it was also mentioned that increased NaCl concentration might have resulted in decreased fatty acid unsaturation rates [56] as confirmed by decreased concentrations of GLA and DGLA in this study. Although slight increases in average EPA and AA accumulation were observed in *C. novae-angliae* exposed to increased salinity, these results were not statistically significant compared to the control group.

Last tested growth parameter was temperature which was lowered from 25 to 17°C. Temperature is one of the most important parameters that affect membrane fluidity, photosynthetic respiratory actions, and fatty acid composition of microalgae species [27, 62]. Increasing fatty acid unsaturation rate is very common behavior among microalgae in order

to adapt to cold environments as double bonds present in unsaturated fatty acids provide membrane fluidity compared to SFAs. Therefore increases in unsaturation rates are mostly observed at exposure to low temperatures [62]. In a study by Thompson, it was shown that shifting temperature from 30 to 12°C during the cultivation of *D. tertiolecta* has led to increase in unsaturated fatty acid levels by 20% [63]. Sushchik and coworkers reported that increasing temperature from 25 to 30°C during the cultivation of *C. vulgaris* and *B. braunii* decreased fatty acid unsaturation rate [64]. In another study by Thompson and colleagues, fatty acid profiles of eight species were investigated by shifting the cultivation temperature from 25 to 10°C [65]. Such decrease in temperature enhanced PUFAs accumulation in *Chaetoceros calcitrans*, *C. gracilis*, *C. simplex*, *D. tertiolecta*, *I. galbana*, *Pavlova lutheri*, *Phaeodactylum tricornutum* and *Thalassiosira pseudonana* [65]. Aussant and coworkers examined optimal temperature for microalgal growth and lipid production where they suggested 14-20°C for optimal EPA production in *D. salina* [66]. However, in this study the growth of *C. novae-angliae* at 17°C was totally inhibited starting on the very first day of cultivation. For most microalgal species, optimal cultivation temperature usually ranges between 25±5°C [67]. Nevertheless, *C. novae-angliae*, was tested at lower temperature ends to evaluate possible impacts on ω-3 and ω-6 fatty acids. Unfortunately, optical density and cell counts were dramatically decreased in short time while the culture color in PBRs turned into yellowish indicating damaged photosynthetic activity. On harvest Day 6, it was impossible to obtain sufficient amounts of biomass for total lipid and FAME profiling, therefore, temperature stress has been excluded from the study as growth of *C. novae-angliae* cells were not acclimated to 17°C, concluding this strain is not tolerant to temperatures lower than ambient.

Conclusions

Polyunsaturated fatty acids cannot be synthesized in humans and other mammals, yet they have numerous positive health impacts on metabolic processes. Therefore, PUFAs should be taken with daily diets at required concentrations and proper ratios. Main motivation for this study was to examine the effects of varying growth conditions on the accumulation of ω-3 and ω-6 fatty acids in *Chlorococcum novae-angliae* SAG 5.85. Although original culture

collection indicated this strain as a potential PUFA producer, this study was the first comprehensive evaluation of varying growth conditions with respect to cell growth, total lipid and FAME profile of *C. novae-angliae*. As most common parameters affecting cellular growth and lipid content in green microalgae, light, nitrogen, salinity, and temperature growth conditions were tested. *C. novae-angliae* has been cultivated in triplicate batch PBRs in order to determine optimal conditions for the control and compared stress conditions. One of the most important outcomes was *C. novae-angliae* ω -3 and ω -6 fatty acid was significantly improved under decreased nitrogen conditions, despite lower total lipid content. Different levels and type of nitrogen sources could be applied in order to achieve large scale production goals. Decreased light and increased salinity test conditions did not improve ω -3 and ω -6 fatty acid content in *C. novae-angliae* compared to the control group, concluding that baseline cultivation conditions have better performance with respect to PUFA accumulation in this strain. Lastly, it was also found that lower than ambient temperatures completely halt the growth of *C. novae-angliae* suggesting temperature control in reactor systems are very critical for this particular strain.

Acknowledgements

This work was financially supported by The Scientific and Technological Research Council of Turkey (TÜBİTAK) 1512 Program (Award No: 2180589). Infrastructure used in this study was supported through Turkish Ministry of Industry and Technology & Directorate General for EU and Foreign Affairs Department of EU Financial Programmes, Competitiveness and Innovation Sector Operational Programme (Award No: EuropeAid/140111/IH/SUP/TR). E.C. was supported by Istanbul Development Agency (Award No: TR10/15/YNK/0062), B.Z.H. was supported by Royal Society Newton Fellowship (Award No: NA140481). We also would like to acknowledge Asst. Prof. Dr. Mehmet Firat Ilker (Department of Chemistry, Bogazici University) for providing access to GC instrument.

Abbreviations

ALA: alpha-linolenic acid; AA: arachidonic acid; DHA: docosahexaenoic acid; DH-GLA: dihomogamma-linolenic acid; DPA: docosapentaenoic acid; EPA: eicosapentaenoic acid; FAME: fatty acid methyl ester; GLA: gamma-linoleic acid; GC-FID: gas chromatography-flame ionization detector; LA:linoleic acid; MUFA: monounsaturated fatty acids; PBR: photobioreactor; PUFA: polyunsaturated fatty acids, SFA: saturated fatty acid

References

1. Abedi, E. and M.A. Sahari, Long-chain polyunsaturated fatty acid sources and evaluation of their nutritional and functional properties. *Food science & nutrition*, 2014. 2(5): p. 443-463.
2. Wiktorowska-Owczarek, A., M. Berezinska, and J.Z. Nowak, PUFAs: structures, metabolism and functions. *Adv Clin Exp Med*, 2015. 24(6): p. 931-941.
3. Robertson, R., et al., Algae-derived polyunsaturated fatty acids: implications for human health. 2013, Nova Sciences Publishers, Inc.: Hauppauge, NY, USA. p. 45-99.
4. Zhou, W., Potential applications of microalgae in wastewater treatments. *Recent advances in microalgal biotechnology*, 2014: p. 1-9.

5. Nichols, P.D., et al., Recent advances in omega-3: Health benefits, Sources, Products and bioavailability. *Nutrients*, 2014. 6(9): p. 3727-3733.
6. Dyall, S.C., Long-chain omega-3 fatty acids and the brain: a review of the independent and shared effects of EPA, DPA and DHA. *Frontiers in aging neuroscience*, 2015. 7: p. 52.
7. Shahidi, F. and P. Ambigaipalan, Omega-3 polyunsaturated fatty acids and their health benefits. *Annual review of food science and technology*, 2018. 9: p. 345-381.
8. Russo, G.L., Dietary n-6 and n-3 polyunsaturated fatty acids: from biochemistry to clinical implications in cardiovascular prevention. *Biochemical pharmacology*, 2009. 77(6): p. 937-946.
9. Araujo, P., et al., The effect of omega-3 and omega-6 polyunsaturated fatty acids on the production of Cyclooxygenase and Lipoxygenase metabolites by human umbilical vein endothelial cells. *Nutrients*, 2019. 11(5): p. 966.
10. Swanson, D., R. Block, and S.A. Mousa, Omega-3 fatty acids EPA and DHA: health benefits throughout life. *Advances in nutrition*, 2012. 3(1): p. 1-7.
11. Shindou, H., et al., Docosahexaenoic acid preserves visual function by maintaining correct disc morphology in retinal photoreceptor cells. *Journal of Biological Chemistry*, 2017. 292(29): p. 12054-12064.
12. Calder, P.C., Omega-3 polyunsaturated fatty acids and inflammatory processes: nutrition or pharmacology? *British journal of clinical pharmacology*, 2013. 75(3): p. 645-662.
13. Winwood, R.J., Recent developments in the commercial production of DHA and EPA rich oils from micro-algae. *Ocl*, 2013. 20(6): p. D604.
14. Adarme-Vega, T.C., et al., Microalgal biofactories: a promising approach towards sustainable omega-3 fatty acid production. *Microbial cell factories*, 2012. 11(1): p. 1-10.
15. Fan, Y.-Y. and R.S. Chapkin, Importance of dietary γ -linolenic acid in human health and nutrition. *The Journal of nutrition*, 1998. 128(9): p. 1411-1414.
16. Simon, D., et al., Gamma-linolenic acid levels correlate with clinical efficacy of evening primrose oil in patients with atopic dermatitis. *Advances in therapy*, 2014. 31(2): p. 180-188.
17. Das, U.N., Essential fatty acids and their metabolites could function as endogenous HMG-CoA reductase and ACE enzyme inhibitors, anti-arrhythmic, anti-hypertensive, anti-atherosclerotic, anti-inflammatory, cytoprotective, and cardioprotective molecules. *Lipids in health and disease*, 2008. 7(1): p. 1-18.
18. Van Hoorn, R., R. Kapoor, and J. Kamphuis, A short review on sources and health benefits of GLA, The GOOD omega-6. *Oléagineux, Corps gras, Lipides*, 2008. 15(4): p. 262-264.
19. Simopoulos, A.P., An increase in the omega-6/omega-3 fatty acid ratio increases the risk for obesity. *Nutrients*, 2016. 8(3): p. 128.
20. Siahbalei, R., G. Kavooosi, and M. Noroozi, Manipulation of *Chlorella vulgaris* polyunsaturated ω -3 fatty acid profile by supplementation with vegetable amino acids and fatty acids. *Phycological Research*, 2021. 69(2): p. 116-123.
21. Akan, J.C., et al., Bioaccumulation of some heavy metals in fish samples from River Benue in Vinikilang, Adamawa State, Nigeria. *American Journal of Analytical Chemistry*, 2012. 3(11): p. 727-736.
22. Nichols, P.D., J. Petrie, and S. Singh, Long-chain omega-3 oils—an update on sustainable sources. *Nutrients*, 2010. 2(6): p. 572-585.
23. Xie, D., E.N. Jackson, and Q. Zhu, Sustainable source of omega-3 eicosapentaenoic acid from metabolically engineered *Yarrowia lipolytica*: from fundamental research to commercial production. *Applied microbiology and biotechnology*, 2015. 99(4): p. 1599-1610.

24. Bucy, H.B., M.E. Baumgardner, and A.J. Marchese, Chemical and physical properties of algal methyl ester biodiesel containing varying levels of methyl eicosapentaenoate and methyl docosahexaenoate. *Algal Research*, 2012. 1(1): p. 57-69.
25. Hu, Q., et al., Microalgal triacylglycerols as feedstocks for biofuel production: perspectives and advances. *The plant journal*, 2008. 54(4): p. 621-639.
26. Mohan, S.V., Devi, M.P, Subhash, G.V., and R. Chandra, Algae Oils as Fuels, in *Biofuels from Algae*, A. Pandey, D. Lee, Y. Chisti, Carlos R. Soccol, Editors. 2014, Elsevier: Amsterdam. p. 155-187.
27. Juneja, A., R.M. Ceballos, and G.S. Murthy, Effects of environmental factors and nutrient availability on the biochemical composition of algae for biofuels production: a review. *Energies*, 2013. 6(9): p. 4607-4638.
28. Singh, S. and P. Singh, Effect of temperature and light on the growth of algae species: a review. *Renewable and sustainable energy reviews*, 2015. 50: p. 431-444.
29. Mishra, A. and B. Jha, Isolation and characterization of extracellular polymeric substances from microalgae *Dunaliella salina* under salt stress. *Bioresource technology*, 2009. 100(13): p. 3382-3386.
30. Li, Y., et al., Effects of nitrogen sources on cell growth and lipid accumulation of green alga *Neochloris oleoabundans*. *Applied microbiology and biotechnology*, 2008. 81(4): p. 629-636.
31. Ren, X., et al., Production, Processing, and Protection of Microalgal n-3 PUFA-Rich Oil. *Foods*, 2022. 11(9): p. 1215.
32. Lu, Q., et al., A state-of-the-art review on the synthetic mechanisms, production technologies, and practical application of polyunsaturated fatty acids from microalgae. *Algal Research*, 2021. 55: p. 102281.
33. Lang, I., et al., Fatty acid profiles and their distribution patterns in microalgae: a comprehensive analysis of more than 2000 strains from the SAG culture collection. *BMC plant biology*, 2011. 11(1): p. 1-16.
34. Ghafari, M., B. Rashidi, and B.Z. Haznedaroglu, Effects of macro and micronutrients on neutral lipid accumulation in oleaginous microalgae. *Biofuels*, 2018. 9(2): p. 147-156.
35. Breuer, G., et al., The impact of nitrogen starvation on the dynamics of triacylglycerol accumulation in nine microalgae strains. *Bioresource Technology*, 2012. 124: p. 217-226.
36. Bligh, E.G. and W.J. Dyer, A rapid method of total lipid extraction and purification. *Canadian journal of biochemistry and physiology*, 1959. 37(8): p. 911-917.
37. Hasan, C.M.M., et al., Triacylglycerol Profile of a Microalga *Chlorococcum* Sp. as a Potential Biofuel Feedstock. *Journal of Bangladesh Academy of Sciences*, 2016. 40(2): p. 147-153.
38. Mahapatra, D.M. and T. Ramachandra, Algal biofuel: bountiful lipid from *Chlorococcum* sp. proliferating in municipal wastewater. *Current Science*, 2013: p. 47-55.
39. Ota, M., et al., Effects of light intensity and temperature on photoautotrophic growth of a green microalga, *Chlorococcum littorale*. *Biotechnology Reports*, 2015. 7: p. 24-29.
40. Rehman, Z.U. and A.K. Anal, Enhanced lipid and starch productivity of microalga (*Chlorococcum* sp. TISTR 8583) with nitrogen limitation following effective pretreatments for biofuel production. *Biotechnology Reports*, 2019. 21: p. e00298.
41. Seyfjadi, J., Z. Ramezanpour, and Z.A. Khoeyi, Protein, fatty acid, and pigment content of *Chlorella vulgaris* under different light regimes. *Journal of Applied Phycology*, 2011. 23(4): p. 721-726.
42. Sukenik, A., Y. Carmeli, and T. Berner, Regulation of fatty acid composition by irradiance level in the eustigmatophyte *Nannochloropsis* sp. 1. *Journal of Phycology*, 1989. 25(4): p. 686-692.
43. Chen, M., et al., Effect of nutrients on growth and lipid accumulation in the green algae *Dunaliella tertiolecta*. *Bioresource technology*, 2011. 102(2): p. 1649-1655.
44. Dean, A.P., et al., Using FTIR spectroscopy for rapid determination of lipid accumulation in response to nitrogen limitation in freshwater microalgae. *Bioresource technology*, 2010. 101(12): p. 4499-4507.

45. Illman, A., A. Scragg, and S. Shales, Increase in *Chlorella* strains calorific values when grown in low nitrogen medium. *Enzyme and microbial technology*, 2000. 27(8): p. 631-635.
46. Bona, F., et al., Semicontinuous nitrogen limitation as convenient operation strategy to maximize fatty acid production in *Neochloris oleoabundans*. *Algal Research*, 2014. 5: p. 1-6.
47. Kiran, B., et al., Influence of varying nitrogen levels on lipid accumulation in *Chlorella* sp. *International journal of environmental science and technology*, 2016. 13(7): p. 1823-1832.
48. Tornabene, T., et al., Lipid composition of the nitrogen starved green alga *Neochloris oleoabundans*. *Enzyme and Microbial Technology*, 1983. 5(6): p. 435-440.
49. Hulatt, C.J., et al., Production of fatty acids and protein by *Nannochloropsis* in flat-plate photobioreactors. *PloS one*, 2017. 12(1): p. e0170440.
50. Rai, M.P., T. Gautom, and N. Sharma, Effect of salinity, pH, light intensity on growth and lipid production of microalgae for bioenergy application. *OnLine Journal of Biological Sciences*, 2015. 15(4): p. 260.
51. Chen, H. and J.G. Jiang, Osmotic responses of *Dunaliella* to the changes of salinity. *Journal of cellular physiology*, 2009. 219(2): p. 251-258.
52. Søggaard, D.H., et al., Growth limitation of three Arctic sea ice algal species: effects of salinity, pH, and inorganic carbon availability. *Polar biology*, 2011. 34(8): p. 1157-1165.
53. Strizh, I., L. Popova, and Y.V. Balnokin, Physiological aspects of adaptation of the marine microalga *Tetraselmis (Platymonas) viridis* to various medium salinity. *Russian Journal of Plant Physiology*, 2004. 51(2): p. 176-182.
54. Erdmann, N. and M. Hagemann, Salt acclimation of algae and cyanobacteria: a comparison, in *Algal adaptation to environmental stresses*. 2001, Springer. p. 323-361.
55. Fabregas, J., et al., Growth of the marine microalga *Tetraselmis suecica* in batch cultures with different salinities and nutrient concentrations. *Aquaculture*, 1984. 42(3-4): p. 207-215.
56. Zhila, N.O., G.S. Kalacheva, and T.G. Volova, Effect of salinity on the biochemical composition of the alga *Botryococcus braunii* Kütz IPPAS H-252. *Journal of Applied Phycology*, 2011. 23(1): p. 47-52.
57. Rismani, S. and M. Shariati, Changes of the total lipid and omega-3 fatty acid contents in two microalgae *Dunaliella salina* and *Chlorella vulgaris* under salt stress. *Brazilian Archives of Biology and Technology*, 2017. 60: e17160555.
58. Takagi, M. and T. Yoshida, Effect of salt concentration on intracellular accumulation of lipids and triacylglyceride in marine microalgae *Dunaliella* cells. *Journal of bioscience and bioengineering*, 2006. 101(3): p. 223-226.
59. Rao, A.R., et al., Effect of salinity on growth of green alga *Botryococcus braunii* and its constituents. *Bioresource technology*, 2007. 98(3): p. 560-564.
60. Ben-Amotz, A., T.G. Tornabene, and W.H. Thomas, Chemical profile of selected species of microalgae with emphasis on lipids 1. *Journal of Phycology*, 1985. 21(1): p. 72-81.
61. Xu, X.-Q. and J. Beardall, Effect of salinity on fatty acid composition of a green microalga from an antarctic hypersaline lake. *Phytochemistry*, 1997. 45(4): p. 655-658.
62. Sharma, K.K., H. Schuhmann, and P.M. Schenk, High lipid induction in microalgae for biodiesel production. *Energies*, 2012. 5(5): p. 1532-1553.
63. Thompson Jr, G.A., Lipids and membrane function in green algae. *Biochimica et Biophysica Acta (BBA)-Lipids and Lipid Metabolism*, 1996. 1302(1): p. 17-45.
64. Sushchik, N., et al., A temperature dependence of the intra-and extracellular fatty-acid composition of green algae and cyanobacterium. *Russian journal of plant physiology*, 2003. 50(3): p. 374-380.
65. Thompson, P.A., et al., Effects of variation in temperature. II. On the fatty acid composition of eight species of marine phytoplankton 1. *Journal of Phycology*, 1992. 28(4): p. 488-497.

66. Aussant, J., F. Guihéneuf, and D.B. Stengel, Impact of temperature on fatty acid composition and nutritional value in eight species of microalgae. *Applied microbiology and biotechnology*, 2018. 102(12): p. 5279-5297.
67. Li, W.K., Temperature adaptation in phytoplankton: cellular and photosynthetic characteristics. *Primary productivity in the sea*, 1980: p. 259-279.

Numanoğlu Çevik, Y. and M. A. Kanat, Discrimination of two species (*Androctonus crassicauda* and *Leiurus abduhbayrami*; Buthidae Scorpions) by MALDI-TOF MS-based PCA. International Journal of Life Sciences and Biotechnology, 2022. 5(3): p. 370-385. DOI: 10.38001/ijlsb. 1077343

Discrimination of two species (*Androctonus crassicauda* and *Leiurus abduhbayrami*; Buthidae Scorpions) by MALDI-TOF MS-based PCA

Yasemin Numanoğlu Çevik^{1*} , Mehmet Ali Kanat¹ 

ABSTRACT

The venoms of the scorpions *Androctonus crassicauda* and *Leiurus abduhbayrami*, scorpion species each of the two members of the Buthidae family, were analyzed by MALDI-TOF MS in a mass range between 1 and 50 kDa. For this, all of the scorpion venoms (n=11) were prepared to equal 2mg/mL concentration. After centrifuging the venoms at 15.000 rpm for 15 minutes at +4 °C, the supernatants (n=11) were mixed with a matrix solution (α -CHCA) in Eppendorf tubes separately. The prepared scorpion venom-matrix (SVMx) samples vortexed. For the biomass analysis, a 1 μ L SVMx sample was spotted onto MALDI 96 MSP was placed in the Microflex MALDI-TOF MS. The system was operated in linear positive ion mode at a 1.000-50.000 Dalton (Da) mass range. A 60 Hz nitrogen laser was employed at 337 nm as the ion source. Interspecies differentiation was evaluated over peptide and protein molecules in this mass range. The similarities and differences between two different scorpion species were revealed with the principal component analysis study, which was conducted with spectral patterns including peptide and protein profiles. The similarity rate of the LAB-123 and the LAB-460 scorpion venoms of the same species was found as 66% while the similarity rates of venoms of the ACR species to the LAB species ranged from zero to 37%. It was demonstrated that scorpion venoms belonging to two different species from the Buthidae family can be differentiated with the help of dendrogram and gel profile, CCI color matrix, 3D or 2D-scattering profile, spectral mass loading data formed by peptide and protein spectral patterns of eleven scorpion venoms. It is anticipated that this approach, which was used for the first time with the application of MALDI-TOF MS-based PCA analysis for the differentiation of scorpion venoms, will be useful in differentiating venoms with different spectral patterns.

ARTICLE HISTORY

Received

22 February 2022

Accepted

20 May 2022

KEYWORDS

Androctonus crassicauda,
Leiurus abduhbayrami,
Scorpion,
Buthidae,
MALDI-TOF MS-
PCA analyse

Introduction

Scorpions are creatures that live widely all over the world, except for the polar regions and some islands. [1] It belongs to a group of arthropods whose phenotype has remained largely unchanged over the past 400 million years. The evolutionary success of these predators is largely due to their venom, which they use to deter predators and immobilize their prey [2].

¹ Microbiology and Reference Laboratory and Biological Products Department, General Directorate of Public Health, Minister of Health, 06430, Ankara, Turkey

* Corresponding Author: Yasemin Numanoğlu Çevik cevikyasemin@yahoo.com

Scorpion venoms are a mixture of complex molecules, many of which are peptides with different biological activities. When scorpions transfer these peptides to their prey, they show neurotoxic effects by affecting ion channels in specific pharmacological target tissues [3]. The Buthidae scorpion family is the largest scorpion family, with about 96 genera and 1230 species diversity. Except for Antarctica and New Zealand, they live in all tropical, subtropical and partially temperate warm landmasses in the World. *Leiurus abduallahbayrami* (LAB), a member of the genus *Leiurus* [4]. It is known as the yellow scorpion, which lives endemic in Syria and Turkey (in the Southeast Anatolia region). *Androctonus crassicauda* (ACR), known as the black scorpion, is widely found in North Africa, the Middle East and Asia [5]. Both scorpion species have peptide structures of medical importance[3]. Analytical methods such as gel electrophoresis [6,7] and liquid chromatography [8] have already been classically used to generate venom profiles. Most toxic peptides contain more than 100 amino acids and therefore venom screening can be performed with mass spectrometry, which makes it easy to detect [2,9,10]. In the last decade, the Matrix Assisted Laser Desorption Time of Flight (MALDI-TOF MS) method has been preferred for the analysis of peptides and proteins in venoms[8,10,11]. MALDI-TOF MS is a sensitive alternative method for biochemical and even molecular based identification approaches, since it requires fewer reagents, fewer steps [12,13]. In addition, it has emerged as a rapid, accurate, easy-to-apply and cost-effective technique for protein and peptide analysis [14]. Smith et al. established peptide profiles of some common scorpion species (*Urodacus elongatus*, *Urodacus yaschenkoi*, *Urodacus armatus* and *Lychas marmoreus obscurus*) in Australia by MALDI-TOF MS using the 1.5-diaminonaphthalene matrix [15]. Schaffrath and Predel analyzed the peptide profiles of *Heterometrus cyaneus* (Vietnam) and *Buthus occitanus* in detail using MALDI-TOF MS/MS and two different matrices (2.5-dihydroxybenzoic acid; DHB and α -cyano-4-hydroxycinnamic acid; CHCA) [16].

In this study, the venoms of the scorpions *Androctonus crassicauda* and *Leiurus abduallahbayrami*, different species each other of two members of the Buthidae family and the most dangerous scorpion species, were analyzed by MALDI-TOF MS. Peptide and protein profiles of two members of Buthidae family, *Androctonus crassicauda* (n=9) and *Leiurus abduallahbayrami* (n=2), were created by MALDI-TOF MS method and it was

demonstrated that they can be differentiated from each other with the help of Principal Component Analysis (PCA).

Materials and Methods

Supply of venom, materials and preparation of venom sample

The Turkish Public Health Institute Antivenom Production Center (TPHIAPC; Ankara, Turkey) has been milking venoms from scorpions kept alive to produce antivenom routinely. For the purpose of this study, the *Androctonus crassicauda* (ACR, n=9) and *Leiurus abduhbayrami* (LAB, n=2) scorpion venom samples were provided as a generous gift by TPHIAPC. The scorpion venom samples were composed of the nine different ACR scorpions (codes are: 47, 57, 117, 134, 168, 176, 243, 405 and 496) and two different LAB scorpions (codes are: 123 and 460). The MALDI matrix, α -cyano-4-hydroxycinnamic acid (CHCA), was obtained from Bruker (Germany). Acetonitrile (ACN, HPLC grade; Sigma-Aldrich), trifluoroacetic acid (TFA; Sigma-Aldrich), Ultra-pure water (UPW) with a 0.1 μ m filter without DNAase and RNAase (Sigma-Aldrich) and Bruker bacterial test solution (BTS) containing *Escherichia coli*, RNAase, and myoglobin protein profiles were also employed. All of the milked scorpion venoms were prepared to equal 2mg/mL concentration with UPW by measuring at 280 wavelengths with Nano Ready Touch (Life Real) instrument. Then, they were centrifuged 15.000 rpm for 15 minutes at +4 °C. The supernatants were transferred to new polypropylene tubes separately. All of the scorpion venom solutions (n=11) were mixed with a matrix solution (18 mg/mL α -CHCA in a 50% ACN and 2.5% TFA mixture, 1:1; v/v) in Eppendorf tubes separately. The prepared scorpion venom-matrix (SVMx) samples vortexed at 3000 rpm for 2 minutes.

Instrumentation and analysis of scorpion venom-matrix samples

For the biomass analysis 1 μ L SVMx sample was spotted onto a special steel 96 micro scout plate (MSP; Bruker Daltonics). This operation was applied to every eleven SVMx samples (both ACRs and LABs) and then allowed to dry completely at room temperature. The SVMx samples loaded MALDI 96 MSP was placed in the Microflex MALDI-TOF MS (Bruker Daltonics; Bremen, Germany) device. The system was operated in linear positive ion mode at a 1.000-50.000 Dalton (Da) mass range. A 60 Hz nitrogen laser was employed at 337 nm

as the ion source. To obtain the spectra, laser pulses consisting of 40 packets of 400 were applied in the measurement of each peptide molecule. Each sample was studied in triplicate, and the highest readings were included in the analysis.

Internal quality control for MALDI-TOF MS was completed with seven peaks (m/z, 5096.39312 Da; 5381.29950 Da; 6255.88327 Da; 7274.94901Da; 10298.9927 Da; 13682.32001 Da and 16953.88117 Da) assigned with a standard deviation of 59.75 and maximum peak error of 79.20 ppm.

Mass spectrum profile and PCA analysis of scorpion venoms

The mass spectra generated from MALDI-TOF MS regarded as multivariate data, in which every mass signal represents a single molecular dimension. The mass spectrum was analyzed using the principal component analysis (PCA) supported by external MATLAB software integrated into MALDI Biotyper software (version 3.1) [13]. Prior to further analysis based on the Biotyper pre-processing standard method (smoothing method: Savitski-Golay; baseline subtraction method; multi polygon; normalization method) was applied [17]. The PCA was based on the peaks acquired from MALDI-TOF MS to find patterns and unique peaks of the spectrum and allows the formation of clustered groups of spectra having similar variation characteristics and the visualization of the differences between them. Cluster analysis was performed by performing PCA dendrograms which represent the relationship and proximity of each spectrum to each other [12]. Accordingly, the mass spectra obtained in this study were further analysed to determine the composite correlation index (CCI) which was used to statistically determine the relationship between the acquired spectra [18].

Results

In this study, the venoms of the scorpions *Androctonus crassicauda* and *Leiurus abduhbayrami* were analyzed by MALDI TOF MS. Peptide and protein profiles of *Androctonus crassicauda* (n=9) and *Leiurus abduhbayrami* (n=2), were obtained by MALDI-TOF MS method. Photographs of 11 scorpion venoms studied in this study (Figure 1) and information including height and weight are presented (Table 1).



Fig 1 The photographs of nine *A. crassicauda* and two *L. abdullahbayrami* were taken by Mehmet Ali Kanat

Table 1 Information about the physical characteristics of the eleven scorpions (nine of *Androctonus crassicauda* and two of *Leiurus abdullahbayrami*)

Scorpion	ACR-47	ACR-57	ACR-117	ACR-134	ACR-168	ACR-176	ACR-243	ACR-405	ACR-496	LAB-123	LAB-460
Weight (g)	6.18	6.77	5.90	4.82	5.36	5.85	5.41	5.73	4.7	4.15	4.68
Dimensions (cm)	9.00	9.00	9.00	8.50	9.00	8.50	8.40	8.00	8.00	7.50	6.00

Potential marker peptides and proteins in discrimination of scorpions

In the present study, two LABs (*LAB-123* and *LAB-460*) and nine ACRs (codes are; 47, 57, 117, 134, 168, 176, 243, 405 and 496) scorpion venoms were analyzed by MALDI-TOF MS. Generally, three readings were performed for each SVMx sample and the analysis of eleven scorpions spectra with the highest intensity were performed. It was observed that peptide

molecules in the range from $2 \cdot 10^3$ to $4 \cdot 10^3$ Da were present in all ten scorpion venoms except *ACR-168*. In addition, in all eleven scorpion venoms, it is seen that peptide molecules are especially concentrated in the range of both from $4 \cdot 10^3$ to $6 \cdot 10^3$ Da and from $7 \cdot 10^3$ to $8 \cdot 10^3$ Da. Unlike the *ACR* species, the third high-intensity peaks were detected in the range of 14300-14500 Da in both *LAB* scorpion species. On the other hand, protein peaks with high intensity from 16000 to 18000 Da, which is not found in the *LAB* scorpion species, were detected in all *ACR* scorpion venoms. Protein peaks in the range from 22000-34000 Da were observed only in four *ACR* (*ACR-47*; *ACR-117*, *ACR-134*; *ACR-176*) scorpion species (Table 2). The top three $(M+H)^+$ molecular basic peptide's/protein's peak (BPP) have high-intensity values for each scorpion venom spectra defined in Table 2. The first highest intensity $(M+H)^+$ molecular peptide/protein peak, the second-highest intensity BPP, and the third-highest intensity BPP were defined as the (1st. BPP), (2nd. BPP), and (3rd. BPP) respectively. Accordingly, while the first three BPP masses of the *LAB* species were compatible with each other, it was observed that there were differences in the scorpion venoms of the *ACR* type (Table 2).

Table 2 Peptides and proteins detected in two *LAB* and nine *ACR* scorpion venoms and their first three main peaks that have highest intensity of $(M+H)^+$

Scorpion Sample Code	$(M+H)^+$									
	2-4 $\times 10^3$ Da	4-6 $\times 10^3$ Da	7-8 $\times 10^3$ Da	13-15 $\times 10^3$ Da	16-18 $\times 10^3$ Da	20-21 $\times 10^3$ Da	22-34 $\times 10^3$ Da	1st. BPP (Da)	2nd. BPP (Da)	3rd. BPP (Da)
<i>LAB-123</i>	++	+	++	++	-	+(21)	-	3583	6492	14454
<i>LAB-460</i>	+	+	+	++	-	-	-	3426	6488	14345
<i>ACR-47</i>	+	+	++	+	+	-	+(27-28)	16936	8472	7161
<i>ACR-57</i>	+	+	++	-	+	-	-	3881	7211	16932
<i>ACR-117</i>	++	+	++	-	++	-	++(33)	16326	8163	7154
<i>ACR-134</i>	+	+	++	-	++	-	++(33)	8468	17074	8063
<i>ACR-168</i>	-	+	++	++	+	-	-	8463	16923	6856
<i>ACR-176</i>	++	+	++	++	+	-	++(33)	16940	8474	3183
<i>ACR-243</i>	+	+	+	+	+	-	-	6703	8476	3610
<i>ACR-405</i>	++	+	++	+	+	-	-	16326	3882	6569
<i>ACR-496</i>	+	+	++	-	++	-	-	16930	8266	5644

(-): not available; (+): available; (++): more available

The dendrogram profile of 11 scorpion venoms of two different species is presented in Figure 2A. Gel profile showing the distribution of peptides and protein peaks of a total of eleven scorpion venoms analyzed by MALDI-TOF MS was presented in Figure 2B. Macroscopic examination revealed both common and differential peaks in the spectra of the *LAB* and the *ACR* scorpion venoms (Figure 2B). In addition, the Composite Correlation Index (CCI) color matrix (Fig. 2C) was shown in Figure 2C. When the closeness and distance percentages of all eleven scorpion venoms were evaluated based on their mass spectra, three distinct similarity matches were evident in the CCI color matrix in Figure 2C. According to this, the most similar (CCI; 81%) venoms belong to the *ACR*-134 and the *ACR*-176 scorpions which were members of the cluster-III in the dendrogram (Figure 2 A). The third scorpion venom, showing more than 70% similarity to these two scorpion venoms (Figure 2C, α -black circle), was the *ACR*-168 scorpion venom in the cluster-I in the dendrogram profile (Figure 2A).

The other member of the cluster-III the *ACR*-405 scorpion venom was most similar to the venoms of the scorpions *ACR*-134 (74%), later *ACR*-47 (68%) and finally *ACR*-176 (52%). The last member of cluster-III, the *ACR*-47 scorpion venom has been included in the cluster with a separate branch in the dendrogram profile (Figure 2A) and its similarity to the *ACR*-496 is 68% (Figure 2C; in a β -black circle) and the *ACR*-134 (CCI; 55%) scorpion venom's similarity is moderate, but it was too dissimilar to the *ACR*-176 scorpion venom with a CCI percentage below 20%.

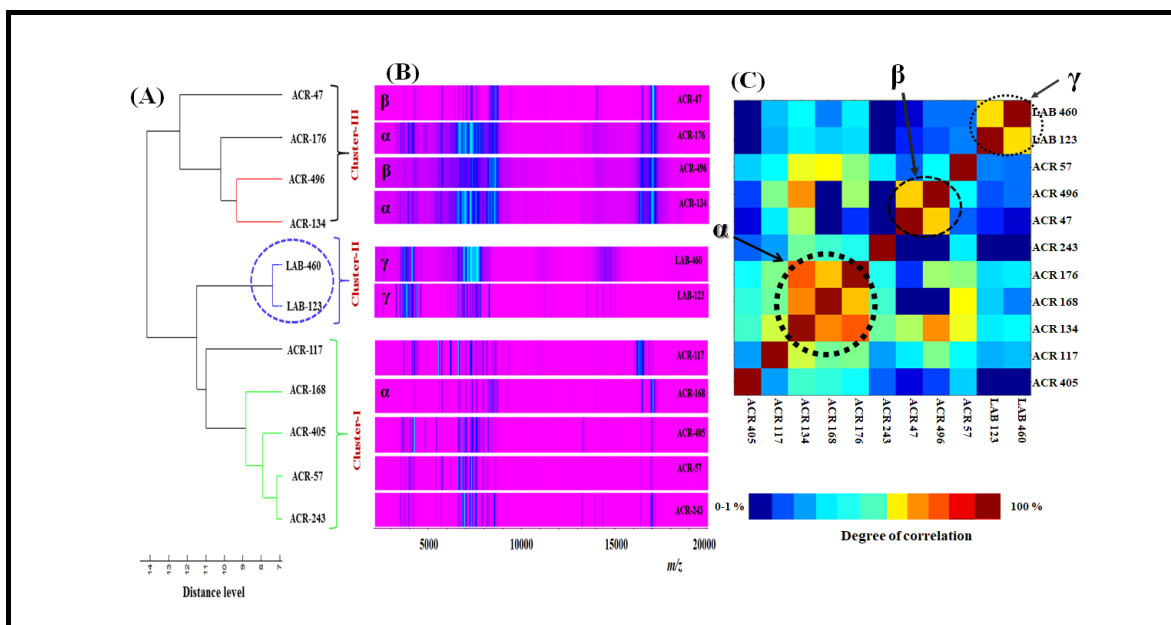


Fig 2 (A) Dendrogram profile, (B) gel profile and (C) CCI color matrix of the two *LAB* and the nine *ACR* scorpion venoms. The degree of similarity between pair mass spectra comparisons ranging from red (very similar) to blue (very dissimilar). Three scorpions (*ACR-134*, *ACR-176* and *ACR-496*) which is best resemble each other in the big black α -circle (C)

The distribution of $(M+H)^+$ peptide and protein molecules found in scorpion venoms confirms each other with both the values in Table 2 and the spectral mass projections in the gel profile (Figure 2B). Accordingly, it is seen that both the first two BPPs in the *ACR-134* and the *ACR-176*'scorpion venom as well as $(M+H)^+$ molecules in general were quite similar. Two of the three clusters formed in the dendrogram profile belong to the *ACR* scorpion venoms (cluster-I and cluster-III). It was determined that the similarity between the scorpions in the cluster-I was lower than the one in the cluster-III. The closest of each other in cluster-I are the scorpions the *ACR-57* and the *ACR-168* (Figure 2B, yellow color). The CCI values of the *LAB-123* and the *LAB-460* scorpion venoms were calculated against both each other and against the *ACR* scorpion venoms were also shown in figures 3A and 3B and 3C respectively. The similarity rate of the *LAB-123* and the *LAB-460* scorpion venoms of the same species was found as 66 % and the CCI color matrix matching was shown in Figure 2C (γ -black circle). In contrast, the similarity rates of venoms of the *ACR* species to the *LAB* species ranged from zero to 37 % (Figures 3B and 3C). On the other hand, when the first three main base peaks in its spectrum were compared with the other nine *ACR* scorpion

venoms and both *LAB* scorpion venoms, the peptide and protein peaks of the *ACR-57* scorpion venom appear to partially resemble the peptide and protein profiles of both of the *LAB* scorpion venoms (Table 2). In contrast, when the CCI values of the *ACR-57* scorpion venom were calculated according to the *LAB* scorpion species were examined, it was seen that the similarity was too low (for the *LAB* 123 is 24 % and the *LAB-460* CCI value is 23%) (Figure 3B and 3C). It is clear that projections of *LAB* species of all biomarker peptides (m/z; 3426, 3583, 6488, 6492 Da) and proteins (m/z; 14345 and 14454 Da) are continuous (Figures 3D and 3E).

Figure 4 shows the 2D-scatter profile of all eleven scorpion venoms and their matching spectral $(M+H)^+$ mass projection values. Consistent with the dendrogram profile (Figure 2A), cluster formations are similar in the 2D-scattering profile. It can be seen that *LAB* scorpion venoms (cluster II) are very clearly separated from cluster-I with 20% variance (PC2) (Figure 3A). In the PCA scattering profile, each dot represents the spectrum of scorpion venoms, while in the spectral loading projection, each dot represents a peptide or protein $(M+H)^+$ molecule. The high-intensity peptide molecules (m/z; 3582-4310 Da and 6492-6500 Da) found in the spectra of the *LAB-123* and the *LAB-460* matched their projections in the 2D-scattering profile, confirming its position. A similar situation is seen in Figure 4B, where the projections of high-intensity peptide and protein molecules of the *ACR* scorpion venoms (cluster-I and cluster-III) are consistent with their positions in Figure 4A.

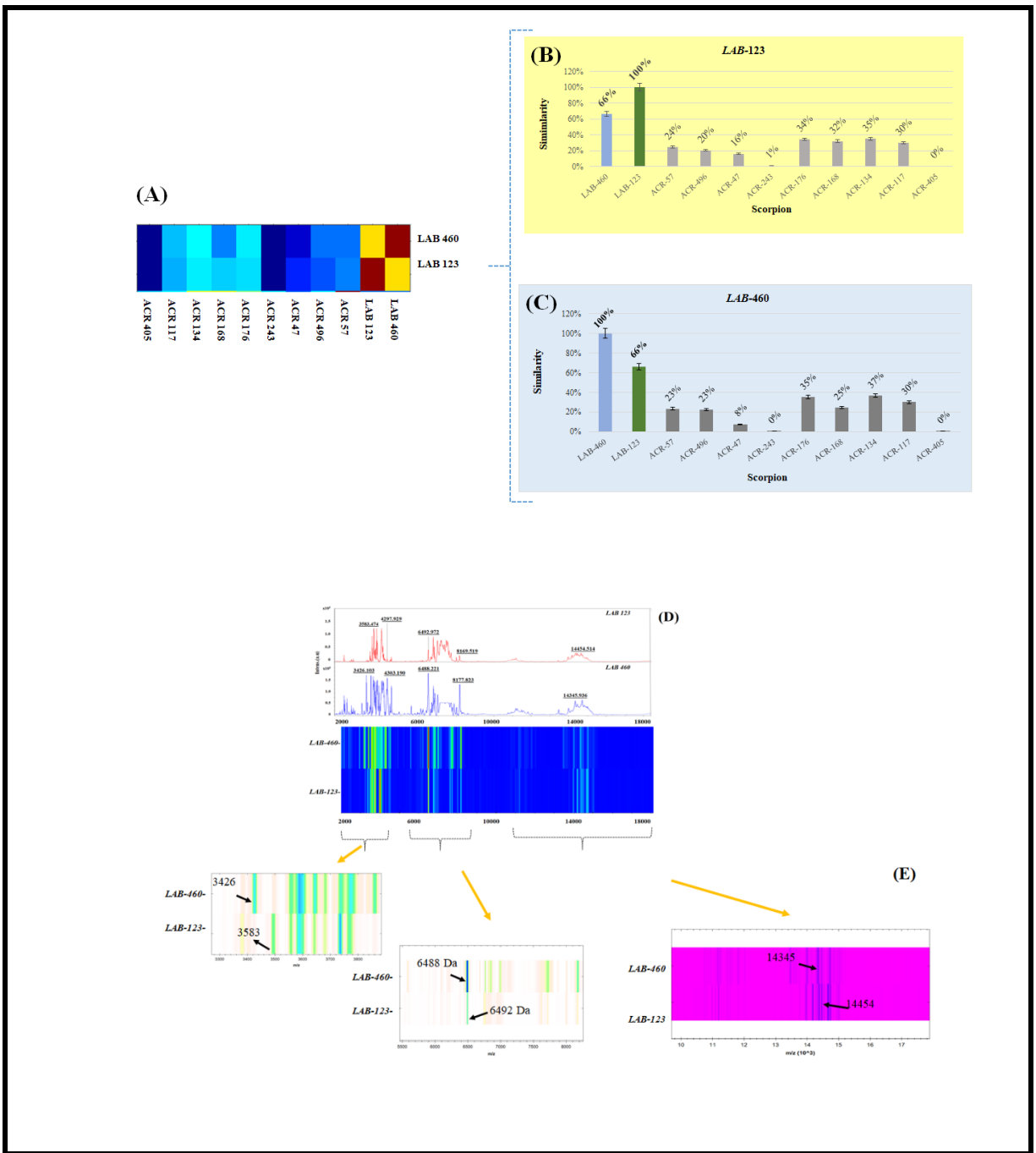


Fig 3 The CCI color matrix (A) and similarity graph for the *LAB-123* (B) and the *LAB-460* (C) scorpion venoms for both the nine *ACR* scorpion venoms and for the *LAB* strains. (D) Representative of whole venom MALDI-TOF MS spectra in the range from 2000 to 18 000 *m/z* and spectral gel images of the *LAB-123* and the *LAB-460* in the range from 2000 to 18 000 *m/z*. (E) The three of the BPPs of two *LABs* scorpion venom gel profiles were detailed

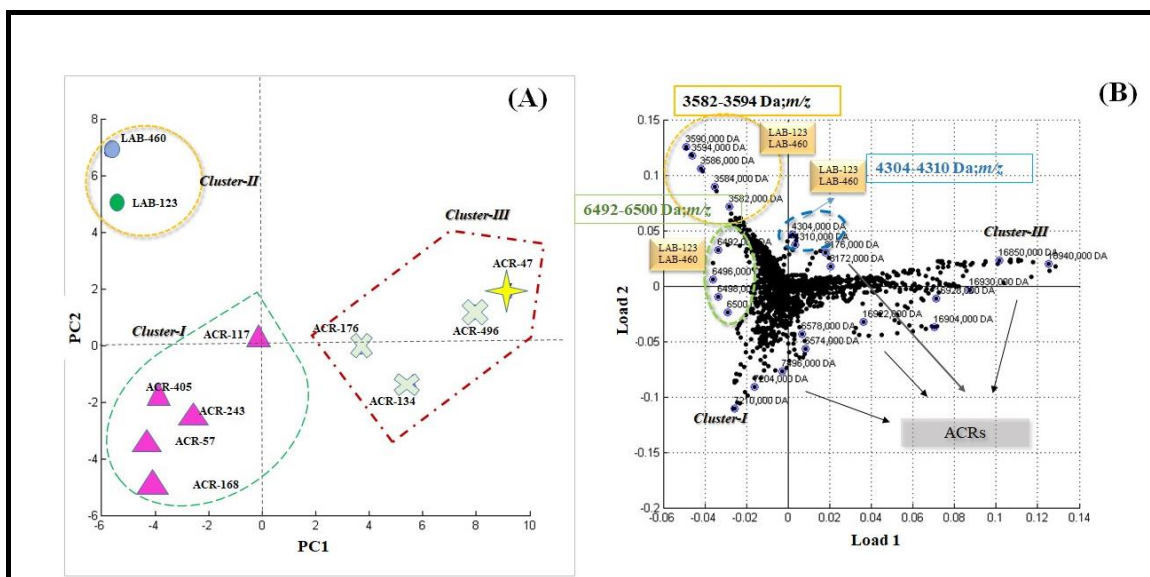


Fig 4 (A) The 2D scatter profile (B) and spectral mass loading projections of two *LAB* and nine *ACR* scorpion venoms. Each spot (triangle, X and star) represents one spectrum. The black plot represents $(M+H)^+$ peptide or protein peak. Both profiles were generated by PCA. The three of BPPs' of two *LAB* scorpion venoms (m/z ; 3426, 3583, 6488, 6492, 14345, 14454 Da) were clearly visible in both spectra and gel profile

The 3880 ± 5 Da $(M+H)^+$ molecule was high in abundance in the *ACR-57*, the *ACR-134*, the *ACR-176*, and the *ACR-405* scorpion venom (Figure 5A), while low in the *ACR-168*, the *ACR-243* scorpion venom was not available in the *LAB-123*, the *LAB-460*, the *ACR-47*. The 6725 ± 5 Da $(M+H)^+$ peptide molecule was also present in other nine scorpion venoms except for the *ACR-176* and the *ACR-405*. The 7210 ± 10 Da peptide molecule was present in all eleven scorpion venoms. The 8170 ± 10 Da peptide was predominant in the *LAB-123*, the *LAB-460*, the *ACR-176*, the *ACR-405* and the *ACR-496*, low abundance in the *ACR-47* and the *ACR-168*, while other *ACRs* (57, 117, 134) scorpion venoms did not have this peptide molecule. When we focused on protein molecules (above 10 000Da), protein peaks between 14000-14500 Da were observed in both *LAB-123* and *LAB-460* scorpion venoms. In contrast, protein molecules were found in high abundance in all *ACR* scorpion venoms, particularly between 16,300 and 16,999 Da (Fig. 5C). These protein peaks were observed as the most significant difference between *ACR* and *LAB* poisons. This difference was also clearly seen in the gel profile in Figure 3A. In addition, the projections of the first 3 BPPs of the *LAB* scorpion venoms in their spectra and gel profile were shown in Figure 3E in detail.

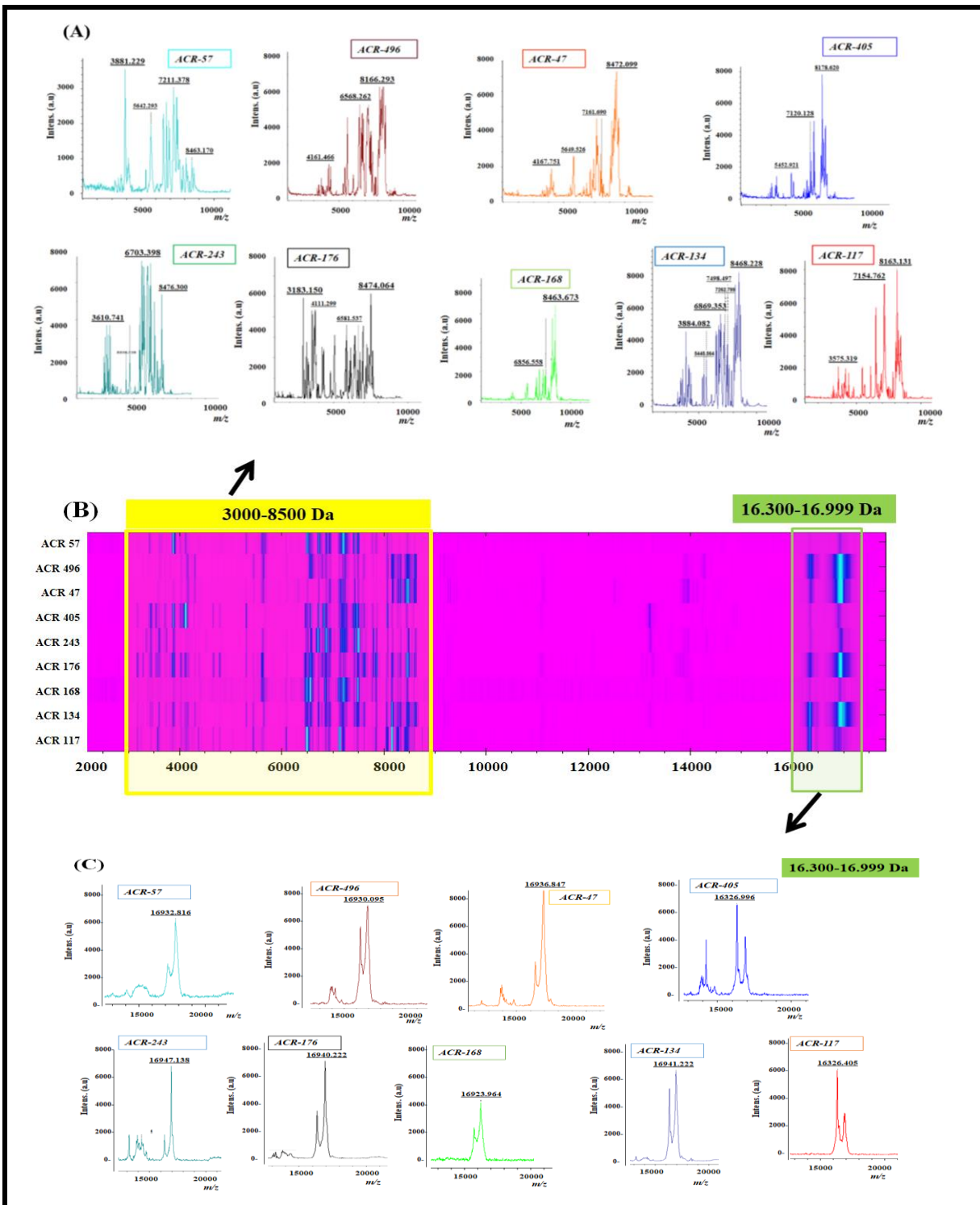


Fig 5 (A) Representative the ACR scorpion venoms MALDI-TOF MS spectra mass ranging from 3000-8500 Da and (C) mass ranging from 16.300-16.999 Da (B) Spectral gel images of the nine ACR scorpion venoms separately

Discussion

MALDI-TOF mass spectrometry has been preferred for many years as a powerful tool for precise molecular mass mapping of complex peptide mixtures [18]. In this study, a mass range between 1 kDa and 50 kDa was studied. Interspecies differentiation was evaluated over peptide and protein molecules in this mass range. Among the eleven Buthidae member scorpion venoms, *LAB*-460 had the lowest mass of peptide molecules (2029 Da), while the protein molecules with the highest mass value m/z , 33938 Da for *ACR*-176 and 33976 Da for *ACR*-134 scorpion venoms were found. While the protein peaks between 14000-14500 Da were observed in the *LAB* scorpion venoms, the protein molecules were found in high abundance in all *ACR* scorpion venoms, particularly between 16300 and 16999 Da). These protein peaks were observed as the most significant difference between the *ACR* and the *LAB* venoms. This difference was also clearly seen in the gel profile.

The peptide toxin molecules found in the venom of scorpions exert neurotoxic effects on the cells of their prey. Small compounds consisting of short polypeptide chains (m/z , 3000-4300 Da) that have been shown to be effective on potassium channels are present in the venom content, albeit in small amounts. On the other hand, peptide toxins known as the main components of scorpion venoms and having a relatively large molecular mass (6000-8000 Da) are active on sodium channels and are abundant [19]. As expected, roughly detected the short polypeptide chains were observed to be less than large molecular mass proteins in the eleven scorpion venoms we studied.

In this study, it was demonstrated that scorpion venoms belonging to two different species from the Buthidae family can be differentiated with the help of dendrogram and gel profile, CCI color matrix, 3D or 2D-scattering profile, spectral mass loading data formed by peptide and protein spectral patterns of eleven scorpion venoms. It is anticipated that this approach, which was used for the first time with the application of MALDI TOF MS-based PCA analysis for the differentiation of scorpion venoms, will be useful in differentiating venoms with different spectral patterns.

In the literature, very valuable analytical studies have been made and continue to be done on both species (*ACR* and *LAB*) belonging to the Buthidae family [20–22]. The contribution of

each study to this field is very important and valuable. For example, microfluidic capillary electrophoresis and LC-ESI-TOF-MS by Erdes et al. performed an extensive analysis of the *L. abduallahbayrami* scorpion venom. According to their results, a total of 45 peptide masses were identified in the *L. abduallahbayrami* scorpion venom[22]. When the results of Erdes et al.'s study and our results were compared, it was observed that 3590 Da peptide was present in both *LAB* (123 and 460) scorpion venoms, among the mass values they detected in *L. abduallahbayrami* scorpion venoms.

Conclusion

This study demonstrated the peptide and protein profiles of some Buthidae family's scorpions by using MALDI-TOF MS for the first time. In addition, using MALDI-TOF mass fingerprint data with multivariate PCA analysis, *Androctonus crassicauda* species and *Leiurus abduallahbayrami* species were discriminated. Using the peptide and protein profiles of scorpion venoms with a fast, practical and low-cost device such as MALDI-TOF MS, revealing the dramatic differences between different species and within the same species will make a very important contribution to this field. Beyond identification, analytical evaluation of the spectral patterns of each species was also performed with PCA-based data and a series of data analyses (dendrogram, clustering, CCI and spectral loading). This comprehensive study, in which this approach has been evaluated for the first time, is open to further development, supported by further analysis and spectral improvement studies. It is also anticipated that the use of mixtures of different scorpions, whose peptide and protein profiles are defined by MALDI-TOF MS, will contribute to more effective antivenom production by using them in the production of scorpion antivenom.

Data availability

The authors confirm that the data supporting the findings of this study are available within the article.

Geolocation information

The scorpions were collected from Şanlıurfa province (GCP coordinates of 39° 56' 0.109" N and 32° 51' 35.07" E) which is located in the eastern part of Turkey. This study was done in Ankara which is the capital of Turkey with GPS coordinates of 39° 55' 28.1280"N and 32° 51' 16.6788" E.

Acknowledgments

The scorpions of the *A. crassicauda* and *L. abduallahbayrami* species were collected from Şanlıurfa province in the eastern part of Turkey for the purpose of antivenom production by Turkish Public Health Institute Antivenom Production Center. We are very grateful to the Turkish Public Health Institute Antivenom Production Center for gifting scorpion venoms.

References

1. Rincón-Cortés, et.al., Structural and Functional Characterization of Toxic Peptides Purified from The Venom of The Colombian Scorpion *Tityus Macrochirus*. *Toxicon*, 2019. 169: p.5–11. <https://doi.org/10.1016/j.toxicon.2019.07.013>.
2. Schaffrath, S., and Predel, R.A., Simple Protocol for Venom Peptide Barcoding in Scorpions. *EuPA Open Proteomics*. 2014. 3: p. 239–245. <https://doi.org/10.1016/j.euprot.2014.02.017>.
3. Oukkache, N. et.al., New Analysis of The Toxic Compounds from The *Androctonus Mauretanicus* Scorpion Venom. *Toxicon*, 2008. 51: p. 835–852. <https://doi.org/10.1016/j.toxicon.2007.12.012>.
4. Yağmur, E.A, Koç, H., and Kunt, K.B., Description of A New Species of *Leiurus* Ehrenberg, 1828 (Scorpiones: Buthidae) from Southeastern Turkey. *Euscorpius*, 2009: p.1–20. <https://doi.org/10.18590/euscorpius.2009.vol2009.iss85.1>.
5. Ozkan, O., and Alcigir, M.E., A Comparative Pathomorphological Findings between *Leiurus abdullahbayrami* and *Androctonus crassicauda* (Scorpion: Buthidae) envenomation in rabbit animal model. *J. Arthropod. Borne Disease*, 2019. 13: p. 104–115. <https://doi.org/10.18502/jad.v13i1.937>.
6. Borges, A., and Rojas-Runjaic, F.J.M., *Tityus Perijanensis* González-Sponga (Scorpiones, Buthidae): Molecular Assessment of Its Geographical Distribution and Venom Lethality of Venezuelan Populations. *Toxicon*, 2007. 50: p. 1005–1010. <https://doi.org/10.1016/j.toxicon.2007.07.019>.
7. Estrada-Gómez, S. et.al., MS/MS Analysis of Four Scorpion Venoms from Colombia: A descriptive approach. *J. Venom. Anim. Toxins Incl. Tropical Disease*, 2021. 27: p. 1–13. <https://doi.org/10.1590/1678-9199-JVATITD-2020-0173>.
8. Bringans, S. et.al., Proteomic analysis of the venom of *Heterometrus longimanus* (Asian black scorpion). *Proteomics*, 2008. 8: p. 1081–1096. <https://doi.org/10.1002/pmic.200700948>.
9. Numanoğlu Çevik, Y. et.al., Salih, B. Identification of Snake Venoms According to their Protein Content Using the MALDI-TOF-MS Method. *Anal. Chemistry Letters*, 2021. 11: p. 153–167. <https://doi.org/10.1080/22297928.2021.1894974>.
10. Martin-Eauclaire, M. F et.al., Achieving Automated Scorpion Venom Mass Fingerprinting (VMF) in The Nanogram Range. *Toxicon*, 2013. 69: p. 211–218. <https://doi.org/10.1016/j.toxicon.2013.03.001>.
11. Favreau, P. et.al., Mass Spectrometry Strategies for Venom Mapping and Peptide Sequencing from Crude Venoms: Case Applications with Single Arthropod Specimen. *Toxicon*, 2006. 47: p. 676–687. <https://doi.org/10.1016/j.toxicon.2006.01.020>.
12. Cheng, K. et.al., Recent development of mass spectrometry and proteomics applications in identification and typing of bacteria. *Proteomics- Clin. Application*, 2016. 10(4): p. 346-357. <https://doi.org/10.1002/prca.201500086>.
13. Taban, B.M., and Y. Numanoglu Cevik, The Efficiency of MALDI-TOF MS Method in Detecting *Staphylococcus Aureus* Isolated from Raw Milk and Artisanal Dairy Foods. *CyTA-J. Food*, 2021. 19: p. 739–750. <https://doi.org/10.1080/19476337.2021.1977392>.
14. Sauget, M., et.al., Can MALDI-TOF Mass Spectrometry Reasonably Type Bacteria? *Trends Microbiology*, 2017. 25: p. 447–455. <https://doi.org/10.1016/j.tim.2016.12.006>.
15. Smith, J.J, Jones, A., and Alewood, P.F., Mass Landscapes of Seven Scorpion Species: The First Analyses of Australian Species with 1,5-DAN matrix., *J. Venom Researche*, 2012. 3: p. 7–14.
16. Schaffrath, S. and Predel, R., A Simple Protocol for Venom Peptide Barcoding in Scorpions. *EuPA Open Proteomics*, 2014. 3: p. 239–245. <https://doi.org/10.1016/j.euprot.2014.02.017>.
17. Jeong, Y.S., Lee, J., and Kim, S.J. Discrimination of *Bacillus Anthracis* Spores by Direct in-situ Analysis of Matrix-Assisted Laser Desorption/Ionization Time-of-Flight Mass Spectrometry, *Bull. Korean Chemical Society*, 2013. 34: p. 2635–2639. <https://doi.org/10.5012/bkcs.2013.34.9.2635>.

18. Samad, R.A, and Al Disi, Z., The Use of Principle Component Analysis and MALDI-TOF MS for The Differentiation of Mineral Forming *Virgibacillus* and *Bacillus* Species Isolated from Sabkhas. *R. Soc. Chemistry*, 2020. 10: p. 14606–14616. <https://doi.org/10.1039/d0ra01229g>.
19. Romi-Lebrun, R. et.al., Characterization of Four Toxins from *Buthus Martensi* Scorpion Venom, Which Act on Apamin-Sensitive Ca^{2+} -Activated K^{+} Channels. *Eur. J. Biochemistry*, 1997. 245: p. 457–64. <https://doi.org/10.1111/j.1432-1033.1997.00457.x>.
20. Caliskan, F. et.al., Characterization of Venom Components from The Scorpion *Androctonus Crassicauda* of Turkey: Peptides and genes. *Toxicon*, 2006. 48: p. 12–22. <https://doi.org/10.1016/j.toxicon.2006.04.003>.
21. Caliskan, F. *Scorpion Venoms*, Springer Netherlands, Dordrecht, 2015. Section:14 p: 327-349. <https://doi.org/10.1007/978-94-007-6404-0>.
22. Erdeş, E. et.al., Characterization of *Leiurus abduhbayrami* (Scorpiones: Buthidae) venom: peptide profile, cytotoxicity and antimicrobial activity, *J. Venom. Anim. Toxins Incl. Trop. Dis.*, 20. 2014: p. 48. <https://doi.org/10.1186/1678-9199-20-48>.

Bozdemir, C., et al., Determination of Yield and Quality Characteristics of Various Genotypes of Black Cumin (*Nigella Sativa* L.) Cultivated Through Without Fertilizers. International Journal of Life Sciences and Biotechnology, 2022. 5(3): p. 386-406. DOI: 10.38001/ijlsb.1111198

Determination of Yield and Quality Characteristics of Various Genotypes of Black Cumin (*Nigella Sativa* L.) Cultivated Through Without Fertilizers

Çiğdem Bozdemir^{1*} , Reyhan B. Bagdat¹ , İlhan Subasi² , Nilufer Akci³ ,
Nurettin Cinkaya⁴ 

ABSTRACT

Black cumin (*Nigella sativa* L.) is one of the essential spice plants used in Turkey. The present study investigated the yield and some agronomic, morphological, and qualitative characteristics of 31 different black cumin genotypes (30 lines and one control variety of Çameli) of domestic and foreign origin under the ecological conditions of the city of Ankara. The study was carried out in the experimental areas of İkizce Research and Application farm of Ankara Field Crops Central Research Institute during the vegetation periods of 2018-2019. The experiment was set up as three replications according to the Experiment Design in Randomized Blocks. According to the results of the research, the plant height of the genotypes in the experiment changed for two years between 17.1-33.5 cm, the height of the first capsule between 11.6-26.6 cm, the number of seeds in the capsule between 28.5-69.6 seeds capsule⁻¹, the number of branches between 2.0-3.4 pieces plant⁻¹, the number of capsules between 1.8-2.9 capsules plant⁻¹, thousand seed weight between 2.0-3.0 g, seed yield between 194.5-505.9 kg ha⁻¹, fixed oil rate between 27.2-35.3%, maturation (growth/harvest) time between 136.5-141.7 days and germination (emergence time) between 27.2-30.7 days. In terms of fatty acids, the most proportional fatty acids were found to be linoleic acid (45.45-55.62%), oleic acid (18.83-25.01%), palmitic acid (6.95-11.72%), stearic acid (3.50-4.77%), respectively. It has been determined as the result of the study that black cumin genotypes with the number 1 (Denizli), 4 (Burdur), 17 (Borsa) and 3 (Burdur) respectively performed better than other black cumin genotypes and Çameli variety in terms of seed yield and genotypes with the number 28 (Kırıkkale), 29 (Ankara) and 26 (Egypt) performed better in terms of fixed oil ratio under the ecological conditions of Ankara.

ARTICLE HISTORY

Received

29 April 2022

Accepted

13 June 2022

KEYWORDS

Black cumin
(*Nigella sativa* L.),
yield,
fixed oil

Introduction

With the use of medicinal and aromatic plants in many different areas and different forms, especially in traditional and modern medicine, their popularity and the demand for them

¹ Central Research Institute for Field Crops, Ankara, Turkey

² Faculty of Agriculture, Department of Seed Growing Science and Technology, Bolu Abant İzzet Baysal University, Bolu, Turkey

³ Directorate of Plant Protection Central Research Institute, Ankara, Turkey

⁴ Çankaya Directorate of County Agriculture and Forestry, Ankara, Turkey

* Corresponding Author: Çiğdem BOZDEMİR, E-mail: cbozdemir72@hotmail.com

around the world are increasing day by day. The importance and therefore consumption of black cumin (*Nigella* spp.) have increased both in our country and the rest of the world owing to its wide range of uses, such as food, cosmetics, and medicinal drugs. The plant's production, which is at the forefront of the list of most exported plants in our country, is at a level that only meets a tiny part of domestic consumption. A significant part of the demand for the product is met through imports [1]. The increasing use of fixed oil obtained from seeds has increased the importance of black cumin cultivation in recent years. While the cultivation area of black cumin was 3261 decares and the production was 352 tons in 2013, these figures decreased to 1717 decares and 140 tons in 2014, and increased to 37.085 decares and 3603 tons in 2019 as a result of increasing demand. Although black cumin, which has an important place in our exports, was exported in an amount of about 65 tons and earned us 219.000 dollars in 2013, 2288 tons were imported in the same year, and we had a foreign exchange outflow of 1.910.000 dollars. In 2019, the black cumin export amount was 592.47 tons (1.236.915 dollars), the import amount was 2647.502 tons (2.531.796 dollars), while in 2020, the exports were 838.372 tons (2.186.684 dollars), and the imports were 3276.232 tons (1.964.851 dollars) [2]. The increase in interest in alternative plants in recent years has made black cumin, which is included in these plants, also popular. The fact that there is only one black cumin variety in our country, not only makes it impossible to meet the export demand but also makes it impossible to meet the requirement on this plant in different industries at the national level. Introduction materials are as important as local materials in obtaining varieties that can adapt to global climate change and meet expectations in terms of quality and yield. Having taken part in adaptation studies, black cumin genotypes grown in different geographies with similar ecological structure; lead obtaining important results with their responses to climate-soil and agronomic practices. At the same time, they play a very important role in the development of new varieties, especially in crossing, which is one of the basic steps of breeding, in increasing genetic variation. Revealing the true genetic potential of the plant in terms of yield and quality and also the presence of the mission of food and medicine, necessitate the cultivation method to be natural and healthy. This study aims to characterize the private sector and introduce black cumin genotypes in terms of agronomic, morphological, and quality, especially many local black cumin lines grown

following without fertilizers and pesticides, and to be a source for research in different fields, especially breeding.

Materials and Methods

The study was carried out in the experimental areas of İıkizce Research and Application farm of Ankara Field Crops Central Research Institute during the vegetation periods of 2018 - 2019. The study area is located at an altitude of 1055 m above sea level and between 39⁰ 12' -43⁰ 6' north latitudes and 35⁰ 58' -37⁰ 44' east longitudes. The experiment was set up as three replications according to the Experiment Design in Randomized Blocks. The parcels were 7.5 m² (5 m×5 rows×30 cm between rows) in size, 250 cm between the blocks, and 50 cm between the parcels. The material used was 30 black cumin (*Nigella sativa* L.) seeds from local domestic populations (Ankara, Burdur, Bursa, Denizli, Konya, Eskisehir, Afyonkarahisar, Diyarbakir, Kırkkale), from abroad (Syria, Egypt, India, Pakistan, Ethiopia) and from gene banks included in the advanced yield experiment of the *Nigella sativa* breeding program of the Central Research Institute of Field Crops (TARM), and the Çameli cultivar was used as a control variable. No fertilization or spraying was applied (Fig 1-2-3).



Fig 1. A view of the field experiments, **Fig 2.** Black cumin flower, **Fig 3.** Black cumin capsule
Sowing was carried out by hand on 20-21 March in 2018 and 12-13 March in 2019. In 2018, irrigation was done twice, the first in March and the other in April (Figure 4).



Fig 4. A view of irrigation treatments in black cumin

The majority of the harvest was collected from the last week of July and through the remaining part of the first week of August. In 2019, irrigation was done once in May, and the harvest was completed, mainly in the first week of August and the rest in the second week of the same month (Figure 5). At the same time, isolation work was carried out against foreign pollination of the plant (Figure 6).



Fig 5. A view of the field experiments (Harvest Time)



Fig 6. A view of isolation treatments in black cumin

Fixed oil ratio was determined by solvent (petroleum ether) extraction method in Soxterm 2000 oil analyzer (ISO 659:2009). Shimadzu GC-2010 (Japan), flame ionization detector (FID), and Technochrome Capillary column (100 m×0.25 mm and 0.2 μm film thickness) were used to determine the fixed fatty acid composition. In identifying fatty acids, Restek 35077, Food Industry FAME mix (USA) was used as a standard. Analysis of variance and LSD test (in MSTAT-C statistical package program) were performed on the analyzed characters. All statistical analyses were first performed separately according to locations, then they were performed jointly.

Soil and climate characteristics of the experimental site

According to the sample extracted from the 0-20 cm depth of the experimental area, the soil texture was clayey-loamy, slightly alkaline, very calcareous, unsalted, low in organic matter, phosphorus, manganese, and zinc, copper was sufficient, iron was moderate, magnesium and calcium were at a reasonable level, and potassium was found to be high (Table 1).

Table 1. Some physical and chemical properties of experiment area soil

Saturation Percentage %	Texture	EC ds/m	pH	Lime (CaCO ₃)	Available								Organic matter %
					P ₂ O	K ₂ O	Ca	Mg	Cu	Fe	Mn	Zn	
					(kg / da)		(ppm)						
64	Clay-loamy	0.64	7.73	30.0	4.50	306	7420	905	1.33	3.38	3.03	0.30	1.97

(Source: Soil, Fertilizer and Water Resources Central Research Institute)

Climatic data of Ankara conditions where the experiment was carried out are given in Table 2. In 2018, flood damage occurred on 26-27 May due to excessive precipitation, hail damage occurred on 28 May, and excessive precipitation damage occurred on 31 July. In 2019, a significant part of the parcels remained underwater and mud, as heavy rain and hail occurred on 12 June and flood damage occurred on 21-22 June and 15-19 July due to excessive precipitation (Table 2). As a result, many yield elements were negatively affected.

Table 2. Climatic figures of the experiment area (Ankara/ Gölbaşı) during the research years

Months	Total Precipitation (mm)			Average Temperature (°C)			Average Relative Humidity (%)		
	2018	2019	Long-Term (2010-2020)	2018	2019	Long-Term (2010-2020)	2018	2019	Long-Term (2010-2020)
March	61.4	20.6	25.8	7.9	4.7	5	65.9	58.4	25.8
April	2.6	23.4	18.1	12.2	7.9	9.6	52.1	61.1	18.1
May	122.8	25.2	51.6	15.3	15.1	14.3	65.8	55.4	51.6
June	27	63.5	19	18.7	18.6	18.4	56.7	58.8	19
July	9.6	7.2	4	21.8	17.8	22.2	48.1	54.3	4
August	2.4	9.2	8.5	22.2	20.7	22.3	41.5	47.3	8.5
Tot./Ave.	225.8	149.1	127	16.35	14.1	15.3	55.0	55.9	21.2

(Source: Agronomy Central Research Institute / Department of GIS and UA)

Result and Discussion

Emergence time

In terms of emergence time, there was a 1% difference in genotypes in 2018 and a 5% significance level in recurrences. There were no statistically significant differences in any respect in 2019. According to the results of the variance analysis performed by combining the years, there were statistically significant differences at the 1% significance level in terms of genotypes and years. In contrast, the recurrence and year \times genotype interaction were not statistically significant. The emergence time of the genotypes varied between 21.3-26.3 days (experimental mean 23.9 days) in 2018, 32.7-37.0 days (experimental mean 33.9 days) in 2019, and 27.2-30.7 days (experimental mean 28.9 days) in the combined analysis. Genotype 13 (Konya) was the genotype that germinated the earliest (Table 4). According to the results of the combined analysis, the number of genotypes that completed emergence 50% earlier than Çameli variety was found to be 14. The results of emergence time (27.2-30.7 days) showed that the genotypes included in the experiment were later than the results reported by Şahin (2013) (16-25 days), Ertuş (2016) (15-16 days) and Telci (1995) (15-16 days) and Gülhan and Taner (2020) (average values of two years 12.5-25 days). Emergence is one of the yield criteria most affected by climatic factors. Compared to 2018, the low rainfall and low soil temperature in the germination period of the plant in 2019 caused a delay in the emergence.

Maturation time

In terms of maturation time, there was a significant difference at the 1% significance level in genotypes in 2018, while there were statistically significant differences at the 1% probability limit only in terms of recurrences in 2019. According to the results of variance analysis made by combining the years, there were 1% statistically significant differences in genotypes, recurrences and years. In contrast, the year \times genotype interaction was not statistically significant. The maturation time of the genotypes varied between 129.0-136.7 days in 2018, 143.3-147.3 days in 2019, and 136.5-141.7 days in the combined analysis. The average of the years was 131.0, 144.5 and combined 137.8 days, respectively. The genotype that reached the earliest maturation efficiency was the number 1 genotype (Denizli) (Table 4). It was

determined that almost all of the materials (26 genotypes) in the experiment were genotypes that reached harvest maturity earlier than Çameli variety. The values (136.5-141.7 days) of the genotypes included in the experiment were later than Telci's (1995) (117-127 days), Safaei et al. (2017) summer plantings in Iranian conditions (103 days), and those of Gülhan and Taner (2020) (average values of two years 87.5-131 days) in terms of maturation time. It has been determined that they are close to the results of Şahin (2013) (115-140 days) and Ertaş (2016) (108-151 days). The factors affecting the harvest time were genotype, agronomic activities, and climate. Untimely and long-term rains also affected the maturation of the plant.

Plant height

Statistically significant differences were found between the genotypes in plant height at the 1% probability limit in both years and, 1% between the recurrences in 2018. According to the results of the combined variance analysis of the years related to the plant height values, there were differences at the 1% significance level between genotypes, years, and replications. In comparison, the year × genotype interaction was statistically significant at the 1% probability limit. While the plant heights of the genotypes varied between 19.2-45.0 cm (experimental mean 31.2 cm) in 2018, 14.9-28.7 cm (experimental mean 20.2 cm) in 2019, and between 17.1-33.5 cm according to the combined analysis results of the two years, the experimental (mean 25.7 cm), Kırıkkale population number 28 was the highest sized black cumini genotype (Table 4). According to the results of two years (25.7 cm), it was determined that 11 genotypes had a taller plant height than Çameli variety.

The values of the genotypes in terms of plant height included in the experiment were lower than the values (17.1-33.5 cm) found by Taqi (2013) (42.98-43.05 cm), Baytöre and Yaver (2014) (34.5-53.6 cm), Tektaş (2015) (63.9-70.4 cm), Ertaş (2016) (45.4-47.6 cm) and Koşar and Özel (2018) (47.8-68.6 cm). The results of Özel and Demirbilek (2000) (18.6-23.8 cm), Özel et al. (2001) (24.5 cm), Özel et al. (2007) (30.6-31.4 cm), Akgören (2011) (16.6-25.2 cm), Koşar et al. (2013) (28.7-39.4 cm) and Gülhan and Taner (2020) (14-35 cm) were consistent with the high results.

These wide variations between the lower and upper limits of the plant heights found in the studies are thought to be due to the untimely and excessive precipitation, although variable across the genotypes used in the research.

First capsule height

In terms of first capsule height, statistically significant differences were found at the 1% probability limit for the genotypes used in the experiment in both years. According to the results of the variance analysis performed by combining the years, statistically significant differences of 1% were found in terms of genotypes, years, and year \times genotype interaction. While the first capsule height of the genotypes changed between 13.6-37.8 cm (experimental mean 25.5 cm) in 2018, and 9.0-22.0 cm (14.4 cm average) in 2019, and between 11.6-26.6 cm according to the combined analysis results of the two years (experimental mean 20.0 cm), the Kırıkkale population numbered 28 was the black cumin genotype with the highest first capsule height (Table 4). Due to the positive relationship between the height of the first capsule and the height of the plant, according to the combined analysis result (test mean 20.0 cm), genotypes with a higher plant height than Çameli are also genotypes with the first capsule height, which are 12 in total. In terms of plant height, the genotypes in the experiment (11.6-26.6 cm) were among the figures found by Şahin (2013) (16.9-41.6 cm) but were lower. The genotypes with the highest first capsule height differed in both years are explained by the statistical significance of the combined analysis results of the genotypes, years, and year \times genotype interaction. It has been determined in many studies that the height of the first pod, which is an important feature for machine harvesting, can vary according to the plant density, ecological conditions, and climate. However, it depends on the genotype structure. The genotypes with the highest first pod height were obtained in 2018, as in the plant length criterion when the years are compared.

Thousand seed weight

Statistically significant differences were found between genotypes in terms of thousand seed weight, at the probability limit of 5% in 2018, 1% in 2019, and 1% in 2018 between replications. According to the results of the combined variance analysis of the years in terms of the plant height figures, there were differences at the 1% significance level between the genotypes, years, and replications. In contrast, the year \times genotype interaction was not

statistically significant. While the thousand seed weight of the genotypes varied between 1.8-2.9 g (experimental mean 2.4 g) in 2018, 1.9-3.3 g (mean 2.7 g) in 2019, and 2.0-3.0 g according to the combined analysis results of the two years (experimental mean 2.6 g), line 19 (material taken from the stock market) was the black cumin genotype with the highest thousand seed weight (Table 4). 11 black cumin genotypes reached a higher per thousand weight than Çameli variety (test mean 2.6 g), and 14 genotypes reached higher than trial average. The values of the genotypes in the experiment in terms of thousand seed weight were within the limits of the values (2.00-3.00 g) reported by Kalçın (2003) (1.59-2.06 g), Özel et al. (2009) (2.07-2.40 g), Ghamarnia et al. (2010)'nın (2.2-2.4 g), Akgören (2011) (1.21-2.62 g), Arslan et al. (2011) (1.97-2.01 g), Kulan et al. (2012) (2.22-2.69 g), Taqi (2013) (2.57-2.78 g), Tavas et al. (2014) (2.34-2.73 g), Baytöre and Yaver (2014) (1.97-2.30 g), Tektaş (2015) (2.40-2.90 g), Ertaş (2016) (2.47-2.67 g), Mehmood et al. (2018) (1.55-2.84 g), Kamçı (2019) (2.12-2.76 g) and higher. It is believed that the statistical difference that emerged as a result of the study resulted from the genetic effects of the genotypes and climatic and environmental conditions, especially the (*Cuscuta* spp.) problem. Damage to the capsules by heavy rain near the harvest time and the sudden overpressing temperature caused the generative cycle to shorten and not fill the pod.

Number of seeds in capsule

Regarding the number of seeds in the capsule, statistically significant differences were found at the 1% probability limit regarding the genotypes used in the experiment in both years. According to the results of the variance analysis performed by combining the years, there were 1% statistically significant differences in terms of genotypes and years. In contrast, the year \times genotype interaction was not statistically significant. The number of seeds in the capsule belonging to the genotypes was 31.3-84.1 seeds capsule⁻¹ in 2018 (experimental mean 55.0 seeds capsule⁻¹), in 2019 25.7-56.7 seeds capsule⁻¹ (mean 41.3 seeds capsule⁻¹), and according to the combined analysis results of the two years, it was 28.5-69.6 seeds capsule⁻¹ (experimental mean 48.1 seeds capsule⁻¹), line 23 (Eskişehir) was the black cumin genotype with the highest number of grains in the capsule (Table 4). It was observed that 14 genotypes taken to study had the number of grains in the capsule above the standard. The values of the genotypes included in the experiment in terms of the number of seeds in the

capsule (28.5-69.6 seeds capsule⁻¹) were similar to the values declared by Kalçın (2003) (91.90-104.05 seeds capsule⁻¹), Ghamarnia et al. (2010) (52.46-64.42 seeds capsule⁻¹), Safaei et al. (2014) (58.73-61.48 seeds capsule⁻¹), and Kamçı (2019) (71.87-102.90 seeds capsule⁻¹). The values reported by Özel et al. (2009) (53.07-89.40 seeds capsule⁻¹), Akgören (2011) (60.5-94.2 seeds capsule⁻¹), and Mehmood et al. (2018) (53.38-106.58 seeds capsule⁻¹) were within the limits and low. It is thought that the difference between the years is due to the precipitation, cold, and dodder grass damage sustained by the plant in different developmental periods.

Number of branches

While the difference between genotypes was at the level of 5% in 2018 in the number of branches in the plant, no statistical difference was detected in 2019. According to the analysis of variance performed by combining the years, 5% significant differences were found between genotypes and 1% in terms of year × genotype interaction between years. In 2018, the number of branches of the genotypes was 2-4.4 pieces plant⁻¹ (experimental mean 3.2 pieces plant⁻¹), in 2019, it was 1.8-3.1 pieces plant⁻¹ (mean 2.1 pieces plant⁻¹), and according to the combined analysis results of the two years, 2.0-3.4 pieces plant⁻¹. While the number of branches varied across the plants (experimental mean 2.6 pieces plant⁻¹), line 4 (Burdur) was the black cumin genotype with the highest number of branches (Table 4). According to the results of the combined analysis, it was found that more than half of the trial material (16 genotypes) reached the number of branches in a single plant above the standard. The values (2.00-3.4 pieces plant⁻¹) of the genotypes in terms of the number of branches, included in the experiment were higher than the values reported by Tavas et al. (2014) (2.96 pieces plant⁻¹); yet close and lower than the values reported by Kalçın (2003) (5.42-6.90 pieces plant⁻¹), Ertaş (2016) (4.15-5.27 pieces plant⁻¹), Özel et al. (2009) (2.30-4.43 pieces plant⁻¹), Akgören (2011) (3.1-4.6 pieces plant⁻¹), Arslan et al. (2011) (1.3-3.5 pieces plant⁻¹), Baytöre and Yaver (2014) (3.45-4.42 pieces plant⁻¹), Koşar and Özel (2018) (2.77-4.63 pieces plant⁻¹), Kamçı (2019) (4.41-5.64 pieces plant⁻¹). Almost all of the experiment was affected by precipitation and weeds in 2019. Still, there was a statistically significant difference at the level of 5% between the 2018 genotypes due to the intense damage caused by the climate only in the populations in some parts of the experiment in 2018. It has been reported in previous studies

that the number of branches, one of the yield criteria, can change depending on the genotype, precipitation, and cultural practices [3,4].

Number of capsules

No statistical difference was found between the genotypes used in the experimental in 2019 in terms of the number of capsules and the combined analysis. In 2018, statistically significant differences were found between the genotypes at the 1% probability limit, between the recurrences at the 5% probability limit, and according to the results of the variance analysis performed by combining the locations, statistically significant differences were found between the years compared to the 1% level. Again in the combined analysis, a statistically significant difference at the 1% probability limit was found in year \times genotype interaction on the number of capsules in the plant. The number of capsules belonging to the genotypes varied between 1.6-3.7 capsule plant⁻¹ in 2018, 1.5-3.3 capsule plant⁻¹ in 2019, and 1.8-2.9 capsule plant⁻¹ in the combined analysis. The average of years was 2.7, 2 and combined 2.4 capsule plant⁻¹, respectively. The black cummin of Line 4 (Burdur) was the genotype with the highest number of branches (Table 4). It was determined that 12 genotypes had more capsules than both Çameli variety and average. The values (1.8-2.9 capsule plant⁻¹) of the genotypes in the experiment in terms of the number of capsules were lower than the values reported by Özel et al. (2009) (2.27-15.97 capsule plant⁻¹), Ghamarnia et al. (2010) (17.52 to 24.24 capsule plant⁻¹), Akgören (2011) (5.6-9.2 capsule plant⁻¹), Arslan et al. (2011) (2.26-5.60 capsule plant⁻¹), Kulan et al. (2012) (2.93-11.05 capsule plant⁻¹), Şahin(2013) (1.1-9.0 capsule plant⁻¹), Baytöre and Yaver (2014) (5.70-7.23 capsule plant⁻¹), Safaei et al. (2014) (5.6-6.1 capsule plant⁻¹), Tavas et al. (2014) (7.62-8.55 capsule plant⁻¹), Ertaş (2016) (7.91-9.44 capsule plant⁻¹), Koşar and Özel (2018) (4.03-7.63 capsule plant⁻¹), Mehmood et al. (2018) (28.47-39.38 capsule plant⁻¹), Kamçı (2019) (8.11-11.53 capsule plant⁻¹). There is a close relationship between the number of capsules and the number of branches, another parameter of the yield criteria. For this reason, the low figures in our branch number results due to climate and weeds were also proportionally low in the number of capsules, and the major genotype was the number 4 genotype, just like the number of branches.

Seed yield

In seed yield per decare, statistically significant differences were found between genotypes at the 1% probability limit in both years and 1% between replications in 2018. According to the results of the combined analysis of variance of the years, statistically significant differences were found between the genotypes, years, and year \times genotype interaction at the 1% significance level and between the recurrences at the 5% probability limit. The seed yield of the genotypes ranged between 126.8-544.8 kg ha⁻¹ (experimental mean 289.3 kg ha⁻¹) in 2018, 188.2-624.4 kg ha⁻¹ (experimental mean 378.9 kg ha⁻¹) in 2019, and 194.5-505.9 kg ha⁻¹ according to the combined analysis results of the two years, the experimental (average 334.1 kg ha⁻¹) number 1 (Denizli) black cumin line was the most fertile black cumin genotype (Table 4). The annual average (334.1 kg ha⁻¹) of 14 genotypes resulted with higher seed yield compared to Çameli variety (328.1 kg ha⁻¹) with the number 16.

Our yield values in the experiment were found to be within the limits of the values reported by (194.5-505.9 kg ha⁻¹) Ertuğrul (1986) (273 kg ha⁻¹), Özel and Demirbilek (2000) (358.6-439.5 kg ha⁻¹), Özel et al. (2001) (336.7-416.7 kg ha⁻¹), Baytöre and Yaver (2014) (284-435 kg ha⁻¹), Ertaş (2016) (301-538 kg ha⁻¹) and high. Also, they were lower than the reported values by Kalçın (2003), (683.9-770.1 kg ha⁻¹), Özel et al. (2009) (1406.3-2482.3 kg ha⁻¹), Akgören (2011) (905-1883 kg ha⁻¹), Kulan et al. (2012) (676.6-903.3 kg ha⁻¹), Taqi (2013) (829-1270 kg ha⁻¹), Tavas et al. (2014) (557.7-689.1 kg ha⁻¹), Tektaş (2015) (719-1188 kg ha⁻¹) and Gülhan and Taner (2020) (623 kg ha⁻¹).

It is thought that the yield values obtained in the research are lower than in some studies due to the adverse weather conditions experienced in both years and the intense dodger weed damage.

Fixed oil ratio

Regarding fixed oil ratio, statistically significant differences were found at the 1% probability limit in genotypes in both years and 1% in terms of recurrences only in 2019. According to the results of the variance analysis performed by combining the years, there were 1% differences in genotypes between years and year \times genotype interaction and 5% between replications. While the fixed oil ratio of genotypes was 21.8%-40.2% (experimental mean 28.3%) in 2018, 27.8%-40.6% (mean 34.8%) in 2019, and according to the combined

analysis results of the two years, it ranged between 27.2% and 35.3% (experimental mean 31.5%), line 28 (Kırıkale) was the black cumin genotype with the highest fixed oil content (Table 4). According to the combined analysis of the materials in the experiment, it was determined that 2/3 (20 genotypes) had a higher fixed oil content than Çameli variety. In terms of fixed oil ratio, the values (27.2-35.3%) of the genotypes in the experiment were similar and higher than the values reported by D'Antuono et al. (2002) (13-19.7-22.9%), Arslan et al.(2011) (21.70-31.50%), Akgören (2011) (19.51-26.34%), Baytöre and Yaver (2014) (16.71-30.08%), Kamçı (2019) (29.58-32.42%). It was found close and low compared to the values reported by Kızıl et al. (2008) (30.2 to 37.9%), Matthaus and Özcan (2011) (28.0- 36.4%), Kulan et al. (2012) (38.91-40.58%), Şahin (2013) (26.90-44.00%), Gharby et al. (2015) (27-37%), Tavas et al. (2014) (36.09-36.37%), Ertaş (2016) (37.5-37.6%), Gülhan and Taner (2020) (two-year average values 26.8%-37.3%). Although similar results were obtained in terms of fixed oil ratio in both years, it is thought that the difference between the lines is due to the genetic structure of the populations.

Fixed fatty acid composition

In the component analysis of fixed oil of the black cumin genotypes in 2018 and 2019, it was determined that the main components were linoleic, oleic, palmitic, and stearic acids. Their rates are respectively 45.45-55.62%, 18.83-25.01%, 6.95-11.72%, and 3.50-4.77%. The highest value in linoleic acid was number 18, and line number 11 in oleic acid was the Burdur line (Table 3).

In previous studies, the main components and ratios of black cumin oil were determined by Kızıl et al. (2008) linoleic acid 43.34%-51.50%, Şahin (2013) linoleic 54.6%, oleic 27.7% and palmitic acid 13.4%, stearic acid 3.46%, Tavas et al. (2014) linoleic acid 57.92%, oleic acid 23.07%, Ertaş (2016) linoleic 57.98%, oleic 24.50% and palmitic acid 12.31%. Safaei et al. (2017) determined linoleic acid as 55.71% in autumn sowing, 55.5% in spring planting, Kamçı (2019) linoleic as 52.47%-55.48%, oleic as 20.57-28.32%, palmitic acid as 12.20-12.63% and stearic acid as 2.99-3.53%. When the results obtained from the research were compared with the previous studies, it was determined that while there were similar figures, there were also positive differences in terms of the main components. These differences are thought to be due to genetic differences.

Table 3. Average fatty acid composition of *Nigella sativa* genotypes in the experiment (%)

Genotypes	Oleic Acid (C18:1n9c)	Linoleic Acid (C18:2n6c)	Palmitic Acid (C16:0)	Stearic Acid (C18:0)
1	23.88	54.15	11.03	4.26
2	22.71	54.30	11.16	4.33
3	22.96	52.73	10.56	4.31
4	23.41	52.79	10.89	4.55
5	22.75	54.26	10.83	4.14
6	23.83	51.46	10.82	4.21
7	22.41	53.53	10.80	4.23
8	23.89	50.93	10.54	4.25
9	21.28	55.19	11.08	4.16
10	22.92	52.89	10.75	4.03
11	25.01	48.54	6.95	4.77
12	22.20	54.21	11.22	4.21
13	21.93	54.13	11.31	4.08
14	21.44	55.11	11.68	4.14
15	22.62	54.17	11.32	4.01
16	20.45	53.96	11.00	4.31
17	22.45	55.28	11.37	4.18
18	22.10	55.62	11.34	4.19
19	22.62	53.69	11.17	4.18
20	18.83	45.45	9.39	3.50
21	22.74	54.59	11.49	3.94
22	22.34	54.11	11.42	4.09
23	21.96	54.82	11.72	4.10
24	22.45	53.65	11.37	4.09
25	22.36	53.62	11.26	4.11
26	23.77	54.34	11.43	3.96
27	22.06	54.24	11.22	4.05
28	21.79	53.90	11.19	4.19
29	22.70	54.27	11.19	3.93
30	22.69	55.12	11.23	3.89
Çameli	23.08	53.73	10.89	4.16
Mean	22.50	53.51	10.96	4.15

Table 4. Average figures of yield and yield components of *Nigella sativa* genotypes in experiments

G	Plant Height (cm)		Seed Yield (kg ha ⁻¹)		First Capsule Height (cm)		Thousand Seed Weight (g)		Number of Branches (pieces plant ⁻¹)		Number of Capsules (capsules plant ⁻¹)		Number of Seeds in Capsule (seeds capsule ⁻¹)		Emergence Time (day)		Maturation Time (day)		Fixed Oil Ratio (%)	
1	30.1	a-f	505.9	a	23.5	a-c	2.6	a-j	2.8	a-f	2.7	a-d	56.3	b-d	28.0	d-g	136.5	e	31.7	c-g
2	29.1	b-g	398.3	a-f	22.8	a-e	2.7	a-h	2.7	b-f	2.4	a-f	51.7	b-h	29.2	a-f	137.5	b-e	33.1	a-e
3	30.1	a-e	440.9	a-c	24.4	a-c	2.8	a-h	2.7	b-f	2.6	a-e	53.7	b-e	29.2	a-f	136.5	e	32.5	b-f
4	26.4	e-i	490.3	a	22.0	b-e	2.5	e-k	3.4	a	2.9	a	53.6	b-f	28.7	b-g	137.3	c-e	33.3	a-d
5	22.3	i-m	215.6	k-l	17.1	f-i	2.9	a-e	2.7	b-f	2.6	a-e	43.6	e-k	30.2	a-b	137.2	c-e	30.8	e-k
6	24.8	h-l	282.5	g-l	19.1	d-g	2.9	a-f	3.0	a-d	2.9	a-b	49.1	b-i	29.3	a-e	137.2	c-e	31.1	d-j
7	20.2	m-o	329.6	d-j	14.9	h-j	2.8	a-g	2.3	e-g	2.0	e-f	38.5	i-l	29.3	a-e	137.7	b-e	29.7	g-k
8	19.9	m-o	298.4	f-l	13.0	i-j	2.9	a-f	2.7	b-f	2.3	a-f	38.6	i-l	29.8	a-c	137.7	b-e	31.9	c-g
9	32.2	a-c	406.5	a-f	24.8	a-c	2.4	g-l	2.7	a-f	2.5	a-f	58.1	b	28.2	c-g	137.8	b-e	33.2	a-d
10	30.2	a-e	415.5	a-d	23.9	a-c	2.0	m	2.6	b-g	2.4	a-f	57.4	b	27.7	e-g	136.5	e	33.7	a-c
11	17.7	n-o	283.6	g-l	11.8	j	3.0	a-b	2.0	g	1.8	f	35.5	k-l	29.9	a-c	137.6	b-e	27.2	l
12	26.1	e-j	366.2	b-g	21.7	b-e	2.3	i-m	2.4	d-g	2.4	a-f	50.0	b-h	27.5	f-g	136.5	e	30.5	f-k
13	28.8	c-h	356.2	c-g	23.8	a-c	2.0	l-m	2.5	c-g	2.1	d-f	54.1	b-e	27.2	g	136.5	e	31.0	d-k
14	26.6	e-h	349.3	c-h	21.5	b-e	2.0	l-m	2.5	b-g	2.2	c-f	52.5	b-h	27.7	e-g	137.3	c-e	28.8	i-l
15	22.0	j-n	338.1	c-i	15.6	g-j	2.6	a-j	2.4	d-g	2.3	a-f	42.7	g-k	29.3	a-e	137.5	b-e	28.7	k-l
16	20.9	l-o	276.2	g-l	14.7	h-j	2.6	a-j	2.9	a-e	2.5	a-f	46.5	c-j	28.7	b-g	137.7	b-e	29.3	h-l
17	21.0	k-o	465.3	a-b	15.2	g-j	2.8	a-g	2.5	c-g	2.3	a-f	42.4	g-k	28.5	b-g	137.5	b-e	28.8	i-l
18	19.4	m-o	246.9	h-l	13.0	i-j	2.9	a-d	2.4	d-g	2.0	e-f	42.8	f-k	30.2	a-b	138.2	b-e	28.7	j-l
19	17.1	o	226.5	j-l	11.6	j	3.0	a	2.1	f-g	1.9	e-f	36.0	j-l	29.7	a-d	137.8	b-e	30.4	f-k

*: P<0.05, **: P<0.01, Y: Year, G: Genotypes, R: Recurrences, NS: Not Significant

Table 4 (Continue.) Average figures of yield and yield components of *Nigella sativa* genotypes in experiments

G	Plant Height (cm)		Seed Yield (kg ha ⁻¹)		First Capsule Height (cm)		Thousand Seed Weight (g)		Number of Branches (pieces plant ⁻¹)		Number of Capsules (capsules plant ⁻¹)		Number of Seeds in Capsule (seeds capsule ⁻¹)		Emergence Time (day)		Maturation Time (day)		Fixed Oil Ratio (%)	
20	19.8	m-o	194.7	l	15.5	g-j	2.6	a-j	2.6	b-g	2.2	b-f	38.8	i-l	29.8	a-c	138.5	b-d	31.1	d-i
21	33.3	a-b	231.0	i-l	26.4	a	2.1	k-m	2.8	a-e	2.5	a-f	56.5	b-c	28.5	b-g	141.3	a	30.5	f-k
22	26.6	e-h	405.6	a-f	21.2	c-f	2.5	d-j	2.5	c-g	2.2	c-f	49.4	b-i	29.2	a-f	137.7	b-e	32.1	c-f
23	32.0	a-d	333.4	c-j	26.5	a	2.4	g-l	3.2	a-b	2.8	a-c	69.6	a	30.7	a	141.7	a	33.5	a-c
24	30.3	a-e	318.1	d-k	24.8	a-c	2.5	f-k	2.3	e-g	2.2	c-f	53.2	b-g	28.3	c-g	138.0	b-e	33.4	a-d
25	25.2	g-k	288.5	g-l	18.8	e-h	2.6	a-j	2.9	a-e	2.4	a-f	45.6	d-k	29.7	a-d	137.3	c-e	31.5	c-h
26	25.9	f-j	311.5	d-k	21.3	b-e	2.5	c-j	3.1	a-c	2.7	a-d	49.0	b-i	28.2	c-g	139.2	b	34.9	a-b
27	29.9	a-f	300.3	e-l	25.4	a-b	2.2	j-m	2.5	c-g	2.3	a-f	52.6	b-h	27.3	g	137.3	c-e	32.7	b-f
28	33.5	a	407.7	a-e	26.6	a	2.4	h-m	3.0	a-d	2.7	a-d	54.2	b-e	29.3	a-e	138.8	b-c	35.3	a
29	27.9	d-h	350.9	c-h	23.0	a-d	2.6	b-j	2.7	a-f	2.4	a-f	41.9	h-k	28.2	c-g	136.8	d-e	34.9	a-b
30	18.8	m-o	194.5	l	12.6	j	2.9	a-c	2.5	c-g	2.2	a-f	28.5	l	30.2	a-b	137.5	b-e	32.4	c-f
Ç	28.2	c-h	328.1	d-j	22.8	a-e	2.6	a-i	2.6	b-g	2.4	a-f	49.9	b-h	28.8	b-g	138.5	b-d	30.6	f-k
Mean	25.7		334.1		20.0		2.6		2.6		2.4		48.1		28.9		137.8		31.5	
F Value	**		**		**		**		*		NS		**		**		**		**	
CV	14.5		28.5		18.2		14.3		21.9		24.1		19.7		5.3		1.1		6.7	
R	**		*		NS		**		NS		NS		NS		NS		**		*	
Y	**		**		**		**		**		**		**		**		**		**	
Y X G	**		**		**		NS		**		**		NS		NS		NS		**	

*: P<0.05, **: P<0.01, Y: Year, G: Genotypes, R: Recurrences, NS: Not Significant, Ç: Çameli

Conclusion

Black cumin seeds, fixed and essential oil have been used in spices, food, cosmetics, and medical fields since ancient times, so they are versatile medicinal plants whose value is increasing every year. For this reason, as in other medicinal plants, quality rather than yield comes to the fore in black cumin as well. Fertilizers and herbicides used pose a risk in terms of food and drugs. This study aimed to increase the black seed cultivation area and production by identifying the genotypes grown in accordance without fertilizers and pesticides, high quality, productive, machine harvested, and suitable for the region. This study tried to identify the yield and yield criteria of different advanced black cumin (*Nigella sativa* L.) lines grown in the ecological conditions of Ankara. According to the results of two years, the average values yield 334.1 kg ha⁻¹, plant height 25.7 cm, number of capsules 2.4 capsule plant⁻¹, the height of the first pod 20 cm, thousand seed weight 2.6 g, number of branches 2.7 pieces plant⁻¹, number of seeds in capsule 48.1 seeds capsule⁻¹, emergence time 28.9 days, maturation time 137.8 days, oil rate 31.5 %, fatty acid components linoleic acid 53.51%, oleic acid 22.50%, palmitic acid 10.96% and stearic acid 4.15%. The obtained values are consistent with many works of literature where fertilization practices are applied. It is thought that the statistical differences between the lines, years, and recurrences may be caused by the adverse and untimely climatic conditions observed during the two years, the genetic differences of the materials, and the difference in the genotypes to these conditions. *Nigella sativa* is a plant that is planted for both its seeds and the fixed oil extracted from these seeds. For this reason, the main purpose of cultivation is to have both characteristics higher and superior to the existing varieties. It has been determined as the result of the study that, out of 31 genotypes examined, black cumin genotypes with the number 1 (Denizli), 4 (Burdur), 17 (Borsa) and 3 (Burdur) respectively became prominent in terms of seed yield and black cumin genotypes with the number 28 (Kırıkkale), 29 (Ankara) and 26 (Egypt) became prominent in terms of essential oil ratio and that they are the genotypes that can be suggested for breeding studies to be continued for the region. In addition, while the genotypes with the number 28 (Kırıkkale)-21 (Borsa)-9 (Denizli) showed maximum performance and took the first three place in terms of plant height, those with the number 28 (Kırıkkale)-23 (Eskişehir)-21 (Borsa)

took the first three place in terms of capsule height, genotypes with the number 19 (Borsa)-11 (Burdur)-30 (Ankara) took the first three place in terms of weight per thousand, genotypes with the number 4 (Burdur)-23 (Eskişehir)-26 (Egypt) took the first three place in terms of number of branches on the plant, genotypes with the number 4 (Burdur)-6 (Syria)-23 (Eskişehir) took the first three place in terms of number of capsules on a plant, genotypes with the number 23 (Eskişehir)-9 (Denizli)-10 (Burdur) took the first three place in terms of number of grains per capsule, genotypes with the number 13 (Konya)-27 (Burdur)-12 (Konya) had the earliest emergence time and genotypes with the number 1 (Denizli)-3 (Burdur)-10 (Burdur) had the earliest harvest maturation time. In terms of the fixed fatty acids, black cumin genotype with the highest oleic acid ratio was measured in Burdur genotype with the number 11 (25.01%), and the highest linoleic fatty acid was measured in black cumin genotype (55.62%) with the number 18, which was obtained from Borsa. There seems to be promise for the genotypes that stood out in our study in the studies to come in future cultivar development studies.

Abbreviations

Y: Year; G: Genotypes; R: Recurrences; NS: Not Significant; Ç: Çameli; TARM: Central Research Institute of Field Crops.

Availability of data and material

Please contact the corresponding author for any data request.

Funding and Acknowledgments

This research was supported by the General Directorate of Agricultural Research and Policies (TAGEM) with project no: TAGEM/17/A07/P06/11. The authors thank to TAGEM for funding and supporting.

References

1. Öztürk, M., ve ark., Tıbbi ve Aromatik Bitkilerin Dış Ticaretimizdeki Yeri. Tıbbi ve Aromatik Bitkiler Sempozyumu Bildiri Kitabı, 2012. S.33 - 44.
2. Anonim, 2021. TÜİK, Türkiye İstatistik Kurumu (www.tuik.gov.tr. Erişim Tarihi 19.01.2021).
3. Yılmaz, G., Tıbbi Aromatik Bitkiler Yetiştiriciliğinde Yeni Yaklaşımlar. Tıbbi ve Aromatik Bitkiler. Lisansüstü Ders Notları (Basılmamış). 2008, Tokat, Türkiye: GOÜ Ziraat Fakültesi, Fen Bilimleri Enstitüsü, Tarla Bitkileri Anabilim Dalı.
4. Küçükemre, D. 2009. Çörek otunda (*Nigella sativa* L.) farklı sıra aralıkları ve ekim normunun verim ve kalite üzerine etkileri. Yüksek Lisans Tezi. Gaziosmanpaşa Üniversitesi, Fen Bilimleri Enstitüsü, Tokat.
5. Ertuğrul, Y., 1986. Çörekotunda (*N. damascena* L.) Farklı Ekim Zamanlarının Verim ve Kaliteye Etkisi Üzerine Bir Araştırma. Çukurova Üniv. Fen Bilimleri Ens. Yüksek Lisans Tezi 34s.
6. Özel, A. ve T. Demirebilek, Harran Ovası Kuru Koşullarında Bazı Tek Yıllık Baharat Bitkilerinin Verim ve Bazı Agronomik Özelliklerinin Belirlenmesi. Harran Üniversitesi Ziraat Fakültesi Dergisi, 2000. 4 (3-4), 21-32.

7. Özel, A., T. Demirbilek. and O. Çopur, Determination of Yield and Agronomic Characters of Some Annual Spice Plants Under The Harran Plain Conditions. Workshop on agricultural and Quality Aspects of Medicinal and Aromatic Plants, 2001. May 29 - June 01 2001, s. 151 - 158. Adana-Turkey.
8. Baytöre, F. ve S. Yaver, 2014. Bazı Çörekotu (*Nigella sativa* L.) Populasyonlarının Verim Ve Verim Kriterlerinin Belirlenmesi. II. Tıbbi Aromatik Bitkiler Sempozyumu Bildiriler Kitabı, 2014. Yalova.
9. Ertaş, M.E., 2016. Tokat Kazova Ekolojik Koşullarında Kışlık ve Yazlık Ekilen Çörek Otu (*Nigella* sp.) Genotiplerinin Agronomik Ve Kalite Özelliklerinin Belirlenmesi. Yüksek Lisans Tezi, G.O.P. Üniv. Fen Bilimleri Enstitüsü, Tarla Bitkileri Anabilim Dalı, Tokat 62.
10. Kalçım F.T., 2003. İki Çörekotu Türünde (*Nigella sativa* L., *Nigella damascena* L.) Ekim Sıklıklarının Verim ve Verim Öğelerine Etkisi. Yüksek Lisans Tezi, A.Ü Fen Bilimleri Enstitüsü, Tarla Bitkileri Anabilim Dalı, Ankara.
11. Özel A., ve ark., Farklı Sıra Aralığı ve Tohumluk Miktarlarının Çörek Otunda (*Nigella sativa* L.) Verim ve Bazı Tarımsal Karakterlere Etkisi. Harran Üniversitesi Ziraat Fakültesi Dergisi, 2009. 13 (1): sayfa: 17-25.
12. Akgören, G., 2011. Bazı çörekotu (*Nigella sativa* L.) populasyonlarının tarımsal özellikleri. Yüksek Lisans Tezi. Eskişehir Osman Gazi Üniversitesi Fen Bilimleri Enstitüsü. Tarla Bitkileri Anabilim Dalı. Eskişehir. S. 92.
13. Kulan, E.G., ve ark., Kuru Koşullarda Yetiştirilen Çörek Otu (*Nigella sativa* L.)'nun Bazı Agronomik ve Kalite Özellikleri. Tıbbi ve Aromatik Bitkiler Sempozyumu, 13 - 15 Eylül, 2011, Gaziosmanpaşa Üniversitesi Ziraat Fakültesi, Tokat. 2012
14. Taqi, H. (2013). Samsun Koşullarında Bazı Çörekotu (*Nigella sativa* L.) Popülasyonlarında Önemli Tarımsal ve Kalite Özelliklerinin Belirlenmesi. Yüksek Lisans Tezi, Ondokuz Mayıs Üniversitesi, Fen Bilimleri Enstitüsü, Tarla Bitkileri Anabilim Dalı, Samsun.
15. Tavas, N., N. Katar, ve Z. Aytaç, Eskişehir Ekolojik Koşullarında Yetiştirilen Çörek Otu (*Nigella sativa* L.)'nda Verim, Verim özellikleri ve Sabit Yağ Bileşenleri. II. Tıbbi ve Aromatik Bitkiler Sempozyumu Bildiri Kitabı, 2014. 23 - 25 Eylül, 2013, s. 623 - 629, Yalova.
16. Tektaş, E., 2015. Harran Ovası Koşullarında Birim Alandaki Tohum Sayısının Çörek Otu (*Nigella sativa* L.)'nun Verim ve Bazı Bitkisel Özelliklerine Etkisi. Yüksek Lisans Tezi, Harran Üniversitesi Fen Bilimleri Enstitüsü, Şanlıurfa 40.
17. Gülhan, M.F. ve S. Taner, Aksaray Ekolojik Koşullarında Farklı Ekim Zamanlarında Çörek Otu'nun (*Nigella sativa* L.) Verim, Kimyasal İçerik Ve Antioksidan Kapasitesinin Belirlenmesi. EJONS International Journal on Mathematic, Engineering and Natural Sciences, 2020. Year 4 (2020) Vol:15, Issued in September, Page: 475 - 488.
18. Koşar, İ. ve A. Özel, Çörekotu (*Nigella sativa* L.) Çeşit ve Popülasyonlarının Karakterizasyonu: I. Tarımsal Özellikler. Harran Tarım ve Gıda Bilimleri Dergisi, 2018. 22 (4), 533-543.
19. Özel, A., ve ark., Harran Ovası Koşullarında Bazı Baharat Bitkilerinde Optimum Tohumluk Miktarının Belirlenmesi. Kesin Sonuç Raporu. 2007, Şanlıurfa, HR.Ü. Ziraat Fakültesi Tarla Bitkileri Bölümü.
20. Koşar, İ., ve ark., Harran Ovası Kuru Koşullarında Çörek otu (*Nigella sativa* L.) Populasyonlarında Verim ve Bazı Tarımsal Karakterlerin Belirlenmesi. 10. Tarla Bitkileri Kongresi. 10 - 13 Eylül 2013.
21. Şahin, B., 2013. Farklı Ekim Zamanlarında Yetiştirilen Bazı Tıbbi Bitkilerin Verim Ve Kalite Özelliklerinin Belirlenmesi. Yüksek Lisans Tezi, Konya Selçuk Üniv. Fen Bilimleri Enstitüsü, Tarla Bitkileri Anabilim Dalı, Konya 153.
22. Ghamarnia, H., H. Khosravy and S. Sephiri, Yield And Water Use Efficiency of (*Nigella sativa* L.) Under Different Irrigation Treatments In A Semi Arid Region In The West of Iran. Journal of Medicinal Plants Research, 2010. 4 (16): 1612 - 1616.

23. Arslan, Y., D. Katar ve İ. Subaşı, Çörek Otu (*Nigella sativa* L.)’nda Farklı Ekim Zamanlarının Verim ve Bazı Bitkisel Özellikler Üzerine Etkileri. Tıbbi ve Aromatik Bitkiler Sempozyumu, 13 - 15 Eylül, 2011, Gaziosmanpaşa Üniversitesi Ziraat Fakültesi, Tokat.
24. Mehmood, A., et al., Sowing Time And Nitrogen Application Methods Impact On Production Traits of Kalonji (*Nigella sativa* L.), 2018. Pure and Applied Biology, 7 (2): 476 - 485.
25. Kamçı, G., 2019. Çörekotu (*Nigella sativa* L.)’da Farklı Ekim Zamanı Ve Sulamanın Verim Ve Kalite Kriterleri Üzerine Etkisinin Belirlenmesi. Yüksek Lisans Tezi, Dicle Üniv. Fen Bilimleri Enstitüsü, Tarla Bitkileri Anabilim Dalı, Diyarbakır 50.
26. Safaei, Z., et al., The Effect Of Different Irrigation Intervals And Anti-Transpiration Compounds On Yield And Yield Components Of Black Cumin (*N. sativa* L.). International journal of Advanced Biological and Biomedical Research, 2014. 4 (2): 326-335.
27. D’Antuono, L.F., A. Moretti and A.F.S. Lovato, Seed Yield, Yield Components, Oil Content and Essential Oil Content and Composition of *Nigella sativa* L. and *Nigella damascena* L. Industrial Crops and Products, 2002. 15: 59-69.
28. Kızıllı, S., et al., Effects of Sowing Periods and P Application Rates on Yield and Oil Composition of Black Cumin (*N. sativa* L.). Journal of Food, Agriculture & Environment, 2008. 6 (2): 242-246.
29. Matthaus, B. and M.M. Özcan, Fatty Acids, Tocopherol and Sterol Contents of Some *Nigella Species* Seed Oil. Czech Journal of Food Science, 2011. 29 (2): 145-150.
30. Gharby, S., et al., Chemical investigation of *Nigella sativa* L. seed oil produced In Morocco. Journal of the Saudi Society of Agricultural Sciences, 2015. 14: 172-177.
31. Telci, İ., 1995. Tokat Şartlarında Farklı Ekim Sıklığının Çörekotu (*Nigella sativa* L.)’nda Verim, Verim Unsurları ve Bazı Bitkisel Özelliklerine Etkisi. Yüksek Lisans Tezi, G.O.P. Üniv. Fen Bilimleri Enstitüsü, Tarla Bitkileri Anabilim Dalı, Tokat 51.
32. Safaei, Z., et al., The Effect of Planting Seasons on Quantitative and Qualitative Characteristics of Black Cumin (*Nigella sativa* L.). Journal of Medicinal Plants and By-products, 2017. 1: 27-33.

Oltulu C., M. Akıncı, B. Elvan, Antitumor Activity of Etoposide, Puerarin, Galangin and Their Combinations in Neuroblastoma Cells, International Journal of Life Sciences and Biotechnology, 2022. 5(3): p. 407-423. DOI: 10.38001/ijlsb.1089164

Antitumor Activity of Etoposide, Puerarin, Galangin and Their Combinations in Neuroblastoma Cells

Cagatay Oltulu^{1*} , Melek Akıncı² , Elvan Bakar³ 

ABSTRACT

In this study we aimed that the evaluation of the mRNA expression levels of apoptosis-related genes by treatment with Etoposide, a topoisomerase 2 α inhibitor, galangin and puerarin, plant-based antioxidants, in neuroblastoma *in vitro*. The effects of etoposide, galangin, puerarin and combinations of etoposide+galangin and etoposide+puerarin on neuroblastoma and astrocyte cells' apoptotic process were examined. IC₅₀ dose was determined by MTT test in neuroblastoma and healthy astrocyte lines from *Mus musculus*. Expressions of apoptosis-related gene topoisomerase 1 and 2 α , caspase 3, caspase 9, BAX, BCL-2, IL-1 β , TNF α , p53 were observed in astrocyte and neuroblastoma cells at the dose of neuroblastoma IC₅₀. The neuroblastoma IC₅₀ dose was lower than the healthy astrocyte cell IC₅₀ dose in all groups. mRNA expression of apoptosis-related genes increased in the neuroblastoma cancer line. The mRNA expression changes in the astrocyte cell line did not cause apoptosis. Antiproliferative effect of etoposide+galangin and etoposide+puerarin combinations were decreased relative to etoposide group. We concluded that single therapy of galangin and puerarin may be promising in the treatment of neuroblastoma.

ARTICLE HISTORY

Received

17 March 2022

Accepted

17 June 2022

KEY WORDS

Etoposide,
galangin,
puerarin,
neuroblastoma,
astrocyte

Introduction

Neuroblastoma is a solid tumor originating from the peripheral sympathetic system mostly seen in children less than 5 years of age [1, 2]. It is the most common extracranial tumors in childhood [3]. In the treatment of neuroblastoma, such methods like chemotherapy, radiation therapy, surgery, immunotherapy, and stem cell transplantation are used. While better treatment results are obtained for those in the low and medium risk groups, the long-term survival rate in the high-risk group neuroblastoma is 50%. Therefore, there is a need to develop new treatment methods [4].

Topoisomerase 1 and 2 are essential for cell survival. It is involved in DNA metabolism and regulation of its topological structure and inhibition of these enzymes creates adverse

¹ Trakya University, Faculty of Pharmacy, Department of Pharmaceutical Toxicology Edirne, Turkey.

² Trakya University, , Faculty of Pharmacy, Department of Pharmacology, Edirne, Turkey.

³ Trakya University, , Faculty of Pharmacy, Department of Basic Phamaceutical Sciences, Edirne, Turkey.

*Corresponding Author: Cagatay OLTULU, e-mail: cagatayo@trakya.edu.tr

effects on cell viability [5]. Topoisomerase 1 disrupts the structure of the DNA by destructing single strand and topoisomerase 2 disrupts the structure of the DNA by destructing double strands to regulate the topological structure of DNA [5]. Etoposide, known to be a topoisomerase 2 inhibitor, belongs to the class of epipodophyllotoxin [6]. Etoposide acts on topoisomerase 2, forming a covalent complex between topoisomerase 2 and DNA [1]. Etoposide inhibits the catalytic activity of topoisomerase 2, creates DNA damage and by impairing DNA metabolism, disrupts transcription and replication. Since etoposide forms a DNA complex with a high amount of topoisomerase 2, it converts topoisomerase 2, an essential enzyme, into a toxic compound. Cells that express topoisomerase 2 at a higher level are more sensitive. The cell may develop resistance against topoisomerase 2 inhibitor drugs by reducing topoisomerase expression [6].

Apoptosis is a form of programmed cell death of damaged and unwanted cells to prevent the formation of substances that will damage the surrounding tissue. Induction of apoptosis is one of the ways used in cancer treatment. The damaged cell identifies the DNA damage caused by topoisomerase 2-DNA complex created by etoposide and it is eliminated via apoptosis [7]. p53 protein can contribute to DNA repair, cell cycle arrest, or apoptosis development [8]. In case of DNA damage, the tumor suppressor gene p53 tries to repair the damage by stopping the cell cycle in G1 phase, and apoptosis occurs if the repair is not successful [9]. Apoptosis can be triggered in two ways. The first one is through an intrinsic pathway. The B-cell lymphoma 2 (BCL-2) protein is antiapoptotic and keeps the cell alive by regulating the potential of the mitochondria outer membrane. Proapoptotic proteins such as BCL-2 associated X (BAX) are normally inactive. Due to various signals, antiapoptotic proteins are suppressed by proapoptotic proteins. BAX protein, which is kept inactive by BCL-2, gets activated with other proapoptotic proteins, leads changes in membrane potential. This leads to activation of initiator caspases such as caspase 9 and effector caspases such as caspase 3, causing to the breakdown of cellular proteins and ultimately apoptosis. The second way is the extrinsic pathway. Apoptosis cascade from the extrinsic pathway is activated by the activation of death receptors such as Tumor Necrosis Factor (TNF) located on the cell surface.

Galangin is reported as plant-based antioxidants induce apoptosis in cancer cells [10, 11]. Galangin is a flavonol, a type of flavonoid, which is antiproliferative, antimutagenic, anticlastogenic, antigenotoxic, antioxidant, neuroprotective and has free radical capturing

quality [10-13]. It is stated that it induces apoptosis of hepatocellular carcinoma cells (HEPG2) in the melanoma cell line [12, 14]. It is also reported that galangin inhibits cell progression in retinoblastoma and induces apoptosis by activating protein of human phosphatase and tensin homolog (PTEN) and caspase 3 pathways [15]. The puerarin found in Pueraria is an isoflavonoid. It is reported that it has antioxidant and estrogenic activity, anti-inflammatory, antidiabetic, and anticancer effects [16, 17].

We hypothesized that combination of etoposide, galangin, puerarin and galangin+puerarin combination with etoposide may have apoptotic and antiproliferative effect on neuroblastoma cell line while do not have apoptotic effect at same dose on healthy astrocyte cell line. The aim of our study was to investigate the effects of etoposide, galangin, puerarin and their combinations with etoposide for 24 hours on apoptotic process in neuroblastoma line and in healthy astrocyte cell lines at the dose of neuroblastoma IC₅₀.

Material and Methods

Groups

The study was planned in six groups as control, etoposide, galangin, puerarin, etoposide+galangin combination and etoposide+puerarin combination.

Chemicals

HAMS F 12 (318-010-CL), Eagle's Minimum Essential Medium (EMEM) (320-026-CL) and trypsin/EDTA (325-542-EL) from Multicell (Wisent Bioproducts, St-Bruno, QC, Canada); Dulbecco's modified Eagle's medium (DMEM) (320-026-CL), L-glutamine (Gibco 25030081), fetal bovine serum (FBS) (Gibco 26140079) and penicillin-streptomycin (Gibco 15070063) from Gibco (Thermo Fisher Scientific, Waltham, MA, USA); Thiazolyl Blue Tetrazolium Bromide (MTT) were obtained from Biocompare (New York, USA). Etoposide (Sigma E1383), galangin (Sigma 282200) and puerarin (Sigma 82435), was obtained from Sigma (St. Louis, MO, USA). Phosphate buffered saline (PBS) (Merck 524650) and dimethyl sulfoxide (DMSO) (Merck 67-68-5) were taken from Merck-Millipore (Darmstadt, Germany). The PureLink RNA Mini Kit (121-830-18A) was supplied from Invitrogen (Thermo Fisher Scientific, Waltham, MA, USA); SYBR Select Master Mix and High Capacity cDNA Reverse Transcription Kit (8368814) from Applied Biosystems (Thermo Fisher Scientific, Waltham, MA, USA).

Cell culture

Mus musculus brain neuroblastoma cell line (N1E-115; ATCC® CRL-2263™) and healthy *Mus musculus* brain astrocyte cells (C8-D1A; ATCC® CRL-2541™) 5% heat-inactivated fetal bovine serum (FBS); nutrient medium contains 100 IU/ml penicillin, 10 mg/ml streptomycin and 1% L-glutamine, 1:1 ratio of Eagle's Minimum Essential Medium (EMEM), DMEM, HAMS F12 are seeded in flasks and they are placed in the incubator that contains 95% moisture and 5% CO₂ at 37 °C. Our study started in the 5th passage and ended in the 12th passage.

Determination of substance concentrations to be administered to cell lines by MTT method

In order to determine IC₅₀ values of all groups to be used in the study, 180 µL cells were seeded in 96 well plates to have 1x10⁶ cells in each well, and they were left to incubate for 24 hours to enable the cells to adhere onto the plate wells. Etoposide, galangin, puerarin were prepared as an aqueous solution containing 0.01% DMSO. Combinations of etoposide+galangin and etoposide+puerarin were prepared in a 1:1 ratio (v/v). All substances were administered to all groups except for the control group, in a volume of 20 µl as 1.25 µM, 2.5 µM, 5 µM, 10 µM, 20 µM and were left in the incubator (37 °C, 5% CO₂) for 24 hours. An aqueous solution containing 0.01% DMSO was applied to the control group. After 3 hours, 200 µl of 0.01% DMSO was added to dissolve the formazan crystals and the absorbance value was determined at 492 nm with the microplate reader (Thermo Scientific Multiskan Go). The control group was considered 100% alive and the IC₅₀ dose was calculated by probit analysis. MTT test was run in four replicates in all groups.

RNA isolation and cDNA synthesis

Neuroblastoma and astrocyte cells were seeded 3 times in culture plates to have 3x10⁶ cells in each well. After 24 hours, the chemical applications of the experimental groups were administered at the dose of neuroblastoma IC₅₀ for 24 hours. RNA isolation from the obtained cells was done with PureLink RNA Mini Kit according to the manufacturer's instructions. Concentrations and purity values of the obtained RNA samples were determined with nanodrop (NaNoQ OPTIZEN). cDNA synthesis was carried out from RNA samples, according to the manufacturer's instructions with the High Capacity cDNA Reverse Transcription Kit.

qRT-PCR analysis

qRT-PCR analysis of gene expressions of the cells associating with topoisomerase 1, topoisomerase 2 α , caspase 3, caspase 9, BCL-2, BAX, Interleukin 1 β (IL-1 β), Tumor Necrosis Factor Alpha (TNF α) and p53 was performed with Quant Studio 6 Flex device of SYBR Select Master Mix. PCR conditions are determined as; 1 cycle is 2 minutes at 50 °C, 10 minutes at 95 °C, afterwards 50 cycles for denaturation are 15 seconds at 95 °C, and 1 second at 60 °C for annealing and extension. mRNA expression levels were analyzed by comparative cycle threshold (2- $\Delta\Delta$ Ct) method (User Bulletin 2, Applied Biosystems). To obtain a copy of the Topoisomerase 1 and Topoisomerase 2 α gene sequences: was selected "Nucleotide" from the National Center for Biotechnology Information (NCBI) website (<http://www.ncbi.nlm.nih.gov/guide/>). After, the relevant organism/gene name was entered in the search box, and FASTA was determined and the relevant genes were designed. Gene expressions were determined as relative fold-change compared to the control group and normalized by β -actin mRNA expression (Table 1).

Table 1. Primer sequences of analyzed genes for qRT-PCR analysis

Gene	Primer sequences (Forward/Reverse)
Topoisomerase 1	5'-TCATACTGAACCCCAGCTCC-3' 5'-GTCCTGCAAGTGCTTGTTC-3'
Topoisomerase 2 α	5'-CTTCTCTGATATGGACAAACATAAGATTCC-3' 5'-GGACTGTGGGACAACAGGACAATAC-3'
p53	5'-CACGAGCGCTGCTCAGATAGC-3' [18] 5'-ACAGGCACAAACACGCACAAA-3'
Caspase 3	5'-GGTATTGAGACAGACAGTGG-3' [19] 5'-CATGGGATCTGTTTCTTTGC-3'
Caspase 9	5'-GAGTCAGGCTCTTCCTTTG-3' [20] 5'-CCTCAAACCTCTCAAGAGCAC-3'
BAX	5'-TTCATCCAGGATCGAGCAGA-3' [21] 5'-GCAAAGTAGAAGGCAACG-3'
BCL-2	5'-ATGTGTGTGGAGAGCGTCAA-3' [22] 5'-ACAGTTCCACAAAGGCATCC-3'
TNF α	5'-TCAGCCTCTTCTCC-3' [23] 5'-TCAGCTTGAGGGTT-3'
IL-1 β	5'-GCACGATGCACCTGTACGAT-3' [24] 5'-CACCAAGCTTTTTTGCTGTGAGT-3'
β -actin	5'-AGAGCTACGAGCTGCCTGAC-3' [25] 5'-AGCACTGTGTTGGGCGTACAG-3'

Immunofluorescence assay

Cell Viability Imaging Kit Caspase 3/7 staining was utilized to determine the morphological changes induced by etoposide, galangin, puerarin and combinations to neuroblastoma (N1E-115) cells. To evaluate the apoptotic activity, cancer cells which were plated at 1×10^5 cells/well into a 24-well chamber plate, and cells were treated with substances and incubated for 24 h. After 24 h of incubation, cells were washed with PBS and stained by Cell Viability Imaging Kit Caspase 3/7 according to manufacturer instruction. To decide the cell death, the cells were seeded in 24-well plates and treated IC_{50} of the concentration of formulations. The morphological change was investigated from stained dead, live and apoptotic cells under a fluorescent microscope (Carl Zeiss, Axio Observer, Germany).

Statistical analysis

IC_{50} value was calculated by applying probit analysis to percent viability data obtained by MTT test. After application of the neuroblastoma line at IC_{50} doses for 24 hours to the astrocyte and neuroblastoma cells, one-way ANOVA test, post hoc Tukey were administered to the relative fold-change values of gene expressions. Values of $p < 0.05$ was considered significant. Probit analysis and ANOVA test were done with SPSS 20 software (IBM).

Results

IC_{50} doses were obtained by applying probit analysis to the results obtained after 24 hours exposure to the N1E-115 neuroblastoma cell line (Fig. 1). IC_{50} doses were determined as 3.75 μM in etoposide, 3.75 μM in galangin, 5.26 μM in puerarin, 5.81 μM in etoposide+galangin, 17.54 μM in etoposide+puerarin. In the MTT test conducted to examine the effects of the dose range applied in neuroblastoma cells on the healthy cell, IC_{50} doses for astrocyte were determined as 14.16 μM in the galangin group and 17 μM in the etoposide+galangin group, while IC_{50} dose for astrocyte was higher than our tested dose scale in the other groups.

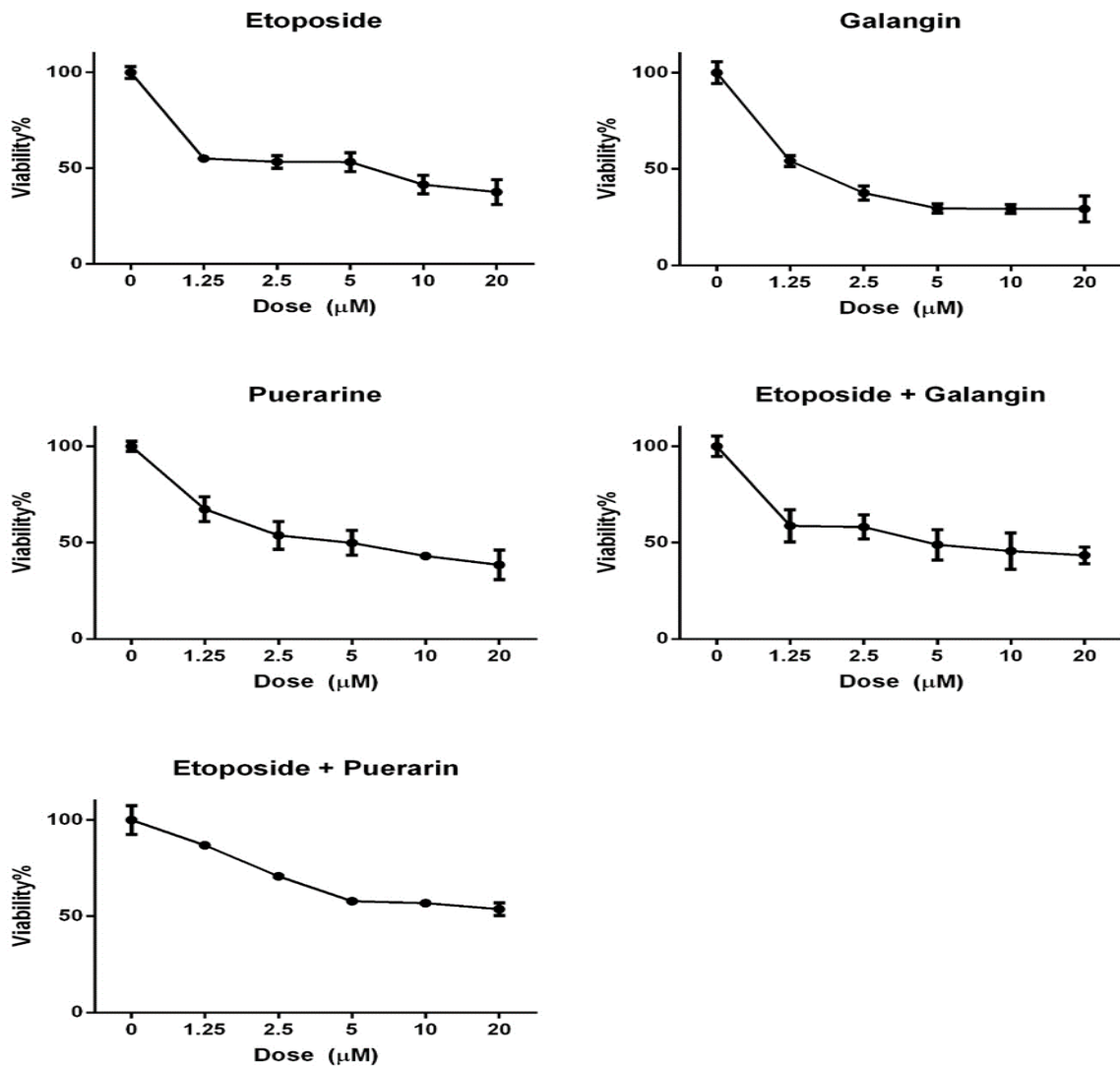


Fig 1. MTT assay results of each treatment group. Vertical bars represent standard deviation. (n=4, mean \pm std dev.) (viability%=sample absorbance average/control absorbance average \times 100)

qRT-PCR

The statistical significance of fold-changes of mRNA expressions of topoisomerase 1, topoisomerase 2 α , caspase 3, caspase 9, BAX, BCL-2, IL-1 β , TNF α , p53 in neuroblastoma and astrocyte cell lines were evaluated in all groups by comparing with control group (Fig. 2). It was observed that expression of topoisomerase 1 in the astrocyte line increased in the puerarin group compared to both the control and the etoposide group (Fig. 2A). A decrease of the expression of topoisomerase 1 on the neuroblastoma line was detected in the etoposide, galangin and etoposide+galangin groups compared to the

control group. It was determined that enzyme expression in the neuroblastoma line was increased in the puerarin and etoposide+puerarin groups compared to the etoposide group.

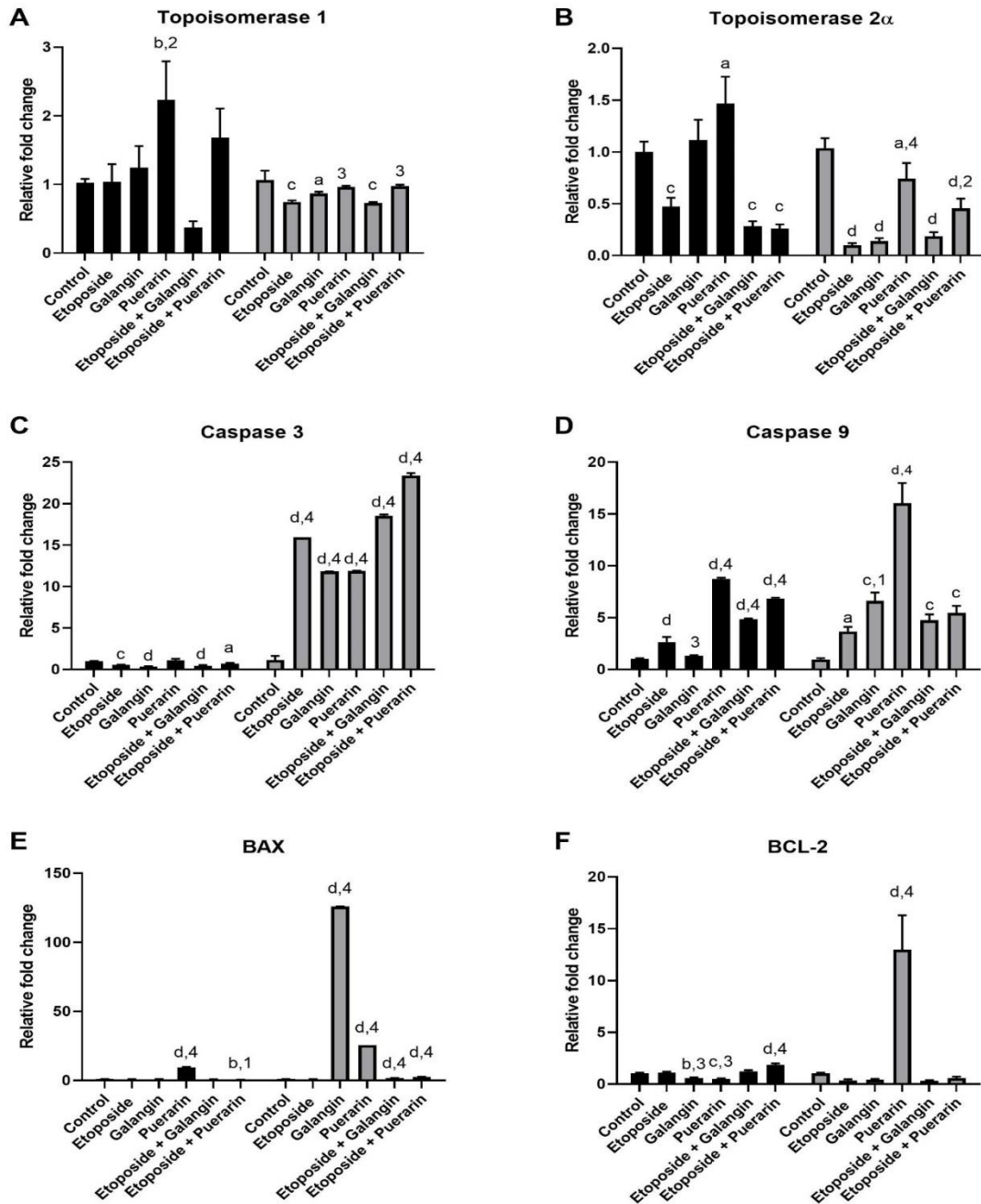


Fig 2. On N1E-115 Neuroblastoma and C8-D1A Astrocyte cell lines, the mRNA expression of topoisomerase 1 (A), topoisomerase 2α (B), caspase 3 (C), caspase 9 (D), BAX (E), BCL-2 (F) genes have been shown as relative fold-change. Black columns represent astrocyte cell line grey columns represent neuroblastoma cell line. (a: $p < 0.05$, b: $p < 0.01$, c: $p < 0.001$, d: $p < 0.0001$ compared with the control group; 1: $p < 0.05$, 2: $p < 0.01$, 3: $p < 0.001$, 4: $p < 0.0001$ compared to the etoposide group; vertical bars show standard deviation; one-way ANOVA post hoc Tukey, $p < 0.05$)

Expression of topoisomerase 1 was significantly increased in the astrocyte cell line Puerarin group compared to the control group. Expression of topoisomerase 1 in the neuroblastoma cell line was decreased in etoposide, galangin and etoposide+galangin groups compared to the control group. Expression of topoisomerase 1 in neuroblastoma cell line was increased in puerarin and etoposide+puerarin groups compared to etoposide group.

Expression of topoisomerase 2 α on the astrocyte cell line decreased in etoposide, etoposide+galangin and etoposide+puerarin groups and increased in the puerarin group compared to the control group (Fig 2B). Topoisomerase 2 α expression was decreased in all groups relative to the control group in neuroblastoma cell lines. On neuroblastoma cell lines, increase of Topoisomerase 2 α expression was determined in the control, puerarin and etoposide+puerarin groups compared to the etoposide group.

The expression of caspase 3 decreased in all groups except puerarin group relative to the control group in the astrocyte cell line but increased in all groups relative to the control group in the neuroblastoma cell line (Fig. 2C). The expression of caspase 3 increased in the etoposide+puerarin and etoposide+galangin groups in the neuroblastoma line but decreased in the galangin and puerarin groups compared to the etoposide group.

Caspase 9 expression increased in etoposide+galangin and etoposide+puerarin groups relative to the control group and expression of caspase 9 increased in both groups compared to etoposide group on the astrocyte cell line (Fig. 2D). Expression of caspase 9 increased in all groups compared to control group and caspase 9 increased in etoposide+puerarin group compared to the etoposide group in the neuroblastoma cell line. mRNA expression of BAX decreased in the etoposide+puerarin group compared to both the control group and the etoposide group, while it increased in the puerarin group on astrocyte cell line (Fig. 2E). An increase on the neuroblastoma line was observed in galangin, puerarin, etoposide+galangin and etoposide+puerarin groups compared to the control and etoposide groups.

BCL-2 gene expression increased in the etoposide+puerarin group compared to both the control group and the etoposide group while it decreased in the galangin and puerarin group in the astrocyte cell line (Fig. 2F). BCL-2 gene expression increased only in the puerarin group in neuroblastoma cell line when compared to the control and etoposide group.

IL-1 β gene expression increased in all groups relative to the control group in the astrocyte cell line (Fig. 3A). IL-1 β gene expression decreased in all groups relative to control group but increased when compared to the etoposide group and etoposide+puerarin group in the neuroblastoma cell line.

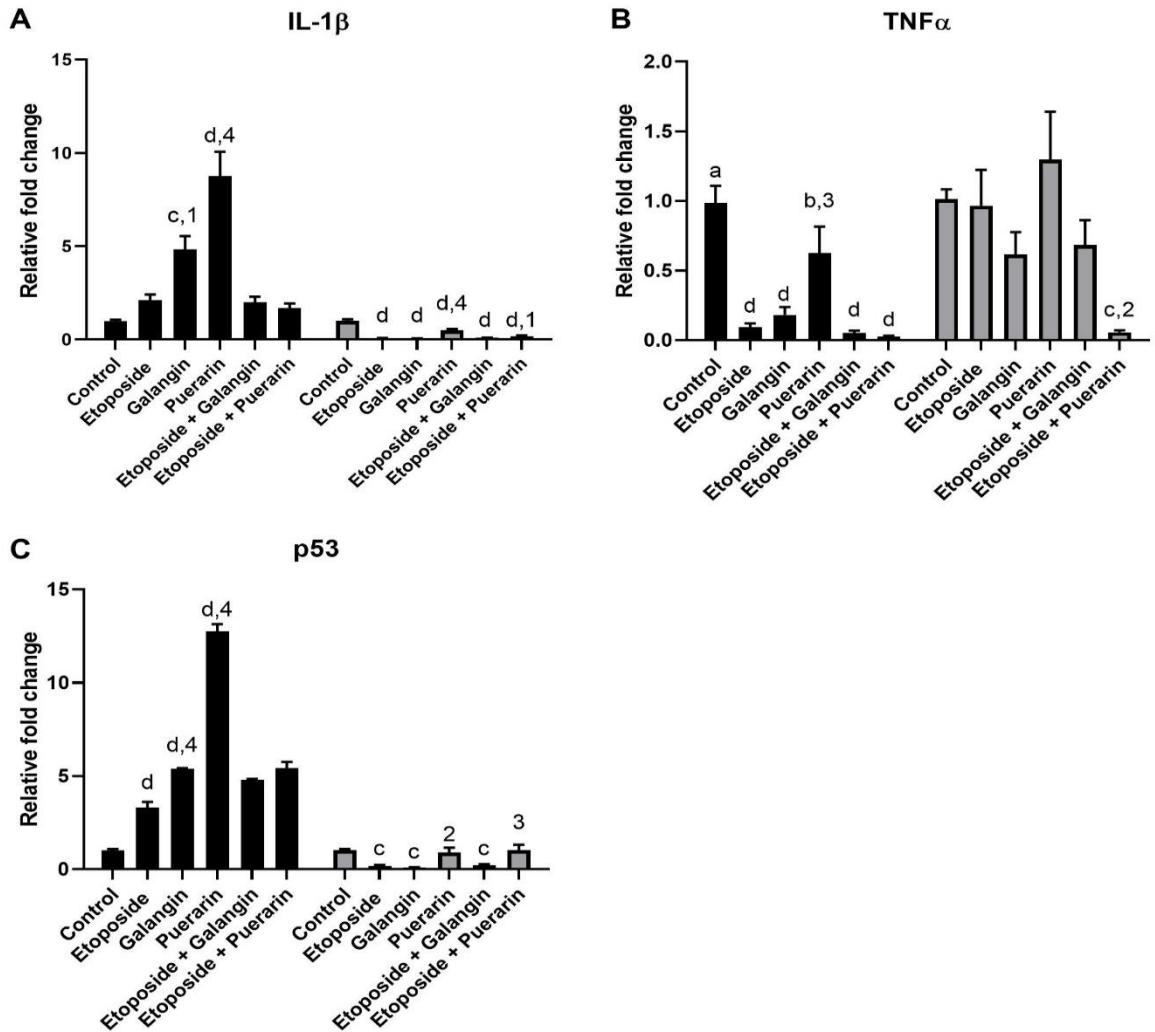


Fig 3. On N1E-115 Neuroblastoma and C8-D1A Astrocyte cell lines, the mRNA expression of IL-1 β (A), TNF α (B), BAX (C), p53 (D) genes have been shown as relative fold-change. Black columns represent astrocyte cell line grey columns represent neuroblastoma cell line. (a: $p < 0.05$, b: $p < 0.01$, c: $p < 0.001$, d: $p < 0.0001$ compared with the control group; 1: $p < 0.05$, 2: $p < 0.01$, 3: $p < 0.001$, 4: $p < 0.0001$ compared to the etoposide group; vertical bars show standard deviation; one-way ANOVA post hoc Tukey, $p < 0.05$)

TNF α expression decreased in all groups relative to the control group in the astrocyte cell line (Fig. 3B). TNF α expression also decreased in the etoposide+puerarin group compared to the control group in the neuroblastoma cell line.

p53 expression increased in all groups relative to the control group (Fig. 3C) also in all groups except the control group when compared to the etoposide group in the astrocyte cell line. p53 gene expression decreased in the etoposide and etoposide+galangin groups compared to the control group in the neuroblastoma cell line.

Immunofluorescence assay

Since cell viability in MTT results is significantly inhibited by etoposide, galangin, puerarin, etoposide+galangin, and etoposide+puerarin, it is critical to classify which cell death is induced in N1E-115 cells. Therefore, an immunofluorescence staining experiment was conducted to determine the type of cell death induced by the administration groups. Apoptotic cells were determined in the viable part of the cell population with treatment groups for 24 hours (Fig. 4). In the immunofluorescence examination, it was observed that the cells in the N1E-115 cell line control group preserved their morphological integrity and were alive. It was observed that the cells in the N1E-115 cell line etoposide, puerarin, galangin, etoposide+galangin and etoposide+puerarin groups could not preserve their integrity, their cytoplasm stained caspase 3/7 positively and the cells were dead (Fig. 4).

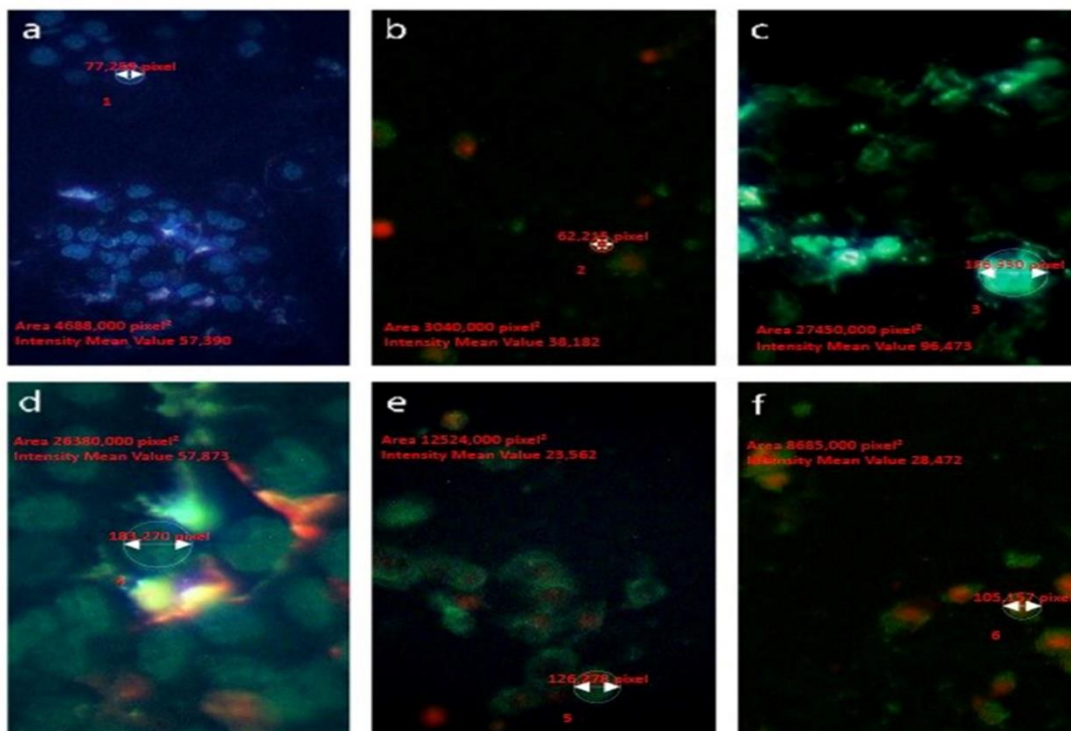


Fig 4. Immunofluorescent staining of control (a), etoposide (b), galangin (c), puerarin (d), etoposide+galangin (e), etoposide+puerarin (f) groups of neuroblastoma (N1E-115) cells by cell viability imaging kit caspase 3/7. (Blue: live cell; Red: dead cell; Green: caspase 3/7 positive)

Discussion

Etoposide is an antineoplastic drug as a topoisomerase 2 inhibitor. Galangin and puerarin are antiproliferative plant-based antioxidants that induce apoptosis in cancer cells [10, 11]. Accordingly, we hypothesized that etoposide and galangin/puerarin combinations with etoposide may have an antiproliferative and apoptotic effect on the neuroblastoma cell line when it is in a non-apoptotic level on a healthy astrocyte cell line in this study. Therefore, we investigated the effects of etoposide, galangin, puerarin and their combinations with etoposide on the mRNA expression of genes which are involved in apoptotic process on neuroblastoma and healthy astrocyte cell lines. The effects of drug administrations at the dose of neuroblastoma IC_{50} on apoptotic process of healthy astrocyte cell line were also examined in our study.

It was observed that topoisomerase 2 α gene expression decreased in the etoposide (3.75 μ M) group on the neuroblastoma and astrocyte cell line. The reduction in topoisomerase 2 α gene expression can be explained by an improved resistance mechanism against anticancer agents acting on the mechanism of non-separation of the topoisomerase-DNA complex. This result obtained from our study is in line with other studies [6, 26]. It is a remarkable finding that the gene expression on the neuroblastoma line significantly decreases while overexpression of p53, the tumor suppressing gene, is observed on the astrocyte line. If astrocyte cell IC_{50} value of etoposide was not determined between administered dose range, this indicates that the IC_{50} value is higher than the administered dose and the decrease of the caspase 3 gene expression shows that etoposide has no effect on apoptotic death at the dose administered in healthy astrocyte cell. It was determined that it caused significant overexpression of caspase 3 in the neuroblastoma line. This result shows that the apoptosis signal pathway is activated. It was determined that p53 decreased significantly in this cell line. The significant increase in caspase 9 expression in the neuroblastoma line indicates that apoptosis occurs through the mitochondrial pathway. Depending on the damage to the mitochondrial membranes in the neuroblastoma line cells, the release of cytochrome c (cyc-c) may have initiated the caspase cascade and thereby led the cell into apoptosis through the mitochondrial pathway. However, it was determined that IL-1 β expression did not change in the astrocyte line and decreased significantly in the neuroblastoma line. At the same time, TNF α gene expression decreased significantly in the astrocyte line, while no difference

was observed on the neuroblastoma line. Reduction of TNF α expression can be interpreted that apoptosis is not triggered through the Extrinsic pathway on the astrocyte cell line. The fact that the etoposide causes apoptosis in the neuroblastoma cell line, not in the astrocyte line, shows its selective effect.

It was determined that IL-1 β , p53 and caspase 9 gene expressions increased and caspase 3, BCL-2, TNF α expressions decreased as a result of the administration of galangin (3.75 μ M) to the astrocyte cell line. The increase of caspase 9 on the astrocyte cell line depending on the administration of galangin can be considered as the cell's attempt to regulate balance with cytoprotective autophagy. Similarly, with the administration to the neuroblastoma cell line, it was determined that caspase 3, caspase 9, BAX expressions increased but IL-1 β , p53, topoisomerase 1 and 2 α expressions decreased. Increased tumor suppressor gene p53 mRNA expression in the astrocyte line and also decreased caspase 3 expression indicate that the apoptosis signal pathway does not cause apoptosis on the astrocyte line. The increase in caspase 3, caspase 9, BAX gene expressions in the neuroblastoma line and decrease in p53 indicate that apoptosis is stimulated. In a study conducted on the HEPG2 cell line, it was reported that cell death occurred via autophagy rather than apoptosis with the administration of galangin at 130 μ mol/L, whereas when it was administered at 370 μ mol/L dose, cell death occurred via apoptosis [27]. In a study on breast cancer, galangin was shown to increase BAX expression and decrease BCL-2 expression, and this result was found to be compatible with our findings [28]. It is demonstrated that the administration of galangin to hepatocellular carcinoma cells (HEPG2), by binding of the proapoptotic protein BAX to the mitochondria membrane, caused the apoptosis-inducing factor and cyc-c to be released into the cytosol [12], and caused apoptosis on B16F10 melanoma line but does not cause any changes on BAX [14]. In the present study, the observation of the increase in BAX gene expression was interpreted as the difference of cell lines. There is no study in the literature about the effect of galangin on neuroblastoma cell line.

In the etoposide+galangin (5.81 μ M 1:1) combination group, mRNA expressions of tumor suppressor gene p53 and caspase 9 increased but topoisomerase 1, topoisomerase 2 α , caspase 3, and TNF α decreased in the astrocyte cell line. However, caspase 3, caspase 9 and BAX gene expressions were significantly increased in the neuroblastoma line. The significant increase of caspase 3, caspase 9 and BAX gene expressions that took place

with the etoposide+galangin administration in the neuroblastoma cell line may be interpreted as apoptosis triggered via mitochondrial pathway. It can be evaluated that the increase in caspase 9 gene expression may depend on the stress of endoplasmic reticulum (ER). The significant decrease of p53 can be interpreted as apoptosis may have occurred independently from p53. Depending on the disruption in the mitochondrial membranes on the neuroblastoma cells, the cyc-c release may have initiated the caspase cascade and thus led the cell via the mitochondrial pathway into apoptosis.

While IL-1 β expression did not change in the astrocyte line but a significant decrease was observed in the neuroblastoma line. It was observed that TNF α gene expression was significantly decreased in the astrocyte line but not changed in the neuroblastoma line. Reduction of TNF α expression on the astrocyte cell line can be interpreted as apoptosis is not triggered from the extrinsic pathway on the astrocyte cell line. We could not find any study investigating the effect of etoposide and galangin combination in neuroblastoma cell line. Therefore, we think that the findings of our study have a significant contribution to the future study.

Increased BCL-2 and p53 expressions and decreased BAX expressions in astrocyte cell line in consequence of etoposide+puerarin (17.54 μ M 1:1) administration can be evaluated as the protective effect of puerarin. Similarly, it was reported that puerarin has a protective effect in astrocyte cells and reduces BAX expression depending on concentration [29]. In the literature, cytotoxicity studies in which the combination of etoposide and puerarin were administered were not found. The significant increase of caspase 3, caspase 9, BAX gene expression that took place with the etoposide+galangin administration in the neuroblastoma cell line may be interpreted as apoptosis triggered via mitochondrial pathway. Compatibly to our study, in another study conducted on human lung adenocarcinoma cell line, puerarin was found to induce apoptosis via mitochondrial pathway [30]. It was also considered that caspase 9 gene expression may have increased due to ER stress. In a study on human colorectal cancer line, the increase in BAX, decrease in BCL-2 and increase in caspase 3 activation are in line with our results [31]. In another study, it was stated that administration of puerarin inhibits proliferation in the bladder cancer T-24 cell line, and apoptosis occurs as a result of decrease in p53 and BCL-2 and increase in BAX protein expression [32]. Decrease in BCL protein expression and increase in BAX expression were consistent with our study. While IL-1 β

expression did not change on the astrocyte line, it decreased significantly on the neuroblastoma line. TNF α gene expression was found to be significantly decreased on the astrocyte line and not changed on the neuroblastoma line. Constancy of IL-1 β expression and reduction of TNF α expression on the astrocyte cell line can be interpreted as apoptosis is not triggered from the extrinsic pathway on the astrocyte cell line. In immunofluorescence examination, the apoptosis and cell death table observed in cells is consistent with the changes in mRNA expression. This result indicates that death in N1E-115 cells of administration groups is due to apoptotic cell death.

Conclusion

In all groups, IC₅₀ dose was lower in neuroblastoma than astrocyte. This suggests that selective effect can occur. Moreover, it shows that the antiproliferative effect is decreased in the combination groups relative to the etoposide group. Available data indicate that apoptosis is triggered by the intrinsic pathway. Etoposide combinations have decreased antiproliferative effect compared to the etoposide group. Thus, the single treatment of galangin and puerarin in neuroblastoma treatment may be promising and proper attention should be paid to the dosage. We also consider that administrations of puerarin and galangin should be evaluated in terms of autophagy and ER stress.

References

1. Urbani, A., et al., A proteomic investigation into etoposide chemo-resistance of neuroblastoma cell lines. *Proteomics*, 2005. 5(3): p. 796-804.
2. Steliarova-Foucher, E., et al., International incidence of childhood cancer, 2001-10: a population-based registry study. *Lancet Oncol*, 2017. 18(6): p. 719-731.
3. Maris, J.M., et al., Neuroblastoma. *Lancet*, 2007. 369(9579): p. 2106-20.
4. Pinto, N.R., et al., Advances in Risk Classification and Treatment Strategies for Neuroblastoma. *J Clin Oncol*, 2015. 33(27): p. 3008-17.
5. Berger, S.J., et al., Green tea constituent (--)epigallocatechin-3-gallate inhibits topoisomerase I activity in human colon carcinoma cells. *Biochem Biophys Res Commun.*, 2001. 288(1): p. 101-5.
6. Nitiss, J.L., Targeting DNA topoisomerase II in cancer chemotherapy. *Nat Rev Cancer*, 2009. 9(5): p. 338-50.
7. Karpnich, N.O., et al., The course of etoposide-induced apoptosis from damage to DNA and p53 activation to mitochondrial release of cytochrome c. *J Biol Chem*, 2002. 277(19): p. 16547-52.
8. Janicke, R.U., D. Sohn, and K. Schulze-Osthoff, The dark side of a tumor suppressor: anti-apoptotic p53. *Cell Death Differ*, 2008. 15(6): p. 959-76.
9. Yonish-Rouach, E., The p53 tumour suppressor gene: a mediator of a G1 growth arrest and of apoptosis. *Experientia*, 1996. 52(10-11): p. 1001-7.
10. Heo, M.Y., S.J. Sohn, and W.W. Au, Anti-genotoxicity of galangin as a cancer chemopreventive agent candidate. *Mutat Res.*, 2001. 488(2): p. 135-150.

11. Bacanli, M., A.A. Basaran, and N. Basaran, The antioxidant, cytotoxic, and antigenotoxic effects of galangin, puerarin, and ursolic acid in mammalian cells. *Drug Chem Toxicol*, 2017. 40(3): p. 256-262.
12. Zhang, H.T., et al., Galangin induces apoptosis of hepatocellular carcinoma cells via the mitochondrial pathway. *World J Gastroenterol*, 2010. 16(27): p. 3377-84.
13. Zeng, H., et al., Galangin-induced down-regulation of BACE1 by epigenetic mechanisms in SH-SY5Y cells. *Neuroscience*, 2015. 294: p. 172-81.
14. Zhang, W., et al., Galangin induces B16F10 melanoma cell apoptosis via mitochondrial pathway and sustained activation of p38 MAPK. *Cytotechnology*, 2013. 65(3): p. 447-55.
15. Zou, W.-W. and S.-P. Xu, Galangin inhibits the cell progression and induces cell apoptosis through activating PTEN and Caspase-3 pathways in retinoblastoma. *Biomed Pharmacother.*, 2018. 97: p. 851-863.
16. Li, J., et al., Anti-colorectal cancer biotargets and biological mechanisms of puerarin: Study of molecular networks. *Eur J Pharmacol*, 2019. 858: p. 172483.
17. Zhou, Y.X., H. Zhang, and C. Peng, Puerarin: a review of pharmacological effects. *Phytother Res*, 2014. 28(7): p. 961-75.
18. Doganlar, Z.B., et al., The Role of Melatonin in Oxidative Stress, DNA Damage, Apoptosis and Angiogenesis in Fetal Eye under Preeclampsia and Melatonin Deficiency Stress. *Curr Eye Res*, 2019. 44(10): p. 1157-1169.
19. Wang, L.M. and R.L. Wang, Effect of rapamycin (RAPA) on the growth of lung cancer and its mechanism in mice with A549. *International Journal of Clinical and Experimental Pathology*, 2015. 8(8): p. 9208-9213.
20. Artym, J., et al., Prolongation of skin graft survival in mice by an azaphenothiazine derivative. *Immunology Letters*, 2019. 208: p. 1-7.
21. Li, R., et al., Bailcalin protects against diabetic cardiomyopathy through Keap1/Nrf2/AMPK-mediated antioxidative and lipid-lowering effects. 2019. 2019.
22. Gong, C., et al., Effects of microRNA-126 on cell proliferation, apoptosis and tumor angiogenesis via the down-regulating ERK signaling pathway by targeting EGFL7 in hepatocellular carcinoma. *Oncotarget*, 2017. 8(32): p. 52527-52542.
23. Sun, X., et al., Activation of the epithelial sodium channel (ENaC) leads to cytokine profile shift to pro-inflammatory in labor. *Embo Molecular Medicine*, 2018. 10(10).
24. Liu, Z.Y., et al., Necrostatin-1 reduces intestinal inflammation and colitis-associated tumorigenesis in mice. *Am J Cancer Res*, 2015. 5(10): p. 3174-85.
25. Jeevannavar, S.S., et al., Response to Wei Y-S, Liu W-L, Bai R, Li D-H, Zhao Z-Q, Wang Y, et al. The use of a transolecranon pin joystick technique in the treatment of multidirectionally unstable supracondylar humeral fractures in children. *J Pediatr Orthop B* 2020; 29:452-457. *Journal of Pediatric Orthopaedics-Part B*, 2022. 31(1): p. E107-E107.
26. Berney, D.M., et al., DNA topoisomerase I and II expression in drug resistant germ cell tumours. *British Journal of Cancer*, 2002. 87(6): p. 624-629.
27. Wen, M., et al., Galangin Induces Autophagy through Upregulation of p53 in HepG2 Cells. *Pharmacology*, 2012. 89(5-6): p. 247-255.
28. Liu, D., et al., Galangin Induces Apoptosis in MCF-7 Human Breast Cancer Cells Through Mitochondrial Pathway and Phosphatidylinositol 3-Kinase/Akt Inhibition. *Pharmacology*, 2018. 102(1-2): p. 58-66.
29. Wang, N., et al., Puerarin protected the brain from cerebral ischemia injury via astrocyte apoptosis inhibition. *Neuropharmacology*, 2014. 79: p. 282-289.
30. Hu, Y.F., et al., Puerarin inhibits non-small cell lung cancer cell growth via the induction of apoptosis. *Oncology Reports*, 2018. 39(4): p. 1731-1738.
31. Yu, Z.L. and W.J. Li, Induction of apoptosis by puerarin in colon cancer HT-29 cells. *Cancer Letters*, 2006. 238(1): p. 53-60.

32. Ye, G.M., et al., Puerarin in inducing apoptosis of bladder cancer cells through inhibiting SIRT1/p53 pathway. *Oncology Letters*, 2019. 17(1): p. 195-200.

Kurt, B., Investigation of The Potential Inhibitor Effects of Lycorine on Sars-Cov-2 Main Protease (Mpro) Using Molecular Dynamics Simulations and MMPBSA. International Journal of Life Sciences and Biotechnology, 2022. 5(3): p. 424-435. DOI: 10.38001/ijlsb.1110761

Investigation of The Potential Inhibitor Effects of Lycorine on Sars-Cov-2 Main Protease (Mpro) Using Molecular Dynamics Simulations and MMPBSA

Bariş Kurt^{1*} 

ABSTRACT

The main protease (Mpro or 3CLpro) plays important roles in viral replication and is one of attractive targets for drug development for SARS-CoV-2. In this study, we investigated the potential inhibitory effect of lycorine molecule as a ligand on SARS-CoV-2 using computational approaches. For this purpose, we conducted molecular docking and molecular dynamics simulations MM-PB(GB)SA analyses. The findings showed that the lycorine ligand was successfully docked with catalytic dyad (Cys145 and His41) of SARS-CoV-2 Mpro with binding affinity changing between -6.71 and -7.03 kcal mol⁻¹. MMPB(GB)SA calculations resulted according to GB (Generalized Born) approach in a Gibbs free energy changing between -24.925-+01152 kcal/mol between lycorine and SARS-CoV-2 which is promising. PB (Poisson Boltzmann) approach gave less favorable energy (-2.610±0.2611 kcal mol⁻¹). Thus, Entropy calculations from the normal mode analysis (ΔS) were performed and it supported GB approach and conducted -23.100±6.4635 kcal mol⁻¹. These results showed lycorine has a druggable potential but the drug effect of lycorine on COVID-19 is limited and experimental studies should be done with pharmacokinetic modifications that increase the drug effect of lycorine.

ARTICLE HISTORY

Received

28 April 2022

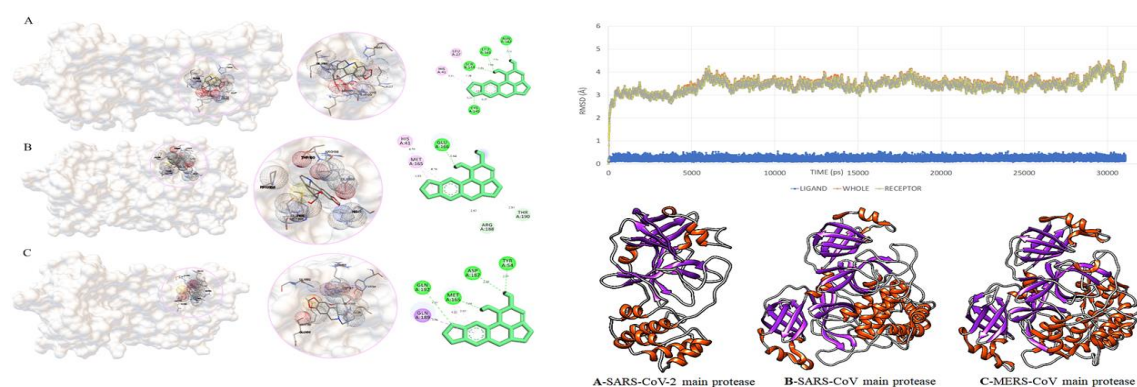
Accepted

13 June 2022

KEYWORDS

Molecular Dynamics Simulation, MMPBSA, Gibbs Energy, SARS-CoV-2

Graphical Abstract



¹ Muş Alparslan University, Faculty of Education, Department of Math, Muş / Turkey

*Corresponding Author: Barış Kurt, e-mail: b.kurt@alparslan.edu.tr

Introduction

Coronaviruses (CoVs) are common pathogens in vertebrates causing various diseases which have been identified as respiratory infections, hepatitis, encephalitis, gastroenteritis [1] and lately COVID-19. The first case of COVID-19 was reported in Wuhan city of Hubei province in China in December 2019 [2] and the outbreak, caused by a novel coronavirus, was declared as global pandemic in 2020 by World Health Organization [3].

The SARS-CoV-2 belonging to β -coronavirus family has an envelope and a non-segmented positive-sense RNA. The genome size of Wuhan-Hu-1 coronavirus (WHCV) is 29.9 kb [4]. The genome encodes 16 non-structural proteins (NSP) along with four structural proteins which are comprised of envelope (E), spike (S) glycoprotein, nucleocapsid (N), and matrix (M) proteins [5]. It is known that ACE-2 (Angiotensin Converting Enzyme-2) receptor is a binding region for SARS-CoV and SARS-CoV-2 viruses [6]. Usually, β -coronaviruses synthesize about 800 kDa long polypeptide [7]. It is determined SARS-CoV-2 is comprised of 16-17 non-structural proteins named as 3-chymotrypsin-like protease ($3CL^{pro}$), papain-like protease (PL^{pro}), helicase, and RNA-dependent RNA polymerase (RdRp). Two proteases ($3CL^{pro}$ and PL^{pro}) serves as probable drug targets since they are of importance in processing two viral proteins in an organized way [8]. Particularly, the $3CL^{pro}$ (main protease or M^{pro}), involved in specific roles in virus replication by cleaving and processing the viral proteins, indicate high-level variations at the 3' side. In MERS-CoV $3CL^{pro}$, His41 and Ala148 residues have been identified as catalytic dyad [9,10]. On the other hand, Cys145 and His41 are catalytic dyad in SARS-CoV-2 $3CL^{pro}$ [11]. The human CoV (HCoV) 229E M^{pro} contains Cys144 and His41 residues as a catalytic dyad [10].

The sequenced virus RNAs obtained from COVID-19 patients around the world indicated that SARS-CoV-2 have undergone slower mutations compared to other RNA viruses and the rates of SARS-CoV-2 mutations are slower compared to transmission rates of the virus. The slower mutations of the virus emanates from the proofreading mechanism of SARS-CoV-2 and earlier genomic sequencing data of the virus showed that the virus averagely undergoes two-single letter mutations each month [12]. The most significant mutation sites

in virus genome are spike proteins since they help virus to enter into host cells by binding to ACE2 receptors and therefore, is the main target of neutralizing antibodies. Alpha, Beta, Gama and Omicron variants have the mutated sites in their spike proteins rendering them more infectious [12].

Lycorine is a pyrrolo[de]phenanthridine ring-type alkaloid and it is found abundant in plants, belonging to Amaryllidaceae family [13]. Lycorine is known to be cytotoxic compound having anti-tumor effects on different cell lines [14]. Lycorine together with other phytochemicals such as trisphaeridine, homolycorine, and haemanthamine from spring snowflake (*Leucojum vernum*) are found to exhibit high antiretroviral activities with low therapeutic indices ($TI_{50} = 1.3 - 1.9$) [15]. Particularly, lycorine exhibits virus inhibitory properties against the enterovirus, the flaviviruses, HIV-1, the hepatitis C virus, and the SARS-CoV [15,16]. Lycorine, like hemanthamine, inhibits viral activities of the H5N1 influenza strain (highly pathogenic avian influenza virus or HPAIV) by impeding export of virus ribonucleoprotein from nucleus to cytoplasm [17]. Also, lycorine decreases the cytopathic effects of viruses, inhibiting the replication of viruses [18,19]. Lycorine and four herbal extracts are suggested as potential candidates for the treatment of SARS as novel anti-SARS-CoV drugs [20]. Jin et al. [21] stated that lycorine exhibits inhibitory properties against SARS-CoV, MERS-CoV, and SARS-CoV-2 by inhibiting the RNA dependent RNA polymerase (RdRp). However, the effects of lycorine on SARS-CoV or SARS-CoV-2 viruses are more effective than those on MERS-CoV. Likewise, gemcitabine, lycorine, and oxysophoridine in cell culture are reported to show antiviral activities against SARS-CoV-2 [16]. Although these mentioned studies suggest that lycorine is a promising drug candidate, it is still emphasized that further studies are needed to gain more insights into the toxicity and safety profile and antiviral activity of lycorine against SARS-CoV-2. Therefore, in this study, the inhibition potential of lycorine as a promising anti-COVID-19 natural compound was tested on the crystal structure of SARS-CoV-2 main protease (3CL^{pro} or M^{pro}) (PDB ID: 6LU7) using docking and molecular dynamics approaches.

Materials and Methods

Receptor and Ligand Preparation

The ligand lycorine (C₁₆H₁₇NO₄) was obtained (Fig. 1) from ZINC (ZINC000003881372) database (<https://zinc.docking.org/>) (Irwin & Shoichet, 2005). The lycorine includes five rings, 21 heavy atoms, and five hetero atoms. As receptor, the 3D structures of SARS-CoV-2 main protease (referred to as the 3C-like protease) [22] obtained by X-ray diffraction was retrieved from Protein Data Bank (PDB ID: 6LU7) (<https://www.rcsb.org/>) (Fig. 2). Similarly, SARS-CoV (PDB ID: 1UK3) and MERS CoV (PDB ID: 4WME) main proteases were also retrieved from Protein Data Bank. The 3D models were visualized using UCSF Chimera v1.14 software [23].

Molecular Docking

The AutoDock 4.2 and MGLTools 1.5.6 [24] were used for docking analysis to predict binding scores and modes. To achieve this, the water molecules of the SARS-CoV-2 main protease protein were deleted and polar hydrogens were added to it. The pdbqt file for the protein including Kollman charges was created using MGLTools 1.5.6 [24]. After that, the ligand (the lycorine) was optimized using GAMESS-US software [25] with HF/6-31G+ basis set [26] and the pdbqt file for the ligand including Gastieger charges was generated [24]. The grid box was created with 126x126x126 Å dimensions (grid center x=-26.358 y=15.363 z=60.52) with 0.5694 spacing. Lamarckian genetic algorithm [27] was selected for the docking process. To visualize docking results, Discovery Studio Visualizer [28] and MGLTools 1.5.6 [24] were used.

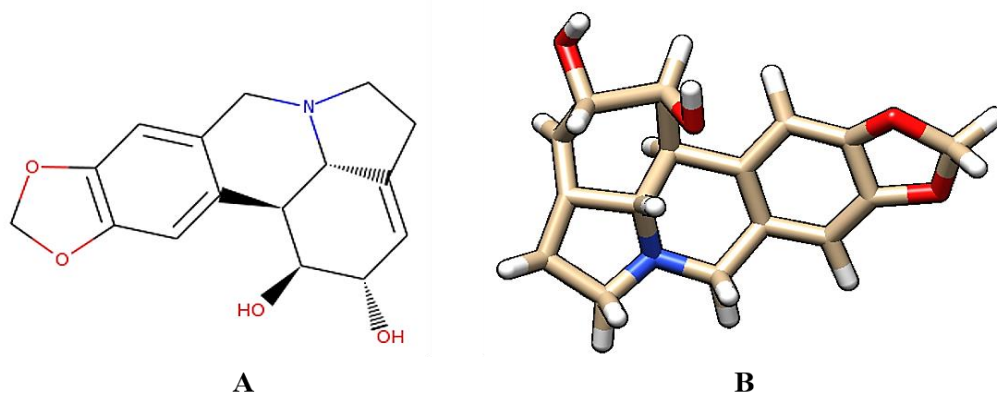


Fig 1. The 2D (A) and 3D structures (B) of lycorine compound

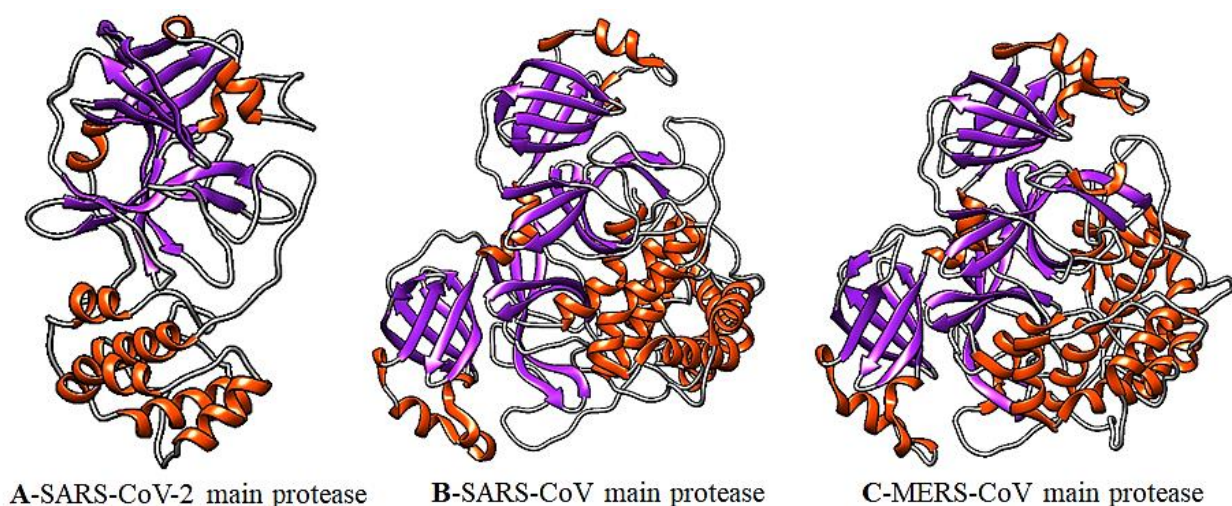


Fig 2. The 3D structure of SARS-CoV-2 (PDB ID: 6LU7), SARS-CoV (PDB ID: 1UK3), and MERS-CoV (PDB ID: 4WME) main proteases. The red, purple, and grey colors show the helices, strands, and coils, respectively. The SARS-CoV-2 showed 95.75% and 95.42% structure overlap with SARS-CoV and MERS-CoV main proteases, respectively (29)

Molecular Dynamics Simulation

After docking process, the lycorine-protein complex with the best docking score was selected for molecular dynamics simulation. The pdb file of this complex was corrected using pdb4amber script in AmberTools 17 package and saved as a new pdb file [30]. Then with tleap program Na^+ ions were added to the complex to provide charge balance and 12 Å TIP3PBOX was used with TIP3P water. AMBER ff14SB and gaff force fields were selected for the protein and the lycorine, respectively [31,32]. To speed up the simulation, after the topology and coordinate files were created, the "hydrogen mass repartitioning" process was applied with the parmed program and the hmassrepartition command [33]. Then two-step minimization was started. In the first step, the complex was restrained, applying $500 \text{ kcal mol}^{-1} \cdot \text{\AA}^2$ force constant. The water molecules were minimized with 1000 steps minimization using the Particle Mesh Ewald (PME) method with 10Å cut-off value. In the second step, force constant was removed from the complex and all system was minimized with the same method as described in the first stage. This time cut-off value was selected as 12Å. Then the heating process was initiated using the Langvein thermostat and selecting SHAKE algorithm while the cut-off value was set to 12Å [30]. Temperature was

increased up to 298K with 1-degree steps. When temperature reached 298K, molecular dynamic simulation was performed for 30 ns with 4 ps relaxation time under 1 atm pressure using the same thermostat and algorithm as mentioned in the heating stage. During the heating and simulation, 10 kcal mol⁻¹.Å² force constant was applied to the complex. Lastly, deltaG and entropy were calculated using MMPBSA [34] and RMSD value was calculated using cpptraj program [35].

Entropy and Relative Free Energy Calculations Using Molecular Dynamics Simulation

After the simulation, ante-mmpbsa.py program was used to obtain mmpbsa compatible prmtop files for complex consisting of the ligand and the receptor molecules. Mbondi radii was set to 2 as it was recommended in Amber Manual. The free energy of binding is calculated by the following equation [36,37,38,39]:

$$\Delta G_{\text{binding}} = \Delta G_{\text{complex}} - \Delta G_{\text{receptor}} - \Delta G_{\text{ligand}} \quad (\text{I})$$

However, since the share of solvent-related energies in the total energy will be greater than the binding energy in solvated states, the solvent effects are included in the calculation and the modified formula is used for the binding free energy [36,37,38,39]:

$$\Delta G_{\text{bind,solv}}^0 = \Delta G_{\text{bind,vacuum}}^0 + \Delta G_{\text{solv,complex}}^0 - (\Delta G_{\text{solv,ligand}}^0 + \Delta G_{\text{solv,receptor}}^0) \quad (\text{II})$$

For hydrophobic contributions, an empirical term is added to the equation after Generalized Born Equation is solved during calculations of solvation free energies [36,37,38]:

$$\Delta G_{\text{solv}}^0 = G_{\text{electrostatic}, \epsilon=80}^0 - G_{\text{electrostatic}, \epsilon=1}^0 + \Delta G_{\text{hydrophobic}}^0 \quad (\text{III})$$

The change of Gibbs energy in the vacuum is calculated by the following formula, which also takes into account the average interaction energy and entropy change between the receptor and the ligand [36,37,38]:

$$\Delta G_{\text{vacuum}}^0 = \Delta E_{\text{MM}}^0 - T\Delta S_{\text{normal mode analysis}}^0 \quad (\text{IV})$$

All energy and entropy calculations were carried out using mmpbsa module in the Amber Tools and the snapshots were taken every 5 ps from the beginning to the end of the simulation.

Results and discussion

Docking analyses

In this study, as a result of molecular docking analyses, it was found that the lycorine molecule was bound to SARS-CoV-2 M^{pro} with binding affinity changing between -6.10 and -7.03 kcal mol⁻¹ and three different lycorine conformations were detected (Fig. 3). For first conformation, the lycorine was bound to Leu141, Asn142, Ser144, and Cys145 residues of the M^{pro} with -6.71 kcal mol⁻¹ docking score. His41, Met165, Glu166, Arg188, and Thr190 were identified as interacting residues in the second conformation with -6.10 docking score whilst Thr54, Met165, Asp187, Gln189, and Gln194 residues were identified as binding sites in the third conformation with -7.03 docking score. Jin et al. [22] reported that substrate-binding pocket of COVID-19 are well-conserved in all M^{pro}s and it shows high potential for drug designing against all CoV-associated diseases. For andrographolide phytochemical from *Andrographis paniculate* (king of bitters), Gly143, Cys145, and Glu166 are the interacting residues for SARS-CoV-2 protease [40]. Cys145 and Glu166 residues were identified in our findings as well. When different phytochemicals in medicinal plants such as isoflavone, myricitrin, methyl rosmarininate, glucopyranoside, calceolarioside, licoleafol, and amaranthin are tested on SARS-CoV-2 CL^{pro} as anti-COVID-19 compounds, two binding sites (His41 and Cys145) are reported as the interacting residues [11]. Consequently, the catalytic dyad (Cys145 and His41) identified in our results also indicate a drug potential of the lycorine against SARS-CoV-2.

Molecular Dynamics Simulation and Energy Calculations

The fact that lycorine has a quite good dock score provides evidence that it may be a good drug candidate. In this regard, molecular dynamics simulation was carried out. The RMSD value was calculated from the simulation with reference to the initial structure (the lowest energy docking complex). Calculated RMSD are shown in Fig. 4. The mean RMSD value during the whole simulation was 3.42 Å for the protein, 3.45 Å for the whole system, and 0.23 Å for the ligand. After 5.8 nanoseconds, it was seen that the RMSD value was fixed and almost unchanged for the protein, while for the ligand this value does not exceed 0.50 Å from the beginning to the end of the simulation. If there were large fluctuations in the

RMSD value, it would indicate that the simulation was stuck at a high energy minimum and therefore, the molecular dynamics simulation should have been continued for a longer period of time. However, the fact that the RMSD value was quite low and remained stable for a long time showed that the simulation progressed quite accurately. Similarly, stabilization in potential energy in Fig. 5 also indicated that the simulation proceeded correctly.

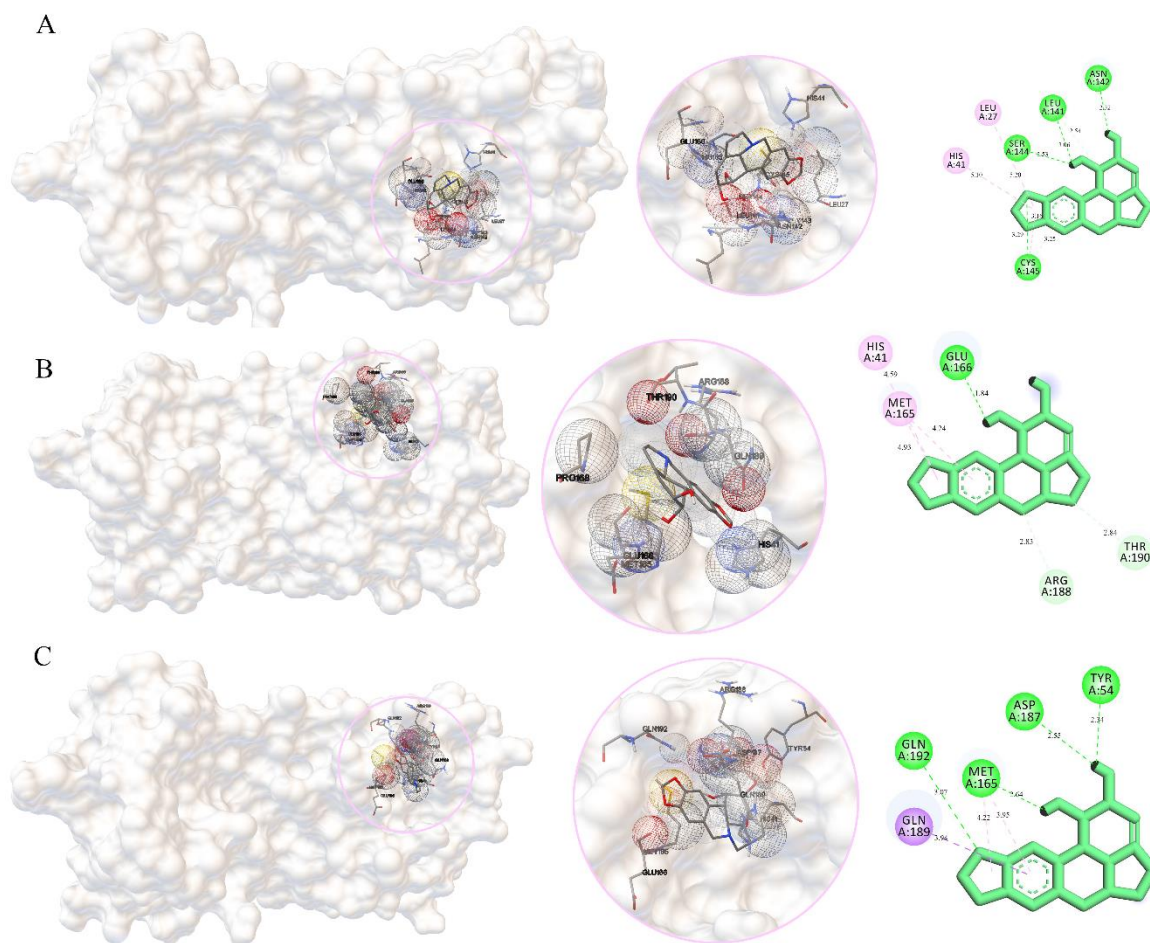


Fig 3. Molecular docking analyses of lycorine ligand with SARSCoV-2 protease with binding affinities of -6.71 , -6.10 , -7.03 kcal mol⁻¹ for A, B, and C, respectively.

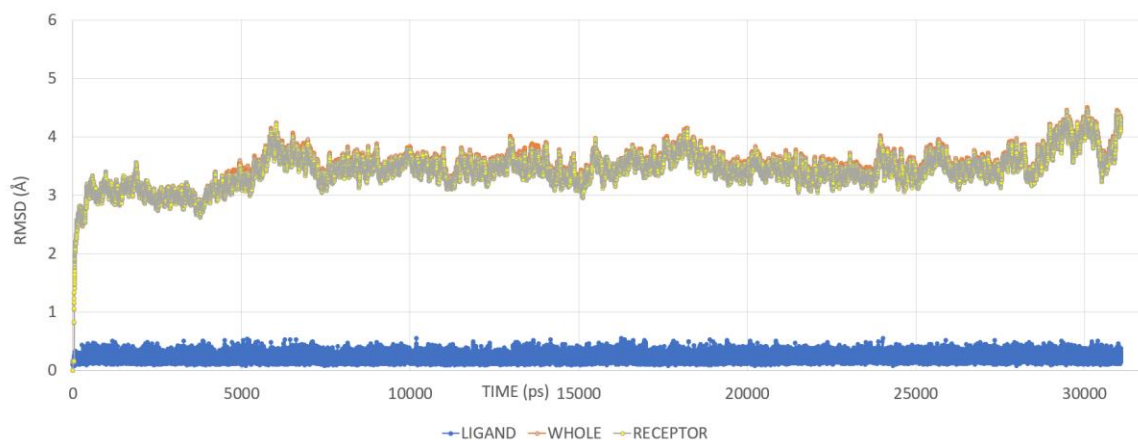


Fig 4. Obtained RMSD value of ligand, receptor, and complex during the simulation

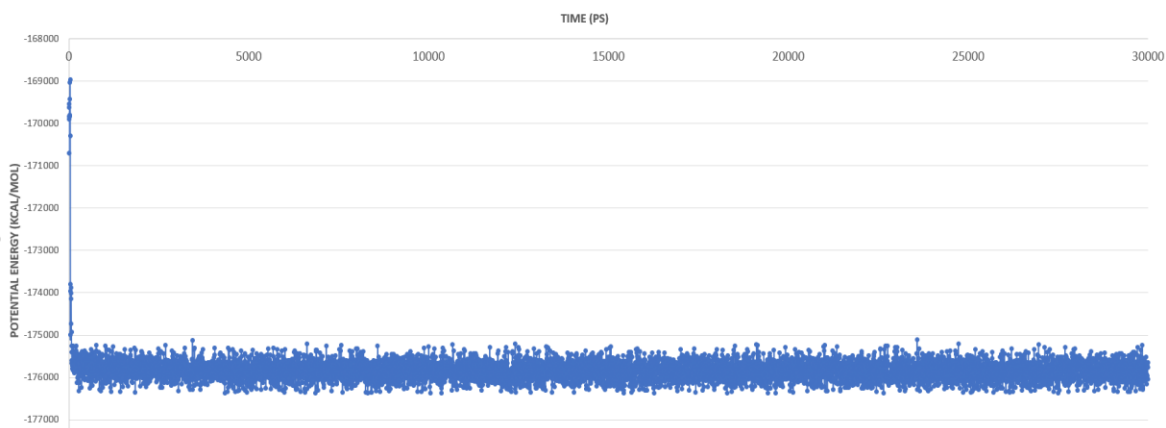


Fig 5. Potential energy profile of lycorine-protein complex

MMPBSA calculations resulted in a Gibbs free energy changing between -24.925 ± 0.1152 kcal mol⁻¹ according to GB (Generalized Born) approach whilst PB (Poisson Boltzmann) approach gives less favorable energy (-2.610 ± 0.2611 kcal mol⁻¹). Entropy calculations from the normal mode analysis (ΔS) were -23.100 ± 6.4635 kcal mol⁻¹ (See Supplementary Material for details). When compared with similar studies [41, 42] in the literature, these values are very reasonable for lycorine to be a drug candidate.

Conclusion

The lycorine molecule has a druggable potential for combating SARS-CoV-2. The binding of lycorine molecule to Cys145 and His41 residues, functioning as catalytic dyad in docking analysis, contributes to the druggable potential of this ligand. Energy calculations via molecular dynamics simulations showed that Gibbs Energy was -24.925 ± 0.1152 kcal mol⁻¹ according to the GB approach and the entropy was -23.100 ± 6.4635 kcal mol⁻¹ between SARS-CoV-2 and lycorine. From these results it can be said that even if the drug effect of the lycorine against COVID-19 is limited, its druggable potential is still remarkable. Therefore, it can be suggested that experimental studies should be conducted by employing pharmacokinetic modifications increasing the drug effect of lycorine.

Abbreviations

MMPBSA: Molecular Mechanics Poisson-Boltzmann Surface Area. RMSD: Root Mean Square Deviation. GB: Generalized Born. PB: Poisson Boltzmann

References

1. Weiss, SR., et al., Coronavirus Pathogenesis and the Emerging Pathogen Severe Acute Respiratory Syndrome Coronavirus. *Microbiology and Molecular Biology Reviews*. 2005. 69(4):635–64.
2. Ji, W., et al., Cross-species transmission of the newly identified coronavirus 2019-nCoV. *Journal of Medical Virology*. 2020. 92:433–440
3. Cucinotta, D. and M. Vanelli, WHO declares COVID-19 a pandemic. *Acta Biomedica*. 2020. 91(1):157–60.
4. Wu, F., et al., A new coronavirus associated with human respiratory disease in China. *Nature*. 2020. 579(7798):265–9.
5. Cui, J., F. Li, and ZL. Shi, Origin and evolution of pathogenic coronaviruses. *Nature Reviews Microbiology*. 2019. 17(3):181–92.
6. Zhou P, Yang X Lou, Wang XG, Hu B, Zhang L, Zhang W, et al. A pneumonia outbreak associated with a new coronavirus of probable bat origin. *Nature*. 2020. 579(7798):270–3.
7. Ghosh, AK., et al., Design and synthesis of peptidomimetic severe acute respiratory syndrome chymotrypsin-like protease inhibitors. *Journal of Medicinal Chemistry*. 2005. 48(22):6767–71.
8. Dömling, A. and L. Gao, Chemistry and Biology of SARS-CoV-2. *Chem*. 2020. 6(6):1283–95.
9. Needle, D., GT. Lountos, and DS. Waugh, Structures of the Middle East respiratory syndrome coronavirus 3C-like protease reveal insights into substrate specificity. *Acta Crystallographica Section D: Structural Biology*. 2015. 71:1102–11.
10. Anand, K., et al., (3CL pro) Structure : Basis for Design of Anti-SARS Drugs. *Science (80-)*. 2003. 300(June):1763–7.
11. Tahir-ul Q., et al., Structural basis of SARS-CoV-2 3CLpro and anti-COVID-19 drug discovery from medicinal plants. *Journal of Pharmaceutical Analysis*. 2020. 4(10) p. 313-319.
12. Callaway E. Beyond Omicron: what's next for COVID's viral evolution. *Nature*. 2021. 600(7888):204–7.
13. Shen, JW., et al., Lycorine: A potential broad-spectrum agent against crop pathogenic fungi. *Journal*

- of Microbiology and Biotechnology. 2014. 24(3):354–8.
14. Shawky, E., In-silico profiling of the biological activities of Amaryllidaceae alkaloids. *Journal of Pharmacy and Pharmacology*. 2017. 69(11):1592–605.
 15. Szlávik, L., and J. Hohman, Alkaloids from *Leucojum vernum* and antiretroviral activity of amaryllidaceae alkaloids. *Planta Medica*. 2004. 70(9):871–3.
 16. Zhang Y-N., et al., Gemcitabine, lycorine and oxysophoridine inhibit novel coronavirus (SARS-CoV-2) in cell culture. *Emerg Microbes & Infections*. 2020. 9(1): 1170-1173
 17. He, J., et al., Amaryllidaceae alkaloids inhibit nuclear-to-cytoplasmic export of ribonucleoprotein (RNP) complex of highly pathogenic avian influenza virus H5N1. *Influenza Other Respi Viruses*. 2013. 7(6):922–31.
 18. Yang, L., et al., Tandem mass tag-based quantitative proteomic analysis of lycorine treatment in highly pathogenic avian influenza H5N1 virus infection. *PeerJ*. 2019(10):1–23.
 19. Liu J., et al., Lycorine reduces mortality of human enterovirus 71-infected mice by inhibiting virus replication. *Virology Journal*. 2011. 8(483):1–9.
 20. Li, SY., et al., Identification of natural compounds with antiviral activities against SARS-associated coronavirus. *Antiviral Research*. 2005. 67(1):18–23.
 21. Jin Y., et al., Lycorine, a non-nucleoside RNA dependent RNA polymerase inhibitor, as potential treatment for emerging coronavirus infections. *Phytomedicine*. 2021. (86):153440.
 22. Jin Z., et al., Structure of Mpro from COVID-19 virus and discovery of its inhibitors. *Nature*. 2020.
 23. Pettersen EF., et al., UCSF Chimera -- A visualization system for exploratory research and analysis. *Journal of Computational Chemistry*. 2004. 25(13):1605–12.
 24. Morris, GM., et al., AutoDock4 and AutoDockTools4: Automated Docking with Selective Receptor Flexibility. *Journal of Computational Chemistry*. 2009. 30:2785–91.
 25. Schmidt MW., et al., General atomic and molecular electronic structure system. *Journal of Computational Chemistry*. 1993. 14(11):1347–63.
 26. Pritchard, BP., et al., New Basis Set Exchange: An Open, Up-to-Date Resource for the Molecular Sciences Community. *Journal of Chemical Information and Modeling*. 2019. 59(11):4814–20.
 27. Santos-Martins, D., et al., AutoDock4 and AutoDockTools4: AutoDock4Zn: an improved AutoDock force field for small-molecule docking to zinc metalloproteins. *Journal of chemical information and modeling*. 2014. 54(8): 2371-2379.
 28. Biovia DS., *Discovery Studio Visualiser*. San Diego: Dassault Systèmes D.S. BIOVIA. 2019.
 29. Nguyen MN, Tan KP, Madhusudhan MS. CLICK - Topology-independent comparison of biomolecular 3D structures. *Nucleic Acids Res*. 2011. 39(SUPPL. 2):24–8.
 30. Case DA., et al., *Amber 2017 reference manual*. Univ California, San Fr. 2017.
 31. Wang, J., et al., Development and testing of a general amber force field. *Journal of Computational Chemistry*. 2004. 25(9):1157–74.
 32. Maier, JA., et al., ff14SB: Improving the Accuracy of Protein Side Chain and Backbone Parameters from ff99SB. *Journal of Chemical Theory and Computation*. 2015. 11(8):3696–713.
 33. Hopkins CW., et al., Long-Time-Step Molecular Dynamics through Hydrogen Mass Repartitioning. *Journal of Chemical Theory and Computation*. 2015.14. 11(4):1864–74.
 34. Miller BR., et al., MMPBSA.py: An Efficient Program for End-State Free Energy Calculations. *Journal of Chemical Theory and Computation*. 2012. 11. 8(9):3314–21.
 35. Roe, DR. and TE. Cheatham, PTRAJ and CPPTRAJ: Software for Processing and Analysis of Molecular Dynamics Trajectory Data. *Journal of Chemical Theory and Computation*. 2013. 9. 9(7):3084–95.
 36. Sharp, KA. and Honig B., Calculating total electrostatic energies with the nonlinear Poisson-Boltzmann equation. *The Journal of Physical Chemistry*. 1990 Sep 1. 94(19):7684–92.

37. Tsui, V., and DA. Case, Theory and applications of the Generalized Born solvation model in macromolecular simulations. *Biopolymers*. 2000. 56(4):275–91.
38. Hou, T., et al., Assessing the Performance of the MM/PBSA and MM/GBSA Methods. 1. The Accuracy of Binding Free Energy Calculations Based on Molecular Dynamics Simulations. *Journal of Chemical Information and Modeling*. 2011. 24. 51(1):69–82.
39. Murugesan, S., et al., Targeting COVID-19 (SARS-CoV-2) main protease through active phytochemicals of ayurvedic medicinal plants – *Emblca officinalis* (Amla), *Phyllanthus niruri* Linn. (Bhumi Amla) and *Tinospora cordifolia* (Giloy) – A molecular docking and simulation study. *Computers in Biology and Medicine*. 2021. 136:104683.
40. Enmozhi, SK., et al., Andrographolide As a Potential Inhibitor of SARS-CoV-2 Main Protease: An In Silico Approach. *Journal of Biomolecular Structure and Dynamics*. 2020.(1):1–10.
41. Gupta, PS., et al., Binding mechanism and structural insights into the identified protein target of COVID-19 and importin- α with in-vitro effective drug ivermectin. *Journal of Biomolecular Structure and Dynamics*. 2020. 28. 1–10.
42. Bera, K., Binding and inhibitory effect of ravidasvir on 3CL pro of SARS-CoV-2: a molecular docking, molecular dynamics and MM/PBSA approach. *Journal of Biomolecular Structure and Dynamics*. 2021. 8. 1–8.

Sarı, Ö., and F. G. Celikel, Karadeniz Bölgesinin İller Düzeyinde Süs Bitkileri Üretimini İncelenmesi. International Journal of Life Sciences and Biotechnology, 2022. 5(1). p. 436-458. DOI: 10.38001/ijlsb.1090043

Karadeniz Bölgesinin İller Düzeyinde Süs Bitkileri Üretimini İncelenmesi

Ömer Sarı^{1*} , Fisun Gürsel Çelikel² 

ÖZET

Türkiye farklı ekolojik ve coğrafi koşulları, özellikle yurtdışı pazarlara yakınlığı ve genç nüfusu ile süs bitkileri sektörü açısından önemli avantajlara sahiptir. Yapılan yatırımlara rağmen ülkemizde süs bitkileri sektörü her kentte aynı düzeyde gelişim göstermemiştir. Bu durum yapılan yatırımların eksik ve plansız olması yanında kent sosyolojilerinin farklılığından da kaynaklanabilmektedir. Çalışmanın amacı süs bitkileri sektörünün genel durumunu ortaya koyarak, Karadeniz Bölgesini il düzeyinde süs bitkileri açısından incelemek ve gelişmesine katkıda bulunmaktır. Çalışma Artvin, Rize, Trabzon, Giresun, Gümüşhane, Bayburt, Ordu, Samsun, Tokat, Amasya, Çorum, Sinop, Kastamonu, Zonguldak, Bartın, Bolu, Karabük ve Düzce illerini kapsamaktadır. Belirtilen bu illerin her birinde süs bitkileri üretim alanları ve üretim yapılan süs bitkisi grupları hakkında bilgi verilerek, süs bitkileri üretimi yapan işletmelerin durumu ortaya konulmuştur. Bu amaçla Tarım ve Orman İl Müdürlükleri ve TÜİK verilerine göre il düzeyinde değerlendirmeler yapılmıştır. İncelenen kentler içerisinde, Samsun, Tokat ve Düzce kentlerinin ulaşım altyapısına ve uygun iklim koşullarına sahip olmaları ve de buldukları konumlar sektörün bu illerde gelişmesinde etkili olmuştur. Bu avantajların yanında turizmin gelişiyor olması da süs bitkileri sektörünün gelişimini olumlu yönde etkilediği tespit edilmiştir. Ancak turizm açısından diğer illere göre önemli atılım içerisinde olan Trabzon ve Rize illerinin süs bitkileri sektörü açısından yeterli gelişmeyi göstermedikleri anlaşılmaktadır. Ordu ili ise yatırımlara rağmen hedeflenen ihracat yapabilirlik durumuna ulaşamamıştır. Bayburt, Gümüşhane, Bolu, Karabük, Sinop ve Amasya illerinde ise süs bitkileri üretimine ait veri bulunmamaktadır. Süs bitkileri sektörünün bölgedeki gelişimi için planlı bir yatırım modeli geliştirilmelidir. Ayrıca yatırım amacıyla iklim koşullarının yanında, nüfus miktarı ve ulaşım alt yapısı gibi kriterlere de dikkat ederek özellikle turizm açısından gelişmekte olan illerin yatırım açısından değerlendirilmesi önerilmektedir.

MAKALE GEÇMİŞİ

Geliş

18 Mart 2022

Kabul

27 Haziran 2022

ANAHTAR KELİMELER

Karadeniz Bölgesi,
İller,
süs bitkileri sektörü,
üretim,
gelişim

¹ Karadeniz Tarımsal Araştırma Enstitüsü, Samsun, Türkiye

² Ondokuz Mayıs Üniversitesi, Ziraat Fakültesi, Bahçe Bitkileri Bölümü, Samsun, Türkiye

*Sorumlu Yazar: omer.sari@tarimorman.gov.tr, omer.sari61@hotmail.com

Investigation of Ornamental Plants Production at the Provincial Level of the Black Sea Region

ABSTRACT

Turkey has important advantages in terms of ornamental plants sector with its different ecological and geographical conditions, especially its proximity to foreign markets and its young population. Despite the investments made, the ornamental plants sector in our country has not developed at the same level in every city. This situation may be due to the incomplete and unplanned investments, as well as the difference in urban sociology. The aim of the study is to reveal the general situation of the ornamental plants sector, to examine the Black Sea Region in terms of ornamental plants at the provincial level and to contribute to its development. The study covers the provinces of Artvin, Rize, Trabzon, Giresun, Gümüşhane, Bayburt, Ordu, Samsun, Tokat, Amasya, Çorum, Sinop, Kastamonu, Zonguldak, Bartın, Bolu, Karabük and Düzce. In each of these provinces, information was given about the ornamental plants production areas and ornamental plant groups, and the situation of the enterprises producing ornamental plants was revealed. For this purpose, evaluations were made at the provincial level according to the data of the Provincial Directorates of Agriculture and Forestry and TUIK. Among the cities examined, the fact that, Samsun, Tokat and Düzce have transportation infrastructure and suitable climatic conditions and their locations have been effective in the development of the sector in these provinces. In addition to these advantages, it was determined that the development of tourism positively affects the development of the ornamental plants sector. However, it is understood that the provinces of Trabzon and Rize, which are in a significant progress compared to other provinces in terms of tourism, do not show sufficient development in terms of ornamental plants sector. Ordu province, on the other hand, could not reach the targeted export capability despite the investments. There is no data on ornamental plants production in the provinces of Bayburt, Gümüşhane, Bolu, Karabük, Sinop and Amasya. For the development of the ornamental plants sector in the region, a planned investment model should be developed rather than scattered and random investments. In addition, it is recommended that developing provinces should be evaluated in terms of investment, especially in terms of tourism, by paying attention to criteria such as population and transportation infrastructure, as well as climatic conditions for investment purposes.

ARTICLE HISTORY

Received

18 March 2022

Accepted

27 June 2022

KEY WORDS

Black Sea Region, provinces, ornamental plants sector, production, development

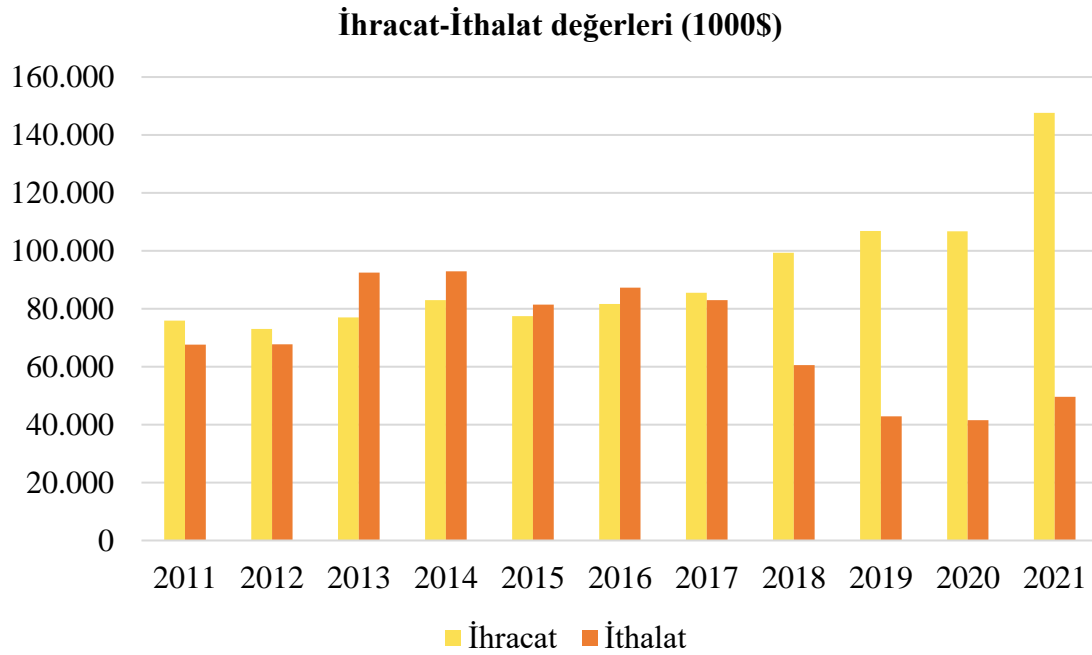
Giriş

Süs bitkileri sektörü ekonomiye yüksek katma değer sağlayan ve önemli istihdam yaratan bir sektör olarak kabul edilmektedir. Dünyada 50'den fazla ülkede yapılan süs bitkileri üretiminin toplam ticaret hacmi 50 milyar dolara ulaşmıştır. Süs bitkileri tüketimi özellikle yüksek satın alma gücü olan Avrupa, Amerika Birleşik Devletleri ve Japonya gibi pazarlara odaklanmıştır [1, 2]. Dünyada kesme çiçek ve saksılı bitkiler üretimi 2021 yılı verilerine göre toplam 734000 ha. alanda yapılmaktadır. Dünya süs bitkileri üretim alanlarının %79'u (580.000 ha.) Asya/Pasifik bölgesinde bulunmaktadır. Asya ülkeleri içinde önemli üreticiler Çin ve Hindistan'dır. Dünya süs bitkileri üretiminin % 11'i Orta ve Güney Amerika ülkeleri tarafından yapılmaktadır. Orta Amerika'da Meksika, Kolombiya, Ekvador, Güney Amerika'da ise Brezilya önemli üretici ülkelerdir. Avrupa Birliği ülkeleri dünya süs bitkileri üretiminin % 8'ini sağlamaktadır. Avrupa Birliği

ülkeleri arasında en önemli üretici ülkeler, Hollanda, İtalya, Almanya ve İspanya'dır. Avrupa Birliği, dünya üzerinde hektar başına verimliliğin en fazla olduğu bölgedir. Afrika ise dünya süs bitkileri üretim alanlarının %2'sine sahiptir. Afrika'da özellikle ekvator kuşağında bulunan Kenya, Tanzanya, Etiyopya, Uganda, Zambiya gibi ülkeler uygun iklimsel koşullar nedeniyle önemli üreticilerdir [1, 2, 3].

Dünyada 2021 yılı verilerine göre, toplam 35 milyar dolar değerinde süs bitkileri üretimi yapılmış ve yaklaşık 28 milyar dolar değerinde ürün ihraç edilmiştir. Dünya genelinde 2021 yılında 11 milyar dolar kesme çiçek, 2 milyar dolar çiçek soğanları, 1.6 milyar dolar değerinde yosun ve ağaç dalları ihracatı yapılmıştır. Canlı bitkiler ihracatı ise 13 milyar dolardır. Dünya süs bitkileri ithalatı ise 25 milyar dolar olarak gerçekleşmiştir [1, 2].

Ülkemizde 2021 yılında 147.6 milyon dolar değerinde ihracat yapmıştır. İhracat 2020 yılına göre %39 oranında artmıştır. İthalat ise 49.570 milyon dolar olarak gerçekleşmiştir. Dış ticaret hacmi yaklaşık 200 milyon dolara ulaşmıştır. İhracatın ithalatı karşılama oranı %298 olmuştur (Şekil 1) [4].

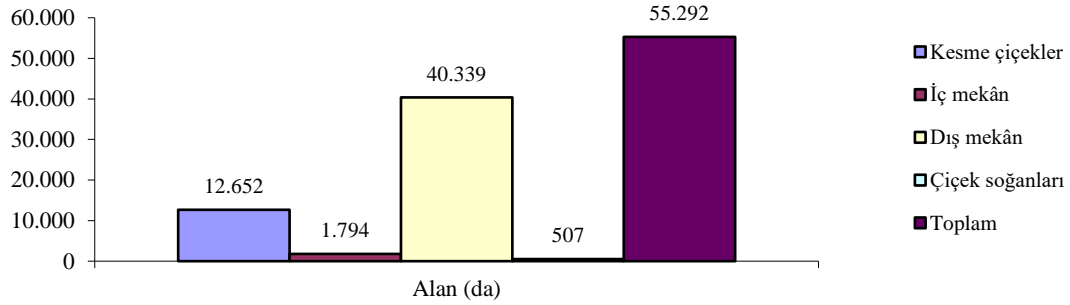


Şekil 1 Türkiye'nin yıllar itibariyle süs bitkileri ihracat-ithalat değerlerinin değişimi [4]

Fig 1 Change of export-import values of ornamental plants by years in Turkey [4]

2005 yılında 26 bin da alanda yapılan üretim 2021 yılı itibariyle 55.292 da'a çıkmış durumdadır. Süs bitkileri üretimi alan bazında en fazla sırasıyla İzmir, Sakarya, Antalya, Bursa ve Yalova illerinde yapılmaktadır. Toplam süs bitkileri üretim alanı içerisinde dış

mekân süs bitkileri %73, kesme çiçekler %23, iç mekân süs bitkileri %3 ve çiçek soğanları %1'lik bir alana sahiptir. Süs bitkileri üretimi 2021 yılında bir önceki yıla göre %2.9 oranında artmıştır. Kesme çiçek üretimi bir önceki yıla göre %5.2, iç mekân süs bitkileri üretimi %11.4 oranında artarken, dış mekân süs bitkileri üretimi ise %1.8 oranında azalmıştır (Şekil 2) [4].



Şekil 2 2021 yılı itibarıyla Türkiye'nin süs bitkileri üretim alanları [4]

Fig 2 Ornamental plants production areas of Turkey as of 2021 [4]

Süs bitkilerinde mevsimlik çiçekler başta olmak üzere bazı kesme çiçekler (şebboy, lisianthus, aslanağzı, Hüsnü Yusuf) ile mavi ladin gibi bazı dış mekân süs bitkilerinde üretim tohumla yapılmaktadır. Üretimde kullanılan hibrit süs bitkisi tohumları ithal edilmektedir. Ayrıca tohum dışında soğanlı (glayöl, lilyum, lale) kesme çiçeklerin üretiminde kullanılan çiçek soğanları da ithal edilmektedir. Fidan olarak kullanılan dış mekân bitkilerinin ithalatı da yüksek miktarlardadır. Süs bitkileri ithalatının 2/3'ü dış mekân bitkileri olup, ithalatın en fazla yapıldığı ülkeler İtalya ve Hollanda'dır. Saksılı süs bitkileri üretiminde kullanılan çelik, fide ve tohumların çoğu ithal edilmektedir. Bu durum süs bitkilerinde dışa bağımlılığı ve üretim maliyetini artıran en önemli faktörler arasındadır [5].

Ülke floramızın, Avrupa ve çevre ülkelere göre oldukça zengin olduğu görülmektedir. Buna karşın doğal bitkilerimizin yeterince değerlendirilmediğini görmekteyiz. Yurt dışından ithal edilen birçok süs bitkisinin ülkemizde de doğal olarak yetiştiği bir gerçektir. Ancak bu bitkilerin üretim yerine ithal edilmesi sektörün gelişmesi önünde önemli engellerden birisidir [6, 7].

Farklı kaynaklarda en yaygın biçimde yer alan süs bitkileri üretiminin sınıflandırması kullanım amaçlarına göre yapılan sınıflandırmadır. Ülkemizde bu sınıflandırma

yaklaşımı benimsenerek süs bitkileri alt sektörü aşağıdaki biçimde sınıflandırılmıştır:

1. Kesme çiçekler: Bu sınıf kesme çiçek amaçlı yetiştirilen türleri içermektedir.
2. İç mekân (saksılı) süs bitkileri: İç mekânda kullanılmak üzere saksı ve kaplarda yetiştirilerek pazarlanan bitki tür ve çeşitlerini kapsamaktadır.
3. Dış mekân süs bitkileri: Dış mekânda peyzaj uygulamalarında kullanılmak üzere üretilip pazarlanan tür ve çeşitleri içermekte, süs ağaç ve ağaççıkları, mevsimlik tek ve çok yıllık çiçekler, çim bitkileri ve yer örtücü olarak kullanılan diğer türler ve süs çimleri bu sınıf içinde değerlendirilmektedir.
4. Doğal çiçek soğanları: Bu sınıf ihraç edilmek üzere doğadan toplanan ve/veya kültür koşullarında üretimi yapılan doğal soğanlı, yumrulu ve rizomlu bitki türlerini (geofitleri) kapsamaktadır. Belirtilen bu dört grup içerisinde üretimi ve ticareti en fazla yapılan sınıf dış mekân süs bitkileri grubudur.

Türkiye, süs bitkileri üretimi için oldukça elverişli ve farklı ekolojik bölgeleri olan bu nedenle çok zengin bir floraaya sahip şanslı bir ülkedir. Akdeniz, Ege ve Marmara Bölgelerinin yanında Karadeniz Bölgesi de iklim özellikleri bakımından süs bitkileri üretimine uygun bir bölgemizdir [9].

Ülkemiz süs bitkileri sektöründe; doğal genetik kaynakları ve ekolojisi, uygun iklim ve coğrafi koşulları, pazarlara yakınlığı ve genç nüfusa sahip olması bakımından önemli avantajlara sahiptir. Ancak sektörün gelişimi her kentte veya bölgede aynı doğrultuda gerçekleşmemektedir. Bunun nedeni sosyo - kültürel sebepler olmasının yanı sıra iklim ve coğrafi koşullar da olabilmektedir [10].

Türkiye’de özellikler Marmara, Ege ve Akdeniz Bölgelerinde süs bitkileri sektörü son yıllarda önemli bir ivme kazanmıştır. Karadeniz Bölgesinde de son yıllarda süs bitkileri sektörünün gelişmesine yönelik farklı ürün gruplarında çalışmalar artmaya başlamıştır. Çalışmanın amacı; süs bitkileri sektörü açısından Karadeniz Bölgesinin durumunu incelemek ve gelişmesine katkıda bulunmaktır. Çalışma Artvin, Rize, Trabzon, Giresun, Gümüşhane, Bayburt, Ordu, Samsun, Tokat, Amasya, Çorum, Sinop, Kastamonu, Zonguldak, Bartın, Bolu, Karabük ve Düzce illerini kapsamaktadır. Belirtilen bu illerin her birinde süs bitkileri üretim alanları ve üretim yapılan süs bitkisi grupları hakkında bilgi verilerek, süs bitkileri üretimi yapan işletmelerin durumu ortaya konmuştur.

Materyal ve Metot

Araştırma alanının özellikleri

Karadeniz Bölgesi Türkiye'deki bölgeler arasında büyüklük olarak üçüncü sırada yer almakta olup, bölgede 18 il bulunmaktadır (Şekil 3). Karadeniz iklimi kıyılarda yıl boyunca yağışlı ve ılımandır. Karadeniz'den gelen nemli hava kütleleri, kıyıya paralel uzanan kuzey Anadolu dağ yamaçlarında bol yağış bırakır. Türkiye'nin en yağışlı bölgesi olan Karadeniz Bölgesi'nde yağışlar bir mevsimde yoğunlaşmayarak yıl boyunca yayılmıştır. Yüksek nem ve bulutluluk nedeniyle yıllık ve günlük sıcaklık farkları en az bu bölgededir. Dağlar kıyıya paralel uzandığından, dağların arkasındaki iç kesimler denizin etkisi altında kalmaz ve iklim karasal ve kurak hale gelir [24, 25]. Bölgenin doğal bitki örtüsü, kıyılardaki yüksek nem ve yağış nedeniyle geniş yapraklı sık ormanlardan oluşmaktadır. Bölge Türkiye ormanlarının %25'ini barındırır ve Türkiye'nin en fazla ormana sahip bölgesidir.



Şekil 3 Karadeniz Bölgesi'nin konumsal haritası

Fig 3 Positional map of the Black Sea Region

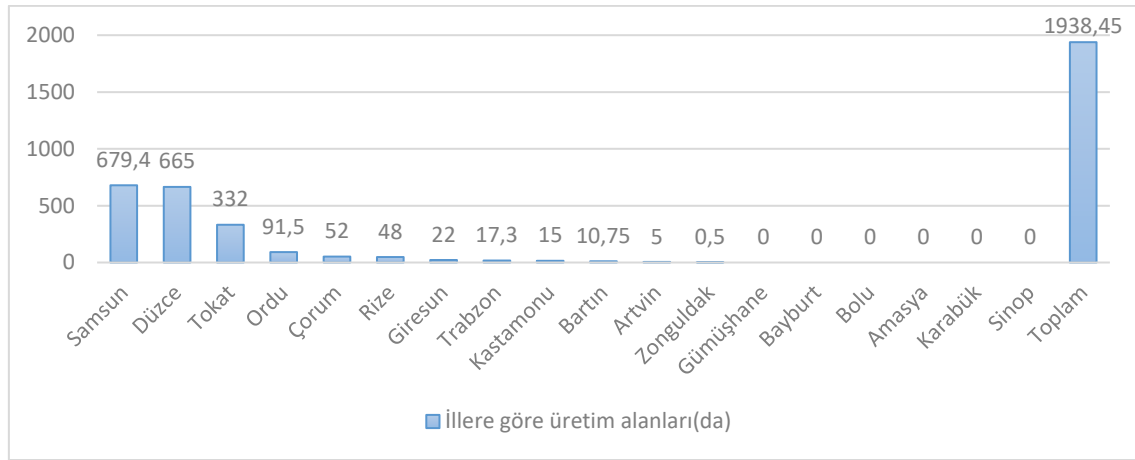
Metot

Bu çalışmanın konusunu, Karadeniz Bölgesi illerinde hâlihazırda süs bitkileri üretimi yapan işletme sayıları, üretilen süs bitkileri ve üretim miktarlarının tespiti oluşturmaktadır. Bu kapsamda tüm Karadeniz Bölgesi illeri çalışmaya dahil edilmiştir. Bu amaçla bilgi toplama formları oluşturularak Tarım ve Orman İl Müdürlükleri aracılığı ile bilgiler toplanmıştır. Bu formlardan elde edilen bilgilerle Karadeniz Bölgesi illerinde süs bitkileri yetiştiriciliğine ilişkin bilgilere ulaşılmıştır. Ayrıca yine bu kapsamda Türkiye İstatistik Kurumu (TÜİK) veri tabanı kayıtları incelenmiştir. Bu iki yöntem ile elde edilen veriler istatistik hesaplama yapılmadan karşılaştırılmış ve bölgenin süs bitkileri üretimi açısından mevcut durumu ortaya konulmuştur.

Bulgular

Karadeniz Bölgesi Süs Bitkileri Üretim Alanları

TÜİK ve Tarım ve Orman İl müdürlüklerinin verilerine göre Karadeniz Bölgesi 1918.45 da'lık süs bitkileri üretim alanına sahiptir. En fazla süs bitkileri üretim alanına sahip iller sırasıyla Samsun (679.4 da), Düzce (665 da), Tokat (332 da) ve Ordu (91.5 da) illeridir (Şekil 4). En düşük üretim alanına ise Artvin (5 da) ve Zonguldak (0.5 da) illerinin sahip olduğu görülmektedir (Şekil 4) [4, 11, 12, 13, 14, 15, 16, 17, 18, 19, 20, 21, 22, 23].



Şekil 4 Karadeniz Bölgesi iller bazında süs bitkileri üretim alanları (da) [4, 11, 12, 13, 14, 15, 16, 17, 18, 19, 20, 21, 22, 23]

Fig 4 Ornamental plants production areas on the basis of provinces in the Black Sea Region (da) [4, 11, 12, 13, 14, 15, 16, 17, 18, 19, 20, 21, 22, 23]

Bölgede 304.86 da alanda 14918900 adet kesme çiçek üretim yapılmaktadır. Kesme çiçek üretim alanı toplam üretim alanlarının %15.7'sini oluşturmaktadır. Bu alanların 82.35 da'ında 8269750 adet kesme yeşillik üretimi yapılmaktadır. Kesme yeşillik üretimi toplam üretim alanlarının ise %4.3'ünü oluşturmaktadır. Üretim tür bazında incelendiğinde, toplam kesme çiçek üretim alanlarının %23'ünü glayöl (Samsun, Tokat), %21.8'ini kasımpatı (Samsun, Tokat), %21.8'ini gypsohilla (Samsun, Tokat), %16.6'sını gerbera (Samsun, Tokat) ve %8.3'ünü gül üretimi (Samsun, Ordu) oluşturmaktadır. Üretim miktarı bakımından ise sırasıyla gypsohilla (%42.5), salidago (%12.9), glayöl (%11.6), gerbera (%8), kasımpatı (%5.6) ve gül (%5) üretimleri en fazla üretimi yapılan türlerdir. Üretim verilerine göre Samsun ve Tokat illeri ön plana çıkmaktadır (Tablo 1) [4].

Tablo 1 Karadeniz Bölgesinde türler bazında kesme çiçek üretim alanları ve miktarları [4]

Table 1 Cut flower production areas and quantities on the basis of species in the Black Sea Region [4]

Ürün adı	İller	Alan (da)	Üretim miktarı (adet)
Gül	Samsun, Ordu	25.35	731750
Lilyum	Samsun	0.50	8000
Karanfil	Samsun	3.07	307000
Glayöl	Samsun, Tokat	70.00	1726000
Gerbera	Samsun, Tokat	50.50	1197000
Kasımpatı	Samsun, Tokat	66.35	830000
Şebboy	Samsun	1.00	4000
Lisianthus	Samsun, Tokat	1.24	120400
Gypsohilla	Samsun, Tokat	66.35	6344750
Salidago	Samsun, Tokat	16.00	1925000
Diğer kesme çiçekler	Samsun, Tokat	9.50	1725000
Toplam		304.86	14918900

Çiçek soğanları üretimi oldukça düşük bir veriye sahiptir. Elde edilen verilere göre Artvin’de 5 da, Trabzon’da 8.25 da, Giresun’da 7.50 da ve Bartın’da 5 da olmak üzere toplamda 25.75 da alanda çiçek soğanı üretimi yapılmaktadır. Çiçek soğanı üretiminin toplam üretim içerisindeki payı ise yaklaşık %1.3’tür (Tablo 2) [4, 11, 13, 14, 20].

Tablo 2 Karadeniz Bölgesinde çiçek soğanları üretim alanları ve miktarları [4, 11, 13, 14, 20]

Table 2 Production areas and quantities of flower bulbs in the Black Sea Region [4, 11, 13, 14, 20]

Ürün grubu	İller	Alan (da)	Üretim miktarı (adet)
Çiçek soğanları	Artvin	5.00	-
	Trabzon	8.25	-
	Giresun	7.50	-
	Bartın	5.00	40000
Toplam		25.75	

Bölgede dış ve iç mekân süs bitkileri üretimi toplam 1607.84 da’lık bir alana sahiptir. Dış mekân ve iç mekân süs bitkileri üretimi Rize, Trabzon, Giresun, Ordu, Samsun, Tokat, Çorum, Bartın, Düzce ve Zonguldak illerinde yapılmaktadır [4, 12, 13, 14, 15, 16, 18, 19, 20, 22, 23]. Dış mekân ve iç mekân süs bitkileri üretiminin toplam üretim içerisindeki payı %83’tür. İç mekân süs bitkileri üretimine ait veriler yetersiz olduğundan üretim alanı ve miktarı tespit edilememiştir. Ancak TÜİK verilerine göre iç mekân süs bitkileri üretimi sadece Samsun ilinde 1.32 da alanda yapılmaktadır. Yine TÜİK verisine göre toplam üretim içerisindeki payı yaklaşık %0,1’dir (Tablo 3) [4].

Tablo 3 Karadeniz Bölgesinde dış ve iç mekân süs bitkileri üretim alanları ve miktarları [4, 12, 13, 14, 15, 16, 18, 19, 20, 22, 23]

Table 3 Production areas and quantities of outdoor and indoor ornamental plants in the Black Sea Region [4, 12, 13, 14, 15, 16, 18, 19, 20, 22, 23]

Ürün grubu	İller	Alan (da)	Üretim miktarı (adet)
Dış mekân ve iç mekân süs bitkileri	Rize, Trabzon, Giresun, Ordu, Samsun, Tokat, Çorum, Bartın, Düzce, Zonguldak	1607.84	2312169
	Toplam	1607.84	2312169

İller bazında süs bitkileri üretim alanları

Artvin

Artvin ilinde süs bitkileri yetiştiriciliği ile ilgili TÜİK kayıtlarında herhangi bir veri bulunmamaktadır. Ancak Artvin Tarım ve Orman İl Müdürlüğü kayıtlarına göre Murgul ilçesinde 5 da açık alanda doğal çiçek soğanları (*Galanthus woronovi* ve *Lilium candidum*) üretimi yapılmaktadır. Artvin'in toplam üretim alanları içindeki payı %0.3'tür (Şekil 4) [11].

Rize

Rize ilinde yaklaşık 48 da alanda dış mekân süs bitkileri üretimi yapılmaktadır. Rize'nin toplam üretim alanları içindeki payı %2,5'tir (Şekil 4) [4, 12].

Trabzon

Trabzon 17.35 da alanda dış mekân süs bitkileri ve doğal çiçek soğanları üretimi yapılmaktadır. Trabzon'un toplam üretim alanları içindeki payı %0,9'dur. Bu alanların 3 da'ı sera, 14.35 da'ı açık alandır. Ayrıca Karadeniz Bölgesinde Samsun'dan sonra kurulan ikinci mezar Trabzon ilinde yer almaktadır (Tablo 4) [13].

Tablo 4 Trabzon ilinde süs bitkileri üreten işletmeler ve üretim alanları [13]

Table 4 Enterprises and production areas producing ornamental plants in Trabzon province [13]

İşletme no	Toplam üretim alanı (da)	Sera (da)	Açık alan (da)	Faaliyet türü	İlçesi
1	9.10	3.00	6.10	Dış mekân	Akçaabat
2	8.25	-	8.25	Doğal çiçek soğanı	Sürmene
Toplam	17.35	3	14.35		

Giresun

Giresun ilinde toplam 22 da alanda süs bitkileri üretimi yapılmaktadır. Giresun'un toplam üretim alanları içindeki payı %1.1'dir. Toplam alanın 14.5 da'ında dış mekân, iç mekân ve kesme çiçek üretimi, 7.5 da'ında ise doğal çiçek soğanı üretimi yapılmaktadır. Toplam alanın 5.8 da'ı sera alanıdır. Sera alanlarının 0.40 da'ı alçak tünel, 1.60 da'ı yüksek tüneldir. Toplam üretim miktarı ise 67000 adettir (Tablo 5) [4, 14].

Tablo 5 Giresun ili süs bitkileri sera üretim alanları ve miktarları [4]

Table 5 Greenhouse production areas and amounts of ornamental plants in Giresun province [4]

Örtü altı türü	Ürün adı	Alan (da)	Üretim miktarı (adet)
Alçak tünel	Dış mekân	0.40	16000
Yüksek tünel	Dış mekân	1.60	51000
Toplam		2.0	67000

İlde 4 işletmeye ait veri bulunmaktadır. İşletmelerin sahip olduğu toplam üretim alanının 16.20'si açık alan, 5.80 da'ı ise sera alanıdır. İşletmelerde dış mekân, iç mekân, kesme çiçek ve doğal çiçek soğanı üretimi yapılmaktadır (Tablo 6) [14].

Tablo 6 Giresun ilinde süs bitkileri üreten işletmeler ve üretim alanları [14]

Table 6 Enterprises producing ornamental plants and their production areas in Giresun [14]

İşletme no	Toplam üretim alanı (da)	Sera (da)	Açık alan (da)	Faaliyet türü	İlçesi
1	2.50	2.30	0.20	Dış ve iç mekân, kesme çiçek	Bulancak
2	12.00	3.50	8.50	Dış ve iç mekân, kesme çiçek	Merkez
3	1.50	-	1.50	Doğal çiçek soğanı	Keşap
4	6.00	-	6.00	Doğal çiçek soğanı	Bulancak
Toplam	22.00	5.80	16.20		

Ordu

Ordu ilinde 91.5 da alanda kesme çiçek, doğal çiçek soğanları ve dış mekân süs bitkileri üretimi yapılmaktadır. Ordu'nun toplam üretim alanları içindeki payı %4.7'dir. TÜİK verilerine göre 6 da alanda kesme gül üretimi yapılmaktadır. Kesme gül üretimi toplam üretim alanlarının yaklaşık %7'sini oluşturmaktadır. Bu alanın 5.5 da alan plastik sera ve 0.5 da ise yüksek tüneldir. Toplam gül üretimi ise 240000 adettir (Tablo 7) [4].

Tablo 7 Ordu ili süs bitkileri sera üretim alanları ve miktarları [4]

Table 7 Ornamental plants greenhouse production areas and quantities in Ordu province [4]

Örtü altı türü	Ürün adı	Alan (da)	Üretim miktarı (adet)
Plastik sera	Gül	5.5	220000
Yüksek tünel	Gül	0.5	20000
Toplam		6.0	240000

İlde 12 işletmeye ait veri bulunmaktadır. İşletmelerin sahip olduğu toplam üretim alanınının 87.1 da'ı açık alan, 4.4 da'ı ise sera alanıdır (Tablo 8) [15].

Tablo 8 Ordu ilinde süs bitkileri üreten işletmeler ve üretim alanları [15]

Table 8 Enterprises producing ornamental plants and their production areas in Ordu [15]

İşletme no	Toplam üretim alanı (da)	Sera (da)	Açık alan (da)	Faaliyet türü	İlçesi
1	2.30	-	2.30	Dış mekân	Altınordu
2	14.00	-	14.00	Dış mekân	Altınordu
3	2.10	0.10	1.90	Dış ve iç mekân, soğanlı bitkiler	Gülyalı
4	25.00	-	25.00	Dış mekân	Perşembe
5	2.00	0.10	1.90	Dış ve iç mekân, soğanlı bitkiler	Altınordu
6	38.30	-	38.31	Dış mekân	Altınordu
7	2.00	0.30	1.70	Dış ve iç mekân, soğanlı bitkiler	Altınordu
8	1.30	0.10	1.20	Dış ve iç mekân, soğanlı bitkiler	Altınordu
9	0.80	0.10	0.70	Dış ve iç mekân, soğanlı bitkiler	Altınordu
10	2.20	2.20	-	Kesme çiçek	Perşembe
11	1.00	1.00	-	Kesme çiçek	Altınordu
12	0.50	0.50	-	Kesme çiçek	Altınordu
Toplam	91.5	4.4	87.1		

Samsun

Samsun ilinde 679.4 da alanda kesme çiçek, iç mekân ve dış mekân süs bitkileri üretimi yapılmaktadır. Samsun'un toplam üretim alanları içindeki payı %35'tir. Kesme çiçek üretim alanı 35.41 da ile toplam üretim içindeki payı %5.2'dir. İç mekân süs bitkileri 1.32 da ile toplam üretim içerisindeki payı %0.2'dir. Dış mekân süs bitkileri ise 642.67 da alanı kapsamaktadır ve %94.6'lik bir paya sahiptir. Türler bazında en fazla üretim 19.35

da alan ve 491750 adet ile kesme gül üretimidir. Yine türler bazında toplam üretim alanının %3.06'sı kesme gül, %0.5 karanfil, %0.6'sı ise gerbera üretimini oluşturmaktadır (Tablo 9) [4, 16].

Tablo 9 Samsun ilinde süs bitkileri toplam üretim alanları ve üretim miktarları [4, 16]

Table 9 Total production areas and production amounts of ornamental plants in Samsun [4, 16]

Ürün adı	Alan (da)	Üretim miktarı (adet)
Karanfil, kesme	3.07	307000
Glavyöl, kesme	2.00	20000
Gerbera, kesme	3.50	210000
Gypsohilla, kesme	0.35	8750
Kasımpatı (Krizantem), kesme	2.00	80000
Lilyum (Zambak), kesme	0.40	2000
Gül, kesme	19.35	491750
Lisianthus, kesme	0.24	20400
Şebboy, kesme	1.00	40000
Solidago, kesme	1.00	50000
Diğer kesme çiçekler	2.50	75000
İç mekân süs bitkileri	1.32	26280
Dış mekân süs bitkileri	642.67	907450
Toplam	679.4	2913630

Örtü altı üretimi (44.77 da) toplam üretimin %7,1'ini oluşturmaktadır. Örtü altı üretiminin 43.45 da'ı plastik sera ve 1.32 da'ı ise yüksek tüneldir. Örtü altı alanlarının 32.76 da'ında kesme çiçek (%73,2), 10.69 da'ında dış mekân (%23.8) ve 1.32 da'ında iç mekân (%3) süs bitkileri üretimi yapılmaktadır [4] (Tablo 10).

Tablo 10 Samsun ili süs bitkileri örtüaltı üretim alanları ve miktarları [4]

Table 10 Ornamental plants greenhouse production areas and amounts in Samsun [4]

Örtü altı türü	Ürün adı	Alan (da)	Üretim miktarı (adet)
Plastik sera	Karanfil, kesme	3.07	125000
Plastik sera	Gerbera, kesme	3.50	210000
Plastik sera	Gypsohilla, kesme	0.10	5000
Plastik sera	Kasımpatı (Krizantem)	2.00	194000
Plastik sera	Gül, kesme	19.35	491750
Plastik sera	Şebboy, kesme	1.00	40000
Plastik sera	Lisianthus, kesme	0.24	20400
Plastik sera	Diğer kesme çiçekler	2.50	75000
Plastik sera	İç mekân süs bitkileri	1.00	26000
Plastik sera	Dış mekân süs bitkileri	10.69	287423
Yüksek tünel	Gül, kesme	1.00	25000
Yüksek tünel	İç mekân süs bitkileri	0.32	1280
Toplam		44.77	4762660

İlde kayıtlı 13 işletmenin faaliyetlerine ilişkin veri bulunmaktadır. İşletme faaliyetlerinde en büyük pay dış mekân süs bitkilerine aittir. Bunun dışında kesme gül ve lilyum üretimi de önemli bir yer tutmaktadır (Tablo 11) [16].

Tablo 11 Samsun ilinde işletmeler bazında süs bitkileri üretim alanları [16]

Table 11 Ornamental plants production areas on the basis of enterprises in Samsun [16]

İşletme no	Toplam üretim alanı (da)	Sera (da)	Açık alan (da)	Faaliyet türü	İlçesi
1	11.00	-	11.00	Dış mekân	Bafra
2	241.00	-	241.00	Yer örtücü/ Rulo çim	Bafra
3	160.00	-	160.00	Dış mekân	Çarşamba
4	120.00	-	120.00	Yer örtücü/ Rulo çim	Çarşamba
5	54.00	-	54.00	Dış mekân	Çarşamba
6	1.00	1.00	-	Keme gül	Çarşamba
7	1.90	-	1.90	Dış mekân	Atakum
8	47.00	-	47.00	Yer örtücü/ Rulo çim	Atakum
9	20.00	-	20.00	Dış mekân	Atakum
10	4.50	-	4.50	Dış mekân	Atakum
11	2.00	1.00	1.00	Lilyum, Ortanca	Terme
12	2.00	1.00	1.00	Kesme gül	Terme
13	15.00	15.00	-	Kesme gül	19 Mayıs
Toplam	679.4	18	661.4		

Samsun da Ondokuzmayıs, Bafra ve Terme ilçeleri süs bitkileri üretimi açısından ön plana çıkmıştır. Mayıs ve Aralık ayları arası başta gül, lilyum, gerbera, karanfil, krizantem ve glayöl olmak üzere kesme çiçek üretimi yapılmaktadır. Diğer illere göre kesme çiçek açısından en geniş çaplı üretimin yapıldığı ilde, Türkiye geneli ile beraber Sinop, Samsun, Ordu, Giresun, Trabzon, Rize, Artvin, Gümüşhane, Tokat, Amasya ve Çorum'daki çiçekçilerin kesme çiçek ihtiyacı karşılanmaktadır [9, 17].

Samsun süs bitkileri üretimi açısından potansiyeli olan bir bölgedir. Uygun iklimi ve zengin doğal florası ile başta Çarşamba ve Bafra olmak üzere Samsun'un verimli ovalarında süs bitkileri yetiştiriciliği yönünden yüksek potansiyel vardır. Sulama ve ulaşım imkânlarının olması, Samsun'u süs bitkileri üretimi için cazip hale getirmektedir. Mevcut geleneksel tarım ürünlerine alternatif olabilecek süs bitkileri, Samsun'da üreticilerin dikkatlerini çekmektedir. Samsun'da gece gündüz sıcaklık farkının yıl boyu düşük kalması gül, karanfil, krizantem gibi türlerde fizyolojik bozuklukların ortaya çıkmasına engel olmaktadır. Samsun'un en büyük avantajlarından biride uluslararası deniz limanına ve hava alanına sahip olmasıdır. Pazar ülkelere yakınlık önemli bir

avantajdır ve Karadeniz’e sınır ülkelere gemiyle kolaylıkla taşıma yapmak mümkündür. Kesme çiçek ihracatında en önemli sorunlardan biri taşıma maliyetinin yüksekliğidir. Deniz yoluyla taşıma maliyeti düşüktür [9]. Ayrıca bölgedeki iller arasında Çiçek Mezat’ının kurulduğu ilk il Samsun ilidir. Samsun mezatında Pazartesi, Çarşamba ve Cuma günleri satış yapılmaktadır (Şekil 5).



Şekil 5 S.S. Flora Çiçekçilik Üretim ve Pazarlama Kooperatifi Samsun çiçek mezarı

Fig 5 S.S. Flora Cicekcilik Production and Marketing Cooperative Samsun flower auction

Tokat

Tokat ilinde yaklaşık 331.90 da alanda kesme çiçek, iç mekân ve dış mekân süs bitkileri üretimi yapılmaktadır. Tokat’ın toplam üretim alanları içindeki payı %17.1’dir. İlde 210 da alanda kesme çiçek üretimi yapılmaktadır. Kesme çiçek üretiminin toplam üretim içerisindeki payı %63.3’tür (Tablo 12) [4, 18].

Tablo 12 Tokat ilinde süs bitkileri üretim alanları ve üretim miktarları [4]

Table 12 Ornamental plants production areas and production amounts in Tokat province [4]

Ürün adı	Alanı (da)	Üretim miktarı (adet)
Glayöl, kesme	68.00	1700000
Gerbera, kesme	47.00	987000
Gypsohilla, kesme	66.00	6336000
Kasımpatı (Krizantem), kesme	6.00	750000
Lisianthus, kesme	1.00	100000
Solidago (Altınbaşak), kesme	15.00	1875000
Diğer kesme çiçekler	7.00	975000
İç mekân süs bitkileri	-	-
Dış mekân süs bitkileri	121.90	508505
Toplam	331.90	13231505

Dış mekân süs bitkileri üretim alanı ise 121.90 da'dır. Dış mekân süs bitkileri üretiminin payı ise %36.7'dir. Tür bazında ise toplam üretim alanının %20.49'u glayöl, %19.88'i gypsohilla, %14.16'sı ise gerbera üretimini oluşturmaktadır. İç mekân süs bitkileri üretimine ait veri ise bulunmamaktadır (Tablo 12). Örtü altı üretim alanları 21.6 da'dır. Toplam üretim alanları içerisindeki örtü altı üretimin payı ise %6.5'tir. Örtü altı alanlarının 19.6 da'ı plastik sera (%90.7), 0.70 da'ı yüksek tünel (%3.3) ve 1.30 da'ı ise cam sera (%6) dır (Tablo 13) [4].

Tablo 13 Tokat ili süs bitkileri örtü altı üretim alanları ve miktarları [4]

Table 13 Ornamental plants greenhouse production areas and amounts in Tokat province [4]

Örtü altı türü	Ürün adı	Alan (da)	Üretim miktarı (adet)
Plastik sera	Gerbera, kesme	4.70	987000
Plastik sera	Gypsohilla, kesme	6.00	6336000
Plastik sera	Kasımpatı (Krizantem)	3.00	750000
Plastik sera	Lisianthus, kesme	1.00	100000
Plastik sera	Diğer kesme çiçekler	3.00	975000
Plastik sera	Dış mekân süs bitkileri	1.90	50000
Yüksek tünel	Dış mekân süs bitkileri	0.70	8500
Cam sera	Dış mekân süs bitkileri	1.30	800
Toplam		21.6	9207300

İlde kayıtlı 5 işletmeye ait veri bulunmaktadır. Dış mekân ve iç mekân süs bitkileri üretimi yapan işletmeler, merkez ve Niksar ilçelerinde faaliyet göstermektedir (Tablo 14).

Tablo 14 Tokat ilinde süs bitkileri üreten işletmeler ve üretim alanları [18]

Table 14 Enterprises producing ornamental plants and their production areas in Tokat province [18]

İşletme no	Toplam üretim alanı (da)	Sera (da)	Açık alan (da)	Faaliyet türü	İlçesi
1	7.00	2.00	5.00	Dış ve iç mekân	Merkez
2	2.50	-	2.50	Dış mekân	Merkez
3	20.00	0.20	19.80	Dış mekân	Niksar
4	21.50	0.15	21.35	Dış ve iç mekân	Merkez
5	12.55	0.80	11.75	Dış ve iç mekân	Merkez
Toplam	63.55	3.15	60.40		

Çorum

Çorum ilinde 52.16 da alanda dış mekân süs bitkileri üretimi yapılmaktadır. Toplam üretim alanları içindeki payı %2,7'dir. Üretim alanının 0.35 da'ı seradır. İşletmeler

merkez ve Osmancık ilçelerinde bulunmaktadır (Tablo 15) [19].

Tablo 15 Çorum ilinde süs bitkileri üreten işletmeler ve üretim alanları [19]

Table 15 Enterprises producing ornamental plants and their production areas in Çorum [19]

İşletme no	Toplam üretim alanı (da)	Sera (da)	Açık alan (da)	Faaliyet türü	İlçesi
1	50.40	-	50.40	Dış mekân	Osmancık
2	1.76	0.35	1.40	Dış mekân	Merkez
Toplam	52.16	0.35	51.80		

Bartın

Bartın ilinde toplam 10.75 da alanda süs bitkileri üretimi yapılmaktadır. Bartın'ın toplam üretim alanları içindeki payı %0.55'tir. İlde üretimin %53.5'ini oluşturan 5.75 da alanda dış mekân, iç mekân ve mevsimlik çiçek süs bitkileri üretimi yapılmaktadır. Çiçek soğanları üretimi ise toplam üretimin %46.5'ini oluşturan 5 da alanda yapılmaktadır. Üretim alanının %12.7'si seradır. İlde iki işletmenin verisi bulunmaktadır [4, 20] (Tablo 16).

Tablo 16 Bartın ilinde süs bitkileri üreten işletmeler ve üretim alanları [20]

Table 16 Enterprises producing ornamental plants and their production areas in Bartın province [20]

İşletme no	Toplam üretim alanı (da)	Sera (da)	Açık alan (da)	Faaliyet türü	İlçesi
1	3.60	0.60	3.00	Dış ve iç mekân, mevsimlik çiçekler	Merkez
2	2.15	0.77	1.38	Dış mekân, mevsimlik çiçekler	Merkez
Toplam	5.75	1.37	4.38		

Kastamonu

Kastamonu ilinde 15.20 da alanda kesme çiçek süs bitkileri üretimi yapılmaktadır. Kastamonu'nun toplam üretim alanları içindeki payı %0.8'dir. Üretimin %20'sini gypsohilla (8100 adet), %13.2'ünü glayöl (6000 adet) ve %6.6'sını solidago (2400 adet) üretimi oluştururken, %55.92'sini diğer kesme çiçekler (60000 adet) oluşturmaktadır (Tablo 17) [4, 21].

Tablo 17 Kastamonu ilinde süs bitkileri üretim alanları ve üretim miktarları [4]

Table 17 Ornamental plants production areas and production amounts in Kastamonu province [4]

Ürün adı	Alan (da)	Üretim miktarı (adet)
Glayöl, kesme	2.00	6000
Gypsohilla, kesme	3.00	8100
Lilyum (Zambak), kesme	0.70	6000
Solidago (Altınbaşak), kesme	1.00	2400
Diğer kesme çiçekler	8.50	60000
Toplam	15.20	136500

İlde iki işletmenin verisi bulunmaktadır. Merkez ilçede faaliyet gösteren işletmeler kesme çiçek üretimi yapmaktadır. İşletme üretim alanlarının 13.70 da'ı açık alan (%90.1) ve 1.50 da'ı seradır (%9.9) (Tablo 18) [21].

Tablo 18 Kastamonu ilinde süs bitkileri üreten işletmeler ve üretim alanları [21]

Table 18 Ornamental plants and production areas in Kastamonu province [21]

İşletme no	Toplam üretim alanı (da)	Sera (da)	Açık alan (da)	Faaliyet türü	İlçesi
1	5.50	-	5.50	Kesme çiçek	Merkez
2	9.70	1.50	8.20	Kesme çiçek	Merkez
Toplam	15.20	1.50	13.70		

Düzce

Düzce ilinde süs bitkileri yetiştiriciliği ile ilgili 665 da alanda dış mekân süs bitkileri üretimi yapılmaktadır. Toplam üretim alanları içindeki payı %34'tür. Üretim alanlarının 663.4 da'ı açık alan (%99.73), 1.10 da'ı yüksek tünel (%0.2) ve 0.50 da'ı ise alçak tüneldir (%0.07). Toplam dış mekân süs bitkileri üretim miktarı 711550 adettir (Tablo 19) [4].

Tablo 19 Düzce ili süs bitkileri örtü altı üretim alanları ve miktarları [4]

Table 19 Düzce province ornamental plants greenhouse production areas and their amounts [4]

Örtü altı türü	Ürün adı	Alan (da)	Üretim miktarı (adet)
Alçak tünel	Dış mekân	0.50	1800
Yüksek tünel	Dış mekân	1.10	49000
	Toplam	1.60	50800

İlde dört işletmeye ait veri bulunmakta ve bu işletmelerin tamamı dış mekân süs bitkileri

üretimi yapmaktadır. İşletmeler merkez ve Gölyaka ilçelerinde faaliyet göstermektedir (Tablo 20) [22].

Tablo 20 Düzce ilinde süs bitkileri üreten işletmeler ve üretim alanları [22]

Table 20 Enterprises producing ornamental plants and their production areas in Düzce [22]

İşletme no	Toplam üretim alanı (da)	Sera (da)	Açık alan (da)	Faaliyet türü	İlçesi
1	15.00	-	14.00	Dış mekân	Merkez
2	102.65	-	102.65	Dış mekân	Merkez
3	58.00	-	58.00	Dış mekân	Merkez
4	15.75	-	15.75	Dış mekân	Gölyaka
Toplam	191.40	-	190.40		

Zonguldak

Zonguldak ilinde 0.5 da alanda 8000 adet dış mekân süs bitkileri üretimi yapılmaktadır. Toplam üretim alanları içindeki payı %0.03'tür. Toplam alanın 0.2 da'nını plastik sera oluşturmaktadır. Üretim miktarı 3000 adettir[4, 23].

Tartışma

Ülkemizde süs bitkileri üretiminde 15 yıllık süreçte toplamda %290'luk bir artış olup bunun içerisindeki en büyük payın dış mekân süs bitkilerine ait olduğu bildirilmiştir [29]. Karadeniz Bölgesi 2015 verilerine göre ülke genelindeki süs bitkisi üretim alanlarının % 2.9'unu (1.422 da) ve süs bitkisi üretiminin ise % 1.05'ini (16.327.119 adet) kapsadığı bildirilmiştir [4, 27]. Yaptığımız çalışmada elde edilen verilere göre, 2021 yılında bölgedeki üretim miktarı 18.976.014 adet olarak gerçekleşmiştir. Üretim miktarı 2015 yılından 2021 yılına kadar yaklaşık % 14 oranında artmıştır. Bölgedeki üretim miktarı ülke üretimimizin %1.1'ini karşılamaktadır. Yine 2015 verilerine göre 1422 da olan üretim alanı yaklaşık %27 oranında bir artış göstererek 1938.45 da'a ulaşmıştır. Bölgedeki üretim alanları 2021 yılı itibariyle ülke süs bitkileri üretim alanlarının % 3.5'ini oluşturmaktadır.

Türkiye genelinde üretim miktarları bakımından kesme çiçekler %60.9'luk bir paya sahipken bunu %31.9 ile dış mekân süs bitkileri, %4.3 ile çiçek soğanları ve %2.9 ile iç mekân süs bitkileri takip etmektedir. Tür bazında ise en fazla üretim %32.3 ile karanfil üretimidir. Bunu %7.2 ile gerbera ve %5.6 ile gül üretimi takip etmektedir.

Karadeniz Bölgesinde ise üretim alanlarının %83'ü dış ve iç mekân süs bitkisi, %15.7

kesme çiçekler ve %1.3'ü çiçek soğanı üretim alanıdır. Üretim alanları 2015 ile 2021 yılları arasında dış mekân süs bitkilerinde %10.5, iç mekân süs bitkilerinde %92.2 ve kesme çiçeklerde %0.6 oranında artarken, çiçek soğanı üretimi %67 oranında azalmıştır [4]. Yine bölgede üretim tür bazında incelendiğinde, toplam kesme çiçek üretim alanlarının 2015 yılında 53.2 da alan ile gypsohilla (% 24) alan bakımından ilk sırada yer alırken [4, 27], 2021 yılında 70 da alan ile glayöl (%23) ilk sırada yer almıştır. Gypsohilla %21.8'lik oranla kasımpatı ile birlikte ikinci sıradadır. Bunu %16.6 ile gerbera ve %8.3 ile gül üretimi takip etmektedir. Karadeniz Bölgesinde üretim miktarı bakımından ise gypsohilla 2015 yılında 4524918 adet ve % 27.5'lik üretim miktarı ile yine ilk sırada yer alırken, 2021 yılında %16.5'lik bir artış göstererek 6344750 adet olmuştur. Salidago üretimi %12.9, glayöl %11.6, gerbera %8, kasımpatı %5.6 ve gül %5 üretimleri en fazla üretimi yapılan diğer türlerdir [2, 3, 4].

Türkiye'de süs bitkilerinin gelişiminde başarıya ulaşmak için; iklim koşulları da dikkate alınarak ülke genelinde uzun vadeli üretim planlamaları yapılmalı, bu sayede uygun standart ve kalitede üretim sağlanmalıdır [29]. Bölgede yaz aylarında yapılacak üretim sıcaklığın düşük olmasından dolayı Akdeniz ve Ege bölgelerine göre avantaj sağlarken kış aylarında yapılacak üretimde ise bazı illerde sıcaklığın 0 °C'nin altına düşmesinden dolayı ısıtmayı zorunlu kılmaktadır. Ayrıca kış aylarında güneşlenme süresinin de Ege ve Akdeniz Bölgelerine göre düşük olması ek aydınlatmaya ihtiyacını arttırmaktadır [26]. Bu nedenle yüksek yatırım maliyeti gerektiren kış üretiminin ısıtma giderlerinin düşük olabileceği mikro klima alanlarda veya jeotermal ısıtma imkânlarının bulunduğu illerde yapılması uygun olacaktır.

Ülkemizde süs bitkileri sektörü tam örgütlü bir yapıya sahip olmadığından süs bitkileri sektörüyle ilgili beyan edilen bazı verilerde tutarsızlıklar söz konusudur [29]. Bu durum Karadeniz Bölgesi içinde geçerlidir. Elde edilen verilere göre TÜİK ve Tarım ve Orman İl Müdürlükleri verileri arasında farklılıklar olduğu görülmüştür. Bölgede mevcut durumun belirlenmesi ve üretim planlamasının yapılması amacıyla üreticinin ve üretim alanlarının kayıt altına alınması oldukça önemlidir.

Bölgede süs bitkileri alanında önemli atılımlar yapan Samsun, Tokat, Düzce, Ordu ve turizm açısından önemli gelişme kaydeden Trabzon süs bitkileri üretimi açısından potansiyelleri yüksek illerdir. Ancak bölgenin başlıca önemli sorunları; pazar arayışının olması, işletmelerin tarımsal birlik ve kooperatifleşmeye sahip olmaması, işletmelerin

küçük aile işletmelerinden oluşması, pazarlama altyapısının yetersizliği, üretim planlamasına dönük sağlıklı bir düzenlemenin olmayışı olarak bildirilmiştir [30]. Bölgenin sahip olduğu avantajların sektörün gelişimi açısından kullanılabilmesi için üretim stratejilerinin geliştirilmesi ve uzun vadeli politikaların oluşturulması gereklidir.

Sonuç ve öneriler

Bu çalışmada TÜİK ve Tarım ve Orman İl müdürlüklerine ait süs bitkileri verileri derlenerek Karadeniz Bölgesinde süs bitkileri üretim alanlarına ait mevcut durum ortaya konulmaya çalışılmıştır.

Bölgedeki süs bitkileri sektöründeki gelişmişlik il büyüklükleri ile kısmi bir paralellik göstermesine rağmen gelişmişliğin asıl sebebinin doğru yatırımlar, bilgi, teknik, satış desteği ve turizm alt yapısı olduğu görülmektedir. İncelenen kentler içerisinde Samsun, Düzce ve Tokat kentlerinin uygun iklim koşulları, nüfusu ve coğrafi konumlarının yanında nispeten daha gelişmiş bir turizm ve ulaşım altyapısına da sahip olmalarının süs bitkisi sektörünün büyüklüğü ve gelişimi üzerine çok önemli katkı yaptığı anlaşılmaktadır. Ancak turizm açısından diğer illere göre önemli atılım içerisinde olan Trabzon, Rize ve Kastamonu illerinin ise süs bitkileri sektörü açısından yeterli gelişmeyi gösteremedikleri de görülmektedir. Ordu ili ise yatırımlara rağmen hedeflenen ihracat yapabilirlik durumuna ulaşamamıştır. Bayburt, Gümüşhane, Bolu, Karabük illerinde ise süs bitkileri üretimi bulunmamaktadır. Sonuç olarak bölgede süs bitkileri sektörünün gelişiminin sağlanması için; Bölgedeki her ilde üretim yerine süs bitkileri üretimi için uygun olan iller seçilmelidir. Bu iller içerisinde planlı üretim bölgeleri oluşturularak bu alanlarda yatırımların eksiksiz yapılmalıdır. Süs bitkileri yetiştiriciliği alanındaki eğitici ve üreticiler tam donanımlı hale getirilmelidir. Bir üretimde en son aşama ve en önemli safha elde edilen ürünün karşılığının alınmasıdır. Bu amaçla sektörün bölgede gelişimi için satış garantisinin sağlanması ile artabileceği düşünülmektedir. Ayrıca bölgenin süs bitkileri açısından ekolojik zenginliğinin yerinde değerlendirilmesi de üretimin geliştirilmesine katkı sağlayacaktır. Bu amaçla bölgede yayılış gösteren ve süs bitkileri açısından ekonomik değeri olan birçok tür kültüre alınarak çoğaltılabilir ve peyzaj alanlarında kullanılabilir.

Karadeniz Bölgesi iklimi, gelişen şehirleri, turizm ve ulaşım altyapısı ile hem bölgesel olarak hem de Rusya ve Orta Asya pazarlarına yakınlığı ile süs bitkileri üretimi ve pazarlanmasına yönelik alternatif sağlayacak önemli bir bölgedir. Elde edilen verilere

göre bölgedeki üretici sayısı 44 gibi düşük bir sayıdır. Marmara bölgesinde sadece Yalova ilinde dış mekân süs bitkisi üretimi yapan yetkilendirilmiş üretici sayısı 43'tür [8]. Bölgede satış yapan işletmelerin birçoğu Marmara, Ege ve Akdeniz'den ürünler getirterek satış yapmaktadır.

Bölgenin süs bitkileri üretimi ve yatırımları ile ilgili önemli sorunları mevcuttur.

Bu sorunlar;

- Üretim altyapısının plansız bir şekilde gelişmesi,
- Bölgede veya her il içerisinde ilin hemen hemen her bölgesinde üretimin teşvik edilmeye çalışılması,
- Üretimin karlılık getirip getirmeyeceğine bakılmadan az veya çok her şekilde yapılmaya çalışılması,
- Süs bitkileri işletmelerinin altyapısının eksik kurulması. Eksik altyapıya sahip işletmelerin ayakta kalamaması ve bu nedenle kısa sürede faaliyetlerine son vermesi,
- Yatırımlar yapılırken ulaşım ve eğitim altyapısının yeterince göz önünde bulundurulmaması,
- Teknik desteklerdeki yetersizlikler. Örneğin teşvik edilen bir üreticiden işletmenin kurulması, üretim materyalinin temini, bitkilerin yetiştirilmesi, hasat edilmesi, paketlenmesi ve pazar bulması ve nihayetinde ürünleri pazara ulaştırması beklenmektedir. Oysa günümüz üretim modelinde süs bitkileri üretimi alanında gelişmiş ülkelerde bu bahsi geçen her bir aşamanın üreticisi ve tedarikçisi farklıdır ve tam bir iş bölümü vardır. Özellikle Antalya'da yapılan üretimde bu model işletilmektedir. Bölgemizde durum değerlendirildiğinde, altyapı olarak eksik kurulan birçok işletmenin problemler ile karşılaştığı görülmüştür. Eksik kurulan işletmeler ilk yatırım yılının sonunda umutsuzluğa kapılmakta, ikinci yıl üretimden çekilmekte veya süs bitkileri üretimi dışında kolay üretebilecekleri ve satabilecekleri ürünlere yönelmektedirler.

Karadeniz Bölgesinde süs bitkileri sektörü açısından tespit edilebilen mevcut durum ve sorunlar karşısında aşağıdaki öneriler geliştirilmiştir;

- Yatırımların planlı bir şekilde yapılması,
- Yatırımların her il veya il içerisinde her bölgeye yapılmaması,
- Planlanan ve yatırım yapılan alanların ulaşım altyapısının ve birbirlerine

yakınlığının mutlaka göz önünde bulundurulması,

- İşletme kuracak olanlara teşviklerin verilmeden önce süs bitkileri yetiştiriciliği ve sektörü kapsamında eğitimin zorunlu tutulması ve eğitimler sırasında çalışma ücreti de ödenerek teşvik edilmesi,
- Eğitimlerin teori ile birlikte kapsamlı biçimde uygulamalı olması eğitim süresinin amaca ulaşacak şekilde uzun süreli verilmesi ve böylece katılımcıların tecrübe edinmelerinin sağlanması,
- Sürdürülebilirliğin sağlanmasında en önemli konu pazar arayışı, ürün pazarlanması ve satışlarıdır. Pazar arayışı tamamıyla üreticiye bırakılmayıp tarım ekonomistlerinden oluşturulacak birimler aracılığıyla üreticiye yol gösterilmelidir. Çünkü pazarı olmayan veya pazarı bulunamayan hiçbir ürünün üretimine yönelik yatırımların başarıya ulaşması mümkün değildir.

Bu öneriler doğrultusunda üniversiteler, araştırma enstitüleri, Tarım ve Orman İl Müdürlükleri ve üreticiler arasında daha fazla işbirliğine ve çalışmaya ihtiyaç duyulduğunu söylemek mümkündür.

Teşekkür

Karadeniz Bölgesindeki tüm Tarım ve Orman İl Müdürlüklerine destekleri için teşekkür ederiz.







Kaynaklar

1. AIPH, The international statistics flowers and plants yearbook. Hannover: Institut für Gartenbauökonomie, 2017.
2. Dünya Süs Bitkileri Sektörü Araştırma Raporu. Süs Bitkileri ve Mamulleri İhracatçıları Birliği, <http://www.susbitkileri.org.tr/images/d/library/ef989b05-0f43-4657-b96b-87c6c6743c14.pdf>, 2021. s.34. [Erişim tarihi: 05.06.2022].
3. Süsbir, Süs Bitkileri Sektör Raporu. <https://www.susbir.org.tr/belgeler/raporlar/susbitkileri-sektor-raporu-2021.pdf>, 2021.s.15 [Erişim tarihi: 05.06.2022].
4. TÜİK, <https://data.tuik.gov.tr/Kategori/GetKategori?p=tarim-111&dil=1>, [Erişim tarihi: 01.03.2022].
5. Balkaya, A., et al., Bahçe Bitkileri Tohumluğu Üretimi ve Kullanımında Değişimler ve Yeni Arayışlar. Türkiye Ziraat Mühendisliği VIII. Teknik Kongresi Bildiriler Kitabı-2, 2015.p 985.
6. Çelikel, F.G, Süs Bitkileri Ders Notları. OMÜ Ziraat Fakültesi Samsun, 2014.
7. Çelikel, F.G, Süs bitkilerinde tohumluk (tohum, fide, fidan, soğan) üretimi ve kullanımı. Süsbir Dergisi, 2015a. (3):32-33.
8. Eroğlu, A, Yalova ilinde dış mekân süs bitkilerinin mevcut durumu, sorunları ve çözüm önerileri, Yüksek Lisans Tezi, Fen Bilimleri Enstitüsü, 2016. s.94.
9. Çelikel, F.G, Samsun ilinin süs bitkileri potansiyeli. In: Bakır T, Duran H, editors. Tarım Hayvancılık Çevre- Ekonomi Sağlık Kadın Öğretim Üyeleri Toplum Konferansları. Bursa: Renkvizyon Matbaacılık Yayıncılık, 2015b. pp.20-31.
10. Gülgün, B, TR83 İllerinde Süs Bitkileri Sektörünün Mevcut Durumu ve Geliştirilmesi Üzerine Bir

- Araştırma, Selçuk Tarım Bilimleri Dergisi, 2016.3(1), 18-24.
11. Artvin Tarım ve Orman İl Müdürlüğü. Bitkisel Üretim Şubesi Kayıtları, 2020.
 12. Rize Tarım ve Orman İl Müdürlüğü. Bitkisel Üretim Şubesi Kayıtları, 2020.
 13. Trabzon Tarım ve Orman İl Müdürlüğü. Bitkisel Üretim Şubesi Kayıtları, 2020.
 14. Giresun Tarım ve Orman İl Müdürlüğü. Bitkisel Üretim Şubesi Kayıtları, 2020.
 15. Ordu Tarım ve Orman İl Müdürlüğü. Bitkisel Üretim Şubesi Kayıtları, 2020.
 16. Samsun Tarım ve Orman İl Müdürlüğü. Bitkisel Üretim Şubesi Kayıtları, 2020.
 17. Hekimoğlu, B. and Altındeğer, M, Süs Bitkileri Sektör Raporu, Samsun Valiliği Gıda, Tarım ve Hayvancılık İl Müdürlüğü,
https://samsun.tarimorman.gov.tr/Belgeler/Yayinlar/Tarimsal_strateji/sus_bitkileri_sektor_rapor_u.pdf, 2019. [Erişim Tarihi: 01.05.2021].
 18. Tokat Tarım ve Orman İl Müdürlüğü. Bitkisel Üretim Şubesi Kayıtları, 2020.
 19. Çorum Tarım ve Orman İl Müdürlüğü. Bitkisel Üretim Şubesi Kayıtları, 2020.
 20. Bartın Tarım ve Orman İl Müdürlüğü. Bitkisel Üretim Şubesi Kayıtları, 2020.
 21. Kastamonu Tarım ve Orman İl Müdürlüğü. Bitkisel Üretim Şubesi Kayıtları, 2020.
 22. Düzce Tarım ve Orman İl Müdürlüğü. Bitkisel Üretim Şubesi Kayıtları, 2020.
 23. Zonguldak Tarım ve Orman İl Müdürlüğü. Bitkisel Üretim Şubesi Kayıtları, 2020.
 24. Sensoy, S., et al., Türkiye iklimi, Turkish State Meteorological Service (DMI), Ankara, 2008.
 25. Öztürk, M. Z., Çetinkaya, G. ve Aydın, S, Köppen-Geiger iklim sınıflandırmasına göre Türkiye'nin iklim tipleri, Coğrafya Dergisi, 2017. (35), 17-27.
 26. Kazaz, S., Kesme Çiçek ve Dış Mekân Süs Bitkileri Yetiştiriciliği Ön Fizibilite Raporu. BAKKA, 2018. s.77.
 27. Akbulut, M., et al., Karadeniz Bölgesi'nde Bahçe Bitkilerinin Mevcut Durumu ve Potansiyeli. Türk Bilimsel Derlemeler Dergisi, 2015. (2), 33-37.
 28. TÜİK., Türkiye İstatistik Kurumu Web Sayfası. Bitkisel Üretim İstatistikleri. <https://biruni.tuik.gov.tr/medas/?kn=92&locale=tr>, 2022. [Erişim Tarihi: 01.03.2022].
 29. Gülgün, B., Dünyada ve Türkiye'de Süs Bitkilerine Genel Bakış, Problemler ve Çözüm Önerileri, TÜRKTOB Dergisi sayı 14 yıl 2015, 2015.
 30. Yazıcı K., ve Gülgün B., TR83 illerinde süs bitkileri sektörünün mevcut durumu ve geliştirilmesi üzerine bir araştırma, Selçuk Tarım Bilimleri Dergisi, 2016. 3(1): 18- 24.

Demirhan I., et al., Antioxidant, Antimicrobial Properties and In Silico Study of a N,N'-(ethane-1,2-diyl)bis(1-(9H-fluoren-2-yl)methanimine). International Journal of Life Sciences and Biotechnology, 2022. 5(3): p. 459-479. DOI: 10.38001/ijlsb.1097396

Antioxidant, Antimicrobial Properties and *In Silico* Study of a N,N'-(ethane-1,2-diyl)bis(1-(9H-fluoren-2-yl)methanimine)

İlter Demirhan^{1*} , Erkan Oner² , Adem Necip³ , Aydin Aktas⁴ ,
Medine Cotak⁵ , Yetkin Gok⁶ 

ABSTRACT

This study aimed to determine the antibacterial and antioxidant activities of the newly synthesized Schiff base and to support the laboratory results with molecular modeling studies. Antibacterial activity of schiff bases was demonstrated using Gram (-) *Pseudomonas aeruginosa* and *Acinetobacter baumannii* bacterial strains. Minimum Inhibition Concentration (MIC) values were determined to evaluate their antimicrobial activity against Gram (-) *Pseudomonas aeruginosa* and *Acinetobacter baumannii* bacterial strains. In antioxidant experiments, the responses to DPPH and ABTS radicals were calculated at certain concentration ranges and graphs were drawn. For the molecular modeling study, Autodock Vina and Discovery Studio 2020 package programs were used. The observed bacterial inhibition activity varied depending on the clinical isolate and the concentration of the samples tested. The highest inhibition activity was achieved at concentration of 75 µl -100 µl. N,N'-(ethane-1,2-diyl)bis(1-(9H-fluoren-2-yl)methanimine) samples. Molecular docking results show that N,N'-(ethane-1,2-diyl)bis(1(9H-fluoren-2-yl) methanimine) binds strongly to the 4ZIIY and 4ZHU structures. It has been proven by molecular docking study that the synthesized Schiff base ligand has antibiotic resistance properties. N, N'-(ethane-1,2-diyl)bis(1-(9Hfluoren-2-yl) methanimine) synthesis compound showed moderate activity against A. baumannii and P. aeruginosa strains. It is known that Schiff bases have strong biological activities and antibacterial activity. In this study, the synthesis of Schiff base showed antibacterial and antioxidant activity. In addition, our results were supported by molecular modeling. Our findings can be taken to a higher level with in vivo and in vitro studies.

ARTICLE HISTORY

Received

6 April 2022

Accepted

20 October 2022

KEYWORDS

Antioxidant,
antimicrobial,
In silico,
molecular docking,
schiff base,

Introduction

As in the whole world, *Pseudomonas aeruginosa* (*P.aeruginosa*) and *Acinetobacter baumannii* (*A.baumannii*) strains have started to be isolated with increasing frequency and multiple resistance in our country in recent years. This rapid increase in antimicrobial resistance reduces

¹ Department of Electronic Automation, Schedule of Biomedical Device Technology, Harran University, Sanliurfa/Turkey

² Department of Biochemistry, Faculty of Pharmacy, Mersin University, Mersin/Turkey.

³ Department of Pharmacy Services, Vocational School, Harran University, Sanliurfa/Turkey.

⁴ Vocational School of Health Service, Inonu University, Malatya/Turkey.

⁵ Department of Medical Services and Techniques, Inonu University, Iğdır/Turkey.

⁶ Department of Biochemistry, Faculty of Science and Literature, Inonu University, Malatya/ Turkey

*Corresponding Author: Dr. İlter Demirhan, ilterdemirhan@harran.edu.tr

and prolongs the treatment options of clinicians, especially in intensive care units (ICU) infections caused by these microorganisms [1,2,3]. ICUs are the units most frequently encountered with nosocomial infections and resistant microorganisms due to the more frequent use of invasive procedures, long hospital stays, and the fact that hospitalized patients are often immunosuppressive, elderly, newborns or patients who have undergone an operation [4,5]. *A.baumannii* and *P.aeruginosa* are Gram (-) microorganisms that are the most common cause of nosocomial infections in ICU [6,7,8,9]. Since these bacteria are resistant to external environmental conditions, they can maintain their vitality for a long time in the hospital environment. In addition, the fact that they are naturally resistant to many antibiotics and can develop acquired resistance in a short time gradually limits the antimicrobials that can be used in the treatment of the infections they cause [11,12,13].

Researching a new drug and putting it on the market involves quite laborious processes. These processes, which require a long time, are also quite expensive. Today, the discovery and development processes of drugs can be realized in a shorter time and at less cost by using special design technologies [14]. Molecular docking studies can define that a drug can be an active ingredient in a structure [15]. By looking at the receptor and ligand structure, it is seen whether the compound carries a functional drug group [16]. Compounds containing the azomethine group (-HC=N-), which were first introduced by Hugo Schiff in 1864 and formed as a result of the reaction of a primary amine with an active carbonyl compound, and which are generally carried out by acid, base catalysis or heat, are called schiff bases [17,18]. Schiff bases are useful chelates because of their ease of preparation, structural variety, and steric and electronic control mechanisms [1]. These are privileged ligands and find a lot of use thanks to their advantages such as versatile synthesis and good solubility [1]. In azomethine derivatives, the C=N bond is required for biological activity. The nitrogen atom of azomethine is involved in the formation of components and interacts in normal cell processes [21]. It is known that heterocyclic structures containing an azole ring system and a phenol derivative have a wide range of biological applications for antifungal, antioxidant, antibacterial, antitumor, anti-inflammatory and antipyretic applications [16].

Reactive oxygen species (ROS) are free radicals produced during oxidative metabolism. ROS can attack nucleic acid, lipids, proteins, polyunsaturated fatty acids and carbohydrates and induce their oxidation, which can lead to oxidative damage such as protein alteration, membrane dysfunction, enzymatic inactivation, and rupture of DNA strains [17]. Therefore, ROS must be cleared by cellular voters. An antioxidant can inhibit or delay the oxidation of other molecules. Antioxidants can inhibit the formation of free radicals and also delay lipid

peroxidation, which leads to deterioration of food and pharmaceutical products during processing and storage. Antioxidants can protect the human body from ROS. Antioxidants are widely used in foods to prevent radical chain reactions that cause food spoilage [18].

In this study, which was carried out for the first time, it was determined that the synthesized *N,N'*-(ethane-1,2-diyl)bis(1-(9*H*-fluorene-2-yl)methanimine) (**1**) schiff base, which is frequently found in ICU (*A. baumannii*, *P. aeruginosa*) bacteria and to investigate the binding affinities and models in bacterial structures by in silico studies. New compounds need to be synthesized and investigated, since existing compounds show weak bacterial resistance.

Material and Methods

Chemistry

Compound **1** which bearing fluorene group was prepared in the air atmosphere. The solvents and all other reagents were commercially available from Sigma-Aldrich and ISOLAB chemical company and used without further purification. Melting point was identified in glass capillaries under air with an Electrothermal-9200 melting point apparatus. FT-IR spectrum was saved in the range 400-4000 cm⁻¹ on Perkin Elmer Spectrum 100 FT-IR spectrometer. Proton (¹H) and Carbon (¹³C) NMR spectra were recorded using either a Bruker AC300P FT spectrometer operating at 300.13 MHz (¹H) and 75.47 MHz (¹³C) in CDCl₃ with tetramethylsilane as an internal reference. Elemental analyses were performed by Inonu University Scientific and Technological Research Center (Malatya, TURKEY).

Synthesis of (*N,N'*-(ethane-1,2-diyl)bis(1-(9*H*-fluorene-2-yl)methanimine), **1**

Compound **1** was synthesized by reacting 1 mL (0.9 g, 15 mmol) ethylenediamine with 2 equivalents of 9*H*-fluorene-2-carbaldehyde (5.83 g, 30 mmol) in ethanol (20 mL) for 2 hours. Then, the compound crystallized by cooling the mixture. The crystals formed were washed by filtration with diethyl ether. As a result white solid was obtained. Yield: 82% (5.07 g); m.p.: 97-98 °C; color: white. Anal. calc. for C₃₀H₂₄N₂: C: 87.35; H: 5.86; N: 6.79. Found: C: 87.07; H: 5.93; N: 6.85. ¹H NMR (400 MHz, CDCl₃, 298 K), δ (ppm): 3.10 and 3.74 (t, 4H, *J*= 5.6 and 5.5 Hz, -NCH₂CH₂N-); 3.93 and 4.05 (s, 4H, Ar-CH₂-Ar); 7.32-8.01 (m, 14H, Ar-*H*); 8.40 and 8.43 (s, -N=CH-*imine*). ¹³C NMR (100 MHz, CDCl₃, 298 K), δ (ppm): 35.2 and 37.6 (Ar-CH₂-Ar); 60.4 and 61.2 (-NCH₂CH₂N-); 119.0, 125.2, 126.9, 127.4, 128.1, 128.6, 129.4, 130.3, 141.1, and 143.4 (Ar-C); 161.6 (-N=CH-*imine*).

Antioxidant study Antimicrobial study

DPPH Radical Scavenging Activity

DPPH• free radical scavenging activity of synthesized compounds and standard antioxidants was performed by Blois method [19,44]. 1 lt of 0.1 mM DPPH• solution was prepared in ethanol and adjusted to 3 ml by adding solutions of different concentrations [9,15]. The prepared solutions were thoroughly vortexed and incubated in the dark for 30 minutes. Absorbance was measured at 517 nm with a spectrophotometer. DPPH• radical scavenging activity was calculated using the following equation:

$$\text{DPPH}\bullet \text{ scavenging effect (\%)} = (\text{Absorbance of control vs. absorbance of sample}) / \text{Absorbance of control} \times 100$$

ABTS•⁺ Scavenging Activity

It was made by the color change method, which is an indication that the dark blue/green colored ABTS•⁺ cation radical has lost its radical property as a result of the treatment with antioxidants [22]. ABTS•⁺ cation radical was obtained by mixing the ABTS solution prepared with 2 mmolL⁻¹ H₂O and 2.45 mmolL⁻¹ potassium persulfate (K₂S₂O₈) solution at a ratio of 1:2 and incubating for 14 hours in the dark and at room temperature. Before using the ABTS•⁺ cation radical, the ABTS•⁺ solution was diluted with sodium phosphate buffer (0.1 molL⁻¹, pH 7.4) to obtain an absorbance of 0.750 ± 0.025 at 734 nm. Then, 10, 20, 30 µL of the stock solutions of the synthesized organic compounds were taken and phosphate buffer was added until the volume was 3 mL, and 1 mL of ABTS•⁺ solution was added to them and vortexed. Inhibition was calculated at 734 nm for each concentration [21,22].

ABTS•⁺ cation radical scavenging activity was calculated using the following equation:

$$\text{ABTS}\bullet^+ \text{ radical scavenging activity (\%)} = ((\text{Absorbance of control} - \text{Absorbance of sample}) / \text{Absorbance of control}) \times 100$$

Antimicrobial study

Bacterial Strains

Pseudomonas aeruginosa and *Acinetobacter baumannii* bacterial strains were used to evaluate the antimicrobial activity. All multidrug-resistant clinical isolates were obtained from Bacteriophage Microlysis Therapeutic Bank (MTBB, Ankara, Turkey): *A. baumannii* (MTBB 120557), *P. aeruginosa* (MTBB 130203). Condalab branded Miller's LB Agar was used as the medium. In the macrodilution method, the effect of different concentrations of antimicrobial agent dilutions prepared using sterile tubes against a certain concentration of microorganism was investigated. With the effective concentrations of the substances synthesized against the used microorganism; MIC value is determined according to the presence or absence of growth

[23,24]. Optical density (OD) measurement and counting of viable microorganisms are the most commonly used methods for monitoring growth. The results obtained are more sensitive than the agar dilution method [23].

Antimicrobial activity

For bacterial inhibition assay, 1 ml of overnight cultures of the tested strains were diluted with 100 ml Luria Broth (LB) and grown until the turbidity equal to 0.1 to 0.3 McFarland at 37°C at 100 rpm. The dilutions of the Compound **1** in concentration range of 25-100 μ l with cell suspensions were added to the test tubes and incubated at 37 °C with shaking at 150 rpm. The turbidity was measured for up to 5 h.

Preparation of medium

Miller's LB Broth (5.5 g) was weighed and diluted to 250 ml, then the density was adjusted according to McFarland standard (0.5).

Molecular modeling method

Ligand System

N,N'-(ethane-1,2-diyl)bis(1-(9*H*fluoren-2-yl) methanimine) material was imported in sdf format in ChemDraw 3d program. Converted from Open Babel GUI program to pdb format.

Protein system

4ZIIY and 4ZHU crystal structures were obtained from the Protein Data Bank (www.rcsb.org). While choosing the crystal structures, care was taken to ensure that the resolution value of the proteins was a maximum of 3 Å.

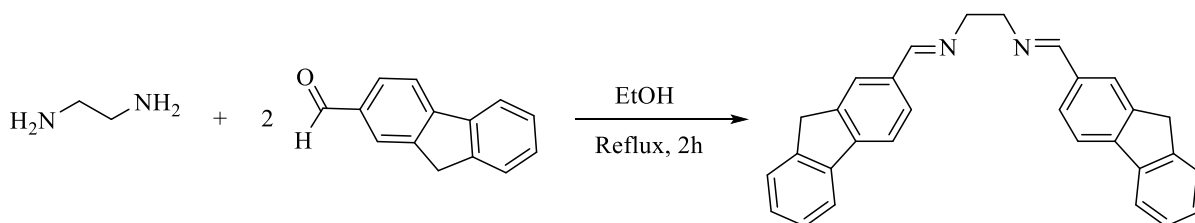
Molecular Modeling

Autodock 4.2.6 is used. AutoDockTools program was used to create modeling data entry files. In all models, a cube divided into squares with 40x40x40 point dimensions in x, y, z directions was created. A length of 0.375 Å (about one quarter the length of the carbon-carbon covalent bond) and a distance dependent function of the dielectric constant were used to calculate the energy of the couplings. 10 processes were carried out using Lamarckian genetic algorithm logic. Randomly placed fragments with an initial population of 50 were used with a maximum energy of 2.5×10^6 and a maximum of 2.7×10^4 formations. A mutation rate of 0.02 and a genetic change rate of 0.8 were chosen. Results that differed less than 0.5 Å in root mean square deviation (RMSD) were pooled and the results of the optimal free energy of coupling were chosen as the final complex structures. Ligand-protein interactions in the active site of **1** were investigated using Autodock Vna 1.1.2 [16] and Discovery Studio 2020 programs [23].

Results and Discussion

Synthesis and characterization study

Compound **1** was synthesized from the ethylenediamine and 2 equivalents of the 9*H*-fluorene-2-carbaldehyde in ethanol (Scheme 1). This compound was obtained in moderate yields 82%. The compound's structure was determined using FT-IR, ¹H NMR, ¹³C NMR spectroscopic methods, and elemental analysis techniques. The proton peak was detected in the ¹H NMR spectra by a characteristic peak at the imine (N=CH), which appeared as a highly downfield shifted singlet at 8.40 and 8.43 ppm. The ethylene group (CH₂) proton peaks were observed as triplets at 3.10 and 3.74 ppm. Aliphatic methylene (CH₂) singlet peaks between two aromatic rings were observed at 3.93 and 4.05 ppm. Proton peaks were observed as multiplets in both aromatic rings, ranging from 7.32-8.01 ppm. In the ¹³C NMR spectra of the compound, a carbon signal at 161.6 was attributed to imine carbon (N=CHN) at a lower area compared to other aromatic carbons. The ethylene group (CH₂) carbon peaks were observed at 60.4 and 61.2 ppm. Aliphatic methylene (CH₂) carbon peaks between two aromatic rings were observed at 35.2 and 37.6 ppm. All data are consistent with the proposed formula.



Scheme 1. *N,N'*-(ethane-1,2-diyl)bis(1-(9*H*-fluorene-2-yl)methanimine), **1**

Antioxidant activity results

DPPH Radical Scavenging Activity Results

The reducing capacity of DPPH• radicals was determined by the reduction in absorbance at 517 nm as a result of the induction of antioxidants. The maximum absorbance of a stable DPPH• radical in ethanol was recorded as 517 nm. They make the antioxidant molecules an inactive radical by donating a hydrogen proton to the DPPH• radical. As a result of this reaction, low absorbance is obtained. A color change from purple to yellow is visually noticeable in this interaction. Therefore, DPPH• is often used as a substrate to evaluate the antioxidant activity of antioxidant molecules [20,23]. DPPH• is a stable free radical and takes an electron or a hydrogen radical to become a stable diamagnetic molecule [23]. Table 1 shows the decrease in the concentration of DPPH• radical due to the radical scavenging capacity of both the **1** extract and

the standards. At the same concentration (0.03 mg/ml), the scavenging effect of **1** extracts and standards on DPPH• radical decreased in the order Trolox(90.5%) > BHA(75.8%) > BHT(73.8%) > **1** (49.8%). As a result of these results, **1** extract showed that it was effective in terms of free radical scavenging activity.

ABTS•⁺ Radical Scavenging Activity Results

The blue-green ABTS•⁺ radical cation scavenging activity of the synthesized compounds was measured according to the radical scavenging activity of the standard antioxidants BHA, BHT and Trolox. In this method, antioxidants oxidize the ABTS•⁺ dark cation radical, resulting in a reduction of dark color. The color change that occurs with this reaction is used as a parameter for the measurement of antioxidant potential [31]. The scavenging effect on ABTS•⁺ radical decreased in the order of Trolox (90.5%) > BHA(75.6%) > BHT(73.7%) > **1** (27%) is seen in Table 1. As a result of these results, **1** extract showed that it has an effect on free radical scavenging.

Table 1 The scavenging activity of compound **1** on ABTS•⁺ radical

Extract	DPPH ^b 0.03 mg/ml	ABTS ^b 0.009 mg/ml
1	49.8 ± 2.6	27 ± 0.5
BHA ^a	75.8 ± 5.9	75.6 ± 6.2
BHT ^a	73.8 ± 5.3	73.7 ± 5.7
TROLOX ^a	90.5 ± 6.4	90.5 ± 6.7

Data mean ± standard deviation,

^astandard antioxidant

^bThe percent (%) of ABTS and DPPH radical scavenging activity

Antimicrobial activity results

The effects of *N,N'*-(ethane-1,2-diyl)bis(1-(9*H*-fluoren-2-yl)methanimine) (**1**) on *P.aeruginosa* and *A.boumannonii* bacteria were evaluated by measuring their optical density. It has been shown that compound **1** has a high inhibitory effect on *A.boumannonii* and a low level inhibitory effect on *P.aeruginosa* (Table 2). The effect of compound **1** on multidrug resistant strains is shown in

Table 3 as IC₅₀ and % inhibition values. The effectiveness of compound **1** for *P.aeruginosa* and *A.boumannii* bacteria is shown in Figure 1 and Figure 2, where the MIC₅₀ values for *P.aeruginosa* at 225 minutes and for *A.boumannii* bacteria at 120 minutes are between 75 µl and 100 µl.

Table 2 Inhibitory effect of compound **1** on *A.boumannii* and *P.aeruginosa*

Compound	<i>P. aeruginosa</i>	<i>A. boumannii</i>
1	--+	-+++

%25 - %50 inhibition -- (less active), %50-%75 inhibition --+ (modarate active), %75 - %100 inhibition -+++ (highly active).

Table 3 % inhibition and IC₅₀ values of compound **1** due to multidrug resistance against bacterial strains

Sample	IC ₅₀ µg/ml		% Inhibition		
	<i>Pseudomonas aeruginosa</i> (MTBB 130203)	<i>Acinetobacter baumannii</i> (MTBB 120557)		<i>Pseudomonas aeruginosa</i> (MTBB 130203)	<i>Acinetobacter baumannii</i> (MTBB 120557)
1	75 µg/ml	80 µg/ml	25 µg/ml	10	20
			50 µg/ml	25	35
			75 µg/ml	30	45
			100 µg/ml	50	70

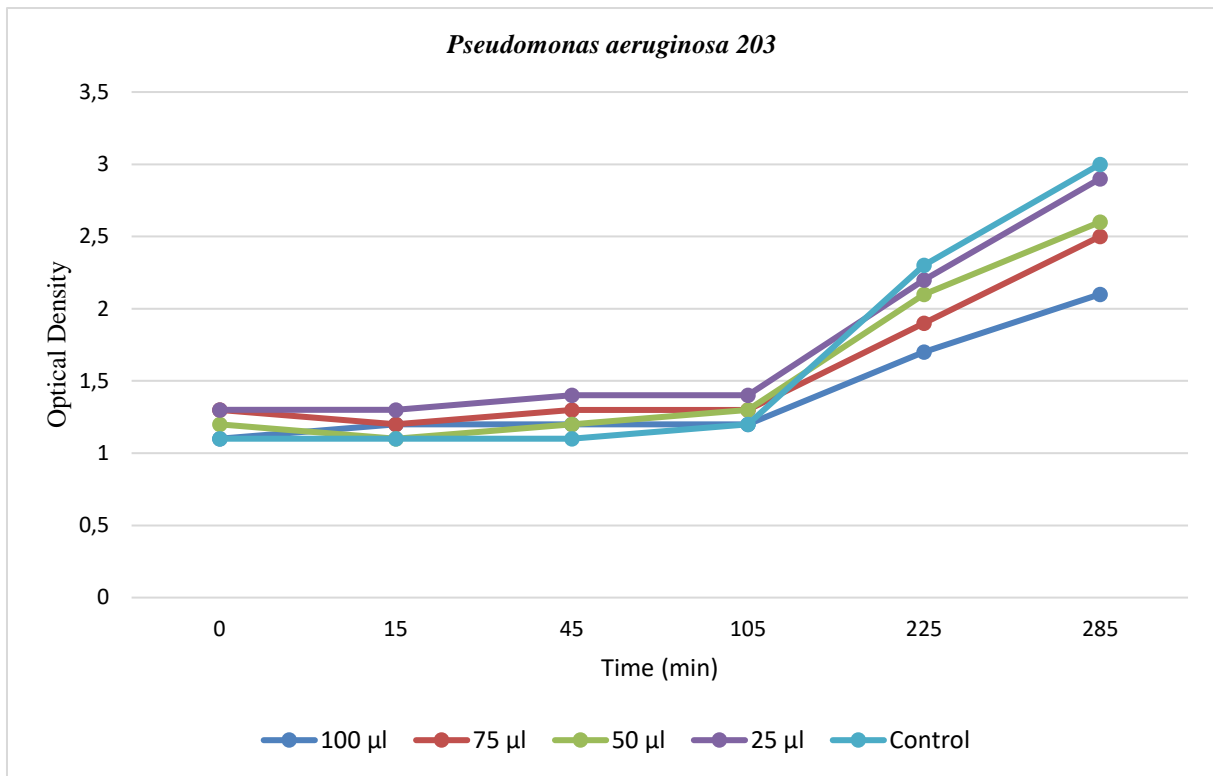


Fig 1 *Pseudomonas aeruginosa* 203 Optical Density of multidrug-resistant bacterial strains.

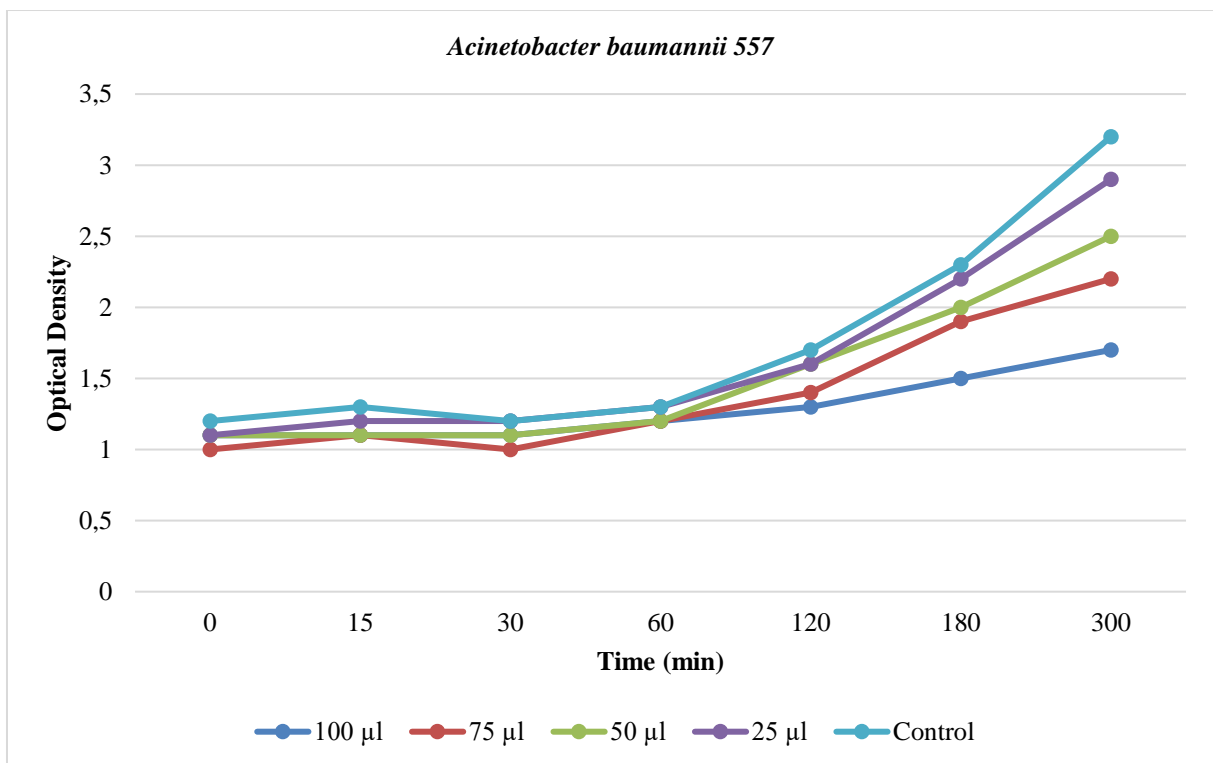


Fig 2 *Acinetobacter baumannii* 557 Optical Density of multidrug-resistant bacterial strains.

In silico Study Results

According to the molecular docking results, the docking score of Compound **1** molecule to the protein structure of 4ZHU (*Pseudomonas aeruginosa*) was found -8.8 kcal/mol (Table 4).

Table 4 In Silico study results of ligand **1** in 4ZHU (*Pseudomonas aeruginosa*)

Results Analysis Software	Visualization Software	Protein	Ligand	Docking Score	Amino Acid Residue
Autodock Vina	3 D BIOVIA Discovery Studio Visualizer	4ZHU	1	-8.8	LEU53, ILE169, VAL176, PRO178
Autodock 4.2	3 D BIOVIA Discovery Studio Visualizer	4ZHU	1	-8.8	PHE127, LEU130, ALA131, VAL135, GLY148, ARG171

Molecular docking model; The protein structure of 4ZHU (*Pseudomonas aeruginosa*) is shown in Figure 3 of the Compound **1** molecule.

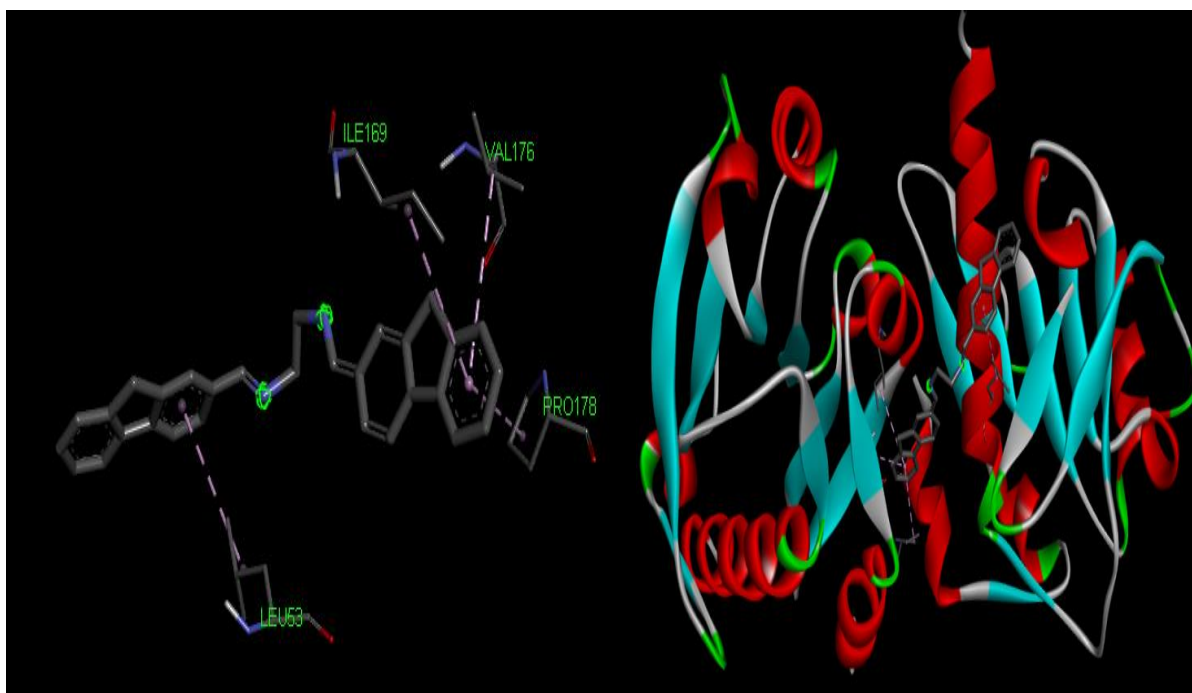


Fig 3 Docking patterns of Compound **1** ligand 4ZHU (amino acid residues of 4ZHU whose binding points were determined by Discovery Studio according to Autodock Vina results)

4ZHU appears to form pi-alkyl bond with LEU53, ILE169, VAL176, PRO178 with Compound ligand **1** (Figure 4).

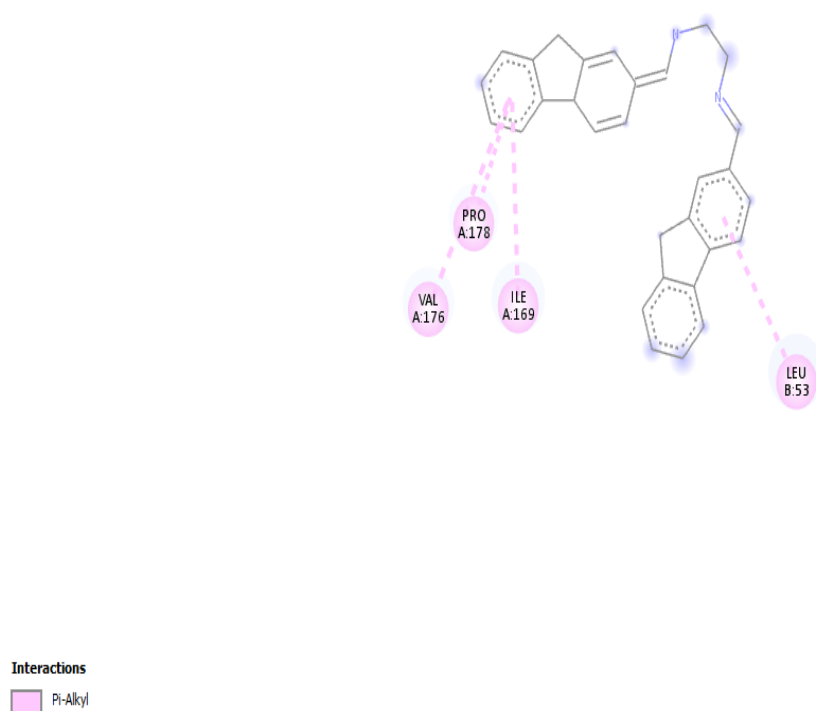


Fig 4 Bond structures of Compound ligand **1** in 4ZHU. (4ZHU appears to form pi-alkyl bond with LEU53, ILE169, VAL176, PRO178 with ligand **1**).

The sites where ligand Compound **1** is thought to be responsible for its biological effect in 4ZHU and where it interacts best with the target site appear (Figure 5).

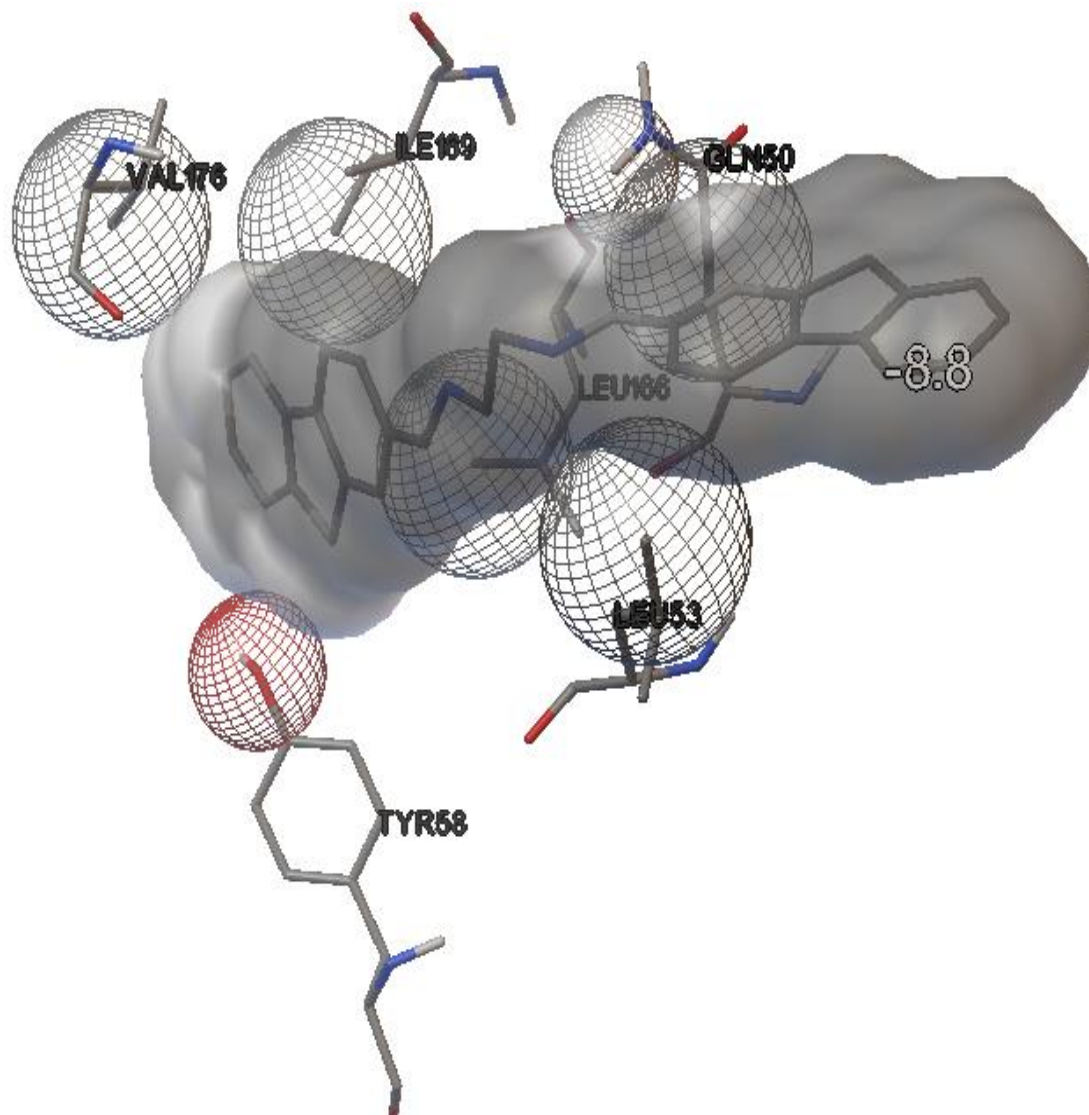


Fig 5 Pharmacophore pattern of ligand Compound **1** in 4ZHU. (The sites where ligand **1** is thought to be responsible for its biological effect in 4ZHU and where it interacts best with the target site appear.)

According to the molecular docking results, the docking score of Compound **1** molecule to the protein structure of 4ZIIY (*A.baumannii*) was found -10.2 kcal/mol (Table 5).

Table 5 In silico study results of ligand Compound **1** in 4ZIIY (*Acinetobacter baumannii*)

Results Analysis Software	Visualization Software	Protein	Ligand	Docking Score	Amino Acid Residue
Autodock Vina	3 D BIOVIA Discovery Studio Visualizer	4ZIIY	1	-10.2	GLY124, LYS125, THR127, HIS292, ARG327
Autodock 4.2	3 D BIOVIA Discovery Studio Visualizer	4ZIIY	1	-10.2	GLY124, LYS125, THR126, PHE288, ALA289, HIS292, ASN293, GLY323, ARG327, LEU328, PHE330, ASN344

Molecular docking model; The protein structure of 4ZIIY (*Acinetobacter baumannii*) is shown in Figure 6 of the **1** molecule.

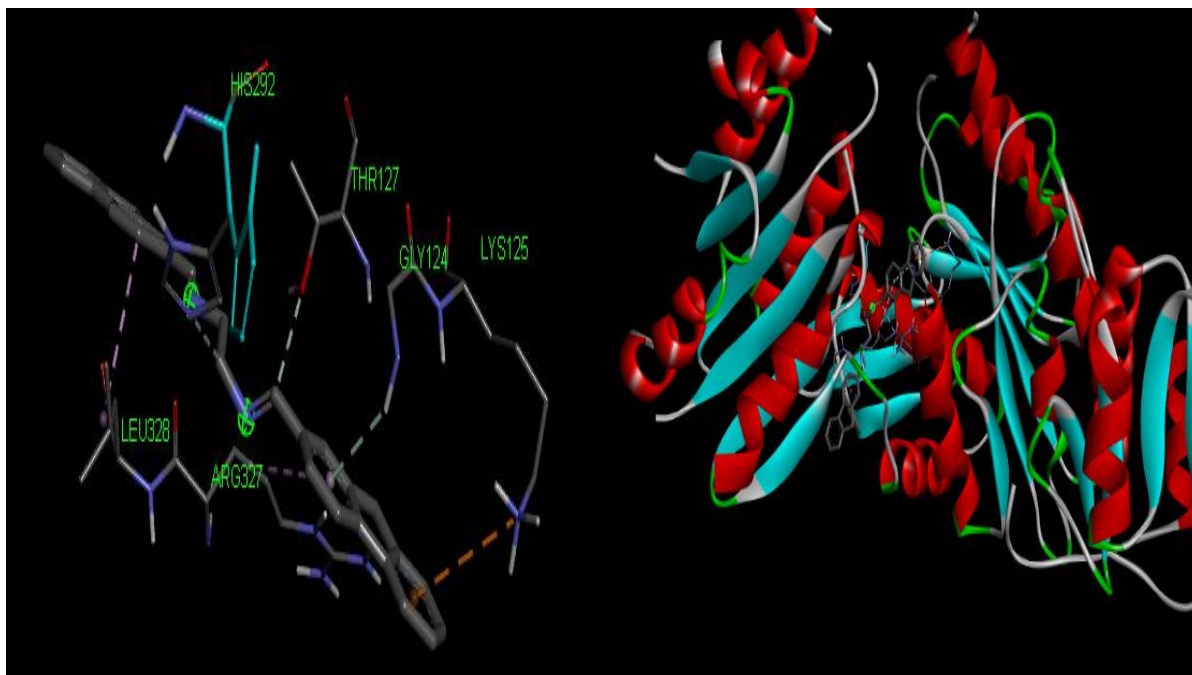
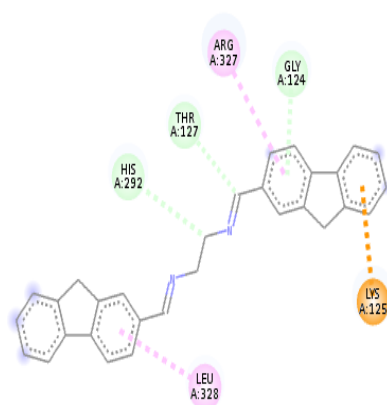


Fig 6 Docking patterns of Compound **1** ligand 4ZIY (amino acid residues of 4ZIY, whose binding points were determined by Discovery Studio according to Autodock Vina results)

To ligand Compound **1** of 4ZIY; It is observed that it forms pi-cation bonds with LYS125, pi-donor hydrogen bonds with GLY124, THR127, HIS292, carbon hydrogen bonds with HIS292, pi-alkyl bonds with LEU328 (Figure 7).



Interactions

Carbon Hydrogen Bond
Pi-Cation

Pi-Donor Hydrogen Bond
Pi-Alkyl

Fig 7 Bond structures of ligand **1** at 4ZIIY (to ligand **1** of 4ZIIY; It is observed that it forms pi-cation bonds with LYS125, pi-donor hydrogen bonds with GLY124, THR127, HIS292, carbon hydrogen bonds with HIS292, pi-alkyl bonds with LEU328).

Where Compound **1** ligand is thought to be responsible for its biological effect in 4ZIIY and where it interacts best with the target site appears (Figure 8).

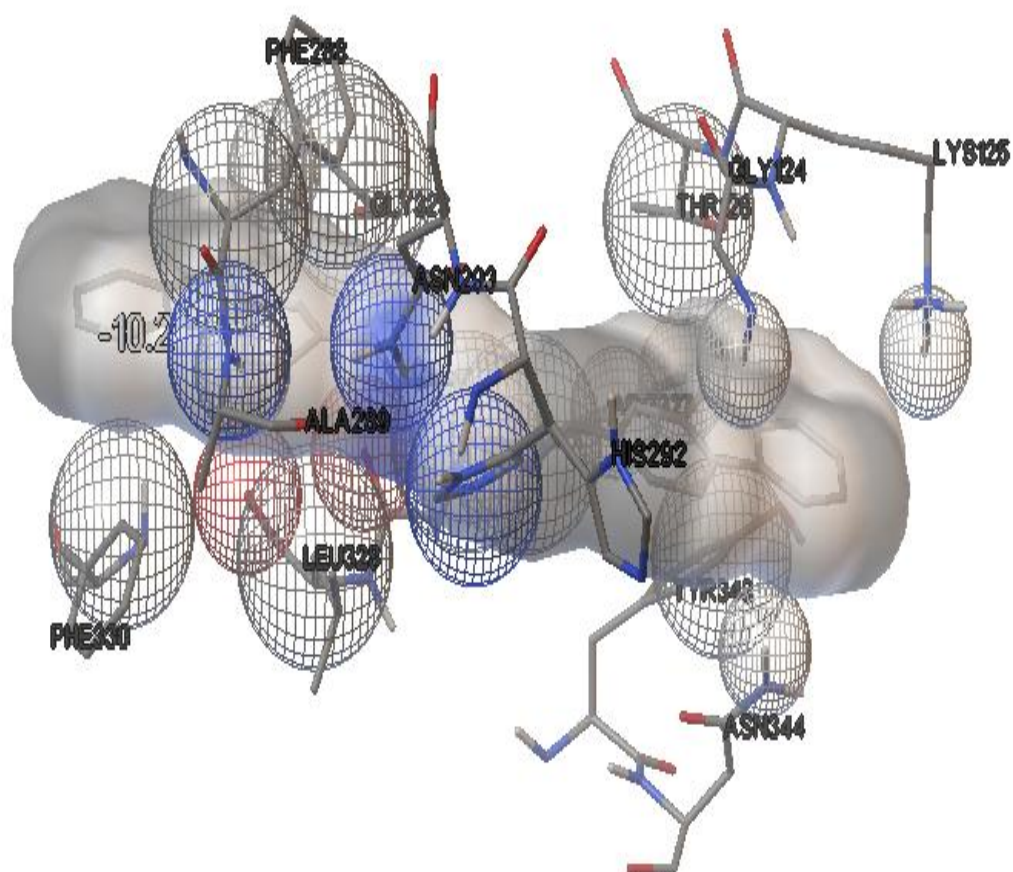


Fig 8 The pharmacophore pattern of ligand **1** in 4ZIIY (where **1** ligand is thought to be responsible for its biological effect in 4ZIIY and where it interacts best with the target site appears.)

Schiff bases are represented by the general formula $RCH=NR'$. In this notation, R and R' are aryl or alkyl substituents. It was observed that Schiff bases synthesized from the reaction of primary amines and carbonyl compounds were synthesized in two main stages. In the first step, a carbonyl amine intermediate is formed from the condensation of the primary amine and the carbonyl group. In the second step, Schiff base is formed as a result of the dehydration of the carbonyl amine intermediate [26].

Shanty et al. In 2017, Schiff bases were stated to have antioxidant activity. [26]. Antibacterial, fungicidal, anti-carcinogenic, catalytic and biological activity is attributed to the presence of the imine group ($N=CH-$) [27,28]. Schiff bases and their complexes are versatile compounds synthesized from the condensation of an amino compound with carbonyl compounds and widely used for industrial purposes, and are known to have antifungal, antibacterial, antimalarial, antiproliferative, anti-inflammatory, antiviral and antipyretic properties [29].

The synthesis of Schiff bases and the measurement of their biological activities have long been of interest to researchers. It is seen that many studies have been conducted in the literature in this area [29,30]. Sharma et al. 2019 determined the antibacterial effects of Schiff base ligands and metal complexes synthesized by the reaction of salicylaldehyde with o-phenylenediamine and p-phenylenediamine, 2-furaldehyde with o-phenylenediamine and p-phenylenediamine against the *E. coli*, *B. subtilis*, *P. Aereuginosa*, *S. aureus* bacteria. They determined the MIC values of some complexes and the minimum inhibitory concentration (MIC) of complex number one against *B. subtilis* and *S. aureus* as 75 $\mu\text{mol mL}$ [31]. It is seen to be compatible with the results obtained in our research. It is recorded in literature studies that Schiff bases show antibacterial and antifungal properties, but this activity is greater with the addition of metal complexes [30, 31]. The antibacterial activity of Schiff bases can be explained by the presence of keto-amine structure. In addition, the fact that they have an enol-imine structure rather than a keto form suggests that they may be effective in showing antibacterial activity. Using the turbidity reduction assay, we showed clinical isolates of *A. baumannii* and *P. aeruginosa* to be considerably affected by **1** regarding the growth inhibition activity. The concentration of **1** had notable impact on bacterial inhibition activity. This study reveals that **1** have potential agent to deal with multidrug-resistant bacteria either alone or in combination with conventional antimicrobials.

In general, it is thought that schiff bases will exhibit good antioxidant properties due to their chelating properties. Antioxidant determination of synthetic compound **1** was made by the method of reducing capacity of DPPH• radicals and ABTS•⁺ radical cation scavenging activity. In this study, in which ethanol was used as a solvent, values of 49.8 and 27 were found for DPPH• and ABTS•⁺, respectively. DPPH• method; It is widely used to measure the ability of antioxidants to scavenge free radicals. In this spectrophotometric method, a stable free radical, DPPH• (2,2-diphenyl-1-picrylhydrazil) reagent is used. It is based on the measurement of antioxidants' ability to reduce the DPPH• radical, which is reduced to hydrazine when this radical interacts with hydrogen donors. According to this method, strong hydrogen donor groups are required for compounds to show good antioxidant properties. The fact that the synthesis compound is close to the BHA compound indicates that its antioxidant property is low. It was found that synthetic compound **1** showed moderate and low inhibitory properties in terms of antioxidant activity compared to DPPH• and ABTS•⁺ methods, respectively. Studies that similar to our findings are available in the literature [32,33]. This situation is thought to be related to the low hydroxyl group in the synthesized compound **1**. It is stated that the ethanolic extract of the synthetic schiff base compound, which has strong hydrogen donors, shows very

strong antioxidant activity [34]. In general, there are many factors that affect antioxidant activity in synthetic compounds. The high number of electron donating groups in the synthesis compound is one of the mechanisms that increase antioxidant activity. The type of solvent used stands out as another factor affecting the antioxidant result. It can be said that this solvent was used in the literature studies as the reason why ethanol was preferred in the research.

A. baumannii and *P. aeruginosa* have an important place among the infectious agents because they are resistant to adverse conditions. These bacteria, in addition to being naturally resistant to many antibiotics, can also develop resistance during antimicrobial use. Therefore, the infections they cause especially in ICU patients progress with high mortality and morbidity. It has been reported that there has been a remarkable increase in antibiotic resistance and multiple resistance in *A. baumannii* and *P. aeruginosa* over the years [35,36]. *A. baumannii* and *P. aeruginosa* are in the priority 1 (critical) group in the list of priority pathogens that urgently need new antibiotics, published by the World Health Organization (WHO) in February 2017 [37]. Centers for Disease Control states that multi-resistant *Acinetobacter* isolates cause 7300 infections and 500 deaths annually, while multi-resistant *Pseudomonas* isolates cause 6700 infections and 440 deaths annually [37].

These factors, which cause hospital-acquired pneumonia in particular, are most commonly isolated from respiratory materials. In studies, it is seen that the most frequently isolated material type is tracheal aspirate [38, 39]. 46% of *A. baumannii* strains and 52% of *P. aeruginosa* strains were isolated from tracheal aspirate samples. It is seen that blood is the sample type from which *A. baumannii* isolates in the second most frequency, while urine is the sample type from which *P. aeruginosa* strains are isolated in the second frequency. While many studies conducted in our country reported that these agents were detected most frequently in the anesthesia department among ICUs, 37% of *A. baumannii* strains and 39% of *P. aeruginosa* strains used in our study were isolated from the general ICU [40, 41, 42].

In vitro resistance rates detected especially against *A. baumannii* isolates isolated from the ICU are quite high [43]. The agents that can be used in the treatment of infections caused by bacteria are very limited, as they are naturally resistant to most antibiotics and develop resistance to almost all other antibiotics.

Conclusion

In studies on Schiff bases and metal complexes, it was concluded that complex Schiff bases are more effective on bacteria than free Schiff bases. However, the degree of action of the metal complexes of Schiff bases varies among themselves. But, in this study, it was concluded that

although Schiff bases showed antibacterial effects at different rates, free Schiff bases could be effective on bacteria as well as metal complexes. It was observed that the synthesized 1 Schiff base ligand showed different levels of activity in terms of reducing capacity of DPPH• radicals and removing ABTS•+ radical cation, especially DPPH• activity was at a normal level. It has been found that the antioxidant activity of synthesis Schiff base 1 is low in general. Molecular modeling insertion studies were conducted to reveal the binding mechanism and effect of ligand 1 to 4ZIIY (*A. baumannii*) and 4ZHU (*P. aeruginosa*). The docking results show that ligand 1 binds strongly to the 4ZIIY and 4ZHU constructs. Due to the binding strength of the 1 ligand, it reveals a unique structure for *A. baumannii* and *P. aeruginosa*, and it is thought that it can be a reference for designing new molecules with antibiotic resistance with the same structure and applying these molecules in in vivo and in vitro studies.

Abbreviations

ICU: Intensive care unit ; ROS: Reactive oxygen species; K₂S₂O₈: Potassium persulfate; MTBB: Bacteriophage Microlysis Therapeutic Bank; MIC: minimum inhibitory concentration; WHO: World Health Organization

Acknowledgements

We sincerely thank the Yetkin GÖK.

Funding

No funding

Availability of data and material

All data and material available

References

1. Sader, H.S., Farrell D.J., Flamm, R.K., Jones, R.N, Antimicrobial susceptibility of Gram-negative organisms isolated from patients hospitalized in intensive care units in United States and European hospitals (2009-2011). *Diagnostic Microbiology Infectious Disease*, 2014. 78:443-8.
2. Karlowsky., et al., Surveillance for antimicrobial susceptibility among clinical isolates of *Pseudomonas aeruginosa* and *Acinetobacter baumannii* from hospitalized patients in the United States, 1998 to 2001. *Antimicrobial Agents*, 2003.47:1681-1688. <https://doi.org/10.1128/AAC.47.5.1681-1688>.
3. Sader, H.S.; Farrell, D.J.; Flamm, R.K.; Jones, R.N. Antimicrobial susceptibility of Gram-negative organisms isolated from patients hospitalized in intensive care units in United States and European hospitals (2009-2011). *Diagnostic Microbiology Infectious Disease*, 2014. 78:443-8.
4. Yesilbağ, Z., et al., Nosocomial infections and risk factors in intensive care unit of a university hospital. *Journal of Clinical and Experimental Investigations*, 2015. 6:233-9.
5. Dereli, N., et al., A 5-Year Evaluation of Invasive Device-Associated Infections Rates in Intensive Care Unit of a Training Hospital in Turkey. *Balkan Military Medical*, 2016. 19:19-24.
6. Tas, S.S., Kahveci, K., Surveillance of Nosocomial Infections in the Long-Term Intensive Care Unit and Palliative Care Center; 3-Year Analysis. *Journal of Contemporary Medicine*, 2018. 8:55-59.
7. Almasaudi, S.B., *Acinetobacter* spp. as nosocomial pathogens: Epidemiology and resistance features. *Saudi Journal of Biological Sciences*, 2018. 25:586-96.

8. Eroğlu, C., Ünal, N., Karadağ, A., Yılmaz, H., Acuner, I.C., Günaydın, M., Acinetobacter species isolated from various clinical specimens between 2006-2011 and their antibiotic susceptibility. *Turkish Hygiene and Experimental Biology Journal*, 2016. 73:25-32.
9. Al Johani, S.M.; Akhter, J.; Balkhy, H.; El-Saed, A.; Younan, A.; Memish, Z. Prevalence of antimicrobial resistance among gramnegative isolates in an adult intensive care unit at a tertiary care center in Saudi Arabia. *Annals of Saudi Medicine*, 2010. 30:364-9. <https://doi.org/10.4103/0256-4947.67073>.
10. Talan, L., Guven, G., Yilmaz, G., Altintas, N.D., Microorganisms Difficult to Control in Intensive Care Units: Acinetobacter. *Journal of Intensive Care Medicine*, 2015. 6:44-7.
11. Doi, Y; Murray, G.L.; Peleg, A.Y. Acinetobacter baumannii: evolution of antimicrobial resistance-treatment options. *Seminars in Respiratory and Critical Care Medicine*, 2015. 36:85-98.
12. Tang, Y., Zhu, W., Chen, K., Jiang, H., New Technologies in Computer-Aided Drug Design: Toward Target Identification and New Chemical Entity Discovery, *Drug Discovery Today: Technologies. Medicinal Chemistry*, 2006. 3:3. <https://doi.org/10.1016/j.ddtec.2006.09.004>.
13. Trott, O., Olson, A.J., AutoDock Vina: improving the speed and accuracy of docking with a new scoring function, efficient optimization and multithreading. *Journal of Computational Chemistry*, 2010. 31, 455-461. <https://doi.org/10.1002/jcc.21334>.
14. İftikhar, B., Javed, K., Khan, M.S.U., Akhter, Z., Mirza, B., Mckee, V., "Synthesis, characterization and biological assay of Salicylaldehyde Schiff base Cu(II) complexes and their precursors," *Journal of Molecular Structure*, 2018. 1155: 337-348.
15. Liu, Y.T.; et al., Ferrocenyl chalcone-based Schiff bases and their metal complexes: Highly efficient, solvent-free synthesis, characterization, biological research. *Journal of Organometal Chemistry*, 2018. 856:27-33.
16. Gao, B.J., Zhang, D.D., and Li, Y.B., Synthesis and photoluminescence properties of novel Schiff base type polymer-rare earth complexes containing furfural-based bidentate Schiff base ligands. *Optical Materials*, 2018. 77:77-86.
17. Avnioglu, S., Güngör, M., Kurutas, E.B, Ozturk, U, Demirhan, I., Bakaris, S., Velioglu, H.A., Cankaya, S., and Yulug, B. (2022). The Effect of Resveratrol on Sphingosine-1 and Oxidative/ Nitrosative Stress in an Experimental Heart Ischemia Reperfusion Model. *Revista Romana de Medicina de Laborator*, **30**: 9-18.
18. Tan, Y.X., Zhang, Z.J., Liu, Y., Yu, J.X., Kuang, D.Z., "Synthesis, crystal structure and biological activity of the Schiff base organotin (IV) complexes based on salicylaldehyde-oaminophenol. *Journal of Molecular Structure*, 2017. 1149:874-881.
19. Blois, M.S., Antioxidant determinations by the use of a stable free radical. *Nature*, 1958. 181: 1199–1200.
20. Re, R., Pellegrini, N., Proteggente, A., Pannala, A., Yang, M., Rice-Evans, C., Antioxidant activity applying an improved ABTS radical cation decolorization assay. *Free Radical Biology and Medicine*, 1999. 26(9), 1231–1237.
21. Isık, M. *Salvia officinalis* L. Anticholinergic and Antioxidant Activity and LC-MS/MS Analysis of Ethanol Extract. *International Journal of Life Science and Biotechnology*, 2020.3(1), 51-61.
22. Necip, A., Isık, M., Güzel, A., Takım, K., Kaygısız, F., LC-MS/MS Analysis, Antioxidant properties and Inhibition Effect of Some Important Metabolic enzymes of *Nicotiana rustica* L. *Sutcu Imam University Journal of Agriculture and Nature*, 2021. 24(5),930-938.
23. Kulkarni, A., Patil, S.A., Badami, PS., Synthesis, characterization, DNA cleavage and in vitro antimicrobial studies of La(III), Th(IV) and VO(IV) complexes with Schiff bases of coumarin derivatives. *European Journal of Medicinal Chemistry*, 2009. 44: 2904–2912.
24. Laskowski, A., Mark, B., LigPlot+: multiple ligand-protein interaction diagrams for drug discovery. *Journal of Chemical Information and Modelling*, 2010. 51(10): 2778-86.
25. Gülçin, I., Antioxidant activity of food constituents: An overview. *Archives of Toxicology*, 2012. 86(3): 345–391.
26. Shanty, A.A., Sneha, E.J., Kurup, M.R., Balachandran, S., Mohanan, P., Synthesis, characterization and biological studies of Schiff bases derived from heterocyclic moiety. *Bioorganic Chemistry*, 2017. 70:67-73.

27. Xiang, L., Jean-René, H., Recent developments in penta-, hexa- and heptadentate Schiff base ligands and their metal complexes. *Coordination Chemistry Reviews*, 2019.389:94-118.
28. Burlov, A., Vlasenko, V., Koshchienko, Y., Makarova, N., Zubenko, A., Drobin, Y., Synthesis, characterization, luminescent properties and biological activities of zinc complexes with bidentate azomethine Schiff-base ligands. *Polyhedron*, 2018. 154: 65-76.
29. Gondia, N., Sharma, S., Comparative optical studies of naphthalene based Schiff base complexes for colour tunable application. *Materials Chemistry and Physics*, 2019. 224: 314-319.
30. Sharma, D., et al., Co (III) and VO(IV) complexes with a new bidentate Schiff base: Interaction with BSA and antimicrobial studies. *Biointerface Research in Applied Chemistry*, 2019. 9:1,3776-3782.
31. Jalbout, F.A., Jarrahpour, A.A., Brunel, J.M., Salmi, C., Rezaei, S., Trzaskowski, B., Synthesis, Physical Characterization, Antibacterial and Antifungal activities of a novel bis(3-((E)-1-(2-hydroxyphenyl) ethylideneamino)phenyl) methanone. *Molbank*, 2006. 484. <https://doi.org/10.3390/M484>.
32. Aslantas, M., Tümer, M., Sahin, M., Spectroscopic, thermal and voltametric studies of crystalline complexes trans-N,N'-bis(salicylidene)-1',2'- cyclohexanediamine with Cu(II). *Spectrochimica Acta Part A*, 2008. 71(1): 263-268.
33. Ali, S.S., et al., Pharmaceutical Potential of a Novel Chitosan Derivative Schiff Base with Special Reference to Antibacterial, Anti-Biofilm, Antioxidant, Anti-Inflammatory, Hemocompatibility and Cytotoxic Activities. *Pharmaceutical Research*, 2019. 36: 18.
34. Yılmaz, S., et al., Antioxidant activities of chemical constituents isolated from *Echinops orientalis*. *Records of Natural Products*, 2014. 8: 32-36.
35. Kurt, B.Z., Synthesis of new schiff bases of cinnamaldehyde and investigation of their antioxidant properties. *Sakarya University Journal of Science Institute*, 2018. 22 (3), 1024-1032.
36. Savcı, U., Ozveren, G., Yenisehirli, G., Bulut, Y., Ozdaş, S., In vitro susceptibility status of *Acinetobacter baumannii* strains isolated from clinical specimens. *Turkish Journal of Clinical and Laboratory*, 2015. 6:24-9.
37. Nguyen, L., Garcia, J., Gruenberg, K., MacDougall, C., Multidrug-Resistant *Pseudomonas* Infections: Hard to Treat, But Hope on the Horizon. *Current Infectious Disease Reports*, 2018. 20:23.
38. Almasaudi, S.B., *Acinetobacter* spp. as nosocomial pathogens: Epidemiology and resistance features. *Saudi Journal of Biological Sciences*, 2018. 25:586-96.
39. Sirin, M.C., et al., The change of antibiotic resistance profiles over the years in *Pseudomonas aeruginosa* and *Acinetobacter baumannii* strains isolated from intensive care units. *Journal of Clinical and Experimental Investigation*, 2015. 6:279-85.
40. Köse, S., Atalay, S., Odemiş, I., Adar, P., Antibiotic susceptibility of *Pseudomonas aeruginosa* strains isolated from various clinical specimens. *Ankem Journal*, 2014;28:100-4.
41. Engin, A., *Acinetobacter*-Associated nosocomial infections in Cumhuriyet University Medical Faculty Research Hospital; Three years' experience. *Cumhuriyet Medical Journal*, 2017. 39:555-63.
42. Demirdal, T., Şen, P., Yula, E., Kaya, S., Nemli, S.A., Demirci, M., Resistance profiles of *Pseudomonas aeruginosa* strains isolated from intensive care units: A five-year evaluation. *Ortadogu Medical Journal*, 2017. 9:108-12.
43. Balcı, M., Bitirgen, M., Kandemir, B., Türk E., Arıbaş, I., Antibiotic susceptibility of nosocomial *Acinetobacter baumannii* strains. *Ankem Journal*, 2010. 24:28-33.
44. Necip, A., and M. Isık, Bioactivities of *Hypericum perforatum* L and *Equisetum arvense* L fractions obtained with different solvents. *International Journal of Life Sciences and Biotechnology*, 2019. 2(3), 221-230.

Guven L., et al., Evaluation of LC-MS/MS Analysis and In Vitro Biological Activities of *Rosa pimpinellifolia* Root, Pseudo-fruit, and Seed extracts. International Journal of Life Sciences and Biotechnology, 2022. 5(3): p. 480-503. DOI: 10.38001/ijlsb.1108547

Evaluation of LC-MS/MS Analysis and *In Vitro* Biological Activities of *Rosa pimpinellifolia* Root, Pseudo-fruit, and Seed extracts

Leyla Guven^{1*}, Ufuk Özgen², Handan Gökben Sevindik³, İclal Ağan⁴, Mehmet Koca⁵, İbrahim Turan⁶, Selim Demir⁷, Yüksel Aliyazıcıoğlu⁸

ABSTRACT

In this study, various extracts of *Rosa pimpinellifolia* antioxidant, anticholinesterase, and antityrosinase properties were determined with the total phenolic and flavonoid contents spectrophotometrically. The phytochemical composition of the methanol extract was analyzed using LC-MS/MS. In addition, the extracts of *R. pimpinellifolia* antimicrobial activity by disc diffusion and microdilution method, and antigenotoxic activities by comet assay were explored. The ethyl acetate extract of the root (EAR) had higher antioxidant activities at 10 µg/mL with inhibition of 39.7, 91.2, and 39.5% respectively in the DPPH[•], ABTS^{•+}, and superoxide anion radical scavenging activity assay than standard antioxidant molecules. The polyphenolic contents of the EAR and the ethyl acetate extract of the seed (EAS) were found to be 378.2 ± 0.477 and 305.39 ± 0.568 µg gallic acid equivalent GAE/mg respectively. The EAR showed butyrylcholinesterase activity with 19% inhibition at 100 µg/mL concentration and higher activity at 500 µg/mL with inhibition of 50% in the tyrosinase inhibitory assay than the other *R. pimpinellifolia* extracts. The extracts of *R. pimpinellifolia* exhibited antimicrobial activity against *Staphylococcus aureus* and *Candida albicans*. The extracts of *R. pimpinellifolia* did not show any antigenotoxic effect up to the concentration of 1000 µg/mL. In LC-MS/MS analysis, cyanidin-3-*O*-Glucoside and isoquercetin in the pseudo-fruit; procyanidin B2 and catechin in the root were the major phenolic compounds.

ARTICLE HISTORY

Received

25 April 2022

Accepted

09 August 2022

KEYWORDS

Rosa pimpinellifolia,
Rosaceae,
biological
activities,
LC-MS/MS

¹ Department of Pharmaceutical Botany, Faculty of Pharmacy, Atatürk University, Erzurum, 25240, Turkey

² Department of Pharmacognosy, Faculty of Pharmacy, Karadeniz Technical University, Trabzon, 61080, Turkey

³ Department of Pharmacognosy, Faculty of Pharmacy, Atatürk University, Erzurum, 25240, Turkey

⁴ Department of Medical Microbiology, Giresun University Prof. Dr. A. İlhan Özdemir Training and Research Hospital, Giresun, 28100, Turkey

⁵ Department of Pharmaceutical Chemistry, Faculty of Pharmacy, Atatürk University, Erzurum, 25240, Turkey

⁶ Department of Biochemistry, Faculty of Pharmacy, University of Health Sciences, Ankara, Turkey

⁷ Department of Nutrition and Dietetics, Faculty of Health Sciences, Karadeniz Technical University, Trabzon, Turkey

⁸ Department of Medical Biochemistry, Faculty of Medicine, Karadeniz Technical University, 61080 Trabzon, Turkey

*Corresponding Author: Leyla Guven, leyla.guven@atauni.edu.tr

Introduction

Rosa pimpinellifolia belonging to the Rosaceae family is presented by 27 species in Turkish flora. It is a deciduous shrub that grows well on calcium soils. It is known as “Karakuşburnu, Koyungözü” in Turkey, “Shrub Rose” in Europe. It is used in the treatments of hemorrhoids, infections, flu, abdominal pain, and anemia in Turkish folk medicine by decoction of the roots and pseudo-fruits of the species [1-3].

Flavonoids [4], aurons [5], phenylethanoids [6], saponosides [7], steroids [8], sesquiterpenes [9], carotenoids [10], tannins [4], fatty acids [11], and volatile compounds [12] were identified in *Rosa* species. Furthermore, according to some studies, *R. pimpinellifolia* has condensed tannins (catechin, epigallocatechin, procyanidin B2) [13], anthocyanidins (cyanidin-3-*O* glucosides) [14,15], phenolic acids (ascorbic acid, caffeic acid) [15], and essential fatty acids (linoleic, oleic, linolenic acids) [16].

With regard to some studies also, *Rosa* species have antibacterial [17], anti-inflammatory [18], antioxidant [19], anticancer [20], antidiabetic [21], hepatoprotective [22], anxiolytic [23], antiobesity [24], anti-conflict [25], purgative [26], kidney stone reducer [27], anti-diarrheal [28], anti-allergic [29], antiproliferative [30], antinociceptive [31], anti-ulcerogenic [32], antihypertensive [33], antifungal [34], anti-HIV, and antitussive [35] activities. It is also reported that *Rosa* species are used in skin disorders [36], atherosclerosis, arthritis, brain dysfunction immunodeficiency [21], and hemorrhoids [37].

Medicinal plants are consumed, because of having thousands of different phenolic components such as reductive agents, free radical scavengers, and quenchers of singlet oxygen formation. It also plays an important role in the control of cancer and other diseases [38]. Oxidative stress is defined as the deterioration of the oxidative balance resulting from the deficiency of antioxidants, which is caused by the increase of reactive oxygen species (ROS) such as hydroxyl radicals, superoxide radicals, and hydrogen peroxides formed during cellular metabolism. ROS causes cell damage and the death of intracellular macromolecules. Moreover, ROS-induced-DNA damage is associated with many diseases. Polyphenolic compounds in plants protect cells against the harmful effects of ROS by donating electrons, chelating metal ions, and stimulating antioxidant enzymes [39].

Many medical professionals seek natural and safe antibiotics due to the increase in antibiotic use and the resistance of bacterial strains [40]. Therefore, the antimicrobial effects of medicinal plants are extensively studied in recent years. In addition, plants are used as an additive in the preservation of raw and processed foods and medicines by making use of their antimicrobial properties [41].

Tyrosinase, commonly found in plants, microorganisms, and animals, is a copper-containing enzyme involved in the synthesis of melanin in the skin, hair, and eyes. The enzyme has a key role in melanization [42, 43]. Recently, the search for safe and effective tyrosinase inhibitors has gained importance in the treatment of hyperpigmentation problems such as skin scarring caused by extreme melanin synthesis in the body and hypopigmentation problems caused by insufficient synthesis of melanin such as psoriasis and vitiligo. These enzyme inhibiting agents can be used in the treatment of hyperpigmentation problems. [44-46]. Tyrosinase inhibitors are utilized in the cosmetics industry due to their skin whitening effect [47] and in the food industry due to their ability to inhibit the enzymatic browning of food products [48]. It has also been reported that tyrosinase may cause dopamine neurotoxicity and that neurodegeneration is associated with Parkinson's disease [49]. Therefore, inhibition of tyrosinase is a popular target in drug development and research for Parkinson's disease [50].

Alzheimer's disease (AD), a neurodegenerative disease, is characterized by a low level of the neurotransmitter acetylcholine (ACh). In the treatment of this disease, it is often aimed to prolong the availability of ACh by stimulating the cholinergic receptors or using agents that increase or improve acetylcholine levels. Therefore, inhibition of acetylcholine degrading enzymes (acetylcholinesterase (AChE) and butyrylcholinesterase (BChE)) is preferred in AD therapy. Potential sources of AChE and BChE inhibitors in natural products, provide for the development of drug molecules. Cheap, safe, alternative AChE and BChE inhibitory plants are researched in this publication [51].

The aim of this study is to reveal the chemical characterization of the root, pseudo-fruit, and seed extracts of *R. pimpinellifolia* by LC-MS/MS and to investigate their *in vitro* antioxidant, antityrosinase, anticholinesterase, antimicrobial, antigenotoxic, and anticancer activities.

Materials and Methods

Chemicals and reagents

Gallic acid monohydrate, sodium carbonate, Folin-Ciocalteu phenol Reagent (FCR) (Sigma-Aldrich) for determination of total phenolic compound quantity. Aluminum chloride; hydrochloric acid (37%), routine hydrate (Sigma-Aldrich) for determination of total flavonoids. Ammonium thiocyanate, 2,2'-azino-bis (3-ethylbenzthiazoline-6-sulfonic acid) diammonium salt (ABTS), 1,1 diphenyl-2-picryl-hydrazole (DPPH), gallic acid monohydrate, (\pm) 6- hydroxy-2,5,7,8-tetramethylchromane-2-carboxylic acid (Trolox), D-methionine, nitrotetrazolium blue chloride (NBT), potassium persulfate, riboflavin, sodium phosphate monobasic (NaH_2PO_4), (\pm) α -tocopherol (Sigma-Aldrich) for determination of antioxidant activity. AChE, acetylthiocholine iodide (ATCI), BChE, butyrylthiocholine iodide (BTCl), 5,5-dithiobis- (2-nitrobenzoic acid) (DTNB), donepezil, tris hydrochloride (Sigma-Aldrich) for determination of anticholinesterase activities. Tyrosinase, 3,4-dihydroxy-L-phenylalanine (L-DOPA), L-tyrosine, α -kojic acid, sodium phosphate monobasic (NaH_2PO_4) (Sigma-Aldrich) for determination of antityrosinase activity.

Fetal bovine serum (Biochrom), penicillin/streptomycin (Gibco), eagle's minimal essential medium (Lonza), polylysine solution (Biochrom), normal boiling point agarose (Lonza), dimethyl sulfoxide (Amresco), low boiling point agarose, NaOH, phosphate buffer tablet, NaCl triton X-100, ethylenediamine tetraacetic acid, H_2O_2 , tris, trypan blue solution, ethidium bromide (Sigma-Aldrich) for investigation of antigenotoxic effects.

1,3-dicaffeoylquinic acid, 4,5-dicaffeoylquinic acid, 7-acetyl sideroxol, apigenin, caffeic acid, catechin, chlorogenic acid, cyanidin-3-*O*-glucoside, emodin, (-)-epicatechin, epigallocatechin, epigallocatechin gallate, eubotriol, fumaric acid, gallic acid, isoquercetin, kaempferol, luteolin, luteolin-5-*O*-glu, luteolin-7-*O*-glu, pelargonin chloride, punicalagin, procyanidin B2, pyrogallol, quercetin, quercetin-3-*O*-arabinoside, quercitrin, ursolic acid, vanillin, p-hydroxybenzoic acid, t-ferulic acid were purchased from Sigma-Aldrich for determination of phenolic compound via LC-MS/MS.

Plant materials

The pseudo-fruits, seeds, and roots of *R. pimpinellifolia* were collected from Erzurum Kosk village in August 2013 (1900 m) and identified by Ufuk Özgen. The voucher specimen (ATA 9876) has been deposited in the herbarium of the Faculty of Sciences, Atatürk University, Erzurum, Turkey.

Preparation of the extracts

20 g pseudo-fruits, seeds, and roots of the plant were extracted separately with 300 mL methanol, ethyl acetate, and water for 12 h at 25°C. The solvents were removed under vacuum.

Determination of the total phenolic content

The Folin-Ciocalteu method, modified by Singleton and Rossi, was used to determine the total phenol content [52-54]. The plant extract was dissolved in distilled water to 1000 µg/mL. Then, 1000 µL of each sample was taken and distilled water was added to 23 mL. After completion, 0.5 mL of Folin-Ciocalteu reagent and after 3 min 1.5 mL of 2% Na₂CO₃ solution were added. After the mixture was stirred for 2 hrs on a magnetic stirrer at room temperature, the absorbances were read on a spectrophotometer against the blindly used distilled water at a wavelength of 765 nm. On the other hand, gallic acid dilutions were prepared at concentrations of 100, 200, 400, and 600 µg/mL to create the calibration curve, and gallic acid dilutions were added to the sample and other solutions were added exactly. The method is based on electron transfer from phenolic compounds to molybdenum in an alkaline environment. The reduced molybdenum turns into a blue complex, which can be measured spectrometrically at a wavelength of 760 nm.

Determination of the total flavonoid determination

The total flavonoid amounts of the plant samples were determined according to the method developed by Lar'kina et al 2009 and were calculated as rutin equivalent (RE) [55]. For this purpose, 30 mL of 70% ethanol was added to the 1 g powdered drug of both parts of the plant and heated at 60 °C for 1 hr under reflux. The process was repeated three times. The extracts were filtered into a 100 mL graduated flask and the volumes were made up to 100 mL with ethanol (solution A).

Sample solution: 2 mL of solution A, 4 mL of 10% ethanolic AlCl₃, and 0.1 mL of dilute HCl were placed in a flask and the volume was completed to 50 mL with 95% ethanol. Absorbances were measured against reference solutions at 410 nm after 20 min.

Reference solution: 2 mL of solution A and 0.1 mL of dilute HCl was placed in a flask and the volume was made up to 50 mL with 95% ethanol.

Rutin sample solution: 0.05 g routinely weighed and placed in a volumetric flask. 10 mL of 95% ethanol was added and dissolved by heating in an 80 °C water bath. After complete dissolution, the volume was made up to 50 mL with 95% ethanol (solution A).

Rutin test solution: 1 mL of solution A was taken into a volumetric flask, 4 mL of 10% AlCl₃ solution was added and the volume was completed to 50 mL with 95% ethanol. Absorbance at 410 nm was measured. The levels of total flavonoid contents in extracts were determined in triplicates and the averages were taken. Calculations were made according to the following equation.

$$X = [D (\text{Sample}) \times M (\text{Rutin}) / D (\text{Rutin}) \times M (\text{Material})] \times 100$$

D (Sample): Absorbance of the sample solution

D (Rutin): Absorbance of rutin test solution

M (Material): Weight of raw material (g)

M (Rutin): Weight of the rutin (g)

X: Total amount of flavonoids calculated over rutin (%)

Evaluation of the antioxidant capacity

DPPH radical scavenging assay

The free radical scavenging activity of the extract was established by DPPH assay according to the method developed by Marsden S. Blois [56]. The extracts were prepared in concentrations of 10, 50, 250, 500, and 1000 µg/mL and the DPPH stock solution at a concentration of 1 mM and dissolved in ethanol. 210 µL of stock solution and 70 µL of DPPH solution were added from each sample. The samples were shaken for approximately 1 min and stored at 37 °C in the dark for 30 min. At the end of the period, the absorbances of the samples were read in a spectrophotometer against Ethanol used blindly at 517 nm wavelength. For the control sample, 210 µL of Ethanol and 70 µL of DPPH solution were used, and tocopherol was used as the standard antioxidant. The % inhibition of the samples

against DPPH free radical was calculated according to the formula given below and tocopherol was used as a reference.

$$\text{DPPH radical scavenging capacity (\%)} = [(A_1 - A_2) / A_1] \times 100$$

A_1 = absorbance value of control sample containing DPPH and Ethanol

A_2 = absorbance value found after sample addition to DPPH solution

ABTS radical cation decolorization assay

ABTS cation radical scavenging capacity was determined according to the method made by Re et al [57]. Firstly, 2 mM ABTS solution was prepared. $\text{ABTS} \cdot^+$ was obtained by adding 2.45 mM potassium persulfate solution to this solution in a ratio of 1:1. The extracts were transferred to the wells with 140 μL of stock solutions at concentrations of 10, 50, 250, 500, and 1000 $\mu\text{g/mL}$, and 100 μL of the $\text{ABTS} \cdot^+$ solution and shaken for 1 min. 140 μL of $\text{ABTS} \cdot^+$ solution and 100 μL (0.1 M pH = 7.4) phosphate buffer were used as control samples. The absorbance value of the control sample at 734 nm should be 0.700 ± 0.025 . At the end of the 30 min waiting period, the absorbances at 734 nm were recorded against the buffer-formed blank. Trolox was used as the standard compound. Calculations of ABTS cation radical scavenging capacities in the percent of the extracts and compounds were made according to the following equation. $\text{ABTS} \cdot^+$ sweeping capacity (%) = $[(A_1 - A_2) / A_1] \times 100$

A_1 = Absorbance value of control sample containing only $\text{ABTS} \cdot^+$ and buffer solution

A_2 = absorbance value found after addition of samples to $\text{ABTS} \cdot^+$ solution

Superoxide anion radical scavenging assay

Superoxide anion radical scavenging tests were performed using the method developed by Zhishen et al [58]. 10, 50, 250, 500, and 1000 $\mu\text{g/mL}$ stock solutions of the extracts and compounds at different concentrations were prepared. 0.5 mL each of riboflavin (1.33×10^{-5} M), methionine (4.46×10^{-5} M) and NBT (8.15×10^{-5} M) solutions were added onto 0.5 mL of sample solution. The resulting reaction mixture was stimulated with 20 W fluorescent light for 40 min at room temperature. At the end of the period, the absorbance of each sample was recorded at 560 nm against a water-based blank. Phosphate buffer (0.05 M, pH=7.8) was used in the control sample instead of the stock solution. The calculations of the superoxide anion radical scavenging capacities in percent of the samples were made according to the following equation.

$$O_2^{\bullet+} \text{ sweeping capacity (\%)} = [(A_1 - A_2) / A_1] \times 100$$

A₁ = Absorbance value of the control sample

A₂ = Absorbance value found after addition of samples

Anticholinesterase activity

AChE inhibitory activity was determined using a modified spectrophotometric Ellman's method [59]. The prepared extracts were dissolved in methanol and diluted to concentrations of 1000, 750, and 500 µg/mL. However, with the solutions to be added to the wells later, final concentrations will be 100, 75, and 50 µg/mL. 50 µL of tris buffer solution, 125 µL of 3 mM DTNB solution, 25 µL of AChE enzyme solution at a concentration of 0.2 U/mL, and 25 µL of dilutions of the samples prepared at concentrations of 500, 750 and 1000 µg/mL were added to the wells. The resulting mixture was allowed to incubate for 15 min at 37 °C. After the 15 min incubation period, 25 µL of 15 mM ATCI solution was added to each well. As controls, 25 µL methanol, 125 µL DTNB, 50 µL tris buffer, 25 µL AChE, and after 15 min 25 µL ATCI were added again with a micropipette. For the blind, 25 µL of methanol, 75 µL of Tris buffer, 125 µL of DTNB, and 25 µL of AChE were added using a micropipette. The absorbances of the reaction mixtures were recorded at 412 nm for 20 min with a microplate reader. Calculations were made using the following formula:

$$\text{Enzyme inhibition (\%)} = [(A_1 - A_2) / A_1] \times 100$$

A₁: Absorbance value of the control sample

A₂: Absorbance value measured in the presence of samples

Antityrosinase activity

The tyrosinase inhibition capacity of the methanol, ethyl acetate, and aqueous extracts of the root and aqueous extracts of the pseudo-fruits of *R. pimpinellifolia* were determined spectrophotometrically with the method modified by Likhitwitayawuid and Sritularak using L-DOPA as substrate [43, 60]. Dilutions of the methanol extracts were prepared as 10 mg/mL in concentrations of 25, 50, 100, and 500 µg/mL in %5 DMSO with potassium phosphate buffer (pH = 6.8). α-Kojic acid (25, 50, 100, and 500 µg/mL) was used for positive control. The concentrations were determined with ELISA. Absorbances of the samples and the control were read at a wavelength of 490 nm and the inhibitions of tyrosinase were calculated according to the formula given. % Inhibition = $[(A-B)-(C-D)]/(A-B) \times 100$.

Antimicrobial activity

The antimicrobial effect of pseudo fruit and root extracts was determined by using Disk diffusion and micro-dilution methods [40].

Microorganisms

Escherichia coli, *Klebsiella pneumoniae*, and *Pseudomonas aeruginosa* from Gram-negative bacteria; *Enterococcus faecalis*, *Staphylococcus aureus*, and *S. epidemidis* strains from Gram-positive bacteria were used to determine the antibacterial activity. *Candida albicans* and *C. tropicalis* strains were used to investigate the antifungal activity. *Staphylococcus aureus* (ATCC BAA977) and *Candida albicans* (ATCC 14053) standard strains were studied in the microdilution method. Oxacillin, standard antibiotic discs; fluconazole, standard antifungal discs were used to determine the sensitivity of each microbial species tested and to control.

Disc diffusion assay

Suspensions were prepared according to 0.5 McFarland (108 CFU/ μ L for bacteria, 106 CFU/ μ L for yeasts) from bacteria and yeast strains were grown on solid media. Sterile swabs were dipped into each of the suspensions, mixed by dipping and the suspensions were spread over the surface of the media with the swab. 15 μ L of extracts at 100 mg/mL concentrations dissolved in DMSO under aseptic conditions were absorbed into sterile discs of 6 mm diameter. After this process, discs impregnated from the extracts and standard antibiotic discs were placed in Petri dishes at regular intervals. The Petri dishes in which bacteria were inoculated were incubated at 37 °C for 24 hrs, and the Petri dishes in which fungi were inoculated at 37 °C for 48 hrs. At the end of the incubation, the diameters of the inhibition zones occurring around the discs were measured. The zone diameters of standard antibiotic discs and only DMSO impregnated discs were used as controls. Only DMSO impregnated disk was used as a control for yeasts.

Broth dilution assay

MIC (Minimum Inhibitory Concentration) values were used to measure the sensitivity of the disk diffusion method. This method was made in accordance with the CLS (Clinical and Laboratory Standards Institute) criteria and Aliyazicioglu et al method [40].

Anti-genotoxic Activity

Cell culture

Human foreskin fibroblast (BJ) cell line was purchased from American Type Culture Collection (Manassas, VA, USA). The cells were grown in EMEM supplemented with 10% FBS, 2 mM glutamine, 1% penicillin, and streptomycin at 37°C.

Determination of H₂O₂ concentration

A total of 2x10⁵ BJ cells were cultured in a T-25 flask. After 24 h, cells were handled with 10-30 µM for 5 min to determine the concentration resulting in DNA damage, but not toxicity. After incubation, cells were trypsinized and centrifuged for comet assay protocol.

Determination of extract concentration

BJ cells were pre-incubated with various concentrations of *R. pimpinellifolia* extracts (25-1000 µg/mL) for 60 min. After that, flasks were washed with PBS, and cells were handled with 20 µM H₂O₂ for 5 min. Then, flasks were washed, trypsinized, and centrifuged for comet assay protocol.

Cell viability and Comet assay

The determination of the possible protective effect of different extracts of *R. pimpinellifolia* on DNA damage induced by hydrogen peroxide (H₂O₂) in BJ cells was carried out using the comet assay. The alkali protocol of the Comet method, it is aimed to determine chain breaks at low levels with high sensitivity. The alkaline comet protocol developed by Singh et al. includes 7 steps: Preparation of microscopic slides, lysis of cells to release DNA, alkaline treatment (pH>13) to reveal lesions such as chain breakage, electrophoresis under alkaline conditions (pH>13), neutralization of alkaline conditions, DNA staining and comet imaging, and comet scoring. For each treatment condition, 100 randomly selected cells from each slide were evaluated for DNA damage visually using a 40x objective on a fluorescent microscope (Nikon Eclipse E800, Tokyo, Japan). The selected cells were classified between 0 and 3, from non-damaged to most damaged, according to tail length. Excessively long tails and DNA spectra scored 4 were not included. All slides were scored with the following formula with a maximum damage possibility of 300 [61, 62].

Comet score = (1 x n₁) + (2 x n₂) + (3 x n₃) (n: cell number for every score)

LC-MS/MS analysis

Preparing standard solutions

Stock solutions of secondary metabolites were prepared in methanol solvent at 100 ppm concentrations. Before starting the study, methanol-water (v:v, 60:40) solutions at different concentrations between 5, 2.5, 1, 0.5, 0.25, and 0.1 ppm were prepared from 10 ppm intermediate stock for each standard compound and prepared in LC-MS / MS. It was kept at + 4 °C before being analyzed.

Determination of the phenolic compounds

The extracts were weighed about 3 mg in weight and placed in Eppendorf tubes. 4000 ppm master stock solutions were prepared in 0.75 mL of methanol solvent. Curcumin was used as the internal standard (IS), a 100 ppm IS stock solution was prepared in methanol solvent and added to the injection vial at a concentration of 5 ppm. All samples were kept at + 4°C before being analyzed. The calibration curve of phenolic compounds was obtained by plotting working standard solutions with LC-MS/MS data.

Instrumental analysis and chromatographic conditions

Zivak Tandem Gold Triple Quadrupole mass spectrometer (Istanbul, Turkey) device was used in the analysis. The Synergy Max C18 column (250 x 2 mm i.d, 5 µm particle size) was used as the chromatography column. The gradient elution steps indicated in Table 1 below were applied.

Table 1 Gradient elution steps for the detection of secondary metabolites

Minute	Mobile Phase A (%)	Mobile Phase B (%)
0.00-1.00	55	45
1.00-20.00	0	100
20.01-23.00	55	40

Mobile phase A	: % 0.05 formic acid -HPLC grade water
Mobile phase B	: % 0.05 formic acid: methanol
Flow rate	: 0.25 mL/min
Injection volume	: 10 µL
Detector	: DAD 280 nm
Column	: RP-C18
Column temperature	: 30 °C

LC-MS/MS Procedure

Zivak Tandem Gold Triple Quadrupole mass spectrometer device was used in the analysis of the samples. During optimization experiments, the best mobile phase composition was determined after satisfactory results were obtained with high ionization abundance and peaks were separated successfully. Optimum electrospray ionization (ESI) parameters were used: CID gas pressure 2.0 mTorr, 4000 V ESI needle voltage, 600 V spray protection voltage, 300 °C drying gas temperature, 55 psi nebulizer gas pressure, and 35 psi drying gas pressure. The measurement method was established by determining the LC-MS/MS characteristics of standard compounds.

Results

Total flavonoid contents of the extracts

The total flavonoid contents of the root and pseudo-fruits of the *R. pimpinellifolia* were calculated as % of the rutin (mg RE/dry drug) and the results are given in Table 2.

Table 2 Total flavonoid contents of the extracts

	Root	Pseudo-fruit
Total Flavonoid Amounts Calculated Over Rutin (%)	0.12	0.21

Total phenolic contents of the extracts

Total phenolic contents of the various extracts of *R. pimpinellifolia* plant were determined as gallic acid equivalents. As shown in Table 3, the phenolic contents of the extracts are higher than flavonoid contents. Among the extracts of *R. pimpinellifolia*, the EAR has the highest total phenolic content (378.2 ± 0.477 µg GAE/mg extract).

Antioxidant activities

The DPPH radical scavenging activity

The DPPH radical scavenging capacities of *R. pimpinellifolia* extracts and the standard antioxidant compound α -tocopherol at a concentration of 10 µg/mL are shown in % inhibition in Table 3.

ABTS⁺ cation radical scavenging capacity

The ABTS radical scavenging capacities of *R. pimpinellifolia* extracts and the standard antioxidant compound trolox at a concentration of 10 µg/mL are shown in % inhibition in Table 3.

Superoxide anion radical scavenging capacity

Superoxide Anion radical scavenging capacities of *R. pimpinellifolia* extracts and the standard antioxidant compound Trolox at a concentration of 10 µg/mL are shown in % inhibition in Table 3.

Table 3 Total phenolic contents and antioxidant activities of *R. pimpinellifolia* various extracts at 10 µg/mL

Samples*	Total Phenolic Compound (µg GAE/mg extract)	DPPH Radical Scavenging Activity	ABTS ⁺ Radical Scavenging Capacity	Cation Superoxide Anion Radical Scavenging Capacity
MR	236.36 ± 0.4	30.9	57.9	21.9
EAR	378.2 ± 0.4	39.7	91.2	39.5
WR	237.087 ± 0.1	15.6	40.2	25.2
WPF	195.6 ± 0.2	30.4	32.9	31.2
MS	224.12 ± 0.2	11.1	56.7	21.1
EAS	305.39 ± 0.5	21.2	39.1	30.0
α-tocopherol		12.5		
trolox			68.4	16.3

(*MR: methanol extract of *R. pimpinellifolia* root, EAR: ethyl acetate extract of *R. pimpinellifolia* root, WR: water extract of *R. pimpinellifolia* root, WPF: water extract of *R. pimpinellifolia* pseudo-fruit, MS: methanol extract of *R. pimpinellifolia* seed, EAS: ethyl acetate extract of *R. pimpinellifolia* seed)

Anticholinesterase activity

The AChE inhibitory activities of the extracts of *R. pimpinellifolia* and the standard donepezil at a concentration of 100 µg/mL are shown in % inhibition in Table 4. The extracts of *R. pimpinellifolia* did not show anticholinesterase activity against AChE but showed BChE with 19% inhibition at 100 µg/mL concentration.

Antityrosinase activity

The α-Kojic acid used as a standard antioxidant shows 92.7% inhibition at 500 µg/mL. the concentration range to be studied has been determined as 25-500 µg/mL. The % inhibition values of the extracts and α-Kojic acid in each dose range are shown in Table 4.

Table 4 BChE and tyrosinase inhibitory activities of *R. pimpinellifolia* extracts

	BChE % Inhibition (100 µg/mL)	Tyrosinase % Inhibition (500 µg/mL)
MR	14	61.5
EAR	19	50
WR	0	37.7
WPF	9	37.9
MS	16	31.9
EAS	18	32.9
Donepezil	97	
α -Kojic acid		92.7

Antimicrobial activity

Extracts of the root, pseudo-fruits, and seeds of *R. pimpinellifolia* plant made by disc diffusion method were found to be effective against *Staphylococcus aureus* and *Candida albicans* in the determination of antimicrobial activity. On the other hand, it was found to be ineffective against bacteria and yeasts such as *Escherichia coli*, *Enterococcus faecalis*, *Candida tropicalis*, *Pseudomonas aeruginosa*, *Klebsiella pneumoniae*, *Staphylococcus epidermidis*.

The MIC (Minimum Inhibitory Concentration) values in the Microdilution method used to measure the sensitivity in the disk diffusion method were compared with the disk diffusion method. The results of both experiments confirm each other.

The results of the Microdilution and Disk diffusion method applied to determine the antimicrobial activity of the extracts are shown in Table 5.

Table 5 Antimicrobial activity (MIC values and zones of inhibition) of extracts of *R. pimpinellifolia* plant against bacteria and yeast species

MIC (µg/mL) and Zone Inhibition (mm), values	MR	EAR	WR	WPF	MS	EAS	Standard Drug (µg/mL)	Negative Control (DMSO)	Positive Control Standard antibiotic disc µg/mL
<i>S. aureus</i> (ATCC BAA977)	1000 7	1000 11	1000 10	1000 8	>1000 8	1000 11		-	0.25 (OKS)
<i>C. albicans</i> (ATCC 14053)	250 20	500 18	250 17	250 15	1000 20	1000 20		-	1 (FLU)

NT: Not tested, OKS: Oxacillin, FLU: Fluconazole

Antigenotoxic Activities

In this study, visual analysis and Comet analysis were performed to reveal the DNA damage created in fibroblast cells with H₂O₂ at a concentration range of 10-30 μM. Comet scoring was made using the scale with 0 for no damage and 3 for the greatest damage. Since the highest comet score according to this scale can be 300 and 20 μM H₂O₂ exhibiting the closest Comet score to this value was determined as the optimum damaging concentration in the next trials. (Table 6, 7)

Table 6 Comet scores (n=3) versus H₂O₂ given to fibroblast cells at increasing concentrations

H ₂ O ₂ Concentration	Comet Score
10 μM H ₂ O ₂	185.7±9.1
20 μM H ₂ O ₂	300±5
30 μM H ₂ O ₂	300+

Table 7 Comet scores (n = 4) showing the potential of different extracts of *R. pimpinellifolia* to inhibit H₂O₂-induced DNA damage

	25	50	100	250	500	1000
	μg/mL	μg/mL	μg/mL	μg/mL	μg/mL	μg/mL
Negative Control	24.2±2.3					
Positive Control (20 μM H ₂ O ₂)	300±5					
WPF→DMSO	300	300	300	300	300	300+
MPF→DMSO	300	300	300	300	300	300+
WPF→ water	300	300	300	300	300	300+
MR→DMSO	300	300	300	300	300	300+

LC-MS/MS analysis

Validation of experiments and uncertainty evaluation

The validation parameters were determined to be LOD (limit of detection), LOQ (limit of quantification), linearity, recovery, and repeatability. The LOD and LOQ values of standards for the LC-MS/MS method are given in Table 8. LOD and LOQ were determined by using the signal-to-noise method. A signal-to-noise ratio of three was accepted for estimation of LOD and signal-to-noise ratio of 10 was used for estimation of LOQ [63]. The repeatability in the intra-day (RSD%) values phenolics ranged between 0.1 – 5 mg/kg were obtained using

the corresponding peak area of 3 replicate analyses at approximately 2.5 mg/kg concentration level.

Table 8 Method validation and uncertainty parameters for phenolic compounds

	Compounds	Linear regression equation	R²	LOD (mg/L)	LOQ (mg/L)	RSD (%)
1	7-acetylsideroxol	y=0.105x+0.0224	0.9834	0.46	1.55	5.61
2	Apigenin	y=0.182x+0.072	0.9940	0.15	0.50	4.01
3	Catechin	y=0.067x+0.035	0.9941	0.06	0.21	6.49
4	Chlorogenic acid	y=0.262x-0.004	0.9981	0.44	1.48	5.45
5	Cyanidin-3-O-glucoside	y=0.35x+0.01	0.9912	0.09	0.29	1.37
6	Emodin	y=0.15x+0.09	0.9806	0.58	1.95	2.46
7	Epigallocatechin Epigallocatechin	y=0.034x+0.022	0.9876	0.04	0.13	5.53
8	gallate	y=0.1175x-0.007	0.9957	0.09	0.32	4.79
9	Eubotriol	y=0.13x+0.09	0.9931	0.31	1.03	3.33
10	Fumaric acid	y=0.056x+0.015	0.9944	0.07	0.23	5.44
11	Gallic acid	y=0.040x-0.020	0.9986	0.54	1.82	7.23
12	Isoquercetin Pelargonin	y=0.323x+0.054	0.9974	0.56	1.87	9.42
13	chloride	y=0.189x+0.0041	0.9928	0.17	0.56	4.45
14	Procyanidin B2	y=0.049x+0.0067	0.9902	0.09	0.31	10.36
15	Pyrogallol	y=0.039x+0.014	0.9875	0.04	0.15	5.47
16	Quercetin Quercetin-3-	y=0.115x+0.027	0.9901	0.303	1.01	1.14
17	arabioside	y=0.33x+0.04	0.9958	0.56	1.87	9.42
18	Quercitrin	y=0.02x-0.004	0.9976	0.02	0.06	4.28
19	Ursolic acid	y=0.015x+0.0044	0.9948	0.07	0.23	3.04

The concentration of each analyte was within the linear range and the concentration of the reported method was obtained from the calibration curve. In conclusion, the calculated concentrations were converted to µg/g of the crude extract sample, by using Equation (X)

$$Amount (\mu/g) = \left(\frac{(C_a \times V \times F)/1000}{m/1000} \right) \quad (X)$$

Where Ca is the analyte concentration obtained by calibration curve (in mg/kg), V is the final diluted volume (in grams) before the analysis, m is the amount of the extract (in milligrams), F is the dilution factor, 1000 is the conversion factor. LC-MS/MS parameters of selected compounds were shown in Table 9.

Table 9 LC-MS/MS parameters of selected compounds

Compounds	Parent ion	Daughter ion	Capillary	Collision energy (V)	ESI mode
7-acetyl sideroxol	385.4	325	100	20	Positive
Apigenin	269	151	100	22	Negative
Catechin	289	245	50	15	Negative
Chlorogenic acid	353	191	80	14	Negative
Cyanidin-3-O-glucoside	449	287	90	19	Positive
Emodin	268.9	224.3	100	30	Negative
Epigallocatechin	305	125	80	18	Negative
Epigallocatechin gallate	457	169	100	14	Negative
Eubotriol	343	343	100	20	Positive
Fumaric acid	115	71	80	8	Negative
Gallic acid	168.6	124	50	13	Negative
Isoquercetin	463.3	300	90	25	Negative
Pelargonin chloride	595	271	80	30	Positive
Procyanidin B2	577.4	288.5	80	20	Negative
Pyrogallol	125	80	100	16	Negative
Quercetin	301	178,5	120	16	Negative
Quercetin-3-arabinoside	463.3	300	80	21	Negative
Quercitrin	471.9	309.9	60	16	Positive
Ursolic acid	455.6	455.1	50	10	Negative

The EURACHEM/CITAC guide was used for the evaluation of sources and quantification of uncertainty of the LC-MS/MS method [64]. The maximum contribution comes from the calibration curve. Detailed procedures of uncertainty evaluation were reported previously in the literature [65]. To obtain expanded uncertainty, combined standard measurement uncertainty has to be multiplied by 2 (coverage factor) at 95% confidence level. The expanded relative uncertainties for all the compounds in each plant sample are given in Table 8. In LC/MS/MS analysis, Cyanidin-3-O-Glucoside and isoquercetin in the pseudo-fruit; procyanidin B2 and catechin in the root were the major phenolic compounds. The results of the chemical compounds were given in Table 10.

Table 10 LC-MS/MS Quantitative Analysis Results of Secondary Metabolites ($\mu\text{g/g}$)

Compounds	Pseudo-fruit	Root
7-acetylsideroxol	18,80 \pm 3,65	83,60 \pm 16,25
Apigenin	37,39 \pm 3,67	41,11 \pm 4,03
Catechin	48,77 \pm 5,71	2211,13 \pm 258,77
Cyanidin-3- <i>O</i> -Glu	2102,35 \pm 232,57	-
Emodin	38,21 \pm 8,29	44,33 \pm 9,62
Epigallocatechin	-	1196,35 \pm 133,88
Epigallocatechin Gallate	-	78,75 \pm 7,09
Eubotriol	-	202,60 \pm 21,93
Fumaric acid	368,22 \pm 34,14	85,06 \pm 7,89
Gallic acid	64,92 \pm 10,36	63,04 \pm 10,06
Isoquercetin	1096,88 \pm 317,66	-
Pelargonin Chloride	8,579 \pm 0,24	88,79 \pm 2,51
Procyanidin B2	382,63 \pm 60,93	5401,88 \pm 860,26
Pyrogallol	-	-
Quercetin	72,57 \pm 11,59	-
Quercetin-3-Arabinoside	188,28 \pm 54,32	-
Quercitrin	85,38 \pm 6,08	-
Ursolic acid	204,54 \pm 18,37	-

Amounts of the samples in μg of secondary compounds per g extract with the expanded ($k = 2$) uncertainty

Discussion

Numerous studies have been carried out on the fruits of the *Rosa* species [66,10,67]. However, in this study, no biological activity studies were conducted on the roots of *R. pimpinellifolia*. Therefore, it can be said that this study is original. Previously, anti-inflammatory and anticancer studies have been conducted on different *Rosa* roots, and it has been observed that the roots are effective in these studies [68, 69].

Previously, total phenolic contents of *R. spinosissima*, *R. canina*, and *R. rugosa* fruits were examined. It has been reported that *R. spinosissima* has the highest total phenolic content and antioxidant activity [70].

In our study, we determined that the roots and fruits were not rich in flavonoids. There are mostly made of catechic and triterpene substances [71].

Antioxidant activities of *Rosa* species's fruits and roots are high [72]. It was reported that methanol extract of *R. davurica* roots showed strong antioxidant activity in DPPH radical scavenging activity assay [73]. The relationship between the rich polyphenol content and antioxidant mechanisms in *R. canina* was investigated, and good antioxidant activity was

demonstrated by H₂O₂ and superoxide anion radical scavenging activity experiments at all concentrations [74].

In our study, we found that *R. pimpinellifolia* roots and fruits did not have cholinesterase activity. In another study, it was reported that *R. canina* fruits are also inactive [75].

In our study, it was observed that the roots and fruits of *R. pimpinellifolia* had moderate antityrosinase activity. Tyrosinase enzyme inhibition values in *R. pimpinellifolia* extracts were the highest at 500 µg/mL. 37.7% in root water extract; 50% in root ethyl acetate extract, 61.5% in root methanol extract, 37.9% in pseudo-fruit extract. At a concentration of 500 µg/mL, α-Kojic acid showed an inhibition of 90%. Inhibitory activity on tyrosinase enzyme at 500 µg/mL. Natural compounds such as kojic acid, arbutin are preferred than chemical substances such as hydroquinone and azelaic acid because they have no inflammatory effects on the skin. Results have shown that *R. pimpinellifolia* extracts can be used as an alternative in the therapy treatment of hyperpigmentation and may be involved in the formulations of cosmetic products used for hyperpigmentation. In our previous study, the antityrosinase activity of *R. pimpinellifolia* petals was shown to be promising [76]

In our study, a weak antimicrobial activity of *Rosa* roots and fruits against bacteria and fungi was determined. In certain studies, *R. rugosa* root extracts were found to exhibit antimicrobial activity against *S. epidermidis*, *S. aureus*, *B. subtilis*, *Micrococcus luteus*, *E. coli*, *Klebsiella pneumoniae*, *Ps. aeruginosa*, *Proteus mirabilis*, and *Candida albicans* [77]. Furthermore, in another study, the activity of alcohol and aqueous extracts of *R. damascena* was determined against 10 pathogenic microorganisms (*S. aureus* ATCC 25923, *Ps. aeruginosa* ATCC 27853, *E. coli* ATCC 25922, *S. pneumoniae* ATCC 55143, *Acinetobacter calcoaceticus*, *Salmonella enteritidis* and *Aspergillus niger* ATCC 1640) MIC, MBC and inhibition area diameter were determined by *in vitro* disc diffusion and microdilution method. While hexane extracts showed very low activity against the microorganisms, it was stated that the aqueous extract inhibited the growth of Gram (+) and Gram (-) bacteria, as well as *A. niger*. With regards to its ethanol extract, it showed antibacterial activity against *P. aeruginosa* ATCC 27853 bacteria (MIC and MBC 62.5 µg/mL, DIZ = 34 mm), *E. coli* ATCC 25922 bacteria (MIC and MBC 62.5 µg/mL, DIZ = 30 mm) according to some studies was reported [78].

According to our results, it was observed that 4 different extracts did not show antigenotoxic effect in the concentration range of 25-500 µg/mL, while extracts at a concentration of 1000 µg/mL showed toxic effects and increased the existing damage. In further studies, we believe that *R. pimpinellifolia* extracts to be prepared using different solvent and extraction techniques should be studied both in different treatment types (simultaneous or post) and different cell types. With this study, antigenotoxic data were obtained for the first time in *Rosa* roots and fruits.

In an LC/MS/MS study, it was reported that Catechin, epicatechin, quercetin-3-glucoside, protocatechuic acid, chlorogenic acid, quercetin, rutin, fumaric acid, and gallic acid are major phenolic compounds in *R. pimpinellifolia* fruits.

In other studies, it has been reported that catechin [68, 79], Cyanidin-3-O-Glucoside [80], and procyanidin [81], are present in different *Rosa* species. In this study, phenolic compounds in *R. pimpinellifolia* roots were first elucidated by LC/MS/MS analysis.

Conclusion

With this study, a start was provided for the studies on the biological activity studies and chemical content of *R. pimpinellifolia* root, pseudo-fruits, and seeds in the literature. By investigating their possible antioxidant, antityrosinase, anticholinesterase, antimicrobial, anti-genotoxic, and anti-cancer properties and determining the chemical content of *R. pimpinellifolia* root, pseudo-fruit, and seed and the deficiency of work in the scientific world was eliminated. Determination of medicinal properties of *R. pimpinellifolia*, production of active substances with biological properties, and application of these substances in the pharmacological field will provide meaningful support. In future studies, *in vitro* and *in vivo* studies of active ingredients to be obtained by plant isolation should be carried out.

Conflict of Interest

The authors declare that there are no conflicts of interest.

Acknowledgments

This study is part of Leyla GÜVEN's PhD thesis. The authors thank Abdulkayyum İdrisu proofreading.

Competing Interests

Authors have declared that no competing interests exist.

Abbreviations

EAR: Ethyl acetate extract of *R. pimpinellifolia* root; MR: Methanol extract of *R. pimpinellifolia* root; WR: Water extract of *R. pimpinellifolia* root; WPF: Water extract of *R. pimpinellifolia* pseudo-fruit; MS: Methanol extract of *R. pimpinellifolia* seed; EAS: Ethyl acetate extract of *R. pimpinellifolia* seed

References



1. Tetik, F., et al., Traditional uses of some medicinal plants in Malatya (Turkey). *Journal of Ethnopharmacology*, 2013. 146(1): p. 331-346.
2. Gürhan, G. and N. Ezer, Halk arasında hemoroit tedavisinde kullanılan bitkiler-I. Hacettepe Üniversitesi Eczacılık Fakültesi Dergisi, 2004. 24(1): p. 37-55.
3. Altundag, E. and M. Ozturk, Ethnomedicinal studies on the plant resources of east Anatolia, Turkey. *Procedia-Social and Behavioral Sciences*, 2011. 19: p. 756-777.
4. Kumar, N., et al., Reversed phase-HPLC for rapid determination of polyphenols in flowers of rose species. *Journal of Separation Science*, 2008. 31(2): p. 262-267.
5. Gao, X., et al., Aurone constituents from the flowers of *Rosa rugosa* and their biological activities. *Heterocycles*, 2012. 85(8): p. 1925-1931.
6. Gao, X.M., et al., Phenylethanoids from the flowers of *Rosa rugosa* and their biological activities. *Bulletin of the Korean Chemical Society*, 2013. 34(1): p. 246-248.
7. Liu, D.L., et al., Triterpenoids from the roots of *Rose odorata* var. *gigantea*. *Chinese Journal of Natural Medicines*, 2010. 8(1): p. 12-15.
8. Stoyanova-Ivanova, B., et al., Content and composition of neutral components in wax from *Rosa canina* flowers. *Doklady Bolgarskoi Akademii Nauk*, 1979. 32(11): p. 1503-1506.
9. Hashidoko, Y., The phytochemistry of *Rosa rugosa*. *Phytochemistry*, 1996. 43(3): p. 535-549.
10. Novruzov, E.N., Pigments of species in the genus *Rosa* and their chemotaxonomic value. *Acta Horticulturae*, 2005. 690(Proceedings of the 1st International Rose Hip Conference, 2004): p. 225-230.
11. Ghazghazi, H., et al., Phenols, essential oils and carotenoids of *Rosa canina* from Tunisia and their antioxidant activities. *The African Journal of Biotechnology*, 2010. 9(18): p. 2709-2716.
12. Al-Rehaily, A.J., et al., Essential oil of *Rosa abyssinica* R. Br. from Saudi Arabia. *Journal of Essential Oil Research*, 2003. 15(5): p. 344-345.
13. Elmastaş, M., et al., Changes in flavonoid and phenolic acid contents in some *Rosa* species during ripening. *Food chemistry*, 2017. 235: p. 154-159.
14. Odabaş, H.İ. and I. Koca, Simultaneous separation and preliminary purification of anthocyanins from *Rosa pimpinellifolia* L. fruits by microwave assisted aqueous two-phase extraction. *Food and Bioproducts Processing*. 125: p. 170-180.
15. Murathan, Z.T., et al., Characterization of bioactive compounds in rosehip species from East Anatolia region of Turkey. *Italian Journal of Food Science*, 2016. 28(2): p. 314.
16. Murathan, Z.T., et al., Determination of fatty acids and volatile compounds in fruits of rosehip (*Rosa* L.) species by HS-SPME/GC-MS and Im-SPME/GC-MS techniques. *Turkish Journal of Agriculture and Forestry*, 2016. 40(2): p. 269-279.
17. Nagaki, M., et al., Composition and antimicrobial activity of the essential oil and water extract from Japanese wild *Rosa rugosa*. *Transactions of the Materials Research Society of Japan*, 2011. 36(3): p. 517-521.
18. Lee, H.J., et al., Anti-inflammatory effects of hexane fraction from white rose flower extracts via inhibition of inflammatory repertoires. *Biomolecules & Therapeutics*, 2011. 19(3): p. 331-335.
19. Park, K.H., et al., Three new stereoisomers of condensed tannins from the roots of *Rosa multiflora*. *Chemical and Pharmaceutical Bulletin*, 2010. 58(9): p. 1227-1231.
20. Hsieh, T.C., et al., Effects of herbal preparation Equiguard on hormone-responsive and hormone-refractory prostate carcinoma cells: mechanistic studies. *International Journal of Oncology*, 2002. 20(4): p. 681-689.

21. Nagai, T., et al., Tea beverages made from Romanas rose (*Rosa rugosa* Thunb.) leaves possess strongly antioxidative activity by high contents of total phenols and vitamin C. *Journal of Food, Agriculture and Environment*, 2007. 5(3 & 4): p. 137-141.
22. Liu, Y.T., et al., Hepatoprotective activity of the total flavonoids from *Rosa laevigata* Michx fruit in mice treated by paracetamol. *Food Chemistry*, 2010. 125(2): p. 719-725.
23. Setzer, W.N., Essential oils and anxiolytic aromatherapy. *Natural Product Communications*, 2009. 4(9): p. 1305-1316.
24. Ninomiya, K., et al., Potent anti-obese principle from *Rosa canina*: Structural requirements and mode of action of trans-tiliroside. *Bioorganic & Medicinal Chemistry Letters*, 2007. 17(11): p. 3059-3064.
25. Umezu, T., et al., Anticonflict effects of rose oil and identification of its active constituents. *Life Science*, 2002. 72(1): p. 91-102.
26. Seto, T., et al., Purgative activity and principals of the fruits of *Rosa multiflora* and *R. wichuraiana*. *Chemical and Pharmaceutical Bulletin*, 1992. 40(8): p. 2080-2082.
27. Tayefi-Nasrabadi, H., et al., The effects of the hydroalcohol extract of *Rosa canina* L. Fruit on experimentally nephrolithiasic wistar rats. *Phytotherapy Research*, 2012. 26(1): p. 78-85.
28. Mandade, R.J., et al., Role of the *Rosa canina* L. leaf extract as an antidiarrheal drug in rodents. *Indian Journal of Pharmacology*, 2011. 43(3): p. 316-319.
29. Jeon, J.H., et al., Anti-allergic effects of white rose petal extract and anti-atopic properties of its hexane fraction. *Archives of Pharmacal Research*, 2009. 32(6): p. 823-830.
30. Tumbas, V.T., et al., Effect of rosehip (*Rosa canina* L.) phytochemicals on stable free radicals and human cancer cells. *Journal of the Science of Food and Agriculture*, 2012. 92(6): p. 1273-1281.
31. Jung, H.J., et al., 19 α -hydroxyursane-type triterpenoids: antinociceptive anti-inflammatory principles of the roots of *Rosa rugosa*. *Biological and Pharmaceutical Bulletin*, 2005. 28(1): p. 101-104.
32. Gürbüz, İ., et al., Anti-ulcerogenic activity of some plants used as folk remedy in Turkey. *Journal of Ethnopharmacology*, 2003. 88(1): p. 93-97.
33. Yoshizawa Y., et al., Anticancer and anti-hypertensive effects of small fruit juices, *American Chemical Society*, 2001,2: 8-23.
34. Trovato, A., et al., In vitro anti-mycotic activity of some medicinal plants containing flavonoids. *Bollettino Chimico Farmaceutico*, 2000. 139(5): p. 225-227.
35. Boskabady, M.H., et al., Pharmacological effects of *Rosa damascena*. *Iranian Journal of Basic Medical Sciences*, 2011. 14(4): p. 295-307.
36. Vlachojannis JE, Duke RK, Tran VH, Duke CC, Chrubasik S. Medicinal properties of *Rosa canina*, *Studium Press*, 2010, 27: 441-463.
37. Vertuani, S., et al., Antioxidant herbal supplements for hemorrhoids developing a new formula. *Nutrafoods*, 2004. 3(3): p. 19-26.
38. Ghasemzadeh, A. and N. Ghasemzadeh, Flavonoids and phenolic acids: Role and biochemical activity in plants and human. *Journal of medicinal plants research*, 2011. 5(31): p. 6697-6703.
39. Park, H.-R., et al., Antioxidant activity of extracts from *Acanthopanax senticosus*. *African Journal of Biotechnology*, 2006. 5(23).
40. Aliyazicioglu, R., et al., Antioxidant, antigenotoxic, antimicrobial activities and phytochemical analysis of *Dianthus carmelitarum*. *Rec. Nat. Prod.*, 2017. 11(3): p. 270-284.
41. Gyawali, R. and S.A. Ibrahim, Natural products as antimicrobial agents. *Food Control*, 2014. 46: p. 412-429.
42. Bao, K., et al., Design and synthesis of biphenyl derivatives as mushroom tyrosinase inhibitors. *Bioorg. Med. Chem.*, 2010. 18(18): p. 6708-6714.

43. Masuda, T., et al., Screening for tyrosinase inhibitors among extracts of seashore plants and identification of potent inhibitors from *Garcinia subelliptica*. *Biosci., Biotechnol., Biochem.*, 2005. 69(1): p. 197-201.
44. Sezer Senol, F., et al., Memory-vitalizing effect of twenty-five medicinal and edible plants and their isolated compounds. *S. Afr. J. Bot.*, 2016. 102: p. 102-109.
45. Tsong-Min, C., Tyrosinase and tyrosinase inhibitors. *Journal of Biocatalysis & Biotransformation*, 2012.
46. Gholamhoseinian, A. and Z. Razmi, Screening the methanolic extracts of some plants for tyrosinase inhibitory activity. *Toxicological & Environmental Chemistry*, 2012. 94(2): p. 310-318.
47. Shimizu, K., et al., Inhibition of tyrosinase by flavonoids, stilbenes, and related 4-substituted resorcinols. Structure-activity investigations. *Planta Med.*, 2000. 66(1): p. 11-15.
48. Martinez, M.V. and J.R. Whitaker, The biochemistry and control of enzymic browning. *Trends Food Sci. Technol.*, 1995. 6(6): p. 195-200.
49. Xu, Y., et al., Tyrosinase mRNA is expressed in human substantia nigra. *Mol. Brain Res.*, 1997. 45(1): p. 159-162.
50. Asanuma, M., et al., Dopamine- or L-DOPA-induced neurotoxicity: the role of dopamine quinone formation and tyrosinase in a model of Parkinson's disease. *Neurotox Res*, 2003. 5(3): p. 165-76.
51. Adewusi, E.A., et al., Medicinal plants with cholinesterase inhibitory activity: a review. *African Journal of Biotechnology*, 2010. 9(49): p. 8257-8276.
52. Singleton, V. and J.A. Rossi, Colorimetry of total phenolics with phosphomolybdic-phosphotungstic acid reagents. *American Journal of Enology and Viticulture*, 1965. 16(3): p. 144-158.
53. Folin, O. and W. Denis, Phosphotungstic-phosphomolybdic Compounds as Color Reagents. *The Journal of Biological Chemistry*, 1912. 12: p. 239-243.
54. Slinkard, K. and V.L. Singleton, Total phenol analysis: automation and comparison with manual methods. *American Journal of Enology and Viticulture*, 1977. 28(1): p. 49-55.
55. Lar'kina, M.S., et al., Quantitative determination of flavonoids from the aerial part of greater knapweed (*Centaurea scabiosa* L.). *Pharmaceutical Chemistry Journal*, 2009. 43(6): p. 320-323.
56. Blois, M.S., Antioxidant determinations by the use of a stable free radical. 1958.
57. Re, R., et al., Antioxidant activity applying an improved ABTS radical cation decolorization assay. *Free Radical Biology & Medicine*, 1999. 26(9-10): p. 1231-1237.
58. Zhishen, J., et al., The determination of flavonoid contents in mulberry and their scavenging effects on superoxide radicals. *Food Chemistry*, 1999. 64(4): p. 555-559.
59. Ellman, G.L., et al., A new and rapid colorimetric determination of acetylcholinesterase activity. *Biochemical Pharmacology*, 1961. 7(2): p. 88-95.
60. Likhitwitayawuid, K. and B. Sritularak, A new dimeric stilbene with tyrosinase inhibitory activity from *Artocarpus gomezianus*. *Journal of Natural products*, 2001. 64(11): p. 1457-1459.
61. Aliyazicioglu, Y., et al., Preventive and protective effects of Turkish propolis on H₂O₂-induced DNA damage in foreskin fibroblast cell lines. *Acta Biologica Hungarica*, 2011. 62(4): p. 388-396.
62. Tice, R.R., et al., Single cell gel/Comet assay: guidelines for in vitro and in vivo genetic toxicology testing. *Environmental and Molecular Mutagenesis* 2000. 35(3): p. 206-221.
63. Ceylan, R., et al., GC-MS analysis and in vitro antioxidant and enzyme inhibitory activities of essential oil from aerial parts of endemic *Thymus spathulifolius* Hausskn. et Velen. *Journal of enzyme inhibition and medicinal chemistry*, 2016. 31(6): p. 983-990.
64. Gören, A.C., et al., HPLC and LC-MS/MS methods for determination of sodium benzoate and potassium sorbate in food and beverages: Performances of local accredited laboratories via proficiency tests in Turkey. *Food chemistry*, 2015. 175: p. 273-279.

65. Binici, B., et al., An efficient GC–IDMS method for determination of PBDEs and PBB in plastic materials. *Talanta*, 2013. 116: p. 417-426.
66. Feng-Zheng, C., et al., Chemical Constituents from Fruits of *Rosa davidii*. *Acta Botanica Sinica*, 2001. 1: p. 19.
67. Larsen, E., et al., An antiinflammatory galactolipid from rose hip (*Rosa canina*) that Inhibits chemotaxis of human peripheral blood neutrophils in vitro. *Journal of Natural Products*, 2003. 66(7): p. 994-995.
68. Çoruh, N. and N. Özdoğan, Identification and quantification of phenolic components of *Rosa heckeliana* Tratt roots. *Journal of Liquid Chromatography & Related Technologies*, 2015. 38(5): p. 569-578.
69. Yeşilada, E., et al., Inhibitory effects of Turkish folk remedies on inflammatory cytokines: interleukin-1 α , interleukin-1 β and tumor necrosis factor α . *Journal of Ethnopharmacology*, 1997. 58(1): p. 59-73.
70. Koczka, N., et al., Total polyphenol content and antioxidant capacity of rosehips of some *Rosa* species. *Medicines*, 2018. 5(3): p. 84.
71. Guven, L., et al., Phytochemical studies on the seeds, pseudofruits, and roots of *Rosa pimpinellifolia*. *Journal of Research in Pharmacy*, 2021. 25(2): p. 153-163.
72. Senol, F.S., et al., Memory-vitalizing effect of twenty-five medicinal and edible plants and their isolated compounds. *South African Journal of Botany*, 2016. 102: p. 102-109.
73. Hu, W., et al., Biological activity and inhibition of non-enzymatic glycation by methanolic extract of *Rosa davurica* Pall. roots. *Journal of Food Sciences and Nutrition*, 2011. 16(3): p. 242-247.
74. Kilicgun, H. and D. Altiner, Correlation between antioxidant effect mechanisms and polyphenol content of *Rosa canina*. *Pharmacognosy Magazine*, 2010. 6(23): p. 238-241.
75. Boğa, M., et al., Antioxidant and anticholinesterase activities of eleven edible plants. *Pharm Biol*, 2011. 49(3): p. 290-5.
76. Guven L., et al., Thyrozinase enzyme inhibitor activity of *Rosa pimpinellifolia* petals, in 5th International Medical and Health Sciences Research Congress (UTSAK). 12-13 December 2020: Ankara.
77. Olech, M., et al., Evaluation of rose roots, a post-harvest plantation residue as a source of phytochemicals with radical scavenging, cytotoxic, and antimicrobial activity. *Industrial Crops and Products*, 2015. 69: p. 129-136.
78. Halawani, E.M., et al., Antimicrobial activity of *Rosa damascena* petals extracts and chemical composition by gas chromatography-mass spectrometry (GC/MS) analysis. *African Journal of Microbiology Research*, 2014. 8(24): p. 2359-2367.
79. He, R.R., et al., Protective effects of radix *Rosa laevigata* against *Propionibacterium acnes* and lipopolysaccharide-induced liver injury. *Bioscience, Biotechnology, and Biochemistry*, 2009. 73(5): p. 1129-1136.
80. Odabaş, H.İ. and I. Koca, Simultaneous separation and preliminary purification of anthocyanins from *Rosa pimpinellifolia* L. fruits by microwave assisted aqueous two-phase extraction. *Food and Bioproducts Processing*, 2021. 125: p. 170-180.
81. Dabić Zagorac, D.Č., et al., Establishing the chromatographic fingerprints of flavan-3-ols and proanthocyanidins from rose hip (*Rosa* sp.) species. *Journal of separation science*, 2020. 43(8): p. 1431-1439.

Diversity Analysis of Common Vetch (*Vicia sativa* L.) Lines and Cultivars Using Pairwise Combinations of Universal Rice Primers

Mustafa Topu¹ , Iskender Tiryaki^{2*} 

ABSTRACT

This study has been conducted to determine genetic diversity of the common vetch lines and cultivars by using pairwise combinations of universal rice primers (URPs). A total number of 37 URP marker pairs were tested and twenty of those provided amplicons in the common vetch genome. The pairs of amplified URP markers provided a total of 83 bands and 62 of them were determined as polymorphic and were scattered to the whole genome. The average polymorphism rate of the primers was calculated as 73.5% while the polymorphism information content (PIC) values have ranged from 0.11 to 0.47 with an average of 0.24. The phylogenetic tree constructed based on UPGMA analysis provided three main clades. Two-dimensional plot of PCA and the UPGMA analysis showed that the URP markers successfully distinguished the genetic material based on their genetic origin. In conclusion, this study revealed that the use of pairwise combinations of URP markers could have a better power to reveal the level of polymorphism in plant genome.

ARTICLE HISTORY

Received

30 May 2022

Accepted

6 August 2022

KEY WORDS

Common vetch,
URP,
genetic diversity,
molecular
characterization

Introduction

Vicia sativa L., common vetch, is considered as one of the most important annual, self-pollinated, diploid forage crop species [1-3]. The common vetch plants have plasticity not only for adaptability to different soil and climate conditions, but it also has diverse use as grain, straw, hay, silage, and green manure along with soil improvement ability with nitrogen fixation [1-3]. Therefore, it is considered one of the most valuable protein and mineral resources for cattle and poultry in Turkey, Australia, New Zealand, China and Eastern Europe [3-7].

PCR based molecular markers are currently one of the best tools to make genetic characterization and to estimate genetic diversity in various organisms including plants [8-11] since they are more reliable than pedigree data to estimate genetic diversity and to

¹ Suleyman Demirel Anadolu Lisesi, Zeybek 4. Cd. No:4, 09020 Efeler/ Aydın / Turkey

² Department of Agricultural Biotechnology, Faculty of Agriculture, Canakkale Onsekiz Mart University, Terzioğlu Campus, 17020 Canakkale, Turkey

*Corresponding Author: Iskender Tiryaki, e-mail: tiryaki46@yahoo.com

discriminate individuals from various breeding sources for parental selection in plants [12, 13]. However, the power of a molecular marker is mainly determined by the level of polymorphism detected [14]. As a complex taxon, *V. sativa* represents a diverse phylogenetic relationship [15, 16]. Various type of molecular markers have been previously used to resolve inter- and intra-specific diversity in common vetch by using random amplified polymorphic DNA (RAPD) [15], sequence-related amplified polymorphism (SRAP) and inter-simple sequence repeat (ISSR) [17], amplified fragment length polymorphism (AFLP) [18], simple sequence repeats (SSRs) [19], expressed sequence tag-simple sequence repeat (EST-SSR) [20], cDNA-simple sequence repeat (cDNA-SSR) [21, 22], start codon targeted polymorphism (SCoT) [23] and single nucleotide polymorphisms (SNPs) [24, 25]. The recent advancements in plant biotechnology also resulted in avalanche of information in terms of DNA sequences and functional gene determination in various plant species [20, 21, 23, 26]. Therefore, not only transferability of the current molecular markers among the species has been studied [19] but new and alternative use of those molecular marker techniques have also been developed in diverse plant species [27-29].

The universal rice primers (URPs) were generated based on repetitive DNA sequences of the rice genome [30-32] and their efficiency as well as universal applicability have been previously tested in various prokaryotic [30-32] and eukaryotic [32, 33] genomes for taxonomic and phylogenetic analysis. However, based on the current literature URP markers have never been tested in pairs so far.

The objective of this study was to reveal genetic relationships of some common vetch lines and cultivars obtained from various genetic resources by using pairwise combinations of URP markers.

Materials And Methods

Materials

A total of 24 common vetch lines and cultivars which were obtained from either national or international genetic resources were used in this study (Table 1). The seeds of lines were propagated by selfing under the same field conditions for 2 years, during the plant growing seasons of 2008 and 2009. The taxonomic confirmation of the lines assured that all lines belong to *V. sativa* (Table 1).

Table 1. Source of 19 lines and 5 varieties of *Vicia sativa* used in this study

Accession number	Source	Register number
TR41968	Izmir Aegean Agricultural Research Institute	GB-3
TR4471	Izmir Aegean Agricultural Research Institute	GB-5
TR35076	Izmir Aegean Agricultural Research Institute	GB-7
TR12447	Izmir Aegean Agricultural Research Institute	GB-8
TR12474	Izmir Aegean Agricultural Research Institute	GB-13
TR33452	Izmir Aegean Agricultural Research Institute	GB-24
TR4392	Izmir Aegean Agricultural Research Institute	GB-25
TR33253	Izmir Aegean Agricultural Research Institute	GB-29
TR33268	Izmir Aegean Agricultural Research Institute	GB-34
IFVS 490 Sel 2003	International Center for Agricultural Research in the Dry Areas	IC-1
IFVS 1293 Sel 2025	International Center for Agricultural Research in the Dry Areas	IC-2
IFVS 1812 Sel 2083	International Center for Agricultural Research in the Dry Areas	IC-3
IFVS 3026 Sel 2490	International Center for Agricultural Research in the Dry Areas	IC-4
IFVS 715 Sel 2556	International Center for Agricultural Research in the Dry Areas	IC-5
TARM-59998	Ankara Field Crops Central Research Institute	TA-1
TARM-59999	Ankara Field Crops Central Research Institute	TA-2
TARM-60265	Ankara Field Crops Central Research Institute	TA-3
TARM-60279	Ankara Field Crops Central Research Institute	TA-4
TARM-60334	Ankara Field Crops Central Research Institute	TA-5
Alinoğlu-2001	Commercial cultivar	ÇE-1
Bakır-2001	Commercial cultivar	ÇE-2
Cumhuriyet – 99	Commercial cultivar	ÇE-3
Karaelçi	Commercial cultivar	ÇE-6
Kubilay-82	Commercial cultivar	ÇE-7

Methods

DNA extraction and quality control

The young leaves of ten plants of each line or cultivar were bulked and were used for genomic DNA extraction by using plant genomic DNA extraction mini kit (Favorgen, Pingtung, Taiwan) based on the manufacturer's instruction. A known concentration of λ DNA on 0.8% agarose gel electrophoresis was used to determine the sample DNA concentrations and DNAs were diluted to 50 ng/ μ l by using dH₂O before stored at -22 °C until used.

Primers and PCR amplification

The primer pairs used in the study were summarized in Table 2. The URP markers were analyzed as described before [32] and was optimized by using 37 URP marker pairs. Amplifications were carried out in a 20 μ l reaction mixture containing 1 x PCR buffer

(10 mM Tris-HCl pH 8.3, 50 mM KCl, %0.01 jelatin); 25 mM MgCl₂; 50 ng (F+R) primer; 0.5 mM each of deoxyadenosine triphosphate (dATP), deoxyguanosine triphosphate (dGTP), deoxycytidine triphosphate (dCTP) and deoxythymidine triphosphate (dTTP); 0.5 unit of Taq DNA polymerase; and 100 ng of genomic DNA.

The PCR analysis was done in a thermal cycler (Favorgen Gradient PCR, Pingtung, Taiwan). The best annealing temperature of each primer pairs was determined by using a gradient PCR before used in the sample DNA amplifications. To determine the reproducibility of the bands, the PCR reactions were repeated twice. The thermal cycler was programmed to five cycles of 1 min at 94 °C, 1 min at 35 °C and 1:30 min at 72 °C, for denaturing, annealing and extension, respectively. Then main cycles followed by 35 cycles of 1 min at 94 °C, 1:30 min at 55–58 °C (depending upon annealing temperature of the primer presented in Table 2, and 1:30 min at 72 °C, followed by a final incubation for 3 min at 72 °C. The URP amplicons were separated with a 2% (w/v) agarose gel in 1 X TBE buffer at 90 V for 3 h and were stained with ethidium bromide before photographed under ultraviolet light.

Data analysis

The DNA amplicons on the gel were scored for the presence (1) or absence (0) of the bands. The evaluation of band patters of URP markers in this study revealed that they inherited in dominant pattern although the original research paper did not define their inheritances as dominant or co-dominant [32]. Therefore, the polymorphism information content (PIC) of each primer pairs was calculated as a dominant marker as described previously [34, 35] by applying the formula $PIC = 1 - (p^2 + q^2)$ where p and q are the frequencies of presence and absence of bands, respectively. The genetic similarity was calculated by using NTSYSpc-2.1 program based on Dice coefficient [36]. The unweighted pair-group method (UPGMA) with arithmetic averages was used to have the dendrogram. The EIGEN and PROJ modules of NTSYSpc-2.1 program were used for the principal component analysis (PCA).

Table 2. The pairwise combinations of 20 URP marker pairs, sequences, GC content, annealing temperature, the numbers of amplified and polymorphic bands, polymorphism rate and PIC values for 19 lines and 5 cultivars of *V. sativa*

No.	Primer Name	The base sequences (5'-3')	GC Rate (%)	Ta (°C)	Amplified bands	Polymorphic bands	Polymorphism Rate (%)	PIC
1	URP25F	GATGTGTTCTTGGAGCCTGT	50	56	5	3	60	0.22
	URP2R	CCCAGCAACTGATCGCACAC						
2	URP30F	GGACAAGAAGAGGATGTGGA	50	56	2	2	100	0.47
	URP2R	CCCAGCAACTGATCGCACAC						
3	URP32F	TACACGTCTCGATCTACAGG	50	55	5	3	60	0.14
	URP2R	CCCAGCAACTGATCGCACAC						
4	URP38F	AAGAGGCATTCTACCACCAC	50	55	1	1	100	0.22
	URP2R	CCCAGCAACTGATCGCACAC						
5	URP2F	GTGTGCGATCAGTTGCTGGG	50	57	4	3	75	0.35
	URP4R	AGGACTCGATAACAGGCTCC						
6	URP30F	GGACAAGAAGAGGATGTGGA	50	56	5	2	40	0.11
	URP4R	AGGACTCGATAACAGGCTCC						
7	URP32F	TACACGTCTCGATCTACAGG	50	56	5	4	80	0.23
	URP4R	AGGACTCGATAACAGGCTCC						

8	URP38F	AAGAGGCATTCTACCACCAC	50	56	4	3	75	0.23
	URP4R	AGGACTCGATAACAGGCTCC						
9	URP1F	ATCCAAGGTCCGAGACAACC	50	57	3	2	67	0.19
	URP6R	GGCAAGCTGGTGGGAGGTAC						
10	URP2F	GTGTGCGATCAGTTGCTGGG	50	57	2	1	50	0.25
	URP6R	GGCAAGCTGGTGGGAGGTAC						
11	URP9F	ATGTGTGCGATCAGTTGCTG	50	55	3	2	67	0.18
	URP6R	GGCAAGCTGGTGGGAGGTAC						
12	URP32F	TACACGTCTCGATCTACAGG	50	55	2	1	50	0.16
	URP6R	GGCAAGCTGGTGGGAGGTAC						
13	URP1F	ATCCAAGGTCCGAGACAACC	50	55	3	2	67	0.33
	URP13R	TACATCGCAAGTGACACAGG						
14	URP2F	GTGTGCGATCAGTTGCTGGG	50	55	5	5	100	0.35
	URP13R	TACATCGCAAGTGACACAGG						
15	URP9F	ATGTGTGCGATCAGTTGCTG	50	55	6	6	100	0.28
	URP13R	TACATCGCAAGTGACACAGG						

16	URP32F	TACACGTCTCGATCTACAGG	50	55	7	6	86	0.16
	URP13R	TACATCGCAAGTGACACAGG						
17	URP38F	AAGAGGCATTCTACCACCAC	50	55	6	6	100	0.33
	URP13R	TACATCGCAAGTGACACAGG						
18	URP2F	GTGTGCGATCAGTTGCTGGG	50	55	8	5	63	0.2
	URP17R	AATGTGGGCAAGCTGGTGGT						
19	URP25F	GATGTGTTCTTGGAGCCTGT	50	55	5	4	80	0.26
	URP17R	AATGTGGGCAAGCTGGTGGT						
20	URP30F	GGACAAGAAGAGGATGTGGA	50	55	2	1	50	0.19
	URP17R	AATGTGGGCAAGCTGGTGGT						
	TOTAL				83	62	-	-
	MEAN				4.15	3.1	73.5	0.24

Results

Genetic diversity based on URP marker analysis

A total of 37 URP marker pairs were tested in this study. Twelve of those (URP1F/URP2R, URP9F/URP2R, URP25F/URP2R, URP1F/URP4R, URP25F/URP6R, URP30F/URP6R, URP30F/URP13R, URP1F/URP17R, URP25F/URP17R, URP32F/URP17R, URP38F/URP6R and URP30F/URP17R) did not provide any amplification in the vetch genome. The marker combinations URP38F/URP17R, URP9F/URP4R, URP25F/URP4R and URP25F/URP13R produced monomorphic bands only. The URP13R marker was tested as a single primer and was removed from application of pairwise combination. Twenty UPR marker pairs gave polymorphic bands in different proportions (Table 2).

The URP marker pairs produced a total of 83 bands and 60 of them were determined as polymorphic (Table 2). The average polymorphism rate of the markers used was 73.5%. The URP marker pairs provided 4.15 bands an average. The number of polymorphic bands was calculated as 3.1 per marker pair. Average PIC value was calculated as 0.24. The lowest PIC value was obtained from URP30F / URP4R marker pair with 0.11 while URP30F/URP2R marker pair had the highest (0.47) (Table 2). The highest number of amplicons (8 amplicons) was obtained from the URP2F/URP17R while the URP38F/URP2R marker pair had the lowest (1 amplicon). The polymorphism rate of the maker pairs ranged from 40% to 100% (Table 2). The lowest polymorphism rate (40%) was determined on the URP30F/URP4R while all of the amplicons of URP30F/URP2R, URP38F/URP2R, URP2F/URP13R and URP9F/URP13R marker pairs were polymorphic.

The 24 common vetch lines and cultivars were divided into 3 main clades based on UPGMA analysis presented in Figure 1. The lines came from GB provided clade I (Fig. 1) while the lines encoded as TA provided clade II. The clade III consisted of the cultivar and the lines encoded as IC. The lines IC1 and IC2 were separated from the others in the clade III while the cultivars Bakır-2001 and Kubilay-82 were determined as the most similar cultivars (0.97). The cultivar Alinoğlu-2001 was separated from the rest of the cultivars (Fig. 1).

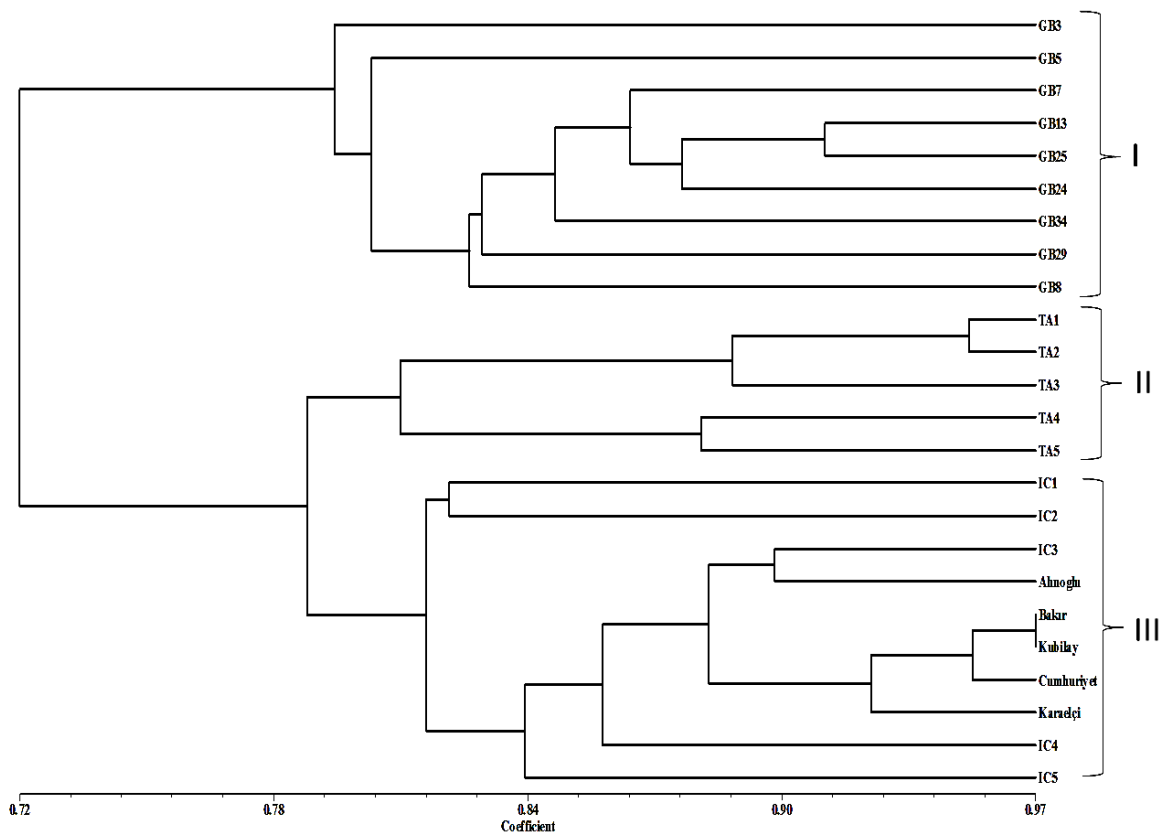


Fig. 1 Genetic similarity dendrogram based given reference [37] for 19 lines and five varieties of *V. sativa* created according to the UPGMA method using 20 pairwise URP markers

The first three components of Eigen values in PCA analysis explained 50.19% of total variation. The PCA analysis revealed that the 20 URP marker pairs as well as their alleles scattered across the vetch genome. For instance, alleles of URP38F/URP13R marker pair provided amplicons came from various loci of different chromosomes (Fig 2). Based on the two-dimensional plot of PCA analysis, the lines GB3 and IC5 were the most distant accessions (Fig. 3).

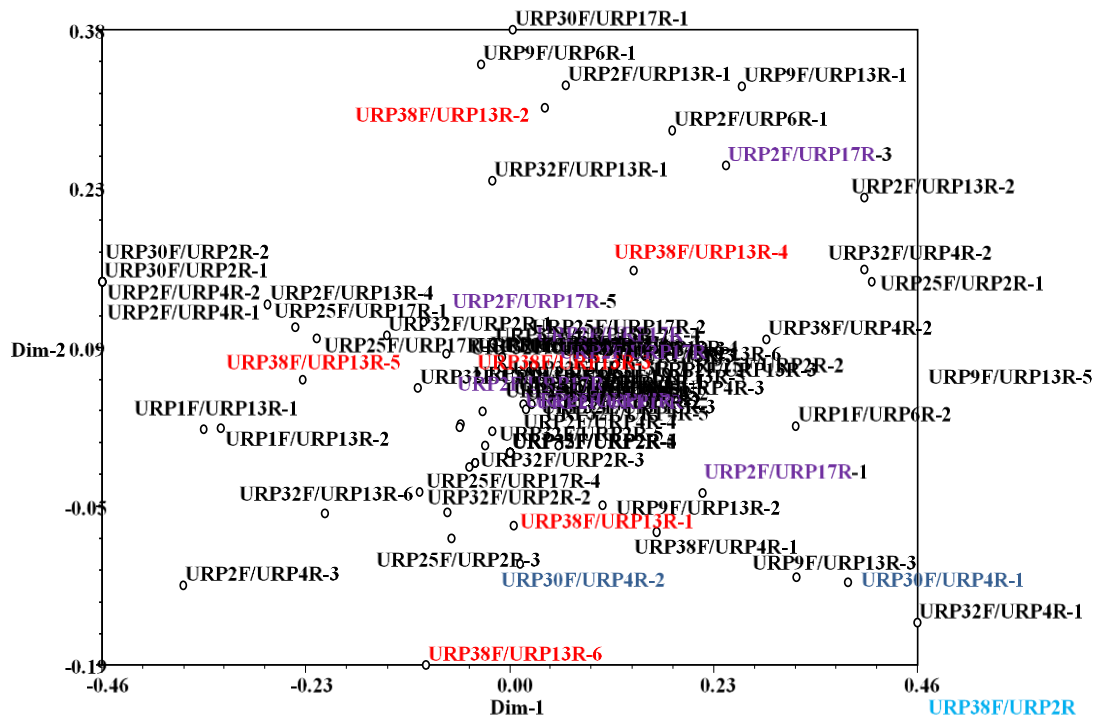


Fig. 2 Two dimensional PCA plot of 20 pair-wise URP markers in the common vetch genome. The 20 pairwise URP markers scattered across the genome. The alleles of URP38F/URP13R, URP2F/URP17R, URP30F/URP4R and URP38F/URP2R markers were given by the same colour along with hyphen and allele numbers

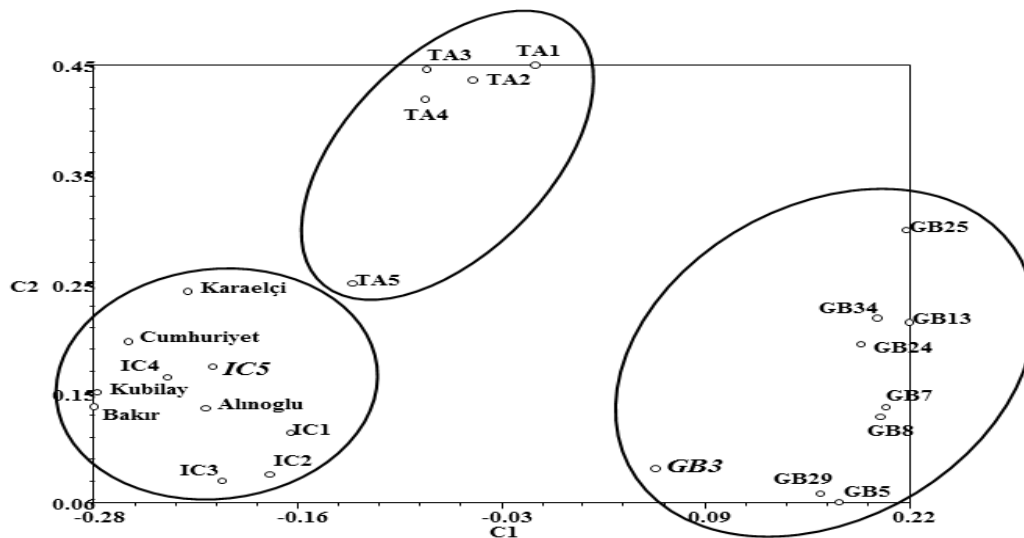


Fig. 3 Two dimensional PCA plot of 19 lines and five varieties of *V. sativa* analyzed by 20 pairwise URP markers. The most distinct lines IC5 and GB3 were indicated in italic

Discussion

The results of the current study revealed that pairwise use of URP markers can successfully be used to determine genetic relationship of common vetch lines and

cultivars. A total of 37 URP marker pairs were tested and twenty of them were amplified in the common vetch genome. Amplified marker pairs produced a total of 83 bands and 62 of them were determined as polymorphic (Table 2). Similar to many other single primer targeting sites such as single primer amplification reaction (SPAR) [38, 39], directed amplification of minisatellite region DNA (DAMD) [40] and random amplified polymorphic DNA (RAPD) [41, 42], URP-PCR method also uses single primer per PCR reaction [32]. Reliability and reproducibility of URP markers were found relatively high since they were used at higher annealing temperatures because of their longer (20 nucleotides) primer sequences and higher GC contents (50% GC) [32, 43]. Therefore, URP markers become a popular DNA marker system for taxonomic and phylogenetic analysis in various prokaryotic [30-32] and eukaryotic [32, 33, 44] genomes. The pairwise use of URP markers in the present study further improved stringency of PCR amplification in comparison to previous reports [43, 45], suggesting that pairwise use of URP markers would provide more unique amplicons for taxonomic and phylogenetic analysis. It was recently reported that pairwise use of RAPD primers provided different patterns of PCR amplifications in soybean genome in comparison to single primer target site of RAPD analysis, indicated that RAPD primers could be used as pairs in various combinations and could provide unique amplicons for phylogenetic analysis [46]. This study first time revealed that URP markers could be used as pairs in various combinations to determine genetic relationship of common vetch lines and cultivars, suggesting that pairwise use of URP markers in various combinations could provide an additional marker resource along with their conventional use in both prokaryotic and eukaryotic genomes. It is also possible that the pairwise use of URP markers may provide new unique amplicons which could be converted into other useful markers such as SCAR (sequence characterized amplified region) and CAPS (cleaved amplified polymorphic sequence) for marker assisted selection in plant breeding after their subsequent cloning and sequencing. The results of this study further indicated that the pairwise use of URP markers should be tested in any specific genome since some of the primer combinations did not provide any amplicon in the vetch genome. Unamplified primer pairs URP25F/URP6R and URP30F/URP6R showed a moderate or very weak primer dimer structure. This might be one of the reasons why those URP pairs did not have any amplification although the other unamplified pairs did not have any such structure. Because of their highest polymorphism

rates (100%) (Table 2), the primer pairs URP30F/URP2R, URP38F/URP2R, URP2F/URP13R, URP9F/URP13R and URP38F/URP13R could be the first candidate to test URP markers in pairs for prokaryotic and eukaryotic genomes. Although URP30F/URP2R marker combination had the highest PIC value (0.47), URP2F/URP17R and URP32F/URP13R marker pairs had the highest number of amplicons and gave medium PIC values (0.20 and 0.13, respectively) than the other URP marker pairs tested. Alleles of URP marker pairs scattered to the whole vetch genome (Fig. 2), indicated that pairwise use of URP markers could have a better power to reveal the level of polymorphism than single primer targeting sites in PCR amplifications.

The PCA analysis showed that the PC1 had the maximum variability (29.21%) followed by PC2 (12.29%) and PC3 (8.68%). Two-dimensional plot of PCA and the UPGMA analysis revealed that genetically the most distinct lines (GB3 and IC5) could be used to create an additional genetic diversity in common vetch breeding programs (Figs 1 and 3). The clades I and II successfully distinguished the vetch lines came from the same genetic resource. The clade III included both the cultivars and the lines (IC), suggesting that the cultivars used in this study were originated from IC genetic resource. The results also revealed that the lines grouped in different clades could be used to develop new and alternative common vetch varieties for various purposes. These results confirmed that the pairwise use of URP markers successfully distinguished the genetic material based on their origin. In conclusion, the results of the current study revealed that pairwise use of URP markers could have a better power to reveal the level of polymorphism in plant genome and could be tested in other eukaryotic as well as prokaryotic genomes.

Abbreviations

URPs: Universal Rice Primers; PIC: Polymorphism Information Content; UPGMA: The Unweighted Pair-Group Method; PCA: Principal Component Analysis; G: Guanine; C: Cytosine; RAPD: Random Amplified Polymorphic DNA; SPAR: Single Primer Amplification Reaction; SRAP: Sequence-Related Amplified Polymorphism; AFLP: Amplified Fragment Length Polymorphism; SSRs: Simple Sequence Repeats; EST-SSR: Expressed Sequence Tag-Simple Sequence Repeat; cDNA-SSR: cDNA-Simple Sequence Repeat; SCoT: Start Codon Targeted Polymorphism; SNPs: Single Nucleotide Polymorphisms

Acknowledgements

The financial support of this study was provided by Kahramanmaraş Sutcu Imam University (KSU, BAP Grant #: 2009/2-3).

Author Contribution Statements

I.T. conceived the idea, granted financial support, planned the experiments, performed the analysis and all the numerical calculations, interpret the data, designed the figures, M.T. carried out the experiments and drafted the manuscript.

Conflicts of Interest

The authors declare that they have no conflict of interest.

Availability of data and material

Please contact the corresponding author for any data request

References

1. Hueze, V., G. Tran, and R. Baumont, Common vetch (*Vicia sativa*). . Feedipedia., 2011. 12: p. 53–56.
2. Sullivan, P., Overview of cover crops and green manures. , in *Fundamentals of sustainable agriculture.*, P. Williams, Editor. 2013, ATTRA, National center for appropriate technology Fayetteville. p. 1–16.
3. Sherasia, P.L., M.R. Garg, and B.M. Bhanderi, Pulses and their by-products as animal feed, edited by T. Calles & H. P. S. Makkar. . 2017, Rome: FAO.
4. Firincioglu, H.K., et al., A selection strategy for low toxin vetches (*Vicia sativa* spp.). *Turkish Journal of Agriculture and Forestry.*, 2007. 31(5): p. 303-311.
5. Georgieva, N., I. Nikolova, and Y. Naydenova, Nutritive value of forage vetch cultivars (*Vicia sativa* L., *Vicia villosa* ROTH.). *Banats Journal of Biotechnology.*, 2016. 7(14): p. 5-12.
6. Huang, Y.F., et al., Potential value of the common vetch (*Vicia sativa* L.) as an animal feedstuff: a review. *Journal of Animal Physiology and Animal Nutrition.*, 2017. 101(5): p. 807-823.
7. Huang, Y.F., et al., Comparative Grain Chemical Composition, Ruminant Degradation In Vivo, and Intestinal Digestibility In Vitro of *Vicia Sativa* L. Varieties Grown on the Tibetan Plateau. *Animals.*, 2019. 9(5).
8. Lenka, S.K., et al., Genome-wide targeted prediction of ABA responsive genes in rice based on over-represented cis-motif in co-expressed genes. *Plant Molecular Biology*, 2009. 69(3): p. 261-71.
9. Zhang, Y.J., et al., DNA isolation and optimization of sequence-related amplified polymorphism-polymerase chain reaction (SRAP-PCR) condition for endangered *Polyporus umbellatus*. *Journal of Medicinal Plants Research.*, 2011. 5(31): p. 6890-6894.
10. Poczai, P., et al., Phylogenetic Analyses of Teleki Grapevine Rootstocks Using Three Chloroplast DNA Markers. *Plant Molecular Biology Reporter.*, 2013. 31(2): p. 371-386.
11. Li, M., et al., A simple method for normalization of DNA extraction to improve the quantitative detection of soil-borne plant pathogenic oomycetes by real-time PCR. *Letters in Applied Microbiology.*, 2015. 61(2): p. 179-85.
12. Tinker, N., M. Fortin, and D. Mather, Random amplified polymorphic DNA and pedigree relationships in spring barley. . *Theoretical and Applied Genetics.*, 1993. 85: p. 976-984.
13. Babic, V., et al., UPOV morphological versus molecular markers for maize inbred lines variability determination. *Chilean Journal of Agricultural Research.*, 2016. 76(4): p. 417-426.
14. Wan, Q.H., et al., Which genetic marker for which conservation genetics issue? *Electrophoresis.*, 2004. 25(14): p. 2165-76.
15. Potokina, E., et al., Population diversity of the *Vicia sativa* agg. (Fabaceae) in the flora of the former USSR deduced from RAPD and seed protein analyses. *Genetic Resources and Crop Evolution.*, 2000. 47: p. 171-183.
16. Kartal, G.K., et al., Hybridization studies in *Vicia sativa* complex. *Euphytica.*, 2020. 216(2).
17. Cil, A. and I. Tiryaki, Sequence-related amplified polymorphism and inter-simple sequence repeat marker-based genetic diversity and nuclear DNA content variation in common vetch (*Vicia sativa* L.). *Plant Genetic Resources-Characterization and Utilization.*, 2016. 14(3): p. 183-191.
18. Potokina, E., et al., AFLP diversity in the common vetch (*Vicia sativa* L.) on the world scale. . *Theoretical and Applied Genetics.*, 2002. 105: p. 58-67.

19. Raveendar, S., et al., Cross-Amplification of *Vicia sativa* subsp *sativa* Microsatellites across 22 Other *Vicia* Species. *Molecules.*, 2015. 20(1): p. 1543-1550.
20. Liu, Z.P., et al., Exploiting Illumina Sequencing for the Development of 95 Novel Polymorphic EST-SSR Markers in Common Vetch (*Vicia sativa* subsp *sativa*). *Molecules.*, 2014. 19(5): p. 5777-5789.
21. Chung, J.W., et al., Development of 65 Novel Polymorphic cDNA-SSR Markers in Common Vetch (*Vicia sativa* subsp *sativa*) Using Next Generation Sequencing. *Molecules.*, 2013. 18(7): p. 8376-8392.
22. Chung, J.W., et al., New cDNA-SSR markers in the narrow-leaved vetch (*Vicia sativa* subsp *nigra*) using 454 pyrosequencing. *Molecular Breeding.*, 2014. 33(3): p. 749-754.
23. Chai, X.T., et al., Optimizing Sample Size to Assess the Genetic Diversity in Common Vetch (*Vicia sativa* L.) Populations Using Start Codon Targeted (SCoT) Markers. *Molecules.*, 2017. 22(4).
24. Kim, T.S., et al., Transcriptome Analysis of Two *Vicia sativa* Subspecies: Mining Molecular Markers to Enhance Genomic Resources for Vetch Improvement. *Genes.*, 2015. 6(4): p. 1164-1182.
25. De la Rosa, L., E. Zambrana, and E. Ramirez-Parra, Molecular bases for drought tolerance in common vetch: designing new molecular breeding tools. *BMC Plant Biology*, 2020. 20(1): p. 71.
26. Abbasi, A.R., et al., Expression Analysis of Candidate Genes in Common Vetch (*Vicia sativa* L.) Under Drought Stress. *Journal of Agricultural Science and Technology.*, 2015. 17(5): p. 1291-1302.
27. Silva, C.C., et al., Leaf-panel- and latex-expressed sequenced tags from the rubber tree (*Hevea brasiliensis*) under cold-stressed and suboptimal growing conditions: the development of gene-targeted functional markers for stress response. *Molecular Breeding*, 2014. 34(3): p. 1035-1053.
28. Poczai, P., et al., Advances in plant gene-targeted and functional markers: a review. *Plant Methods.*, 2013. 9(1): p. 6.
29. Wang, T.Z., et al., Identification and characterization of long non-coding RNAs involved in osmotic and salt stress in *Medicago truncatula* using genome-wide high-throughput sequencing. *BMC Plant Biology.*, 2015. 15: p. 131.
30. Aggarwal, R., et al., URP based DNA fingerprinting of *Bipolaris sorokiniana* isolates causing spot blotch of wheat. *Journal of Phytopathology*, 2010. 158: p. 210-216.
31. Kang, H.W., PCR Fingerprinting of diverse genomes from bacterial strains using universal rice primer (URP). *International Journal of Bioscience and Biotechnology*, 2018. 6: p. 51-64.
32. Kang, H.W., et al., Fingerprinting of diverse genomes using PCR with universal rice primers generated from repetitive sequence of Korean weedy rice. *Molecules and Cells*, 2002. 13(2): p. 281-7.
33. Sharma, A., et al., Analysis of genetic diversity in earthworms using DNA markers. *Zoolog Sci*, 2011. 28(1): p. 25-31.
34. Dawson, I.K., et al., Detection and pattern of interspecific hybridization between *Gliricida sepium* and *G. maculata* in Meso-America revealed by PCR-based assays. *Mol Ecol*, 1996. 5(1): p. 89-98.
35. Powell, W., et al., Genepool variation in genus *Glycine* subgenus *Soja* revealed by polymorphic nuclear and chloroplast microsatellites. *Genetics*, 1996. 144(2): p. 793-803.
36. Dice, L.R., Measures of the Amount of Ecologic Association Between Species. *Ecology*, 1945. 26: p. 297-302.
37. Nei, M., Genetic distance between populations. *American Naturalist* 1972. 106: p. 283-292.
38. Devi, S.P., et al., Single primer amplification reaction (SPAR) methods reveal subsequent increase in genetic variations in micropropagated plants of *Nepenthes khasiana* Hook. f. maintained for three consecutive regenerations. *Gene.*, 2014. 538(1): p. 23-29.

39. Sharma, S.K., et al., Single primer amplification reaction (SPAR) reveals inter- and intra-specific natural genetic variation in five species of *Cymbidium* (Orchidaceae). *Gene.*, 2011. 483(1-2): p. 54-62.
40. Heath, D.D., G.K. Iwama, and R.H. Devlin, PCR primed with VNTR core sequences yields species specific patterns and hypervariable probes. *Nucleic Acids Research.*, 1993. 21(24): p. 5782-5.
41. Zhang, Y., et al., Assessment of cyto- and genotoxic effects of Cesium-133 in *Vicia faba* using single-cell gel electrophoresis and random amplified polymorphic DNA assays. *Ecotoxicology and Environmental Safety.*, 2020. 197: p. 110620.
42. Yildirim, N. and G. Agar, Determination of genotoxic effects of fipronil in *Vicia faba* using random amplified polymorphic DNA analysis. *Toxicology & Industrial Health.*, 2016. 32(8): p. 1450-1455.
43. Xiong, F., et al., Molecular profiling of genetic variability in domesticated groundnut (*Arachis hypogaea* L.) based on ISJ, URP, and DAMD markers. *Biochem Genet*, 2013. 51(11-12): p. 889-900.
44. Lee, H.H., et al., Characterization of Newly Bred *Cordyceps militaris* Strains for Higher Production of Cordycepin through HPLC and URP-PCR Analysis. *Journal of Microbiology and Biotechnology.*, 2017. 27(7): p. 1223-1232.
45. Saleh, B., Molecular Characterization using Directed Amplification of Minisatellite-region DNA (DAMD) Marker in *Ficus sycomorus* L. (Moraceae). *The Open Agriculture Journal.*, 2019. 13: p. 74-81.
46. Sharma, R., S. Sharma, and S. Kumar, Pair-wise combinations of RAPD primers for diversity analysis with reference to protein and single primer RAPD in soybean. *Annals of Agrarian Science.*, 2018. 16: p. 243-249.

Surmeli, M. and N. Demirel, Controlling with Mass Trapping and Determination of Damage Rates of *Cydia pomonella* L. (Lepidoptera: Tortricidae) at Good Agricultural Practices of Walnut Orchards. 2022, 5(3): p. 519-525. DOI: 10.38001/ijlsb.1124392

Controlling with Mass Trapping and Determination of Damage Rates of *Cydia pomonella* L. (Lepidoptera: Tortricidae) at Good Agricultural Practices of Walnut Orchards

Mustafa Sürmeli¹ , Nihat Demirel^{1*} 

ABSTRACT

The current study was carried out in 2018-2019 at good agricultural practices of walnut orchards to control mass-trapping and determination of damage rates of codling moth, *Cydia pomonella* L. (Lepidoptera: Tortricidae) in Hatay province of Turkey. The study was conducted at 312.43 decares good agricultural practices of walnut orchards containing 3,928 Chandler varieties tree, located at the Kışlak village of the Yayladağ district of Hatay province. Delta traps with codling moth pheromones were used. Traps were hung 1.5 m high; pheromone capsules were replaced with new ones in every forty days. In the first year, a total of 235 codling moth adults were caught by the 50 delta traps during the sampling period. The average population density of adults caught by traps was determined to be 4.61. In the second year, a total of 70 codling moth adults were caught by the 50 delta traps during the sampling period. The average population density of adults caught by traps was determined to be 1.4. In the first year, a total of 38,400 walnut fruits were harvested and 100 walnut fruit was harmed by the codling moth larvae. Thus, the damage rates of the codling moth were estimated as 0.26 percent. In the second year, a total of 443,100 walnut fruits were harvested and 9,065 walnut fruit was harmed by the codling moth larvae. Thus, the damage rates of the codling moth were estimated as 2.04 percent.

ARTICLE HISTORY

Received

1 June 2022

Accepted

12 August 2022

KEYWORDS

Walnut,
Cydia pomonella,
pheromone,
damage rate,
Hatay

Introduction

The walnut, *Juglans regia* L., (Juglandaceae: Fagales) is one of the most significant nut trees in the world. In 2022, the worldwide production of shells was 4.498.442 tonnes, China contributed 50% (2.521.504 tonnes); other major producers were the United States (592,390 tonnes), Iran (321,074 tonnes), Turkey (225,000), and Mexico (171,368) of the world total [1]. The walnut is one of the significant nut trees in Turkey which production consisting of approximately 86.852,8 ha with a total production of 195.000 tons of fruit per annum, and Hatay province's share is 236,1 ha and 1428 tons

¹ Hatay Mustafa Kemal University, Faculty of Agriculture, Department of Plant Protection, Antakya-Hatay, Turkey.

*Corresponding author: N.Demirel, ndemirel@mku.edu.tr; Tel:+90 533 663 66 55

[2]. The codling moth, *Cydia pomonella* L. (Lepidoptera: Tortricidae) is the most serious pest of apple, pear, peach, plum, quince and walnut [3,4,5,6,7,8,9,10,11,12,13,14,15]. Codling moth larvae directly feed on walnut fruit. The first instar larvae feed inside of the fruit. The second and third instar larvae generally feed on the green peel of the fruit. Therefore, crop loss of up to 20-50% may occur if no management strategy is applied [12,13,16]. The compound (E, E)-8,10-dodecadien-1-ol (codlemone) of the codling moth pheromone was developed by [17]. Monitoring the adult population of codling moths is conducted by pheromone traps, mating disruption dispensers, and mass-trapping [7,14,15,18,19]. Mass-trapping of *C. pomonella* has been attempted for several years with varying degrees of success [15,19,20,21,22,23,24,25,26,27,28,29]. Previous reports have shown that trapping isolated, low-density *C. pomonella* populations are more successful than attempting to mass-trap high high-density actions [29,30]. The purpose of the current study was to evaluate controlling with mass trapping and determination of damage rates of codling moth, *Cydia pomonella* L. (Lepidoptera: Tortricidae) at good agricultural practices of walnut orchards in Hatay province of Turkey.

Material and Methods

The study was carried out in 2018-2019 at good agricultural practices of walnut orchards to control with mass-trapping and determination of damage rates of codling moth, *Cydia pomonella* L. (Lepidoptera: Tortricidae) in Hatay province of Turkey. The study was conducted at 312.43 decares good agricultural practices of walnut orchards containing 3,928 number of Chandler varieties tree, located at the Kışlak village [35°94'40''K; 36°18'78''W]of the Yayladağ district of Hatay province. The walnut orchards contain seven-year-old tree. Delta traps with codling moth pheromones (E, E)-8,10-dodecadien-1-ol (codlemone) [17] were used. Traps were hanged 1.5 m high, pheromone capsules were replaced with new ones in every forty days. A totally 50 pheromone traps were used each of the sampling year. In the first year, the pheromone traps were set up on 15 May 2018 and removed on 11 September 2018. In the second year, the pheromone traps were set up on 7 May 2019 and removed on 10 September 2019. The percentage of damage rates was calculated by dividing the number of infested walnut fruits by the total number of harvested walnut fruits. All data were analyzed by analysis of variance (ANOVA) with using the SAS software (SAS Institute Inc., [31].

Results and Discussion

Mass-trapping of *C. pomonella* was studied for two years in Hatay province of Turkey. In the first year, a total of 235 codling moth adults were caught by the 50 delta traps during the sampling period. The average population density of adults caught by traps was determined to be 4.61. In the second year, a total of 70 codling moth adults were caught by the 50 delta traps during the sampling period. The average population density of adults caught by traps was determined to be 1.4. Pheromones have been applied in different ways in the control of codling moths. Capturing and killing the codling moths with pheromones has been practiced by many researchers [32,33,34,35,36,37,38,39,40,41,42,43]. The mass-trapping of the Codling moth has been attempted for several years with varying degrees of success [20,22,23,29].

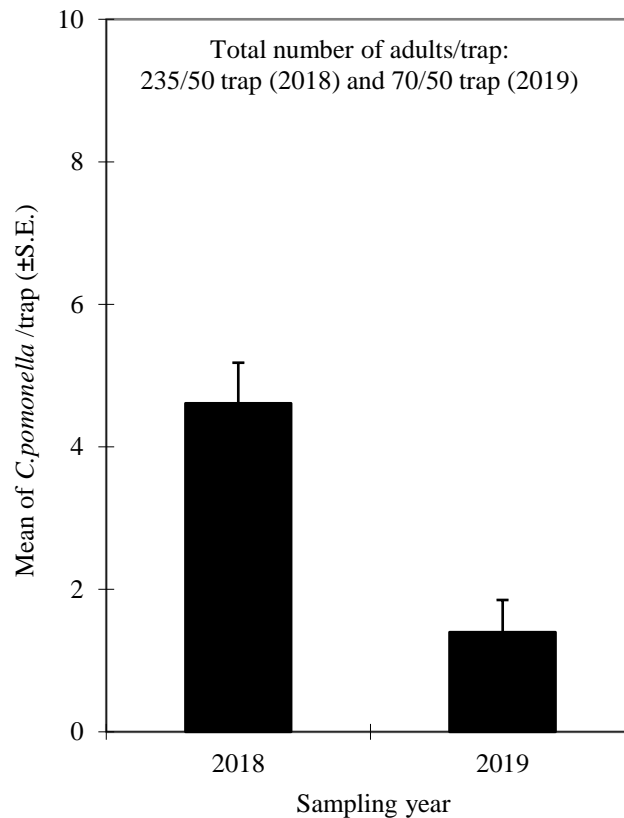


Fig 1. Population density of Codling moth on Chandler walnut orchard in 2018-2019.

The mass-trapping was used to control *C.pomonella* by many researchers [21,24,25,26,27,28,30,34,44,45]. Gilik [15] reported that the population density of codling moths on walnut was changed for the sampling times. According to the results,

the population density of codling moths was the highest in June with 35.93%, followed by July (33.12%), August (18.75%), September (6.25%), and May (5.93%) in 2016. Moreover, the population density of codling moths was the highest in May with 26.27%, followed by July (25.7%), June (20.33%), August (17.51%), and September (10.17%) in 2017.

In the first year, a total of 38,400 walnut fruits were harvested and a 100 walnut fruit was harmed by the codling moth larvae. Thus, the damage rate of the codling moth was estimated as 0.26 percent. In the second year, a total of 443,100 walnut fruits were harvested and a 9,065 walnut fruit was harmed by the codling moth larvae. Thus, the damage rates of the codling moth were estimated as 2.04 percent. Codling moth is an economically important pest on the walnut fruit (*Juglans regia* L.) in Turkey. Crop loss of 20-50% may occur, if no management strategy is applied [12-13-16]. Gilik [15] reported that the larvae of codling moths caused significant damages on walnut in Mersin. The damage rates were changed from 0,6 to 0,2 % in 2016. The damage rates were changed from 5,6 to 0,3 % in 2017.

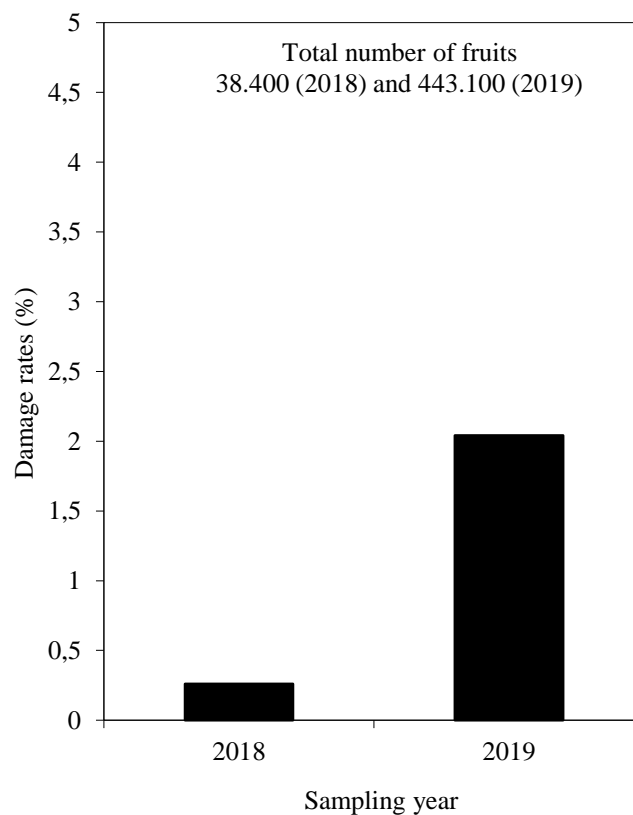


Fig 2. Damage rates of Codling moth on Chandler walnut orchard in 2018-2019

Conclusion

As a result of two years of investigation, the population density of codling moth varied each of the sampling years. In the first year, a total of 235 codling moth adults were caught by the 50 delta pheromone traps. The average population density of adults caught by traps was determined to be 4.61. In the second year, a total of 70 codling moth adults were caught by the 50 delta traps. The average population density of adults caught by traps was determined to be 1.4. In addition, the damage rates of codling larvae were changed each of the sampling years. In the first year, the damage rates of the codling moth were estimated as 0.26 percent. In the second year, the damage rates of the codling moth were estimated as 2.04 percent.

References

1. FAOSTAT, Production of walnut with shell by countries; 2019, Browse data, World. <https://www.nationmaster.com/nmx/ranking/walnuts-production>, Acces Date: [26.07.2019]
2. Anonymous, Bitkisel Üretim İstatistikleri, 2016, Ankara. Erişim tarihi: [29.12.2016]
3. Hoyt SC, et al., Basic biology and management components for insect IPM. In: Integrated Management of Insect Pests of Pome and Stone Fruits (Eds Croft BA & Hoyt SC), 1983, p. 93–151.
4. Barnes, M.M., Codling moth occurrence, host race formation and damage. In: van der Geest, L.P.S., Evenhuis, H.H. (Eds.), World Crop Pests, Vol. 5: Tortricid Pests. Their Biology, Natural Enemies and Control. Elsevier, Amsterdam, 1991, p. 313–327.
5. Quarles, W, Mating disruption success in codling moth IPM. IPM Practioner, 2000, 22 (5/6):1–12.
6. Van Frankenhuyzen, A. and H. Stigter, Schadliche undnutzliche Insekten und Milben an Kern- und Steinobst in mitteleuropa, Ulmer Verlag, Stuttgart (German), 2002, pp. 288.
7. Witzgall, P. et al., Codling moth management and chemical ecology. Annual Review of Entomology, 2008, 53:503–522.
8. Çevik T., Orta Anadolu Bölgesi ceviz ağaçlarında zararlı ve faydalı faunanın tespiti üzerinde araştırmalar. Bitki Koruma Bülteni, 1996, 36 (1-2):55-72.
9. Dindar İ. and O. Ecevit, *Cydia pomonella* (L.) (Lepidoptera: Tortricidae)' nin cevizdeki biyolojisi ve zararı üzerinde araştırmalar. Türkiye 3. Entomoloji Kongresi 24-28. Eylül 1996, Ankara, 692-699.
10. Ginzal, M.D., Walnut Insects: Ecology and Control, Encyclopedia of Pest Management, 2010, 1(1): 1-3.
11. Mamay M, and E. Yanık, Determination of population development and infestation rates of codling moth [*Cydia pomonella* (L.) (Lepidoptera: Tortricidae)] by using different sampling methods in Şanlıurfa province. Journal of Agricultural Science, 2013, 19:113–120.
12. Zeki, C. and A. Ozdem, Studies on the formation of prediction and warning system in the struggle of codling moth (*Cydia pomonella* L.) (Lepidoptera: Tortricidae) in walnut orchards. Plant Protection Bulletin, 2013, 53 (3):127-140.
13. Canihoş, E., et al., Walnut. Türkiye Bilimsel ve Teknik Araştırma Kurumu (TÜBİTAK) Tarım, Ormançılık ve Veterinerlik Araştırma Grubu Yayını, 2014, p. 69.
14. Demir, P. and O.B. Kovancı, Evaluation of the effectiveness of alternative methods in the fight

- against Apple worm (*Cydia pomonella* L.) (Lepidoptera: Tortricidae) in walnut orchards. Plant Protection Bulletin, 2015, 55 (4):277-304.
15. Gilik, A. Mersin ili Ceviz bahçelerinde elma içkurdu, *Cydia pomonella* L. (Lepidoptera: Tortricidae)'nın yayılışı, populasyon yoğunluğu ve zarar oranının belirlenmesi. Yüksek Lisans Tezi, Hatay Mustafa Kemal Üniversitesi, 2019, p. 69.
 16. Anonymous, UC IPM Pest Management Guidelines: Walnut, Codling moth, *Cydia pomonella* (Reviewed 7/17, updated 7/17). UC ANR Publication 3471, UC IPM Online Statewide, Statewide Integrated Pest Management Program, Agricultural and Natural Resources University of California. www.ipm.ucanr.edu. Acces Date: [30.07. 2017]
 17. Roelofs, W., et al., Sex Attractant of the Codling Moth: Characterization with Electroantennogram Technique. Science, 1971, 174 (4006): 297–299.
 18. Light D., et al., Kairomone-augmented mating disruption control for codling moth in Californian walnuts and apples. IOBC WPRS Bulletin, 2005, 28 (7):341-344.
 19. Sürmeli, M, Hatay ilindeki iyi tarım uygulamaları yapılan ceviz bahçelerinde elma içkurdu, *Cydia pomonella* L. (Lepidoptera: Tortricidae)'nın kitlesel tuzaklama ile kontrolü ve zarar oranının belirlenmesi. Yüksek Lisans Tezi, Hatay Mustafa Kemal Üniversitesi, 2020, p. 46.
 20. Proverbs, M.D. et al., A study to suppress codling moth (Lepidoptera: Olethreutidae) with sex pheromone traps. The Canadian Entomologist, 1975, 107: 1265–1269.
 21. Maitlen, J.C. et al., Codling moth sex pheromone: baits for mass trapping and population survey. Environmental Entomology, 1976, 5:199-202.
 22. Madsen, H. F., and B.E. Cary, Codling moth (Lepidoptera: Olethreutidae) suppression by male removal with sex pheromone traps in three British Columbia orchards. The Canadian Entomologist, 1979, 111:627–630.
 23. Willson, H. R., and K. Trammel, Sex Pheromone trapping for control of codling moth, oriental fruit moth, lesser appleworm, and three tortricid leafrollers in a New York apple orchard. Journal of Economical Entomology, 1980, 73:291–295.
 24. Ghizdavu, I., Investigations on the control of codling moth, *Laspeyresia pomonella* L., by means of the specific sex pheromone. Bulletin Protection of Plant, 1984, 3: 7-14.
 25. Pawar, A.D., and N.C. Tuhani, Codling moth (Lepidoptera: Olethreutidae) - suppression by male removal with sex pheromone traps in Ladakh, Jammu and Kashmir. Indian Journal of Entomology, 1985, 47: 226-229.
 26. Gut, L.J., et al., Mating disruption as a control for codling moth and leafrollers. Good Fruit Grower, 1992, 43:56-60.
 27. Mottus, E., et al., Performance of *Cydia pomonella*, *Argyresthia conjugella*, *Plutella xylostella*, and *Archips podana* attractant dispensers in Estonia. Proceedings of the Estonian Academy of Sciences, Biology, 1996, 45:155-170.
 28. Kilic, M., et al., Research on the application possibilities of mass trapping methods against codling moth [(*Cydia pomonella* L.) (Lepidoptera: Tortricidae)] in the Black Sea region. Bitki Koruma Bulteni, 1999, 39: 45-55.
 29. El-Sayed, A.M., et al., Potential of “lure and kill” in long-term pest management and eradication of invasive species. Journal of Economical Entomology, 2009, 102: 815–835.
 30. Hagley, E.A.C., Sex pheromones and suppression of the codling moth (Lepidoptera: Olethreutidae). The Canadian Entomologist, 1978, 110:781–783.
 31. SAS Institute, User's Guide, version 6. SAS Institute, 1998, Cary, NC, USA.
 32. Losel, P.M., et al., Factors affecting the field performance of an attracticide against the codling moth *Cydia pomonella*. Pest Management Science, 2002, 58:1029-1037.
 33. Alma, A., et al., "Attract and kill" a new IPM method in apple orchards against *Cydia pomonella* (L.). IOBC WPRS Bulletin, 2001, 24:139-143.
 34. Angeli, G., et al., Control of *Cydia pomonella* L. in walnuts (*Juglans regia* L.) with mating disruption technique. Atti delle Giornate Fitopatologiche, 2000, 20: 361-366.

35. Angeli, G., et al., Control of *Cydia pomonella* (L.) and *Cydia molesta* (Busck) by false trail following and attract & kill techniques. *Informatore Fitopatologico*, 2003, 53:45-50.
36. Trematerra, P., et al., Control of codling moth, *Cydia pomonella*, with an attracticide (attract and kill) method. *Informatore Fitopatologico*, 1999, 49:41-44.
37. Ebbinghaus, D., et al., Appeal: efficacy and mode of action of attract and kill for codling moth control. *IOBC WPRS Bulletin*, 2001, 24:95-99.
38. Puciennik, Z., et al., "Attract and kill" as control method of codling moth *Cydia pomonella* (L.) in home gardens and allotments. *Journa of Fruit Ornamental Plant Research*, 2002, 10:173-176.
39. Charmillot, P.J., et al., Control of codling moth *Cydia pomonella* L. by an attract and kill technique. *Revue suisse de viticulture, arboriculture, horticulture*, 1998, 29:111-117.
40. Charmillot, P.J., et al., Attract and kill: a new method for control of the codling moth *Cydia pomonella*. *Entomologia Experimentalis et Applicata*, 2000, 94: 211-216.
41. Knight, A.L., Testing an attracticide hollow fibre formulation for control of codling moth, *Cydia pomonella* (Lepidoptera: Tortricidae). *Journal of the Entomological Society of British Columbia*, 2003, 100: 71-78.
42. Knight, A.L., et al., Modeling the impact of a sex pheromone/kairomone attracticide for management of codling moth (*Cydia pomonella*). *Acta Horticulturae*, 2002, 584: 215-220.
43. Krupke, C.H., et al., Field and laboratory responses of male codling moth (Lepidoptera: Tortricidae) to a pheromone-based attract-and-kill strategy. *Environmental Entomology*, 2002, 31:189-197.
44. Shorey, H.H., and R.G., Gerber, Use of puffers for disruption of sex pheromone communication of codling moths (Lepidoptera: Tortricidae) in walnut orchards. *Environmental Entomology*, 1996, 25: 1398-1400.
45. Grant, J.A., et al., BIOS approach tested for controlling walnut pests in San Joaquin valley. *California Agriculture*, 2003, 57:86-92.

Parmaksız, A., A. Demir, and D. Ulusal, mtDNA COI and Cyt b Analysis of *Carassius auratus* (Linnaeus, 1758) Species Living in Atatürk Dam Lake (Turkey). *International Journal of Life Sciences and Biotechnology*, 2022. 5(3): p. 526-532. DOI: 10.38001/ijlsb.1129879

mtDNA COI and Cyt b Analysis of *Carassius auratus* (Linnaeus, 1758) Species Living in Atatürk Dam Lake (Turkey)

Arif Parmaksız^{1*} , Aynur Demir¹ , Dilara Ulusal¹ 

ABSTRACT

Today, biological invasion is one of the leading threats to biodiversity and is an issue that is gaining more and more importance. In recent years, molecular techniques have been widely used in the identification and monitoring of invasive species in many parts of the world. This study aimed to detect the infested species, *Carassius auratus*, in Atatürk Dam Lake and to reveal the population status. For these purposes, 10 *Carassius auratus* specimens were randomly selected from Atatürk Dam Lake. After DNA isolation of the selected samples, mtDNA COI and cyt b gene regions were sequenced and analyzed. In this study, sequence analyzes of individuals belonging to the *C. auratus* species living in Atatürk Dam Lake were performed for the first time using mtDNA COI and cyt b markers. Analyzed sequence results were compared with databases and it was concluded that the results obtained for both mtDNA markers were compatible. No other variation was observed. When the results are evaluated as a whole, it is possible to say that this species has spread recently. In future studies, it is recommended to determine the invasive species populations that are intensely found in Atatürk Dam Lake and other lakes and to determine the necessary strategies to combat these invasive species.

ARTICLE HISTORY

Received

13 June 2022

Accepted

10 August 2022

KEYWORDS

Invasive species,
Carassius auratus,
mtDNA,
Atatürk Dam Lake

Introduction

Carassius auratus (Linnaeus, 1758) is a fish species whose homeland is China and is widely found in Japan, and it has been taken to almost all parts of the world [1,2]. *C. auratus* is a species belonging to the Cyprinidae family and varies greatly in size, body shape, fin configuration and color. They have formed a natural population in many countries around the world due to conscious vaccinations made to water resources and individuals escaping from breeding systems [2]. This species was first domesticated in China and has become one of the important and common farmed fish [3]. It was introduced in Europe and Japan in the 17th century and in the Americas in about 1850, then quickly spread all over the World [4].

¹ Harran University, Faculty of Science-Literature, Department of Biology, Şanlıurfa / Turkey

*Corresponding Author: Arif Parmaksız, e-mail: aprmksz@gmail.com

The *C. auratus* species can produce thousands of eggs and can cohabit and be reared in small areas. Periods of domestication have generated significant artificial and natural selection [5]. There are hundreds of varieties according to body shape, fins, eyes, and color of scales [3]. These different features make *C. auratus* a valid model for genetic, evolutionary, and biological research [6].

The presence of *C. auratus*, an invasive fish, has been reported in Turkish inland waters in different regions [7]. It is estimated that this species spread as a result of accidentally or deliberately releasing it into Turkish waters or escaping from fish production farms [8]. The Southeastern Anatolia Project has increased its agricultural production capacity and has become a great aquaculture potential thanks to the Atatürk Dam Lake [9,10]. Invasive fish species have settled in the lake water due to fisheries or other factors. The invasion of freshwater ecosystems by foreign fish can have important consequences for natural biodiversity, including local extinctions of endemic and native species [11, 12, 13].

In recent years, pond fish (*Carassius* sp.) have become an important threat in inland waters, including endemic species found in our country [14]. This threat significantly affects the habitats of natural species and causes the rapid decline of local species and the termination of fishing activities in the basins [15]. Natural fish species living in Atatürk Dam Lake; due to factors such as overfishing, the dominance of invasive species, and habitat loss, it is exposed to increasing pressures day by day, the number of individuals in economic species populations is decreasing, along with species losses [16]. Depending on their biological and ecological characteristics, invasive species negatively affect the population density of native fish species in the environments they enter [17]. Invasive fish species are a threat to both fisheries and biodiversity [18]. For this reason, it is important both scientifically and economically to determine the species of invasive fish in the environment and to put forward a control program. For this program, a certain genetic data must first be obtained. Sequences of COI and cyt b gene regions among mitochondrial genes are used for kinship relationships among fish.

The aim of this study; For *C. auratus*, by performing sequence analyses with mtDNA COI and cyt b markers, (i) species identification, (ii) upload the obtained sequences to the gene bank, and (iii) make predictions about where it came to Atatürk Dam Lake by comparing it with the data in the gene bank.

Material and Methods

In this study, 10 randomly selected *C. auratus* samples, which were sold at the stalls of local fishermen fishing in the Bozova region of Atatürk Dam Lake in December 2021, were used as material. The samples were brought to Zoology Laboratory of Harran University, Faculty of Science- Literature, Department of Biology by applying a cold chain. After the species were identified, muscle tissue was taken from the samples, placed in microcentrifuge tubes containing 90% ethanol, and stored at -20°C until DNA was obtained.

DNA isolation and PCR

Total DNA isolation was performed from muscle tissue using the GeneJET Genomic DNA Purification Kit (Thermo Scientific) according to the protocol instructions. To check the presence of DNA after the protocol, DNA samples from all individuals were loaded into the wells of 0.8% agarose gel added to SYBR Green, carried out in electrophoresis, and visualized in a (UV) light device (Smart View Pro Imager System, Major Science).

In this study, PCR was performed in Thermal Cycler (BIO-RAD T100TM). The primer sequence used for amplification of the mtDNA COI gene region was reported by Darabi et al. (2014) (COI-625F: 5' TCA ACC AAC CAC AAA GAC ATT GGC AC-3'; COI-625R: 5' GAC TTC TGG GTG GCC AAA GAA TCA-3') [19]. PCR conditions and chemicals were applied according to the study of Parmaksız and Eskici (2018) and the product was obtained [20]. The primer sequence used for the mtDNA cyt b gene region was taken from Briolay et al., (1998) (L15267 F: 5' GTT TGA TCC CGT TTC GTG TA-3'; H15891 R: 5'AAT GAC TTG AAG AAC CAC CGT-3'), PCR conditions and chemicals were applied according to the study of Parmaksız and Şeker (2018) and the product was obtained [21, 22].

Data analysis

The obtained PCR products were sent to the commercial firm and sequence analysis was performed with the 3500 XL Genetic Analyzer device. Then, raw data of mtDNA COI and cyt b sequences were evaluated using the FinchTV 1.4 program. Furthermore, sequences of all individuals were aligned using BioEdit software version 7.2.5. The sequences of mtDNA COI and cyt b gene region of the target species in the gene bank were included in the study and similarity rates were determined.

Results and Discussion

In this study, sequence analyzes of the mtDNA COI and cyt b gene regions of individuals belonging to the *C. auratus* species, which live invasively in Atatürk Dam Lake and whose number of individuals have increased recently, were performed for the first time and compared with the data in the gene bank. An average of 600 bp (Figure 1) and 570 bp long sequences were obtained for the mtDNA COI and cyt b gene regions, respectively. Similarities were revealed by BLASTing these sequence results (Table 1).

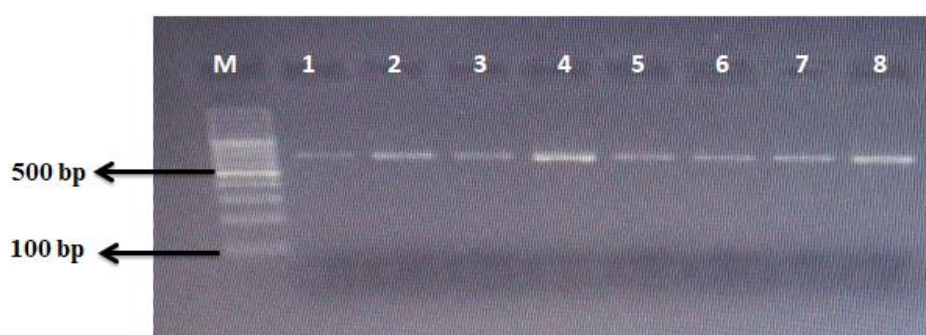


Fig 1. Image of mtDNA COI PCR Products (M: Marker; bp: Base Pair)

Table 1 Comparison of the sequences obtained in this study with the sequences in the NCBI database

Marker	Country	Access Number	Similarity Rate (%)	Source
COI	Bangladesh	MN171366.1	100	Unpublished
	Chinese	MF443771	100	Unpublished
	Chinese	KJ874430	100	Unpublished
	India	MN562051	100	Unpublished
	Japan	AB379921	100	Komiyama et al., 2009 [23]
	Australia	KF227945	100	Loh ve ark., 2014 [24]
	Korean	HQ536310	100	Unpublished
	United States	KF558297	100	Brandl et al., 2015 [25]
cyt b	America	MG281934	100	Halas et al., 2018 [26]
	Germany	KX688782	100	Knytl et al., 2013 [27]
	England	JN412524	100	Rylková et al., 2013 [28]
	Japan	AB379921	100	Komiyama et al., 2009 [23]
	Chinese	MT612437	100	Unpublished

In Table 1, the sequences of both mtDNA markers obtained from the *C. auratus* species caught from Atatürk Dam Lake are shown with 100% similarity to the sequences in the

Genbank. Accordingly, it is possible to say that this fish species is the same in terms of both markers in different continents and countries, does not show a different variation, and has recently spread. In other words, no different variation or mutation was detected between the fish in our study and the fish belonging to the same species in different countries shown in Table 1. It shows 100% similarity in terms of both markers. Thus, it raises the idea that all of these fish originated from the same ancestral fish. However, since the gene exchange is interrupted due to the difference in the environment, there is a high probability that different mutations and variations will occur in the future.

Biological invasions have caused significant disruption to natural ecosystems around the world through habitat change, competition and hybridization with native species. Especially species of the *Carassius* genus such as *C. auratus*, *C. carassius*, and *C. gibelio* have been transported to many inland water bodies throughout Turkey and are seen as a threat factor for native species [7]. The effects of these fish species, which form a continuous population, on local species and especially endemic species in the habitats should be investigated and awareness should be increased to prevent the human-induced spread of exotic species [8, 29]. In addition, in fisheries studies, only target species should be included in the study. Because it is seen that six aquarium fish species are spread in Turkish waters [8]. If species other than these aquarium fish enter the reservoir, it will be inevitable that natural species will be seriously affected. It will cause greater damage both economically and in terms of biodiversity.

In the study of Tarkan et al., (2012), the density of the *Carassius gibelio* species living in Ömerli Dam Lake in the Marmara Region, which was followed for six years, and the density of native and economic species were studied [30]. On the contrary, it was found to increase. It is estimated that similar results occurred for both *C. gibelio* and *C. auratus* in Atatürk Dam Lake. Therefore, a serious control program should be organized against invasive species. In particular, it should be ensured that the populations that are concentrated in the dam lake are detected and removed from the environment as much as possible before they enter the breeding period.

Conclusion

Since the reproductive capacity of invasive fish species is very high, the number of individuals is increasing rapidly. Therefore, in future studies, populations of *C. auratus* species should be determined along the Atatürk Dam Lake and Euphrates river, genetic

diversity levels of populations should be determined by using marker systems such as mtDNA D-loop and microsatellite, and the struggle should be started quickly to start with the population with the highest diversity recommended.

Funding

This study was funded by Harran University Research Fund (Project No: 22124).

References

1. Dogac, E., et al., Mitochondrial genetic variations of an introduced freshwater fish, goldfish *Carassius auratus* at the frontier between Europe and Asia (western Anatolia, Turkey): proximity to Europe rather than East Asia? Mitochondrial DNA Part A: DNA Mapping, Sequencing, and Analysis, 2016. 27(6):4008-4014.
2. Aktop, Y., Japon balığının (*Carassius auratus* L. 1758) büyümesi ve Gonad gelişimi üzerine çakşır otunun (*Ferula elaeochytris* K. 1947) etkisinin araştırılması. Akdeniz Üniversitesi, Fen Bilimleri Enstitüsü, 2017.
3. Alesci, A., et al., Mast cells in goldfish (*Carassius auratus*) gut: Immunohistochemical characterization. Acta Zoologica. 2022; 00:1–14.
4. Chen, Z., et al., De novo assembly of the goldfish (*Carassius auratus*) genome and the evolution of genes after whole-genome duplication. Science Advances, 2019. 5(6):1-12.
5. Luo, J., et al., From asymmetrical to balanced genomic diversification during rediploidization: Subgenomic evolution in allotetraploid fish. Science Advances, 2020. 6(22):1-11.
6. Wu, DS., Current situation and prospect of the standardization research and application of Laboratory red crucian carp. Laboratory Animal Science, 2016. 33(03):56–60.
7. Innal, D., Distribution and impacts of *Carassius* species (Cyprinidae) in Turkey: a review. Management of Biological Invasions, 2011. (2):57-68.
8. Bostanci, D., et al., Ordu ili iç sularında *Carassius auratus* (Linnaeus, 1758) türünün ilk kaydı ve türün Ulugöl Yaylası Göleti popülasyonu ile ilgili bazı veriler. Aquatic Research, 2021. 4(3):279-285.
9. Oymak, S. A., Atatürk Baraj Gölü' nde yaşayan *Chondrostoma regium* (Heckel, 1843) un büyüme özellikleri. Turkish Journal of Zoology, 2000. 24(supp):41-50.
10. Oymak, S. A., A Study on the Age, Growth and Reproduction of *Aspius vorax* (Heckel, 1843) (Cyprinidae) in Atatürk Dam Lake (Euphrates River), Turkey. Turkish Journal of Fisheries and Aquatic Sciences, 2011. 11:217-225.
11. Gozlan, R. E., et al., Current knowledge on non-native freshwater fish introductions. Journal of fish biology, 2010. 76(4):751-786.
12. Mollot, G., Pantel, J. H., and Romanuk, T. N., Chapter Two - The Effects of Invasive Species on the Decline in Species Richness: A Global Meta-Analysis. Advances in Ecological Research, 2017. 56:61-83.
13. Jackson, M. C., et al., Chapter Two - Novel and Disrupted Trophic Links Following Invasion in Freshwater Ecosystems. Advances in Ecological Research, 2017. 57:55-97.
14. Ugurlu, S., and Polat, N., Samsun İli Tatlı Su Kaynaklarında Yaşayan Egzotik Balık Türleri. Journal of FisheriesSciences.com, 2007. 1(3):139-151.
15. Leung, B., et al., An ounce of prevention or a pound of cure: bioeconomic risk analysis of invasive species. Proceedings of the Royal Society of London. Series B: Biological Sciences, 2002. 269:2407-2413.

16. Parmaksiz, A., et al., Phylogenetic analysis of *Luciobarbus* Heckel, 1843 and *Barbus* Cuvier & Cloquet, 1816 species in the Euphrates River (Turkey) based on mtDNA COI gene sequences. *Aquatic Research*, 2022. 5(2):129-135.
17. Tarkan, A. S., et al., Are introduced gibel carp *Carassius gibelio* in Turkey more invasive in artificial than in natural waters? *Fisheries Management and Ecology*, 2012. 19:178–187.
18. Erdem, Y., Samur, M., and Özdemir, S., İçsularda İstilacı Balık Türleriyle Mücadelede Seçici Avlama Yöntemlerinin Etkinliği. *Journal of Fisheries & Aquatic Sciences*, 2014. 29(2): 49-63.
19. Darabi, A. R., et al., Investigation of Phylogenetic Relationship Among Two *Barbus* Species (Cyprinidae) Populations with Mitochondrial Dna Using Pcr-Sequencing. *International Journal of Biology, Pharmacy and Allied Sciences*, 2015. 4(2):302-311.
20. Parmaksiz, A., and Eskici, H. K., Genetic Variation of Yellow Barbell (*Carasobarbus Luteus* (Heckel, 1843)) From Four Populations Using Mitochondrial Dna Coi Gene Sequences. *Applied Ecology and Environmental Research*, 2018. 16(2):1673-1682.
21. Briolay, J., et al., Molecular phylogeny of Cyprinidae inferred from cytochrome b DNA sequences. *Molecular Phylogenetics and Evolution*, 1998. 9(1):100-108.
22. Parmaksiz, A., and Seker, Ö., Genetic Diversity of the Endemic Species Shabbout (*Arabibarbus grypus* (Heckel, 1843)) Based on Partial Cytochrome B Sequences of Mitochondrial DNA. *Aquatic Research*, 1(3):103-109.
23. Komiyama, T., et al., An evolutionary origin and selection process of goldfish. *Gene*, 430(1-2):5-11.
24. Loh, W. K. W., et al., DNA barcoding of freshwater fishes and the development of a quantitative qPCR assay for the species-specific detection and quantification of fish larvae from plankton samples. *Journal of Fish Biology*, 2014. 85(2):307-328.
25. Brandl, S., et al., Ten real-time PCR assays for detection of fish predation at the community level in the San Francisco Estuary-Delta. *Molecular Ecology Resources*, 2015. 15(2):278-284.
26. Halas, D., Lovejoy, N., and Mandrak, N. E., Undetected diversity of goldfish (*Carassius* spp.) in North America. *Aquatic Invasions*, 2018. 13(2):211–219.
27. Knytl, M., et al., Chromosome studies of European cyprinid fishes: cross-species painting reveals natural allotetraploid origin of a *Carassius* female with 206 chromosomes. *Cytogenetic and Genome Research*, 2013. 139(4):276-83.
28. Rylková, K., et al., Phylogeny and biogeographic history of the cyprinid fish genus *Carassius* (Teleostei: Cyprinidae) with focus on natural and anthropogenic arrivals in Europe. *Aquaculture*, 2013. 380-383: 13-20.
29. Türkmen, G., First record of the Guppy (*Poecilia reticulata* Peters, 1859) in inlandwaters of Turkey. *Ege Journal of Fisheries and Aquatic Sciences*, 2019. 36(4):397-400.
30. Tarkan, A. S., et al., Circumstantial evidence of gibel carp, *Carassius gibelio*, reproductive competition exerted on native fish species in a mesotrophic reservoir. *Fisheries Management and Ecology*, 2012. 19:167-177.

Ozdemir Bahadır, A., Developing selection strategy for CHO-K1 cell line that secretes scfv-Fc fusion antibodies using ClonePix2. International Journal of Life Sciences and Biotechnology, 2022. 5(3): p. 533-545. DOI: 10.38001/ijlsb.1112823

Developing selection strategy for CHO-K1 cell line that secretes scfv-Fc fusion antibodies using ClonePix2

Aylin Özdemir Bahadır^{1*} 

ABSTRACT

In the pharmaceutical industry, biopharmaceuticals (biologics) are gaining market share. There has been a dramatic increase in the sale and market penetration of monoclonal antibodies in particular. Typically, therapeutic antibodies are produced using high-expression, clonal, or recombinant CHO cell lines. CHO cells dominate the market as a commercial production host due to their ease of use, built-in regulatory records, and security profiles. While traditional limiting-dilution and cloning-ring regulations are frequently used to select mammalian cell lines that produce high levels of proteins, they have a number of drawbacks. ClonePix2 is a fully automated, single cell-based clone selector that significantly increases the likelihood of rapidly selecting high-production clones with high monoclonality. Scfv-Fc recombinant antibody structures with a variety of therapeutic advantages have gained prominence in recent years. Single cell cloning of CHO cells expressing the scfv-Fc fusion protein, which differs from the classical immunoglobulin structure, was performed *in situ* using the ClonePix2 device using FITC-tagged anti-Fc and anti-H+L antibodies. The fluorescent intensity parameters of the resulting cell clones were analyzed. Additionally, ELISA was used to determine the production capacities of the best clones. As a result, it was established that anti-Fc antibody recognizes the scfv-Fc fusion protein in a semi-solid environment, enabling the identification of higher production clones.

ARTICLE HISTORY

Received

6 May 2022

Accepted

8 October 2022

KEYWORDS

Biopharmaceuticals,
cell-line,
high-producer,
scfv-Fc antibody,
ClonePix2

Introduction

A critical step in the production of commercial therapeutic antibodies (Ab) is the selection of clones that produce high levels of protein. Various methods are used to select a stable cell line that produces recombinant proteins. Although laborious and time consuming, the limiting-dilution and cloning-ring methods are still widely used due to their simplicity and low cost. These methods, however, do not allow for the separation of high, low, and non-productive clones prior to cell culture growth [1,2]. Recently, an alternative cell-cloning method that contains fluorescent-labeled antibodies against the interest protein secreted by cells, coated with a semi-solid medium, and then presented to an automated

¹ TÜBİTAK, Marmara Research Center, Medical Biotechnology Department of Life Sciences, Kocaeli/Turkey

*Corresponding Author: Aylin Özdemir Bahadır, e-mail: aylin.ozdemir@tubitak.gov.tr

colony selector such as ClonePix2 has been developed to increase the likelihood of obtaining high protein-producing clones [3,4,5]. This robotic selection system can identify all productive colonies derived from single cells based on parameters such as colony size, roundness, and proximity to neighbors, as ascertained by bright-field and fluorescent images of relative protein expression [3,6] . The semi-solid environment keeps dividing cells in place during single-cell cloning, allowing control of the parameters mentioned above and increasing the likelihood of collecting high-producer clones. The most significant advantage of automatic clone collection is the capture of rare clones that perform high expression [2].

Single-chain variable fragment (scfv) is a class of engineered antibodies generated by the fusion of the heavy (VH) and light chains (VL) of immunoglobulins through a short polypeptide linker (10-25 amino acid). The benefits of scfv stem from their small size. Because they are smaller, they can be cleaned from the blood more quickly in treatment approaches, penetrate the tissues more effectively, and have low immunogenicity [7]. The scfv-Fc fusion protein is made up of a scfv linked to the CH2 and CH3 regions of the immunoglobulins (IgG) fixed region, which can then form a homodimer with another copy. Fragment crystallizable (Fc) parts of immunoglobulins are composed of the heavy chain fixed zone (Fc region) and mediate cellular effector functions. Fc contains common protein sequences for all IgG as well as class-specific determinants. These regions are known as fixed regions because they do not differ significantly between IgG molecules of the same class [3]. The fusion of scfv and Fc provides several advantages, including two valuable bindings to scfv structures, a longer half-life, and Fc-mediated effector functions. In addition, the scfv-Fc format can be used in the clinic for therapeutic purposes [4,5].

Many studies on the choice of single cell-based cloning of IgG in a semi-solid environment have been conducted using the ClonePix2 system. In these cases, the selection can be made by marking with antibodies conjugated with fluorescence provided by the vendor. Clone-Detect reagents, which each contain an antibody specific to different parts of immunoglobulins (Fc, H+L chain, etc.) or the antibody's subtype (such as Kappa), are among the antibodies offered by the vendor [6,7]. The Scfv-Fc fusion protein, however, differs from the classical IgG structure and has not been studied until now to identify these structures using Clone-Detect reagents unique to the Clonepix2 system.

Two antibodies supplied by the vendor were compared in this study to identify highly productive clones from the same stable cell pool.

Material and Methods

Cells, cell culture and transfection

CHO-K1 cells are transfected with using plasmid DNA containing single copies of the fusion of scfv and Fc genes. The CMV promoter directed the expression of the scfv-Fc fusion protein. The plasmid pTK-Hyg (Clontech, USA, 631750) was also used in transfection to create a stable cell line, which is a selection vector that confers hygromycin resistance in mammalian cells and is used for the selection of stably transformed cells. All cell counts were either performed using the trypan blue exclusion method via the Luna II™ cell counter (Logos biosystems, South Korea) or estimated based on well confluency using the Clone Select Imager (CSI, Molecular Devices, USA).

3×10^4 CHO-K1 cells (ATCC, CCL-61, USA) were seeded into each well of a 6-well plate one day before transfection. The cells were grown in Dulbecco's modified eagle and F12 medium (DMEM-F12) (Thermo Fisher, Gibco, USA), 1% Penicillin-Streptomycin, and 10% fetal bovine serum (FBS) (Cytiva HyClone, South America Origin) in a 37°C, 5% CO₂ environment with high humidity. On the day of transfection, the culture medium was replaced with Opti-MEM Reduced-Serum Medium (Thermo Fisher, 31985062, USA). The Lipofectamine LTX (Thermo Fisher, A12621, USA) protocol was used to create transfection complexes with 3 µg scfv-Fc fusion and 0.3 µg pTK-Hyg plasmids. The mixture was then incubated for 5 minutes at room temperature (15-20 °C). Drop by drop, the transfection complex was added to CHO-K1 cells. Cells were then incubated for 48 hours at 37°C, 5% CO₂, and high humidity. The medium was then replaced with 2 ml of DMEM-F12 medium containing 10% FBS and 350 µg/ml Hygromycine (Thermo Fisher, 10687010, USA). Antibiotic selection was carried out for 10 days, and surviving cells were directly used for subsequent clonal isolation [8,9].

Clonal isolation

Methylcellulose-based semi-solid medium used in conceived with the ClonePix2 (Molecular Devices, USA) device, was used for the isolation of the resulting clones. CloneMatrix concentrate (2,5X) (Molecular Devices, K8600, USA) is diluted to 1X with DMEM-F12 medium containing 10% FBS and supported by anti-Fc CloneDetect™ (anti-Human IgG (Fc) Specific, Fluorescein antibody, 10000U/ml) (Molecular Devices,

K8205, USA) or anti-H+L CloneDetect™ (anti-Mouse IgG (H+L) Specific, Fluorescein antibody, 10000U) (Molecular Devices, K8220, USA). Following the 10-day selection period, the transfected, stable pools are plated at 200 cells/mL in 6-well tissue culture plates (Corning, 657185, USA) containing 2 ml 1X semi-solid media at each well. Before coating, the media and CHO cells are thoroughly mixed to ensure that all components are evenly distributed. After plating, plates were observed with CSI (Molecular Devices, USA) to verify single cells were well distributed. The plates were incubated at 37 °C with 5% CO₂ for 12 days [6].

ClonePix 2 isolation of single high-producing clones

Prior to each cloning procedure, the ClonePix2 device was sanitized and calibrated according to the manufacturer's instructions to ensure that the selected colonies were isolated accurately and without contamination. After 12 days, individual 6-well plates were analyzed using ClonePix2™ software (Molecular Devices, USA). Each plate was divided into 36 sections; each section was imaged for 1 ms under white light and then fluorescence measured for 2000 ms with the LED intensity set to 81. A “local threshold” algorithm was used to detect each colony. Colonies were chosen based on their exterior mean fluorescence intensity (EMFI), their size, their compactness, and their proximity to neighboring colonies. Colonies that met the picking criteria were seeded into individual wells of a 96-well plate containing 150 µL of DMEM-F12 containing 10% FBS medium. Cell growth was monitored using the CSI device. Confluent wells appeared after 6–10 days, and cells were expanded to 6-well plates for titer testing [7,8].

Scfv-Fc expression control by Protein L/Fc capture ELISA

Scfv-Fc expression was monitored using the enzyme linked immunosorbent assay (ELISA). "Recombinant Protein L Type-1 Protein" (Novus Biologicals, USA) was coated onto an immunoplate (Corning, 3690, USA) overnight at a concentration of 250 ng/50 µl in 0.1 M NaHCO₃. Skim milk was used to block all plates, and PBS-T was used to wash them (0.1 % Tween 20 in Phosphate Buffered Saline). In designated wells, 50 µl of sample (undiluted supernatants) from each clone (top 25 colonies of anti-human IgG (Fc) specific (Fc-1 to Fc25) and anti-human (H+L) specific (HL1- to HL-25) with cell densities of 3 x 10⁶ cells/ml were added in duplicate. For 90 minutes, the plates were incubated at 37°C. Wells were washed three times with PBS-T before adding 50 µl of secondary antibody: anti-Human IgG conjugated to alkaline phosphatase enzyme (Sigma,

A9544, Germany) to each well. The secondary antibody used is specific to the Fc of human mAbs and was diluted to a 1:50.000 ratio prior to use. The mixtures were incubated for another 60 minutes at 37°C. Washing was used to remove unbound secondary antibodies, and 50 µl of 4-Nitrophenyl phosphate disodium salt hexahydrate substrate solution (Sigma, N2765, Germany) was added. For 30 minutes, the mixture was incubated at room temperature in the absence of light. Finally, the enzyme-substrate reaction was stopped by adding 50 µl of 3 N NaOH, and absorbance at 405 nanometers was measured with microplate reader (Bio-Tech EIA Reader, USA) [10].

Results and Discussion

The VH and VL heavy- and light-chain variable domain constructs (scfv) used in this study were obtained from a mouse phage display library. The Fc region, where it is fused, contains the human IgG's second and third constant domains (CH2 and CH3), as well as a hinge region (H) that allows the formation of two disulfide bonds. After this structure is established, the two fusion proteins form a homodimeric structure with sulfide bonds, similar to IgGs. The resulting homodimeric fusion protein contains two scfv structures that can be recognized by the "anti-Mouse IgG (H+L) Specific" antibody (anti-H+L) and an Fc structure that can be recognized by the "anti-Human IgG (Fc) Specific" antibody (anti-Fc) (Figure 1). In this study, it was determined which of these antibodies recognizes the scfv-Fc fusion protein better in a semi-solid environment.

To ensure the stability of the construct, CHO-K1 cells are transfected with two plasmids, one containing the scfv-Fc construct containing plasmid and the other containing the Hygromycin phosphotransferase gene. Following transfection, the cells were grown for 10 days in a selection medium containing Hygromycine, ensuring the death of unstable cells. A stable cell pool expressing untagged scfv-Fc fusion protein (Figure 1) is obtained in this manner. When the viability of cells reached % 65 in the post-transfection selection process, the selection was stopped and the cells were placed in a 6-well plate containing anti-Fc or anti-H+L CloneDetect™. After that, the plates were incubated to form distinct colonies. Four 6 well plates were studied for each antibody. After the fifth day, colony formations began to be controlled by the CSI device.

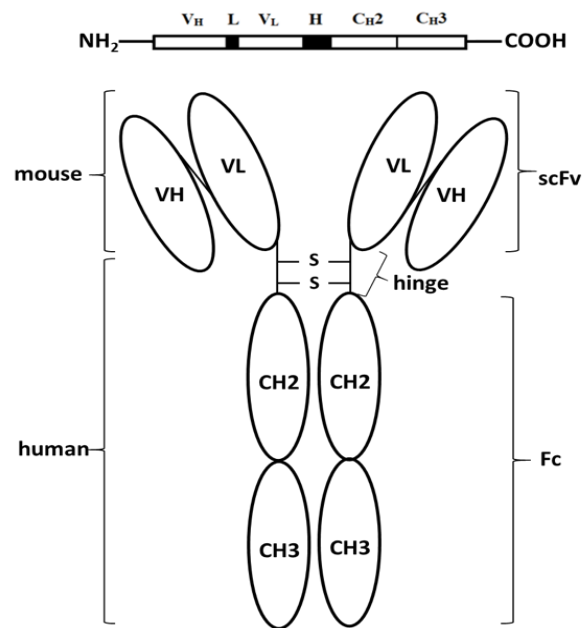


Fig 1 The scfv-Fc fusion protein is schematically displayed. VH and VL variable domains of mouse scfv; H hinge area of human IgG containing two disulfide bridges; and CH2 and CH3 second and third constant domains of human IgG, respectively

The colonies that formed on the 12th day were isolated clonally. Plates labeled with both antibodies were analyzed with CSI prior to isolation to ensure that the estimated cell numbers were in the same ranges. It has also been demonstrated that colonies in both groups are generally distributed evenly to plate wells, and that colony numbers are equally dense (**Figure 2**). Thus, it has been demonstrated that different CloneDetect™ antibodies added to the environment have no effect on cell growth.

Because of the semi-solid environment, the secreted recombinant proteins remain around the colonies where they are secreted. Cells coated with semi-solid media with a high viscosity that reduces secretion diffusion and incubated to form discrete colonies were shown under white light and fluorescence, respectively. Precipitation occurs around the relevant colonies in colonies that produce fusion protein due to the interaction of Scfv-Fc antibodies secreted from colonies and the capture antibody conjugated to FITC. As a result, the higher the fluorescent density, the greater the amount of antibodies secreted [11].

Following imaging with Clonepix2, each colony is classified primarily based on criteria such as size, proximity, irregularity, and fluorescent intensity. Table 1 summarizes the colony groups that resulted from this classification.

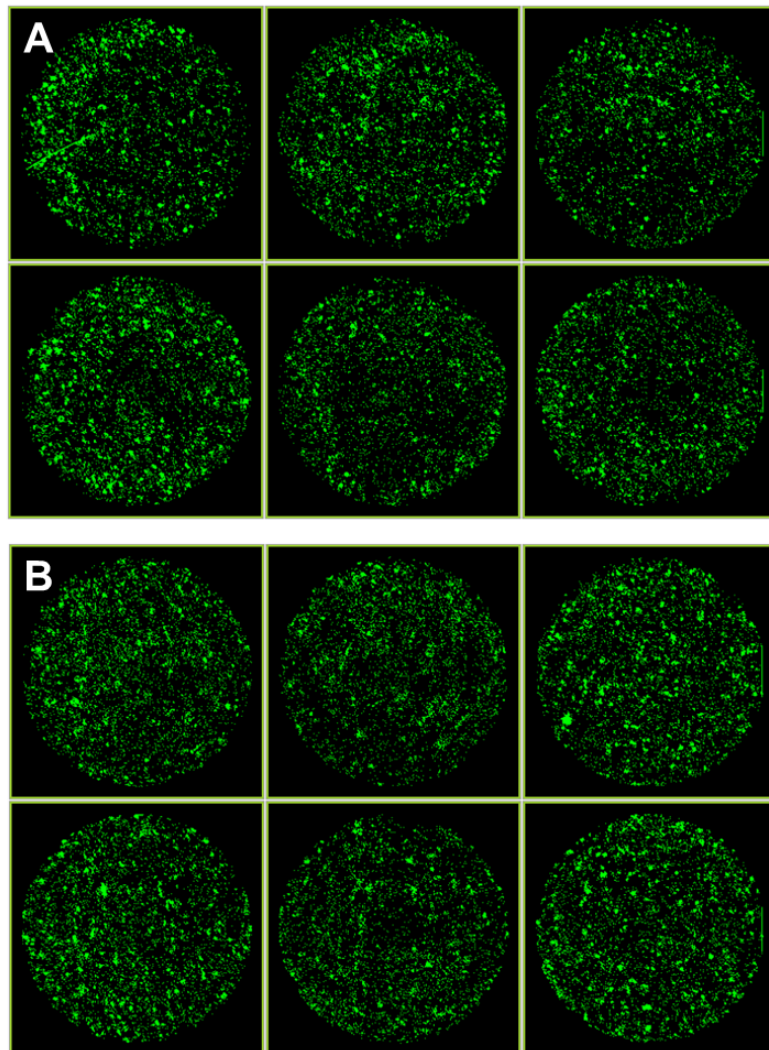


Fig 2 Images from the Clone Select Imager (CSI) grown in a 6-well plate with detection antibodies Anti-Human IgG (Fc) Specific (**A**) or Anti-Mouse IgG (H+L) Specific (**B**)

When compared to colonies grown in both antibodies, it has been determined that most colonies do not reach sufficient size, despite the passage of sufficient time. Colonies that are very close to each other and have irregular shapes have also been identified. Individual clones that are excluded from all of these clones and have the highest EMFI values are aspirated with the ClonePix2 system's micro-pins. Each of the 48 colonies identified by the anti-Fc and the 43 colonies identified by the anti-H+L antibody was transferred to a 96-well plate well. The fact that approximately 4000 clones were screened and approximately 50 colonies (~1%) exceeded the threshold indicates that the high number

of producers is extremely low. This clearly demonstrates the reasoning behind scanning a large number of clones with a highly efficient selection method.

Table 1 Colony group distribution of "Human IgG (Fc) Specific, Fluorescein antibody" and "Mouse IgG (H+L) Specific, Fluorescein antibody"

Conditions	anti-Human IgG (Fc)	anti-Mouse IgG (H+L)
Too small (excluded colonies too small)	3436	3966
Proximity (excluded colonies too close to each other)	187	186
Irregular colonies (roundness & axis ratio)	436	469
Screened and picked clones (best expressed)	48	43
Grown colonies after picked	31	33

The "Exterior Mean Fluorescence Intensity" (EMFI) values used in the selection of colonies expressing a high amount of protein are divided by the number of pixels in the exterior area (arithmetic mean). This statistic approximates how bright the area immediately surrounding a given colony is. Colonies' "Interior Mean Fluorescence Intensity" (IMFI) values can also be used to identify colonies that produce a high quantity of proteins. IMFI is calculated by dividing Interior Total Intensity by colony area (in pixels). It is the arithmetic mean of the 'average' brightness of all pixels in the colony [7,12]. When the EMFI values of the top 25 colonies from both selection groups were compared, it was discovered that the proteins expressed by the colonies identified by the anti-Fc antibody had a higher intensity (Figure 3A). Similarly, the IMFI values of the top 25 colonies were compared, and it was discovered that the scfv-Fc structure, which is also defined by the anti-Fc antibody, had a higher intensity (Figure 3B). The values after the 25th colony in both colony groups were low (for EMFI and IMFI<15) and were not included in the comparison results.

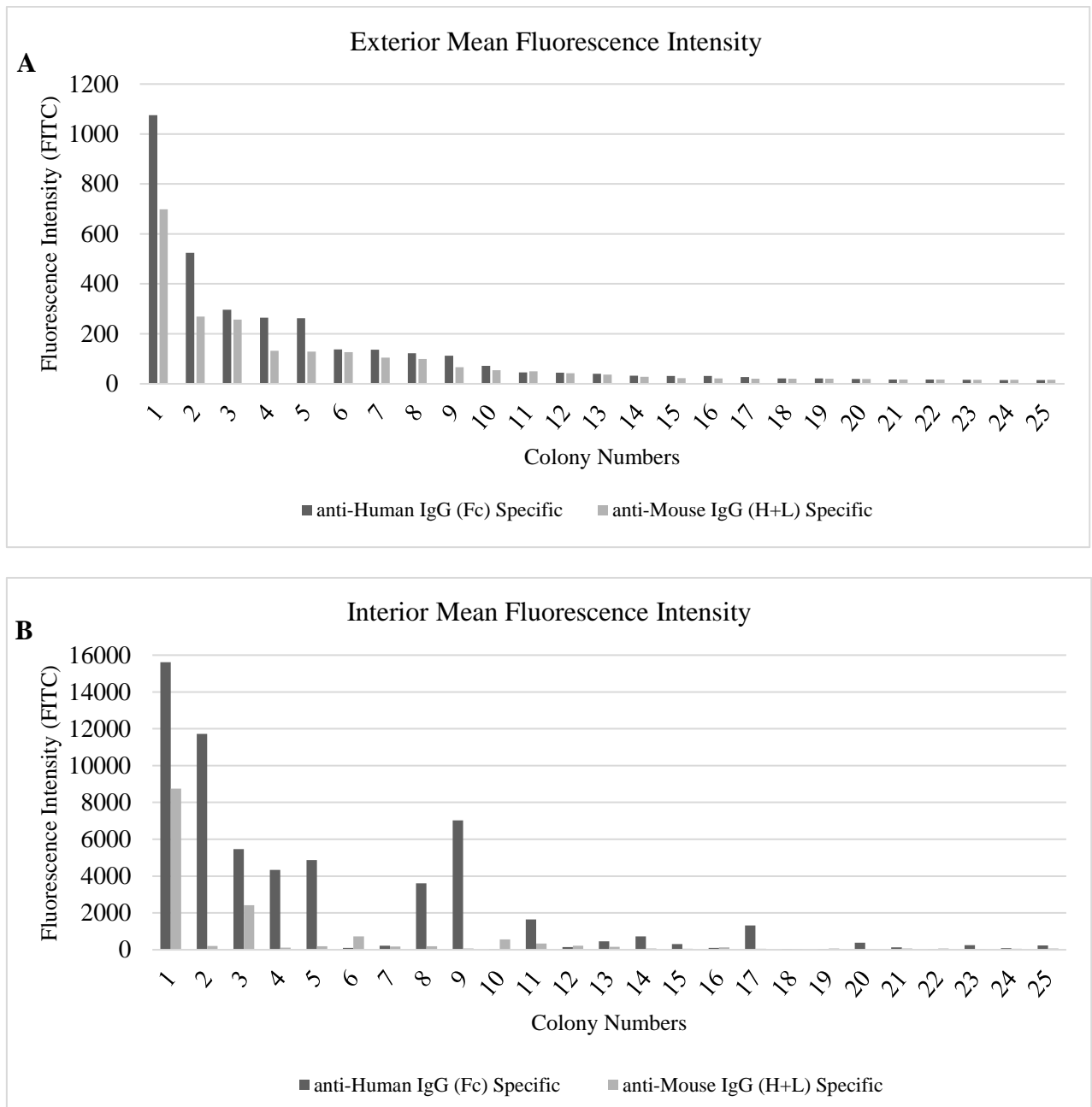


Fig 3 Comparison graphs of the top 25 colonies identified by the anti-Human IgG (Fc) Specific and the anti-Mouse IgG (H+L) Specific antibody's EMFI (A) and IMFI (B) values

Colonies were grown in 96 well plates for 7 days while being monitored for growth with a CSI device. However, when high-producer clones are detected and collected, they may change their production profiles or cease to grow when returned to their original environment. After being removed from the semi-solid environment, 31 of the 48 colonies identified by the Anti-Fc antibody and 33 of the 41 colonies identified by the Anti-H+L antibody were able to continue their development in liquid medium.

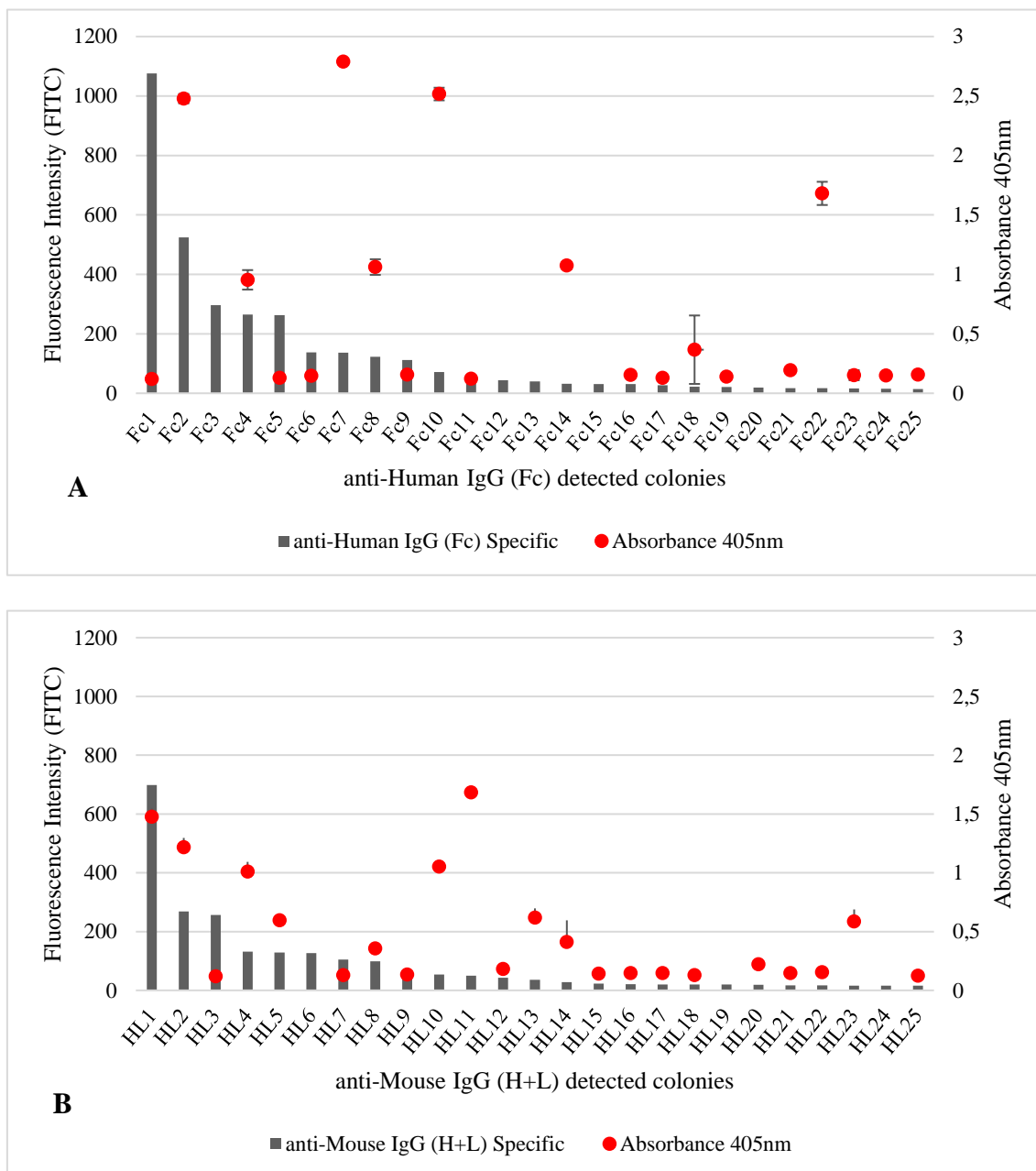


Fig 4 EMFI (column) and antibody productivity (red dot) (OD_{405}) graphs of top 25 colonies selected with anti-Human IgG (Fc) Specific antibody (**A**) and anti-Mouse IgG (H+L) Specific antibody (**B**)

The relationship between fluorescence intensity and scfv-Fc productivity was also investigated in the top 25 clones using the ELISA method to measure antibody levels in cell supernatants at a concentration of 3×10^6 cells/ml. At equivalent cell densities, clones with higher exterior fluorescence intensities should have a higher concentration of

antibodies secreted [11]. This correlation was found in some colonies in this study. When protein expressions were evaluated using the EMFI value of the top 25 colonies in both groups, it was discovered that clones detected with the anti-H+L antibody had an absorbance value of 0.5 or less, with the exception of one clone less than 10 fluorescence intensity (Figure 4A). Except for one, all of the clones with less than 50 fluorescence intensity identified by the anti-Fc antibody had a value of 0.5 or less (Figure 4B). Seven of the remaining clones have an absorbance value greater than 0.9; the Fc2 clone has an absorbance of 2.47, the Fc7 clone has an absorbance of 2.78, and the Fc10 clone has an absorbance of 2.51, making them the highest producer clones obtained from all scans performed within the scope of this study. Despite the fact that the scfv structure in the scfv-Fc structure is compact and dimeric, it has a lower identifiability capacity. This could be due to scfv's conformation. Scfv molecules are held together by a flexible linker, which allows them to oscillate between open and closed states [13,14]. This study can also be done with scfv structures with different linker lengths to see if the scfv conformation differs in identifying with anti-H+L antibodies.

As a result, this study demonstrated that targeting Fc is more appropriate in identifying the best producing clone from colonies that secrete scfv-Fc in the semi-solid medium. This could be because the Fc structure is more stable.

Conclusion

It is critical to have an antibody that can detect scfv-Fc well secreted from colonies in a semi-solid environment. The ClonePix2 system was used to select the CHO-K1 cell line, which expresses a high level of the scfv-Fc protein. Two antibodies supplied by the vendor were used concurrently to identify highly productive clones from same stable cell pool. It was discovered that the antibody "anti-Human IgG (Fc) Specific" detects homodimeric scfv-Fc fusion antibody better and allows for the selection of higher-producing clones.

Abbreviations

CHO: Chinese Hamster Ovarian, scfv: Single-chain variable fragment, Fc: Fragment crystallizable, Ab: antibody, VH: heavy chain, VL: light chains, CH2: second constant domain, CH3: third constant domain, a.a: amino acid, IgG: immunoglobulin, H+L chain: heavy and light chain, anti-Fc: anti-Human IgG (Fc) Specific, Fluorescein antibody, FITC: Fluorescein, anti-H+L: anti-Mouse IgG (H+L) Specific, Fluorescein antibody, DNA: Deoxyribo nucleic acid, CMV: Cytomegalovirus, CSI: Clone Select Imager, FBS: fetal bovine serum, MEM: Modified Eagle Medium, DMEM-F12: Dulbecco's Modified Eagle Medium/Nutrient Mixture F-12, EMFI: exterior mean fluorescence intensity, IMFI: interior mean fluorescence intensity, ELISA: enzyme linked immunosorbent assay, PBS: Phosphate Buffered Saline, LED: light-emitting diode

Acknowledgements

I would like to express my gratitude to Esin Bayralı, Gökhan Güler and Evrim Tekel for their excellent technical assistance, as well as to Koray B. Balcioglu, H. Ümit Öztürk, Hivda Ülbeği Polat, Müge Serhatlı, Hilal Yazıcı Malkoçoğlu and Melis Denizci Öncü for their comments on this article.

Funding

This work has been supported by the TÜBİTAK, Marmara Research Center, Medical Biotechnology Department of Life Sciences.

Availability of data and material

Please contact the corresponding author for any data request.



References

1. Wurm, F. M., Production of recombinant protein therapeutics in cultivated mammalian cells. *Nature Biotechnology*, 2004. 22(11): p. 1393–1398.
2. Dharshanan, S. and C. S. Hung, Screening and subcloning of high producer transfectomas using semisolid media and automated colony picker. *Methods Mol. Biology*, 2014. 1131: p. 105–112.
3. Nakamura, T. and T. Omasa, Optimization of cell line development in the GS-CHO expression system using a high-throughput, single cell-based clone selection system. *Journal of Bioscience and Bioengineering*, 2015. 120(3): p. 323–329.
4. Tsuruta L.R., et al., Genetic analyses of Per.C6 cell clones producing a therapeutic monoclonal antibody regarding productivity and long-term stability. *Applied Genetics and Molecular Biotechnology*, 2016. 100: p. 10031–11041.
5. Tejwani, V., et al., High-throughput and automation advances for accelerating single-cell cloning, monoclonality and early phase clone screening steps in mammalian cell line development for biologics production. *Biotechnology Progress*, 2021. 37(6): p. 3208.
6. O'Rourke, S. M., et al., Robotic selection for the rapid development of stable CHO cell lines for HIV vaccine production. *PLoS One*, 2018. 13 (8): p.1–22.
7. Ahmad, Z. A., et al., ScFv antibody: Principles and clinical application. *Journal of Immunology Research*, 2012. 2012: p. 1-15.
8. Yu, J., Y. Song, and W. Tian, How to select IgG subclasses in developing anti-tumor therapeutic antibodies. *Journal of Hematology and Oncology*, 2020. 13(45): p.1-10.
9. Diebold, P., et al., Preclinical Evaluation of an Engineered Single-Chain Fragment Variable-Fragment Crystallizable Targeting Human CD44. *Journal of Nuclear Medicine*, 2021. 62: p. 137–143.
10. Wang, M., et al., The preparation and therapeutic roles of scFv-Fc antibody against *Staphylococcus aureus* infection to control bovine mastitis. *Biotechnological Products and Process Engineering*, 2019. 103(1703): p.1703-1712.
11. Hou, J. J. C., et al., High-throughput ClonePix FL analysis of mAb-expressing clones using the UCOE expression system. *New Biotechnology*, 2014.31(3): p. 214–220.
12. Dharshanan, S., et al., Rapid automated selection of mammalian cell line secreting high level of humanized monoclonal antibody using Clone Pix FL system and the correlation between exterior median intensity and antibody productivity. *Electronic Journal of Biotechnology I*, 2011. 14(2): p. 1-10.
13. Roy, G., et al., Sequential screening by ClonePix FL and intracellular staining facilitate isolation of high producer cell lines for monoclonal antibody manufacturing. *Journal of Immunological Methods*, 2017. 451: p. 100-110.
14. Erdag, B., et al., Identification of novel neutralizing single-chain antibodies against vascular endothelial growth factor receptor 2. *Biotechnology Applied Biochemistry*, 2011. 58(6): p. 412–22.
15. Caron, A. W., et al., Fluorescent labeling in semi-solid medium for selection of mammalian cells secreting high-levels of recombinant proteins. *BMC Biotechnology*, 2009. 9: p. 1-11.

16. Lavoie, R. A., et al., Multiplexed competitive screening of one-bead-one-component combinatorial libraries using a ClonePix 2 colony sorter. *International Journal of Molecular Sciences*, 2019. 20(20): p. 1-9.
17. Arndt, K. M., K. M. Müller, and A. Plückthun, Factors influencing the dimer to monomer transition of an antibody single-chain Fv fragment. *Biochemistry*, 1998. 37(37): p. 12918–12926.
18. Schmiedl, A., et al., Effects of unpaired cysteines on yield, solubility and activity of different recombinant antibody constructs expressed in *E. Coli*. *J. Immunological Methods*, 2000. 242 (1–2): p. 101-114.

Aksoy, B. T. and O. Ates Sonmezoglu, Comparison of Modified DNA Isolation Methods for the Detection of GMO in Processed Foods. *International Journal of Life Sciences and Biotechnology*, 2022. 5(3): p. 546-561. DOI: 10.38001/ijlsb.1166275

Comparison of Modified DNA Isolation Methods for the Detection of GMO in Processed Foods

Begum Terzi Aksoy^{1*} , Ozlem Ates Sonmezoglu¹ 

ABSTRACT

The highly degraded DNA content in processed food samples results in limited efficiency in detecting GMOs. Generally, conventional DNA isolation techniques from transgenic plant seeds or raw materials were available in the literature, whereas studies on DNA isolation techniques from processed food samples were more limited. Also, many processed food products contain genomic DNA from numerous complex plants or animal sources. In the present study, we proposed some beneficial modifications for high-quality DNA isolation of processed foods such as biscuits, cakes, crackers, corn chips, and flours. For this purpose, isolation protocols were investigated to obtain high molecular weight and quality DNA from food samples, the first step of GMO analysis in processed foods. To control the gene region of the target organism from the obtained DNA samples, PCR detection was performed with soybean and maize-specific primers. According to the statistical analysis, the A260/A280 ratios were the lowest in cake (1.58) and highest in biscuit (1.83). The highest values of the total DNA presence belong to soy flour samples (211.80 ug/ul), and the lowest amount belongs to corn flour, cake, and corn chips samples. Among the four isolation methods tested, the modified Wizard-CTAB method showed better results in most of the tested food products. Results showed that the modified Wizard-CTAB could be used in different food products for studies on corn and soybean specific genes and GMO detection.

ARTICLE HISTORY

Received

24 August 2022

Accepted

18 October 2022

KEYWORDS

DNA isolation, genetically modified food (GMO), lectin, nucleic acid extraction, PCR detection

Introduction

According to the definition of the World Health Organization (WHO), genetically modified organisms (GMO) is defined as the unnatural modification of DNA. According to ISAAA (2021), Genetically modified (GM) seeds were sown in an area of 190.4 Mha in 29 countries in 2019. Soybean, corn, canola, and cotton are the main commercially grown genetically crops. GM soybeans are the most cultivated crop globally, accounting for 48.2% and 91.9 Mha of the global GM crop area. Corn has the most production area following soybeans. It accounts for 32% and 60.9 Mha of the international GMO crop area [1].

¹ Karamanoglu Mehmetbey University, Faculty of Engineering, Department of Bioengineering, Karaman/Turkey

*Corresponding Author: Begüm Terzi Aksoy, e-mail: begumterzi19@gmail.com

In general, labeling GM products is mandatory or optional, up to a threshold GMO content level that varies between countries, although there is much debate [2]. The EU was one of the first regions to monitor and regulate the use of GMOs. Regulations on the use and law of GMOs in food, (EC) 1829/2003 and 1831/2003, have been in force since 2004. EU rules require that all ingredients in foodstuffs, including source materials, are well documented, and necessary precautions are taken for GMO traceability. Although according to the manufacturer food samples do not contain GMOs, GMO traces may be present in the products incidentally or unavoidably during transportation, storage, seed harvesting, planting, and processing of the food product. For this reason, according to EU law, the mandatory labeling requirement has been established at 0.9% per ingredient [3]. This labeling requirement applies to permitted GMOs. GMOs not authorized by the EU cannot be included in food samples. In Turkey, only accepted soybean and corn varieties are allowed to be used as animal feed within the framework of biosecurity law, but not for food consumption [4].

Food products have different polymerase chain reaction (PCR) inhibitors, such as polyphenols, proteins, and polysaccharides. Accurate detection of GMO presence depends on the specificity and sensitivity of the PCR, DNA isolation method, and the amount and quality of the obtained genomic DNA [5]. Proper sampling methods, inhibitors, biological factors, sample size, and matrix type in GMO detection affect the efficiency of DNA extracted from food, feed, and grain/seed samples. In the processed food industry, the addition of certain flavors and chemical components also changes the DNA quality and creates an inhibitor for amplification. Corn and soy content find wide use as food preservatives and additives. [6-7]. For this reason, it is important to use standardized test methods applied in feed and food products. The use of these food components in the food industry and the fact that processed products have many contents simultaneously make detection difficult due to the process [8]. If the amount and purity of DNA obtained from the DNA extraction according to the GMO detection procedures are unsuitable, a plant DNA-specific detection method should be performed. If DNA cannot be detected, it should be appropriately reported in the relevant reports that the product does not contain DNA at a level that can be amplified in PCR [9].

Sönmezoğlu and Keskin [10] compared DNA extraction methods specific to processed foods in food products consisting of different varieties. Using six DNA isolation

methods and two commercial DNA extraction kits, Sönmezoğlu and Keskin [10] stated that the DNA yield varied according to the type of food and processing. Arun et al. evaluated the effect of different cooking temperatures on GMO detection in products by preparing cookies containing various amounts of GM soy and cooking them at different temperatures and at different times [11]. As a result, the heating process affected the sensitivity of the PCR screen of GM organisms and increased the detection limit. Three DNA extraction methods were compared to detect GMOs in 35 food products sold in the Equator. As a result of their PCR studies, they stated that DNA extraction with the DNeasy mericon food kit provided higher amplification efficiency and emphasized that other DNA extraction methods may be needed for PCR studies used in various food products [12].

Saadedin et al. [13] detected CaMV-35 promoter and T-nos terminator sequences that control gene expression in genetically engineered tomatoes using qualitative PCR. In the study, 78 tomato genotypes were collected from Iraqi institutions and markets, and DNA isolations were completed by the CTAB DNA isolation method [13]. Matthes et al. [14] focused on the efficiency of DNA extraction methods from corn gluten of protein-rich corn-containing feed samples. Ashrafi Dehkordi et al. [15] in their study for DNA extraction from soybean samples, compared phenol/chloroform methods, CTAB and modified CTAB method. Their results showed that the modified CTAB method is more promising than the other two DNA extraction methods [15].

In this study, standard DNA isolation methods previously mentioned in the literature for food products were used, and these methods were modified for use in some processed food samples. In addition, a new modified isolation protocol (modified Wizard-CTAB) in which Wizard and CTAB methods are used as a hybrid has been tried. In the modified protocol, soybean and corn gene content in packaged food products belonging to different brands was determined to verify the DNA quality and determine the qualitative PCR amplification efficiency in GMO detection. It aims to obtain preliminary information on the isolation efficiency of the methods applied in general isolation protocols on processed foods and provide preliminary data for molecular studies on this subject.

Packaged food products containing soy or corn, such as biscuits, crackers, cakes, corn chips, corn and soy flour were used for DNA extraction. The products were obtained

from local markets between 2019-2020. The products used in DNA extraction consist of 20 different products with different brands and different processing levels (Table 1).

Material and Methods

Food materials

GM maize and GM soybean seed residues used as positive controls were obtained by request from Tubitak-MAM Biotechnology Institute. Wheat (Gediz-75) DNA was used as a negative control in PCR. Food samples were ground into flour by grinding in a mortar, and the experiments were carried out in three repetitions for each food product.

Table 1 Sample samples used in GMO analysis

Sample No	Food Product	Sample No	Food Product
1	Biscuit (brand 1)	12	Cracker (brand 2)
2	Biscuit (brand 2)	13	Cracker (brand 3)
3	Biscuit (brand 3)	14	Corn chips (brand 1)
4	Biscuit (brand 4)	15	Corn chips (brand 2)
5	Biscuit (brand 5)	16	Corn flour (brand 1)
6	Biscuit (brand 6)	17	Corn flour (brand 2)
7	Cake (brand 1)	18	Soy flour (brand 1)
8	Cake (brand 2)	19	Soy flour (brand 2)
9	Cake (brand 3)	20	GM Soy
10	Cake (brand 4)	21	GM Corn
11	Cracker (brand 1)	22	Negative control

Reagents

Preparation of 200 ml TNE Buffer: After adding 150 mM NaCl, 0.315 g Tris-HCL, 2 mM EDTA, 1% SDS, the total volume was made up to 200 ml with ddH₂O (pH: 8) and then the prepared buffer was autoclaved an than. After autoclaved the 1% β-mercaptoethanol (BME) was added to this solution. Chloroform-isoamyl alcohol (24:1 v/v), NaCl (1.2 M), cold 100% isopropyl alcohol, 70% ethanol, agarose (molecular grade) were used in DNA isolations. CTAB precipitation solution was prepared with NaCl (40 mM) and CTAB (0.5%) and the pH was adjusted by to 8.0. For the CTAB Lysis buffer, Tris/HCl (100 mM), Na₂EDTA (20 mM), NaCl (1.4 M), CTAB (2% w/v) was used, then the pH was adjusted to 8.0.

DNA extraction methods

Method-1; Modified Wizard method [16, 10] method-2; CTAB isolation method [14], method-3; modified Wizard-CTAB and the method-4; modified classical CTAB method [17] are used for this study.

Food samples were prepared as homogenized samples, 50-100 mg each, in equal proportions. The reason why this amount is relatively low is to ensure homogeneous distribution in buffer solutions. For example, samples such as corn chips over-absorb the buffer solution and limit the amount of supernatant after centrifugation. To overcome this situation, the amount of buffer solution can be increased if needed.

For the repeatability of the extraction, the DNA isolation methods were applied in three repetitions. Distilled water was put in place one sample in each set during the experiment against possible contamination risks caused by the environment.

The Modified wizard method (method-1) [16, 10], CTAB isolation method (method-2) [14], and modified classical CTAB method (method 4) [17] used in DNA extraction of the food products examined in the study were applied based on the procedures specified in the source articles. Modified Wizard-CTAB method is explained in this study.

DNA isolation method-3 (modified Wizard-CTAB)

50-100 mg sample was weighed and mixed with 1000 μ l TNE buffer and 30 μ l Proteinase K (20 mg/ml). This mixture was kept in a 65 °C water bath for three hours and stirred every 15 minutes. Samples were incubated at 65 °C for an additional one hour by adding 5 μ l (10 mg/ml) of RNase to the mixture. After centrifuging at 15 000 rpm for 15 minutes, the supernatant was taken into a new sterile Eppendorf tube. The same volume of Chloroform/isoamyl alcohol (24: 1) was added to it. After 10 minutes of centrifugation at 13 000 rpm, the supernatant was taken into new tubes. 2/3 isopropanol was added. Further sedimentation at 13 000 rpm for 20 minutes, the pellet was dissolved in 400 μ l TE buffer and incubated overnight at 4°C. The next day, sample tubes were dissolved in a 60 °C water bath, and Chloroform/isoamyl alcohol (24:1) was added again to the tubes. After 15 minutes of centrifugation at 13 000 rpm, the supernatant was taken into new tubes. Nine μ l of 3M sodium acetate (pH 5.2) and 30 μ l of absolute ethanol solution were added to the supernatants taken for the precipitation step and mixed. The mixture is incubated on ice for 15 min to precipitate the DNA. Afterward, it is centrifuged at 13 000 rpm for 10 minutes. The supernatant was taken

into a new tube. Three μl of sodium acetate and 500 μl of pure ethanol solution were added and incubated on ice for 15 minutes again. The samples were precipitated by centrifugation at 13 000 rpm for 10 minutes, and the pellet was washed with 70% alcohol. Samples were re-centrifuged, dried thoroughly free from alcohol, and dissolved in 100 μl ddH₂O and used.

Purity and concentration of DNA

Gel electrophoresis method and spectrophotometric techniques were used for the amount and purity determination of the isolated DNA. For this purpose, the samples were measured with NanoDrop (Denovix, DS-11 Spectrophotometer) at 260-280 nm wavelengths, and quantitative determinations were made [18]. Genomic DNAs obtained were run in 1% agarose gels with 1 X TBE buffer. Gels were stained with ethidium bromide (20 mg/ml) for visualization. After running, the gels were visualized using a UV transilluminator (BioRad, ChemiDocTMMP Imaging System).

Molecular screening of soy and corn gene

PCR processes were carried out using the Bio-RAD C1000 Touch Thermal Cycler. All primers used in the study were synthesized by Iontek company according to the base sequence in the reference articles. LEC1 / LEC2 primer pairs (164 bp) [19] were used to screening the presence of the lectin gene in the determination of soy content, and the ZEIN03 / ZEIN04 (277 bp)[20] primer pairs were used for corn.

Mixture solution prepared for PCR amplification for soy and corn determination of food samples; 10x Taq Buffer (Thermo Fisher Scientific), 25 mM MgCl₂ (Thermo Fisher Scientific), 3.2 μl of dNTP mix solution (Sigma Aldrich), 1 μl of 10 mM forward and reverse primer (Iontek Company), 0.5 U of Taq DNA polymerase (Thermo Fisher Scientific), 100 ng of DNA template. The mixing volume of the reaction was 40 μl . PCR cycles for the Lec1/Lec2 primers are as follows; Initial denaturation at 95 °C for 12 min followed by 95 °C for 60 s, 72 °C for 30 s and 72 °C for 30 s; in the last step, it is completed by extension at 72 °C for 10 minutes. PCR cycle for primer pair Zein03/Zein04, incubation at 95 °C for 10 minutes, followed by 60 seconds at 96 °C, 60 seconds at 60 °C, and 60 seconds at 72 °C, final extension of 72 °C was applied at for 10 minutes. The number of cycles for both primer pairs is planned as 40 cycles.

GMO screening

For the amplification of the 35S promoter region, primers P35s-cf3/cr4 [21-22] were used. The band sizes expected to be seen in a positive control due to PCR using these primers are expected to be 123 base pairs for the 35SP primer.

The PCR were based on the conditions specified in the source articles. The total reaction volume for the PCR mix was set to 25 μ L and included 10x Taq Buffer, 0.24 μ M of each reverse and forward primers, 160 μ M of each dNTP, 1.5 mM MgCl₂, 0.5 U of Taq DNA polymerase, 100 ng of template DNA and ddH₂O.

Statistical analysis

Two-way analysis of variance (ANOVA) was used to evaluate the spectrophotometric data. Measurements were taken in duplicate, using SPSS 15.0 software according to random block design, and the Duncan test was used to compare the mean data.

Results and Discussion

High-density DNA fragments were visualized using gels with 1% agarose concentrations from samples obtained from various food products. Different DNA isolation protocols were applied for DNA isolation from the food products examined. It was determined that the high-density distinct band profiles for the Wizard method (a) and the modified Wizard-CTAB method (c) (this study) belonged to the soy flour samples (Fig. 1). The classical CTAB DNA isolation method is primarily suitable for DNA extraction from green plants or seeds. For this reason, its effectiveness on processed food samples is relatively low compared to other isolation methods on agarose gel images. According to the agarose gel images, the classical CTAB isolation method (Fig 1d) yielded clean band profiles for the GM corn sample (lane 21). However, according to the other three DNA isolation methods, the GM corn sample (lane 21) did not show a clean and dense band profile only the GM soy sample. This result may be because the GM corn sample was obtained with unprocessed cornmeal. The quantity and quality of DNA isolated from food, seed/cereal, or feed samples are affected by sample size, optimal sampling method, biological factors, inhibitors, and matrix type [23, 24, 8].

There are drifts towards the gel's lower molecular weight portions for the biscuit, cake, and cracker samples (Fig 1). In addition, the presence of a higher molecular weight and thick band in the gel means that genomic DNA is intact and minimally contaminated

[25]. For the corn chips sample (lane 14), a band profile was not obtained in all the DNA extraction methods. Corn chips sample (lane 15) showed a slight band presence only for the Wizard isolation method. It is reported that baking affect negatively the DNA isolation yield and PCR test results [8, 11, 26, 27].

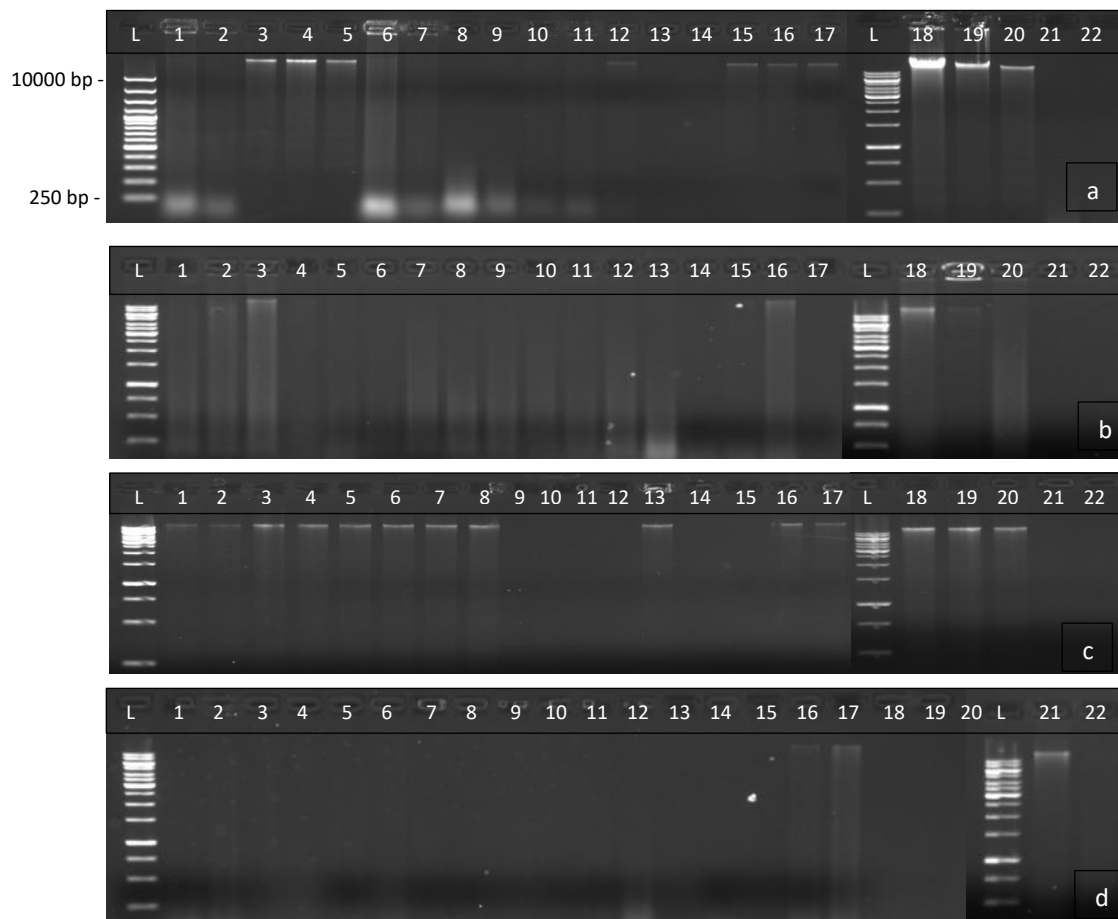


Fig 1 Agarose gel images of different DNA isolation protocols a) DNA Isolation Method-1, b) DNA Isolation Method-2, c) DNA Isolation Method-3 and d) DNA Isolation Method-4, respectively. Lane L, The GeneRuler™ 1 kb DNA Ladder (Thermo scientific). Lane 1-6 biscuit, 7-10 cake, 11-13 cracker, 14-15 corn chips, 16-17 corn flour, 18-19 soy flour, 20 GM soy, 21 GM corn, and the 22 is negative control (dH₂O)

The DNA concentrations, 260/280 ratios obtained due to the DNA isolation methods examined in this study vary according to product type (Table 2). The 260/280 ratio provides information on the purity and quality of the DNA. According to this ratio, values of 1.7 or greater can be considered acceptable [28]. The 1.8 ratio is a DNA grade with high purity in the absence of protein and phenolic compounds. As this ratio rises above 2, RNA contamination can be mentioned [29]. The range of calculated DNA

yields was between 8.27 ug/ul (Method-2, Cake) and 593.58 ug/ml (Method-1, Soy flour). According to the statistical analysis, the A260/A280 ratios were the lowest in cake (1.58) and highest in biscuit (1.83). The highest values of the total DNA presence belong to soy flour samples (211.80 ug/ul), and the lowest amount belongs to corn flour, cake, and corn chips samples (Tablo 2). In addition to ingredients such as chocolate and sauces, it is difficult to obtain quality and intact whole genomic DNA from samples containing starch and lecithin [30]. For this reason, it is supported that besides the negative effect of the product processing level, the differences arising from the product composition may cause different results in terms of sample type. Turkec et al., [31] also pointed out that although the DNA yield among the products they examined differed according to the isolation method examined, generally lower purity values were obtained in products with medium and high processed corn content [32]. Subsequently, as expected, the lowest DNA yield was in the samples of cake (52.55 ug/ul) and corn chips (58.16 ug/ul), which are food samples with high processed levels. This result confirms a decrease in the amount of DNA depending on the processing levels in foods.

A purity ratio of > 1.9 indicates RNA, while a ratio of < 1.7 in the extracted DNA sample indicates the presence of proteins in these samples [33]. According to all modified isolation methods examined in this study, the average 260/280 ratio of cake (1.58) and corn chips (1.68) in food samples was less than 1.7. The average ratio of 260/280 for other food samples examined were among 1.7 and 2.0, and these results indicate insignificant contamination levels by protein and polysaccharides in genomic DNA extracted [34]. The mean values of the 260/280 ratio for all samples were below 2.0, and this result indicates the minimal nucleic acid contamination in food samples in terms of the isolation protocols examined.

Spectrophotometric measurement results (Table 2) obtained from Method-4 showed lower or non-optimal values compared to the other three isolation methods. These results are consistent with the unclear band profiles obtained from the agarose gel electrophoresis images (Fig. 1d). Method-1, on the other hand, gave very high values in terms of DNA yield compared to other DNA isolation methods. Still, it should be considered that these high rates may be due to contamination when compared with agarose gel photographs (Fig 1a).

Turkec et al. [31] examined DNA extraction methods to evaluate GMO detection in Turkey's commercially available food and feed products containing corn. According to their observations, the CTAB method was the most suitable for raw soy and corn and highly processed food samples than commercial kits. The purity of the CTAB method was found to be above 1.5 for the samples examined, excluding the cornbread, indicating the suitability of the extracted DNA for amplification analysis [31, 35]. For the samples examined in this study, the mean was above 1.7 in all samples except soy flour and cake.

Mathess et al. [14] proposed a modified CTAB protocol for DNA extraction from protein-rich corn feeds. This DNA extraction protocol was used in this study with minor modifications (DNA isolation method-2). Accordingly, while the DNA yields were between 20.67 and 82.14 ng/ml in method-2, the 260/280 ratio was found between 1.45 and 1.88 (Table 2).

Table 2 Concentration and purity genomic DNA extracted various protocols

Food Product	DNA Isolation Method-1		DNA Isolation Method-2		DNA Isolation Method-3		DNA Isolation Method-4		Mean* ng/ul	Mean* 260/280
	ng/ul	260/280	ng/ul	260/280	ng/ul	260/280	ng/ul	260/280		
Biscuit	125.22ab	1.80a	52.19ab	1.88c	68.43ab	1.77b	35.05b	1.86c	70.22	1.83
Cake	118.87ab	1.72a	45.26ab	1.61ab	37.81ab	1.58ab	8.27a	1.4a	52.55	1.58
Cracker	274.58bc	1.80a	26.08ab	1.76c	57.83ab	1.58ab	68.02b	1.79bc	106.62	1.73
Corn chips	81.80ab	1.67a	45.24b	1.76c	58.98ab	1.72ab	46.65ab	1.57a	58.16	1.68
Corn flour	36.16a	1.75a	25.40ab	1.76c	25.03ab	2.05c	16.86a	1.67ab	32.86	1.81
Soy flour	593.58d	1.89a	82.14b	1.75abc	107.12cd	1.71bc	63.98ab	1.47a	211.80	1.71
GM Soy	380.77c	1.83a	78.53b	1.81bc	159.47e	1.75a	12.65a	2.14d	157.86	1.81
GM Corn	150.84ab	1.81a	20.67a	1.45a	134.61d	1.94c	13.66a	1.74abc	79.85	1.74

DNAs of the samples extracted by DNA extraction method-3 were used as template DNA for PCR studies (Fig 2). Most processed food products contain different genomic DNA content from various animal and plant sources. Within this complex matrix, only a small fraction of the genomic DNA used as a template for PCR contains the appropriate target for amplification. For this reason, in this research, the lectin gene's presence to determine the content of soy products and the presence of the zein gene to determine the content of corn products were performed (Fig. 2).

The samples containing soy content were biscuit, cake, crackers, corn chips, and soy flour (Fig. 2a). Soy flour and biscuit samples showed more apparent band profiles, showing the correct band profile in the expected base pair range. On the other hand, cake samples did not show significant band profiles in the agarose gel in soy content. Compared to average of the four isolation protocols, DNA quality has the lowest for cake samples (1.58). The DNA quality results showed that the DNA quality ratios of biscuit and soy flour samples, which are the sample groups with the cleanest band profile in determining the soy content, were 1.83 and 1.81, respectively (Table 2). These results suggest that DNA quality may be adequate in PCR results, a sensitive detection method depending on the product type and processing level.

According to the agarose gel image of the PCR results (Fig. 2b), the presence of the Zein gene was detected in the biscuit, corn chips and the cornflour. A band profile of the corn content was not obtained among cake and cracker. Although these results are expected for the cornflour samples, the corn content compared to the soybean content was less.

Arun et al. [36] analyzed soy-specific lectin and corn-specific zein sequences found in GM and non-GMO soy and corn, respectively, in CaMV 35S and nos negative samples to eliminate false-negative results. The distribution of positive products in soy and corn content from the screened products were, 14 (32.6%) of 43 corn samples and 11 (19.3%) of 57 soybeans. Transgenes of food products such as sugar, vegetable oils, and highly processed carbohydrates exposed to mechanical, high temperature, and chemical factors are degraded and damaged [37, 38]. Although this situation can be overcome with the efficiency of the isolation protocol, phenolic acid residues or polysaccharides cannot be removed entirely from the genomic DNA during DNA isolation. These contaminants affect and even inhibit the activation of DNA polymerase during PCR amplification [36, 39, 40]. However, small amounts of DNA can be amplified by PCR, but there may be differences in DNA quality and yield in band profiles according to the agarose gel results.

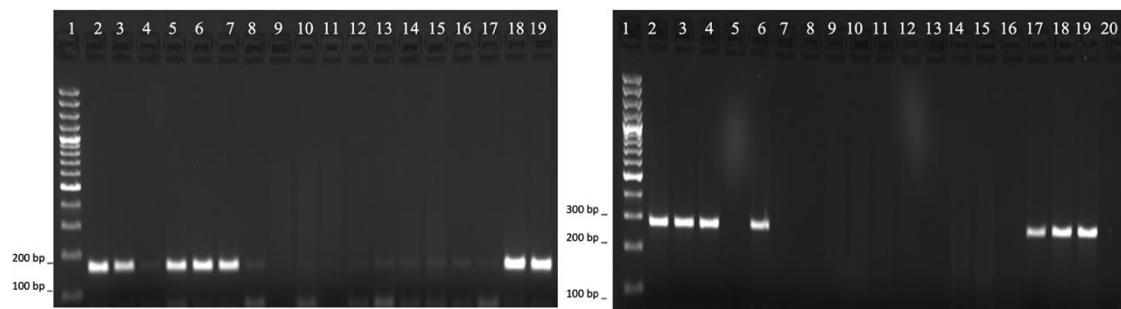


Fig 2 Agarose gel image of PCR samples with lectin (a) and zein (b) primer a)- 1) Thermo 100 bp DNA Ladder 2) GM Soy (positive control); 3-8) biscuit; 9-12) cake; 13-15) cracker; 16-17) corn chips; 18-19) soy flour. b)- 1) Thermo 100 bp DNA Ladder 2) GM Corn (positive control); 3-8) biscuit; 9-12) cake; 13-15) cracker; 16-17) Corn chips; 18-19) Corn flour; 20) Wheat DNA (negative control)

As a result of the GMO screening for the 35S promoter gene region, the expected band size was determined was only the corn flour (Fig 3). There are strict legal measures on using GMO in food products in Turkey [4]. In this study, GMO screening of genomic DNA samples obtained according to the Method-3 isolation protocol was evaluated using the amplification results of the 35S promoter region (Fig. 3).

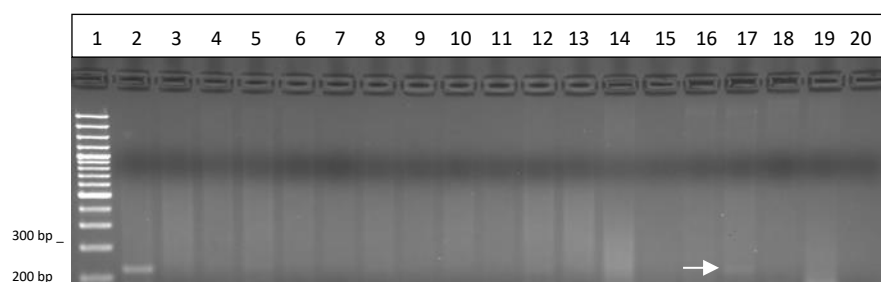


Fig 3 Agarose gel image of PCR samples with 35s cf3/cf4 primer 1) Thermo 100 bp DNA Ladder 2) GM Soy positive control); 3-8) biscuit; 9-11) cake; 12-14) cracker; 15) Corn chips; 16-17) Corn flour; 18-19) Soy flour; 20) Wheat DNA (negative control)

GMO content was not found in any tested food samples, except for one corn sample (sample 17). CTAB and commercial kit isolation methods were applied to the samples examined in a study in which GMO detection was performed in chips and breakfast products offered for sale in Turkey. A sufficient quality and amount of DNA could not be obtained in any of the samples examined so this study results support that product processing processes cause DNA damage [41]. Artuvan and Aksay, in which GMO content was screened in baby formulas and baby continue milk offered for sale in markets in Turkey, p35S, tNOS and pFMV transgenic contents were not found [42]. In other studies, on GMOs in food products in Turkey, no GM content was found in terms

of soy and corn content [10, 11, 31, 45]. It is recommended to examine the low amount of GMOs determined by qualitative and quantitative studies by sequence analysis in the next step. It should be noted that the band 17th sample (Fig 3) in this study may be positive for GMO content at low concentrations, which can be attributed to accidental contamination in the transfer or the same production line. However, the complex zygotic structure of corn is a limiting factor for GMO content because not all tissue types have the same GMO content. In the production of corn starch, maize flour, seed coat and embryo are separated. In snacks containing corn, the endosperm is milled and used as a raw material [43]. Embryo is diploid, endosperm is triploid and pericarp is haploid [44]. Therefore, the GMO content of the corn sample may be higher than in the other processed food samples studied. It is recommended to perform quantitative analyses to determine the limit threshold value determined by the relevant laws in GMO analysis studies conducted with the traditional PCR method and sequence analyzes for the result [36, 45].

Conclusion

In the present study we investigated the most suitable DNA isolation protocols for different types and brands samples at different processing levels. Although the most suitable isolation method for different sample types varies, it was determined that the appropriate isolation protocol was the modified Wizard-CTAB method among the four isolation methods tested. It was determined that the highest DNA content was obtained from the biscuit samples, and the lowest DNA content was obtained from the cake samples among the biscuit, cake, cracker, and chips samples examined.

Such studies are important to determine the market situation of food products in terms of food safety and legal control. In this study, the traditional PCR method, which is one of the methods used for routine control analysis, was used. It is desired to draw attention to DNA isolation yield or quality on PCR yield in screening corn and soybean assets, which is essential for GMO analysis in food samples with complex matrix content.

Abbreviations

ANOVA: Analysis of variance; BME: Beta-mercaptoethanol; CaMV: Cauliflower mosaic virus; CTAB: Cetyltrimethylammonium Bromide; DNA: Deoxyribonucleic acid; dNTP: Deoxynucleotide triphosphates; EC: European commission; EDTA: Ethylenediamine tetraacetic acid; EU: European union; GMO: Genetically modified organisms; ISAAA: International service for the acquisition of agri-biotech applications; Mha: million hectares; NaCl: sodium chloride; PCR: Polimerase chain reaction; RNA: Ribonucleic acid; RNase: Ribonuclease; rpm: revolutions per minute; SDS: Sodium dodecyl sulfate;

SPSS: Statistical package for the social sciences; TBE: Tris-Boric acid EDTA; UV: Ultraviolet; WHO: World health organization.

Acknowledgements

In this article, data belonging to the study of Begum TERZI AKSOY's doctoral thesis were used.

Funding

This study was supported by Karamanoglu Mehmetbey University Scientific Research Projects Commission (Project No: 03-D-21).

Availability of data and material

Please contact the corresponding author for any data request.

References

1. ISAAA, ISAAA Brief 55-2019: Executive Summary Biotech Crops Drive Socio-Economic Development and Sustainable Environment in the New Frontier. 2019. In: <https://www.isaaa.org/resources/publications/briefs/55/executivesummary/default.asp>.
2. Mahgoub, S.E., Regulation of GMOs. Testing and Analysis of GMO-containing Foods and Feed, S.E. Mahgoub, and L.M., Nollet, Editors. 2019, CRC Press. Boca Raton: Florida. p. 22-25.
3. Davison, J., GM plants: Science, politics and EC regulations. *Plant Science*, 2010. 178(2): p. 94-98.
4. Regulation (TR). Turkish regulation on genetically modified organisms and their products; Official Gazette No: 27671. 2010. Accessed June 20, 2020. <http://www.resmigazete.gov.tr/eskiler/2010/08/20100813-4.htm>.
5. Singh, M., et al. Development and Utilization of Analytical Methods for Rapid GM Detection in Processed Food Products: A Case Study for Regulatory Requirement. *Research Square* (in press, 2022), 2022.
6. Ramos-Gómez, S., et al. Development of a method to recovery and amplification DNA by real-time PCR from commercial vegetable oils. *Food Chemistry*, 2014. 158, p. 374-383.
7. Singh, M., et al. Efficient DNA Extraction Procedures for Processed Food Derivatives—a Critical Step to Ensure Quality for GMO Analysis. *Food Analytical Methods*, 2021. 14(11): p. 2249-2261.
8. Gryson, N., Effect of food processing on plant DNA degradation and PCR-based GMO analysis: a review. *Analytical and Bioanalytical Chemistry*, 2010. 396(6): p. 2003-2022.
9. Linnhoff, S., et al., An examination of millennials' attitudes toward genetically modified organism (GMO) foods: is it Franken-food or super-food? *International Journal of Agricultural Resources, Governance and Ecology*, 2017. 13(4): p. 371.
10. Sönmezoğlu, Ö. and H. Keskin, Determination of genetically modified corn and soy in processed food products. *Journal of Applied Biology & Biotechnology*, 2015. (3): p. 32-37.
11. Arun, Ö.Ö., The effect of heat processing on PCR detection of genetically modified soy in bakery products. *Journal of Food and Health Science*, 2016. p. 130-139.
12. Pacheco Coello, R., et al. Comparison of three DNA extraction methods for the detection and quantification of GMO in Ecuadorian manufactured food. *BMC Research Notes*, 2017. 10(1): p. 758.
13. Saadedin, S., M. Abbas and A. Suleiman, Detection of CaMV-35S Promoter and NOS Terminator in Genetically Modified Tomato Seed in Iraqi Markets. *Iraqi Journal of Biotechnology*, 2019. 18(2): p. 160-168.
14. Matthes, N., et al. Validation of a modified CTAB method for DNA extraction from protein-rich maize feedstuffs. *Journal of Consumer Protection and Food Safety*, 2020. 15(4): p. 331-340.

15. Ashrafi-Dehkordi, E., S.M. Mazloomi, and F. Hemmati, A comparison of DNA extraction methods and PCR-based detection of GMO in textured soy protein. *Journal of Consumer Protection and Food Safety*, 2021. 16(1): p. 51-57.
16. Tung Nguyen, C., et al. Comparison of DNA Extraction Efficiencies Using Various Methods for the Detection of Genetically Modified Organisms (GMOs). *International Food Research Journal*, 2009. 16: p. 21-30.
17. Doyle, J.J. and J.L. Doyle, Isolation of Plant DNA From Fresh Tissue. *Focus (Madison)*, 1990. 12: p. 13-15.
18. Wilfinger, W.W., K. Mackey, and P. Chomczynski, Assessing the Quantity; Purity and Integrity of RNA and DNA following Nucleic acid purification. *DNA sequencing II optimising preparation and cleanup*, 2006. p. 291-312.
19. Vollenhofer, S., et al. Genetically Modified Organisms in Food Screening and Specific Detection by Polymerase Chain Reaction. *Journal of Agricultural and Food Chemistry*, 1999. 47(12): p. 5038-5043.
20. Pauli, U., et al. Extraction and Amplification of DNA From 55 Foodstuffs. *Mitteilungen aus Lebensmitteluntersuchung und Hygiene*, 2000. 91: p. 491-501.
21. Cardarelli, P., et al. Detection of GMO in food products in Brazil: the INCQS experience. *Food Control*, 2005. 16(10): p. 859-866.
22. Lipp, M., et al. Validation of a method based on polymerase chain reaction for the detection of genetically modified organisms in various processed foodstuffs. *European Food Research and Technology*, 2001. 212(4): p. 497-504.
23. Ahmed, F.E., *Testing of Genetically Modified Organisms in Food*. 2004, Binghamton, New York: Food Products Press.
24. Laffont, J.L., et al. Testing for adventitious presence of transgenic material in conventional seed or grain lots using quantitative laboratory methods: statistical procedures and their implementation. *Seed Science Research*, 2005. 15(3): p. 197-204.
25. Shokere, L.A., M.J. Holden, and G. Ronald Jenkins, Comparison of fluorometric and spectrophotometric DNA quantification for real-time quantitative PCR of degraded DNA. *Food Control*, 2009. 20(4): p. 391-401.
26. Bauer, T., The effect of processing parameters on DNA degradation in food. *European Food Research and Technology*, 2003. 217(4): p. 338-343.
27. Gryson, N., K. Dewettinck, and K. Messens, Detection of Genetically Modified Soy in Doughs and Cookies. *Cereal Chemistry Journal*, 2007. 84(2): p. 109-115.
28. Sambrook, J., and D. Russell, *Molecular cloning: a laboratory manual*, 3rd ed. 2001, New York, ABD: Cold Spring Harbor Laboratory Press.
29. Ateş Sönmezoğlu, Ö., and B. Terzi, Characterization of some bread wheat genotypes using molecular markers for drought tolerance. *Physiology and Molecular Biology of Plants*, 2018. 24(1): p. 159-166.
30. Greiner, R., U. Konietzny, and A.L.C.H. Villavicencio, Qualitative and quantitative detection of genetically modified maize and soy in processed foods sold commercially in Brazil by PCR-based methods. *Food Control*, 2005. 16(8): p. 753-759.
31. Turkec, A., et al. DNA extraction techniques compared for accurate detection of genetically modified organisms (GMOs) in maize food and feed products. *Journal of Food Science and Technology*, 2015. 52(8): p. 5164-5171.
32. DiBernardo, G., et al. Comparative Evaluation of Different DNA Extraction Procedures from Food Samples. *Biotechnology Progress*, 2007. 23(2): p. 297-301.
33. Abdel-Latif, A., and G. Osman, Comparison of three genomic DNA extraction methods to obtain high DNA quality from maize. *Plant Methods*, 2017. 13(1): p. 1.

34. Pervaiz, Z.H., et al. Methodology A modified method for high-quality DNA extraction for molecular analysis in cereal plants. *Genetics and Molecular Research*, 2011. 10(3): p. 1669-1673.
35. Querci, M., et al. From sampling to quantification: developments and harmonisation of procedures for GMO testing in the European Union. *Collection of Biosafety Reviews*, 2007. 3: p. 8-14.
36. Arun, Ö., F., Yılmaz, and K. Muratoğlu, PCR detection of genetically modified maize and soy in mildly and highly processed foods. *Food Control*, 2013. 32(2): p. 525-531.
37. Anklam, E., et al. Analytical methods for detection and determination of genetically modified organisms in agricultural crops and plant-derived food products. *European Food Research and Technology*, 2002. 214(1): p. 3-26.
38. Rastegar, H., et al. Investigation of transgenic elements in genetically modified maize germ (*Zea mays*) and maize germ oil distributed in local market by qualitative PCR method. *Human, Health and Halal Metrics*, 2021. 1(2): p.64-70.
39. Jia, R., et al. Microbiologically influenced corrosion and current mitigation strategies: A state of the art review. *International Biodeterioration & Biodegradation*, 2019. 137: p. 42-58.
40. Aboul-Maaty, N.A.F., and H.A.S. Oraby, Extraction of high-quality genomic DNA from different plant orders applying a modified CTAB-based method. *Bull Natl Res Cent*, 2019. 43(1): p. 25.
41. Mutlu, Ş., O., Şimşek, and Ö. Öksüz, Investigating The GMO Existence in Chips and Breakfast Cereals Marketed in Turkey. *Tekirdağ Ziraat Fakültesi Dergisi*, 2021. 18(3): p. 375-385.
42. Artuvan, E., and S., Aksay, Investigation of the Genetically Modified Organism (GMO) Existence in Baby Foods on the Market in Turkey. *Turkish Journal of Agriculture-Food Science and Technology*, 2021. 9(10): p. 1945-1952.
43. Yoshimura, T., et al. Applicability of the quantification of genetically modified organisms to foods processed from maize and soy. *Journal of Agricultural and Food Chemistry*, 2005. 53(6): p. 2052-2059.
44. Zhang, D., A., Corlet and S., Fouilloux, Impact of genetic structures on haploid genome-based quantification of genetically modified DNA: theoretical considerations, experimental data in MON 810 maize kernels (*Zea mays* L.) and some practical applications. *Transgenic Research*, 2008. 17(3): p. 393-402.
45. Avsar, B., et al. Identification and quantitation of genetically modified (GM) ingredients in maize, rice, soybean and wheat-containing retail foods and feeds in Turkey. *Journal of Food Science and Technology*, 2020. 57(2): p.787-793.

Taş, N., et al., A Current and Common Cause of Secondary Spontaneous Pneumothorax: Covid- 19 Pneumonia. International Journal of Life Sciences and Biotechnology, 2022. 5(3). p. 562-571.
DOI: 10.38001/ijlsb.1116153

A Current and Common Cause of Secondary Spontaneous Pneumothorax: Covid- 19 Pneumonia

Nurmuhammet Taş^{1*}, Muhammet Emin Naldan², Fatih Öner³,
Yener Aydın⁴, Hülya Naldan⁵

ABSTRACT

This study evaluated cases of spontaneous pneumothorax developing secondary to SARS-CoV-2 pneumonia. Sixteen cases presenting to our hospital due to spontaneous pneumothorax developing secondary to SARS-CoV-2 pneumonia between March 2020 and February 2020 were evaluated retrospectively. Ten patients (62.5%) were men, and six (37.5%) were women, with a mean age of 68 ±20.3 years (range 18 - 90 years). Pneumothorax was in the right hemithorax in 11 cases (68.75%), in the left hemithorax in two (12.5%), and bilateral in three (17.75%). Pneumothorax developed during active SARS-CoV-2 pneumonia in all 16 cases (100%). No pneumothorax was detected following the healing of SARS-CoV-2 infection. Pneumothorax was observed while patients were not intubated in 15 cases (93.75%), but pneumothorax developed during mechanical ventilation in one case (6.25%). Tube thoracostomy was performed on all patients in treatment. Air leakage from the tube was observed in 14 cases (87.5%). The mean duration of tube thoracostomy was 18.3 ±20.1 days (range 1 - 81 days). Pneumothorax resolved after treatment in seven cases (43.75%), while mortality occurred in nine (56.25%). Pneumothorax recurred after treatment in one case (6.25%). Pneumothorax is widely seen in the active period or after healing in cases infected with COVID-19. Aggressive treatment is generally required for this clinical manifestation with high mortality.

ARTICLE HISTORY

Received

13 May 2022

Accepted

22 October 2022

KEYWORDS

SARS-CoV-2 pneumonia, pneumothorax, management

Introduction

Pneumothorax occurring due to any underlying pulmonary disease without trauma or iatrogenic intervention is secondary spontaneous pneumothorax (SSP). The annual incidence of SSP is reported at 6.3 and 2 per 100,000 in men and women, respectively

¹ Department of Physical Medicine and Rehabilitation, Erzurum Regional Education and Research Hospital, Erzurum, Türkiye

² Department of Anesthesiology and Reanimation, Erzurum Regional Education and Research Hospital, Erzurum, Türkiye

³ Department of Otorhinolaryngology, Erzurum Regional Education and Research Hospital, Erzurum, Türkiye

⁴ Department of Thoracic Surgery, Medical Faculty, Ataturk University, Erzurum, Türkiye

⁵ Medicinal and Aromatic Plants Specialist, Erzurum Regional Education and Research Hospital, Erzurum, Türkiye

[1]. The most frequently detected causes of SSP are pulmonary emphysema, interstitial lung disease, lung cancer, and tuberculosis [1, 2].

The disease caused by Severe Acute Respiratory Syndrome-Coronavirus 2 (SARS-CoV-2) and first reported from the Chinese city of Wuhan in December 2019 was given the name Coronavirus Disease 2019 (COVID-19) by the World Health Organization (WHO) [3]. The infection that then spread rapidly across the world can exhibit a broad clinical spectrum, from an asymptomatic form to fatal complications. Pulmonary symptoms such as cough, dyspnea, and chest pain, and severe cases of pneumonia are frequently encountered symptoms and findings. Large numbers of cases of pneumothorax associated with SARS-CoV-2 have recently begun being reported worldwide [4-6]. This study evaluated cases of SSP developing in cases with previous or current SARS-CoV-2 pneumonia in the light of the current literature.

Material and Methods

This retrospective and a single-center study was performed in Erzurum Training and Research Hospital, Turkey. The study protocol was approved by the Institutional Review Board of the Ministry of Health Human Subjects Research and Ethical Committee. The research was performed in compliance with the ethical principles of the Declaration of Helsinki. Sixteen consecutive cases treated in our hospital, a pandemic hospital in the city of Erzurum, due to SARS-CoV-2-related SSP, between March 2020 and February 2021 were evaluated retrospectively.

The SARS-CoV-2 diagnosis was made in the laboratory using real-time reverse transcription-polymerase chain reaction (RT-PCR) of nasopharyngeal swab samples. Cases with primary spontaneous pneumothorax or SSP for any reason other than COVID-19, a negative real-time reverse transcriptase polymerase chain reaction test result for COVID-19, and identified iatrogenic pneumothorax were not included in the study. Direct posteroanterior chest x-rays and thoracic computed tomography (CT) were used for preoperative diagnosis in all cases. Tube thoracostomy was decided by the clinical team responsible for the patient. Large diameter chest tubes were placed in patients for pneumothorax. Thoracic drains were connected to watertight chest drainage systems. Age, gender, comorbidity, pneumothorax location, radiological characteristics, the treatment applied, and morbidity, mortality, and recurrence rates were reviewed retrospectively.

Results

Ten (62.5%) of the cases were male, and six (37.5%) were female, with a mean age of 68 ± 20.3 years (range 18 - 90). A history of smoking was present in 10 (62.5%) cases. In terms of comorbidities, chronic obstructive pulmonary disease (COPD) was detected in six cases (37.5%), heart failure in four (25%), and diabetes mellitus in one (6.25%). Dyspnea was present in all 16 cases (100%) at the time of presentation, cough in 16 (100%), and chest pain in nine (56.25%).

Pneumothorax was located in the right hemithorax in 11 cases (68.75%), in the left hemithorax in two (12.5%), and bilateral in three (18.75%) (Figure 1). Pneumothorax developed during active SARS-CoV-2 pneumonia in all 16 cases. No pneumothorax was detected following SARS-CoV-2 infection treatment. Pneumothorax was observed while the patient was not intubated in 15 cases (93.75%) and developed during mechanical ventilation in one (6.25%). Accompanying mediastinal emphysema was present in five cases (31.25%), subcutaneous emphysema in four (25%), and pleural effusion in 10 (62.5%) (Figure 1).

Discussion

Covid-19 pneumonia-related pneumothorax was detected in 16 cases. The mean age of the patients was 68. Ten (62.5%) had a history of smoking, and comorbidities such as COPD, heart failure, hypertension, and diabetes mellitus were observed in all 16 (100%). Pneumothorax developed spontaneously rather than when the patient was intubated in 15 cases (93.75%) and developed in association with barotrauma during mechanical ventilation in one case (6.25%). Accompanying mediastinal emphysema was present in five cases (31.25%), subcutaneous emphysema in four (25%), and pleural effusion in 10 (62.5%). Tube thoracostomy was applied in all cases during treatment. The mortality rate was 56.25%.

The clinical course of COVID-19 is unpredictable and ranges from asymptomatic to subclinical symptoms to acute disease with acute respiratory distress syndrome (ARDS) and organ failure. The SARS-CoV-2 virus has been shown to enter the cell through angiotensin-converting enzyme 2 (ACE-2) receptors in humans. The virus, therefore, first causes interstitial damage in the lungs, followed by parenchymal damage. Due to its high

sensitivity and rapid availability, thoracic CT plays an essential role in diagnosing and treating COVID-19 infection, showing pulmonary involvement and its severity. It is also the most sensitive imaging technique for determining small amounts of pneumomediastinum and pneumothorax [7]. Due to the more widespread recognition of thoracic CT findings, various CT algorithms have been developed. Typical and atypical disease findings have been determined. Typical findings at thoracic CT include ground-glass opacity, consolidation, a reticular pattern, a crazy-paving appearance, air bronchograms, airway changes, and nodules (maybe with halo and reversed halo signs). Reported atypical findings include lymphadenopathy, pleural effusion, pericardial effusion, and cavitation [8, 9].

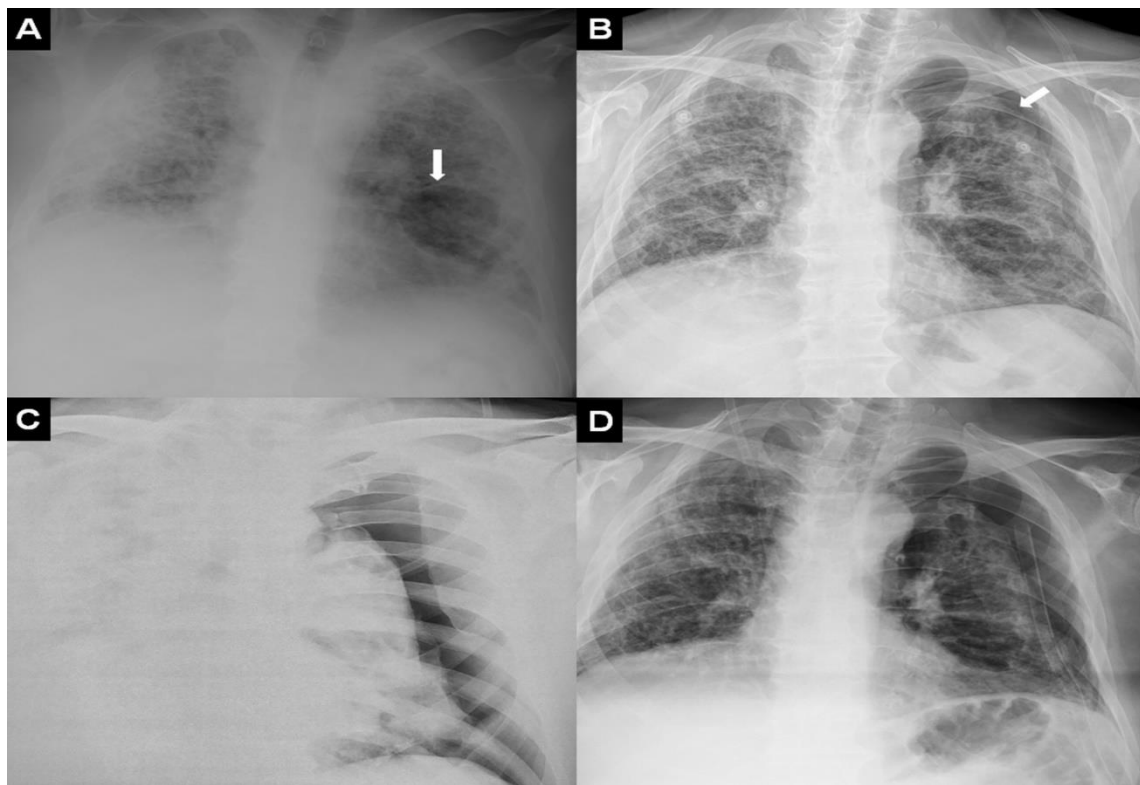


Fig 1 (A) Widespread pulmonary involvement and an air cyst (arrow) on the left side associated with COVID-19 pneumonia in a 65-year-old male patient. (B) Pneumothorax (arrow) developed at x-ray three days later. (C) The pneumothorax became more pronounced at control x-ray. (D) Direct x-ray following tube thoracostomy

Tube thoracostomy was performed in the treatment of all patients. Air leakage from the chest tube was observed in 14 cases (87.5%). The mean duration of tube thoracostomy was 18.3 ± 20.1 days (range 1 - 81 days). Pneumothorax resolved after treatment in seven

cases (43.75%), while mortality occurred in nine (56.25%). Pneumothorax recurred after treatment in one case (Table 1).

Table 1 Patient characteristics

		Count	%
Gender	Male	10	62.5%
	Female	6	37.5%
Age (years)		68±20.3(18-90)	
Localization of pneumothorax	Right	11	68.75%
	Left	2	12.5%
	Bitateral	3	18.75%
Smoking status	Yes	10	62.5%
	No	6	37.5%
Comorbidities	COPD	6	37.5%
	Asthma	0	0%
	Systemic hypertension	6	37.5%
	Coronary artery disease	4	25%
	Type 2 diabetes mellitus	1	6.25%
	Hyperlipidemia	1	6.25%
	Chronic kidney disease	1	6.25%
Symptoms	Dyspnea	16	100%
	Chest pain	9	56.25%
	Cough	16	100%
	Backache	3	18.75%
	Sputum	10	62.5%
	Asymptomatic	0	0%
	Yes	1	6.25%

Unilateral or bilateral, peripheral, subpleural ground-glass opacities are the most common finding in COVID-19 infection, being seen in approximately 90% of patients. Ground glass opacity is also known to be the earliest radiological finding of the disease. This appearance is thought to be associated with edema in the lungs and the hyaline membrane. Ground glass can be seen alone or also together with findings such as interlobular septal thickening and consolidation. Consolidations are generally multifocal, segmental, or patchy in patients with COVID-19 infection and are generally subpleural or peribronchovascular in location. In terms of pathophysiology, consolidations are thought to be associated with fibromyxoid exudates in alveoli. In addition, the presence of consolidation is associated with disease prognosis and may be an indication of progressive disease [8-10]. A ground-glass appearance was observed in 100% of our case series, consolidation in 43.74%, and fibrosis in 81.25%.

The most frequent symptoms of SARS-CoV-2 infection are fever, cough, and respiratory difficulty. Pneumothorax development is reported in a very small proportion of these patients [4]. COVID-19 patients developing SSP more commonly present with dyspnea, tachypnea, and hypoxia. However, all these features are frequently seen in patients with severe COVID-19. Interestingly, chest pain has been observed significantly more frequently in association with pneumothorax development [6].

The proposed mechanism involved in spontaneous pneumothorax in patients with COVID-19 disease has been linked to structural changes in the lung parenchyma. These include cystic and fibrotic changes leading to tearing of the alveolar wall associated with an increasing pressure difference between the alveoli and the pulmonary interstitium. The possibility of pneumothorax development has been emphasized in the case of bronchiolar distortion and narrowing caused by SARS-CoV-2, leading to COVID-19 pneumonia and pulmonary blistering resulting from severe alveolar damage. Increased intrathoracic pressure deriving from prolonged cough and/or mechanical ventilation is another significant factor [4, 7, 10-12]. Both pneumothorax and pneumomediastinum are known mechanical ventilation complications associated with intubation. Additionally, pneumothorax or pneumomediastinum, or more rarely both, can be seen in COVID-19 even in the absence of barotrauma [4].

Among patients requiring prolonged respiratory support, such as in COVID-19 pneumonia, mechanical ventilation creates a persistent alveolar pressure trend capable of accelerating cyst rupture, causing air leakage from the pulmonary tissue. This air can pass through the visceral pleura and give rise to subpleural air cysts. Pneumothorax frequently occurs due to the tearing of these subpleural air cysts. Escaping air sometimes leads to pneumomediastinum, pneumoperitoneum, or subcutaneous emphysema, respectively, by dissection through the perivascular and peribronchial vascular sheath into the mediastinum, retroperitoneum, and subcutaneous tissue. Pneumothorax can also occur in the case of mediastinal pleura rupture following pneumomediastinum development.

Moreover, the probability of such destructive complications is particularly exacerbated by prolonged high-pressure mechanical ventilation. This is because it triggers the formation and progression of new alveolar cysts that eventually rupture, causing the air to spread to various interconnected body cavities [13]. Ozdemir et al. [14] reported a rate of pneumothorax development of 7.5% in patients undergoing mechanical ventilation following diagnosis of COVID-19 pneumonia in the intensive care unit. Talan et al. [15] reported admitting 161 patients to the intensive care unit due to COVID-19 pneumonia that 96 patients underwent mechanical ventilation, and that pneumothorax, pneumomediastinum, and/or subcutaneous emphysema developed in nine of these.

Pneumothorax is a potential complication in some pulmonary infections and is particularly frequently seen in *Pneumocystis jirovecii* pneumonia. The true incidence of SSP in patients with COVID-19 is currently unknown. Some sporadic cases of pneumothorax development in COVID-19 patients have been reported. Invasive or non-invasive mechanical ventilation was applied before pneumothorax developed in some cases, while in others, pneumothorax appeared after pulmonary involvement lasting several weeks with extensive inflammatory infiltration in the pulmonary parenchyma and cyst formation [6]. Pneumothorax seen after recovery from Covid-19 pneumonia is not yet fully understood but is thought to result from persistent chronic inflammatory changes and a delayed alveolar tear as part of the ongoing chronic disease process [16]. These cases suggest that pneumothorax is a complication of COVID-19.

One study from the UK evaluated six cases of pneumothorax from 16 centers. Two consecutive pneumothorax episodes were observed in two cases, and additional accompanying pneumomediastinum was present in six. The incidence of pneumothorax

was higher among male patients. Thirty-two percent of the patients developing pneumothorax consisted of cases in which pneumothorax developed spontaneously without any non-invasive ventilation or intubation. The estimated incidence of pneumothorax in COVID-19 cases is 0.91% [17]. Miró et al. [6] reported spontaneous pneumothorax development in 40 (0.056%) out of 71,904 cases diagnosed with COVID-19. This was higher than the rate of pneumothorax development in patients without COVID-19. Zantah et al. [11] reported that pneumothorax developed spontaneously in six (0.66%) out of 3368 cases of suspected COVID 19 pneumonia presenting to institutions. Consistent with the previous literature, pneumothorax was more common in males in the present study. This may be due to men in large series of patients with COVID-19 being more frequently affected by severe forms of the disease.

Pneumothorax can range from asymptomatic to a life-threatening condition. Small pneumothoraces in clinically stable patients can be managed with observation. However, larger pneumothoraces with hemodynamic imbalance require active intervention in order to avoid destructive sequelae. Delayed pneumothorax can be treated with tube thoracostomy alone in some cases. However, the treatment of pneumothorax in patients with ARDS undergoing mechanical ventilation may represent a clinical difficulty. If the air leak is permanent despite drainage, bleb resection and thoracoscopy with pleural scratch may be one therapeutic option [16-18]. Tube thoracostomy was performed in all cases in the present study.

There are various particular difficulties in the operative management of recurring pneumothoraces in patients recovering from COVID-19. Significant problems include health workers being exposed to aerosol-producing procedures, maintenance of single-lung ventilation, the risk of contralateral pneumothorax development, and the suitability for resection of the underlying lung tissue [16, 17].

Although the primary cause of death in COVID-19 infections is ARDS, the early diagnosis and treatment of severe complications such as pneumothorax, pneumomediastinum, or pulmonary embolism are also highly important [13]. The mortality rate in pneumothorax developing in association with SARS-CoV-2 infection is much higher than in previously reported SSP cases [1, 6]. Onuki et al. [1] reported a mortality rate of 4.59% in 327 cases of SSP. That rate was approximately 30 times higher compared to primary spontaneous pneumothoraces. Miró et al. [6] reported mortality

rates of 32.5%, 13.8%, and 1.6% in COVID-19 patients developing pneumothorax, COVID-19 patients without pneumothorax development, and non-COVID-19 pneumothorax cases, respectively. Rafiee et al. [7] reported a mortality rate of 30%. They identified male gender, advanced age, and pre-existing lung disease, particularly COPD, as risk factors. Martinelli et al. [17] reported a general survival rate of 63.1%. No difference was determined in 28-day survival between the genders, although 28-day survival was significantly higher in patients aged 70 or more than young individuals. The mortality rate due to spontaneous pneumothorax in the present study was 56.25%.

Some limitations need to be considered when interpreting the results of this study. First, due to the retrospective nature of the study, it is not easy to evaluate factors capable of affecting pneumothorax development. The second limitation is the relatively low case number. Another factor is that the effect of pneumothorax on mortality cannot be thoroughly evaluated since this was an observational study and due to multiorgan involvement.

Conclusion

Pneumothorax is a potential complication of COVID-19 pneumonia. It can emerge during active COVID-19 infection or after the completion of treatment. It can worsen prognosis, particularly in patients with underlying lung disease, and the mortality rate is higher compared to other spontaneously developing pneumothoraces. The incidence of pneumothorax in COVID-19 cases is higher than that in the normal population, and diagnosis and treatment must not be delayed.

References

1. Onuki, T., et al., Primary and secondary spontaneous pneumothorax: Prevalence, clinical features, and in-hospital mortality. *Canadian Respiratory Journal* 2017. 2017: 6014967
2. Türkyılmaz, A., et al., Treatment of secondary spontaneous pneumothorax: 100-patient experience. *Eurasian Journal of Medicine* 2007. 39: p. 97-102.
3. Elhakim, TS., et al., Spontaneous pneumomediastinum, pneumothorax and subcutaneous emphysema in covid-19 pneumonia: A rare case and literature review. *British Medical Journal Case Reports* 2020. 13: e239489.
4. Quincho-Lopez, A. , et al., Case report: pneumothorax and pneumomediastinum as uncommon complications of covid-19 pneumonia—literature review. *The American Journal of Tropical Medicine and Hygiene* 2020. 103: p. 1170–76.
5. Alhakeem, A., et al., Case report: Covid-19–associated bilateral spontaneous pneumothorax—a literature review. *The American Journal of Tropical Medicine and Hygiene* 2020. 103: p. 1162–65.

6. Miró, Ò. , et al., Frequency, risk factors, clinical characteristics, and outcomes of spontaneous pneumothorax in patients with coronavirus disease Chest 2021.159: p. 1241-1255.
7. Rafiee, MJ., et al., Spontaneous pneumothorax and pneumomediastinum as a rare complication of covid-19 pneumonia: Report of 6 cases. Radiology Case Reports 2021. 16: p. 687–92.
8. Akçay, Ş., T. Özlü, and A. Yılmaz., Radiological approaches to covid-19 pneumonia. Turkish Journal Of Medical Sciences 2020. 50: p. 604–10.
9. Salehi, S., et al., Coronavirus disease 2019 (COVID-19): A systematic review of imaging findings in 919 patients. American Journal of Roentgenology 2020. 215: p. 87–93.
10. Vahidirad, A. , et al., Tension pneumothorax in patient with covid-19 infection. Radiology Case Reports 2021. 16: p. 358–60.
11. Zantah, M., et al., Pneumothorax in Covid-19 disease- incidence and clinical characteristics. Respiratory Research 2020. 21: 236.
12. Al-Shokri, SD., et al., Case report: Covid-19–related pneumothorax—case series highlighting a significant complication. The American Journal of Tropical Medicine and Hygiene 2020.103: p. 1166–69.
13. Akdogan, RE., et al., Pneumothorax in mechanically ventilated patients with covid-19 infection. Case Reports in Critical Care 2021. 2021: 6657533.
14. Özdemir, S., et al., Pneumothorax in patients with coronavirus disease 2019 pneumonia with invasive mechanical ventilation. Interactive CardioVascular and Thoracic Surgery 2020. 19: p. 351–55.
15. Talan, L., et al., Covid-19 pneumonia and pneumothorax: Case series. Tuberk Toraks 2020. 68: p. 437–43.
16. Kasturi, S., et al., Delayed recurrent spontaneous pneumothorax post-recovery from covid-19 infection.” Indian Journal of Thoracic and Cardiovascular Surgery 2021. 37: p. 1–3.
17. Martinelli, AW., et al., COVID-19 and pneumothorax: a multicentre retrospective case series European Respiratory Journal 2020. 56: 2002697.
18. Aiolfi, A., et al., Management of persistent pneumothorax with thoracoscopy and bleb resection in covid-19 patients. The Annals of Thoracic Surgery 2020. 110: p.413-415.

Hassan, M., et al., Antibacterial Activity of Ethanol Leaf Extract of *Sida acuta* Against Some Clinical Bacterial Isolates. International Journal of Life Sciences and Biotechnology, 2022. 5(3). p. 572-580.
DOI: 10.38001/ijlsb.1115771

Antibacterial Activity of Ethanol Leaf Extract of *Sida acuta* Against Some Clinical Bacterial Isolates

Maimuna Hassan¹ , Fatima M. Musa¹ , Firdausi Aliyu² , Aliyu Adamu^{1*} 

ABSTRACT

Persistent evolution of multidrug resistance bacteria due to inappropriate use of conventional antibiotics is undermining treatment intervention for infectious diseases, thus constituting substantial proportion of the global public health problem. This necessitated the search and development of new drugs particularly from plant origin that are effective against such superbugs. Therefore, the present study is designed to determine the phytochemical constituents in *Sida acuta* and their antibacterial effects on pathogenic bacterial species of *Escherichia coli*, *Staphylococcus aureus*, *Pseudomonas aeruginosa* and *Bacillus subtilis*. The phytochemical components of the extract were identified using standard methods. Furthermore, the antibacterial activity of the leaf extract against the bacterial pathogens were assessed using agar well diffusion and broth dilution methods, at varying concentrations of the extract (37.50, 75, 150 and 300 mg/ml), and using Commercially obtained ciprofloxacin as control. Preliminary screening revealed that ethanolic leaf extract possesses many secondary metabolites such as alkaloids, flavonoids, phenol, tannins, terpenoids, glycosides and cardiac glycosides. The extract exhibited significant inhibitory effects at ($p < 0.05$) against the reference isolates of bacteria. The highest antibacterial activity was exhibited by the highest concentration of the extract (300mg/ml). The minimum inhibitory concentrations (MIC) and minimum bactericidal concentrations (MBC) of ethanol crude extract of *Sida acuta* was found to be 37.5 and 75mg/ml, respectively against all the reference isolates of tested bacteria. The observed antibacterial activity suggests that *Sida acuta* could be used for the treatment of tested bacterial infections.

ARTICLE HISTORY

Received

12 May 2022

Accepted

22 October 2022

KEYWORDS

Phytochemical constituents, antibacterial activity, *Sida acuta*, ethanolic extract

Introduction

Medicinal plants represent the source of medical practice and are globally distributed, but mostly abundant in the tropics [1]. Historically, most native doctors were botanists, using medicinal plants to treat various kinds of diseases, if not all diseases. Currently, there are estimated 422,000 flowering plants distributed globally, out of which 50,000 were used

¹ Department of Microbiology, Kaduna State University Kaduna, Tafawa Balewa Way Nigeria

² Department of Biotechnology, Nigerian Defence Academy, Kaduna Nigeria

* Corresponding Author: Aliyu Adamu, E-mail: aliyuadamu@kasu.edu.ng

as primary source of medicine as chewing sticks for dental care, anti-inflammatory, antimicrobials and anticancer [2].

The use of conventional drugs in chemotherapy for the treatment diseases is being undermined by the evolution of antimicrobial resistance. Microorganisms particularly bacteria have the ability to evolved into a resistance strains by either genetic adjustments such as mutations as a result of selective pressure incited by inappropriate antimicrobial use [3]; or acquisition of resistance genes [4][5]. Therefore, there is need to identify more therapeutic options especially from plant origin in order to ensure effective treatment.

Sida acuta, otherwise called in Hausa “Kalkashin kwado” and “Stubborn grass” in English is an important medicinal plant in Africa, for treatment some ailments [6]. This plant is a member *malvaceae* family, genus *Sida* species and species *acuta*. It can grow in almost all soil types except that originated from limestone and flooded soil. All the plant parts, including root, stem bark, leaf and flower were reported to be used for medicinal purposes [7]. It was gathered from various studies that the plant is used for management of sperm cell related fertility problems, cold, cough, abdominal pain, headache, tuberculosis, malaria, asthma, blood disorders, respiratory diseases, dysentery and diarrhea, cancer and inflammation, among others[8]. These biological activities were associated with phytochemical compounds contained within the plant including essential oil, tannins, flavonoids and alkaloids [9]. In India, hot water extract of the dried plant is administered orally as febrifuge and diuretic; and the leaf juice is taken to manage vomiting [10]. The plant fresh root is used for dysentery treatment in Guinea. It is therefore based on this, this study assessed the antibacterial efficacy of the plant leaf extract against some pathogenic bacterial species

Materials and Methods

Collection, authentication and preparation of plant material

Fresh leaves of *Sida acuta* plant was collected within kawo, Kaduna North Local Government area of Kaduna State. The plant was identified and authenticated by a taxonomist at the Department of Biological Science, Kaduna State University. The leaves were washed thoroughly under running water and dry under room temperature for 14 days.

It was grinded into coarse powder using mortar and pestle and stored in separate airtight bottles.

Extraction of plant material

The leaves phytochemicals were extracted by percolation method as we described previously [11]. 150 g of the leaf powder was mixed with 2000 ml of 70% Ethanol in a flask and vigorously mixed. The mixture was kept in tightly sealed vessels for 72 hours at room temperature and constantly shaking. Whatman no 1 filter paper was used to filter the mixture and the solvent was removed from the filtrate at 28°C by evaporation in rotary vacuum evaporator and the recovered extract finally dried in air.

Phytochemical screening of *Sida acuta*

Phytochemical components of the leaf extract were screened using the appropriate chemical test as we described previously [11]. The components analysed were Alkaloids, Flavonoids, Saponins, Phenol, Tannins, Steroids, glycosides, Terpenoids, Phlobatannins and Cardiac glycosides.

Collection of test bacteria

The organism used in this study were reference bacterial isolates consisting of *Escherichia coli* (ATCC 43888), *Staphylococcus aureus* (ATCC 6538), *Pseudomonas aeruginosa* (ATCC 9027) and *Bacillus subtilis* (ATCC 6633). They were obtained from National Veterinary Research Institute (NVRI), Vom, Jos, Plateau State.

Preparation of extract concentrations

In a test tube, 3 g of leaf crude extract was dissolved in 10 ml of 10% Dimethyl Sulfoxide (DMSO) to obtain 300 mg/ml as the stock concentration. From the stock solution and using 10 % DMSO as a diluent, two-fold dilutions was used to obtain 150 mg/ml, 75 mg/ml and 37.5 mg/ml concentrations [12].

Standardisation of bacterial inoculums

The number of bacterial cells in the inoculums were standardised using the McFarland Scale No.1. The bacterial cells from overnight growth culture suspended separately, in 2 mL of sterile physiological saline. The turbidity of the bacterial suspensions were then adjusted to match that of 0.5 McFarland standards.

Antibacterial activity of crude extracts

The antibacterial activity of the ethanolic crude extract of leaves of *Sida acuta* against the reference, *S. aureus*, *E. coli*, *B. subtilis* and *P. aeruginosa* was determined using agar well diffusion method [13]. 100 µl of standardised bacterial suspension was inoculated (in triplicates) into MH agar. Using swab stick, the inoculum was spread evenly over the entire surface of the plates and allow to stay for 10 minutes, after which a sterile cork borer was used to dig wells of 9 mm. 100 µl 300 mg/ml, 150 mg/ml, 75 mg/ml and 37.5 mg/ml extract concentrations were each filled into the wells. DMSO was used as negative control and was used to fill in separated well in the plate. To ensure appropriate diffusion of the well content (extract) in to the agar, the plates were allowed to stay at room temperature for 10 minutes. The plates were then incubated for 24 hours at 37°C. For each bacteria tested and concentration, the zone of inhibition of growth was measured using a meter rule and the means were computed.

Determination of minimum inhibitory concentration (MIC)

Using broth dilution method as described in (Slue and Agbabiaka 2018), the MICs of crude extract the test bacteria. 1ml of the different concentrations () were added to separate tubes containing 9 ml of Mueller Hinton broth and 100 µl of the standardized bacterial inoculum. The test tube was incubated for 24 hours at 37°C, after which were observe for turbidity as indication of bacterial growth. The lowest concentration of extract which inhibited the growth of a test bacteria was recorded as the MIC. Negative and positive controls constituting of the broth and extract; and broth, inoculum, and ciprofloxacin, respectively were used.

Determination of minimum bactericidal concentration (MBC)

The MBC was determined by plate method as described by [14]. The tubes that yielded no growth from MIC were sub-cultured on nutrient agar plates for 24 hours at 37°C, after which were examined for growth. The tube with minimum concentration of extract, in which the growth was completely stopped was considered as the MBC.

Results and Discussion

The phytochemical screening carried out on the crude extract of *Sida acuta* leaves using qualitative methods, revealed the presence of many compounds as shown in Table 1, which include alkaloids, flavonoids, phenol, tannins, terpenoids, glycosides, cardiac glycosides, alkaloids, flavonoids, phenol, tannins, terpenoids, glycosides, cardiac glycosides steroids and phlobatannins. However, saponins were found to be absent. The phytochemicals detected in *S. acuta* leaf extract are similar to the compounds detected in many medicinal plants [15][16]. These phytochemicals are known to be biologically active and could confer antibacterial activities via various mechanisms. Alkaloids for example, being one of the compounds present in *Sida acuta* is one of the largest groups of phytochemicals in plants, with amazing effects in humans, which is used for development of a powerful pain killer medication [15].

One of the most common biological properties of alkaloids is their toxicity against cells of foreign organisms, which have been widely studied for their potential use in the elimination and reduction of human cancer cells [17]. Table 2 summarises the antibacterial activities of the plant extract against the test bacteria. The ethanolic extract was observed to produce visible zone of inhibition against all the four test bacteria and across all concentrations tested. The effect of the extract against all the test bacteria was found to be bactericidal with MIC and MBC values of 37.5 mg/ml and 75 mg/ml, respectively (Table 3). Being *E. coli* and *P. aeruginosa* Gram negative, and *B. subtilis* and *S. aureus* Gram positive, indicates the extract has broad spectrum activity. This could probably be the explanation why *S. acuta* is effective traditional treatment of tested bacterial infections.

E. coli was highly susceptible to the extract with mean zones of inhibition of 29.25 ± 0.35 , while *B. subtilis* was less susceptible to the extract with mean zones of inhibition of 21.50 ± 0 . The highest antibacterial activity was exhibited by the highest concentration of the extract (300 mg/ml). Also, it has been reported by [18] that the nature and composition of some biologically active components (saponins, alkaloids, phenol etc) are enhanced in the presence of ethanol due to the stronger extraction capacity as well as solubility of the compound in the solvent.

In addition, the differences in susceptibilities of bacterial isolates to varied concentrations of crude extracts of *S. acuta* could be attributed to mode of actions and structural properties of the bacteria. Ethanol leaf extract of *S. acuta* was active against both Gram positive and Gram negative bacteria as observed in this study. Gram positive bacteria (*Staphylococcus aureus* and *B. subtilis*) with no lipopolysaccharrides tend to allow more diffusion of the active components and Gram negative bacteria (*E. coli* and *P. aeruginosa*) possess lipopolysaccharrides that might have minimized penetration of active components of the extracts which shows the effectiveness of this plant. Similar antibacterial activities by ethanolic extract of various plant were also observed in many studies [16].

Table 1 Phytochemical Constituents of Ethanol leaf extract of *Sida acuta*

S/NO	Constituents	Test	Ethanolic Extract
1	Alkaloids	Mayer's	+
2	Flavonoids	Sodium hydroxide	+
3	Saponins	Frothing	-
4	Phenol	Ferric chloride	+
5	Tannins	Ferric chloride	+
6	Steroids	Sulphuric acid	+
7	Terpenoids	Salkowski	+
8	Cardiac glycosides	Keller Killani	+
9	Glycosides	Ferric chloride	+
10	Phlobatannins	HCL	+

Key: + = present, - = Absent

Table 2 Antibacterial Activity of *Staphylococcus aureus*, *Escherichia coli*, *Bacillus subtilis* and *Pseudomonas aeruginosa* to test concentration of Ethanol leaf extract of *Sida acuta*

Bacterial Isolates treated	Mean zone of Inhibition (mm)				
	37.5 mg/ml	75 mg/ml	150mg/ml	300mg/ml	Ciprofloxacin 50µg
<i>E. coli</i> (ATCC 43888)	13.50±1.41	20.50±0.71	24.50±1.41	29.25±0.35	35.00±0.00
<i>P. aeruginosa</i> (ATCC 9027)	12.25±1.77	20.50±0.00	21.00±0.71	22.50±1.41	28.00±0.00
<i>S. aureus</i> (ATCC 6538)	11.75±1.06	17.25±0.35	20.25±1.00	26.50±0.71	27.00±0.00
<i>B. subtilis</i> (ATCC 6633)	13.00±1.41	15.50±0.00	19.50±0.00	21.50±0.71	30. 00±0.00

KEY: Values are means ± Standard deviation

Table 4 Minimum Inhibitory Concentration (MIC) and Minimum Bactericidal Concentration (MBC) of Ethanol leaf Extract of *Sida acuta* against Reference isolates of bacteria

Bacteria	MIC (mg/ml)	MBC (mg/ml)
<i>E. coli</i>	37.50	75.00
<i>S. aureus</i>	37.50	75.50
<i>P. aeruginosa</i>	37.50	75.50
<i>B. subtilis</i>	37.50	75.50

Conclusion

The current study found that leaf extract of *Sida acuta* contains different phytochemicals including alkaloids, flavonoids, phenol, tannins, terpenoids, glycosides and cardiac glycosides. *In vitro* antibacterial assay shown the ethanolic plant extract to be active against *Escherichia coli*, *Staphylococcus aureus*, *Pseudomonas aeruginosa* and *Bacillus subtilis* with MIC and MBC of approximately 37.5 and 75mg/ml, respectively, suggesting it potential use for treatment of infectious diseases.

References

1. Calixto, J. B., Efficacy, safety, quality control, marketing and regulatory guidelines for herbal medicines (phytotherapeutic agents). *Brazilian Journal of Medical and Biological Research*, 2000. 33(2): p. 179–189.
2. Cunningham, A. B., P. Shanley, and S. Laird, Health, habitats and medicinal plant use. *Human health and forests: a global overview of issues, practice and policy*, 2008. p. 35–62.
3. Lekshmi, M., et al., The food production environment and the development of antimicrobial resistance in human pathogens of animal origin. *Microorganisms*, 2017. 5(1): p. 11
4. Tenover, F. C., Mechanisms of antimicrobial resistance in bacteria. *American Journal of Medicine*, 2006. 119 (6): p. S3–S10.
5. Tanwar, J., S. Das, Z. Fatima, and S. Hameed, Multidrug resistance: An emerging crisis. *Interdisciplinary Perspectives on infectious disease*. *Infect*, 2014. p. 1-7.
6. Mbajiuka, C., et al., The Antibacterial Activity of Leaf Extracts of *Ocimum Gratissimum* and *Sida Acuta*. *Journal of Dental Medical Sciences*. 2014. 13: p. 80–85.
7. Onajobi, F. D., Smooth muscle contracting lipid-soluble principles in chromatographic fractions of *Ocimum gratissimum*. *Journal of Ethnopharmacology*, 1986. 18(1): p. 3–11.
8. Tcheghebe, O. T., A. J. Seukep, and F. N. Tatong, Ethnomedicinal uses, phytochemical and pharmacological profiles, and toxicity of *Sida acuta*. *The Pharma Innovation*, 2017. 6(6): p. 1-6
9. Okigbo, R. N., and D. I. Igwe, Antimicrobial effects of *Piper guineense* ‘Uziza’ and *Phyllanthus amarus* ‘Ebe-benzo’ on *Candida albicans* and *Streptococcus faecalis*. *Acta Microbiologica and Immunologica Hungaria*, 2007. 54(4): p. 353–366.
10. Okwu, D. E. and O. Ekeke, Phytochemical screening and mineral composition of chewing sticks in South Eastern Nigeria. *Global Journal of Pure Applied Science*, 2003. 9(2): p. 235–238.
11. Hassan, M., et al., “Phytochemical analysis and antibacterial activity of fractions of *sida acuta* against some

- reference isolates of bacteria. *Science World Journal*, 2022. 17(1): p. 26–30.
12. Srinivasan, K., et al., Antibacterial, Preliminary Phytochemical and Pharmacognostical Screening on the Leaves of *Vicoa indica* (L.) DC. *Iranian Journal of Pharmacology and Therapeutics*, 2007. 6: p. 109-113.
 13. Bauer, A. W., et al., Antibiotic susceptibility testing by a standardized single disk method. *American Journal of Clinical Pathology*, 1966. 45(4): p. 493–496.
 14. Andrews, J. M. Determination of minimum inhibitory concentrations. *Journal of Antimicrobial Chemotherapy*. 2001. 48(1): p. 5–16.
 15. Musa, F. M., et al., “Antibacterial activities of ethanol leaf and bark extracts of *Terminalia avicennioides* against methicillin resistant *Staphylococcus aureus*. *Science World Journal*. 2020. 15(3): p. 119-123.
 16. Musa, F. M., et al., “Antimicrobial Activity of *Mitracarpus scaber* Leaf Extract against Some Human Pathogenic Microorganisms,” *African Sciences*, 2022. 22(1): p. 23-30.
 17. Akinpelu, D. A., A. O. Aiyegoro, and A. I. Okoh, Studies on the biocidal and cell membrane disruption potentials of stem bark extracts of *Azela africana* (Smith). *Biological Research*, 2009. 42(3): p. 339-349, 2009.
 18. Ncuba, N. S., A. Afolayan, and A. Okoh, “Assessment techniques of antimicrobial properties of natural compounds of plant origin: Current Methods and Future Trends. *African Journal Biotechnology*, 2008. 7: p. 1797–1806.

Turk S. and M. Ozacar, Nitrogen-Doped Carbon Quantum Dots-Gellan Gum As An Innovative Self-Healable Hydrogel Composite. *International Journal of Life Sciences and Biotechnology*, 2022. 5(3): p. 581-590. DOI: 10.38001/ijlsb.1143572

Nitrogen-Doped Carbon Quantum Dots-Gellan Gum As An Innovative Self-Healable Hydrogel Composite

Serbulent Turk^{1,2*} , Mahmut Ozacar^{2,3} 

ABSTRACT

Tension sensors can be widely applied to detect body movements and monitor physiological signals. Hydrogels with conductive properties draw attention among the studies in this field. However, their application is limited because hydrogels can be easily damaged during use. In this study, a self-healing conductive hydrogel was produced by adding nitrogen-doped carbon quantum dots (NCQDs) to gellan gum (GG) polymer. The self-healing property of the hydrogen bonds in the prepared polymeric matrix network to a certain extent and the conductivity were supported by the addition of NCQDs. The electrical recovery process of the hydrogel in the 1, 2, and 3 cut/healing cycles was illustrated by a visually designed LED bulb serial circuit. As a result of connecting the obtained 3D hydrogel to a real-time resistance change measurement system, the resistance changes in the cut/healing cycles were monitored. The duration of the total cut-healing process, including cut and contact time, was 2.12 s. In addition, a free-standing gel bridge was formed after joining the two cut pieces of cylindrical hydrogels. Due to the resulting hydrogel composite properties, it has promising potential in various applications such as personal health diagnosis, human activity monitoring, and human-motion sensors.

ARTICLE HISTORY

Received

13 Temmuz 2022

Accepted

1 Kasım 2022

KEYWORDS

Self-healable, hydrogel composite, conductivity

Introduction

Self-healing and recovery after damage is an essential feature of living tissues. In nature, biological systems can self-heal at both the molecular level (DNA repair) and the macroscopic level (healing of a graze or broken bone in the skin). Inspired by such systems, self-healing materials have been developed for various applications. Self-healing hydrogels, which can regain their structure and function after damage, have been developed as “smart” soft materials that can extend the persistence time and have attracted great interest recently. As a typical soft material with good viscoelasticity, transparency and biocompatibility properties, self-healing gels are increasingly being

¹ Sakarya University, Biomedical, Magnetic and Semiconductor Materials Application and Research Center (BIMAS-RC), 54187 Sakarya, Turkey

² Sakarya University, Biomaterials, Energy, Photocatalysis, Enzyme Technology, Nano & Advanced Materials, Additive Manufacturing, Environmental Applications and Sustainability Research & Development Group (BIOENAMS R & D Group), 54187 Sakarya, Turkey

³Department of Chemistry, Faculty of Science & Arts, Sakarya University, 54187, Sakarya, Turkey

*Corresponding Author: Gülfidan Kuyumcu, e-mail: serbulentturk@sakarya.edu.tr

investigated for its potential applications in tissue engineering, biomedicine, artificial intelligence, wearable devices and soft robotics [1].

While self-healing materials can recover their original state by healing the damage done to them, this healing process is driven by thermodynamic parameters and depends on dynamic/reversible chemical bonds or physical interactions. These interactions allow the material to be cut into pieces and reassembled after contact, and mechanical properties are restored by restructuring the gel network after the rheological deformation treatment. This property extends the life of materials and makes them ideal candidates for applications with repeated mechanical stress. Compared to conventional hydrogels, self-healing hydrogels can recombine and regain their initial structures and functions once damaged. Given their durability and long-term stability, self-healing hydrogels have emerged over the past few years as a promising material for many fragile hydrogels being used in preclinical or clinical trials. Looking at the hydrogels produced for use in the field of biotechnology and biomedicine; depending on the target tissue, self-healing hydrogels must conform to a wide variety of properties, including electrical, biological, and mechanical.

Wearable devices should maintain their structural properties after possible damages in the area where they are applied. After any damage, it can return to its original structural and functional state and add features that repair themselves, giving wearable devices more durability and a longer lifespan [2]. Due to this requirement, the self-healing feature in wearable devices has taken its place among the most sought-after features. In recent years, self-healable wearable devices, which can restore their functionality and structure after damage, have gained increasing interest [3–5]. Soft and flexible materials attract attention in the field of self-healing wearable devices. Self-healing materials as soft materials with properties such as biocompatibility and good viscoelasticity are frequently used in this field due to their potential applications in wearable devices, biomedicine, and artificial intelligence [6,7]. The field of materials with excellent electrical and biocompatibility properties and self-healing properties is still in its infancy. Based on this field, conductive hydrogels with good biocompatibility and high-water retention have attracted the attention of many researchers in recent years as promising materials [8–10]. Due to their conductivity and similarity to natural tissues, conductive hydrogels are applied in various applications such as biological tissue

engineering [11]. In addition, hydrogel-based wearable strain sensors connected to a wireless transmitter can wirelessly monitor and record body movements.

Gellan gum (GG) is a polymer that has potential applications in many areas recently due to its biocompatibility and functional reactive groups suitable for easy modification / functionalization of the polymer backbone. In fact, the major advantage of this biopolymer is its incredible versatility to be processed into new derivatives with different properties, making it possible to tailor its physicochemical and biological properties to suit the specific needs of a particular tissue [12]. GG is a versatile biopolymer that can be easily modified into new derivatives with different properties than the natural polymer, due to its free carboxyl and hydroxyl groups in its repeater unit. These different features, which are associated with high availability and low production costs, have made its application to different areas widespread. GG is an anionic microbial polysaccharide composed of repeat unit of two β -D-glucose, a β -D-glucuronic acid, and an α -L-rhamnose tetrasaccharide. GG is capable of physical gelation. Upon temperature drop, a random helix transition takes place with more aggregation of helices leading to the formation of junctional sites. The sol-gel transition of GG polymer is ionotropic. Therefore, the presence of cations in polymeric environment is necessary for the formation of a stable hydrogel.

Adding conductive nanomaterials such as graphene, carbon nanotubes, and metallic nanoparticles to the conductive polymers network is one widely used approach to obtaining hydrogel-based electronic skin and strain sensors [13–15]. New studies are still needed to increase the wearable technology field's material diversity and introduce more suitable materials.

In this study, nitrogen-doped carbon quantum dots/gellan gum (NCQDs/GG) hydrogel was obtained as an innovative self-healing hydrogel composite that can be a promising candidate for wearable sensors. Rapid self-healing feature was observed as a result of the addition of NCQDs added to affect the fast self-healing capacity of the nanocomposite hydrogel. With the addition of NCQDs, which increases the self-healing property of the composite hydrogel, a composite hydrogel with also conductivity was obtained.

Material and Methods

As previously reported [16], N-doped carbon quantum dots were synthesized using a green and convenient "oil bath" strategy. Briefly, for this process, 2 g of urea powder and 10 g of sucrose powder were added to 20 mL of cooking oil preheated at approximately 250°C and mixed for 5 min. After cooling to room temperature, 30 mL of purified water was added to the reaction system to transfer the N-CQDs to the aqueous phase. It was then centrifuged (HETTICH) for 15 min at 11000 rpm to remove any clumped particles. The oil, which is the upper phase in the reaction system, was removed with the help of a separatory funnel. NCQDs synthesized in aqueous solution stored at 4°C were lyophilized using a lyophilizer (BIOBASE) to obtain solid products. As a lyophilization step, it was first frozen at -20°C for 24 hours, then frozen at -60°C for 12 hours, and then lyophilized in a low pressure environment for freeze-drying.

Pure water preheated to 85°C and in a closed environment was pre-prepared for the preparation of GG solutions. Then, 2.0% (w/v) Gellan gum (GG, Sigma Aldrich) was added to the preheated distilled water and the solution was stirred at 85° for 15 min. Then, for the preparation of NCQDS/GG hydrogels, 5% (wt) of pre-synthesized NCQDs were added and mixing was continued for another 15 min at 85°C in closed containers to ensure homogeneity. It was observed that the color of the solution changed with the addition of NCQDs during this time. Prepared solutions were poured into pre-prepared cylindrical and cube-shaped molds while hot to obtain 3D hydrogel shapes and left to cool at room temperature. After waiting for about 2 h at room temperature, the hydrogel samples were removed from the molds and made ready for analysis. For self-renewal characterizations, hydrogels were cut into two parts with a scalpel and the cut surfaces were joined. Real-time resistance changes of 3D NCQDS/GG hydrogels obtained using the Keithley 2612A Source Meter were analyzed during cut/healing cycles.

Results and Discussion

One of the techniques in which the electrical self-renewal of the sample is demonstrated is to place the prepared sample into a series circuit [17–20]. As shown in Figure 1, a series circuit consisting of a light-emitting diode (LED) indicator and a commercial 3 V dry cell was set up to demonstrate the electrical recovery process of the hydrogel

visually. It is known that GG has good conductivity due to the ions such as Na^+ , K^+ , Ca^{2+} in its content and is effective in a led circuit in an established circuit [21]. The prepared hydrogels, which were divided into two parts and subjected to cut/healing processes 1, 2, and 3 times and integrated into the circuit, are shown in Figure 1a, b and c, respectively. It has been observed that when the bifurcated parts of the hydrogels with different cut/healing cycles come into contact with each other, the series circuit is completed, and the LED emits light of equivalent brightness. In addition, since it is known that human soft tissue has electrical conductivity [22], the conductivity of the hydrogels obtained for the biomedical field is also important.

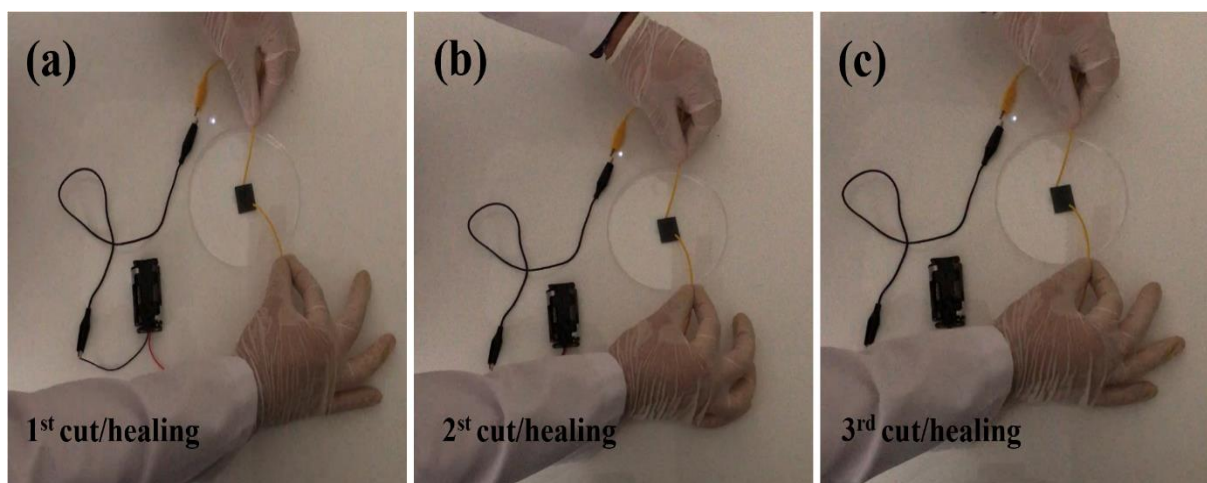


Fig 1 Self-healing behavior of a series-connected hydrogel in a designed LED lamp circuit after cut/healing operations. (a) after 1st cut/healing, (b) after 2nd cut/healing, and (c) after 3rd cut/healing

To further investigate the electrical recovery of the hydrogel, the NCQDs-GG hydrogel was connected to a real-time resistance change measurement system, and the resistance changes in the cut/healing cycles were monitored. As shown in Figure 2, the strength of the hydrogel was recorded over three cut/healing cycles performed with the polyester film slice. The hydrogel was repeatedly completely bifurcated at the same location, and the two separate pieces were soon joined together. Figure 2b shows the time evolution of real-time resistance change during the self-healing process. It was observed that the resistance of the hydrogel attached to the analyzer increased rapidly when cut by the polyester film slice. Then, the resistance value decreased rapidly with the removal of the polyester film. The resistance change of the hydrogel was observed to be relatively stable during the cut/healing cycle. The duration of the total cut/healing process,

including cut and contact time, was observed as 2.12 seconds. In Table 1, comparisons of the sample in the current study with some of the hydrogels in the literature are given. Overall, the results show that the hydrogel with added NCQDs has reproducible electrical self-healing property. Thanks to this feature, the hydrogel obtained for wearable electronics devices becomes an interesting material.

Samples with self-healable feature are materials that have the ability to regain their previous properties after cutting. In this respect, there are visuals in the literature showing that cylindrical samples can form a gel bridge without disintegrating after self-healable [28–31].

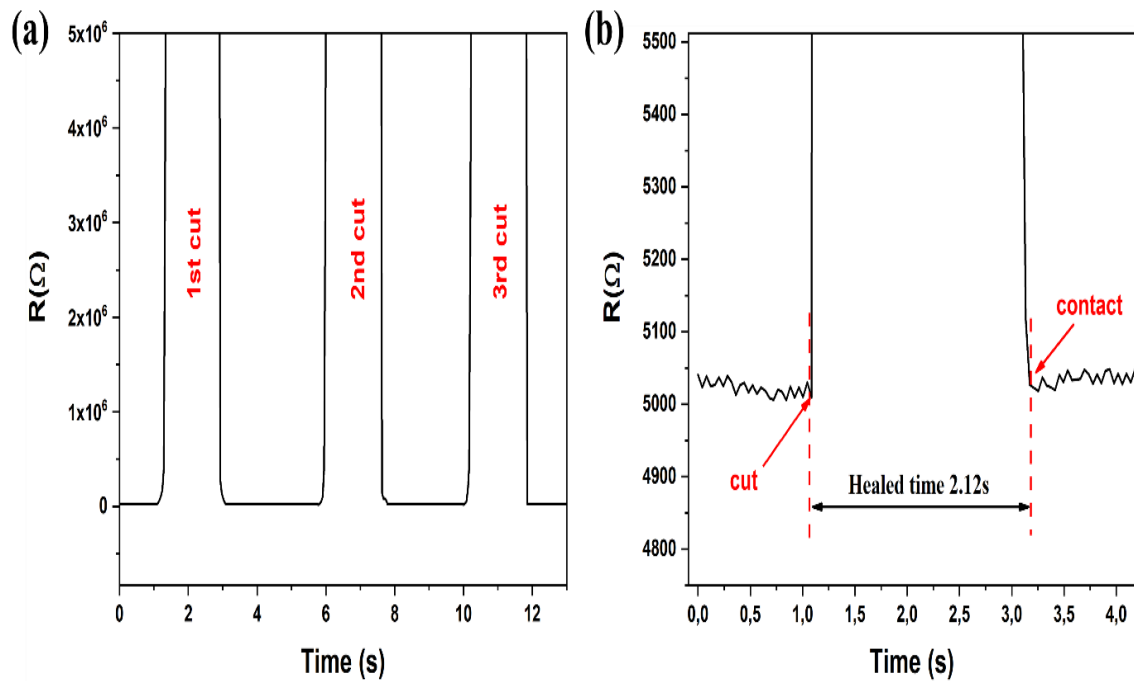


Fig 2 Time evolution of self-healing process by Real-time resistance measurements for NCQDs/GG hydrogel. (a) co-located cut/healing cycles, (b) regional magnified self-healing process

As shown in Figure 3, the two pieces separated after cutting were joined together, and the two bottle caps formed a free-standing gel bridge. Thus, it has been observed that they stick together as a single piece of self-healing gel.

Table 1 Comparison of the contents and cut/healing properties of some hydrogel studies in the literature with the current study

Hydrogel	Component	Cut/Healing Time	Ref.
L4S90	<ul style="list-style-type: none"> •[2-Methacryloyloxy ethyl]dimethyl-(3-sulfopropyl) ammonium hydroxide •2- hydroxyethyl methacrylate •Laponite XLG 	11s (including cut time)	[23]
PVA/PDA	<ul style="list-style-type: none"> •Polyvinyl alcohol •Polydopamine 	250 ms (including cut time)	[24]
PVA-PDA-pRGO	<ul style="list-style-type: none"> •Polyvinyl alcohol •Polydopamine •Graphene oxide 	4.2 s (after the contact moment)	[25]
CSH	<ul style="list-style-type: none"> •Polypyrrole •Poly(acrylic acid) •Chitosan 	30 s (including cut time)	[26]
SWCNT	<ul style="list-style-type: none"> •Single wall carbon nano-tube •Graphene •Silver nanowire 	3.2 s (after the contact moment)	[27]
NCQDs/GG	<ul style="list-style-type: none"> •Gellan Gum •Nitrogen-doped carbon quantum dots 	2.12s (including cut time)	This study

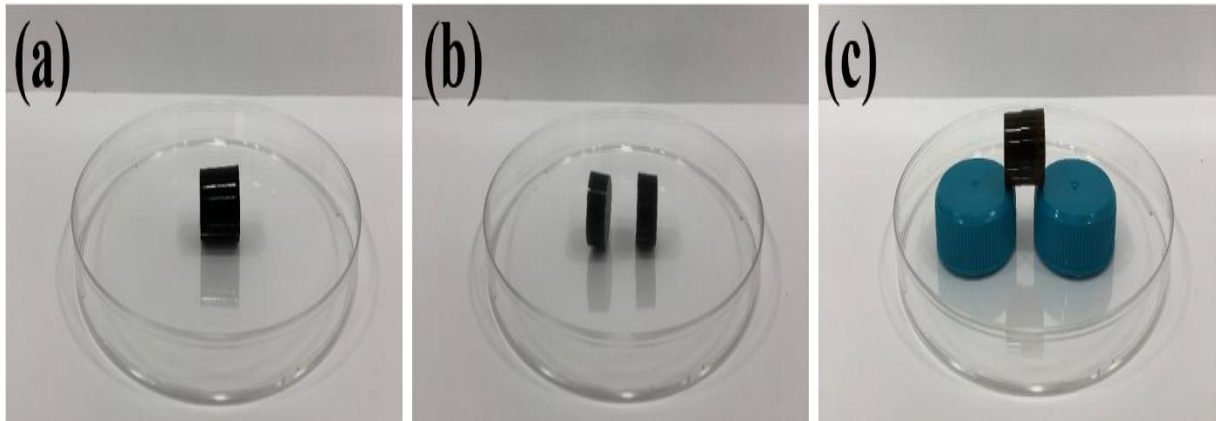


Fig 3 (a) Obtained cylindrical hydrogel (b) cut hydrogel blocks (c) self-healing cylindrical hydrogel sample able to form a bridge

Conclusion

In summary, an innovative self-healable NCQDS/GG hydrogel was produced by adding NCQDs to the hydrogel medium. It was observed that the conductive hydrogel was able to regenerate itself after the cut/healing cycles returned to their initial resistance. It was observed that the obtained hydrogels had reproducible self-healing properties after 2.12 s. For these reasons, there is great potential for the application of the NCQDS/GG hydrogel as a wearable body motion tension sensor to monitor body movements.

For future studies, it is planned by our group to analyze the recovery times in environments where external environmental conditions such as body sweat are imitated. In addition, the evaluation of sensitivity in the perception of under-eye, neck and pulse movements by using the existing hydrogel with an innovative composition is considered to be of great importance in terms of adding an additional innovation to the literature. By varying the NCQDs ratios in its content, hydrogels with adjustable conductivity can also be prepared and used in application areas such as drug-delivery system, bone regeneration, stimulation of tissue growth, artificial muscle.

Acknowledgements

This work was supported by the Scientific Research Projects Commission of Sakarya University (Project number: 2019-6-23-223).

References

1. Tu, Y., et al., Advances in injectable self-healing biomedical hydrogels. *Acta Biomaterialia*, 2019. 90(2019): p.1–20.
2. Mohan, AMV., et al., Recent advances and perspectives in sweat based wearable electrochemical sensors. *TrAC Trends in Analytical Chemistry*, 2020. 131(October 2020): p.116024.
3. Lu, C., et al., A tough hydrogel with fast self-healing and adhesive performance for wearable sensors. *Colloids and Surfaces A: Physicochemical and Engineering Aspects*, 2022. 632(2 January 2022): p.127793.
4. Wang, J., et al., Polysaccharide-based high-strength, self-healing and ultra-sensitive wearable sensors. *Industrial Crops and Products*, 2022. 178(April 2022): p.114618.
5. Jia, Y., et al., Highly efficient self-healable and robust fluorinated polyurethane elastomer for wearable electronics. *Chemical Engineering Journal*, 2022. 430(15 February 2022): p.133081.
6. Raho, R., et al., Reusable flexible dry electrodes for biomedical wearable devices. *Sensors and Actuators A: Physical*, 2022. 333(1 January 2022): p.113157.
7. Liu, W., et al., A novel anisotropic saturation magnetization phenomenon in flexible Mn-doped BiFeO₃ thin films for wearable device. *Journal of Magnetism and Magnetic Materials*, 2022. 551(1 June 2022): p.169134.
8. Wang, H., et al., Stretchable, freezing-tolerant conductive hydrogel for wearable electronics reinforced by cellulose nanocrystals toward multiple hydrogen bonding. *Carbohydrate Polymers*,

2022. 280(15 March 2022): p.119018.
9. Wang, J., et al., Tannic acid-Fe³⁺ activated rapid polymerization of ionic conductive hydrogels with high mechanical properties, self-healing, and self-adhesion for flexible wearable sensors. *Composites Science and Technology*, 2022. 221(12 April 2022): p.109345.
 10. Zhang, C., et al., Highly adhesive and self-healing γ -PGA/PEDOT:PSS conductive hydrogels enabled by multiple hydrogen bonding for wearable electronics. *Nano Energy*, 2022. 95(May 2022): p.106991.
 11. Distler, T. and Boccaccini, AR., 3D printing of electrically conductive hydrogels for tissue engineering and biosensors – A review. *Acta Biomaterialia*, 2020. 101(1 January 2020): p.1–13.
 12. Lv, Y., et al., Locust bean gum/gellan gum double-network hydrogels with superior self-healing and pH-driven shape-memory properties. *Soft Matter* 2019;15(Jul): p.6171– 6179.
 13. Guan, R., et al., Understanding the sensitivity of thin-film graphene/polymer nanocomposite strain sensors to ultrasonic waves: Analytical and experimental analysis. *Composites Science and Technology*, 2021. 216(10 November 2021): p.109079.
 14. Sankar, V., K. Balasubramaniam, and R. Sundara, Insights into the effect of polymer functionalization of multiwalled carbon nanotubes in the design of flexible strain sensor. *Sensors and Actuators A: Physical*, 2021. 322(1 May 2021): p.112605.
 15. Idumah, CI., Novel trends in conductive polymeric nanocomposites, and bionanocomposites. *Synthetic Metals*, 2021. 273(March 2021): p.116674.
 16. Liu, X., et al., N-Doped carbon dots: green and efficient synthesis on a large-scale and their application in fluorescent pH sensing. *New Journal of Chemistry*, 2017. 41(Aug): p.10607–10612.
 17. Jing, X., et al., Highly Stretchable and Biocompatible Strain Sensors Based on Mussel-Inspired Super-Adhesive Self-Healing Hydrogels for Human Motion Monitoring. *ACS Applied Materials Interfaces*, 2018. 10(24): p.20897–909.
 18. Xia, S., et al., A flexible, adhesive and self-healable hydrogel-based wearable strain sensor for human motion and physiological signal monitoring. *Journal of Materials Chemistry B*, 2019. 7(Jun): p.4638–48.
 19. Wang, Z. and Q. Pan, An Omni-Healable Supercapacitor Integrated in Dynamically Cross-Linked Polymer Networks. *Advanced Functional Materials*, 2017. 27(April): p.1–8.
 20. Jing, X., et al., Biocompatible, self-healing, highly stretchable polyacrylic acid/reduced graphene oxide nanocomposite hydrogel sensors via mussel-inspired chemistry. *Carbon*, 2018. 136(September 2018): p.63–72.
 21. Liu, S., et al., Highly Stretchable and Self-Healing Strain Sensor Based on Gellan Gum Hybrid Hydrogel for Human Motion Monitoring. *ACS Applied Polymer Materials*, 2020. 2(3): p.1325–34.
 22. MacDonald, RA., et al., Carbon nanotubes increase the electrical conductivity of fibroblast-seeded collagen hydrogels. *Acta Biomaterialia*, 2008. 4(6): p.1583–92.
 23. Wang, L., et al., Tough, Adhesive, Self-Healable, and Transparent Ionically Conductive Zwitterionic Nanocomposite Hydrogels as Skin Strain Sensors. *ACS Applied Materials Interfaces*, 2019. 11(3): p.3506–15.
 24. Liu, S., et al., A compliant, self-adhesive and self-healing wearable hydrogel as epidermal strain sensor. *Journal of Materials Chemistry C*, 2018. 6(Mar): p.4183–90.
 25. Wang, M., et al., A fast self-healing and conductive nanocomposite hydrogel as soft strain sensor. *Colloids and Surfaces A: Physicochemical and Engineering Aspects*, 2019. 567(20 April 2019): p.139–49.
 26. Darabi, MA., et al., Skin-Inspired Multifunctional Autonomic-Intrinsic Conductive Self-Healing Hydrogels with Pressure Sensitivity, Stretchability, and 3D Printability. *Advanced Materials*, 2017. 29(31): p.1–8.
 27. Cai, G., et al., Extremely Stretchable Strain Sensors Based on Conductive Self-Healing Dynamic

- Cross-Links Hydrogels for Human-Motion Detection. *Advanced Science*, 2017. 4 (2): p. 1600190.
28. Yan, L., et al., Self-healing supramolecular heterometallic gels based on the synergistic effect of the constituent metal ions. *Chemical Communications*, 2015. 51(Oct):p.17627– 17629.
 29. Biswas, S., DB. Rasale, and AK. Das, Blue light emitting self-healable graphene quantum dot embedded hydrogels. *RSC Advances*, 2016. 6(May):p.54793–800.
 30. Liu, S. and L. Li, Ultrastretchable and Self-Healing Double-Network Hydrogel for 3D Printing and Strain Sensor. *ACS Applied Materials and Interfaces*, 2017. 9(31): p.26429–37.
 31. Karan, CK. and M. Bhattacharjee, Self-Healing and Moldable Metallogels as the Recyclable Materials for Selective Dye Adsorption and Separation. *ACS Applied Materials and Interfaces*, 2016. 8(8): p.5526–35.

Koprululu Kucuk, G. and N. I. Giritlioglu, Homology Modeling of L18F Mutation on SARS-CoV-2 Spike Protein Receptor-Binding Domain. International Journal of Life Sciences and Biotechnology, 2022. 5(3): p. 591- 601. DOI: 10.38001/ijlsb.1159060

Homology Modeling of L18F Mutation on SARS-CoV-2 Spike Protein Receptor-Binding Domain

Gizem Koprululu Kucuk^{1*} , Nazlı Irmak Giritlioglu² 

ABSTRACT

Proteins have unique properties to participate in many structural and physiological processes. Knowledge of the three-dimensional structure of proteins is important to understand their roles in the physiological processes and the functions of these processes. Any structural defect in proteins due to mutations can cause diseases, treatment unresponsiveness, and drug resistance development. The recent emergence of the new SARS-CoV-2 variants containing mutations that accelerate the spread of the virus by affecting infectiousness has been of concern. In the study, visualization of the homology model and investigation of the chemical properties of L18F mutation responsible for the formation of mutant type SARS-CoV-2 spike protein via *in silico* approach was intended. In this study, amino acid number, molecular weight, theoretical pI value, the percentage composition of amino acids, total negatively charged residue number, total positively charged residue number, atomic composition, formula, total atomic number, molar extinction coefficient, aliphatic index, and the average hydrophathy were calculated via ProtParam. The FASTA amino acid sequence was used for visualization of the homology models via UCSF Chimera in wild-type and mutant-type spike proteins. Basic chemical calculations also were displayed on BIOVIA Discovery Studio Visualizer. $\Delta\Delta G$ value and the changes in the stability in L18F mutation were predicted via I-Mutant Suite software. We detected that location of the mutant residue is near a highly conserved position and the L18F mutation may not cause the damage.

ARTICLE HISTORY

Received

8 August 2022

Accepted

2 November 2022

KEYWORDS

in silico,
spike protein,
homology
modeling,
SARS-CoV-2,
mutation

Introduction

Proteins are molecules that participate in many physiological processes and are found in all organisms. Proteins participate in many physiological processes such as cell structure, cell viability, cell signals, ligand binding, and enzyme catalysis [1]. All proteins consist of amino acid sequences called polypeptide chains. In proteins in biological organisms, there are 20 types of amino acids with different characteristics, all of which have a common central carbon atom, an amino group, and a carboxyl group [2]. Each amino acid has its

¹ Department of Radiotherapy, Istanbul Sisli Vocational School Istanbul, Turkey

² Department of Molecular Biology and Genetics, Graduate School of Science and Engineering, Yildiz Technical University, Istanbul, Turkey

*Corresponding Author: Gizem Koprululu Kucuk, e-mail: gzm0507@gmail.com

properties [3]. The three-dimensional structure (3D) is important for understanding protein structure [4]. The specific order of amino acids determines the 3D structure of a protein [5]. The folding of a protein into a certain conformation depends on physicochemical properties such as hydrogen bonds, ionic interactions, Van der Waals forces and hydrophobic interactions, and covalent interactions between amino acids [6]. The amino acid sequence determines how these interactions occur. The way a protein folds also depends on environmental influences such as the presence of water or lipids and the pH of the environment [7]. Knowing this structure is vital in understanding the function of the protein. Changing any amino acid can disrupt the entire structure or function of the protein by disrupting the protein and its environment, as well as the forces of interaction within the protein [8].

Knowing the three-dimensional structure of proteins is important in understanding their role in the physiological process and the functioning of this process [9]. Three-dimensional structures of proteins can be revealed by various experimental studies. However, besides these experimental studies, there are also important developments in studies on determining the three-dimensional structural models of proteins using bioinformatics methods. Any structural defect in proteins due to mutations can cause diseases, treatment unresponsiveness, and drug resistance development [10].

The emergence of new variants of SARS-CoV-2, which have emerged recently and contain mutations that affect transmissibility and accelerate the spread of the virus, has been a matter of concern [11]. Especially with the identification of two independent strains that emerged in the United Kingdom and South Africa, studies on the detection of new mutations gained momentum. SARS-CoV-2 strains B.1.1.7 emerged in the UK (HV 69-70 deletion, Y144 deletion, N501Y, A570D, P681H, T716I, S982A, D1118H) and B.1.351 in South Africa (L18F, D80A, D215G, R246I, K417N, E484K, N501Y, and A701V) were detected in the spike protein receptor binding site (RBD) [12].

Within the scope of the study, homology modelling studies of the L18F mutation responsible for the formation of mutant type coronavirus occurring in the receptor-binding domain (RBD) of spike protein by Swiss Model and amino acid number, molecular weight,

theoretical pI value, the percent composition of amino acids, the total amino acid content of wild and mutant type were calculated via ProtParam.

Materials and Methods

The L18F mutation was detected in the B chain in the receptor-binding domain (RBD) of the spike protein of the Sars CoV2 virus that causes Severe Acute Respiratory Syndrome (SARS). The homology model of L18F mutation was created by bioinformatics tools. In the study, the Uniprot website and GenBank database of the National Center for Biotechnology Information (USA, NCBI) website were used detection of the amino acid sequence of the SARS CoV2 spike RBD protein [13]. Sequence information was arranged according to wild type and mutant type. Homology models of Spike protein types (wild and mutant types) were created with the Swiss Model Program which is a web-based bioinformatics tool, and the obtained three-dimensional models were examined with the UCSF Chimera program which is a visualization tool [14, 15]. Physico-chemical properties of models were obtained by ExPASy-ProtParam which is a bioinformatic tool and results were evaluated. sequence with accession numbers P0DTC2 was used for wild type in this study [16].

Swiss model analysis

The homology modelling study was carried out using Swiss-Model [17] database and the Chimera program. Wild and mutant type sequence sets were loaded into the system separately and their three-dimensional structures were obtained. The selection was made by looking at the Qualitative Model Energy Analysis (QMEAN) values of the three-dimensional structures obtained.

Homology Modelling by Chimera Program

Using UCSF Chimera program tools, all proteins were superimposed with each other, and visualization of three-dimensional structures was provided. The structural differences of the mutant protein were observed by visualizing the wild-type and mutant protein structures with a ribbon display.

Detection of Physico-chemical Properties

In the study, the Physico-chemical properties of Spike protein were calculated to understand the functional diversity. For this purpose, the ProtParam program of the ExPASy database, which is one of the bioinformatics tools, was used. FASTA formats of wild and mutant types were obtained on the GeneBank database. Physico-chemical properties of models were calculated. In both models (wild and mutant type); amino acid number, molecular weight, theoretical pI value, the percent composition of amino acids, total number of negatively charged residues, the total number of positively charged residues, atomic composition, formula, total atomic number, molar extinction coefficient, aliphatic index, and average hydropathy were calculated.

Result and Discussion

In homology modelling, protein sequence and three-dimensional structure information previously obtained by methods such as X-ray are used. Although a nature-like structure is not fully met in modelling, these studies are of great importance for clinical drug development studies. Mutations occurring in the RBD region are an important issue affecting sustained ligand binding and thus virus infectivity [18]. The changes caused by these mutations on the binding surface give us information about the degree of danger of the variation.

The amino acid sequence format that will be used as a basis in bioinformatics studies has been created based on the NCBI-P30518 accession number sequence. These arranged sequence sets were used to create the three-dimensional structure and extract the physico-chemical properties of the models. The sequence of wild-type and mutant-type proteins is shown in Figures 1 and 2.

Wild Type

```

MFVFLVLLPL VSSQCVNLTT RTQLPPAYTN SFTRGVYYPD KVFRSSVLHS
TQDLFLPFFS NVTWFHAIHV SGTNGTKRFD NPVLPFNDGV YFASTEKSNI
IRGWIFGTTL DSKTQSLIIV NNATNVVIKV CEFQFCNDPF LGVYYHKNNK
SWMESFRVY SSANNCTFEY VSQPFIMDLE GKQGNFKNLR EFVFKNIDGY
FKIYSKHPTI NLVRDLPQGF SALEPLVDLP IGINITRFQT LLALHRSYLT
PGDSSSGWTA GAAAYYVGYL QPRTFLLKYN ENGTITDAVD CALDPLSETK
CTLKSFTVEK GIYQTSNFRV QPTESIVRFP NITNLCPFGE VFNATRFASV
YAWNRRKRIS CVADYSVLYN SASFSTFKCY GVSPTKLNLD CFTNVYADSF
VIRGDEVROI APGQTGKIAD YNYKLPDDFT GCVIAWNSNN LDSKVGGNYN
YLYRFRKSN LKPFERDIST EIIYQAGSTPC NGVEGFNCYF PLQSYGFQPT
NGVGYQPYRV VVLSFELLHA PATVCGPKKS TNLVKNKCVN FNFNGLTGTG
VLTESNKKFL PFQQFGRDIA DTTDAVRDPQ TLEILDITPC SFGGVSVITP
GTNTSNQVAV LYQDVNCTEV PVAIHADQLT PTWRVYSTGS NVFQTRAGCL
IGAHEVNNSY ECDIPIGAGI CASYQTQNS PRRARVASQ SIIAYTMSLG
AENSVAYSNN SIAIPTNFTI SVTTEILPVS MTKTSVDCTM YICGDSTEC
NLLQYGSFC TQLNRALTGI AVEQDKNTQE VFAQVKQIYK TPKIKDFGGF
NFSQILPDP KPSKRSPED LFNKVTLDL AGFIKQYGDG LGDIAARDLI
CAQKFNGLTV LPPLLTDEMI AQYTSALLAG TITSGWTFGA GAALQIPFAM
QMAYRFNGIG VTQNVLYENQ KLIANQFNSA IGKIQDSLSS TASALGKLQD
VVNQNAQALN TLVKQLSSNF GAISSVLNDI LSRLDKVEAE VQIDRLITGR
LQSLQTYVTQ QLIRAAEIRA SANLAATKMS ECVLGQSKRV DFCGKGYHLM
SFPQSAPHGV VFLHVTYVPA QEKNTTAPA ICHDGKAHFP REGVFSVNGT
HWFVTQRNFY EPQIITDNT FVSGNCDVVI GIVNNTVYDP LQPELDSFKE
ELDKYFKNHT SPDVDLGDIS GINASVVNIQ KEIDRLNEVA KNLNESLIDL
QELGKYEQYI KWPWYIWLGF IAGLIAIVMV TIMLCCMTSC CSCCLKGCCSC
GSCCKFDEDD SEPVLKGVKL HYT

```

Fig 1 Wild-type sequence for the formation of the three-dimensional structure

L18F Mutation

```

MFVFLVLLPL VSSQCVNFTT RTQLPPAYTN SFTRGVYYPD KVFRSSVLHS
TQDLFLPFFS NVTWFHAIHV SGTNGTKRFD NPVLPFNDGV YFASTEKSNI
IRGWIFGTTL DSKTQSLIIV NNATNVVIKV CEFQFCNDPF LGVYYHKNNK
SWMESFRVY SSANNCTFEY VSQPFIMDLE GKQGNFKNLR EFVFKNIDGY
FKIYSKHPTI NLVRDLPQGF SALEPLVDLP IGINITRFQT LLALHRSYLT
PGDSSSGWTA GAAAYYVGYL QPRTFLLKYN ENGTITDAVD CALDPLSETK
CTLKSFTVEK GIYQTSNFRV QPTESIVRFP NITNLCPFGE VFNATRFASV
YAWNRRKRIS CVADYSVLYN SASFSTFKCY GVSPTKLNLD CFTNVYADSF
VIRGDEVROI APGQTGKIAD YNYKLPDDFT GCVIAWNSNN LDSKVGGNYN
YLYRFRKSN LKPFERDIST EIIYQAGSTPC NGVEGFNCYF PLQSYGFQPT
NGVGYQPYRV VVLSFELLHA PATVCGPKKS TNLVKNKCVN FNFNGLTGTG
VLTESNKKFL PFQQFGRDIA DTTDAVRDPQ TLEILDITPC SFGGVSVITP
GTNTSNQVAV LYQDVNCTEV PVAIHADQLT PTWRVYSTGS NVFQTRAGCL
IGAHEVNNSY ECDIPIGAGI CASYQTQNS PRRARVASQ SIIAYTMSLG
AENSVAYSNN SIAIPTNFTI SVTTEILPVS MTKTSVDCTM YICGDSTEC
NLLQYGSFC TQLNRALTGI AVEQDKNTQE VFAQVKQIYK TPKIKDFGGF
NFSQILPDP KPSKRSPED LFNKVTLDL AGFIKQYGDG LGDIAARDLI
CAQKFNGLTV LPPLLTDEMI AQYTSALLAG TITSGWTFGA GAALQIPFAM
QMAYRFNGIG VTQNVLYENQ KLIANQFNSA IGKIQDSLSS TASALGKLQD
VVNQNAQALN TLVKQLSSNF GAISSVLNDI LSRLDKVEAE VQIDRLITGR
LQSLQTYVTQ QLIRAAEIRA SANLAATKMS ECVLGQSKRV DFCGKGYHLM
SFPQSAPHGV VFLHVTYVPA QEKNTTAPA ICHDGKAHFP REGVFSVNGT
HWFVTQRNFY EPQIITDNT FVSGNCDVVI GIVNNTVYDP LQPELDSFKE
ELDKYFKNHT SPDVDLGDIS GINASVVNIQ KEIDRLNEVA KNLNESLIDL
QELGKYEQYI KWPWYIWLGF IAGLIAIVMV TIMLCCMTSC CSCCLKGCCSC
GSCCKFDEDD SEPVLKGVKL HYT

```

Fig 2 Mutant-type sequence for the formation of the three-dimensional structure

3D structures of the spike protein were obtained by using wild and mutant-type sequence sets. 3D structure of Spike protein homology modelling was performed using the Swiss-Model (www.swissmodel.expasy.org) database and the Chimera program, By examining the QMEAN values of the three-dimensional structures obtained, high models were selected and used as models (Table 1). We used the P0DTC2 accession number sequence for the wild type as the basis. The selection was made by evaluating the QMEAN values of the 3D structures obtained as a result of Swiss Homology modelling. The QMEAN for the wild type was detected at -1.59 and the mutant type was detected at -1.58.

Table 1 QMEAN values of the models that homology modeling was built by Swiss-Model

	QMEAN
Wild-type	-1,59
L18F	-1,58

Basic chemical calculations were displayed on BIOVIA Discovery Studio Visualizer (Table 2). Leucine is a more hydrophobic amino acid than phenylalanine (Hydrophobicity values are 3.8 and 2.8, respectively). Protein-ligand binding needs hydrophobic interactions. L18F mutation at the RBD site of the spike protein gains more hydrophilic character to the protein. Changing the stability and $\Delta\Delta G$ value in L18F mutation was predicted via I-Mutant software. The conditions were selected as 25°C, pH: 7.0 (default settings), and the software showed that the stability of the mutant spike protein decreased. Also, the graph of temperature- $\Delta\Delta G$ was created in Microsoft Excel. According to the data, $\Delta\Delta G$ is increased when the temperature is decreased. The increased temperature causes a more unstable mutation at the B: 18F site.

Table 2 Calculation of hydrophobicity by BIOVIA Discovery Studio Visualizer

	Full name	Hydrophobicity	Secondary structure
Wild-type	B:Leu18	3.8	Coil
Mutant-type	B:Phe18	2.8	Coil

Also HOPE web service was utilized for determining the structural effects of the mutant protein in this study. The location of the mutant residue is near a highly conserved position and L18F mutation may not cause damage. Receptor-ligand interactions could be changed negatively in the structural base because the mutant residue is bigger than the wild-type residue. The amino acid change was detected for the mutant type (Figure 3).

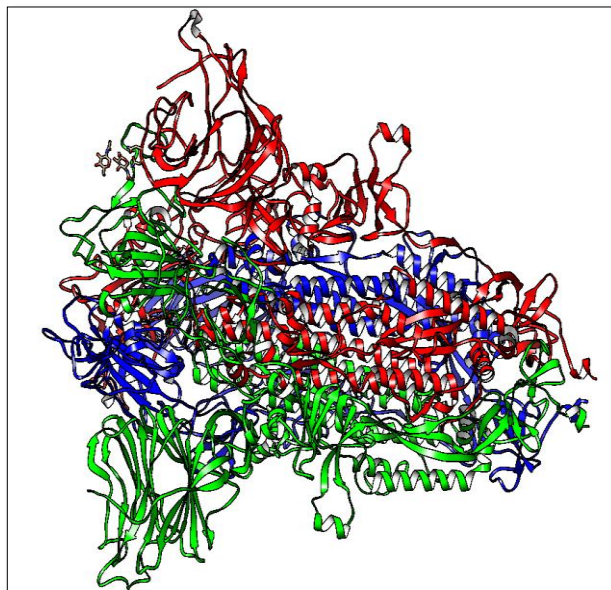


Fig 3 Wild-type ribbon structure

The change in the receptor-binding domain of the mutant type Spike protein is shown in Figure 4. The amino acid Leucine at position 18 in the wild-type receptor-binding domain of the spike protein was converted to mutant-type as phenylalanine. When the ribbon structure of both models was examined, conformational change was not observed.

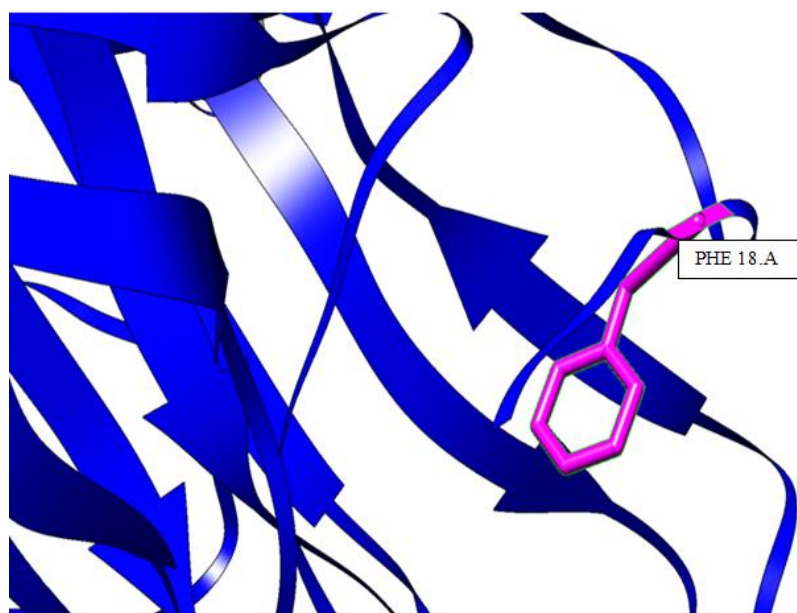
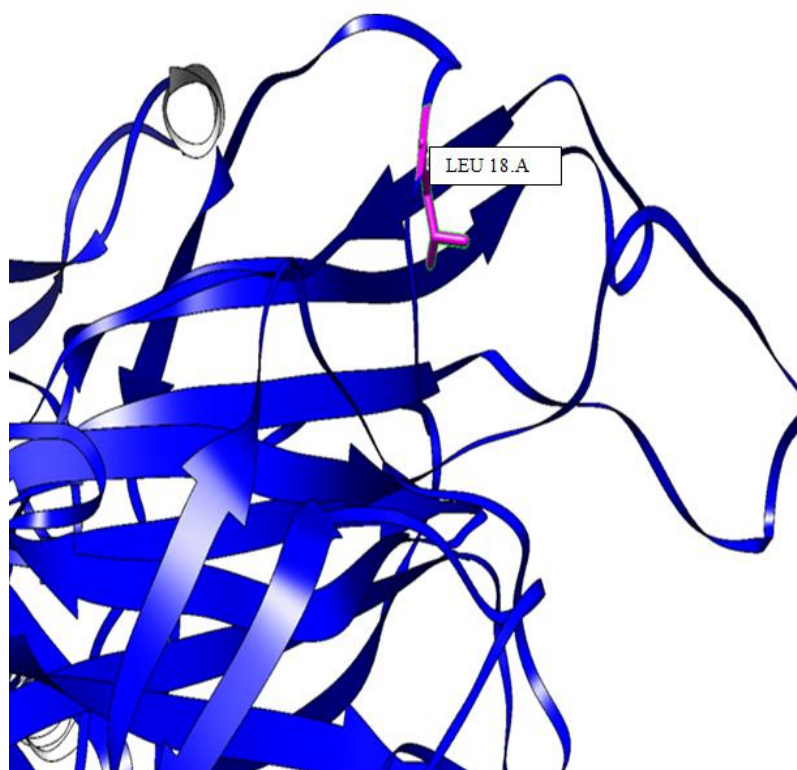


Fig 4 Amino acid changes

Leucine is a more hydrophobic amino acid than phenylalanine (Hydrophobicity values are 3.8 and 2.8, respectively). Protein-ligand binding needs hydrophobic interactions. L18F

mutation at the RBD of the spike protein gains more hydrophilic character to the protein. Also HOPE web service was utilized for determining the structural effects of the mutant protein in this study. The location of the mutant residue is near a highly conserved position and L18F mutation may not cause damage. Receptor-ligand interactions could change negatively in the structural base because the mutant residue is bigger than the wild-type residue.

Travel restrictions have been imposed in most countries since the pandemic was declared. However, the SARS-CoV-2 virus continued to mutate. New SARS-CoV-2 variants occurred and continued to spread across continents.

Substitution of phenylalanine with aromatic ring instead of leucine with aliphatic chain impairs steric elasticity in the protein chain. It may cause the ligand not to cleave. It breaks conformational elasticity sterically. Aromatic rings increase stability [19]. As the increased stability also strengthens the ligand-protein bonds, continuous binding takes place. This increases the damage of the mutation. It is a negative situation in methods such as xray in the study of protein ligand interactions. Because the relaxed structure of the protein cannot be visualized. There is no such disadvantage in homology modelling [20].

In a study, Kuzmina A. et al. detected that the L18F mutation (B. 1. 351 variant) is more resistant to greater infectivity and antibody neutralization [21]. Moreover, they showed that when K417T/E484K mutants were compared with L18F, it was detected that these mutants resisted the post-vaccination serum neutralization similarly to L18F.

On the contrary, Thomson EC. et al. found that N439K facilitated resistance to antibody neutralization [22]. Boon S. et al. speculated that N439S, T478S, and N501K mutations gave the virus a chance to infect host cells more efficiently and with low antigenicity. They detected that these mutations allow SARS-Cov2 to enter the host cell easily and make it easier to infect the cell [23].

Shahhosseini N. et al. used the SWISS-MODEL database to create homology models for SARS-CoV-2 Spike protein mutants [24]. We also used the SWISS-MODEL database for homology modelling. However, we cannot obtain hydrophobic interactions, hydrophobic structure, or atom-bond visualizing for protein by SWISS-MODEL. Because of this situation, we used the Chimera program and we backed up our models with Chimera.

Conclusion

Detection of the effects of changes in the protein sequences of the SARS-CoV-2 virus is an important element in determining the spread and severity of COVID-19. In particular, since spike protein is closely related to receptor proteins such as ACE2, FURIN, and TMPRSS2 in humans, it is extremely necessary to determine the rate and direction of change in this protein. The change from leucine to phenylalanine at amino acid 18 is found in the VOC strain that has a replicative advantage, and it is clear that such mutations result in subspecies with novel properties. When we consider the drug development process from a technological point of view, vaccine studies against COVID-19 are at the beginning and it is a matter of debate whether they are sufficient against variants. We think that it is important to model all newly formed variants just like in our study and to examine them from all chemical aspects. In addition to our *in silico* study, performing *in vitro* studies will be important in terms of understanding the beta coronavirus species and subspecies that are likely to occur in the future.

References

1. Lee, M. J., and M.B. Yaffe, Protein regulation in signal transduction. Cold Spring Harbor Perspectives in Biology, 2016. 8(6).
2. Alberts, B., A. Johnson, and J. Lewis, The Shape and Structure of Proteins. 2002, United States: Molecular Biology of the Cell.
3. Lopez, M J. and S.S. Mohiuddin, Biochemistry; Essential Amino Acids. StatPearls. Retrieved, 2020.
4. Schmidt, T., A. Bergner, and T. Schwede, Modelling three-dimensional protein structures for applications in drug design. Drug Discovery Today Elsevier Ltd., 2014.
5. Suryanto, C. H., H. Saigo, and K. Fukui, Structural Class Classification of 3D Protein Structure Based on Multi-View 2D Images. IEEE/ACM Transactions on Computational Biology and Bioinformatics, 2018. 15(1): p. 286–299.
6. Englander, S. W., and L. Mayne, The nature of protein folding pathways. Proceedings of the National Academy of Sciences of the United States of America. National Academy of Sciences, 2014.
7. Sun, P. D., C.E. Foster, and J.C. Boyington, Overview of protein structural and functional folds. Current Protocols in Protein Science, 2004.
8. Fuentes-Prior, P., and G.S. Salvesen, The protein structures that shape caspase activity, specificity, activation, and inhibition. Biochemical Journal, 2004.
9. Torrisi, M., G. Pollastri, and Q. Le, Deep learning methods in protein structure prediction. Computational and Structural Biotechnology Journal, 2020.

10. Longley, D. B., and P. G. Johnston, Molecular mechanisms of drug resistance. *Journal of Pathology*, 2005.
11. Khandia, R., et al., Emergence of SARS-CoV-2 Omicron (B.1.1.529) variant, salient features, high global health concerns and strategies to counter it amid ongoing COVID-19 pandemic. *Environmental Research*, 2022.
12. Naveca, F., et al., Phylogenetic relationship of SARS-CoV-2 sequences from Amazonas with emerging Brazilian variants harboring mutations E484K and N501Y in the Spike protein. *Virological*, 2021. p. 1–12.
13. <https://www.ncbi.nlm.nih.gov/> Access date: 15.06.2022.
14. Waterhouse, A., et al., SWISS-MODEL: homology modelling of protein structures and complexes. *Nucleic Acids Research*, 2018. p.296-303
15. Pettersen, EF, et al., UCSF Chimera—A Visualization System for Exploratory Research and Analysis. *Journal of Computational Chemistry*, 2004. 25(13): p.1605-12.
16. Gasteiger, E., et al., Protein Identification and Analysis Tools on the ExPASy Server, J.M. Walker, Editor. 2005, Humana Press. U.S.: U.S. p. 571-607.
17. www.swissmodel.expasy.org. Access date: 15.06.2022.
18. <https://bmcmolcellbiol.biomedcentral.com/articles/10.1186/s12860-021-00403-4>, Accessed: 18.10.2022 .
19. Biancalana, M., et al., Aromatic cluster mutations produce focal modulations of β -sheet structure. *Protein Science*, 2015. 24(5): p. 841–849.
20. Celej, MS., G.G. Montich, and G.D. Fidelio, Protein stability induced by ligand binding correlates with changes in protein flexibility. *Protein Science*, 2003. 12(7): p. 1496–1506.
21. Kuzmina, A., et al., SARS-CoV-2 spike variants exhibit differential infectivity and neutralization resistance to convalescent or post-vaccination sera. *Cell Host Microbe*, 2021. 29:p. 522–528.
22. Thomson, EC., et al., COVID-19 Genomics UK (COG-UK) Consortium, et al. Circulating SARS-CoV-2 spike N439K variants maintain fitness while evading antibody-mediated immunity. *Cell*, 2021. 184: p. 1171–1187.
23. Boon, S. S., et al., Temporal-Geographical Dispersion of SARS-CoV-2 Spike Glycoprotein Variant Lineages and Their Functional Prediction Using in Silico Approach. *American Society for Microbiology*, 2021. 12(5).
24. Shahhosseini, N., et al., Mutation signatures and in silico docking of novel sars-cov-2 variants of concern. *Microorganisms*, 2021. 9(5).

Uzun, O. F, and F. Alay, Meralarda Kentsel Dönüşüm ve Gelişim Amaçlı Tahsis Amacı Değişikliği Talebinin Değerlendirilmesi: Doyran ve Kızılcaören Köy Meraları Örneği. International Journal of Life Sciences and Biotechnology, 2022. 5(3): p. 602- 610. DOI: 10.38001/ijlsb.1180257

Meralarda Kentsel Dönüşüm ve Gelişim Amaçlı Tahsis Amacı Değişikliği Talebinin Değerlendirilmesi: Doyran ve Kızılcaören Köy Meraları Örneği

Ömer Faruk Uzun¹ , Fatih Alay^{2*} 

Özet

Bu çalışmada, Samsun Büyükşehir Belediye Meclisi tarafından “kentsel dönüşüm ve gelişim proje alanı” olarak ilan edilen; Vezirköprü ilçesi, Doyran ve Kızılcaören Mahalleleri sınırları içerisinde yer alan sırasıyla 108/51 ve 108/66 numaralı mera parsellerinde, tahsis amacının değişimi isteğine binaen “Mera durum” sınıfı belirlenerek yapılan işin 4342 sayılı Mera Kanuna uygunluğu incelenmiştir.

Etüt, 2017 yılı haziran ayı içerisinde yapılmış olup, göz ile tahmin yöntemi kullanılmıştır. Vejetasyon etüdü verilerine göre yapılan hesaplama göre mera durumu % 40 ile “Orta” sınıfta yer almıştır. Mera Kanunu’nun 14. maddesine göre mera alanının “Mera durum sınıfı”nın “Çok iyi” veya “İyi” değil de “Orta” çıkması, çalışılan mera alanında tahsis amacı değişikliği yapılabileceğini göstermiştir. Bu sonuca göre Mera Komisyonu, alan için tahsis amacında değişiklik yapılması talebini kabul etmiş ve kararı onay için Tarım ve Orman Bakanlığına göndermiştir. Ancak Bakanlık; bu tür her başvuruda olumlu görüş bildirilme gibi bir zorunluluğun olmadığını ifade ederek; bu alanın sanayi yatırımı için zorunlu olup olmadığı, alternatif bir alanın bulunup bulunmadığı, istenilen alanın gereğinden büyük olup olmadığı ve mera bütünlüğünün bozulup bozulmadığı gibi kriterler bakımından yeniden değerlendirilmesini istemiştir. Mera komisyonu, Belediyenin gerekçeli raporunu incelendikten sonra tahsis amacı değişikliği hususunda yeniden “Olumlu” görüş bildirmiştir. Ancak Bakanlık kararı uygun bulunmamış ve mera alanı Samsun Büyükşehir Belediyesine tahsis edilmemiştir.

ARTICLE HISTORY

Received

1 Eylül 2022

Accepted

15 Kasım 2022

Anahtar Kelimeler

Bitki örtüsü,
kentsel planlama,
kentsel gelişim,
mera durumu,
mera kanunu,
taşınmaz hukuku

¹ Sinop Üniversitesi, Boyabat Meslek Yüksekokulu, Mimarlık ve Şehir Planlama Bölümü, Sinop, Türkiye

² Karadeniz Tarımsal Araştırma Enstitüsü Müdürlüğü, 55300, Samsun, Türkiye

*Corresponding Author: Fatih ALAY, e-mail: fatih.alay@tarimorman.gov.tr

Legislative Compliance Assessment of the Request for Urban Transformation and Development in the Purpose of Allocation for Development Purposes in Rangelands: Example of Doyran and Kızılcaören Village Rangelands

ABSTRACT

In the study, the decision was taken by the Samsun Metropolitan Municipality Council to be an "Urban transformation and development project area"; In the rangeland parcels numbered 108/51 and 108/66 in Doyran and Kızılcaören villages of Vezirköprü sub-province, the "Rangeland condition" class was determined based on the request for change of allocation purpose, and the compliance of the process with the Rangeland Law legislation numbered 4342 was evaluated. The study of the rangeland vegetation was carried out in June 2017 with the visual estimation method. According to the data obtained from the vegetation of the rangeland parcels studied together, the average rangeland condition class of the parcels was "Fair" with 40%. According to the 14th article of the rangeland Law, the rangeland condition class of the rangeland area is "Fair", indicating that the purpose of allocation can be made in the rangeland area that is legally studied. According to this result, the Rangeland Commission accepted the request for a change in the allocation purpose for the area and sent the decision to the Ministry of Agriculture and Forestry for approval. However, the Ministry; expressing that there is no obligation to give a positive opinion to every request for a change in the purpose of allocation, taking into account only the rangeland condition class criterion; It requested that this area be re-evaluated in terms of criteria such as whether it is compulsory for industrial investment, whether there is an alternative area, whether the desired area is larger than necessary and whether the integrity of the rangeland is impaired. Rangeland Commission, after examining the reasoned report of the Municipality, gave a "Positive" opinion again on the change of purpose of allocation. However, the Ministry did not approve of the decision and the rangeland area was not allocated to Samsun Metropolitan Municipality.

ARTICLE HISTORY

Received

1 September 2022

Accepted

15 November 2022

KEYWORDS

Plant cover, urban planning, rangeland condition, rangeland law, real estate law

Giriş

4342 sayılı Mera Kanununun 1998 yılında yürürlüğe girmesiyle birlikte mera, yaylak ve kışlakların kullandırılması, ıslahının yapılarak verimliliklerinin artırılması, sürdürülebilirliği, kullanımlarının denetlenmesi, korunması ve gerektiğinde tahsis amacı değişiklik yetkisini Tarım ve Orman Bakanlığına vermiştir [2]). Mevzuata göre bazı durumlarda meraların kullanım amacı, bir takım toplumsal ihtiyaçların giderilmesi adına değiştirilebilmektedir.

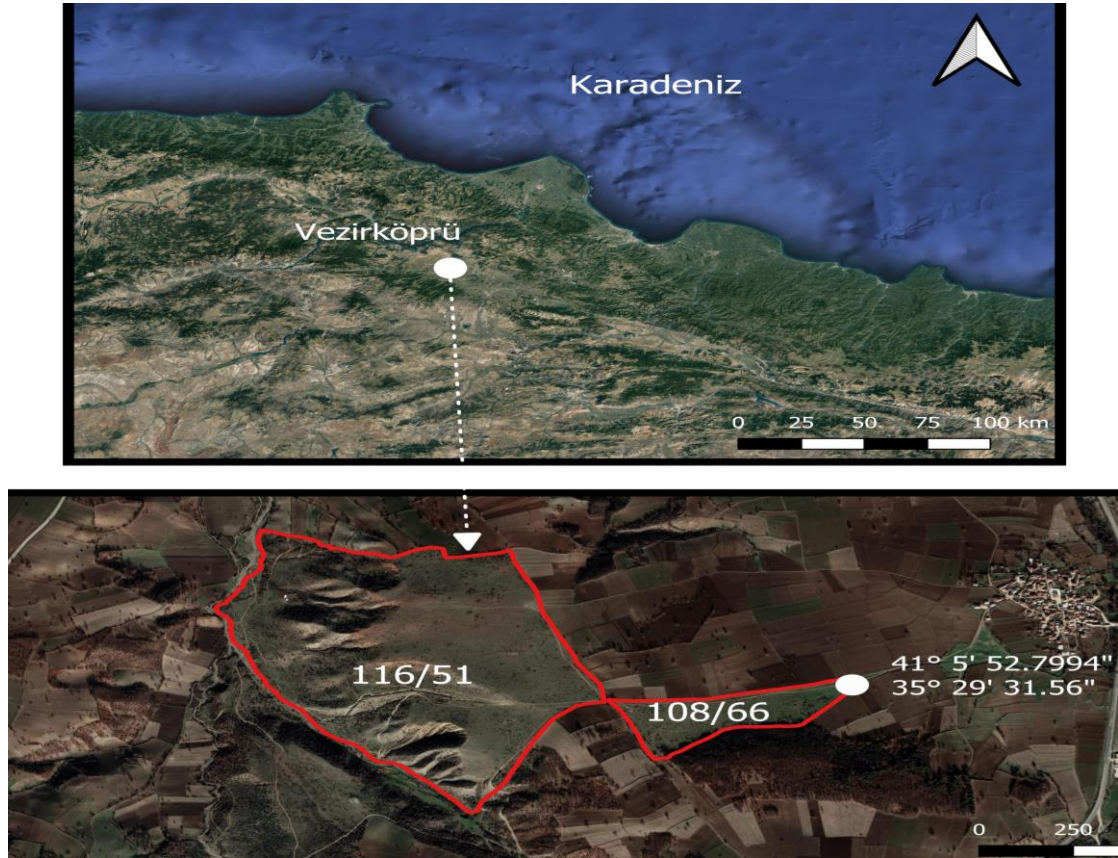
"Kentsel dönüşüm ve gelişim proje alanı" olarak Bakanlar Kurulu'nca ilan edilen mera, yaylak ve kışlaklardaki tahsis amacı değişiklik işlemleri Mera Kanunu'nun 14/1 ve Mera Yönetmeliği'nin 8. maddesi genel hükümlerince yapılmaktadır [2, 3]. Buna göre belirtilen proje alanlarında tahsis amacı değişiklik işlemleri Kanunun 14. ve Yönetmeliğin 8. maddesi hükümlerince gerçekleştirilir. Mera durum sınıfı çok iyi veya iyi olan mera, yaylak ve kışlaklarda tahsis amacı değişikliği yapılamamaktadır. Bu

alanlarda tahsis amacı değişikliği yapabilmek için öncelikle kentsel dönüşüm ve gelişim proje alanı ilan edilmesi, düşünülen alanın 1/5000 ölçekli haritasının çıkarılması ve Mera Komisyonuna başvurularak uygun görüş alınması gerekmektedir. Tahsis amacı değişikliği başvurularında, Bakanlar Kuruluna ait kamu yararı yazısı, kentsel dönüşüm ve gelişim proje alanı krokisi, bu alan içerisindeki taşınmazların bilgisi, belediye meclis kararı, çevre parselleri gösterir 1/5000 ölçekli harita ile komisyonca istenilen diğer bilgi ve belgeler başvuru dosyasına eklenerek Tarım ve Orman Bakanlığı Çayır ve Mera Dairesine sunulur ve son karar Tarım ve Orman Bakanlığınınındır. Tahsis amacının değiştirilmesinden sonra, valilik tarafından 20 yıllık ot bedelinin yatırılması sağlanmaktadır. Ot bedelinin ödenmesine müteakip iki yıl süre içinde uygulama imar planının, komisyona sunulması gerekmektedir. Bu süre içinde belirtilen planların sunulmaması halinde tahsis amacı değişikliği talebi iptal edilmektedir. İmar planlarının, tahsis amacı değişikliğine uygunluğunun kesinleşmesi halinde belirtilen meraların tescilleri hazine adına, vakıf meralarının tescilleri ise vakıf adına yapılmaktadır. 5393 sayılı Belediye Kanunu'nun 73. maddesine göre [4], Samsun Büyükşehir Belediyesi, İmar ve Şehircilik Dairesi Başkanlığı, Samsun İl Tarım ve Orman Müdürlüğü (SİTOM)'ne Ağustos 2017 tarihli yazısında Vezirköprü ilçesinin Doyran ve Kızılcaören mahalleleri sınırları içerisinde yer alan 82 hektarlık mera alanında sanayi alanı yapılmasını Belediye Meclisinde kararlaştırdıklarını bildirmiştir. Belediye ayrıca, Ekim 2017 tarihindeki yazıya ek olarak 1/5000 ölçekli F34c.15c, F34c.15d, F34c.20a ve F34c.20b kadastro paftalarına isabet eden alan için “Kentsel Dönüşüm ve Gelişim Proje Alanı” ilan etmeyi düşündüklerini bunun için anılan mera parsellerinde tahsis amacı değişikliği için Çevre ve Şehircilik Bakanlığı'na sunulmak üzere Mera Komisyonu'nda görüşülerek bir karar oluşturulması hususunda istekte bulunmuştur. SİTOM tarafından Defterdarlığa alanın Hazine adına tescil edilmesinde bir sakınca bulunmadığına dair cevap verilmiştir. Ekim 2018 tarihinde toplanan Mera Komisyonu, Mera Kanununun 14. madde, 5. fıkrasındaki “Mera durum sınıfı” “İyi” ve “Çok iyi” olan mera, yaylak ve kışlaklarda (birinci fıkranın a, f, g, ğ ve h bentleri hariç) “tahsis amacı değişikliği yapılamaz” hükmü gereğince meranın, durum sınıfının belirlenmesi istenmiştir. Bunun için konu mera teknik ekibine intikal ettirilmiştir.

Bu çalışma, parsel numaraları yukarıda verilen mera alanında vejetasyon etüdü yapılarak mera durumu sınıfının belirlenerek tahsis amacı değişikliğinin yapıp yapılamayacağını ortaya konulması amacıyla 2017 yılında yürütülmüştür.

Yöntem

Tahsis amacı değişikliği istenilen Samsun ili, Vezirköprü ilçesinin Doyran Mahallesi'ne ait mera parselinin; Taşınmaz numarası: 114809226, Pafta numarası: F34-C-20-B-1, Zemin tipi: Ana Taşınmaz, 116 Ada, 51. Parsel ve parsel büyüklüğü 71.05 ha'dır (Parsel numarası değişmiştir. Eski parsel numarası 347'dir). Kızılcaören Mahallesi'ne ait mera parselinin ise; Taşınmaz numarası: 114809226, Pafta numarası: F34-C-20-B-2, Zemin tipi: Ana Taşınmaz, 108 Ada, 66. Parsel ve büyüklüğü 9.61 ha'dır (Parsel numarası değişmiştir. Eski parsel numarası 437'dir).



Şekil 1 Tahsis amacı değişikliği istenilen Doyran ve Kızılcaören köyü mera parsellerinin görüntüsü

Mera alanında koordinat ve rakım ölçümleri “South S82 Plus” GPS ile yapılmış, veriler QGis 3.16.8 programına işlenmiş ve harita çıktıları oluşturulmuştur (Şekil 1). Eğim, yükseklik ve mesafe ölçümleri ise “Leica DISTO D810” lazer metresi ile ölçülmüştür. Mera parsellerinde yer alan bitki türleri, gözle tahmin yöntemi kullanılarak teşhis edilmiştir. Serin iklim bitkilerinin teşhisi çiçeklenme evresini devam ettirdiği, sıcak iklim bitkilerinin teşhisi ise haziran ayı içerisinde yaprak alanına göre Koç ve Çakal (2004) ile Aydın ve Uzun (2002)’un belirttiği esaslara göre yapılmıştır. Bitkilerin teşhis edilmesinde Davis (1970) ve Serin (2008)’den istifade edilmiştir. Teşhis edilen her bir bitki türüne ait sayılar, o türün toplam bitki sayısına oranlanarak türlerin botanik kompozisyondaki oranları bulunmuştur. Vejetasyon etüdü sonucu belirlenen türler azalıcı, çoğalıcı ve istilacı türler olarak sınıflamaya tabi tutulmuştur. Tespit edilen bitkilerden azalıcıların tamamı, çoğalıcıların 19’a kadar kendisi 20-40 arası 20 ve 40’tan yukarıda ise yarısı dikkate alınarak mera durum sınıfı belirlenmiştir. “Mera durum sınıfı, ”Koç ve ark. (2003) ile Holecek ve ark. (2010)’ın belirttiği ve mera yönetmeliğinin, uygulama esaslarını düzenleyen 2. bölüm (Uygulama normları)’ün 6/c. maddesindeki esaslara [3] göre belirlenmiştir (Tablo 1).

Tablo 1 Mera durum sınıfı

Azalıcı + Çoğalıcı Bitki Türlerinin oranı (%)	Mera durum sınıfı
76-100	Çok İyi
51-75	İyi
26-50	Orta
0-25	Zayıf

Meralarda eğim düz (% 0-2), hafif eğimli (% 3-6), orta eğimli (% 7-12), dik eğimli (% 13- 20), çok dik eğimli (% 21-30), sarp eğimli (%30-45) ve çok sarp eğimli (46+) cetveline göre sınıflandırılmıştır [5].

Bulgular

Mera lokasyon bulguları

Birbirine bitişik olan mera parselerinden Doyran Mahallesi sınırları içerisinde kalan ve 116/51 ada/parsel numaralı mera alanı düz ve düze yakın (% 0-1) eğim derecesine sahiptir. Kızılcäören sınırları içerisinde yer alan, 108/66 ada/parsel numaralı mera alanının yarısı % 20-45 eğime sahip olduğundan yüksek su erozyonu nedeniyle su

oyuntuları gözlemlenmiş, diğer yarısında ise % 3-10 arasında eğim olduğundan su oyuntuları gözlemlenmemiştir. (Şekil 1). Doyran mahallesi sınırları içerisinde kalan mera parselinin eğim derecesinin, sığırların meradan faydalanabilmesi için uygun olduğu söylenebilir [8, 10]. Bilindiği üzere sığırlar % 10 eğim derecesine kadar olan mera alanlarından sorunsuz bir şekilde faydalanabilmektedir. Ancak Kızılcaören Mahallesi sınırları içerisinde kalan mera parselinin % 50'si tüm hayvan türlerinin faydalanabileceği eğim derecesine (% 3-10), diğer kısmı ise küçükbaş hayvanların daha iyi değerlendirebileceği eğim derecesine (% 25-50) sahiptir. Her iki mera parselinin yaklaşık % 20'si çalı ile kaplı olduğundan özellikle keçi istihdamı, alandan faydalanmayı çok daha üst seviyelere çıkaracağından meranın sürdürülebilirliği ve ıslahı açısından da daha faydalı olacaktır [22].

Mera durumu sınıfı

Her iki mera parselinin birlikte etüt edildiği çalışmada, vejetasyonda yer alan bitki türleri ve oranları Tablo 2'de verilmiştir.

Tablo 2 Azalıcı, çoğalıcı ve istilacı bitki türlerinin botanik kompozisyondaki oranları (%)

Azalıcı Bitki Türleri (%)			
<i>Bothriochloa ischaemum</i>	10.4	<i>Bromus catharticus</i>	2.4
<i>Sangiosorba minor</i>	4.0	<i>Lotus corniculatus</i>	0.8
<i>Chrysopogon gryllus</i>	2.4	<i>Onobrychis armena</i>	0.8
Toplam			20.8
Çoğalıcı Bitki Türleri (%)			
<i>Festuca ovina</i>	12.0	<i>Brachypodium pinnatum</i>	3.2
<i>Plantago lanceolata</i>	2.4	<i>Dorycnium graecum</i>	1.6
Toplam			19.2
Azalıcı+Çoğalıcı Toplamı			40.0
İstilacı Bitki Türleri (%)			
<i>Trifolium resupinatum</i>	8.0	<i>Tanacetum sp.</i>	1.6
<i>Globularia orientalis</i>	6.4	<i>Trifolium dubium</i>	1.6
<i>Tymus spyleus</i>	4.8	<i>Scorpiurus muricatus</i>	1.6
<i>Carex sp.</i>	3.2	<i>Helianthemum nummularium</i>	0.8
<i>Fumana arabica</i>	2.4	<i>Noaea mucronata</i>	0.8
<i>Bellis perennis</i>	2.4	<i>Anthemis cretica</i>	0.8
<i>Teucrium chamaedrys</i>	2.4	<i>Teucrium polium</i>	0.8
<i>Taraxacum aleppicum</i>	2.4	Çalı	20.0
Toplam			60.0
Genel Toplam			100

Sonuçlar ve Tartışma

Vejetasyon etüdü değerlerine göre yapılan hesaplama göre mera durumu sınıfı % 40.0 ile “Orta” sınıfta yer almıştır (Azalıcı % 20.8 + Çoğalıcı % 19.2 = % 40.0). Vejetasyonda yer alan bitki örtüsünün % 60.0’lık kısmı ise istilacı türlerden oluşmuştur. Vejetasyonda teşhis edilen azalıcı bitki türleri içerisinde en fazla bulunan yem bitkileri % 10.4 ve % 4.0’lık oranlarla sırasıyla *Bothriochloa ischaemum* ve *Sangiosorba minor*’dur.

Bitki türleri içerisinde ortama en iyi adapte olabilen çoğalıcı tür ise % 12.0’lık oranla *Festuca ovina* ve % 3.2 ile *Brachypodium pinnatum*’dur.

Mera yüzeyinde % 4 taş ve % 28 boş alan mevcuttur. Bu değerlere göre mera yüzeyinin bitki ile kaplılık oranı % 68’dir. Bu sonuç özellikle eğimi yer yer % 45’leri bulan Kızılcaören sınırları içerisinde kalan 108/66 ada/parsel numaralı mera alanının erozyona maruz kalabileceğini ifade etmektedir. Nitekim adı geçen alanda su akış izleri görülmüştür.

Karadeniz bölgesinde yürütülen birçok çalışmada istilacı türlerin mera vejetasyonlarının çoğunluğunu oluşturduğu ifade edilmiştir. Çalışılan merada, otlatma süre ve kapasitesine dikkat edilmeden yapılan otlatma yanında, uygun olmayan sayı ve türde hayvan ile otlatma bunun en başta gelen sebeplerinden olduğu birçok çalışmada bildirilmiştir [1, 6, 9, 12, 13, 14, 15, 20, 21, 22, 23, 24, 25, 26, 27].

Mera Kanunu’nun 14/1 (Ek: 10/09/2014-6552/112 md.) maddesi ve Değişik 4. Fıkra: 26/3/2008-5751/3 md.’ye göre mera alanının “mera durum sınıfı”nın “Çok iyi” veya “İyi” değil de “Orta” çıkması, çalışılan mera alanının “tahsis amacının değiştirilmesi” hususuna açık olduğu anlamına gelmektedir [2, 3].

Bu çalışmalardan sonra Mera komisyonu 15.02.2019 tarihli oturumunda Belediyenin talebi uygun bulunmuş ve konu SİTOM tarafından Tarım ve Orman Bakanlığına gönderilmiştir. Bakanlık’ta bu tür her başvuruda olumlu görüş bildirilme gibi bir zorunluluğun olmadığını ifade ederek; Belediyece bu alana yatırımın zorunlu olup olmadığını, alternatif bir alanın bulunup bulunmadığı, meranın vasfı, yatırım istenilen alanın gereğinden büyük olup olmadığı ve mera bütünlüğünün bozulup bozulmadığı gibi kriterler bakımından alanın yeniden değerlendirilmesini istemiştir. Konu Mera komisyonunda yeniden görüşülerek, bu alanın seçiminde Belediyece dikkate alınan hususlar hakkında bilgi istenilmiştir. Belediyenin gerekçeli raporu incelendikten sonra Mera komisyonu yeniden tahsis amacı değişikliği hususunda “olumlu” görüş bildirmiştir.

Ancak Tarım ve Orman Bakanlığı kararı uygun bulmadığından alan “Kentsel Dönüşüm ve Gelişme Proje Alanı” olarak kullanım için Samsun Büyükşehir Belediyesine tahsis edilmemiştir.

Teşekkür

Verilerin elde edilmesinde ve yazım işlemlerindeki destekleri için Samsun İl Tarım ve Orman Müdürlüğü Çayır Mera ve Yem Bitkileri Şube Müdürlüğü personelleri; Müdür V. Namık AKGÜL, Ziraat Mühendisleri Hakan UZUN, Nuri DEMİRCİ, Bayram AY ve Mehmet YOLCU, Karadeniz Tarımsal Araştırma Enstitüsü personeli Zir.Yük.Müh. Kadir İSPİRLİ'ye teşekkür ederiz.

Kaynaklar

1. Alay, F., et al., Uzun süreli serbest otlatmanın doğal meralar üzerine etkileri (Effects of long-term free grazing on natural rangelands). Gaziosmanpaşa Üniversitesi, Ziraat Fakültesi Dergisi, 2016. 33(1): 116-124.
2. Mera Kanunu. Resmî Gazete Tarih: 28/2/1998, Sayı: 23272, Tertip: 5, Cilt: 38, Kanun Numarası: 4342, Kabul Tarihi: 25/2/1998. URL: <https://www.mevzuat.gov.tr/MevzuatMetin/1.5.4342.pdf> (erişim tarihi: 02.08.2021).
3. Mera Yönetmeliği. Resmî Gazete Tarihi: 31.07.1998, Resmî Gazete Sayısı: 23419. T.C. Cumhurbaşkanlığı Mevzuat Bilgi Sistemi. <https://www.mevzuat.gov.tr/mevzuat?MevzuatNo=5057&MevzuatTur=7&MevzuatTertip=5> (erişim tarihi: 01.08.2021).
4. Belediye Kanunu. <https://www.mevzuat.gov.tr/mevzuatmetin/1.5.5393.pdf> (erişim tarihi: 15.05.2022)
5. Toprak ve arazi sınıflaması standartları teknik talimatı. URL: http://www.tarim.gov.tr/Belgeler/Mevzuat/Talimatlar/Toprak_Arazi_Sınıflaması_Standartları_Teknik_Talimatı_ve_Ilgili_Mevzuat_yeni.pdf (erişim tarihi: 28.07.2021).
6. Aydın, I. and F. Uzun, Lâdik ilçesi Salur Köyü merasında farklı ıslah metotlarının ot verimi ve botanik kompozisyon üzerine etkileri. Turkish Journal of Agricultural and Forestry, 2000. 24(2): 301-307.
7. Aydın, I. and F. Uzun, Çayır-Mera Amenajmanı ve Islahı. 2002, Ders Kitabı No:9, Ziraat Fak. Basımevi, Samsun, 313.
8. Davis, P., Flora of Turkey and East Aegean Islands. 1970, University Press, Edinburg, UK, 3: 518-531.
9. Dönmez, B. and F. Uzun, Meralarımızda görülen sütleğen türlerinin (*Euphorbia ssp.*) bitkisel özellikleri ve kontrolü. Türkiye 10. Tarla Bitkileri Kongresi. 2013. 10-13 Eylül, 254-259. Konya.
10. Farazmand, A., et al., Determining the factors affecting rangeland suitability for livestock and wildlife grazing. Applied Ecology & Environmental Research, 2019. 17(1): 317-329.
11. Holechek, J.L., R.D. Pieper, and Herbel, C.H. 2010, Range Management: Principles and Practices (6th Edition). Prentice Hall, one Lake Street, Upper Saddle River, Amsterdam, Netherland.
12. İspirli, K., et al., Doğal meralardaki vejetasyon örtüsü ve yapısı üzerine otlatma ve topoğrafyanın etkisi (Impacts of livestock grazing and topography on vegetation cover and structure in natural rangelands). Türkiye Tarımsal Araştırmalar Dergisi, 2016. 3: 14-22.
13. İspirli, K., et al., Orta ve Batı Karadeniz Bölgesi mera ıslah çalışmalarının etkinliğinin belirlenmesi. T.C. Tarım ve Orman Bakanlığı, Tarımsal Araştırmalar ve Politikalar Genel Müdürlüğü, Entegre Proje Sonuç Raporu, 2021a. TAGEM/TBAD/B/19/A7/P7/2128.
14. İspirli, K., F. Uzun, and Ö.F Uzun, Aşdağul beldesi merası için tahsis amacı değişikliği talebinin mevzuata uygunluk değerlendirilmesi. ISPEC 7th International Conference on Agriculture, Animal Sciences and Rural Development. 2021b.18-19 September 631-644, Muş, Turkey.

15. İspirli, K., et al., Nemli-mezotermal iklim kuşağında yer alan hasanlar köyü mera ıslahı çalışmalarının etkinliğinin belirlenmesi. *Anadolu Tarım Bilimleri Dergisi*. Basımda. 2022.
16. Koç, A., A. Gökkuş, and M. Altın, Mera durumu tespitinde dünyada yaygın olarak kullanılan yöntemlerin mukayesesi ve Türkiye için bir öneri. *Türkiye 5. Tarla Bitkileri Kongresi*, 2003. 13-17 Ekim, Diyarbakır, Türkiye, 36-42.
17. Koç, A. and Ş. Çakal, Comparison of some rangeland canopy coverage methods. In: *International Soil Congress Natural Resource Management for Sustainable Development*, 2004. 7-10 June, Erzurum, Turkey, 41-45.
18. Lyons, R.K. and R.V. Machen, Livestock grazing distribution: considerations and management. *Texas Farmer Collection*. 2002. URL: <https://hdl.handle.net/1969.1/87089> (erişim tarihi: 08.06.2021)
19. Serin, Y., Türkiye'nin Çayır ve Mera Bitkileri. *Tarım ve Köyişleri Bakanlığı Tarımsal Üretim ve Geliştirme Genel Müdürlüğü Yayınları*. 2008, 486, Ankara.
20. Şahinoğlu, O. and F. Uzun, Taban mera ıslahında farklı metotların etkinliği: I. Agronomik özellikler. *Anadolu Tarım Bilimleri Dergisi*, 2016. 31(3): 423-432.
21. Uzun, F., A.V. Garipoğlu, and D. Algan, Meralarımızda görülen sarı peygamber çiçeği (*Centaurea solstitialis* L.)'nin bitkisel özellikleri ve kontrolü. *Anadolu Tarım Bilimleri Dergisi*, 2010. 25(3): 213-222.
22. Uzun, F., A.V. Garipoğlu, and H.B. Dönme,.. Mera yabancı otlarının kontrolünde keçilerin kullanımı. *Uluslararası Tarım ve Yaban Hayatı Bilimleri Dergisi*, 2015.1(1): 40-50.
23. Uzun, F., F. Alay, and K. İspirli, Bartın ili meralarının bazı özellikleri. *Türkiye Tarımsal Araştırmalar Dergisi*. 2016a. 3(2) 173-184.
24. Uzun, F., et al., The rates of desirable grazing plant species in rangelands: effect of different animal species and grazing pressures. *Ecosystem services and socio-economic benefits of Mediterranean grasslands*. Ed. A. Kyriazopoulos, A. Lopez-Francos, C. Porqueddu, P. Sklavou. *Options Mediterraneennes*, 2016b. Series A, No:114, 83-86.
25. Uzun, F., F. Alay, and K. İspirli, Rangeland Characteristic of open for grazing area for long years of West Black Sea Region. I. *International Agricultural Science Congress*. 2018. 9-12 May, 295, Van, Türkiye.
26. Uzun, F. ve N. Ocak, Some vegetation characteristics of rangelands subjected to different grazing pressures with single-or multi-species of animals for a long time (A case of Zonguldak province, Turkey). *Anadolu Tarım Bilimleri Dergisi*, 2019. 34(3): 360-370.
27. Uzun, F., et al., Meralarda Tahsis Amacı Değişikliği Talebinin Mevzuata Uygunluk Değerlendirmesi: Kayı Köyü Merası Örneği, Çorum, Türkiye. *Black Sea Journal of Engineering and Science*, 2022. 5(1) 1-6. DOI: 10.34248/bsengineering. 980787.

Budak B. and E. Dinckaya, L-Askorbik asit (C vitamini) Tayinine Yönelik Kalem Grafit Elektrot – Askorbat Oksidaz Temelli Yeni Bir Biyosensör Geliştirilmesi. International Journal of Life Sciences and Biotechnology, 2022. 5(3). p. 611-626. DOI: 10.38001/ijlsb.1189195

L-Askorbik asit (C vitamini) Tayinine Yönelik Kalem Grafit Elektrot – Askorbat Oksidaz Temelli Yeni Bir Biyosensör Geliştirilmesi

Burhan Budak^{*1} , Erhan Dinckaya² 

ÖZET

Bu çalışmada, biyosensör teknolojisi için özgün ve yeni bir bakış açısı katmak amacıyla PGE kullanılarak L-askorbik asit analizi için yeni bir sensör geliştirildi. Askorbat oksidaz enzimi glutaraldehid ve jelatin kullanılarak çapraz bağlandı, kalem grafit elektrot yüzeyinde tutturuldu ve geliştirilen biyosensör L-askorbik asit tayini için kullanıldı. Ölçümler amperometrik yöntem kullanılarak tüketilen oksijen miktarı ile orantısal akım değerlerindeki azalmanın belirlenmesi ile yapıldı. Tasarlanan biyosensör ile L-askorbik asit ölçümleri -0.7 V'ta amperometrik yöntem ile gerçekleştirildi. Optimizasyon çalışmalarından PGE/jelatin-glutaraldehit/askorbat oksidaz modifiye biyosensör için askorbat oksidaz konsantrasyonu, glutaraldehitte bekletme süresi, jelatin miktarı ve glutaraldehit tabakalandırma sayısı sırasıyla $1,5$ U/mL, 3 dakika, 20 mg ve 3 kez olarak belirlendi. Kullanılan Potasyum fosfat tamponu (pH:7, 50 mM) ve 30°C optimum çalışma koşullarını olarak belirlendi. PGE/jelatin-glutaraldehit/askorbat oksidaz biyosensörü için karakterizasyon çalışmalarında doğrusal tayin aralığı $25\mu\text{M}$ - $500\mu\text{M}$ bulundu. Sonuçlarına ilişkin olarak % varyasyon katsayısı (V.K) = 0,44 ve standart sapma (S.S) = $\pm 1,46$ μM olarak belirlendi. Depolama kararlılığına ilişkin yapılan denemeler sonucunda 4 haftalık sürecin sonunda %75'lik aktivitenin korunduğu tespit edildi.

MAKALE GEÇMİŞİ

Geliş

14 Ekim 2022

Kabul

30 Kasım 2022

ANAHTAR KELİMELER

Kalem grafit elektrot, askorbat oksidaz, amperometrik, biyosensör, askorbik asit

¹ Hatay Mustafa Kemal University, Hatay Vocational Health School, Department of Medical Laboratory, Hatay / Turkey

² Ege University, Faculty of Science, Department of Biochemistry, İzmir / Turkey

*Corresponding Author: Burhan BUDAK, e-mail: burhanbudak_dr@hotmail.com

A New Biosensör Development Pencil on Based Graphite Electrode – Ascorbate Oxidase for Determination of L-ascorbic acid (C Vitamin)

ABSTRACT

In this study, in respect to provide an novel and inventive viewpoint, a new assay for analysis of L-ascorbic acid enhanced using PGE. Ascorbat oxidase was crosswise bounded using gluteraldehyde and gelatine, stable to the surface of pencil graphite electrode and devised biosensor used for the detection of ascorbic acid. L-ascorbic acid measuring done amperometrically at -0.7 V using the improved biosensor. For the PGE/gelatine- glutaraldehyde /ascorbate oxidase biosensor ascorbate oxidase concentration, holding time in glutaraldehyde, gelatine amount and glutaraldehyde stratifying repeat cycle determined to be 1.5 U/mL, 3minutes, 20 mg and 3 times stratification in turn after optimization works. Potassium phosphate buffer (pH:7, 50 mM) and 30°C warmth determined to procure optimum labouring conditions. After the characterization labours, 25 µM - 500 µM detection space provided to be linear for PGE/gelatine- glutaraldehyde/ascorbate oxidase biosensor. Regarding the results, the % coefficient of variation (V.K) = 0.44 and the standard deviation (S.S) = ±1.46 µM. As a result of the experiments on storage stability, it determined that 75% activity was preserved at the end of the 4-week period.

ARTICLE HISTORY

Recieved
14 October 2022
Accepted
30 November 2022

KEY WORDS

Pencil graphite electrode,
ascorbate oxidase,
amperometric,
biosensör,
ascorbic acid

Giriş

Askorbik asit, serbest radikalleri indirgeyici ve radikalleri süpürücü gibi antioksidan özelliklere sahip olduğundan dolayı hücrelerde hayati fonksiyon gösteren yaygın bir vitamindir [1-4]. Vitamin C olarak bilinen L-askorbik asit (AA), doğal yolla oluşan bir organik bileşiktir ve gıdalarda bulunan önemli bir besin koruyucusudur. Yaşlanmayı geciktirmede, gen regülasyonunu düzenlenmesinde, aterosklerozun azaltılmasında, kollajen biyosentezinin düzenlenmesinde ve kolesterol metabolizmasında önemli bir biyolojik rolü vardır. Ayrıca kalp damar hastalıkları ve kanser gibi ciddi hastalıkların önlenmesinde hayati bir role sahiptir [4-9]. Ancak insan vücudunda askorbik asit sentezlenmez ve vücutta depolanmaz. Bu nedenlerden dolayı günlük gerekli miktarlarda düzenli olarak C vitamini alınmalıdır [10].

Literatüre göre, askorbik asitin elektrokimyasal oksidasyonu altın, karbon, platin, paladyum ve polianilin gibi iletken polimerler gibi çeşitli elektrotlarla analiz edildi. İletim polimerleri, iyi elektrokimyasal, yüksek elektriksel iletkenlik ve çevresel kararlılık gibi önemli özellikleri nedeniyle araştırmacılar için özel bir ilgi kaynağıdır [11-14].

Askorbat oksidaz (AA-Ox) bir tür çoklu bakır oksidaz ailesinde yer alır ve AA-Ox, askorbik asidin dehidroaskorbik aside (DHAA) oksidasyonunu katalize eder [15]. Bitkilerde, AA-Ox hem sitoplazmada serbest halde hem de hücre duvarında sınırlı bir zara bağlı bir halde bulunur. Askorbat oksidaz bitki hücrelerinin oksidasyon durumunu

düzenler [15,16]. Şimdiye kadar Askorbat oksidazı tespit eden bazı yöntemler vardır. Bunlar kromatografi, elektrokimya, kemilüminesans kolorimetri ve floresan yöntemleridir [17-23].

L-Askorbik asidin oksidasyonunu katalize eden askorbat oksidaz enzimine dayalı bazı biyosensörler geliştirildi. Bu biyosensörler genellikle amperometriktir ve biyosensör üretiminde askorbat oksidaz enziminin çeşitli immobilizasyon yöntemleri kullanıldı. [24-31]. Amperometrik biyosensörler çok hızlı, ucuz ve spesifiktirler. Bu cihazlar, şarap endüstrisinde sıklıkla kullanılır. Şarap gibi organik asitleri spesifik olarak algılar ve ölçerler. Bu yöntemlere kıyasla, kalem grafit elektrot rahat ulaşılabilir, ucuz, kolay modifikasyon olabilme, yüksek elektrokimyasal aktivite ve minyatürize edilebilme gibi kolaylıklarından dolayı hem elektrokimyasal sensör tasarımında hem de DNA etkileşimlerine dayalı biyosensör tasarımlarında sıklıkla kullanılır.[32]

Gulsah Congur vd. PGE (kalem grafit elektrot yüzeyi) için süksinamik asit kullanılarak yapısını değiştirdiler. Bu sayede işlevselleşmiş ikinci nesil poli (amidoamin) G2-PS dendrimer yapısına sahip tek kullanımlık elektrokimyasal DNA biyosensörü geliştirdiler [33]. Abdel-Nasser Kawde vd. İse enzimatik olmayan (non enzimatik) platin nanopartikül yapıyla modifiye PGE (kalem grafit elektrot) (PtNP-GPE) geliştirdiler ve hidrojen peroksit (H_2O_2) ölçümlerini yapmayı ve belirlemeyi amaçladılar [34].

Bu çalışmada, enzimin kalem grafit elektroduna immobilizasyonu, biyosensör kararlılığını arttırmış ve daha düşük konsantrasyonlarda ölçüm hassasiyeti sağlamıştır. Ayrıca maliyeti düşük ve taşıma kolaylığı sağlamıştır. Bu çalışmadaki veriler, diğer çalışmalar için enzimlerin kalem grafit sensöründe kullanılmasına referans oluşturabilecektir.

Materyal ve Metot

Ekipmanlar

Çalışmalarda potansiyostat (IVIUM Compactstat), manyetik karıştırıcı(IKA-KIMO 2), Kalem(Rotring), Termostat(Lauda ecoline RE106), 0,5 grafit uç(Magnum) kullanılarak ölçümler gerçekleştirildi.

Kimyasallar

Deneysel çalışmalarda KH_2PO_4 , glutaraldehit, jelatin, NaOH, 4-(2-hidroksietil)-1-piperazinetansülfonik asit, L-askorbik asit, Tris, glutamik asit, aspartik asit ve diğer

kimyasallar Sigma'dan (ABD) satın alındı. Deneylerde kullanılan tüm çözeltiler saf su ile hazırlandı.

Çözeltiler

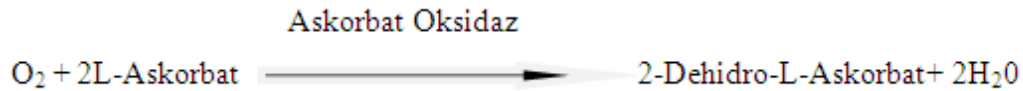
DeneySEL çalışmalarında potasyum fosfat tamponları (pH: 6.0-8.0; 25mM, 50mM ve 75mM), askorbat oksidaz (0,5U/mL, 1U/mL ve 1,5U/mL), glutaraldehit (% 1,25, % 2,5 ve %5), askorbik asit (40mM), sodyum fosfat tamponları (pH 7; 50mM), Redoxon tablet (1000 mg C vitamini) ve diğer kimyasallar saf su ile hazırlandı.

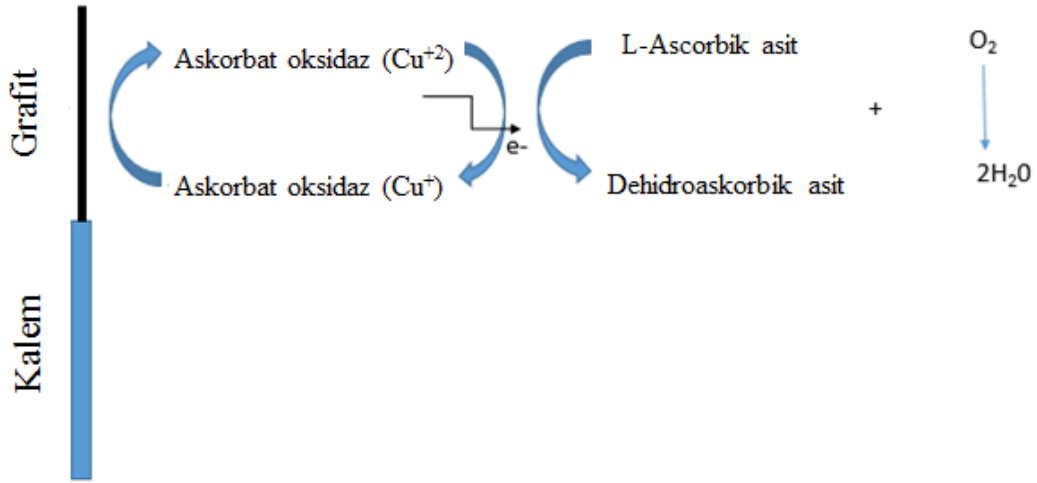
PGE/jelatin-glutaraldehit /askorbat oksidaz modifiye biyosensörün hazırlanması

PGE (Kalem grafit elektrot)'un grafit kısmı yaklaşık 1,5 cm dışarıda kalacak şekilde kalem elektrota yerleştirildi. PGE, 50 mM 200 µL pH fosfat tamponu içerisinde 1,5 U/mL olacak şekilde L-askorbat oksidaz enzimi ve 20 mg jelatin içeren 40 °C' de hazırlanmış enzim çözeltisi içerisine daldırılıp çıkartıldı. Daha sonra % 2,5 lük glutaraldehite 3dk bekletildi. Glutaraldehit ve enzim çözeltisine daldırma işlemi 3 kez tekrar edildi. Modifiye biyosensör kullanılmadığı zamanlarda + 4 °C sıcaklık da buzdolabında saklandı.

Geliştirilen biyosensörün çalışma prensibi

Hazırlanan biyosensörün çalışma ilkesi, ölçüm hücresinde bulunan oksijenin azalmasına dayalı ve amperometrik olarak -0,7 V potansiyelde ölçüm alınması esasına dayanır. Kalem grafit ucuna immobilize edilen askorbat oksidaz enzimi, askorbik asitten 2 elektronun oksijene aktarılmasını sağlar. Bu sayede askorbik asit dehidroaskorbik aside yükseltgenirken, oksijende suya indirgenir ve ortamdaki oksijen azalması gerçekleşir. Kapalı kap içerisinde ölçümler alındığından dolayı ortamdaki oksijen miktarı sadece enzimin dönüştürdüğü askorbik asit oranında değişkenlik gösterir. Kalem grafit yüzeyindeki askorbat oksidaz enziminin askorbik asidi dönüştürme mekanizması Şekil 1'de gösterildi.





Şekil 1 Kalem grafit elektrodun yüzeyine sabitlenmiş askorbat oksidaz enziminin çözelti içerisindeki L-askorbik asidi dehidroaskorbik aside dönüştürmesi.

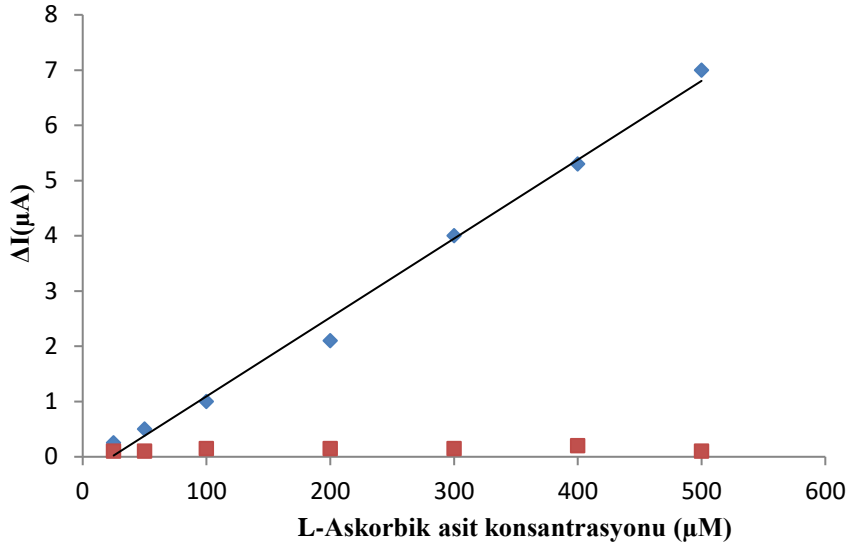
Fig 1 The conversion to dehydroascorbic of L-ascorbic acid in the solution by the enzyme ascorbate oxidase fixed on the surface of the pencil graphite electrode.

Sonuçlar ve Bulgular

Enzim İmmobilizasyon Etkisi

Öncelikle geliştirilen kalem grafit biyosensör ile elde edilen sinyallerin enzimatik reaksiyon kaynaklı olduğunun doğrulanması amacıyla PGE/glutaraldehit/jelatin ile PGE/jelatin-glutaraldehit/askorbat oksidaz elektrotlar kıyaslandı ve alınan sinyallerin askorbat oksidaz enziminden kaynaklandığı doğrulandı. Elde edilen sonuçlar Şekil 2’de gösterildi.

Ölçüm sonuçlarında anlaşıldığı gibi enzim bulunmayan elektrot ile enzim bulunan biyosensör arasında büyük bir sinyal farklılığı vardır. Ayrıca enzim içeren elektrotta ortamda bulunan substrat ile orantılı bir sinyal farklanmasının olması enzimin sinyal üzerindeki etkisini ortaya koydu.



Şekil 2 Enzimli ve enzimsiz elektrotun biyosensör yanıtına etkisi. (Fosfat tamponu; pH 7.0, 50 mM; T:30 °C), (◆) PGE/jelatin-askorbat oksidaz/glutaraldehit ($R^2 = 0,9927$); (■) PGE/jelatin/glutaraldehit

Fig 2 The effect of between enzymes and without enzymes electrode on the biosensor response. (Phosphate buffer; pH 7.0, 50 mM; T:30 °C), (◆) PGE/gelatin/L-ascorbate oxidase/glutaraldehyde ($R^2 = 0,9927$); (■) PGE/gelatine/glutaraldehyde)

Kalem Grafit Biyosensöründe Enzim Miktarının Optimizasyonu

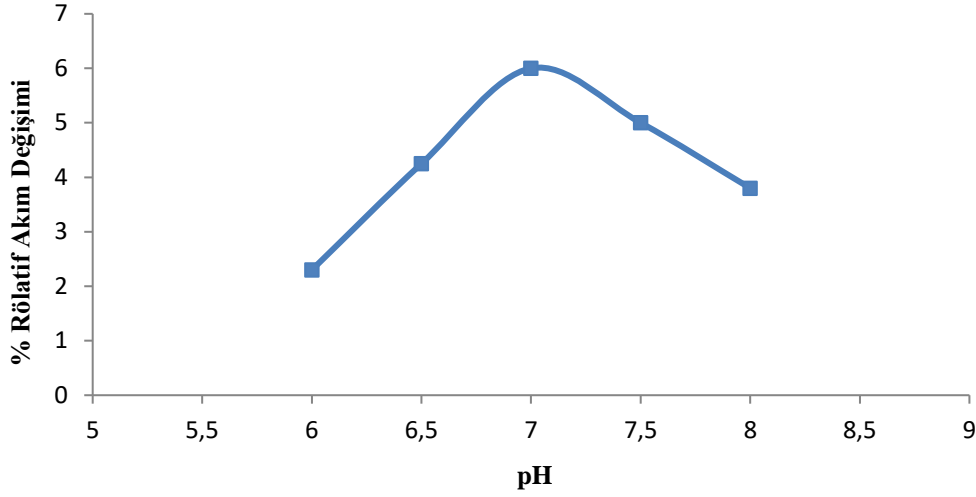
Yapılan ölçümler pH 7, 50mM fosfat tamponu içerisinde 30°C' de alındı. 20mg jelatin, % 2,5'luk glutaraldehitte 3 dk bekletme süresi sabit tutularak enzim miktarı (1, 1,5 ve 2 U/mL) olarak şekilde değiştirilerek enzim miktarı optimizasyonu gerçekleştirildi ve kullanılan askorbat oksidaz enzim (U/mL) miktarının modifiye biyosensör cevabı üzerindeki etkisi tespit edildi.

Ölçümler sonrası elde edilen yanıtlara göre en yüksek elektrot cevabının 1,5 U/ml ve 1 U/mL askorbat oksidaz enzim kullanılarak hazırlanan biyosensörler olduğu tespit edildi. İki biyosensörde alınan cevapların bir birine yakın olmasına rağmen düşük enzim miktarında substrat doygunluğuna çabuk ulaşabileceği için düşük enzim miktarları tercih edilmedi. Ayrıca diğer bir faktör ise, protein içeriğinin düşük olması çapraz bağ sayısını ve membran kararlılığını olumsuz etkileyeceğinden enzim miktarı fazla olan biyosensör tercih edildi.

Kalem grafit biyosensöründe pH optimizasyonu

PGE/jelatin-glutaraldehit/askorbat oksidaz modifiye biyosensör 20 mg jelatin, 1,5 U/mL enzimi çözeltisi kullanarak %2,5'luk glutaraldehitte 3 dk bekletilerek hazırlandı.

Ölçümler 50 mM fosfat tamponu içerisinde 30°C’ de alındı. Jelatin miktarı, enzim miktarı, glutaraldehitte bekletme süresi sabit tutularak pH 8; 7,5; 7; 6,5; 6 aralığı değiştirilerek optimum pH 7 olarak belirlendi. Sonuçlar Şekilde 3’de gösterildi.



Şekil 3 Biyosensör cevabına pH’nın etkisi. (Fosfat tamponu; pH 7.0, 50 mM; T:30 °C)

Fig 3 The effect of pH on the biosensor response. (Phosphate buffer; pH 7.0, 50mM; T:30 °C)

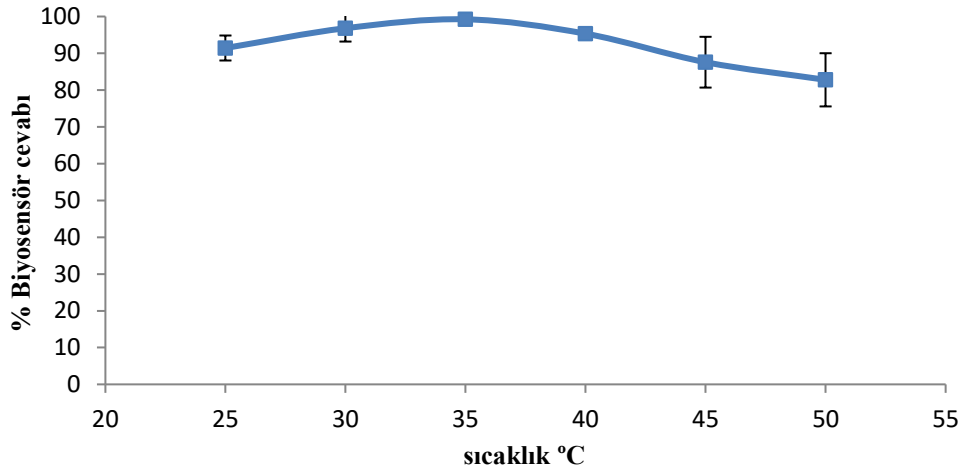
Enzimlerin katalitik etkisine ve üç boyutlu yapısına etki eden en önemli faktörlerden bir tanesi pH’dır. Enzimler protein yapılı makromoleküllerdir. Optimum pH’ın belirlenmesi, enzimlerin immobilizasyonun ve ölçümlerin verimliliği açısından önemlidir.

En iyi sinyal pH 7 de alındı. Yüksek asitlik ya da bazlık değerlerinde H⁺ ve OH⁻ konsantrasyonlarının yüksek olması enzimle etkileşime girip aktif merkezini etkileyebilir. Hatta enzimi denatüre edebilir.

Sıcaklığın Kalem Grafit Biyosensör Üzerindeki Etkisi

PGE/jelatin-glutaraldehit/askorbat oksidaz modifiye biyosensör 20 mg jelatin, 1,5 U/mL enzimi çözeltisi kullanarak %2,5’luk glutaraldehitte 3 dk bekletilerek hazırlandı. Membran tabakalandırma işlemi 3 kez gerçekleştirildi. Ölçümler değişen sıcaklıklarda pH 7, 50mM potasyum fosfat tamponu içerisinde de alındı. Analiz Bulguları Şekil 4’de gösterildi.

Jelatin miktarı, enzim miktarı, glutaraldehitte bekletme süresi, tampon konsantrasyonu ve pH sabit tutularak sıcaklık (50 °C, 45 °C, 40 °C, 35°C, 30°C ve 25°C) olacak şekilde değiştirilerek sıcaklık optimizasyonu gerçekleştirildi.



Şekil 4 Biyosensör yanıtına sıcaklığın etkisi. (Fosfat tamponu; pH 7.0, 50mM;)

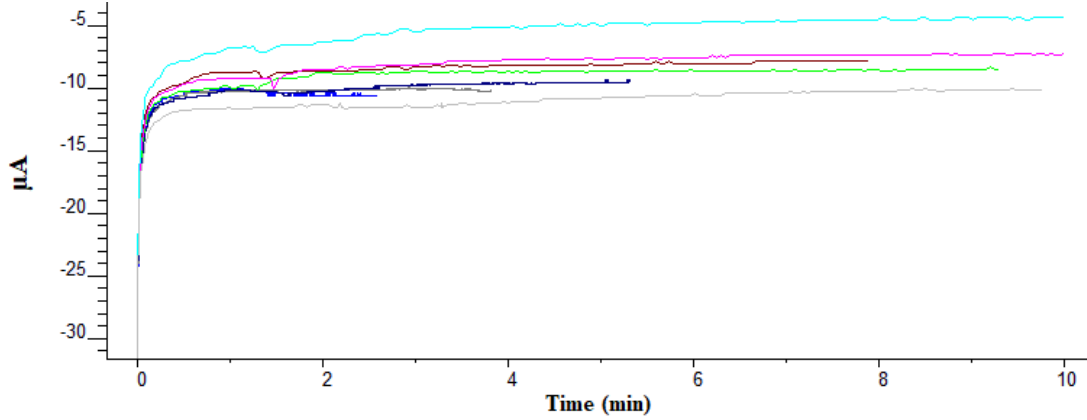
Fig 4 Effect of temperature on biosensor response. (Phosphate buffer; pH 7.0, 50mM;)

Şekil 4' de görüldüğü gibi en yüksek sinyal 35°C sıcaklığında alındı. Fakat yüksek sıcaklık değerlerine doğru çıkıldıkça enzimin doğası gereği kararlılığı düşmektedir. Bundan dolayı hem 35°C hem de 30°C değerlerinde standart grafiği çizildi. Elde edilen değerlerin kıyaslanması sonucu 30°C değerinin seçilmesinde karar kılındı.

L-askorbik asidin Lineer Aralığı

Geliştirilen PGE/jelatin-askorbat oksidaz /glutaraldehit biyosensörlerinin hazırlama ve çalışma koşullarının optimizasyonu sonrasında, karakterizasyonu amacıyla L-askorbik asit için ölçüm aralığı belirlendi. Şekil 5'de 25 µM - 500 µM arası kronoamperometrik ölçümler ve PGE/jelatin-askorbat oksidaz /glutaraldehit modifiye biyosensörüne ilişkin doğrusal tayin aralık grafiği verildi.

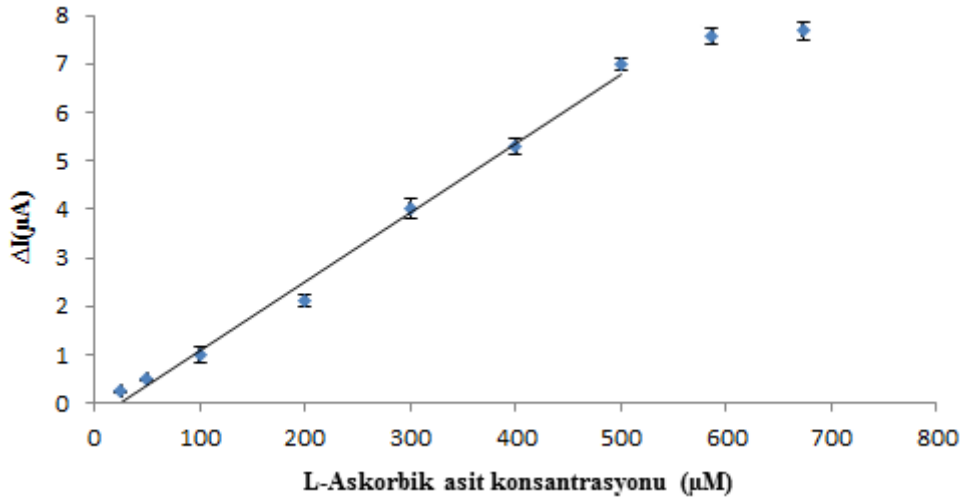
PGE/jelatin-glutaraldehit/askorbat oksidaz modifiye biyosensör 20 mg jelatin, 1,5 U/mL enzimi çözeltisi kullanarak %2,5'luk glutaraldehitte 3 dk bekletilerek hazırlandı. Membran abakalandırma işlemi 3 kez yapıldı. Ölçümler 50 mM, pH 7, 50 mM fosfat tamponu içerisinde de 30°C sıcaklığında alındı.



Şekil 5 Karıştırılan potasyum fosfat tamponu (50 mM, pH 7.0) içinde kalem grafit biyosensörünün amperometrik tepkileri. Uygulanan potansiyel: - 0,7 Voltaj. (A) 25µM-500 µM L-Askorbik asidin amperometrik yanıtı ve (B) akım ile L-Askorbik asit konsantrasyonu arasındaki kalibrasyon eğrisi ($R^2 = 0,9927$)

Fig 5 Typical amperometric responses of the pencil graphite biosensor in a blended potassium phosphate buffer (pH 7, 50 mM). Applied potential: - 0.7 Voltage. (A) Amperometric response of 25µM-500 µM L-Ascorbic acid and (B) calibration curve between the current and the concentration of L-Ascorbic acid ($R^2 = 0.9927$)

Şekil 5’de anlaşıldığı gibi artan yüksek L-askorbik asit derişimine bağılı olarak enzimin gösterdiği reaksiyon sonucunda zaman bağılı azalan O_2 miktarı artar. O_2 miktarındaki bu azalış kalem elektrot yüzeyinde meydana gelen reaksiyon uyarınca amperometrik ölçümlerde pozitif yönde doğrusal artış olarak gözlemlendi.



Şekil 6 Biyosensör yanıtında 30°C’de elde edilen doğrusal tayin aralığı. (Fosfat tamponu; pH 7.0, 50 mM; T:30 °C)

Fig 6 Linear detection range obtained of 30°C on the biosensor response. (Phosphate buffer; pH 7.0, 50 mM; T:30 °C)

Şekil 6'dan anlaşıldığı gibi PGE/jelatin-askorbat oksidaz/glutaraldehit biyosensörüne ilişkin doğrusal tayin aralığı 25 µM - 700 µM arasında yapılan ölçümler (n=3) sonucunda 25 µM – 500 µM olarak bulundu.

Tekrarlanabilirlik

Bu çalışmada tasarlanan L-askorbik asit biyosensörünün tekrarlanabilirlik özelliği incelendi. Ölçüm haznesi içerisinde 300 µM askorbik asit olacak şekilde eklemeler yapılarak ölçümler -0,7 voltajda amperometri yöntemi kullanılarak potasyum fosfat tamponu (pH 7, 50 mM; 30° C)'de gerçekleştirildi. Art arda sekiz kez alınan ölçümler ve elde edilen sonuçlara göre çizilen standart grafik yardımıyla örnek derişimleri tespit edildi. Standart sapma (S.S), ortalama değer (\bar{x}) ve varyasyon katsayısı (% V.K.) Tablo 1'de verildi. Elde edilen sonuçlar kabul edilebilir değerlerdedir.

Tablo 1 L-Askorbik asit numunesi için kalem grafit biyosensörünün tekrarlanabilirlik tayini

Table 1 Repeatability determination of the pencil graphite biosensor for Ascorbic acid sample

Aritmetik ortalama (\bar{x})	Standart sapma (S.D)	Varyasyon katsayısı (%)
327 µM	±1,46 µM	0,44

Yeniden üretilebilirlik

Bu çalışmada benzer yöntemle PGE/jelatin-glutaraldehit/askorbat oksidaz ayrı üç biyosensör hazırlandı ve -0,7V'ta amperometri yöntemiyle yapılan ölçümlerde 300 µM askorbat konsantrasyonuna verdiği cevaplar kıyaslandı.

Aynı yöntemle ayrı ayrı hazırlanmış üç PGE/jelatin-glutaraldehit /askorbat oksidaz biyosensörün L-askorbik asit konsantrasyonuna verdiği cevaplar arasında benzerlik vardır. Sonuçlar biyosensör için seri üretim yapılabileceğini gösterdi.

Biyosensörün Substrat Seçiciliği

Bu çalışmada benzer yöntemle PGE/jelatin-glutaraldehit/askorbat oksidaz biyosensör hazırlandı ve -0,7V'ta amperometri yöntemiyle yapılan ölçümlerde 300 µM askorbat konsantrasyonunda ve farklı dokuz substrata ayrı bir şekilde verdiği yanıtlar kıyaslandı. Elde edilen bulgular Tablo 2'de gösterildi.

PGE/jelatin-glutaraldehit/askorbat oksidaz biyosensör 20 mg jelatin, 1,5 U/mL enzimi çözeltisi kullanarak %2,5'luk glutaraldehitte 3 dk bekletilerek hazırlandı. Membran

tabakalandırma işlemi 3 kez yapıldı. Ölçümler pH 7, 50 mM fosfat tamponu içerisinde 30°C sıcaklığında alındı.

Tablo 2 L-Askorbik asit numunesi ve diğer numuneler için kalem grafit biyosensörünün substrat aktivitesi

Table 2 Relative activity of the pencil graphite biosensor for L-Ascorbic acid sample and other samples

Substratlar	Rölatif aktivite %
L-Askorbik asit	100
Sitrik asit	0,1
Hidrokinon	10,1
D-Glukoz	0,1
D- Fruktoz	9,8
Okzalik asit	0,3
Glikolik asit	0
Aspartik asit	0,2
Glutamik asit	9,85
Kateşol	16,2

Üç ölçümün ortalaması.

Tablo 2’de anlaşıldığı gibi PGE/jelatin-glutaraldehit/askorbat oksidaz biyosensörün dokuz tane farklı substrattan sadece dört tanesine düşük sinyal verdiği gözlemlendi.

Örnek Analizi

Tasarlanan PGE/jelatin-glutaraldehit/askorbat oksidaz biyosensör ile dışarıdan satın alınan Redoxon C vitamini ilacında, taze sıkılmış limon suyunda, portakal suyunda ve greylfurt suyunda L-askorbik asit analiz yapıldı.

Satın alınan C vitamini (1000mg) tabletinin çözündüğü çözeltilerden ölçüm hücresinde 300 µM konsantrasyon olacak şekilde eklemeler yapıldı ve dört ölçüme ilişkin alınan cevaplar standart grafiği ile kıyaslanarak değerlendirilmesi yapıldı. Bulgular Tablo 3’de verildi.

Table 3 Kalem grafit - askorbat oksidaz enzim biyosensörü ve DCIP yöntemleri kullanılarak Vitamin-C tabletlerinde L-Askorbik asit tayini.

Table 3 L-Ascorbic acid determination in Vitamin-C tablets by using the pencil graphite – ascorbate oxidase enzyme biosensor and DCIP methods.

Örnek	Askorbik asit konsantrasyonu (µM)	DCIP yöntemi (n=4)		Askorbat oksidaz biyosensörü (n=4)	
		SD	CV (%)	SD	CV(%)
Redoxon Tablet	300	±7,8	2,55	±0,262	0,087
		X _{ort} =305µM		X _{ort} =301,62µM	

İnsan metabolizmasının gereksinimi olan C vitamini farklı sebeplere bağlı olarak 30–105 mg arasında değişiklik göstermektedir. Bu değer yetişkinler için 65 mg, bebekler için 35-40 mg, emzirme döneminde anneler için 100-110 mg olacak şekilde ön görülmüştür. Yapılan epidemiojik, klinik ve biyokimyasal çalışmalar göz önünde bulundurularak askorbik asidin günlük alımı (RDA) günde 120-140 mg olarak önerilmektedir. Günlük ihtiyacını giderecek kadar vitamin C alındığında hücre doyunluğa ulaşır, kanser, kalp hastalıkları ve felç riskleri azalma gösterir. Bu değerler dikkate alınarak yapılacak ölçümler için 1000 mg C vitamini tableti kullanıldı. Ölçümler -0,7 V'ta amperometri yöntemi kullanılarak pH 7, 50mM fosfat tamponu; 30 °C sıcaklıkta gerçekleştirildi. Bulgular Tablo 3'de ve 4'de verildi.

Tablo 4 Kalem grafit-askorbat oksidaz enzim biyosensörü kullanılarak meyve sularında L-askorbik asit tayini

Table L-Ascorbic acid determination in fruit juices by using the pencil graphite – ascorbate oxidase enzyme biosensor

Meyve suları	Askorbat oksidaz biyosensörü		
	Ortalama (mg/100ml) (n=4)	SD	CV(%)
Portakal	38,3	0,041	0,107
Greyfurt	28,2	0,029	0,102
Limon	28,3	0,028	0,098

Meyvelerde bulunan askorbik asit miktarı meyvenin çeşitliliğine göre önemli farklılık göstermektedir. Yumuşak ve sert çekirdekli meyvelerin yaklaşık 12mg-110mg/100g düzeylerinde askorbik asit içermelerine rağmen, limon, greyfurt ve portakal yaklaşık 35mg - 55mg/100g düzeylerinde vitamin C içermektedirler. Fakat bu değerler meyvelerin türüne göre de değişiklik gösterebilmektedir.

Tartışma

Bu çalışma, insan vücudunda sentezlenmeyen ve dışarıdan sürekli düzenli olarak alması gereken C vitaminin (askorbik asit) [35] sıvılarda kolay, hızlı ve hassas tespiti için tasarlandı ve kalem grafit elektroda enzim/jelatin/glutaraldehit yapısı kullanıldı.

Kalem grafit elektrot genel olarak affinite esaslı DNA etkileşimlerine dayalı ve elektrokimyasal sensörler olarak kullanılmıştır [36]. İlk kez bu çalışmada, kalem grafit

elektrot enzim (askorbat oksidaz) temelli biyosensör tasarlanmış, kullanım yönü araştırılmış ve denenmiştir.

Song ve ark. (2020) [37] geliştirdikleri grafen oksit/poli (anilin ko-tionin) nanokompozit elektrokimyasal biyosensöründe, L-askorbik asitin lineer aralığını $500\mu\text{M} - 5000\mu\text{M}$, hassasiyetini $242\mu\text{M}$ olarak tespit etmişlerdir. Ancak bu çalışmada kullanılan PGE/jelatin-glutaraldehit/askorbat oksidaz biyosensörünün L-askorbik asitin lineer aralığı $25\mu\text{M} - 500\mu\text{M}$, hassasiyeti $25\mu\text{M}$ olarak tespit edildi. Buda geliştirdiğimiz kalem grafit askorbat oksidaz biyosensörünün düşük konsantrasyonlar da daha hassas ölçümler yaptığını göstermiştir. Geliştirilen biyosensör sistemleriyle ölçümler $-0,7$ voltajda amperometrik metotla yapılmıştır. Enzim tarafından kullanılan L-askorbik asit konsantrasyonu ile orantısal olarak kullanılan oksijen miktarının negatif yönde artan akım değerlerinden çıkılarak tayin edilmiştir.

Kaçar ve Erden (2020) [38] geliştirdikleri poli(L-aspartik asit), nanoelmas parçacıklı, karbon fiber, askorbat oksidaz temelli amperometrik biyosensörünün, askorbik asitin tekrarlanabilirlik denemelerinde standart sapmasını 3.4% tespit etmişlerdir. Bu çalışmada kullanılan PGE/jelatin-glutaraldehit/askorbat oksidaz temelli biyosensörünün L-askorbik asitin tekrarlanabilirlik denemelerinde standart sapması 0.44% tespit edildi. Buda geliştirdiğimiz biyosensörün diğer sensörlere kıyasla artarda daha hassas ve doğru ölçümler yapabileceğini göstermiştir.

Mu ve ark. (2018) [39] geliştirdikleri askorbik asit tayinine yönelik kolorimetrik ‘‘kapalı’’ biyosensöründe, portakal suyunun askorbik asit analizinde standart sapmasını 1.9% tespit etmişlerdir. Çalışmalarında yer alan HPLC analiz verilerinde ise ortalama bağıl hata oranı 3.3% göstermişlerdir. Bu çalışmada kullanılan kalem grafit askorbat oksidaz temelli modifiye biyosensörün portakal suyunun askorbik asit analizinde standart sapma 0.107% tespit edildi. Bu değerler geliştirdiğimiz biyosensörün diğer sensörlere ve klasik yöntemlere kıyasla meyve sularında askorbik asitin daha hassas ve doğru tespit edileceğini göstermiştir.

Sonuç olarak bu çalışma, kalem grafit elektrotların L-askorbik asit tayini için askorbat oksidazın kullanıldığı biyosensörlerin hazırlanmasında ve kullanılmasında genelde ise enzim temelli biyosensörlerin hazırlanmasında başarıyla kullanılabileceğini göstermiştir.

Kaynaklar

1. Abd-Allah, H., et al., Nicotinamide and ascorbic acid nanoparticles against the hepatic insult induced in rats by high fat high fructose diet: A comparative study, *Life Sciences*, 2020. 263. p. 118540.
2. El-Gendy, Z.A., et al., Potential hepatoprotective effect of combining vitamin C and l-carnitine against acetaminophen induced hepatic injury and oxidative stress in rats, *International Journal of PharmaTech Research*, 2016. 9. p. 33–47.
3. Abdulrazzaq, A.M., et al., Hepatoprotective Actions of Ascorbic Acid, Alpha Lipoic Acid and Silymarin or Their Combination Against Acetaminophen-Induced Hepatotoxicity in Rats, *Medicina (B. Aires)*, 2019. 55. p. 181.
4. Zou, M.Y., et al., Ascorbic acid induced degradation of polysaccharide from natural products: a review, *International Journal of Biological Macromolecules*, 2020. 151. p. 483–491.
5. Valko, M., et al., Redox- and non-redox-metal-induced formation of free radicals and their role in human disease, *Archives of Toxicology*, 2016. 90. p. 1–37.
6. Schoenfeld, J.D., et al., Redox active metals and H₂O₂ mediate the increased efficacy of pharmacological ascorbate in combination with gemcitabine or radiation in pre-clinical sarcoma models, *Redox Biology*, 2018. 14. p. 417–422.
7. Du, J., Cullen, J.J., and Buettner, G.R., Ascorbic acid: Chemistry, biology and the treatment of cancer, *Biochimica et Biophysica Acta (BBA)-Reviews on Cancer*, 2012. 1826. p. 443–457.
8. Minor, E.A., et al., Ascorbate induces ten-eleven translocation (Tet) methylcytosine dioxygenase-mediated generation of 5-hydroxymethylcytosine, *Journal Biological Chemistry*, 2013. 288. p. 13669–13674.
9. Moser, M. and Chun, O., Vitamin C and Heart Health: A Review Based on Findings from Epidemiologic Studies, *International Journal of Molecular Sciences*, 2016. 17. p. 1328.
10. Karakurt, I., et al., Stereolithography (SLA) 3D printing of ascorbic acid loaded hydrogels: A controlled release study, *International Journal of Pharmaceutics*, 2020. 584. p. 1–9.
11. Lin, W., et al., Hemin-intercalated layer-by-layer electropolymerized co-deposition of bisphenol A on carbon nanotubes for dual electrocatalysis towards ascorbate oxidation and oxygen reduction, *Electrochimica Acta*, 2020. 340. p. 135946.
12. Rueda, M., Aldaz, A. and Sanchez-Burgos, F., Oxidation of L-ascorbic acid on a gold electrode, *Electrochimica Acta*, 1978. 23. p. 419–424.
13. Mondal, S. K., et al., Electrooxidation of ascorbic acid on polyaniline and its implications to fuel cells, *Journal Power Sources*, 2005. 145. p. 16–20.
14. Osial, M., et al., Hybrid polyindole-gold nanobrush for electrochemical oxidation of ascorbic acid, *Journal of Electroanalytical Chemistry*, 2020. 877.
15. Zhang, J., et al., Determination of ascorbic acid and ascorbate oxidase based on quaternary CuInZnS QDs/thiochrome ratiometric fluorescence sensing system, *Talanta*, 2020. 214. p. 120814.
16. Wang, Y. H., et al., Chlorine disinfection significantly aggravated the biofouling of reverse osmosis membrane used for municipal wastewater reclamation, *Water Research*, 2019. 154. p. 246–257.
17. Qian, X., et al., Separation/Determination of Flavonoids and Ascorbic Acid in Rat Serum and Excrement by Capillary Electrophoresis with Electrochemical Detection, *Analytical Sciences*, 2010. 26. p. 557–560.
18. Liu, K., et al., Online electrochemical monitoring of dynamic change of hippocampal ascorbate: Toward a platform for in vivo evaluation of antioxidant neuroprotective efficiency against cerebral ischemia injury, *Analytical Chemistry*, 2013. 85. p. 9947–9954.
19. Sun, C. L., et al., Microwave-assisted synthesis of a core-shell MWCNT/GONR heterostructure for the electrochemical detection of ascorbic acid, dopamine, and uric acid, *ACS Nano*, 2011, 5.

- p. 7788–7795.
20. Koblová, P., et al., Development and validation of a rapid HPLC method for the determination of ascorbic acid, phenylephrine, paracetamol and caffeine using a monolithic column, *Analytical Methods*, 2012. 4. p. 1588–1591.
 21. Wang, Z., Teng, X. and Lu, C., Carbonate interlayered hydrotalcites-enhanced peroxy-nitrous acid chemiluminescence for high selectivity sensing of ascorbic acid, *Analyst*, 2012. 137. p. 1876–1881.
 22. Peng, J., et al., Ding, A rapid, sensitive and selective colorimetric method for detection of ascorbic acid, *Sensors and Actuators B:Chemical*, 2015. 221. p. 708–716.
 23. Chen, J., et al., Reduced graphene oxide nanosheets functionalized with poly(styrene sulfonate) as a peroxidase mimetic in a colorimetric assay for ascorbic acid, *Microchimica Acta*, 2016. 183. p. 1847–1853.
 24. Wang, X., Watanabe, H. and Uchiyama, S., Amperometric L-ascorbic acid biosensors equipped with enzyme micelle membrane, *Talanta*, 2008. 74. p. 1681–1685.
 25. Chauhan, N., Dahiya, T. and Priyanka-Pundir, C. S., Fabrication of an amperometric ascorbate biosensor using egg shell membrane bound *Lagenaria siceraria* fruit ascorbate oxidase, *Journal of Molecular Catalysis B:Enzymatic*, 2010. 67. p. 66–71.
 26. Liu, M., et al., A stable sandwich-type amperometric biosensor based on poly(3,4-ethylenedioxythiophene)-single walled carbon nanotubes/ascorbate oxidase/nafiion films for detection of L-ascorbic acid, *Sensors and Actuators B:Chemical*, 2011. 159. p. 277–285.
 27. Dodevska, T., Horozova, E. and Dimcheva, N., Electrochemical behavior of ascorbate oxidase immobilized on graphite electrode modified with Au-nanoparticles, *Materials Sciences and Engineering B:Solid-State Materials for Advanced Technology*, 2013. 178. p. 1497–1502.
 28. Liu M., et al., An Amperometric Biosensor Based on Ascorbate Oxidase Immobilized in Poly(3,4-ethylenedioxythiophene)/Multi-Walled Carbon Nanotubes Composite Films for the Determination of L-Ascorbic Acid, *Analytical Sciences*, 2011. 27. p. 477.
 29. Csiffáry, G., et al., Ascorbate oxidase-based amperometric biosensor for L-ascorbic acid determination in beverages, *Food Technology Biotechnology*, 2016. 54. p. 31–35.
 30. Kannoujia, D. K., Kumar, S. and Nahar, P., Covalent immobilization of ascorbate oxidase onto polycarbonate strip for L-ascorbic acid detection, *Journal of Bioscience Bioengineering*, 2012. 114. p. 402–404.
 31. Akyilmaz, E., Guvenc, C. and Koylu, H., A novel microbial biosensor system based on *C. tropicalis* yeast cells for selective determination of L-Ascorbic acid, *Bioelectrochemistry*, 2020. 132.
 32. Gao, W., Song, J. and Wu, N., Voltammetric behavior and square-wave voltammetric determination of trepibutone at a pencil graphite electrode, *Journal Electroanalytical Chemistry*, 2005. 576. p. 1–7.
 33. Erdem, A., Congur, G. and Mese, F., Electrochemical Detection of Activated Protein C Using an Aptasensor Based on PAMAM Dendrimer Modified Pencil Graphite Electrodes, *Electroanalysis*, 2014. 26. p. 2580–2590.
 34. Kawde, A. N., et al., A facile fabrication of platinum nanoparticle-modified graphite pencil electrode for highly sensitive detection of hydrogen peroxide, *Journal Electroanalytical Chemistry*, 2015. 740. p. 68–74.
 35. Abbas, S., et al., Ascorbic acid: microencapsulation techniques and trends-a review. *Food Reviews International*, 2012. 23. p. 343-374.
 36. Yaman, Y. T., Nano-elektrokimyasal Biyosensörler Kullanılarak DNA ile Doksorubisin Etkileşiminin Araştırılması, Süleyman Demirel University, 2022. 26. p. 229-235.
 37. Song, N., et al., A novel electrochemical biosensör for the determination of dopamine and ascorbic acid based on graphene oxide / poly(aniline-co-thionine) nanocomposite, *Journal of Electroanalytical Chemistry*, 2020. 873. p. 114352.

38. Kaçar, C. and E, P. E., An amperometric biosensor based on poly(L-aspartic acid), nanodiamond particles, carbon nanofiber, and ascorbate oxidase-modified glassy carbon electrode for the determination of L-ascorbic acid, *Analytical and Bioanalytical Chemistry*, 2020. 412. p. 5315-5327.
39. Mu, C., et al., Visual colorimetric 'turn-off' biosensor for ascorbic acid detection based on hypochlorite-3,3',5,5'-Tetramethylbenzidine system, *Spectrochimica Acta Part A: Molecular and Biomolecular Spectroscopy*, 2018. 201. p. 61-66.

Kimsanaliev, D., S. Maraklı, and Y. Kaya, *Fritillaria* cinsinin ve bu cinsin bir üyesi olan Aygül lalesi'nin (*Fritillaria eduardii*) dünü, bugünü ve yarını. International Journal of Life Sciences and Biotechnology, 2022. 5(3): p. 627-642. DOI: 10.38001/ijlsb.1121393

***Fritillaria* Cinsinin ve Bu Cinsin Bir Üyesi Olan Aygül Lalesi'nin (*Fritillaria Eduardii*) Dünü, Bugünü ve Yarını**

Daniel Kimsanaliev^{1*} , Sevgi Maraklı² , Yılmaz Kaya^{1,3} 

Özet

Fritillaria, Avrasya ve Kuzey Amerika olmak üzere iki kıtada dağılım gösteren ve yaklaşık 140 soğanlı otsu çok yıllık türden oluşan bir cinstir. Şimdiye kadar kaydedilen en büyük diploid genom boyutlarına sahip bitkilerden oluşan bu cins, son yıllarda araştırmacılar tarafından çok fazla ilgi görmektedir. *F. eduardii* bitkisi de bu cinsin içinde yer alan bir türdür. Bu tür ile ilgili literatürde az çalışma bulunmaktadır. Kırgızistan, yüzölçümü olarak birçok dünya ülkesinden küçük olmasına karşın çok zengin biyolojik çeşitliliğe sahip bir ülkedir. Batken bölgesi de bu biyolojik çeşitliliğe katkıda bulunan önemli bir merkezdir. Aygül bitkisi gibi yüzlerce endemik ve yerel bitkiye ev sahipliği yapmaktadır. Aygül bitkisi, güzelliğinden dolayı Batken bölgesinde tanınan bir endemik bitki olmasının yanı sıra tüm Kırgızistan için de değerli bir bitkidir. Aygül bitkisinin isimlendirilmesi araştırmacılar tarafından tartışılan konulardan biridir. Bu bitkinin ismi literatürde; *Petillium eduardii*, *Fritillaria imperialis* var. *eduardii*, *Fritillaria imperialis* var. *inadora*, *Fritillaria imperialis* var. *purpurea* ve *Fritillaria eduardii* olarak geçmektedir. Sınırlı sayıda yetişen Aygül bitkisi, yetiştiği doğal ortamında kuvvetli sağanak yağmurlara ve sert iklim koşullarına maruz kalmaktadır. Ayrıca bu bitki türü Kırgız Cumhuriyeti Başkanlığı'nın 28 Nisan 2005 tarihli, 170 no'lu tebliği ile Kırmızı Kitap listesine de eklenerek nesli tükenme tehlikesi altında ve doğada toplanması yasak olan çiçek soğanları listesine dâhil edilmiştir. Bu derleme çalışmasında amaç, *Fritillaria* cinsi ile bu cinsin bir üyesi ve Kırgızistan'ın endemik türü olan Aygül bitkisi hakkında gen kaynaklarının korunması ve biyoçeşitlilik içerisindeki devamlılığının sağlanması için uygulanabilecek biyoteknolojik metotların belirtilerek bu alanda yapılacak araştırmalar için temel bilginin sağlanmasıdır.

MAKALE GEÇMİŞİ

Geliş

25 Mayıs 2022

Kabul

10 Ağustos 2022

Anahtar Kelimeler

Fritillaria eduardii,
Fritillaria imperialis
var. *eduardii*,
endemik bitki

¹ Kırgızistan-Türkiye Manas Üniversitesi, Fen Fakültesi, Biyoloji Bölümü Bışkek, Kırgızistan

² Yıldız Teknik Üniversitesi, Fen Edebiyat Fakültesi, Moleküler Biyoloji Ve Genetik Bölümü, Esenler, İstanbul

³ Ondokuz Mayıs Üniversitesi, Ziraat Fakültesi, Tarımsal Biyoteknoloji Bölümü, Samsun, Türkiye

*Sorumlu yazar: Daniel KIMSANALIEV, e-mail: danielkimsanaliev@gmail.com

Past, present and future of *Fritillaria* genus and Aygül tulip (*Fritillaria eduardii*), a member of this genus

ABSTRACT

Fritillaria is a genus of about 140 bulbous herbaceous perennial species distributed in two continents, Eurasia and North America. This genus of plants with the largest diploid genome sizes ever recorded has received much attention from researchers in recent years. *F. eduardii* plant is also a species in this genus. There are few studies in the literature related to this species. Although Kyrgyzstan is smaller than many other world countries in terms of surface area, it has very rich biological diversity. The Batken region is also an important center that contributes to this biodiversity. It is home to hundreds of endemic and local plants such as the Aygül plant. Aygül plant is an endemic plant known in the Batken region due to its beauty and also a valuable plant for all of Kyrgyzstan. Naming the Aygul plant is one of the issues discussed by researchers. The name of this plant is *Petillum eduardii*, *Fritillaria imperialis* var. *eduardii*, *Fritillaria imperialis* var. *inadora*, *Fritillaria imperialis* var. *purpurea* and *Fritillaria eduardii* in the literature. The Aigul plant growing in limited numbers is exposed to heavy rains and harsh climatic conditions in its natural environment. In addition, this plant species was also added to the Red Booklist with the Communiqué of the Kyrgyz Republic Presidency dated 28 April 2005 with numbered 170 and included in the list of flower bulbs in danger of extinction prohibited from being collected in nature. This review study aims to provide basic information for research in this field by specifying the biotechnological methods that can be applied to protect the gene resources and ensure their continuity in biodiversity of *Fritillaria* genus with Aygül plant which is a member of the this genus, and an endemic species of Kyrgyzstan.

ARTICLE HISTORY

Received

25 May 2022

Accepted

10 August 2022

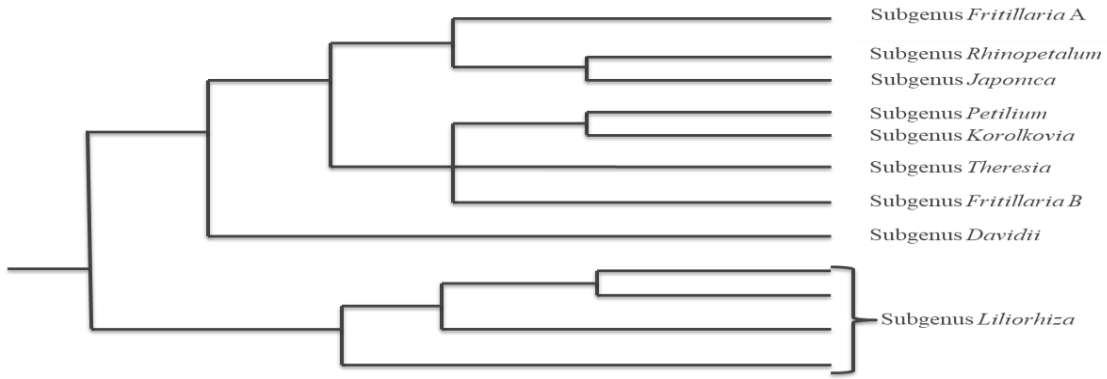
KEYWORDS

Fritillaria eduardii,
Fritillaria imperialis
var. *eduardii*,
endemic plant.

Fritillaria cinsi

Fritillaria cinsi, yaklaşık 140 soğanlı otsu çok yıllık türden oluşmaktadır [1, 2, 3]. Cins genel olarak iki dala ayrılmakta ve bu iki dalda *Fritillaria*, *Rhinopetalum*, *Japonica*, *Petillum*, *Korolkovia*, *Theresia*, *Davidii* ve *Liliorhiza* olmak üzere sekiz tür bulunmaktadır (Şekil 1). Bir dal, ağırlıklı olarak Kuzey Amerika'nın batı bölgelerinde bulunan *Liliorhiza* alt cinsine ait türleri içerir. Diğer türler ise ikinci dalda bulunur ve Avrasya'ya dağılmıştır [1, 4, 5].

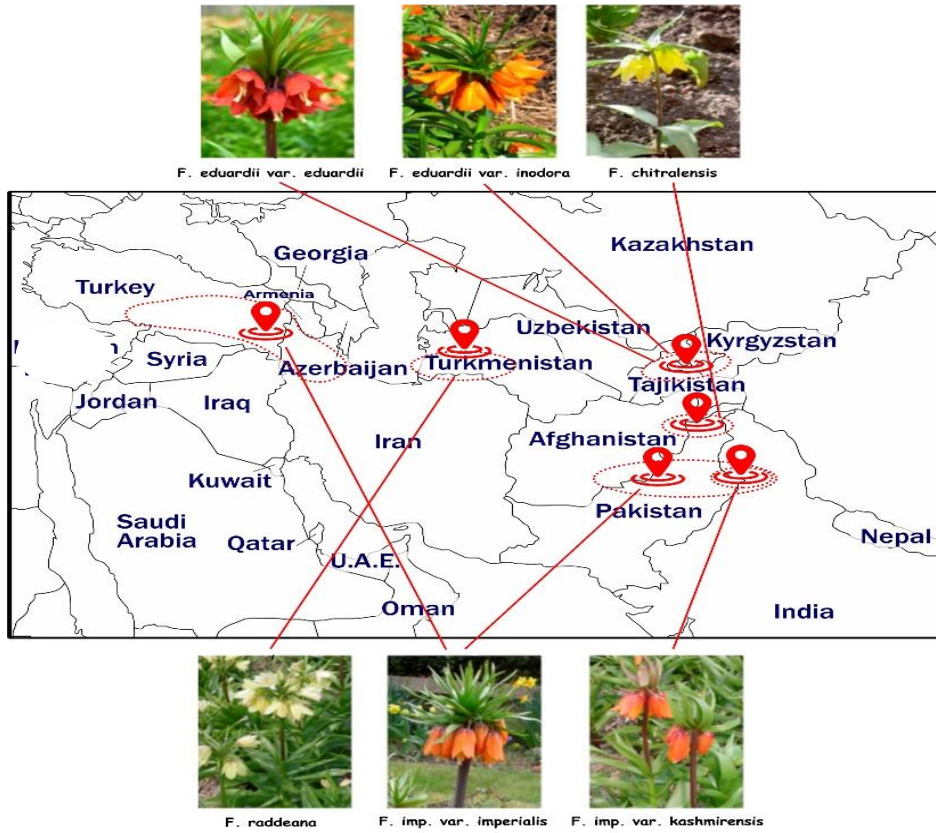
Avrupa (çoğunluk Akdeniz bölgesinde), Orta Asya, Çin ve Japonya gibi bölgelerde *F. chitralensis*, *F. eduardii*, *F. imperialis* ve *F. raddeane* olmak üzere dört farklı *Fritillaria* türü bulunmaktadır (Şekil 2). *F. chitralensis*, Afganistan ve Pakistanın kuzey bölgelerinde bulunmaktadır. *F. eduardii* (*Regel ex Lozinsk.*) nadir görülmesiyle özellik kazanmıştır.



Şekil 1 *Fritillaria*'nın alt tür sınıflandırması [5]

Fig. 1 Subspecies classification of *Fritillaria* [5]

F. imperialis türü, Anadolu'dan Himalaya dağlarına kadar yer alan geniş bir bölgede yer almaktadır. *F. raddeana* (Regel) Vved. ex Pazij türü, Kopetdag (Aşhabat. Türkmenistan) bölgesinin endemik bitkisidir. Bu türün öbürlerinden farkı, çiçeklerinin yeşil sarımtırak renginde olmasıdır [6].



Şekil 2 Orta Asya'da var olan başlıca *Fritillaria* türleri [7]

Fig. 2 The main *Fritillaria* species existing in Central Asia [7]

***Fritillaria* yapısı ve gelişiminin tarihsel süreci**

Fritillaria cinsine ait bitkiler, Dağ yamaçlı yüksekliklerde ve çalılıklarda deniz seviyesinden 1200-2500 metre yüksekliklerde yetişmektedir. Batı Avrupa, İran, Afganistan ve Türkiye'nin dağlarında büyüyen bu bitkilerden Aygöl lalesi gibi bazı türleri bir metreye kadar uzayabilmektedir. Bitkinin gövdesinin tepesinde ve çiçeklerin üstünde ince mızrak şeklindeki yaprakları bulunmaktadır. Gövdenin tepesinde yer alan çiçekleri ağzı aşağıya eğik, çan şeklinde 5-9 adettir. Çiçeklerin renkleri çeşitli tonlarda olur. En çok karşılaşılanları da sarı, kırmızı ve turuncu renkleridir. Bu cinse ait türlerin başka tür bitkilerden ayırt eden karakteristik özelliklerinden biri de hoş olmayan kokuya sahip olması ve bazı türlerinde hiç kokusunun olmamasıdır [8].

Fritillaria 16. yüzyılda Türkiye'den Batı Avrupa'ya getirilmiştir ve süs bitkisi olarak kullanılmaya başlanmıştır. 1553'de İtalya'nın Vener padişahının bahçesinde Leyden Karl Kluziust tarafından yetiştirilmeye başlanmıştır. 1573'ten itibaren "Padişah tacı" olarak tanınmıştır. Çünkü bitkinin çiçekleri taca benzer bir şekilde çiçek açar. 1574'ten itibaren ise botanik literatürlerinde *Corona imperialis* olarak adlandırılmaya başlanmıştır [9].

Fritillaria, 1753'te Linnaeus tarafından tanımlanan Avrupa'daki ilk bahçe bitkilerinden biriydi. Bu tarihten itibaren bitki, çeşitli taksonomik sınıflandırmalar altında yer almıştır [10]. Türkiye'deki en büyük dördüncü geofit bitki cinsidir. Türkiyede, %36,53 endemizm oranı ile *Fritillaria*'nın 41 taksonu bulunmaktadır ve bu oran cins için çeşitlilik merkezi olarak kabul edilebilir [11].

***Fritillaria* Genomu**

Fritillaria cinsine ait türler, başka diploid bitki türlerine kıyasla son derece büyük genom boyutuyla (1C-value: c. 29.7 pg to 100.1 pg (c. 29 Gb ile c. 98 Gb arası)) karakterize edilir. Angiosperm türleri ile karşılaştırıldığında *Fritillaria* cinsinde yer alan türlerden bazılarının daha büyük genoma sahip olduğu görülmektedir [12]. Bitki genom boyutlarının büyük ölçekli karşılaştırmalı analizlerinde büyük genomlara sahip olan bitkilerin, küçük boyutlu genoma sahip bitkilere kıyasla daha fazla yok olma riski altında olduğu, besin elementlerinin yeterli miktarda olmayan topraklarda büyüme ve adapte olma imkanlarının az olduğu ve ayrıca değişen çevre şartlarına adaptasyonlarının da düşük olduğu belirlenmiştir [13]. Bu bakımdan, *Fritillaria*'nın

genom büyüklüğü, genom evrimini destekleyen mekanizmaları incelemek açısından önemlidir [12].

***Fritillaria*'nın Tıbbi ve Aromatik Önemi**

Fritillaria soğanları Uzakdoğu başta olmak üzere yayılış gösterdiği ülkelerde, binlerce yıldan beri geleneksel tıpta yaygın olarak kullanılmaktadır. *Fritillaria* türlerinin soğanlarından; öksürük ve boğaz ağrısı giderici, balgam söktürücü, ateş düşürücü, akciğeri nemlendirici, yüksek tansiyon düşürücü, astım, sıraca ve bronşit tedavi edici olarak yararlanıldığı bilinmektedir. *Fritillaria* türlerinden alınan doğal ürünler, öksürük tedavisinde kullanılan ilaçlarla karşılaştırıldığında avantajlarının çok olduğu ve daha az yan etki gösterdiği veya hiç yan etki göstermediği görülmektedir [14, 15, 16]. *Fritillaria* türlerinin en büyük fotokimyasal bileşeni olan ve tüm bileşenlerin yaklaşık %42,32'sini oluşturan alkaloidler, çeşitli yollarla indüklenen akciğer hasarını azaltan potansiyel ajanlar olarak kabul edilmektedir [17]. İçerdiği steroidal alkaloidler nedeniyle *Fritillaria*'ların, modern tıpta ilaç sanayinde de kullanım alanı söz konusudur. Bazı *Fritillaria* türlerinde alkaloidlerin dışında ayrıca saponin, sterol, polisakkarit, nişasta, flavonoid, yağ asitleri, organik asitler ve uçucu yağların bulunduğu da belirlenmiştir [18].

Antibakteriyel ve antiviral etkiler

Bakterilere, mantarlara ve virüslere karşı biyoaktif bileşenleri tanımlamak için dünya çapında şifalı bitkiler üzerinde yapılan farmakolojik araştırmalar, antibiyotik direnciyle mücadele için alternatif hale gelebilir [19]. *Fritillaria* cinsine ait bitkilerden alınan ekstraktların bakteri ve virüslere karşı etkisinin olduğu tespit edilmiştir. *F. thunbergii* ile ilgili yapılan çalışmalarda, bu bitkiden elde edilen ekstraktların altı *Helicobacter pylori* suşuna karşı oldukça inhibe edici olduğunu görülmüştür [20]. Bu bitkinin antibakteriyel etkisinin yanı sıra *in vitro*, *in ovo* veya *in vivo* toksisiteyi indüklemeyen antiviral etkisinin de olduğu H1N1 virüsünde yapılan araştırmalar sonucunda belirlenmiştir [21]. Kim ve diğ. [21] tarafından yapılan başka bir çalışmada ise *Fritillaria verticillata* bitkisinin; *Bacillus subtilis*, *Staphylococcus aureus* ve *Micrococcus luteus* dahil olmak üzere üç bakteriye karşı antibakteriyel aktivite sergilediği rapor edilmiştir [22].

Antioksidan etki

Antioksidan etkinin *Fritillaria* cinsinde türe bağlı olarak farklı olduğu bildirilmiştir. Li ve diğ. [23] yaptıkları çalışmada, *F. ussuriensis* ekstraktlarının antioksidan aktivitesinin farklı polarite ile azaldığı rapor edilmiştir (ham favonoid ekstraktı>ham saponin ekstraktı>etanol ekstraktı). *Fritillaria* soğanlarında bol miktarda üç izosteroidal alkaloidin (peimisine, peimine ve peiminine) bulunduğu belirlenmiştir. Ayrıca, *F. pallidiflora*'dan elde edilen FPSP-H2-1 molekülünün de DPPH (1,1-difenil-2-pikrilhidrazil), hidroksil ve ABTS (2,2'-azinobis-(3- etilbenzotiazolin-6-sulfonik asit)) radikallerine karşı güçlü antioksidan özellik gösterdiği de rapor edilmiştir [24, 25, 26]. *F. cirrhosa*'dan elde edilen farklı kimyasal yapılara sahip altı izosteroidal alkaloidin (vertisinon, vertisin, imperyalin-3-β-D-glikozid, delavin, imperyalin ve peimisin) karşılaştırma analizleri; bitkide bulunan bu kimyasalların antioksidan etkilerinin olduğunu ve bu alkaloidlerin arasından vertisinon, vertisin, imperyalin-3-β-D-glikozid, delavin ve peimisinin oksidatif strese karşı imperyaline göre daha güçlü etki gösterdiği belirlenmiştir. Bu bulgular ilk kez *F. cirrhosa*'nın, Nrf2 aracılı antioksidan yolağını aktive ederek hücrel oksidatif streste koruyucu bir rol oynayabileceğini göstermiştir. Bu çalışmada, *F. cirrhosa*'nın oksidatif stresle ilişkili hastalıkların önlenmesi için umut verici bir terapötik tedavi olabileceği de rapor edilmiştir [27].

Toksisite

Fritillaria cinsine ait türlerin kurutulmuş soğanları son derece düşük bir toksisite sergiler. Li ve diğ. [28], *Fritillaria* cinsinin başlıca şifalı bitkilerinden biri olan *F. thunbergii*'nin toksisite özelliklerini araştırmıştır. Farklı bir çalışmada da *F. thunbergii*'nin su ekstraktının tahmini öldürücü dozu (LD₅₀) 52.2 mg kg⁻¹ olarak bildirilmiştir [29]. *F. cirrhosae* ve *F. pallidiflora* özleri arasındaki toksisite ve geleneksel farmakolojik etkilerin karşılaştırmalı bir değerlendirmesinde ise farelerde (LD₅₀) değeri 213.57g kg⁻¹ ve maksimum uygulanabilir doz değeri ise 452.14g kg⁻¹ olarak hesaplanmıştır [30]. *Fritillaria* türleri, çeşitli tümör hücrelerine belirli sitotoksositeye sahiptir. *F. cirrhosa*'nın sulu özütünün, mitotik kontrol noktasını işlevsiz hale getirerek insan kolon epitelyal NCM460 hücrelerinde mitotik sapmaları, anormallikleri ve kromozomal kararsızlığı indüklediği rapor edilmiştir [31, 32]. *F. imperialis*'in sulu ve alkollü özlerinin ise insan karaciğer kanseri hücrelerine ve meme

kanseri hücrelerine karşı sitotoksik, sitostatik ve proapoptotik etkilere sahip olduğu ve ayrıca alkollü özütün sulu özütten daha etkili olduğu da kanıtlanmıştır [33].

Diğer etkiler

Antihipertansif etki, *Fritillaria* türlerinin geleneksel etnofarmakolojik özelliklerinden farklı olan yeni bir farmakolojik etkidir. *F. ussuriensis*'in su ekstraktının, sistolik kan basıncının artışını önleyebildiği rapor edilmiştir [34]. Ticari tür olan *F. cirrhosa* ve *F. pallidiflora*'dan elde edilen etanol ekstraktlarının kulak ödemi gelişimini engellediği de tespit edilmiştir [35]. Başka bir çalışmada; *F. unibracteata* ve *F. yuminensis* kaynaklı perimisin-3-O- β -d-glikopiranozidinin, rotenondan etkilenen PC12 hücrelerinde nörotoksisiteye karşı orta koruyucu etki gösterdiği belirlenmiştir [36]. *F. ussuriensis*'in etanolden elde edilen özütünün sıçan mast hücrelerindeki pasif anafilaksi tepkisini ve histamin salınımını önemli ölçüde inhibe ettiği görülmüştür [37]. *Fritillaria* türlerinden ekstrakte edilen ve tanımlanan vertikinonun, muhtemelen periferik ve merkezi mekanizmalar yoluyla inflamatuvar ve kansere bağlı nöropatik ağrıda iyi bir antinosiseptif etkiye sahip olabildiği de rapor edilmiştir [38]. *F. imperialis*'in soğanlarından izole edilen beş izosteroidal alkaloidin (imperiyalin, fortisin, persikanidin, imperisin ve delavin) arasından fortisin, persikanidin, imperisinin anti-asetilkolinesteraz ve anti-butirilkolinesteraz inhibe edici etki gösterdiği de tespit edilmiştir [39].

***Fritillaria* Üzerinde Yapılan Moleküler ve Sitogenetik Çalışmalar**

Fritillaria'nın sitogenetik ve moleküler karakterizasyonu çeşitli araştırmacılar tarafından incelenmiştir. Çalışmalardan biri Rønsted ve diğ. [4] tarafından gerçekleştirilmiştir. Bu çalışmada, *Fritillaria* bitkilerinin plastid ve nükleer DNA bölgeleri analiz edilmiştir. Genetik ilişkileri belirlemek ve doğal bitki popülasyonlarının yapısını göstermek için moleküler markırların kullanıldığı çalışmalar da bulunmaktadır. Metin ve diğ. [40], AFLP (Amplified Fragment Length Polymorphism-Çoğaltılmış Parça Uzunluk Polimorfizmi) markır yöntemini kullanarak Türkiye florasındaki *Fritillaria* türlerini incelemişlerdir [40].

Roguz ve diğ. [41] yaptığı çalışmada ise filogenetik ağaç çizmek için matK, rpl16, rbcL, 18S ve ITS olmak üzere beş DNA markırından oluşan bir veri tabanı hazırlamışlardır. Bu genetik markırlar, *Fritillaria*'daki filogenetik ilişkileri analiz etmek için başka araştırmacılar tarafından da başarıyla kullanılmıştır [4, 5, 42, 43].

Bununla birlikte, Zhang ve diğ. [44] yapmış olduğu araştırmada *Fritillaria* türlerinde tüm kloroplast (CP) genomlarını belirleyerek elde edilen *ycf1*, *trnL*, *trnF*, *ndhD*, *trnN-trnR*, *trnE-trnT*, *trnN*, *psbM-trnD*, *atpI* ve *rps19* moleküler markırlarının taksonomik çalışmalarda yararlı olacağını rapor etmişlerdir [44].

Aygül Lalesi (*Fritillaria eduardii*)

Zambakgiller ailesine ait *Fritillaria* cinsinin bir türü olan Aygül lalesinin bilimsel adı “*Fritillaria eduardii*”– Eduard çiçeğidir. *F. eduardii*; karbonat içeren topraklarda, nemli, kireç ve taşlı toprağa sahip olan orman bölgelerinde, çalılar arasında, ağaçların altında, bazen çalılar ve ağaçların bulunmadığı açık alanlarda, dağların genelde batı ve kuzey kısımlarında deniz seviyesinden 700-2500 metre yükseklikte yetişir. Kırgızistanda da deniz seviyesinden 1550-2000 m yükseklikteki dağların güneş görmeyen kuzey kısımlarında bulunur. Çiçek açma zamanı Mart ayının başından Mayıs ayının sonuna kadardır [45]. Çiçeklerinin kokusu vardır ama çok fark edilmez. Nektarının içeriğinde şekerin konsantrasyonu çok yüksektir. Bitkinin tozlaşmasında böceklerin, kelebeklerin ve haşerelerin yeri büyüktür. Bazı kaynaklar, 13 çeşit haşerenin tozlaştırmada görev aldığını bildirmektedir. Bununla birlikte kuşlar da tozlaşmaya katkıda bulunmaktadır. Meyve verme zamanı Mayıs ve Haziran aylarıdır. Yaz mevsiminin sonuna doğru Aygül bitkisinin toprağın üst kısmında yer alan gövdesi kurur [46].

F. eduardii tüm *Fritillaria* cinsine ait türler gibi soğanlı bir polikarpiktir ve bitki örtüsünün doğası gereği tipik bir efemeroiddir. *F. eduardii*'nin soğanı büyük, küresel veya ovaldir, soğanı 8 cm çapında, kökleri ise 15-30 cm derinlikte bulunur. En büyük soğanlı bitkilerden biri olarak kabul edilmiştir [47]. Bazı bitkileri, çiçeklenme dönemindeyken yaklaşık 15 çiçek açabilir. Genel olarak çiçek açma Mart ayında başlar ve Mayıs ayına kadar sürebilmektedir. Bu bitki, deniz seviyesinden 2500 metre yüksekliklere kadar doğal olarak bulunabilir. Tohum verme zamanı ise Mayıs-Haziran aylarıdır. Tohumu, küçük yassı ve kahverengidir [9, 48, 49]. Doğada sadece tohumla çoğalır, fideler 7-9 yaşlarında çiçek açar [47, 49] ve tohumun çimlenme oranı %60'a kadar çıkabilmektedir [49].

***Fritillaria eduardii* Tarihçesi**

F. eduardii ve çeşitlerinin isimlendirme tarihi 1884 senesine dayanmaktadır. Eduard Regel 1884'te *F. eduardii*'yi ilk olarak tanımlamıştır ve o zamandan beri bitkinin adı üzerinde farklılıklar bulunmaktadır. 1884'te Eduard Regel tarafından bu yeni *Fritillaria*'ların tartışıldığı dört makale yayınlanmıştır. İlk üçü Gartenflora'da ve dördüncüsü Acta Horti Petropolitani'de yayınlanmıştır. Yeni keşfedilen tür, 30-60 cm yüksekliğe, çok yapraklı bir gövdeye ve büyük mor renkli çiçeklere sahip, iyi bilinen *F. imperialis*'in yakın akrabası olarak kayıt altına alınmıştır. Eduard Regel, bu yeni bitkiyi *F. imperialis* türüne benzer olarak görmemiştir. Bunun nedenini de hem soğanlarda hem de çiçeklerinde *F. imperialis*'e has olan bir kokusunun olmaması ve daha kısa, yapraksız gövdesinin olması olarak açıklamıştır. 1884'te yayınlanan sonraki makalelerde aynı bitkiden tekrar bahsedilmiş, ancak makalede kokusu olmayan *Fritillaria*'nın bu türleri *Fritillaria imperialis inodora* ve *Fritillaria imperialis L. var. inodora purpurea Rgl* olarak *F. imperialis*'in bir varyetesi olarak sınıflandırılmıştır. Bu yeni keşfedilen kahverengi-mor çiçekli *Fritillaria* bitkisi, *F. imperialis*'e kıyasla daha kısa, yapraksız bir gövdeye sahiptir ve çiçekleri başlangıçta, tomurcuk aşamasında daha dik olarak gelişim göstermektedir. Acta Horti Petropolitani'deki son yayında, biri safran sarısı aşağıya eğik haldeki çiçeklere sahip ve diğeri mor, dik veya yatay çiçekleri olan iki renk çeşidi olan bitki ayırt edilmiştir. Makale, "*Fritillaria Eduardi A. Rgl.*" olarak kaydedilmiştir, ancak Regel'in kendisi bu ismin kaldırılması gerektiğini belirtmiştir [50, 51, 52, 53]. 1878 ve 1879 yılları arasında ise Albert Regel, Tacikistan'daki Darwas ve Baldschuan dağlarında ve Özbekistan'daki Doğu Buhara dağlarında *Fritillaria* bitkisini toplamıştır ve onları Rusya'nın Saint Petersburg kentine ekim için getirmiştir. *F. eduardii* adı Albert Regel tarafından babasının onuruna önerilmiştir. Bitkinin kokusuz bir soğana sahip olduğunu ve parlak kırmızı bir çiçek örtüsü ile dik veya incelmış çiçekler (*F. imperialis*'teki gibi başını sallamadan) olarak tanımlanmıştır [33]. Flora Uzbekistanika'da Vvedensky, *F. eduardii*'yi Petilium cinsindeki bir tür olarak bahsetmiştir [54]. Bitkinin üç çeşit çiçek renginden bahsedilir: turuncu-kırmızı, tuğla kırmızısı ve mor-kahverengi. Sonradan Wietsma ve diğ. [7], *F. eduardii* adını yeniden kabul etmiştir ve önce yayınlanan çalışmalarda bahsedilen bitkinin isimlerinin *Fritillaria eduardii* olduğunu ve önceden kullanılan isimlerin eş anlamlı isimler olduğunu belirtmiştir.

Eduard Regel tarafından bahsedilen kokusuz *Fritillaria* bitkilerinin de *F. eduardii*'nin biri *Fritillaria eduardii* var. *eduardii* ve diğeri *F. eduardii* var. *inodora* olan iki varyetesinin olduğunu belirtilmiştir. *Fritillaria eduardii* var. *eduardii* bitkisinin; çan şeklinde ve sarkık mor-kırmızı veya kırmızı çiçeklere sahip olduğu, yaklaşık 60-70 cm yüksekliğinde olduğu rapor edilmiştir. Bununla birlikte *F. eduardii* var. *inodora* bitkisinin ise yaklaşık 50-70 cm yüksekliğinde sarıdan turuncuya, geniş çapta çan şeklinde, dik veya sarkık çiçeklere sahip olduğu belirtilmiştir. *Fritillaria eduardii* türünün Orta Asya'ya, özellikle Tacikistan, Özbekistan, Kırgızistan ve muhtemelen Afganistan'ın dağlık bölgelerine özgü olduğu da vurgulanmıştır [7].

***Fritillaria eduardii*'nin Biyolojik Özellikleri**

Aygül lalesi, zambakgiller ailesinin bir üyesi olan çok senelik bir bitkidir. Çiçek tablası ve taç yapraklarının çeşitli renklerde olması ve ayrıca gelişmiş kök ve sürgün sistemleri Aygül lalesinin bilinen özellikleridir. Bitkinin karakteristik özelliklerinden bir de çiçeklerinde koku olmamasıdır [47]. Bu çiçeğin filizleri, tohumları toprağa düştükten yedi yıl sonra yüzeye çıkar ve yedi yıl sonra, üzerinde parlak turuncu renkli ilk çiçek tomurcuğu belirir. Bitkide yılda birden fazla tomurcuk görünmez, bu nedenle bitkinin yaşı çiçek sayılarına göre belirlenebilir [57]. Mart ayından itibaren yeşillenmeye başlar, Nisan ve Mayıs aylarında çiçeklenir.

Milko [6] tüm popülasyon alanı boyunca 200'den fazla çiçek açan ve rastgele seçilen *F. eduardii* bireylerinde bitki boylarını ve çiçek sayılarını eşit kriterlere göre ölçmüştür. Bu çalışmada, bitki yüksekliği 65 cm ve bir bireydeki/örnekteki çiçek sayısı 4 olacak şekilde ortalama değerler kaydedilmiştir. Rapor edilen en küçük örnek ile ilgili veriler şu şekildedir: yükseklik 37 cm, çiçek sayısı 1 adet, apikalde 5 ve gövdede 20 adet yaprak. En uzun örneğin değerleri ise yükseklik 95 cm, çiçek sayısı 13, apikalde 27 ve gövdede 38 adet yaprak olacak şekilde belirlenmiştir. İncelenen popülasyondaki *F. eduardii*'nin alt yapraklarının genişliği 5-12 cm ve orta kısımları ise (yukarı doğru boyut olarak küçülme gözlemleniyor) 2,5-4 cm'dir. Gölgede büyüyen bitkilerde yaprak laminanın maksimum uzunluğu 22,5 cm, çiçeğin çapı 10 cm ve taç yaprağının uzunluğu ise 6,5 cm olarak belirlenmiştir.

Büyük, parlak renkli çiçekleri, bu bitkinin entomofil olmasının bir işaretidir ve tozlaştırıcı böceklerin yaşam döngülerinin kütlesi ve eşzamanlılığı, tohum yenilenmesinin önemli sınırlayıcı faktörlerinden biridir. Çiçeklenmenin başlangıcında,

açıldıktan sonraki 2-3 gün içinde çiçeklerin dibinde büyük nektar damlaları belirlenir. Nektarı çok sıvıdır (şeker içeriği yaklaşık %8'dir), bu nedenle beslenme için değil susuzluğu gidermek için daha uygundur ve hem özel nektarofajları hem de ara sıra damlayan su (çiğ), tüketicilerini (arı, böcek ve sinekleri) çeker. Nektar damlaları ve üzerlerinde toplanan böcekler ile bazen kuşları da çektiği belirlenmiştir [57].

***Fritillaria eduardii*'nin Yaşam Döngüsü**

Çiçeklenme dönemindeyken yaklaşık 15 adet çiçek açılabilir. Bu bitkinin soğanları havaların sıcak olmaya başladığı mart ayından itibaren büyümeye başlar (Şekil 3.01 ve Şekil 3.02). Şekil 3.03 ve Şekil 3.04' de görüldüğü gibi mart ayı boyunca toprak üstü aksamı büyümeye devam eder. Genelde Nisan ayında gövdelerinin tepesinde ve çiçeklerinin üstünde ince mızrak şeklinde yapraklardan oluşan tuğ şeklinde bir yaprak demeti oluşmaya başlar (Şekil 3.05). Genel olarak çiçek açma nisan ayı ile başlar ve mayıs ayına kadar sürebilmektedir (Şekil 3.06 ve Şekil 3.07). Bununla beraber tohum verme zamanı ise Mayıs-Haziran aylarıdır (Şekil 3). Çiçekleri 4-6 gün arasında tozlaşır ve tohumlanır. Tohumlandıktan bir gün sonra dişi organını tepeciği kuruyarak kahverengi hale gelir. Yağmurlu günlerde de bitkinin çiçek taçları dökülmez. Genelde çiçeklerinin %40-60'ı dökülmektedir [58, 59].



Şekil 3 Aygül bitkisinin yaşam döngüsü.
Fig. 3 Life cycle of Aigul plant

***Fritillaria eduardii* Üzerinde Yapılan Çalışmalar**

Farklı disiplinlerden yapılan çalışmalar genelde *Fritillaria* cinsi kapsamında gerçekleştirildiğinden dolayı günümüze kadar Kırgızistan'a özgü *F. eduardii* üzerinde yapılmış olan ve yayınlanmış olan makale ve çalışmalar neredeyse yok denecek kadar azdır. Yayınlanmış olan araştırmalarda da sadece bitkinin biyolojik özellikleriyle ilgili bilgiler yer almaktadır. İmanberdieva [57], *F. eduardii* bitkisini Batkenden Bişkek şehri Alamedin bölgesine getirilerek yetiştirmiş ve biyolojik özellikleri başta olmak üzere bitkinin yeni bölgede yetiştirme ile büyüme sürecini gözlemiştir. Sadykova [56], Kırgızistan'ın Özgün Florası konulu çalışmasında Kırgızistan için tipik olan bazı otsu bitki türlerini tanımlarken *F. eduardii* hakkında da bilgi vermiştir. Fergana Vadisi'nin Nadir Bitki Türleri Atlas Sözlüğünde (2021) ise *F. eduardii*'nin biyolojik özellikleri, sistematigi ve durumu hakkında bilgi verilmiştir [60]. Roguz ve diğ. [41] tarafından yapılan çalışmada ise *Fritillaria* türlerinin çiçek özelliklerinin yeni tozlayıcılar için çekiciliği değerlendirilmiş ve çiçek özelliklerinin evrimi izlenmiştir. *Fritillaria* türlerinin çiçek renk değişimlerinin izlenmesi sonucunda diğer bitki aileleri ile kıyaslandığında bu cinste renk kaybının geri dönüşümlü olabileceği belirtilmiştir.

Sonuç ve Öneriler

Önemli *Fritillaria* türlerinden olan ve Kırgızistan için ekonomik değeri bulunan *F. eduardii* bitkisi ile detaylı bilgi vermek için yapılan bu derleme çalışmasında; bu bitkinin korunması ve biyoçeşitlilik içerisindeki devamlılığın sağlanması için moleküler düzeyde çok az çalışmanın yapıldığı belirlenmiştir. Araştırmaların genel olarak sadece bitkinin taksonomik değerlendirilmesi, sitolojik yapısı ve morfolojik özellikleri ile kısmi sekonder metabolitlerin varlığı ve bunların aktiviteleri yönünde olduğu gözlenmiştir. *Fritillaria* türleri hem geleneksel tıpta hem modern tıpta kullanılmaktadır. Ayrıca, bu bitki türlerinin çoğu sadece doğada bulunmaktadır ve sınırlı bölgelerde endemik olarak bilinen türlerinin sayısı da çoktur. *Fritillaria* türlerinin çoğu doğada yetiştiğinden dolayı, bitkinin genetik çeşitliliğinin ve gen kaynaklarının korunması önem arz etmektedir.

Bu çalışmada belirtildiği gibi *F. eduardii* soyu tükenme tehlikesi ile karşı karşıyadır. Geleneksel çoğaltım yöntemlerinin çoğaltım katsayısı ve çoğaltım hızı bakımından yetersiz kaldığı bilinmektedir. Bu yüzden öncelikle bitki doku kültürü kullanılarak *F.*

eduardii için etkin bir çoğaltım tekniği geliştirmesi önerilmektedir. Ayrıca moleküler analizler sayesinde nesli tükenmekte olan bu bitkiyle ilgili detaylı genom bilgisinin elde edilmesi önemlidir. Özellikle endemik tür sayısı bakımından Kırgızistan'ın sahip olduğu zenginliğin farkına varılarak güncel problemlerin olumsuz etkilerini en aza indirmek için kapsamlı biyoteknolojik önlemler alınmalıdır.

Teşekkürler

Yazarlar, Kırgızistan-Türkiye Manas Üniversitesi'ne projeye sağladıkları mali destek için teşekkürlerini sunarlar (KTMU-BAP-2022.FB.01).

Kaynakça

1. Rix, EM., E. Frank, G. Webster, *Fritillaria*: A revised classification: together with an updated list of species. 2001, Worcestershire, UK: Fritillaria Group of the Alpine Garden Society.
2. Hill L (2013). *Fritillaria*: A list of published names. Version 5.7. Available at: <http://www.fritillariaicones.com/info/names/frit.names.pdf> (last accessed July 2022).
3. WCSP (2017). World Checklist of Selected Plant Families. Facilitated by the Royal Botanic Gardens, Kew. Available at: <http://wmsp.science.kew.org> (last accessed July 2022).
4. Rønsted, N., et al., Molecular Phylogenetic Evidence for The Monophyly of *Fritillaria* and *Lilium* (*Liliaceae*; *Liliales*) and the Infrageneric Classification of *Fritillaria*, *Molecular Phylogenetics and Evolution*, 2005. 35: p. 509–527
5. Day, P. D., et al., Evolutionary Relationships in The Medicinally Important Genus *Fritillaria* L. (*Liliaceae*), *Molecular Phylogenetics and Evolution*, 2014. 80: p. 11–19.
6. D. Mil'ko., Eduard's Imperial Crown (*Petillum Eduardii*, *Liliaceae*) In Kyrgyzstan, *Turczaninowia*, 2005. 8.2: p. 44-53.
7. Wietsma, Willem A., et al., The nomenclatural history of *Fritillaria eduardii* and the correct names of its varieties, *Taxon*, 2011. 60.6: p. 1754-1759.
8. Alp, Ş., Doğal Çiçeksoğanları ve Ters Lale Koruma Önlemleri ve Yetiştiriciliği, Yalova: Doğal Çiçek Soğanlıları Derneği, 2006. Yayın No: 2, ISBN : 975 - 00731 - 1 - 8
9. Butkov A. IA., *Petillum Eduardii*. – Ozvek SSSRnin Kyzyl Kitebi. Tashkent, , 1984: p. 33 (Бутков. А.Я. Петилиум Эдуард. –Өзбек СССР инин Кызыл Китеби. Ташкент, 1984. - 33-б)
10. Kevin, Pratt, and Jefferson Brown MJ., *The gardener's guide to growing fritillaries*, 1997. USD, Timber Press Publishing. ISBN-10: 0881923877
11. Tekşen, M., and Z. Aytac, The revision of the genus *Fritillaria* L. (*Liliaceae*) in the Mediterranean region (Turkey), *Turkish Journal of Botany*, 2011. 35: p. 447–78.
12. Bennett, MD., and IJ Leitch, (2012), *Plant DNA C-values Database* (Release 6.0, Dec. 2012). Available at: <http://data.kew.org/cvalues> (last accessed July 2022)
13. Day, Peter D., *Studies in the genus Fritillaria L. (Liliaceae)*. 2018, Diss. Queen Mary University of London.
14. Marco, R., et al, Incidence of Chronic Obstructive Pulmonary Disease in a Cohort of Young Adults According to The Presence of Chronic Cough and Phlegm, *The American Journal of Respiratory and Critical Care Medicine*, 2007. 175: p. 32–9.
15. Li, H., Y. Jiang, and P. Li, Chemistry, Bioactivity and Geographical Diversity of Steroidal Alkaloids from the *Liliaceae* Family, *Natural Product Reports*, 2006. 23: p. 735.
16. Hao, D., et al., Phytochemical and Biological Research of *Fritillaria* Medicine Resources, *Chin Journal Natural Medicine*, 2013. 11: p. 330–44.
17. Majnooni, MB., et al., Phytochemicals: potential therapeutic interventions against coronavirus-associated lung injury, *Front Pharmacol*, 2020. 11: p. 1–22.

18. Gurlek, D., A. Muhammad, and O. Sebahattin, *In vitro* rooting without exogenous auxins and acclimatization of *Fritillaria* species of Turkey, *Current Opinion in Biotechnology*, 2011. 22: p. S140.
19. Abdalla, M. A., and C. Zidorn, The genus *Tragopogon* (Asteraceae): a review of its traditional uses, phytochemistry, and pharmacological properties. *Journal of Ethnopharmacology*, 2020. 250, 112466.
20. Li, Y., et al., *In vitro* Anti-*Helicobacter Pylori* Action of 30 Chinese Herbal Medicines Used to Treat Ulcer Diseases, *Journal Ethnopharmacology*, 2005. 98: p. 329–33.
21. Kim, M., et al., Antiviral Activity of *Fritillaria thunbergii* Extract Against Human Influenza Virus H1N1 (PR8) *in vitro*, *in ovo* and *in vivo*, *Journal of Microbiology and Biotechnology*, 2020. 30: p.172–7.
22. Kim, S., et al., Inhibition of Sortase, a Bacterial Surface Protein Anchoring Transpeptidase, by β -itosterol3-O-glucopyranoside from *Fritillaria verticillata*, *Bioscience Biotechnology Biochemistry*, 2003. 67: p. 2477–9.
23. Li, X., et al., *In vitro* Antioxidant and *in vivo* Anti-inflammatory Potential of Crude Non-alkaloid Fractions from *Fritillaria ussuriensis* Maxim, *Latin American Journal of Pharmacy*, 2010. 8: p. 1328–35.
24. Pan, F., et al., Extraction, Purification and Antioxidation of A Polysaccharide from *Fritillaria unibracteata* var. *wabuensis*, *International Journal of Biological Macromolecules*, 2018. 112: p. 1073–83.
25. Ruan X., et al., Optimization of supercritical fluid extraction of total alkaloids, peimisine, peimine and peiminine from the bulb of *Fritillaria thunbergii* Miq, and evaluation of antioxidant activities of the extracts, *Materials*, 2016. 9: p. 524.
26. Rozi, P., et al., Sequential Extraction, Characterization and Antioxidant Activity of Polysaccharides from *Fritillaria pallidiflora* Schrenk, *International Journal of Biological Macromolecules*, 2019. 131: p. 97–106.
27. Liu, S., et al., Isosteroid Alkaloids from *Fritillaria cirrhosa* bulb as Inhibitors of Cigarette Smoke Induced Oxidative Stress, *Fitoterapia*, 2020. 140: p.104-434.
28. Li H., et al., *Fritillariae Thunbergii* Bulbus: traditional Uses, Phytochemistry, Pharmacodynamics, Pharmacokinetics and Toxicity, *International Journal of Molecular Sciences*, 2019. 20: p. 16-67.
29. Li, Z., et al., Acute and Sub-chronic Toxicity Studies of The Extract of Thunberg Fritillary Bulb, *Regulatory Toxicology and Pharmacology*, 2014. 68: p. 370–7.
30. Xu, Y., et al., A Comparative Assessment of Acute Oral Toxicity and Traditional Pharmacological Activities Between Extracts of *Fritillaria cirrhosae* Bulbus and *Fritillaria pallidiflora* Bulbus, *Journal Ethnopharmacology*, 2019. 238: p. 111853.
31. Guo, X., et al., Extract of bulb *Fritillaria cirrhosa* Perturbs Spindle Assembly Checkpoint, Induces Mitotic Aberrations and Genomic Instability in Human Colon Epithelial Cell Line, *Toxicologic Pathology*, 2017. 69: p. 163–71.
32. Guo, X., et al., Aqueous extract of bulb *Fritillaria cirrhosa* induces cytokinesis failure by blocking furrow ingression in human colon epithelial NCM460 cells. *Mutation Research-Genetic Toxicology and Environmental Mutagenesis*, 2020: p. 850–851: 503147.
33. Zarei, O., and MM. Yaghoobi, Cytotoxic effects of *Fritillaria imperialis* L. extracts on human liver cancer cells, breast cancer cells and fibroblast-like cells, *Biomed Pharmacother*, 2017. 94: p. 598–604.
34. Kang, DG., et al., Effects Of Bulbus *Fritillaria* Water Extract on Blood Pressure and Renal Functions in the L-NAME-Induced Hypertensive Rats, *Journal of Ethnopharmacology*, 2004. 91: p. 51–6.

35. Wu, X., et al., Investigation of Association of Chemical Profiles with The Tracheobronchial Relaxant Activity of Chinese Medicinal Herb Beimu Derived from Various *Fritillaria* Species, *Journal Ethnopharmacology*, 2018. 210: p. 39–46.
36. Zhang, Q., Z. Zheng, and D. Yu, Steroidal alkaloids from the bulbs of *Fritillaria unibracteata*, *Journal of Asian Natural Products Research*, 2011. 13: p. 1098–103.
37. Cho, I., et al., *Fritillaria ussuriensis* Extract Inhibits The Production of Inflammatory Cytokine And Maps in Mast Cells, *Bioscience Biotechnology Biochemistry*, 2011. 75: p. 1440–5.
38. Xu, F., et al., Antinociceptive Efficacy of Verticinone in Murine Models of Inflammatory Pain and Paclitaxel Induced Neuropathic Pain, *Biological and Pharmaceutical Bulletin*, 2011. 34: p. 1377–82.
39. Atta-Ur-Rahman, et al., New Steroidal Alkaloids from *Fritillaria imperialis* and Their Cholinesterase Inhibiting Activities, *Chemical Pharmacological Bulletin*, 2002. 50: p. 1013–6.
40. Metin, Ö. K., et al., Evaluation of the genetic relationship between *Fritillaria* species from Turkey's flora using fluorescent-based AFLP, *Turkish Journal of Biology*, 2013. 37.3: p. 273-279.
41. Roguz, K., et al., Evolution of bird and insect flower traits in *Fritillaria* L.(Liliaceae), *Frontiers in plant science*, 2021. 12: p. 656783.
42. Khourang, M., et al., Phylogenetic relationship in *Fritillaria* spp. of Iran inferred from ribosomal ITS and chloroplast trnL-trnF sequence data, *Biochemical Systematics and Ecology*, 2014. 57: p. 451-457.
43. Kim, Jung Sung, and Joo-Hwan Kim., Updated molecular phylogenetic analysis, dating and biogeographical history of the lily family (*Liliaceae: Liliales*), *Botanical Journal of the Linnean Society*, 2018. 187.4: p. 579-593.
44. Zhang, T., et al., Identification of evolutionary relationships and DNA markers in the medicinally important genus *Fritillaria* based on chloroplast genomics, *PeerJ*, 2021. 9: p. e12612.
45. Imanberdieva N. A., and Maadaliyeva A. M., Sovremennoe Sostoianie Endema *Fritillaria eduardii* i Ego Introducisia v Chuiskuiu Dolinu (Kyrgyzskaia Respublika) // Mejdunarodnyi jurnal prikladnyh i fundamentalnyh issledobanii, 2020. 2: p. 17-20. (Иманбердиева Н.А., Маадалиева А.М. Современное Состояние Эндема *Fritillaria Eduardu* И Его Интродукция В Чуйскую Долину (Кыргызская Республика) // Международный журнал прикладных и фундаментальных исследований. – 2020. – № 12. – С. 17-20)
46. M. V. Baranova., The Ecologo-Morphological Peculiarities of the Underground Organs of the Representatives of the Genus *Fritillaria* (Liliaceae), 2008.
47. Bondarenko L. Imperatoridun taajjysy- Gul osturuuchuluk, Moskva, 2002: (Бондаренко.Л. Императордун таажысы –Гүл өстүрүүчүлүк. Москва, 2002. - 12-б.)
48. Lozina-Lozinkaja A. S., Rabchik – *Fritillaria* L. SSSR, 1935: p. 302. (Лозина-Лозинская А.С. Рябчик – *Fritillaria* L. СССР, 1935. - 302–б.)
49. Kamelin R. V., and Belousova L. S., Rabchik Eduard. Krassnaia Kniga SSSR 2-Том. Moskva, 1984. - 240-б (Камелин. Р.В., Белоусова Л.С. Рябчик Эдуард. Красная Книга СССР. 2-Том. Москва, 1984. - 240-б.)
50. Regel, E., Kurze Nachrichten über die letzten Sammlungen von A. Regel. *Gartenflora*, 1884a. 33: p. 68–73.
51. Regel, E., Internationale Gartenbau-Ausstellung der Kaiserlichen Gartenbau-Gesellschaft in St. Petersburg vom 5. /17.–17. /29. Mai 1884. *Gartenflora*, 1884b. 33: p. 163–170.
52. Regel, E., *Fritillaria imperialis* L. var. *inodora purpurea* Rgl. *Gartenflora*, 1884c. 33: p. 257–258, Tafel 1165.
53. Regel, E., Descriptiones plantarum novarum et minus cognitarum, IX. *Trudy Imp. S.-Peterburgsk. Bot. Sada* [= *Acta Horti Petropolitani*], 1884d. 8: p. 639–702.

54. Losina-Losinskaja, A.S. Genus 271. *Fritillaria* L. 1935: p. 232–246. in: Komarov, V.L. (ed.), *Flora of the U.S.S.R.*, vol. 4. Leningrad: Izdatel'stvo Akademii Nauk SSSR.
55. Vvedensky, A.I., Petilium. P. 473 in: Schreder, R.R. & Kudr-jashev, S.N. (eds.), *Flora Uzbekistanica*, vol. 1. Tashkent: Editio Academiae Scientiarum UzSSR, 1941.
56. Sadykova, A., Unique Flora of Kyrgyzstan. Materials of The All-Russian Youth Scientific And Practical Conference "Modern Problems of The Ecology of The Animal And Plant World", 2021. Russian.
57. Baranova M. V., K sistematike roda *Lilium*. Leningrad, 1990: p 74. (Баранова. М.В. К систематике рода *Lilium*. Ленинград, 1990. - , 74-6.)
58. Imanberdieva N. A., Current state of the endem *P. eduardii* and its introduction to the Chui valley (Kyrgyz Republic). IV. International Eurasian Agriculture and Natural Sciences Congress. Congress Book. Turkish 2020: p. 75.
59. Kimsanaliev, D., et al., Biotechnological Approaches on Aigul Flower (*Fritillaria eduardii*), 8th International Congress on Fundamental and Applied Sciences 2021 (ICFAS2021) Proceeding Book. 2021 Antalya, Turkey. p. 176
60. Ro'zimatov, E. Yu., Foziljonov, Sh., and Yuldashev, X.E., Farg'ona vodiysi kamyob o'simlik turlari“ atlas lug'ati //Uslubiy qo'llanma. - Toshkent: «Fan ziyosi» nashriyoti, 2021: p. 84.

Erdogan, E., et al., Hava Bazlı Proteinin Alternatif Bir Protein Kaynağı Olarak Kullanım Olanaklarının İncelenmesi. International Journal of Life Sciences and Biotechnology, 2022. 5(3): p. 643-668
DOI: 10.38001/ijlsb.1096533

Hava Bazlı Proteinin Alternatif Bir Protein Kaynağı Olarak Kullanım Olanaklarının İncelenmesi

Elif Erdogan¹ , Orhan Kaya^{1,2} , Esra Derin^{1,2} , Busra Cakaloglu Ebcim^{1,2,*} 

ÖZET

Sürdürülebilir kaynakların araştırılması gıda endüstrisinde günden güne artan bir öneme sahip olmaktadır. Bu noktada alternatif protein kaynakları, üretimde kullanılan doğal kaynakların sınırlı olması ve hızlı nüfus artışı nedenleriyle popüler araştırma konusu olmuştur. Yapılan araştırmalara göre mevcut tüketim alışkanlıkları ve nüfus artışıyla devam edilirse; 2050 yılına gelindiğinde dünya nüfusuna yeterli protein kaynağının sağlanması için protein mahsullerinin 2005 yılına göre %110 daha fazlasına ihtiyaç duyulacaktır. Tarımsal alanların azalması ve küresel ısınma neticesinde biyoçeşitliliğin zarar gördüğü gerçeği hesaba katıldığında, gelecekte kaliteli protein ve içilebilir su kaynaklarına erişim konusunda sıkıntı çekileceği öngörülebilmektedir. Tek hücre proteini (THP); biyoprotein, mikrobiyal protein veya biyokütle olarak adlandırılan kurutulmuş hücre topluluğudur. THP; mantarlar, mayalar, algler ve bakteriler gibi birçok farklı mikroorganizmalardan elde edilebilmektedir. Hava bazlı protein (HBP) ise Hidrojen Oksitleyici Bakteriler (HOB)'in biyoreaktörlerde çoğaltılıp, saflaştırılıp kurutulması ile elde edilen bir THP'dir. Elde edilen biyokütle, proteine ek olarak lipid, karbonhidrat, vitamin ve mineral kaynağı da sağlamaktadır. Bu sebeple HBP, alternatif ve sürdürülebilir bir protein kaynağı olma potansiyeli taşımaktadır. Bu çalışmada; THP, HOB ve HBP hakkında yapılan araştırmalar derlenmiş ve HBP'lerin kullanım potansiyeline bir ışık tutulması hedeflenmiştir.

MAKALE GEÇMİŞİ

Geliş

04 Nisan 2022

Kabul

22 Temmuz 2022

ANAHTAR KELİMELER

Tek hücre proteini, hidrojen oksitleyici bakteriler, hava bazlı protein, alternatif protein kaynakları, sürdürülebilirlik

¹ Pınar Entegre Et ve Un Sanayi A.Ş., 35730, İzmir, Türkiye

² Ege Üniversitesi, Mühendislik Fakültesi, Gıda Mühendisliği Bölümü, 35040, İzmir, Türkiye

* Corresponding Author: Büşra Çakaloğlu Ebcim busra.cakaloglu@pinaret.com.tr

An Investigation of the Possibilities of Using Air-Based Protein as an Alternative Protein Source

ABSTRACT

Day by day, the researches on sustainable sources are gaining more importance in the food industry. At this point, alternative protein sources became a popular research topic due to the limitation of natural resources used in food processing and rapid population growth. It is stated that, If the current consumption trends and population growth are maintained, 110% more protein crops will be needed compared to 2005 to provide sufficient protein for the world population in 2050. Considering the damaging results of decrease in agricultural areas and global warming to biodiversity, it is predictable that there will be difficulties to access of qualified protein and potable water in the future. The single-cell protein (SCP) refers to dried cells of microorganism and also called as bioprotein, microbial protein, or biomass. SCP can be obtained by many different microorganisms such as fungi, yeasts, algae, and bacteria. Air-based protein (ABP) is an SCP obtained by growing, purifying, and drying of Hydrogen Oxidizing Bacteria (HOB) in bio-reactors. The obtained biomass is a source of lipids, carbohydrates, vitamins and minerals in addition to protein. For this reason, ABP has a potential as an alternative and sustainable protein source. In this study, besides reviewing of researches on SCP, HOB and ABP, it was aimed to shed a light on the potential areas of the ABP usage.

ARTICLE HISTORY

Received
04 April 2022
Accepted
22 July 2022

KEYWORDS

Single cell protein,
hydrogen oxidizing
bacteria,
Air-based protein,
Alternative protein
sources,
Sustainability

Giriş

Dünya nüfusunda meydana gelen hızlı artış ve iklim değişiklikleri nedeniyle meydana gelebileceği düşünülen tarımsal verimlilikteki düşüş küresel gıda güvenliği ile ilgili endişeleri artırmaktadır [1]. Dünya nüfusundaki bu artışın önümüzdeki yıllarda da devam edeceği ve Birleşmiş Milletler (BM)'in tahminine göre bugün 7,7 milyar olan insan nüfusunun 2050 yılına kadar 9,7 milyara ulaşacağı öngörülmektedir [2]. Tilman ve arkadaşlarının [3] tahminine göre artan nüfusa yeterli miktarda protein kaynağı sağlamak için 2050 yılında gerekecek olan tarımsal protein mahsulü 2005 yılına göre % 110 fazla olacaktır. Öte yandan tarımsal alanlar günümüzde çöl olmayan ve buzla kaplı olmayan arazinin yaklaşık %43'ünü kapsamaktadır. Tarımsal üretimin, dünya nüfusunun artmasına paralel olarak artacak olan tarımsal protein talebini karşılaması durumunda ise bu yüzde daha da yükselecek ve biyoçeşitlilik olumsuz yönde etkilenecektir [4]. Ayrıca hayvansal kaynaklı protein arzının küresel tüketim talebini karşılayabilmesi için et üretimi miktarının 2050 yılına kadar iki katına çıkması beklenmektedir. Mevcut durumda 1 kg dana eti üretimi için yaklaşık 15,5 ton su kullanılması, 1 kg tavuk eti üretimi için ise 3,9 ton su kullanılması, temiz su kaynaklarının gelecekte daha hızlı tükeneceğini göstermektedir [5]. Buna bağlı olarak,

zaten kısıtlı olan arazi kaynaklarının hayvancılık ve su ürünleri yetiştiriciliğinde kullanılan protein ağırlıklı yem üretimi için de ayrılması gerekmektedir [6, 7].

Proteinler, hücre onarımı ve yenilenmesinde, çocukların büyüme ve gelişiminde etkili olup diyetle yer alması gereken temel besin öğeleridir [8]. Özellikle içerdikleri fenilalanin, valin, treonin, triptofan, izolösin, metionin, histidin, lösin ve lizin gibi zorunlu amino asitler, insan vücudu tarafından üretilmediği için yaşam boyu besinler yoluyla alınması gerekmektedir [9-11]. Günlük beslenmeyle alınması gereken protein ihtiyacı yaş, kilo, cinsiyet ve fizyolojik durumlar (hamilelik, emzirme, spor yapma, hastalık) gibi faktörlere bağlı olarak değişkenlik göstermektedir [11, 12]. Beslenmeyle alınabilecek protein kaynakları hayvansal ve bitkisel olmakla birlikte hayvansal kaynaklı proteinler zorunlu amino asitler bakımından daha zengindir [13]. Tablo 1’de çeşitli faktörlere bağlı kilogram vücut ağırlığı başına günlük alınması gereken protein miktarı (g) verilmiştir. Tablo 2’de ise yaş gruplarına göre gerekli zorunlu amino asit miktarları (mg/g protein) görülmekte olup büyüme çağında zorunlu amino asitlere gereksinimin daha fazla olduğu anlaşılmaktadır [11].

Tablo 1 Değişik faktörlere göre günlük gerekli protein miktarları [8]

Table 1 Daily protein requirements based on different factors[8]

Gruplar	Alt grup	Protein (g/kg-gün)
Bebekler	6-12 ay	1,0
Çocuklar	1-3 yaş	0,87
	4-8 yaş	0,76
Erkekler	9-13 yaş	0,76
	14-18 yaş	0,73
	>19 yaş	0,66
Kadınlar	9-13 yaş	0,76
	14-18 yaş	0,71
	>19 yaş	0,66
Hamilelik dönemi	14-50 yaş	0,88
Emzirme dönemi	14-50 yaş	1,05

Dünya nüfusunun hızlı artışı ve iklim değişikliğinin, günümüzde zaten var olan gıda güvenliği ve yetersiz beslenme gibi olguların artmasına neden olacağı öngörülmektedir [14]. Dünyada eşit olmayan gelir dağılımı nedeniyle kaliteli proteine erişim

sağlanamaması, özellikle gelişmekte olan ülkelerde yetersiz beslenmeye neden olmaktadır [15]. Kişinin diyetinde yeterli protein kaynağı bulunmaması da kas güçsüzlüğü, büyüme geriliği ve bağışıklık sisteminin zayıflaması gibi ciddi klinik sorunlara neden olabilmektedir [16].

Tablo 2 Çeşitli yaş gruplarına göre zorunlu amino asit gereksinimleri [11]

Table 2 Essential amino acid requirements based on various age groups [11]

Amino asit (mg/g protein)	0-5 yaş	1-2 yaş	3-10 yaş	11-14 yaş	15-18 yaş	>18 yaş
Histidin	20	18	16	16	16	15
İzolösin	32	31	31	30	30	30
Lösin	66	63	61	60	60	59
Lizin	57	52	48	48	47	45
Metionin+Sistein*	28	26	24	23	23	22
Fenilalanin+Tirozin*	52	46	41	41	40	38
Treonin	31	27	25	25	24	23
Triptofan	8,5	7,4	6,6	6,5	6,3	6,0
Valin	43	42	40	40	40	39

*Metionin vücutta sistein yapımında kullanıldığı için, fenilalanin ise tirozin yapımında kullanıldığı için birlikte verilmiştir.

Gelecek yıllarda etkileri daha çok görülecek olan iklim değişikliği ve nüfus artışı ile meydana gelecek olan protein talebindeki artış, yüksek kaliteli proteine erişimi daha da zorlaştıracaktır. Bu nedenlerden dolayı bazı araştırmacılar çalışmalarını, geleneksel gıda ve yem katkı maddelerine alternatif olacak besin kaynakları üzerine odaklamışlardır. Minimum çevresel etki ile gıda güvenliğini koruyan ve yüksek kaliteli proteinlerin üretimine olanak sağlayan tek hücre proteinleri, geleneksel hayvan ve bitki bazlı proteinlere kıyasla umut verici alternatifler olarak görülmektedir [17]. Bu makalede, tek hücre proteinlerinden biri olan hava bazlı protein üretiminin ortaya çıkışı, gelişim süreci, üretim yöntemleri, beslenmedeki yeri, kullanım alanları ve çevresel etkileri hakkında yapılan araştırmalar derlenmiş ve HBP'lerin kullanım potansiyeline ışık tutulmaya çalışılmıştır.

Tek Hücre Proteini (THP)

Tek hücre proteini (THP) kurutulmuş hücre topluluğudur. Bu kavram aynı zamanda biyoprotein, mikrobiyal protein veya biyokütle olarak da ifade edilmektedir [18, 19].

Yüksek ham protein içeriği (%60-70), hayvansal proteinlere benzer amino asit profili, B grubu gibi zengin vitamin içerikleri ve düşük miktarda yağ seviyeleri sayesinde insan ve hayvanlar için alternatif bir besin potansiyeli oluşturmaktadır [18, 20]. THP'lerin amino asit profili incelendiğinde ise çoğu hayvan ve bitki kaynağında yeterli miktarda bulunmayan lizin, metiyonin gibi çeşitli amino asitler açısından zengin olduğu saptanmıştır [21]. Ayrıca THP'nin balık unu ve soya fasulyesi unu gibi protein kaynaklarının iyi bir ikamesi olduğu bildirilmiştir [22].

Protein kaynaklarını artırmanın etkili yollarını aramak, teknolojik ilerlemenin ana hedeflerinden olmuştur. Mikrobiyolojik sentez ile protein üretimi; geleneksel et üretimine göre su, toprak, enerji gibi kaynakları daha verimli kullanan, iklim ve hava şartlarına bağlı olmayan bir üretim şeklidir. Gıda güvenliği açısından ise hormonlar, pestisitler ve patojenler gibi kimyasal ve biyolojik tehlikelerin de önüne geçilebilmektedir [23].

İnsanların ve hayvanların beslenmesinde önemli bir yeri olan proteinin geleneksel üretimden daha sürdürülebilir alternatif kaynakları uzun yıllardır araştırılmaktadır [18]. Mikroorganizmalar yoğurt, peynir, kefir, ekmek, fermente sebzeler ve fermente balık ezmesi gibi birçok geleneksel gıdanın bileşenleri olarak binlerce yıldır insan beslenmesinin bir parçası olmuştur [24]. Ekmek ve içecek üretimi için kullanılan mayaların tarihi ilk çağlara kadar dayanmaktadır. Ayrıca mayalar, hayvan yemi takviyesi olarak önemi neredeyse bir asır önce anlaşılan ilk mikroorganizmalardır. 16. yüzyılda bugünkü Meksika başkentinin yerlileri, Texcoco Gölü'nün yakınlarındaki alkali sularından *Arthrospira* (yaygın olarak *Spirulina* olarak bilinir) cinsine ait siyanobakterileri toplamıştır [25]. *Spirulina* biyokütlesinin toplanması ve bisküvi şeklinde kurutularak insan tüketimi için kullanımı günümüzde hala devam etmektedir [26]. Birinci Dünya Savaşı sırasında Almanlar *Candida utilis*'i çorbalarda ve sosislerde kullanmışlardır. Savaş sırasında Alman askerlerinin diyetleriyle aldıkları proteinin yarısı mayalar ile ikame edilmiştir. İkinci Dünya Savaşı sırasında da bu ikame yöntemi yoğun olarak kullanılmıştır [27, 28]. 1960'lı yıllarda protein, yağ ve vitamin kaynağı olarak bakteriyel biyokütleyi doğrudan kullanmak için ilk adımlar atılmıştır ve daha sonra THP terimi ortaya çıkmıştır [29]. Mikroorganizmaların kuru maddesinin büyük bir çoğunluğunun proteinden meydana gelmesi, bu canlıların tek hücre olarak yüksek protein içeriğinde olmasını sağlamaktadır [30].

THP üretiminde optimum ortam koşulları sağlanırsa, bitkisel veya hayvansal protein kaynaklarına kıyasla daha hızlı bir şekilde üretim gerçekleştirilebilmektedir. Ayrıca gıda işletmelerinde sistemden ayrılan atık nitelikli yan ürünlerin tek hücre proteini üretimi sırasında besi ortamı olarak kullanılması ekonomik olarak fayda sağlamaktadır. İncelenen mikrobiyal gelişim ortamlarının bazıları portakal kabukları, şeker kamışı, patates, Hindistan cevizi, üzüm, mango vb. işlenmesi sırasında ortaya çıkan tarımsal yan ürünlerdir. Ayrıca alkol, kâğıt, petrol vb. sanayi atıkları da besi yeri olarak kullanılmaktadır. Bu tarımsal ve sanayi atıklarının değerlendirilmesi ile ekonomik kazanım artmakta, çevre kirliliğinin artışı engellenebilmekte ve yüksek kaliteli hayvansal ürünlere alternatif bir protein üretimi gerçekleştirilebilmektedir [31-37]. Ek olarak, THP üretim süreci kapalı sistemlerde gerçekleştiği için mevsimsel değişikliklerden etkilenmemektedir. Ayrıca hayvansal protein üretiminde görülen hayvan hastalıkları da bu üretim modelinde görülmemektedir. Böylelikle THP dört mevsim boyunca, talep edilen miktarda verimli bir şekilde üretilebilmektedir [38-40]. THP üretimi geniş arazi ve büyük su kaynakları gerektirmediğinden, THP'nin bitkisel ve hayvansal protein kaynaklarına iyi bir alternatif olacağı düşünülmektedir [41, 42]. THP üretimi sırasında hayvansal hastalıkların görülme olasılığı olmasa da üretim sırasında yüksek kontaminasyon riski mevcuttur. Fermentasyon ortamının dış ortamda bulunan mikroorganizmalarla, dış ortamın da biyoreaktör içerisindeki mikroorganizmalarla kontaminasyonunun engellenmesi için biyoreaktör içerisindeki hava giriş ve çıkışlarında steril hava filtreleri kullanılmaktadır. Bu durumun yanı sıra kontaminasyonu engellemek için yapılan uygulamalardan biri biyoreaktör boşken sterilize etmek, daha sonra kesikli veya sürekli sistemle steril edilen besiyerini mikroorganizmaların kullanması için fermentasyon kabına aktarmaktır. Diğer bir yöntem ise biyoreaktörün fermentasyon ortamı ile doldurulması ve ikisinin beraber tek seferde sterilize edilmesidir. Bir başka açıdan bakıldığında ise fermentasyon için gereken hava, inokulum ve besin maddelerini taşıyan bütün borular buhar ile sterilize edilmektedir. Ortamda bulunması istenmeyen mikroorganizmaların inaktive edilebilmesi için, biyoreaktör bağlantıları buharla muameleye uygun şekilde dizayn edilmekte ve sistem aseptik inokülasyon, örnek alma ve ürün ayrılmasına uygun olarak tasarlanmaktadır [43].

THP'nin zengin protein, vitamin ve esansiyel amino asit içeriği, bu ürünün besin değerini yükseltmektedir. Ancak içeriğinde fazla miktarda nükleik asit bulunması, bilim insanlarını geleneksel protein kaynaklarına alternatif olmaları konusunda daha fazla araştırma yapmaya sevk etmiştir. İnsan vücuduna fazla miktarda nükleik asit alınması halinde ürik asit çökmesi ve böbrek taşı oluşumu gibi bazı sağlık problemleri görülebilmektedir [44]. Katabolizmayla birlikte nükleik asitler hipoksantin ve ksantine parçalandıktan sonra bu ürünler ksantin oksidaz enziminin etkisiyle ürik aside dönüşmektedir. Ürik asit suda çok az çözünmektedir ve ürik asit kristalleri renal dolaşımında yoğunlaştığında çökme meydana gelerek böbrekte tübül tıkanması, glomerüler filtrasyon ve idrar çıkışında azalmaya neden olabilmektedir [45]. Ham THP'lerdeki bu yüksek nükleik asit oranı bazı kimyasal, enzimatik veya ısıl işlemler ile azaltılabilmektedir [27]. Bakteri kaynaklı THP'lerin yüksek nükleik asit içeriği bakterilerin RNA'larından kaynaklanmaktadır. THP'lerin RNA içeriğini ve böylece içerdiği nükleik asit miktarını azaltmak amacıyla çeşitli metotlar geliştirilmiştir. Isıl işlem (60-70°C) ile aktivasyondan sonra ribonükleaz kullanılarak RNA degradasyonu gerçekleştirilebilmektedir. Ancak bu işlem sonrasında degrade olan RNA bileşenleri hücrenin dışına dağılır ve %35 ile %38 arasında bir biyokütle kaybı yaşanabilmektedir. Oluşan bu kaybı azaltmak amacıyla araştırmacılar prosesi daha yüksek (72-74°C) sıcaklık aralığında uygulamış ve biyokütle kaybını %30 ile %33 düzeylerine indirmeyi başarmışlardır. Alkali hidroliz ve kimyasal ekstraksiyon metotları da benzer amaçlar doğrultusunda incelenmiştir. Yapılan bir çalışmada 65°C, 7,5-8,5 pH aralığında yapılan işlemde RNA içeriği %2'nin altına düşürülmüş olup protein içeriği %50 olarak korunabilmiştir [46].

Bu işlemlerin sonucunda, işlenmiş mikrobiyal biyokütle ağırlıklı olarak ölü hücrelerden oluşmaktadır [44]. Tablo 3'te mikroorganizma gruplarının bazı ortalama besin değerleri kuru ağırlık (%) cinsinden verilmiştir [27].

THP birçok farklı mikroorganizma ile elde edilebilmektedir. Önemli THP kaynağı olan bakterilerin jenerasyon süreleri oldukça kısadır. Bu mikroorganizmalar geniş bir substrat kullanım alanına sahip olmakla birlikte cinslerine bağlı olarak 20 ile 120 dakika içerisinde sayılarını iki katına çıkarabilmektedirler. Nişasta, şeker gibi organik atıkları ve hatta etanol, metanol ve nitrojen gibi petrokimyasal atıkları dahi substrat olarak

kullanabilen THP kaynağı bakteriler mevcuttur [47] ve bu bakterilerden elde edilen THP'nin amino asit profili balık proteini ile benzerlik göstermektedir [48].

Tablo 3 THP üretiminde kullanılan mikroorganizmaların ortalama bazı besin öğeleri

Table 3 Some approximate amount of nutrients of microorganisms used in SCP production

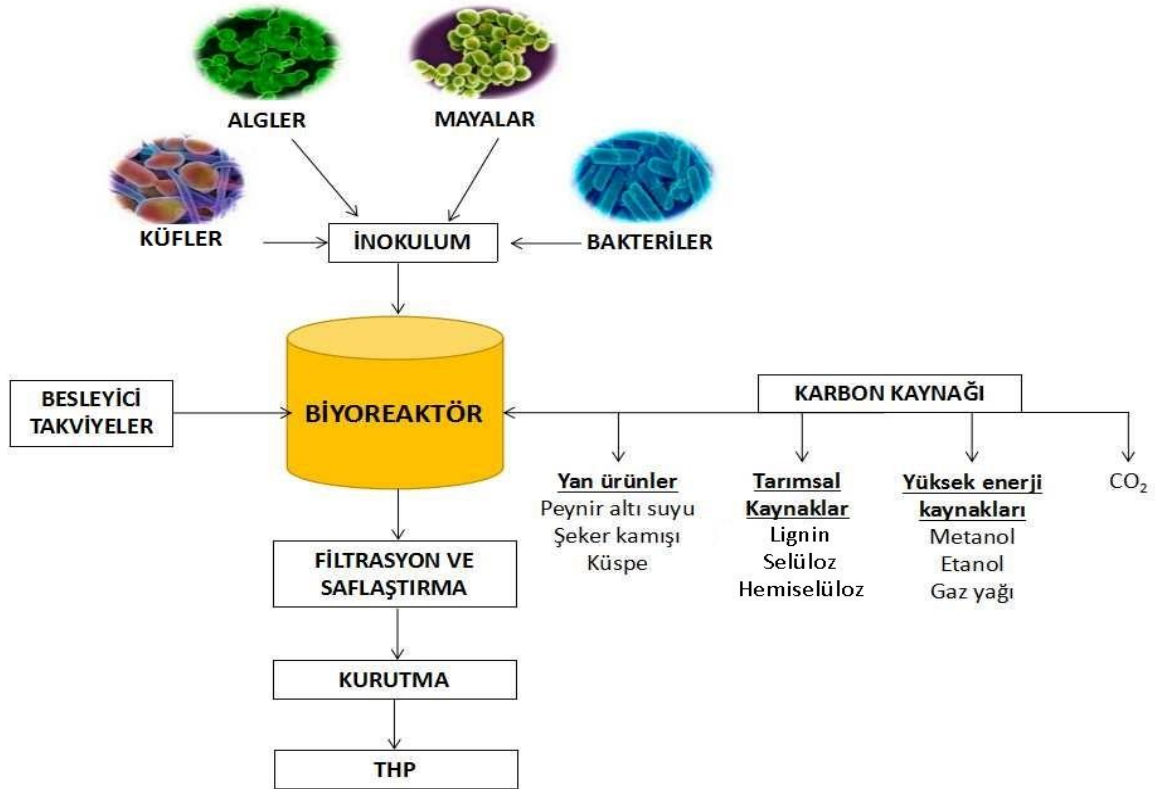
	Küfler	Algler	Mayalar	Bakteriler
Protein (%)	30-45	40-60	45-50	50-80
Yağ (%)	2-8	7-20	2-6	1-3
Kül (%)	9-14	8-10	5-10	3-7
Nükleik asit (%)	7-10	3-8	6-12	8-12

Önemli bir THP kaynağı da küflerdir. Küflerden elde edilen THP mikoprotein olarak isimlendirilmektedir ve %30-50 oranında protein içermektedir. Mikoproteinler sofralarda tüketilmek üzere 'Genel Olarak Güvenli' (GRAS) gıda sınıfında kabul edilmesinin yanı sıra amino asit profili de Gıda ve Tarım Örgütü'nün (FAO) standartlarını karşılamaktadır [27]. Son yıllarda özellikle vegan diyet için oldukça dikkat çeken, sürdürülebilir protein kaynaklarına önemli bir alternatif sunan mikoproteinler, her ne kadar *Agaricus bisporus*, *Auricularia fuscusuccinea*, *Neurospora intermedia* ve *Pleurotus albidus* türleri kullanılarak üretilse de *Fusarium venenatum* adlı küf türü, mikoprotein üretiminde en çok bilinen ve gıdalarda ticari olarak kullanılan türdür [49-53].

Bazı mikroalg türlerinden elde edilen THP'ler de hayvan ve insan tüketimi için üretilmekte ve genellikle %70 oranına kadar protein içerebilmektedir. Protein içeriğinin yanı sıra, omega-3 yağ asiti içermesi nedeniyle yağ kaynağı olarak sağlıklı bir profil oluşturmaktadır. Bununla birlikte, alglerde, %3 ile %8 arasında değişen nispeten düşük miktarda nükleik asit içeriği bulunmaktadır [54]. Texcoco Gölü yakınlarındaki Meksikalı insanlar tarafından hasat edilen ve insan diyetinde kullanılması için kurutulan bir alg cinsi olan *Spirulina* uzun yıllardır tüketilmektedir. Dünyanın farklı yerlerinde *Chlorella* ve *Senedesmus* gibi diğer alg cinslerinin biyokütlesi de yem kaynağı olarak kullanılmıştır. Alglerin yüksek protein içeriği, hızlı büyüme hızı ve basit yetiştiriciliği dünya çapında yem bileşeni olarak kabul görmelerinde kolaylık sağlamıştır [55]. Dünyada tüm mikroalg türlerinin yıllık üretiminin 10 bin ton olduğu tahmin edilmektedir. Yıllık alg biyokütlesinin %75'ten fazlası toz, tablet, kapsül veya pastil

üretiminde kullanılmaktadır [56]. Ayrıca yeşil algler iyi bir antioksidan kaynağı olarak da değerlendirilmektedir. Nutrasötikler ile birlikte *Spirulina maxima* adlı alg türü içeren bir diyet ile birlikte progenitör hücreler korunabilmektedir. Ek olarak yağlı karaciğer sendromunu önleme yeteneğine de sahiptirler. Alglerin yukarıda bahsedilen avantajları bulunmasına rağmen kuru maddesinde bulunan selülozik hücre duvarları insanlar tarafından sindirilememektedir. Ayrıca bileşimde yüksek düzeyde ağır metaller bulunabilmektedir [57].

THP üretiminin başlangıç aşamasında, çalışılacak olan mikroorganizmaya uygun karbon kaynağını içeren besi ortamı hazırlanmaktadır. Daha sonra biyoreaktörde üreme için optimum koşullar sağlanarak istenilen mikroorganizmanın üretimi gerçekleştirilir ve işlem sonunda biyokütle ayrılarak hasat edilir. Fermantasyondan sonra biyokütle; yıkama, hücre parçalanması, protein ekstraksiyonu ve saflaştırma gibi işlemlere tabi tutulmaktadır [27, 47, 58]. THP üretimi temel olarak Şekil 1’de gösterilmiştir [18].



Şekil 1 THP üretim şeması

Fig 1 SCP production chart

Ototrof mikroorganizmalar karbon ve besin döngüsü için oldukça önemlidir. Bu mikroorganizmalar inorganik karbondioksiti (CO₂) atmosferden alıp biyolojik ve

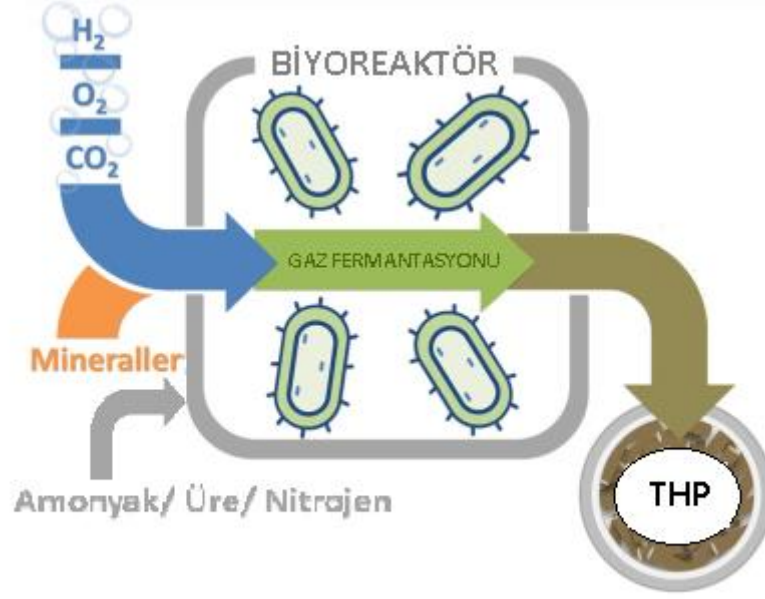
kimyasal reaksiyonlarda kullanarak organik biyokütle besinleri olan azot (N) ve fosfora (P) geri dönüştürmekte ve daha yüksek yaşam formları için yiyecek üretilmesini sağlamaktadırlar [59]. Algler ve ototrof bakteriler THP formunda hem hayvan yemi olarak hem de insan gıdası olarak alternatif bir protein kaynağı olmaktadır [60, 61]. Proteinin yanı sıra, bu mikroorganizmalar bünyelerinde dikkate değer bir miktarda prebiyotik materyal de biriktirebilmektedir [17].

Hidrojen Oksitleyici Bakteriler (HOB)

İnsanoğlu neredeyse bin yıldır diyetinde geleneksel fermente gıdalar ile (yoğurt, peynir, turşu, vb.) bakterilerden faydalanmaktadır [62]. 1960'lı yıllarda bakteri biyokütlesinin protein, yağ ve vitamin kaynağı olarak kullanımı keşfedilmiştir [63]. Son yıllarda, artan protein ihtiyacı ve sürdürülebilirlik konuları gıda endüstrisinin THP üretimine olan ilgisinin ve araştırmalarının artmasını sağlamıştır. THP üretiminde ototrof hidrojen oksitleyen bakteriler (HOB), özellikleri ve kullanım potansiyeli ile araştırmacıların dikkatini çekmektedir. Ototrof HOB'ler, metabolik özellikleri sayesinde hidrojen (elektron vericisi) ve oksijeni (elektron alıcısı) kullanarak karbondioksiti hücre materyaline bağlayıp, nitrojeni yüksek, kaliteli bir proteine dönüştürebilmektedir [64].

Ototrof HOB'ler tarafından üretilen THP; insan beslenmesi için önem teşkil eden ve besinlerle alınması gereken tüm esansiyel amino asitleri içeren, yüksek kaliteli, besin değeri hayvansal proteinlere benzer bir amino asit profiline sahip bir proteindir. Ototrof HOB'lerin karbon kaynağı olarak karbonhidrat yerine atmosferde bulunan substratları kullanabilmesi ve yapısındaki proteinin özellikleri sebebiyle 1966 yılında ABD Ulusal Havacılık ve Uzay Dairesi (NASA) tarafından uzun süreli uzay görevlerinde kullanılması planlanan kapalı karbon döngüsünün temeli olarak araştırılmıştır [23, 62].

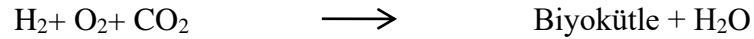
THP'nin en sürdürülebilir örneklerinin üretimini mümkün kılan ototrof HOB'ler Şekil 2'de şematik olarak gösterildiği gibi CO₂'i hücresele bünyelerine sabitleyebilmektedir [62].



Şekil 2 HOB'lerin THP üretimi

Fig 2 SCP production by HOB's

Bazı hücrelerdeki H₂ ve CO₂ ile beslenen anaerobik metabolizma, karbon kaynağının %70-80'ini asetat gibi indirgenmiş bileşiklere dönüştürmekte ve yalnızca %20 oranında THP sentezleyebilmektedir. Protein üretimi açısından incelendiğinde bu üretilen asetat, tekrar karbon kaynağı olarak kullanılmıyor ise pek verimli bir durum sergilenmemektedir. H₂ ve CO₂ arasındaki reaksiyondan salınan enerji sayesinde aerobik H₂ temelli ototrofi, herhangi önemli bir yan ürün üretmeden hücre üreterek biyokütleyi, dolayısıyla da elde edilen THP miktarını artırır. H₂ ve O₂ gazlarının optimal koşullardaki karışımı "Knallgas" olarak bilinmekte ve aerobik H₂ ototrofları, Knallgas bakterileri veya HOB'ler olarak tanımlanmıştır. Genel olarak aerobik H₂ oksidasyonu ile CO₂ bağlanma reaksiyonu aşağıdaki şekilde gösterilmektedir [62, 65]



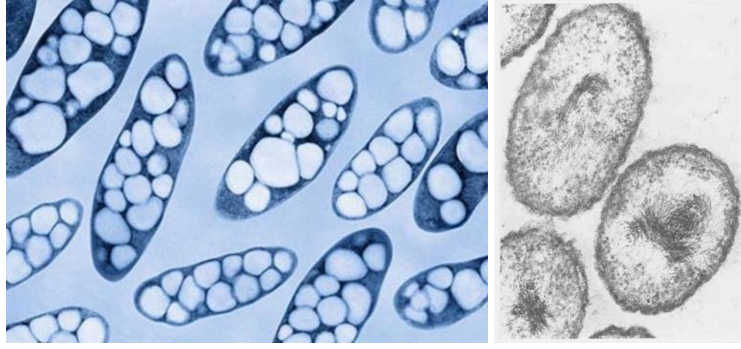
HOB'ler Antarktika buzul altı gölleri, ılıman topraklar ve sıcak hidrotermal menfezler gibi pek çok farklı alanda tespit edilebildiği için kolayca izole edilebilmektedirler. *Rhodococcus opacus* ve *Xantobacter autotrophicus*, endüstriyel kullanım potansiyeli nedeniyle araştırılan bazı bakteri türleridir. *R. opacus* beslenme ögesi ve biyoyakıt gibi ürünlere lipid kaynağı sağladığı için dikkat çeken bir HOB'dir. *X. autotrophicus* ise

gıda boyası olarak kullanılan bir karotenoid olan zeaksantin üretebilmektedir. Bu örnekler arasında kullanım potansiyeli sayesinde uluslararası projelere konu olan ve kısmen endüstride kullanımı onaylanmış ve araştırmalara en çok konu olan HOB *Cupriavidus necator* türüdür [62]. Bazı çalışmalar *C. necator* türünü THP üretimi kapsamında öne çıkartırken, bazı araştırmalar bu bakteri türünün petrol bazlı plastiklere alternatif olabilecek, biyolojik olarak parçalanabilen biyoplastik veya polihidroksialkonoat üretebilme kapasitesine odaklanmıştır [66].

Hava Bazlı Protein (HBP)

Biyoreaktörlerde yenilebilir mikrobiyal biyokütle üretimi, tatlı su tüketicisi, sera gazı yayıcısı ve ötrofikasyona (eutrophication) sebep olan tarımsal üretime önemli bir alternatiftir. Hava bazlı protein (HBP) ise HOB'lerin biyoreaktörlerde çoğaltılıp, saflaştırılıp kurutulması ile elde edilen bir THP'dir. Elde edilen biyokütle, proteine ek olarak lipid, karbonhidrat, vitamin ve mineral kaynağı da sağlamaktadır. Bu proses için Gram-negatif ve Gram-pozitif HOB'ler kullanılmaktadır. HOB'lerin ototrof olarak üretilmesi için gazların (H_2 ve O_2) üretim ortamına sabit hızda verilmesi gerekmektedir. Bu gazlar rüzgâr ve güneş enerjisi kullanılarak su elektrolizi sayesinde elde edilebilmektedir. Suyun elektrolizi, geliştirme ortamından ayrı olarak veya içerisinde kültür bulunan biyoreaktör içinde biyo-elektrokimyasal sistemler (BES) ile gerçekleştirilebilmektedir. BES'de gazların kütle transferi daha etkin olduğu için biyokütle verimi daha yüksek olmasına rağmen, bu sistemlerde su elektrolizi sırasında bakteri gelişimini inhibe edebilecek H_2O_2 veya hidroksil radikaller gibi reaktif oksijen türleri oluşabilmektedir [62, 67-69].

Dikkat çeken bazı çalışmalarda Gram-negatif, *Betaproteobacteria* sınıfına ait, mezofilik, spor oluşturmeyen, fakültatif ve kemolitotrofik bir toprak bakterisi olan *Cupriavidus necator* kullanılmıştır (Şekil 3) [68, 69]. Bovell tarafından 1957 yılında izole edilen bu bakteriye ilk olarak *Hydrogenomonas eutropha* adı verilmiş ancak taksonomik sinonimler sebebiyle yıllar içerisinde *Alcaligenes eutropha*, *Ralstonia eutropha*, *Wautersia eutropha* ve son olarak *Cupriavidus necator* olarak kabul görmüştür [70, 71].



Şekil 3 *Cupriavidus necator*

Fig 3 *Cupriavidus necator*

C. necator ilk olarak *Hydrogenomonas eutropha* adı ile 1960'lı yıllarda Ulusal Havacılık ve Uzay Dairesi tarafından Kaliforniya Ames Araştırma Merkezi tarafından yayınlanan raporda, ortamdaki üre ve CO₂'i kullanacak ve astronotlar için gıda üretebilecek “Kapalı Sistem Karbon Döngüsü (Closed Loop Carbon Cycle)” prototipinin temelini oluşturmuş ve araştırmacıların dikkatini çekmiştir. NASA'nın “Kapalı Sistem Karbon Döngüsü” projesi; o yıllarda biyoreaktörler ve biyoreaktörlerin çalışma prensipleri uzay programı için verimli ve uygulanabilir olmaması, *C. necator*'un insan gıdası olarak tüketiminin *in vivo* çalışmalar ile yeterince desteklenmemesi ve *C. necator* kullanılarak üretilen ilk THP'nin nükleik asit içeriğinin insan tüketimi için gereğinden fazla olması gibi endişeler sebebiyle rafa kaldırmış ve hayata geçirilememiştir [70-72]. NASA'nın bu araştırmalarından yaklaşık 50 yıl sonra, birkaç bilim insanı dünyanın da kıt kaynaklı bir uzay aracı olduğunu düşünerek bu projeyi hayata geçirmiş ve Kaliforniya'da Kiverdi-Air Protein adlı start-up firmasını kurmuşlardır [73].

C. necator'un en önemli özelliği CO₂'i karbon kaynağı olarak kullanarak gelişmesine ek olarak toprakta bulunan süksinat, fumarat ve malat gibi birçok organik bileşiği de substrat olarak kullanabilmesidir. Bu mikroorganizmanın CO₂ bağlama kapasitesi Calvin döngüsünün bir parçası olarak Rubisco enzimi sayesinde oluşmaktadır. Biyokütle oluşturmak için hücrelerin ihtiyacı olan enerji H₂ gazının hidrojenaz enzimi ile oksidasyonu sayesinde elde edilirken, nitrojen ise amonyak, üre ve hatta N₂ gazından sağlanabilmektedir [62, 74].

Belirli kısıtlayıcı koşullar altında *C. necator* polihidroksialkanoat (PHA) üretmekte ve bu bileşik, hücrelerin %90'ını kapsamaktadır [62]. PHA'lar, çok sayıda bakteri tarafından hücre içi karbon ve enerji depolama bileşikleri olarak sentezlenen, hücre

sitoplazmasında granüller halinde biriken hidroksialkanoatların poliestерleridir [75]. Yapılan çalışmalara göre *C. necator*'un salgıladığı bu PHA memeliler tarafından sindirilememekte ve dolayısıyla da elde edilen THP'nin besin değeri düşmektedir [76]. Ancak kontrollü ve optimal şartlar sağlandığında hücreler tarafından sentezlenen PHA minimum seviyeye indirilerek kuru madde olarak %75 oranında protein içeren biyokütle elde edilebilmektedir [62]. *C. necator* gibi HOB'lerin de aerobik H₂ oksidasyonu ile yakıt ve farklı kimyasalların biyoteknolojik olarak üretiminde kullanımı popüler araştırma konusu olmuştur [69].

Tüm bu olumlu yanlarına rağmen son yapılan araştırmalara göre gram-negatif bakteriler, tipik olarak lipopolisakkarit ekzotoksinler içermektedir ve bakteriyel lipopolisakkaritlerin de diyabet, karaciğer hasarı, nörolojik bozukluklar ve kronik bağırsak enfeksiyonu gibi hastalıklarla bağlantılı olduğu belirtilmiştir bildirilmiştir. Dolayısıyla lipopolisakkarit içermeyen gram-pozitif bakterilerin gıda üretimine daha uygun olduğu ileri sürülmüştür [69].

Hava bazlı proteinlerin elde edilmesi ve besin içeriği

HOB'ler hidrojen oksidasyonu ile ortaya çıkan enerjiyi kullanarak CO₂ gazından substrat olarak faydalanıp çoğalmaktadır ve belirli bir konsantrasyona ulaştığında mikroorganizma-besiyeri karışımı filtreden geçirilerek veya santrifüj edilerek besiyerinden arındırılmaktadır. Ayrıştırılan peletin kurutulması ile hava bazlı protein elde edilmektedir. Biyoreaktörlerde, inkübasyon koşulları kontrol altında tutularak çoğaltılan bakteriler üretim ortamından ayrılıp kurutulduktan sonra tatsız ve kokusuz bir ürün ortaya çıkmaktadır. Bu ürünün tercih edilirliliğini ve kalite özelliklerini iyileştirmek için tekstür kazandırmak ve form vermek gibi ileri işlemlere ihtiyaç olabileceği göz önünde bulundurulmalıdır [17, 27, 62, 77, 78].

Günümüzde sürdürülebilirlik kapsamında THP üretiminde kapalı sistemler dikkat çekmektedir. Bu kapalı sistemler, sürdürülebilirliği artırmak ve gıda üretiminin çevresel etkilerini azaltmak amacıyla atmosferdeki havadan direkt olarak karbon bağlamakta ve proses için gerekli olan hidrojen ve oksijen gazını suyun yenilenebilir enerji kaynakları ile hidrolizi sayesinde ortaya çıkarıp kullanmaktadır. Üretimde kullanılan mineral karışımları ise biyoreaktörlere dışarıdan ek olarak verilmektedir [62, 78].

Hibrit biyolojik inorganik sistemler katma değerli ürünler elde etmek için çeşitli mikroorganizmalar ve elektrik enerjisi ile oluşturulmaktadır. Bu sistemler

sürdürülebilir, verimli, çok yönlü ve ekonomik kimyasal sentez platformlarıdır. Temel olarak, biyoyumlu elektrotlar ile elektrik enerjisini direkt veya dolaylı olarak biyolojik olarak kullanılabilir enerjiye dönüştürmektedir. Buna ek olarak, bazı spesifik bakteriler kullanılarak CO₂, çok karbonlu organik bileşenlere sabitlenebilmektedir. Ototrofik mikroorganizmaların metabolizmalarını H₂ ve CO₂ kullanarak devam ettirebilmeleri sayesinde ortamdaki CO₂ kullanımını artar ve böylece pahalı hammadde ihtiyacı azaltılabilmektedir. Liu ve arkadaşları [65] prosesdeki CO₂'i bağlama verimliliğini karşılaştırmak için hibrit biyolojik inorganik sistem kullanarak atmosferdeki CO₂'i ve saf CO₂ gazını kullanmışlardır. Hibrit biyolojik inorganik sistem kullanılarak yapılan işlemlerde %50 olan CO₂'i bağlama verimliliğinin, saf CO₂ kullanıldığında %20'ye kadar düştüğü gözlemlenmiştir. Bu sistemlerde HOB için toksik etki oluşturan reaktif oksijen türleri (ROT) oluşabileceği bilinmektedir. ROT oluşmasının engellenmesi amacıyla Nangle ve arkadaşları [79], ROT üretimi yerine H₂ üretimi için seçici katalizörlerin geliştirilmesi üzerine çalışmışlardır. Bu amaçla kobalt-fosfor (Co-P) alaşımı katot olarak kullanılmış, sonuç olarak alkali koşullarda bu alaşımın hidrojen üretimini desteklediği, nötral koşullarda ise hidrojen üretimini minimum ROT üretimi ile artırdığı gözlemlenmiştir.

THP'lerin besleyici değeri ve kullanılabilirliği ürün bileşimine bağlıdır. Besin içeriği, vitaminler, nitrojen içeriği, karbonhidratlar, yağlar, hücre duvarı içeriği, nükleik asitler, protein konsantrasyonu ve amino asit profili gibi parametrelerin THP'lerin gıdalarda kullanılmasından önce tespit edilmesi gerekmektedir. Örneğin azot kaynağı kısıtlı ortamda üretilen *H.eutropha*, insan vücudunun stres ortamında yağ biriktirmesine benzer şekilde β-hidroksibütirik asit salgılamaktadır ve memelilerin bu yapıdaki ürünleri sindiremediği bilinmektedir [77]. Ayrıca belirli bir mikroorganizma türünün THP üretiminde kabul edilebilirliği; büyüme hızına, kullanılan substrata, meydana gelebilecek kontaminasyonlara ve mikroorganizma ile ilişkili toksinlere bağlıdır [60].

Hydrogenomonas eutropha kullanılarak elde edilen hava bazlı protein ürününün 100 gram kuru madde temelindeki içeriği, Tablo 4'te gösterilmiş olup protein miktarının 74 gram olduğu dikkat çekmektedir [71, 80]. Tablo 5'te HBP ile bazı protein kaynaklarının 100 gram kuru madde temelinde içerdiği zorunlu ve zorunlu olmayan amino asit miktarları verilmiştir [81, 82].

Tablo 4 HBP'nin bazı besin öğeleri

Table 4 Some nutrients of ABP

Besin İçeriği	100 g kuru madde HBP
Protein (g)	74
Yağ (g)	9
Kül (g)	2
Nükleik asit (g)	8
Ca (mg)	66
Mg (mg)	98
Na (mg)	280
K (mg)	590

HBP'nin tüm zorunlu amino asitleri içermesinin yanı sıra metiyonin ve triptofan içeriğinin bezelye proteinine, lizin içeriğinin ise glütene göre daha fazla olduğu görülmektedir. Zorunlu olmayan amino asit profiline bakıldığında ise çeşitlilik göstermekle birlikte genel olarak diğer protein kaynaklarına göre düşük değerlerin olduğu görülmektedir. Beş yıl sonra yapılan bir çalışmada [83] *Hydrogenomonus eutrophu*'nun aminoasit kompozisyonunun Tablo 5'te verilen değerlerden %50 fazla olduğu gözlenmiştir. Bu farkın, daha önceki çalışmada, proteinin tamamlanmamış hidrolizinden veya daha büyük olasılıkla, kalıntı substrattan bakteriyel proteinin, protein olmayan nitrojen (üre) ile seyreltilmesinden kaynaklanabileceği bildirilmiştir. Bu durumla birlikte çeşitli çalışmalarda, HBP'nin hayvansal proteine benzer bir protein profilinin olduğu, soyadan elde edilen proteinle karşılaştırıldığında 2 kat daha fazla amino asit içerdiği ve amino asit bileşiminin kazein proteinine benzer olduğu belirtilmektedir. *H. eutropha*'dan elde edilen HBP'nin içeriğinde kalsiyum, magnezyum, sodyum, potasyum gibi minerallerin bulunduğu da tespit edilmiştir [71, 80].

Beslenme açısından incelendiğinde, araştırmacılar hava bazlı proteinin, mevcut bir gıda maddesinden daha zararlı olmadığını belirtmektedirler. Hâlihazırda hayvan beslenmesi için kullanılan hava bazlı proteinin insan beslenmesi için yeni bir gıda olarak tanımlanması ve GRAS listesine girmesi için otoritelerin çalışmaları devam etmektedir [84]. Yapılan araştırmalarda hava bazlı proteinin farelerde, domuzlarda, köpeklerde, maymunlarda ve şempanzelerde herhangi bir akut toksisite oluşturmadığı belirtilmiş,

farelerle yapılan deneylerde hava bazlı proteinin sindirilebilirliğinin %93 olduğu tespit edilmiştir [85]. İnsanlar ile yapılan deneylerde ise 25-30g ham haldeki hava bazlı proteini tüketen kişilerde 24 saat içinde karın ağrısı, ishal, baş ağrısı ve halsizlik görülmüştür. Araştırmacılar bir insanın herhangi bir belirti göstermeden 1 günde maksimum tüketebileceği işlem görmemiş hava bazlı protein miktarının 6 gram olduğunu belirtmişlerdir [72]. Bu durumun yanı sıra sadece hava bazlı protein içeren bir diyet uygulamasında tüketilen nükleik asit içeriğinin normal diyete göre yaklaşık 25 kat daha fazla olacağı saptanmıştır. Nükleik asidin metabolizmaya dahil olması, kandaki ürik asit seviyesinin yükselmesine ve idrar yolunda kristalleşme riskine neden olmaktadır [72]. Diyetle alınan nükleik asit miktarının günde 3-4 g'dan fazla olmaması gerektiği belirtilmektedir. Bu durum, fermentasyon sonucu elde edilen hava bazlı proteinin içeriğindeki yüksek nükleik asit miktarının kimyasal, enzimatik veya ısı uygulamaları ile azaltılmasını zorunlu hale getirmektedir [46].

Hava bazlı proteinin ham halinin tüketicilerin tercih etmeyeceği bir tat ve görüntüye sahip olduğu, tüketilmesi için mutlaka şekil verme, kalıplama gibi işlemlerin uygulanması ve kıvam ve tekstürün iyileştirilmesi gerektiği belirtilmektedir. Tatmin edici bir karbonhidrat/protein oranı için ürün geliştirme kapsamında çeşitli lif ve karbonhidrat içeriklerinin eklenmesi de önerilmektedir [85].

Finlandiya'da bulunan bir firma olan Solar Foods, Solein olarak isimlendirdikleri HBP ürününün tadı ve görünüşünün buğday ununa benzer olduğunu belirtmişlerdir. Solar Foods firmasının ürettiği HBP'nin de tüm esansiyel amino asitlerini içerdiği belirtilmiştir. Üretilen HBP ile ilgili yapılan araştırmalara göre soya proteine kıyasla, bir yetişkinin günlük amino asit gereksinimlerinin karşılamak için daha küçük bir Solein porsiyonunun yeterli olduğu ileri sürülmüştür. Ürün %65-75 oranında protein içerirken, sırasıyla %10-20, %4-10 ve %4-10 oranlarında karbonhidrat, yağ ve mineraller içermektedir [85].

Çevresel etkileri

Tarım endüstrisi günümüzde çöl veya buzul olmayan toprakların yaklaşık %43'ünü kullanmaktadır. Artan protein ihtiyacını karşılamak için kullanılan tarım alanlarının Dünya üzerindeki oranı daha da artacak ve biyoçeşitlilik üzerinde negatif bir etki yaratacaktır. Dünya'da iklim krizine sebep olan sera gazları %36-70 su buharı, %9-26 CO₂, %4-9 metan ve %3-7 ozondur [62]. Paris İklim Anlaşması'nın iklim krizi

etkilerini azaltma hedefine ulaşmak için yılda 4-5 Gigaton CO₂ depolanması gerekmektedir. Hükümetlerarası İklim Değişikliği Paneli'ne (IPPC) göre toplam antropojenik sera etkisine 2007-2016 yılları arasında sebep olan gaz emisyonlarının %23'ü tarım, ormancılık ve diğer arazi kullanımından dolayı ortaya çıkmıştır. Biyoreaktörlerde üretilen protein kaynaklarına geçiş ile gıda üretiminin çevre üzerinde oluşturduğu baskının azalacağı öne sürülmektedir [78].

Tablo 5 HBP ve bazı protein kaynaklarının amino asit profili

Table 5 Amino acid composition of ABP and some protein sources

Amino asit	HBP	Bezelye	Pirinç	Soya	Glüten	Peynir altı suyu	Yumurta
Zorunlu amino asitler							
Histidin	0.95	2.4	2.2	2.5	1.9	1.8	2.3
Treonin	2.15	4.0	4.0	3.9	2.4	7.4	4.6
Valin	3.03	3.9	5.5	3.9	3.6	5.1	6.4
Metiyonin	1.14	0.9	2.1	1.2	1.3	1.5	3.4
Izolösin	2.17	3.4	3.7	3.7	3.1	5.7	5.7
Fenilalani	2.20	4.6	4.9	4.9	5.7	2.7	5.8
Triptofan	0.78	0.4	1.3	1.3	1.2	1.4	1.2
Lösin	4.04	7.3	8.0	7.5	6.7	9.8	8.5
Lisin	2.65	8.4	3.9	6.6	1.2	9.5	6.9
Zorunlu olmayan amino asitler							
Aspartik asit	4.32	11.7	10.1	12.1	2.5	11.0	10.2
Serin	1.80	5.7	5.7	5.2	5.2	5.7	7.0
Glutamik asit	7.67	19.9	20.0	19.7	38.4	18.6	13.3
Glisin	2.76	4.0	4.5	4.3	3.3	1.8	3.5
Arginin	3.41	9.8	8.1	7.4	2.6	2.3	5.4
Alanin	4.47	5.4	6.0	4.4	2.2	5.3	5.8
Tirozin	1.79	3.7	4.7	3.1	3.0	2.6	3.9
Prolin	2.06	4.0	4.5	6.4	14.7	6.6	3.9
Sistin	0.08	0.6	0.9	2.2	1.1	1.4	2.2

Atmosferde biriken sera gazlarından biri olan CO₂'in bağlanarak kullanılması için enerji gerekmektedir. Konvansiyonel gıda tedarikinin temelinde ışığı, enerji kaynağı olarak kullanan bitkiler bulunmaktadır. HOB'ler, karbon enerji kaynağı olarak maliyeti yüksek bitki bazlı karbon kaynakları (şekerler veya karbonhidratlar) yerine karbondioksit gazını

kullanılmaktadır. THP üretiminde kullanılan enerji ise yenilenebilir enerji kaynakları kullanılarak hidrolize edilen sudan ortaya çıkan hidrojen gazından elde edilebilmektedir. Böylece üreticiler karbon nötr bir ürün elde edebilmektedir [62].

Sillman ve ark. [86] yapmış oldukları çalışmada, havadaki CO₂ gazını tutan mikrobiyal protein üretimi ve soya fasulyesi üretimi işlemleri sırasında kullanılan suyu ve alan miktarlarını karşılaştırmışlardır. Çalışma sonunda, mikrobiyal protein üretimi sırasındaki arazi kullanımı ve su tüketiminin, soya fasulyesi üretiminin arazi kullanımı ve su tüketiminden daha düşük olduğu saptanmıştır. Güneş enerjisi ve rüzgâr enerjisi kullanılarak üretilen mikrobiyal proteinde kullanılan su miktarı 0.82 L/kg protein iken, soya fasulyesi üretiminde kullanılan su miktarının 2.67-6.67 L/kg protein arasında olduğu tespit edilmiştir. Alan kullanım miktarları ise güneş enerjisi ve rüzgâr enerjisi kullanılarak üretilen mikrobiyal proteinde sırasıyla 0.04-0.26 m²/kg protein olduğu tespit edilirken, soya fasulyesi üretiminde kullanılan alan miktarının 6.40-15.86 m²/kg protein olduğu belirlenmiştir. Bir HBP üreticisi olan Solar Foods şirketi de Solein olarak isimlendirdikleri ürünlerinin çevreye olan etkilerinin hayvansal ve bitkisel bazlı protein kaynaklarına göre daha düşük olduğunu belirtmektedirler. Solein üretiminde bitkisel protein üretiminden 100 kat, sığır eti üretiminden 700 kata kadar daha az su kullanıldığı tespit edilmiştir. Ayrıca Solein üretimi için arazi kullanımının, bitkisel üretime göre 20 kat, sığır eti üretimine göre 200 kat daha verimli olduğu saptanmıştır. Sera gazı emisyonları açısından ise bitkisel üretimden beş kat, sığır eti üretiminden 200 kat daha az çevreyi kirlettiği belirtilmiştir. Ek olarak Solein'in bitkisel protein üretimden 10 kat daha az, sığır eti üretiminden ise 1000 kata kadar daha az ötrofi emisyonuna (azot oksitleri, nitrat, amonyum, fosfor ve azot gazları) neden olduğu bildirilmiştir [4, 84].

Hava bazlı proteinin ticarileştirilmesi ve endüstrideki yeri

Son 10 yıl içerisinde H₂, O₂ ve CO₂ karışımlarının HOB'ler için substrat kaynağı olarak kullanıldığı ve HOB'lardan gıda ve yem bileşenleri üretiminin gerçekleştirildiği şirketlerin sayısında artış meydana gelmiştir. 2011 yılında kurulan Kaliforniya merkezli bir şirket, THP ürünleri olan AirProtein™ ve CO₂ Aquafeed'in yanı sıra yağlar ve biyoplastikler üzerine de çalışmaktadır [73]. HBP'nin sürdürülebilir gıda üretiminin yeni evrim basamaklarından biri olacağını düşünen firma, ürünlerinin gelecek yıllarda süpermarketlerde olmasını hedeflemektedir. Kaliforniya merkezli diğer bir firma ise

THP'yi su ürünleri üretiminde kullanılan yemlerde kullanılması üzerine geliştirmişlerdir. Firmanın ilk yem denemeleri, balık büyüme oranı dikkate alındığında soya ve alg içeren kontrol diyetlerine kıyasla THP'nin daha üstün olduğunu göstermiştir [87]. Finlandiya'da 2017 yılında kurulan bir şirket ise insan tüketimine uygunluk için AB Gıda Lisansı onayı bekleyen Solein'i üretmişlerdir. Ticari ölçekte üretime geçmeye 2023'te başlamayı planlayan şirket Mars görevlerinde NASA'nın gıda tedarikçisi olmayı ve 2026 yılında yıllık gelirlerinin 80 milyon dolar olmasını hedeflemektedir [88]. Belçika'da kurulan bir firma da maliyeti düşük substratlardan birkaç THP geliştirmiştir. Firma, Hollanda'da bulunan Su Araştırma Enstitüsü KWR ile işbirliği yaparak "Power to Protein" projesi kapsamında THP üretmek için hidrojen oksitleyici bakteriler kullanmıştır [89]. 2018 yılında İngiltere'nin Nottingham şehrinde hem gaz fermantasyonu hem de sentetik biyoloji konusunda geçmişi olan bir ekip tarafından kurulan bir diğer firma da HOB'ları kullanarak ürettiği THP'ye Proton™ adını vermiştir. Firma önemli bir sürdürülebilirlik örneği olarak 2019 yılında bir enerji üretim şirketi ile ortaklık kurarak baca gazından elde edilen CO₂ ile THP üretimi projesine başlamıştır [90]. Mevcut üreticiler, kuruluş yılları ve HBP ürünleri Tablo 6'da özetlenmiştir.

Tablo 6 HBP Üretimi Gerçekleştiren Firmalar

Table 6 ABP Producing Firms

Firma adı	Ülke	Kuruluş Yılı	Ürün
Avecom	Belçika	1995	ProMic, ValProMic, Eximium, Chlorella
Unibio	Danimarka	2001	Uniprotein®
Kiverdi	ABD	2011	Air Protein™
Calysta	Birleşik Krallık	2016	Feedkind
Novonutrients	ABD	2017	Novomeal
Solar Foods	Finlandiya	2017	Solein
Deep Branch	Birleşik Krallık	2018	Proton™

Sonuç

Yapılan araştırmalarda bugüne kadar gıda üretimini sürdürülebilir hale getirebilmek için çok sayıda çözüm önerisi sunulmuştur. Daha düşük çevresel etkiye sahip gıda ve yem kaynakları olarak yenilebilir mikrobiyal biyokütle örneklerinden biri olan HBP,

geleneksel gıda üretim yöntemlerine bir alternatif olarak görülmektedir. Artan dünya nüfusu ve protein kaynaklarının giderek azalması tüketici ve üreticilerin daha sürdürülebilir olan protein kaynaklarına yönelimi nedeniyle THP ve HBP arařtırmaları daha da önem kazanmıştır. Mikroorganizmaların metabolik çeşitliliği sayesinde THP üretimi birçok farklı substrat ile gerçekleştirilebilmektedir. THP üretiminde genel olarak; heterotrof bakteriler kullanılmaktadır. Bu bakteriler doğası gereği CO₂ salınımı yapmakta ve substrat olarak karbonhidrat, yağ, metan veya etanolü kullanmaktadırlar. Ancak, ototrof bakterilerin CO₂ tutma yetenekleri bu canlıları sürdürülebilir THP ve HBP üretimi için en uygun adaylardan biri olarak öne çıkartmaktadır. Endüstride HBP ile bağlantılı son 10 yıllık ivme göz önünde bulundurulduğunda, gelecek yıllarda THP ve HBP ile ilgili daha çok araştırma yapılarak literatürün zenginleştirileceği ve dolayısıyla gıda işletmelerinin sürdürülebilir protein üretimi konusunda aydınlatılacağı düşünülmektedir.

Tarım ve sanayi atıklarının THP üretimi sırasında besi ortamı olarak kullanılması ekonomik faydanın yanı sıra çevre kirliliğinin azaltılmasına da katkı sağlamaktadır. Üretimde kapalı sistemlerin kullanılması mevsimsel değişikliklerden bağımsız olarak üretimi sürekli hale getirebilmektedir. Hayvansal ve bitkisel protein üretiminde karşılaşılan sağlık ve hijyen riskleri THP üretimiyle ortadan kalmakta, bu duruma karşılık mikrobiyal bir üretim söz konusu olduğu için kontaminasyon riski ortaya çıkmaktadır. THP üretimi için optimum koşullar sağlandığında bitkisel veya hayvansal kaynaklı protein üretimine göre daha hızlı bir şekilde üretim gerçekleştirilebilmektedir. Geleneksel üretimde kullanılan geniş arazi ve su kaynaklarının gerekliliği THP üretiminde ortadan kalkmaktadır. Bir THP olan HBP'nin üretimi, atmosferdeki CO₂'i sisteme bağlayıp kapalı bir karbon döngüsüne kazandırarak bakteri hücreleri üretimine dayanmaktadır. Üretim aşamalarında sürdürülebilir enerji kaynakları kullanıldığı takdirde HBP üretimi karbon negatif bir üretimdir.

Proteinler için alternatif üretim yöntemleriyle ilgili çalışmalar, artan nüfus, mevcut üretim koşulları ve çevreye olan etkileri göz önüne alındığında dengeli ve yeterli beslenmenin sürdürülebilirliği için önem kazanmaktadır. Mevcut durumda hayvan yemlerinde kullanılan ve insan beslenmesinde kullanımı için çalışmaların devam ettiği HBP'nin kalorisi düşük olup protein içeriği ve sindirilebilirliği yüksektir. Bu durumun doğal bir getirisi olarak sadece HBP içerikli bir diyetin nükleik asit miktarı insan sağlığı

açısından risk teşkil etmektedir. Bu durumun iyileştirilmesi ve HBP'nin duyuşsal olarak geliştirilmesi için ilave işleme yöntemleri gerekmektedir. Araştırmacıların insan tüketimine uygun HBP üretimi ile ilgili araştırmalarını üretim sonrası işleme koşulları üzerine de yoğunlaştırması gerektirdiđi düşünölmektedir.

Kaynaklar

1. Godfray, H., et al., Food Security: The Challenge of Feeding 9 Billion People. *Science*, 2010. 327(5967): p. 812-818.
2. Birleşmiş Milletler, Department of Economic and Social Affairs, World Population Highlights. 2019.
3. Tilman, D., Balzer, C., Hill, J. and Befort, B., Global food demand and the sustainable intensification of agriculture. *Proceedings of the National Academy of Sciences*, 2011. 108 (50): p. 20260-20264.
4. Poore, J. and Nemecek, T., Reducing food's environmental impacts through producers and consumers. *Science*, 2018. 360(6392): p. 987-992.
5. Gruener, O., The water footprint: water in the supply chain. *The Environmentalist*, 2010. (93): p. 12.
6. Boland, M., Rae, A. and Vereijken, J., The future supply of animal derived protein for human consumption. *Trends in Food Science & Technology*, 2013. 29(1), 62-73.
7. Henchion, M., et al., Future protein supply and demand: strategies and factors influencing a sustainable equilibrium. *Foods*, 2017. 6(7): p. 53.
8. Bohrer, B., Nutrient density and nutritional value of meat products and non-meat foods high in protein. *Trends in Food Science & Technology*, 2017. 65: p. 103-112.
9. Reeds, P., Dispensable and indispensable amino acids for humans. *The Journal of Nutrition*, 2000. 130(7): p. 1835-1840.
10. Elango, R., Ball, R. and Pencharz, P., Amino acid requirements in humans: with a special emphasis on the metabolic availability of amino acids. *Amino acids*, 2009. 37(1): p. 19-27.
11. Henley, E., Taylor, J. and Obukosia, S., The importance of dietary protein in human health: Combating protein deficiency in sub-Saharan Africa through transgenic biofortified sorghum. *Advances in Food and Nutrition Research*, 2010. 60: p. 21-52.
12. Moughan, P. J., Dietary protein for human health. *British Journal of Nutrition*, 2012. 108(S2): p. 1-2.
13. Neacsu, M., McBey, D. and Johnstone, A. M., Meat reduction and plant-based food: replacement of meat, nutritional, health and social aspects, in *Sustainable Protein Sources*, Nadathur S. R., Scanlin L. and Wanasundara, J. P. D., Editors. 2017, Elsevier, London, United Kingdom. p. 359-375.
14. Porter, J. R., et al., Food Security and Food Production Systems, in *Climate Change: Impacts, Adaptation and Vulnerability. Part A: Global and Sectoral Aspects*, Field C. B., Barros V. R., Dokken D. J., Mach K. J. and Mastrandrea M. D. Editors. 2014, Cambridge University Press, New York. p. 485-533.
15. Semba, R., The rise and fall of protein malnutrition in global health. *Annals of Nutrition and Metabolism*, 2016. 69(2): p. 79-88.
16. Wu, G., et al., Arginine deficiency in preterm infants: biochemical mechanisms and nutritional implications. *The Journal of Nutritional Biochemistry*, 2004. 15(8): p. 442-451.

17. Matassa, S., et al., Autotrophic nitrogen assimilation and carbon capture for microbial protein production by a novel enrichment of hydrogen-oxidizing bacteria. *Water Research*, 2016. 101: p. 137-146.
18. Sharif, M., et al., Single cell protein: Sources, mechanism of production, nutritional value and its uses in aquaculture nutrition. *Aquaculture*, 2021. 531: p. 735885.
19. Saeed, M., et al., Single cell protein: a novel value added food product. *Pakistan Journal of Food Sciences*, 2016. 26: p. 211-217.
20. Çalışkaner, Ş., et al., Etil alkol vasatında üretilen tek hücre proteini (Erpin) üzerinde biyolojik bir araştırma. *Türk Tarım ve Ormancılık Dergisi*, 1998. 22(3): p. 299-304.
21. Gao, Y., Li, D. and Liu, Y., Production of single cell protein from soy molasses using *Candida tropicalis*. *Annals of Microbiology*, 2012. 62(3): p. 1165-1172.
22. Goldberg, I., *Single Cell Protein*. 2013, Berlin, Germany: Springer Science & Business Media.
23. Volova, T. and Barashkov, V., Characteristics of proteins synthesized by hydrogen-oxidizing microorganisms. *Applied Biochemistry and Microbiology*, 2010. 46: p. 574-579.
24. Campbell-Platt, G., *Fermented Foods-a world perspective*. *Food Research International*, 1994. 27(3): p. 253-257.
25. Ciferri, O., *Spirulina, the edible microorganism*. *Microbiological Reviews*, 1983. 47(4): p. 551-578.
26. Abdulqader, G., Barsanti, L. and Tredici, M., Harvest of *Arthrospira platensis* from Lake Kossorom (Chad) and its household usage among the Kanembu. *Journal of Applied Phycology*, 2000. 12(3): p. 493-498.
27. Nasser, A. T., et al., Single cell protein: production and process. *American Journal of Food Technology*, 2011. 6(2): p. 103-116.
28. Srividya, Y., et al., Rapid and concurrent detection of *Listeria* species by Multiplex PCR. *International Journal of Pharma and Bio Sciences*, 2013. 4(1): p. 106-116.
29. Matelbs, R. and Tannenbaum, S., Single-cell protein. *Economic Botany*, 1968. 22(1): p. 42-50.
30. Patel, S. and Cook, P., The DNA-protein cross: a method for detecting specific DNA-protein complexes in crude mixtures. *The EMBO journal*, 1983. 2(1): p. 137-142.
31. Steinkraus, K., *Microbial biomass protein grown on edible substrates: the indigenous fermented foods*, in *Microbial Biomass Proteins*, Moo-Young, M. and Gregory K. F., Editors. 1986, Elsevier Applied Science, Essex, England. p. 33-45.
32. Bekatorou, A., Psarianos, C. and Koutinas, A. A., Production of food grade yeasts. *Food Technology and Biotechnology*, 2006. 44(3): p. 407-415.
33. Overland, M., Potential of microbial ingredients as protein sources for farmed animals and fish. *International Symposium on European Protein Position*, 2021.
34. Upadhyaya, S., et al., Microbial protein: a valuable component for future food security, in *Microbes and Environmental Management*, Singh J.S. and Singh D. P., Editors. 2016, Studium Press, New Delhi, India. p. 259-279.
35. Reihani, S. F. S. and Khosravi-Darani, K., Mycoprotein production from date waste using *Fusarium venenatum* in a submerged culture. *Applied Food Biotechnology*, 2018. 5(4): p. 243352.
36. Souza Filho, P. F., et al., Vegan-mycoprotein concentrate from pea-processing industry byproduct using edible filamentous fungi. *Fungal Biology and Biotechnology*, 2018. 5(1): p. 1-10.
37. Hashempour-Baltork, F., et al., Safety assays and nutritional values of mycoprotein product by *Fusarium venenatum* IR372C from date waste as substrate. *Journal of the Science of Food and Agriculture*, 2020. 100(12): p. 4433-4441.
38. Israelidis, C., Nutrition-Single cell protein, twenty years later. *Proceedings from First Biointernational Conference*, 2003.

39. Vermeulen, S. J., Campbell, B. M. and Ingram, J. S., Climate change and food systems. *Annual Review of Environment and Resources*, 2012. 37: p. 195-222.
40. Pikaar, I., et al., Microbes and the next nitrogen revolution. *Environmental Science and Technology*, 2017. 51(13): p. 7297-7303.
41. Mekonnen, M. and Hoekstra, A., Water footprint benchmarks for crop production: A first global assessment. *Ecological*, 2014. 46: p. 214-223.
42. Demirel, R. and Demirel, D., Tek hücre proteinlerinin insan ve hayvan beslemede kullanımı. *Journal of the Institute of Science and Technology*, 2018. 8(3): p. 327-336.
43. Turhan İ., *Endüstriyel Mikrobiyolojiye Giriş*. 2015, Ankara, Turkey: Palme Yayıncılık-In Turkish
44. Edozien, J., et al., Effects of high levels of yeast feeding on uric acid metabolism of young men. *Nature*, 1970. 228(5267): p. 180-187.
45. Öztürk, N. and Arıkan, F., Tümör Lizis Sendromunda Hemşirelik Yaklaşımı, *Ordu Üniversitesi Hemşirelik Çalışmaları Dergisi*, 2021. 4(1): p. 113-122.
46. Ritala, A., et al., Single cell protein state of the art, industrial landscape and patents 2001-2006. *Frontiers in Microbiology*, 2017. 8: p. 2009.
47. Adedayo, M. R., et al., Single cell protein: as nutritional enhancer. *Advances in Applied Science Research*, 2011. 2(5): p. 396-409.
48. Yousufi, M. K., To determine protein content of single cell protein produced by using various combinations of fruit wastes and two standard food fungi. *International Journal of Advanced Biotechnology and Research*, 2012. 3: p. 533-536.
49. Trinci, A. P. J., Quorn mycoprotein. *Mycologist*, 1991. 5(3): p. 106-109.
50. Kim, K., et al., Bioproduction of mushroom mycelium of *Agaricus bisporus* by commercial submerged fermentation for the production of meat analogue. *Journal of the Science of Food and Agriculture*, 2011. 91(9): p. 1561-1568.
51. Stoffel, F., et al., Production of edible mycoprotein using agroindustrial wastes: Influence on nutritional, chemical and biological properties. *Innovative Food Science and Emerging Technologies*, 2019. 58: p. 102227.
52. Hellwig, C., et al., Fungi burger from stael bread? A case study on perceptions of a novel protein-rich food product made from an edible fungus. *Foods*, 2020. 9(8): p. 1112.
53. Stoffel, F., et al., Use of *pleurotus albidus* mycoprotein flour to produce cookies: Evaluation of nutritional enrichment and biological activity. *Innovative Food Science and Emerging Technologies*, 2021. 68: p. 102642.
54. Sousa, I., et al., Microalgae in novel food products, in *Food Chemistry Research Developments*, Papadopoulos K. N., Editor. 2008, Nova Science Publishers, USA. p. 75-112.
55. Raja, R., et al., A perspective on the biotechnological potential of microalgae. *Critical Reviews in Microbiology*, 2008. 34(2): p. 77-88.
56. Becker, E., Micro-algae as a source of protein. *Biotechnology Advances*, 2007. 25: p. 207-210.
57. Mahasneh, I. A., Production of single cell protein from five strains of the microalga *Chlorella* spp. (Chlorophyta). *Cytobios*, 1997. 90: p. 153-161.
58. Faust, U., Production of microbial biomass, in *Fundamentals of Biotechnology*, Prave P., Faust U., Sittig W. and Sukatsch D., Editors. 1987, VCH Publishers, Germany. P. 601-622.
59. Elser, J. J., et al., Nutritional constraints in terrestrial and freshwater food webs. *Nature*, 2000. 408: p. 578-580.
60. Anupama, R. P., Value-added food: single cell protein. *Biotechnology Advances*, 2000. 18: p. 459-479.
61. Walsh, B. J., et al., New feed sources key to ambitious climate targets. *Carbon Balance and Management*, 2015. 10: p. 1-8.
62. Pander, B., et al., Hydrogen oxidising bacteria for production of single-cell protein and other food and feed ingredients. *Engineering Biology*, 2020. 4(2): p. 21-24.

63. Synder, H. E., Microbial sources of protein. *Advances in Food Research*, 1970. 18: p. 85-140.
64. Parkin, A. and Sargent, F., The hows and whys of aerobic H₂ metabolism. *Current Opinion in Chemical Biology*, 2012. 16(1-2): 26-34.
65. Takors, R., et al., Using gas mixtures of CO, CO₂ and H₂ as microbial substrates: the do's and don'ts of successful technology transfer from laboratory to production scale. *Microbial Biotechnology*, 2018. 11(4): p. 606-625.
66. Hafuka, A., et al., Effects of feeding regimens on polyhydroxybutyrate production from food waste by *Cupriavidus necator*. *Bioresource Technology*, 2011. 102(3): p. 3551-3553.
67. Liu, C., et al., Water splitting-biosynthetic system with CO₂ reduction efficiencies exceeding photosynthesis. *Science*, 2016. 352(6290): p. 1210-1213.
68. Little, G., et al., Complete Genome Sequence of *Cupriavidus necator* H16 (DSM 428). *Microbiology Resource Announcements*, 2019. 8(37).
69. Nyssöla, A., et al., Production of endotoxin-free microbial biomass for food applications by gas fermentation of Gram-positive H₂-oxidizing bacteria. *ACS Food Science & Technology*, 2021. 1(3): p. 470-479.
70. Raberg, M., et al., *Ralstonia eutropha* H16 in progress: applications beside PHAs and establishment as production platform by advanced genetic tools. *Critical Reviews in Biotechnology*, 2017. 38(4): p. 494-510.
71. Chee, J., et al., The potential application of *Cupriavidus necator* as polyhydroxyalkanoates producer and single cell protein: A review on scientific cultural and religious perspectives. *Applied Food Biotechnology*, 2018. 6(1): p. 19-34.
72. Calloway, D. and Margen, S., Investigation of the Nutritional Properties of *Hydrogenomonas eutropha* Final Report to National Aeronautics and Space Administration. NASA, 1968.
73. Air Protein, <https://www.airprotein.com>, Erişim tarihi: [24.05.2021].
74. Matassa, S., et al., Can direct conversion of used nitrogen to new feed and protein help feed the world? *Environmental Science & Technology*, 2015. 49: p. 5247-5254.
75. Lee, S. Y., Bacterial polyhydroxyalkanoates. *Biotechnology and Bioengineering*, 1996. 49(1): p. 1-14.
76. Waslien, C. I. and Calloway, D. H., Nutritional Value of Lipids in *Hydrogenomonas eutropha* as measured in the rat. *Applied Microbiology*, 1969. 18(2): p. 152-155.
77. Lu, Y. and Yu, J., Comparison analysis on the energy efficiencies and biomass yields in microbial CO₂ fixation. *Process Biochemistry*, 2017. 62: p. 151-160.
78. Ruuskanen, V., et al., Neo-Carbon food concept: a pilot-scale hybrid biological-inorganic system with direct air capture of carbon dioxide. *Journal of Cleaner Production*, 2021. 278: p. 1-11.
79. Nangle, S. N., et al., Biological-inorganic hybrid systems as a generalized platform for chemical production. *Current Opinion in Chemical Biology*, 2017. 41: p. 107-113.
80. Drake, G. L., et al., Study of life support systems for space missions exceeding one year in duration, in *The Closed Life-Support System*, Klein H., Editor. 1966, NASA, USA. p. 1-74
81. Foster, J. F. and Litchfield, J. H., A continuous culture apparatus for the microbial utilization of hydrogen produced by electrolysis of water in closed-cycle space systems. *Biotechnology and Bioengineering*, 1964. 6(4): p. 441-456.
82. Claessens, M., et al., Glucagon and insulin responses after ingestion of different amounts of intact and hydrolysed proteins. *British journal of nutrition*, 2008. 100(1): p. 61-69.
83. Calloway, D. H. and Kumar, A. M., Protein Quality of the Bacterium *Hydrogenomonas eutropha*. *Applied Microbiology*, 1969. 17(1): p. 176-178.
84. Ercili-Cura, D., Hakamies, A., Sinisalo, L., Vainikka, P., Pitkanen, J. Food out of thin air. *Food Science and Technology*, 2020, 34(2), 44-48.
85. Waslien, C. and Oswald, W., Unusual sources of proteins for man. *Food Science and Nutrition*, 1975. 6(1): p. 77-151.

86. Sillman, J., et al., Bacterial protein for food and feed generated via renewable energy and direct air capture of CO₂: Can it reduce land and water use? *Global Food Security*, 2019. 22: p. 25-32.
87. Novonutrients. <https://www.novonutrients.com>, Eriřim tarihi: [15.04.2021].
88. Solar Foods. 2021. <https://solarfoods.fi>, Eriřim tarihi: [26.05.2021].
89. Avecom. 2021. <https://avecom.be/feed-and-food>, Eriřim tarihi: [22.06.2021].
90. Deep Branch. 2021. <https://deepbranch.com>, Eriřim tarihi: [22.06.2021].

Basturk, M. H., S. F. Arslanoglu, and R. Ozturk, Karbon Noktaların Tarımsal Üretimde Kullanılması. International Journal of Life Sciences and Biotechnology, 2022. 5(3): p. 669-679. DOI: 10.38001/ijlsb.1134751

Karbon Noktaların Tarımsal Üretimde Kullanılması

Mehmet Han Basturk^{1*} , Sahane Funda Arslanoglu¹ , Rumeysa Ozturk¹ 

ÖZET

Birleşmiş Milletler Gıda ve Tarım Örgütü'ne (FAO) göre dünya nüfusunun 2050 yılında 10 milyara ulaşacağını ve özellikle gelişmekte olan ülkelerde gıda ihtiyacının %50 oranda arttıracağı tahmin edilmektedir. Bu durum Dünya'da tarımsal anlamda köklü değişimlere gidilmesi gerekliliğini ortaya koymaktadır. Son yıllarda tarımsal alanlarda girdi verimliliğini arttırarak, gıda üretimini ve güvenliliğini arttırmak, tarım ve çevresel sorunlara çözüm sunmak amacıyla tarımda nanoteknoloji kullanılması umut verici bir gelişmedir. Nanoteknolojinin bir ürünü olan nano parçacıklar yeni kimyasal ve fiziksel özellikleri sayesinde tıp, elektronik, malzeme bilimi, biyoteknoloji ve enerji sektörlerinde kullanımı hızla artmaktadır. Karbon malzemeler arasında son zamanlarda çok popüler olan Karbon noktaları (Carbon dots), boyutları genellikle 0.1-20 nm aralığına sahip yarı karbon bir malzeme olarak tanımlanmaktadır. Yapıları, özellikleri, görüntüleme ve karakterizasyon seçenekleri bakımından daha önce çalışılmış karbon formlarına göre önemli farklılıklara sahip Karbon Noktalar çeşitli fizikokimyasal özellikleri, yüksek biyo-uyumluluk, yüksek stabilite ve optik özellikleri ile öne çıkmaktadır. Karbon noktalar bitkilerin verimini önemli ölçüde arttıran kül bileşenidir. Tarımsal üretimde tohum çimlenmesi, kök uzaması, bitki hastalıklarına karşı direnç ve karbon fiksasyonu artırma gibi pozitif etki göstererek bitki büyümesini desteklemektedir. Son zamanlarda Karbon noktalar tarımda, kimyasal ilaç kullanımı azaltma, gübrelemede bitki besin elementi kaybını minimuma indirmede, su ve besin elementinden etkin yararlanmayı sağlayarak verimi arttırmak amacıyla kullanılmaktadır. Bu derlemede, yeni bir nanogübre olarak tanımlayabileceğimiz Karbon noktaların, sentezi, tarımsal üretimde kullanımı ve etkileri üzerine yaptığımız literatür incelemeleri sonucunda elde ettiğimiz bilgiler mevcuttur.

MAKALE GEÇMİŞİ

Geliş

24 Haziran 2022

Kabul

22 Kasım 2022

ANAHTAR KELİMELER

Çimlendirme,

gübre,

karbon noktalar,

nanoteknoloji

¹ Samsun Ondokuz Mayıs Üniversitesi, Ziraat Fakültesi, Tarla Bitkileri Bölümü, Samsun / Türkiye

* Sorumlu yazar: Mehmet Han Basturk, e-mail: mehmethanbasturk75@gmail.com

The Use of Carbon Dots in Agricultural Production

ABSTRACT

According to the United Nations Food and Agriculture Organization (FAO), it is estimated that the world's population will reach 10 billion in 2050 and that the need for food, especially in developing countries, will increase by 50%. This situation shows the need for fundamental changes in the agricultural sense in the world. In recent years, the use of nanotechnology in agriculture has been a promising development in order to increase input efficiency in agricultural fields, increase food production and safety, and provide solutions to agricultural and environmental problems. Nanoparticles, which are a product of nanotechnology, are rapidly increasing in use in medicine, electronics, materials science, biotechnology and energy sectors due to their new chemical and physical properties. Carbon dots, which have recently become very popular among carbon materials, are defined as a semi-carbon material, the dimensions of which usually have a diameter of 0.1-20 nm. Structures, properties, characterization, and imaging options in terms of various physicochemical properties of Carbon Dots with significant differences according to the form previously studied carbon, high bio-compatibility, high stability, and optical properties stand out. Carbon is the component of ash, which significantly increases the yield of plants. It supports plant growth by showing positive effects such as seed germination, root elongation, resistance to plant diseases and increasing carbon fixation in agricultural production. Recently, carbon dots have been used in agriculture to reduce the use of chemical drugs, minimize the loss of plant nutrients in fertilization, and increase yields by providing effective use of water and nutrients. In this review, the information we have obtained as a result of literature reviews on the synthesis, use and effects of carbon dots, which we can define as a new nanogubber, in agricultural production, is available.

ARTICLE HISTORY

Received

24 June 2022

Accepted

22 November 2022

KEYWORDS

Carbon dots,
nanotechnology,
fertilizer,
germination

Giriş

Dünya'da tarımsal üretim, iklim değişikliği, çevresel kirlilik, girdi maliyetlerinin yüksekliği, pestisitlerin kontrolsüz kullanımı ve tarım arazilerinin azalması nedenleriyle büyük bir sorunla karşı karşıyadır [1]. Birleşmiş Milletler Gıda ve Tarım Örgütü'ne [2] göre dünya nüfusunun 2050 yılında 10 milyara ulaşacağı ve özellikle gelişmekte olan ülkelerde gıda ihtiyacının %50 oranda artacağı tahmin edilmektedir. Günümüz verilerine göre yaklaşık 1 milyar insan gıda kıtlığı yaşamaktadır. Bunun 2050 yılında 2 milyar olması beklenmektedir [2]. Bu durum Dünya'da tarımsal üretimde köklü değişimlere gidilmesi gerekliliğini ortaya koymaktadır [1]. Araştırmacılar son zamanlarda tarım ve çevre sorunlarına çözüm bulmak amacıyla tarımsal girdi verimliliğini, tarımsal üretimi ve gıda güvenliğini artırmak için nanoteknolojik gelişmelerden yararlanmak gibi farklı çözüm önerileri sunmaktadır [3-5].

Nanoteknoloji, konusu biyoloji olsun veya olmasın 0.1-100 nanometre (nm) boyutlara sahip yapıları üretmek, karakterize etmek ve fonksiyonel hale getirmek için kullanılmaktadır [6]. Boyutlarının bir sonucu olarak nanoteknolojik malzemeler fiziksel

dayanıklılık, kimyasal reaktivite, elektriksel iletkenlik, optik ve manyetizma gibi özellikler bakımından mikrometrik veya daha büyük moleküllerden çok farklı kimyasal ve fiziksel özellikler sergilemektedir [3, 7, 8]. Bu özellikleri nedeniyle nano parçacıkların tıp, elektronik, malzeme bilimi, biyoteknoloji ve enerji sektörlerinde kullanımı hızla artmaktadır [9]. Bu sektörlerde yaşanan umut verici gelişmeler, araştırmacıları tarımsal üretimde yaşanan sorunların çözümü yönünde nanoteknolojinin kullanılabilirliğine yönlendirmiştir [9].

Neolitik çağdan bu yana karbon parçacıkları ve iyonik besin içeriği nedeniyle kül, tarımsal üretimi iyileştirmek amacıyla kullanılmıştır. Bu bilgiden yola çıkarak yapılan çalışmalarda, karbon nano malzemelerin, kül etkilerine benzer şekilde bitkilerin su ve besin alımını artırdıkları gözlemlenmiştir [10]. Geleneksel karbon (aktif karbon) ile endüstriyel karbon (karbon fiber, grafit ve karbon nanotüpler) gibi karbon bazlı malzemeler sağlam ve çevre dostu olmaları sebebiyle kimya, malzeme bilimi ve diğer disiplinlerin gelişmesinde önemli rol oynamaktadırlar. Makroskobik karbon malzemeleri etkili bir floresan ışımadan yoksundur, bu sebeple biyolojik çalışmalarda optik uygulamalar için uygun değildir. Karbon malzeme grubuna 2004 yılında eklenen karbon noktaları, floresan ışımaya özelliği ile bu açıklığı gidermiş ve biyolojik uygulamalarda etkili bir biçimde kullanılmasını sağlamıştır [11].

Karbon Noktalar (Carbon Dots)

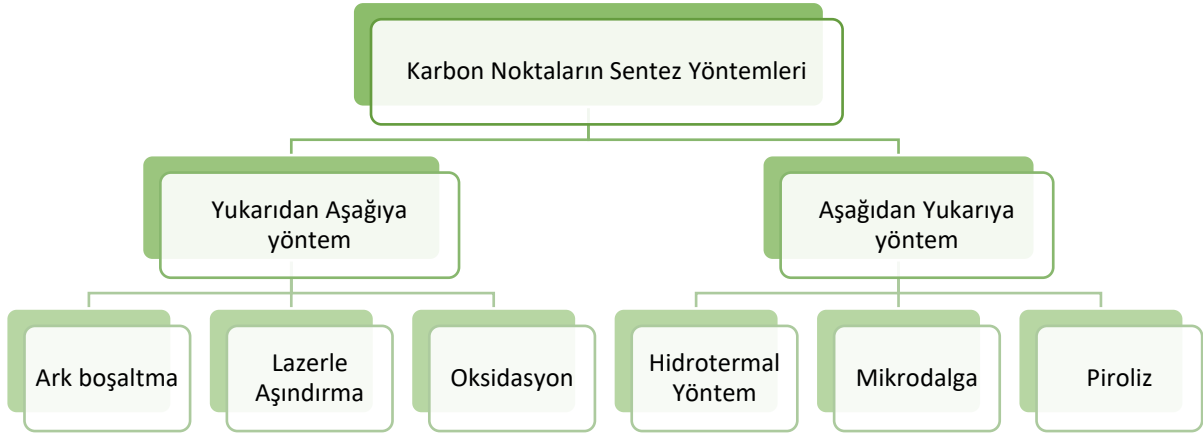
İlk defa tesadüfen 2004 yılında, tek duvarlı karbon nanotüplerin saflaştırılması ile floresan karbon nano parçacıklar elde edilmiştir [12]. Sun ve ark., [13], karbonun lazer ablasyonu ile sentezlenen nano ölçekli karbon parçacıklarını ‘‘Karbon Noktalar (Carbon Dot)’’ olarak adlandırmışlardır. Genellikle 20 nm’ den küçük boyutlara sahip yarı karbon bazlı bir malzeme olarak tanımlanan karbon noktalarının en önemli özelliği doğal fotoluminesans olmalarıdır [11].

Karbon noktaları (KN); fotostabilite, küçük boyut, biyo uyumluluk, suda çözünürlük, biyo moleküller ile kolay etkileşime girmesi ve yüksek kuantum verimi gibi özellikleri nedeniyle biyo izleme, algılama, ilaç ve gen dağıtımı gibi optik araştırmalara konu olmuştur [14, 15].

Karbon noktaların sentezi

Karbon malzemelerden, karbon noktaların sentezlenmesinde yukarıdan aşağıya ve aşağıdan yukarıya olmak üzere iki yöntem kullanılmaktadır [16]. Sentez yöntemi Şekil 1’ de şematik olarak gösterilmiştir.

Lazer ablasyonu, asidik aşındırma ve elektrokimyasal aşındırma yöntemlerinin uygulandığı yukarıdan aşağıya sentezlenmesi metoduyla kaliteli ve saf karbon noktalar üretilebilmektedirler [10]. Ancak bu yöntem, fazla enerji kullanımı, fazla atık madde oluşumu, sentez yolunun karmaşık olması ve maliyetinin yüksekliği gibi nedenlerden dolayı çok tercih edilmemektedir. Bunun yerine hidrotermal, mikrodalga, piroliz gibi yöntemlerin uygulandığı aşağıdan yukarıya sentez yöntemi kullanılmaktadır (Şekil 1) [10, 16].



Şekil 1 Karbon noktaların sentez yöntemleri

Fig 1 Methods of synthesis of carbon dots

Bu yöntemde karbon noktalar, karbonhidrat, organik asitler ve polimerler gibi organik maddelerden yüksek sıcaklık altında çözücü olarak su veya etanol kullanılmasıyla kolayca sentezlenmektedir [5, 16].

Karbon noktalarının fiziksel ve kimyasal özellikleri, sentez yöntemi, reaksiyon süresi, çözücü madde, sıcaklık, boyut ve yüzeylerinde bulunan fonksiyonel gruplara (hidroksil, eter, karbonil, karboksilik asit) göre farklılık göstermektedir. Bu farklılıklar sebebiyle teorik ve pratik uygulamalar için gerekli standartlar her zaman sağlanamamaktadır [10]. Ancak şimdiye kadar yapılan çalışmalarda karbon noktaların bitkilerin bütün kısımlarına girerek, besin ve su alınımlarını arttırdığını, bitkilerde büyüme ve gelişmeyi desteklediğini, hücre ve doku görüntülemeye kullanımı konularında oldukça başarılı

bulunmuştur [17]. Bu sonuçlar doğrultusunda KN' lerin tarımda gübre olarak iyi bir aday olabileceği ve biyoteknolojide büyük potansiyel uygulamaları olduğunu göstermektedir [18].

Karbon Noktaların Tarımsal Üretime Etkileri

Tarımsal anlamda ilk olarak sitrik asit ve üreden hazırlanan karbon noktaları model bitki olarak fasulyede denenmiş ve toksik olmadığı bildirilmiştir [19]. Bu çalışma sonrasında karbon noktalarının bitki büyümesi üzerine potansiyel etkilerinin araştırılma süreci başlamıştır [20]. Aşağıda karbon noktaların bitki büyümesi, fotosentez, biyotik ve abiyotik stres, *Azotobacter chroococum*'un aktivitesi üzerine etkileri hakkında yapılan çalışmalara yer verilmiştir.

Karbon noktaların bitki büyümesi üzerine etkileri

Maş fasulyesi, hızlı büyümesi nedeniyle çalışmalarda sıklıkla model bitki olarak kullanılmıştır [18, 21]. Karbon noktaları (KN) kök ve gövde uzamasını teşvik ederek bitkilerde biyokütle artışını desteklemektedir. Örneğin; Wang ve ark., [18], 0.02 mg ml⁻¹ KN uygulaması ile birlikte maş fasulyesinde kök uzunluğu, gövde uzunluğu ve bitki yaş ağırlığını sırasıyla %29.9, %18.3, %14.9 oranında arttırdığını (Şekil 2A), Zheng ve ark. [22], 3.5 mg L⁻¹ KN uygulamasının Çin lahanasında sürgün ve kök yaş ağırlıklarını sırasıyla %69.9 ve %66.12 oranda arttırdığını (Şekil 2B), marula KN uygulamasında konsantrasyon arttıkça biyokütle artışının olduğunu ve 30 mg L⁻¹ konsantrasyonda %48.09'lük bir artış olduğunu (Şekil 2C) ve Su ve ark. [23], Yer fıstığında 180 mg L⁻¹ KN uygulaması ile birlikte kök aktivitesi bakımından 3.5 kat, kök uzunluğu, fide yüksekliği, kök sayısı, kök kuru ağırlığı, kök yaş ağırlığı ve sürgün yaş ağırlığı bakımından ise 1.5 kat (Şekil 2D) daha iyi sonuç aldıklarını bildirmişlerdir.

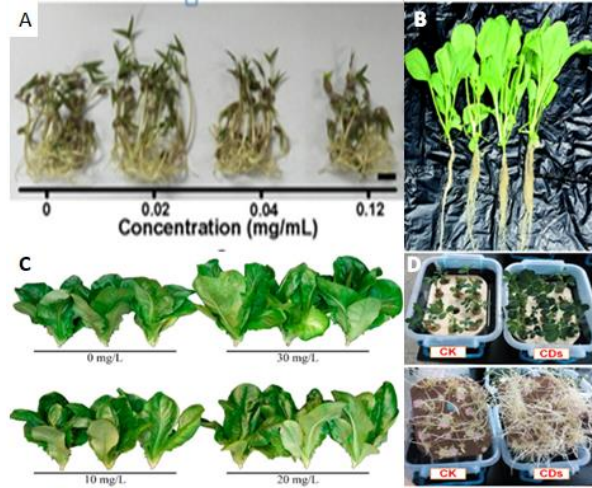
Karbon noktaların bitkilerde fotosentez üzerine etkileri

Fotosentez, bitkilerin güneş enerjisini kimyasal enerjisine çevirdiği, bu sırada bitki büyümesi ve biyokütle birikiminde önemli rol oynadığı bilinmektedir. Karbon noktalar hem iyi bir elektron verici hem de alıcı olarak ışık enerjisinin dönüşüm uygulamalarını desteklemektedir [20].

Fotosentezde elektrik enerjisinin kimyasal enerjiye dönüştürülmesinde karbondioksit (CO₂) fiksasyonu önemli bir role sahiptir. Ribuloz bifosfat karboksilaz oksijenaz (RuBisCo) enzimi fotosentezin calvin döngüsü sırasında CO₂ sabitleyen önemli bir

enzimdir. RuBisCo aktivitesi fotosentez hızı ve karbonhidrat birikimini doğrudan etkilemektedir [18].

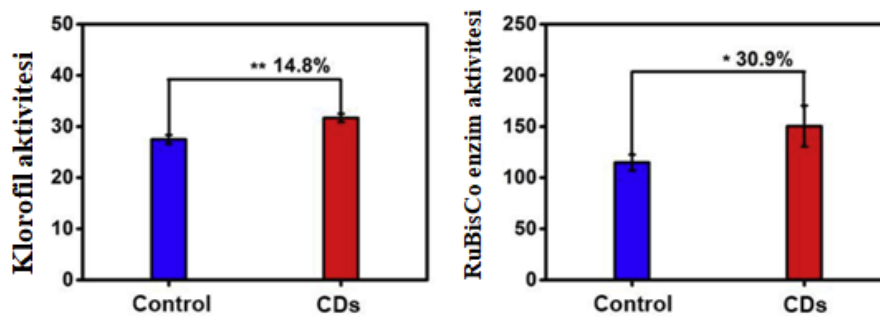
Wang ve ark., (18), Karbon noktaları uyguladıkları Maş fasulyesinde klorofil içeriğinin ve RuBisCo aktivitesinin sırasıyla %14.8 ve %30.9'a (Şekil 3) kadar arttığını bildirmişlerdir.



Şekil 2 Karbon noktaların; (A) maş fasulyesi [18], (B) çin lahanası [22], (C) marul [22], (D) yer fıstığı [23] bitkilerinde büyüme üzerine etkileri

Fig 2 Karbon dots; (A) mung beans [18], (B) Chinese cabbage [22], (C) lettuce [22], (D) peanuts [23] effects on plant growth

Li ve ark., [24], karbon noktaların çeltik üzerindeki etkilerini incelemiş ve RuBisCo enzim aktivitesinin %42 oranda artması sonucunda %14.8 lik bir verim artışı gözlemlenmiştir.



Şekil 3 Karbon noktaların mas fasulyesinde klorofil ve RuBisCo enzim aktivitesi üzerine etkileri (18)

Fig 3 The effects of carbon dots on the enzyme activity of chlorophyll and RuBisCO in mas beans [18]

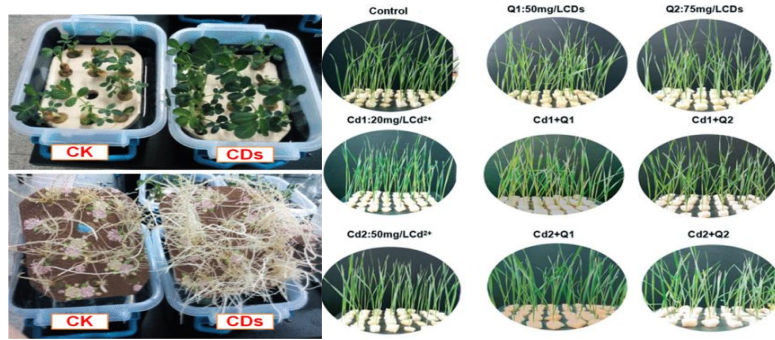
Karbon noktaların bitkilerde abiyotik ve biyotik streslere karşı toleransı

Bitkilerde stres, bitkilerin büyümesini, gelişmesini veya üretkenliğini olumsuz yönde etkileyen dış koşulları ifade etmektedir. Bitkilerde biyotik (mantar, bakteri, nematod vb.) ve abiyotik (sıcaklık, kuraklık, tuzluluk vb.) olmak üzere iki tür stres vardır. Bitkiler, bu çevresel streslerin üstesinden gelmek için bir takım savunma mekanizmaları geliştirmişlerdir [25].

Birleşmiş Milletler Gıda ve Tarım Örgütü' nün (FAO) 2007 yılında hazırlanmış olduğu rapora göre Dünya'da tarımsal alanların %96 sı çeşitli abiyotik streslerden etkilenmekte, bunun sonucu olarak %50'ye varan verim kayıplarına uğramaktadır [26].

Reaktif oksijen türlerinin (ROS) oluşumundaki artış, bitki büyümesini etkileyen abiyotik streslerin ana faktörüdür ve ROS' un birikmesi genellikle proteinler, lipidler, karbonhidratlar ve DNA' da oksidatif hasara yol açar [27]. Son yıllarda yüzeylerindeki karboksil ve amino grupları nedeniyle radikal süpürücü özelliğe sahip KN' ler abiyotik strese karşı direnci arttırabileceği bildirilmiştir [28, 29].

Bu bilgiler doğrultusunda [23], karbon noktaların, yer fıstığında kuraklık stresi üzerine etkisini inceledikleri çalışmada, karbon nokta (CD) uygulanmış yer fıstığı bitkilerinde süperoksit dismutaz (SOD), peroksidaz (POD) ve katalaz (CAT) aktivitelerinin arttığı ve malondialdehit (MDA) içeriğinin azaldığı görülmüştür. Araştırmacılar, yer fıstığında CD uygulamasının stres direncini arttırdığı ve kuraklık stresini azalttığı sonucuna varmışlardır (Şekil 4). Xiao ve ark., (30)'nın buğday'da kadminyum toksisitesinin negatif etkilerine karşı yaptıkları çalışmada, karbon noktalarının Kadminyum'u absorbe ettiğini, bitkide çözünür şeker ve protein içeriğini arttırdığını, bunun yanı sıra buğday yapraklarında askorbat peroksidaz (APX), katalaz (CAT) ve peroksidaz'ı (POD) arttırarak bitkide kadminyum toksisitesine karşı toleransı yükselttiğini belirlemişlerdir.

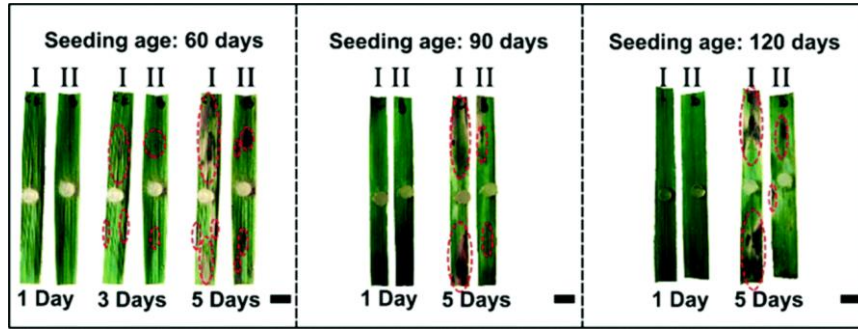


Şekil 4 Karbon noktaların abiyotik stres üzerine etkileri; yerfıstığı [23], buğday [30]

Fig 4 The effects of carbon dots on abiotic stress; peanut [23], wheat [30]

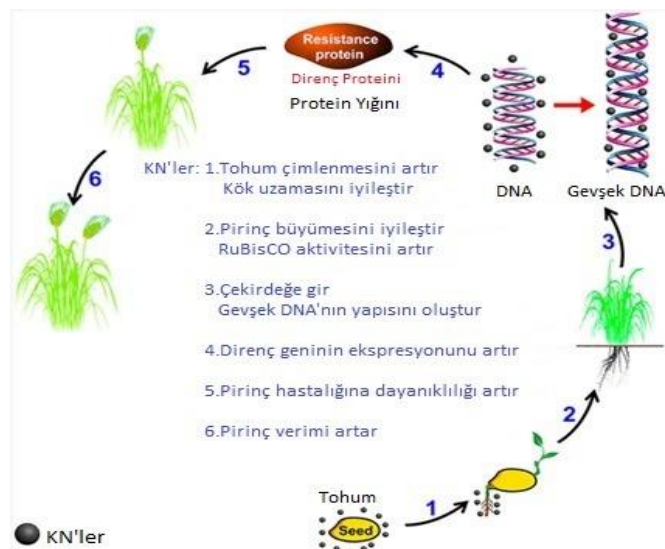
Bitkiler farklı büyüme evrelerinde böcek, bakteri, fungus, virüs veya nematod gibi organizmalar tarafından besin kaynağı olarak kullanılmaktadırlar, bununla birlikte bitkilerde biyotik stres oluşumuyla birlikte hastalıkların ortaya çıkması ve sonucunda da ürün kayıpları meydana gelmektedir [31]. Bitkiler biyotik streslere karşı dayanıklılık genleri geliştirmişlerdir. Bu genlerin ürünü olan proteinler, hastalık etmeninin bitkiye girmesiyle birlikte savunma sistemini harekete geçirerek antimikrobiyal etkiye sahip birçok proteinin bitkide üretilmesini sağlamaktadır [32].

Fitopatojenlerle enfeksiyon, tarımsal üretimde ciddi kayıplara yola açan biyotik bir streştir (Şekil 5) [11]. Çeltik üzerinde bir dizi deney sonucunda [24], Karbon noktalarının hücre çekirdeği içerisine girerek DNA'nın yapısını gevşettiğini ve bunun sonucunda bitki hastalık direnç genlerinin ifade düzeyinde bir artış sağlandığını bildirmişlerdir (Şekil 6) [24].



Şekil 5 Karbon noktalarının biyotik stres üzerine etkileri [24]

Fig 5 The effects of carbon dots on biotic stress [24]

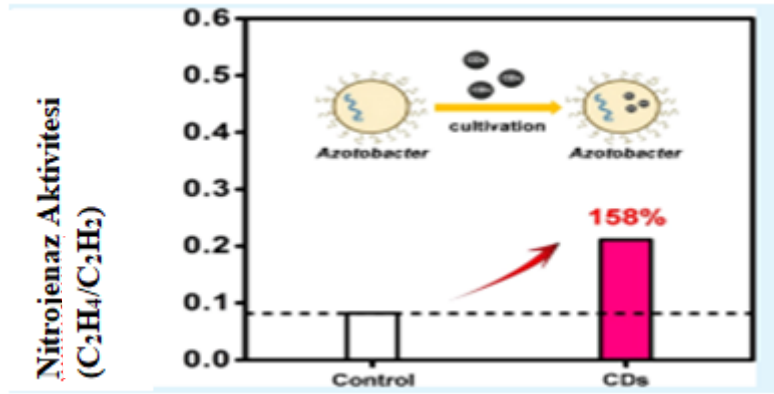


Şekil 6 Karbon noktalarının zamana göre çeltik üzerindeki etkisi [24]

Fig 6 The effect of carbon dots on paddy with respect to time [24]

Karbon noktaların *azotobacter chroococum*'un azot fiksasyonu üzerine etkileri

Azot, bitkiler için en önemli bitki besin elementlerinden birisidir. Azotlu gübrelerin fazla kullanımı çevresel kirlilik ve yüksek girdi maliyeti sebebiyle endişe kaynağıdır. Atmosfer bol miktarda azot (Nitrojen formda) içermektedir. Ancak, bitkiler bu azotu doğrudan kullanamazlar. Azot sabitleyici bakteriler azot fiksasyonu ile birlikte serbest atmosferdeki serbest azotu toprağa bağlayarak bitkilerin alımı için uygun hale getirebilmektedirler [33]. Wang ve ark., [18], *Azotobacter chroococum*'un aktivitesi üzerine karbon noktaların etkisini inceledikleri araştırmada, KN uygulamasının %158 oranında azot fiksasyonu aktivitesininin artırdığı bildirmişlerdir (Şekil 4). Buna ek olarak karbon noktaların nitrojenaz ile birleşerek nitrojenazın ikincil yapısını etkileyebileceği, biyokatalitik süreçte elektron transferini iyileştirebileceği ve son olarak azot fiksasyonu için nitrojenaz aktivitesini geliştirebileceği sonucuna varmışlardır(Şekil 7) [18].



Şekil 7 Karbon noktaların *Azotobacter chroococum*' un aktivitesi üzerine etkileri [18]

Fig 7 Effects of carbon dots on the activity of *Azotobacter chroococum* [18]

Sonuç

Yapılan literatür çalışmalarında karbon noktaların yüksek konsantrasyonlarda kullanılmadığı takdirde tarımsal üretimde bitki büyümesi, verim artışı, su ve besin emilimini artması, hastalık ve zararlılara karşı direncin artması, biyotik ve abiyotik strese karşı tolerans gibi konularda pozitif yönlü etkilerinin olduğu görülmüştür.

Başlangıç materyallerinin ucuz ve kolay temin edilebilir olmasıyla birlikte karbon noktaların hazırlanması için çok yönlü sentez yöntemleri geliştirilmiştir. Bununla birlikte, standart boyut, şekil ve fonksiyonel gruplara sahip yüksek kaliteli ve saf karbon noktaları için sistematik ve ölçeklenebilir bir sentez yöntemi henüz yoktur. Bu sebeple

çalışmalar çimlendirme veya saksı denemeleri ile sınırlı kalıp tarla koşullarında çalışmaya rastlanmamıştır. Yaptığımız literatür çalışmaları arasında ürün kalitesi üzerine yapılan bir çalışma bulunamamıştır.

Ancak, günümüzde tarımsal üretimde kuraklık, su kısıtı, kimyasal ilaç kullanımının yarattığı olumsuz etkileri azaltmak, gübre girdi maliyetleri düşürmek, hastalık ve zararlılara dayanıklılık sağlamak gibi konularda olumlu katkılar sağladığı laboratuvar ve saksı çalışmaları ile belirlenmiş olan karbon noktaların çevre dostu, biyoyumluluk özelliği ve toksisitesinin olmaması özellikleri dikkate alınarak, kullanımıyla ilgili tarla-sera koşullarında, verim ve kaliteyi artırmak yönünde fizyolojik çalışmaları da kapsayan daha geniş kapsamlı araştırmalara ihtiyaç olduğu görülmüştür.

Kaynakça

1. Usman, M., et al., Nanotechnology in agriculture: Current status, challenges and future opportunities. *Science of the Total Environment*, 2020. 721: p. 137778.
2. FAO, F., The future of food and agriculture—Trends and challenges. *Annual Report*, 2017. 296: p. 1-180.
3. Demirbilek, M.E., Tarımda ve gıdada nanoteknoloji. *Gıda Ve Yem Bilimi Teknolojisi Dergisi*, 2015(15).
4. Erdem, S. and G.T. Gülel, Gıda endüstrisinde nanoteknoloji uygulamaları. *Etlık Veteriner Mikrobiyoloji Dergisi*, 2015. 26(2): p. 52-57.
5. Li, Y., et al., Magnesium-nitrogen co-doped carbon dots enhance plant growth through multifunctional regulation in photosynthesis. *Chemical Engineering Journal*, 2021. 422: p. 130114.
6. Yildirim, N., Nanoteknoloji ve geleceğin çevreci polimeri nanoselüloz. *Ormancılık Araştırma Dergisi*, 2018. 5(2): p. 185-195.
7. Modi, S., et al., Recent Trends in Fascinating Applications of Nanotechnology in Allied Health Sciences. *Crystals*, 2021. 12(1): p. 39.
8. Wu, D., et al., Phenolic-enabled nanotechnology: Versatile particle engineering for biomedicine. *Chemical Society Reviews*, 2021. 50(7): p. 4432-4483.
9. Parisi, C., M. Viganı, and E. Rodríguez-Cerezo, Agricultural nanotechnologies: what are the current possibilities? *Nano Today*, 2015. 10(2): p. 124-127.
10. Kang, Z. and S.-T. Lee, Carbon dots: advances in nanocarbon applications. *Nanoscale*, 2019. 11(41): p. 19214-19224.
11. Liu, J., R. Li, and B. Yang, Carbon dots: A new type of carbon-based nanomaterial with wide applications. *ACS Central Science*, 2020. 6(12): p. 2179-2195.
12. Xu, X., et al., Electrophoretic analysis and purification of fluorescent single-walled carbon nanotube fragments. *Journal of the American Chemical Society*, 2004. 126(40): p. 12736-12737.
13. Sun, Y.-P., et al., Quantum-sized carbon dots for bright and colorful photoluminescence. *Journal of the American Chemical Society*, 2006. 128(24): p. 7756-7757.
14. Zheng, X.T., et al., Glowing graphene quantum dots and carbon dots: properties, syntheses, and biological applications. *small*, 2015. 11(14): p. 1620-1636.
15. Peng, Z., et al., Carbon dots: biomacromolecule interaction, bioimaging and nanomedicine. *Coordination Chemistry Reviews*, 2017. 343: p. 256-277.

16. Dinç, S. and M. Kara, Synthesis and applications of carbon dots from food and natural products. *Journal of Apitherapy and Nature*, 2018. 1(1): p. 33-37.
17. Verma, S.K., et al., Applications of carbon nanomaterials in the plant system: A perspective view on the pros and cons. *Science of the Total Environment*, 2019. 667: p. 485-499.
18. Wang, H., et al., Carbon dots promote the growth and photosynthesis of mung bean sprouts. *Carbon*, 2018. 136: p. 94-102.
19. Qu, S., et al., A biocompatible fluorescent ink based on water-soluble luminescent carbon nanodots. *Angewandte Chemie international edition*, 2012. 51(49): p. 12215-12218.
20. Li, Y., et al., A review on the effects of carbon dots in plant systems. *Materials Chemistry Frontiers*, 2020. 4(2): p. 437-448.
21. Li, W., et al., Phytotoxicity, uptake, and translocation of fluorescent carbon dots in mung bean plants. *ACS applied materials & interfaces*, 2016. 8(31): p. 19939-19945.
22. Zheng, Y., et al., Pollen derived blue fluorescent carbon dots for bioimaging and monitoring of nitrogen, phosphorus and potassium uptake in *Brassica parachinensis* L. *RSC advances*, 2017. 7(53): p. 33459-33465.
23. Su, L.-X., et al., Carbon nanodots for enhancing the stress resistance of peanut plants. *Acs Omega*, 2018. 3(12): p. 17770-17777.
24. Li, H., et al., Impacts of carbon dots on rice plants: boosting the growth and improving the disease resistance. *ACS Applied Bio Materials*, 2018. 1(3): p. 663-672.
25. Gull, A., A.A. Lone, and N.U.I. Wani, Biotic and abiotic stresses in plants. *Abiotic and biotic stress in plants*, 2019: p. 1-19.
26. Van Velthuisen, H., Mapping biophysical factors that influence agricultural production and rural vulnerability. 2007: Food & Agriculture Org.
27. Choudhury, F.K., et al., Reactive oxygen species, abiotic stress and stress combination. *The Plant Journal*, 2017. 90(5): p. 856-867.
28. Das, B., et al., Carbon nanodots from date molasses: new nanolights for the in vitro scavenging of reactive oxygen species. *Journal of Materials Chemistry B*, 2014. 2(39): p. 6839-6847.
29. Zhao, S., et al., Green synthesis of bifunctional fluorescent carbon dots from garlic for cellular imaging and free radical scavenging. *ACS applied materials & interfaces*, 2015. 7(31): p. 17054-17060.
30. Xiao, L., et al., Carbon dots alleviate the toxicity of cadmium ions (Cd²⁺) toward wheat seedlings. *Environmental Science: Nano*, 2019. 6(5): p. 1493-1506.
31. Sarikaya, F., Domates (*solanum lycopersicum* l.)te virüs enfeksiyonu ve kuraklık stresi sırasında mirnalar ve hedefledikleri myb transkripsiyon faktörlerinin ekspresyonlarının belirlenmesi. 2020, Isparta Uygulamalı Bilimler Üniversitesi, Lisansüstü Eğitim Enstitüsü.
32. Esra, K. and A.S. Üstün, Patojenlere Karşı Bitkilerde Savunma Ve Antioksidanlar. *Erciyes Üniversitesi Fen Bilimleri Enstitüsü Fen Bilimleri Dergisi*, 2008. 24(1): p. 82-100.
33. Bohlool, B., et al., Biological nitrogen fixation for sustainable agriculture: A perspective. *Plant and soil*, 1992. 141(1): p. 1-11.

Bir sonraki sayıda grşmek midiyle..
Hope to see you in the next issue..

Author Guidelines

General Principles

1. The article should be submitted by the responsible author responsible as Microsoft Word (Doc, Docx).
2. The responsible author is responsible for monitoring all the processes of the article.
3. The main section headings should be bold and the first letter in capital letters, the first letter of the first word in the 2nd-degree headings should be large. If a third-degree title is required, the title should be in italics and only the first letter of the first word should be capitalized. If possible, articles with fourth-degree titles should not be used in our journal.
4. The main headings and sub-headings should not be numbered.
5. Turkish and English titles of the articles should be short, descriptive, and not more than fourteen words (except prepositions).
6. In the Pre-Control and Evaluation processes, the authors must submit the proposed corrections within 30 days at the latest. Otherwise, the article will be rejected.
7. Please click here to see the article written according to the rules of our journal.

Note: The general similarity rate should not exceed 20% except the bibliography part of the submitted articles. It is necessary to inform the journal editor if the rate specified in the necessary cases is exceeded. All articles submitted to the journal are screened with iThenticate plagiarism program.

8. Except for the Turkish and English titles of the work, all remaining parts should be written on the right side.
9. The text should be written on an A4-size page, in 12-font size Times New Roman, and double-spaced.
10. There should be 3 cm margin on the left, right, and top of the page.
- 11 Text should be written in a single column, all pages should be given a page number.
There is no page limit in publishing an article in our journal.

Names Section

A double-blind peer reviewer system is applied in our journal. Therefore, the names and addresses of authors should not be given in the main text when loading the Manuscript to the system. Author names and contact information should be written on a separate cover page. The cover page is available in the article submission section of our journal.

Abstract

The article can be written in Turkish and English. English and Turkish abstracts should be written at the beginning of the Turkish manuscripts.

The abstract should contain brief and clear information about the purpose, method, and results of the article. 10 font size, single line spacing and maximum 300 words should be written. No reference should be made to the "Abstract".

Keywords: Keywords should be 10 font sizes, minimum 3, and maximum of 5 words. Keywords must be separated with a comma (,) sign and should be in lowercase.

Introduction

The sections of the main part of the study should be written in 14 font sizes; Bold and the first letter should be capitalized; Article should have Introduction, Methods, Results, Discussion, and Conclusion sections. The second level titles should be written in the left, in 12 font sizes, the first letter of the first word should be capitalized, bold, and numbered. A line in the previous paragraph must be separated by a space.

Figures and Tables

In the Turkish article for Figures and Tables;” Şekil“, ”Tablo“; whereas in The English article “Fig”, “Table” should be used (Table 1, Fig 1).

Figure and Table words should be written in bold, and at the end of the description of figures and tables should not have a dot (.)

Figures, graphics, photographs and the like should be written under Figures and written with 11 fonts. Figure and Table should be given in the main document in the relevant places, should not be uploaded as separate files or should not be added to the end of the text.

Examples;

Table 1 Possible effects of genetically modified organisms

Table 2 Methods of tissue culture in tomato plants

Fig. 1 Amount of GMO products in the world

Fig. 2 Countries with the highest number of GM cultivation in the world

Citation Inside the Text

In the text, the author should be numbered. Name and year should not be specified.

Example: Potatoes produced on a global scale are used in many basic areas [1, 2, 3]. Fifty percent of primarily produced potatoes are used for fresh consumption, such as baking, frying, boiling [4, 5, 6, 7].

References

The references section should be written in 10 font sizes and without hanging indentations. In the references section, italics should not be written except in italic words such as “in vivo, in vitro, ex-situ” and species names. References should be written according to the “Chicago style”. Besides, there is an endnote style preparing for "International Journal of Life Sciences and Biotechnology". You can prepare your references using that style. For Endnote style, you can reach it by clicking on the endnote at the bottom right part of the main page of the journal.

Examples

Example of an article with 1 author;

Marakli, S., A Brief Review of Molecular Markers to Analyze Medicinally Important Plants. International Journal of Life Sciences and Biotechnology, 2018. 1 (1): p. 29-36.

Example of an article with 2 authors;

Kocacaliskan, I. and I. Tailor, Allelopathic effects of walnut leaf extracts and juglone on seed germination and seedling growth. The Journal of Horticultural Science and Biotechnology, 2001. 76 (4): p. 436-440.

Example of an article with 3 authors;

Segura-Aguilar, J., I. Hakman, and J. Rydström, The effect of 5OH-1,4-naphthoquinone on Norway spruce seeds during germination. Plant Physiology, 1992. 100 (4): p. 1955-1961.

Example of articles with 4 or more authors

Arasoglu, T., et al., Synthesis, characterization, and antibacterial activity of juglone encapsulated PLGA nanoparticles. Journal of applied microbiology, 2017. 123 (6): p. 1407-1419.

Example for the book;

Kocalishkan, I., Allelopathy. 2006, Ankara, Turkey: Our Office Press-In Turkish.

Example for Book Chapter;

Kaya, Y., F.Z. Huyop, and M.F. Edbeib, Genetic Diversity in Plants, in Advances in Biosciences, F.Z. Huyop and S. Mohammed, Editors. 2019, Penerbit UTM Press. Malaysia: Malaysia. p. 04-24.

Ethical Principles and Publication Policy

Ethical standards for publication exist to ensure high-quality scientific publications, public trust in scientific findings, and that people receive credit for their ideas. In addition, the authors are encouraged to follow the ethic guidelines of the Committee on Publication Ethics (COPE) which can be viewed on the COPE website.

International Journal of Life Sciences and Biotechnology (Int J. Life Sci. Biotechnol.) is an electronic peer-reviewed international journal trying to have the highest standards of publication ethics. For that, we affirm the following principles of the Publication Ethics and Malpractice Statement.

If malpractice is discovered at any time even after the publication, the articles not in accordance with these standards will be removed from the publication. Int J. Life Sci. Biotechnol. is checking all papers in a double-blind peer-review process. We also check for plagiarisms, research fabrication, falsification, and improper use of any organisms in research. We will also report any cases of suspected plagiarism or duplicate publishing. Int J. Life Sci. Biotechnol. reserves the right to use plagiarism detecting software to screen submitted papers at all times.

Author's responsibilities: The author or authors must guarantee that they have written a unique study. Moreover, they must make sure that the article has not been submitted and evaluated elsewhere at the same time. Literature of the other researchers, all contributors and sources (including online sites) should be appropriately credited and referenced. All submitted manuscripts should be edited for language. All references should be cited without been copied or plagiarized. If needed, any financial sources or another conflict of interest should be disclosed. In order to correct the paper, any significant error or inaccuracy in the published works should be notified by the related authors. An author agrees to the license agreement before submitting the article. All articles must be submitted using the online submission procedure. Submitting a paper simultaneously to more than one publication at a time is a violation of publications' ethics.

Editorial responsibilities: Editors along with Editor-in-Chief and Editorial Board have publication decisions. Editors must guarantee a fair double-blind peer-review of the submitted articles for publication. They have to prevent any potential conflict of interests between the author and editors and reviewers. They have to guarantee the confidentiality of submitted articles before publishing. Editor-in-Chief will coordinate the work of the editors.

Peer review/responsibility for the reviewers: They have to review the manuscripts based on content without regard to ethnic origin, gender, sexual orientation, citizenship, religious belief, or political philosophy of the authors. They have to guarantee the confidentiality of submitted articles before publishing. They have to report any plagiarisms, research fabrication, falsification, and improper use of any organisms in research to the editors and/or the Editor-in-Chief. They have to review the papers objectively and state their opinions clearly in the forms and on the paper. A reviewer having inadequate time or feeling unqualified should notify the editors as soon as possible and excuse her/himself from the review process.

Plagiarism

All journals published by IJLSB are committed to publishing only original material, i.e., material that has neither been published elsewhere nor is under review elsewhere. Manuscripts that are found to have been plagiarized from a manuscript by other authors, whether published or unpublished, will incur plagiarism sanctions.

Manuscripts are checked by Ithenticate Plagiarism System.

Duplicate Submission

Manuscripts that are found to have been published elsewhere, or to be under review elsewhere, will incur duplicate submission/publication sanctions. If authors have used their own previously published work or work that is currently under review, as the basis for a submitted manuscript, they are required to cite the previous work and indicate how their submitted manuscript offers novel contributions beyond those of the previous work.

Citation Manipulation

Submitted manuscripts that are found to include citations whose primary purpose is to increase the number of citations to a given author's work or articles published in a particular journal, will incur citation manipulation sanctions.

Data Fabrication and Falsification

Submitted manuscripts that are found to have either fabricated or falsified experimental results, including the manipulation of images, will incur data fabrication and falsification sanctions.

Improper Author Contribution or Attribution

All listed authors must have made a significant scientific contribution to the research in the manuscript and approved all its claims. It is important to list everyone who made a significant scientific contribution, including students and laboratory technicians.

Redundant Publications

Redundant publications involve the inappropriate division of study outcomes into several articles.

Sanctions

In the event that there are documented violations of any of the above-mentioned policies in any journal, regardless of whether or not the violations occurred in a journal published by Int J. Life Sci. Biotechnol., the following sanctions will be applied:

Immediate rejection of the infringing manuscript.

Immediate rejection of every other manuscript submitted to any journal published by Int J. Life Sci. Biotechnol. by any of the authors of the infringing manuscript.

The prohibition against all of the authors for any new submissions to any journal published by IJLSB, either individually or in combination with other authors of the infringing manuscript, as well as in combination with any other authors. This prohibition will be imposed for a minimum of 36 months. Prohibition against all of the authors from serving on the Editorial Board of any journal published by Int J. Life Sci. Biotechnol.

In cases where the violations of the above policies are found to be particularly egregious, the publisher reserves the right to impose additional sanctions beyond those described above.

Publication Charge

"International Journal of Life Sciences and Biotechnology" is an Open Access Journal and does not charge any printing charges from authors, during article delivery, assessment and printing stages.

Aim and Scope

International Journal of Life Sciences and Biotechnology (Int J. Life Sci. Biotechnol.) is an international peer-reviewed journal that publishes original articles from all biology and molecular biology studies, particularly in the fields of life sciences and biotechnology. The language of publication is Turkish and English. Also the main objective of Int J. Life Sci. Biotechnol. is to provide quality publications to scientists, researchers, and engineers from both academia and industry who want to communicate the latest developments and practices in their field.

Int J. Life Sci. Biotechnol. publishes original papers in various fields of Life Sciences and Biotechnology that covers, but is not limited to, the following areas:

- Agricultural Biotechnology
- Animal (livestock and fish production, physiology, breeding and genetics, biotechnology, etc),
- Animal Biotechnology
- Biochemical Genetics,
- Biochemistry
- Biodiversity and biodiscovery
- Bioinformatics and system biology
- Biology and Molecular Biology,
- Bioremediation and biodegradation
- Biotechnology
- Bioethics (Life Sciences and Biotechnology)
- Botany,
- Evolution and Population Genetics,
- Food Biotechnology
- Genetic engineering and cloning
- Lichens
- Genetics,
- Biotechnological product and Halal Food
- Industrial Biotechnology
- Medical Biotechnology
- Molecular Genetics
- Plant (Plant production, physiology, breeding and genetics, biotechnology, agronomy, horticulture, plant protection, etc.),
- Plant Biotechnology
- Soil (soil ecology, physics, and chemistry, etc)
- Polar Science (Life Sciences and Biotechnology)

DECLARATION: This work is part of Gülfidan KUYUMCU's MA thesis. Articles on 27-29 September 2017 held in Bayburt in Turkey was presented as a Oral Presentation I. International Organic Agriculture and Biodiversity Symposium

Genetic Analysis Related To Organized Genetic Changes in Potato And Processed Potatoes

Gulfidan Kuyumcu^{1*}, Muhammed Majed Abed²

Author Addresses: ¹ Samsun Ondokuz Mayıs University, Faculty of Agriculture, Department of Agricultural Biotechnology, Samsun / Turkey

² Samsun Ondokuz Mayıs University, Faculty of Agriculture, Department of Agricultural Biotechnology, Samsun / Turkey

*Corresponding Autor: Gulfidan Kuyumcu, e-mail: ijlsb@intsa.org

Please write the e-mail addresses and Orcid ID numbers of all authors **(required fields)**

Author 1 mail and Orcid ID:

Author 2 mail and Orcid ID:

Author 3 mail and Orcid ID:

Ethics Committee Report

Article If an Ethics Committee Report is required to conduct a research on animals and humans and to conduct this research, it is mandatory that the **Ethics Committee Report be scanned and uploaded as a PDF file**. Otherwise, the article is returned to the author at the preliminary examination and other stages.

1.REVIEWER SUGGESTION

DEGREE:
FIRST NAME:
LAST NAME:
MAIL ADDRESS:
INSTITUTION:
DEPARTMENT:
SUBJECTS:

2.REVIEWER SUGGESTION

DEGREE:
FIRST NAME:
LAST NAME:
MAIL ADDRESS:
INSTITUTION:
DEPARTMENT:
SUBJECTS:

3.REVIEWER SUGGESTION

DEGREE:
FIRST NAME:
LAST NAME:
MAIL ADDRESS:
INSTITUTION:
DEPARTMENT:
SUBJECTS: